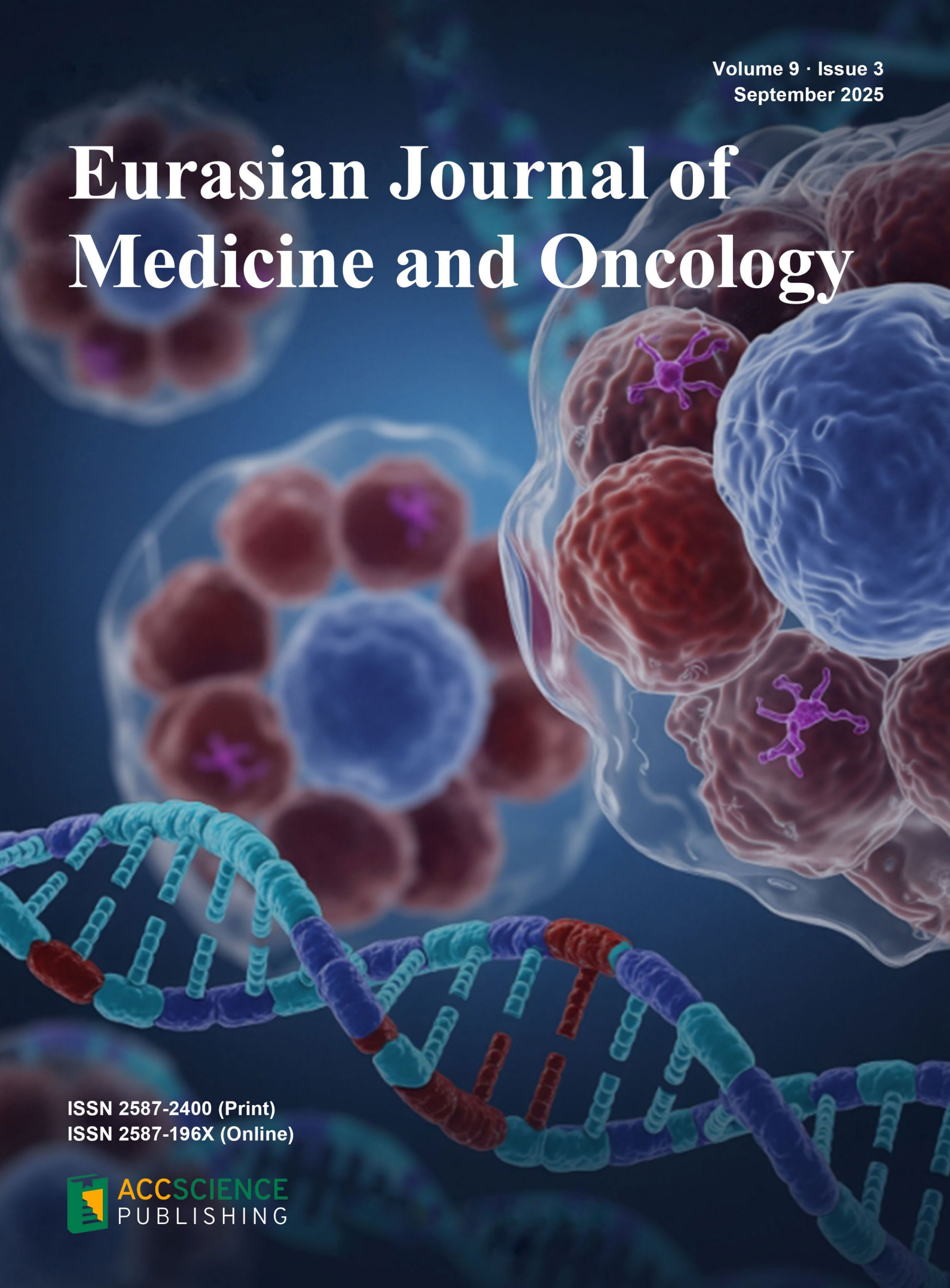
Volume 9 · Issue 3
September 2025

Eurasian Journal of Medicine and Oncology



ISSN 2587-2400 (Print)
ISSN 2587-196X (Online)

ACCSCIENCE PUBLISHING

ACCSCIENCE PUBLISHING

Eurasian Journal of Medicine and Oncology

Print ISSN: 2587-2400
Online ISSN: 2587-196X

The ***Eurasian Journal of Medicine and Oncology (EJMO)*** is an international peer-reviewed journal that publishes high-quality research across the full spectrum of oncology and general medicine. *EJMO* accepts submissions in English only and aims to disseminate impactful research and clinical insights to an international readership, promoting advancements in both cancer-specific and general medical fields. *EJMO* is committed to bridging the gap between basic research and clinical applications, advancing developments in the field of medical and cancer research, and communicating scientific knowledge to researchers and the public alike, to empower scientific breakthroughs of the future.



About the Publisher

AccScience Publishing is a publishing company based in Singapore. We publish a range of high-quality, open-access, peer-reviewed journals and books from a broad spectrum of disciplines.

Contact Us

Managing Editor
ejmo.office@accscience.sg

AccScience Publishing
9 Raffles Place, Republic Plaza 1 #06-00 Singapore 048619.

Volume 9 • Issue 3 • September 2025
ISSN 2587-2400 (print) ISSN 2587-196X (online)

Eurasian Journal of Medicine and Oncology

Editors-in-Chief

Bernd Kaina
Universitätsmedizin Mainz, Mainz, Germany

Hilmi Kodaz
Department of Medical Oncology, Eskisehir, Turkey

Mingzhu Yin
School of Medicine Chongqing University, China

ACCSCIENCE PUBLISHING

Access Science Without Barriers

Full issue copyright © 2025 AccScience Publishing
All rights reserved. Without permission in writing from the publisher, this full issue publication in its entirety may not be reproduced or transmitted for commercial purposes in any form or by any means, electronic or mechanical, including photocopying, recording, or any information storage and retrieval system. Permissions may be sought from ejmo.office@accscience.sg.

Article copyright © Respective Author(s)
See articles for copyright year. All articles in this full issue publication are open-access. There are no restrictions in the distribution and reproduction of individual articles, provided the original work is properly cited. However, permission to reuse copyrighted materials of an article for commercial purposes is applicable if the article is licensed under Creative Commons Attribution-NonCommercial License. Check the specific license before reusing.



EURASIAN JOURNAL OF MEDICINE AND ONCOLOGY

ISSN: 2587-2400 (print)
ISSN: 2587-196X (online)

Editorial and Production Credits

Publisher: AccScience Publishing
Managing Editor: Qingbo Li
Production Editor: Samyuktha Balakrishnan
Article Layout and Typeset: Sinjore Technologies (India)

For all advertising queries, contact.
ejmo.office@accscience.sg.

Supplementary file

Supplementary files of articles can be obtained at https://accscience.com/journal/EJMO/9/3.

Disclaimer

AccScience Publishing is not liable to the statements, perspectives, and opinions contained in the publications. The appearance of advertisements in the journal shall not be construed as a warranty, endorsement, or approval of the products or services advertised and/or the safety thereof. AccScience Publishing disclaims responsibility for any injury to persons or property resulting from any ideas or products referred to in the publications or advertisements. AccScience Publishing remains neutral with regard to jurisdictional claims in published maps and institutional affiliations.

Eurasian Journal of Medicine and Oncology

Editorial Board

Editors-in-Chief

Bernd Kaina, *Germany*
Hilmi Kodaz, *Turkey*
Mingzhu Yin, *China*

Associate Editors

Hu Zhou, *China*
Murat Dincer, *Turkey*
Gaetano Isola, *Italy*
Bulent Erdogan, *Turkey*
Donghai Wu, *China*
Yi Zhang, *China*

Editorial Board Members*

Ibrahim A. Abdelazim, *Kuwait*
Fathinul Fikri Ahmad Saad, *Malaysia*
Mamoun Ahram, *Jordan*
Habban Akhter, *India*
George A Alexiou, *Greece*
Surya Prakash Amarachintha, *USA*
Maqood Ali Ansari, *Pakistan*
Zafer Arik, *Turkey*
Babak Asadi-Azarbaijani, *Norway*
Majid Asadi-Shekaari, *Iran*
Nuri Faruk Aykan, *Turkey*
Muhammad Bilal, *China*
Gulcan Bulut, *Turkey*
Abdullah Buyukcelik, *Turkey*
Ronald C. Desrosiers, *USA*
Wei Cao, *China*
Donatella Caserta, *Italy*
Long-Sheng Chang, *USA*
Xiaojun Chen, *China*
Chung-Yi Chen, *China*
William Cho, *China*
Maoquan Chu, *China*
Havva Yesil Cinkir, *Turkey*
Ugo Cioffi, *Italy*
Roberto Cuomo, *Italy*
Vito D' Andrea, *Italy*
Olga D. Savvidou, *Greece*
Paolo De Simone, *Italy*
Meran Keshawa Ediriweera, *Sri Lanka*
Mehmet Ali Erkurt, *Turkey*
Onur Esbah, *Turkey*
Alfio Ferlito, *Italy*
Pedro Fonte, *Portugal*
Rosario Fornaro, *Italy*
Izzo Francesco, *Italy*
Liwu Fu, *China*
Vittorio Gebbia, *Italy*
Hatef Ghasemi Hamidabadi, *Iran*
Anar Gojayev, *USA*
Mahmut Gumus, *Turkey*
Simona Gurzu, *Romania*
Ilhan Hacibekiroglu, *Turkey*
Hakan Harputluoglu, *Turkey*
Jing He, *China*
Daniel Wai-Hung Ho, *China*
Jason Chia-Hsun Hsieh, *China*
Shen (Steve) Hu, *USA*
Hannah Xiaoyan Hui, *China*
Alice Indini, *Italy*
Orestis Ioannidis, *Greece*
Marcello Iriti, *Italy*
Aasems Jacob, *USA*
Miaomiao Jiang, *China*
Weilin Jin, *China*
Abolghasem Jouyban, Iran
Venkataramana Kandi, *India*
Surya Kant, *India*
Aziz Karaoglu, *Turkey*
Samander Kaushik, *India*
Rovshan I. Khalilov, *Azerbaijan*
Naveed Ahmed Khan, *Turkey*
Â Rabia Sannam Khan, *UK*
Shashank Kumar, *India*
Anupam Kumar, *India*
Jeng Kuo-Shyang, *China*
Giuseppe Lanza, *Italy*
Carl J. Lavie, *USA*

Chen-Hua Liu, *China*
Dong-Xu Liu, *New Zealand*
Baohua Liu, *China*
Li Liu, *China*
Zhenyu Luo, *China*
Xuelei Ma, *China*
Clelia Madeddu, *Italy*
Saurav Mallik, *USA*
Francesco Marotta, *Italy*
Fabio Martinelli, *Italy*
Mohammad Waheed Mohammad El-Anwar, *Egypt*
Tapan Kumar Mohanta, *Oman*
Roberto Montalti, *Italy*
Mohammad Amin Moosavi, *Iran*
Ghulam Murtaza, *Pakistan*
Handan Onur, *Turkey*
Chunlin Ou, *China*
Sibel Ozden, *Turkey*
Ashok K Pandurangan, *India*
Chiara Pane, *Italy*
Semra Paydas, *Turkey*
Raja Affendi Raja Ali, *Malaysia*
Hasan Mahmud Reza, *Bangladesh*
Michela Roberto, *Italy*
Rommel Mario Rodriguez Burbano, *Brazil*
Umberto Romeo, *Italy*
Cinzia Valeria Russo, *Italy*
Emilio Sacco, *Italy*
Saeid Safiri, *Iran*
Alexander M. Seifalian, *UK*
Bogdan Socea, *Romania*
John Spiliotis, *Greece*
Masahiro Sugimoto, *Japan*
Mauro Tognon, *Italy*
Aytug Uner, *Turkey*
Mihai Dorin Vartolomei, *Switzerland*
Panagiotis J. Vlachostergios, *USA*
Yin Ping Wong, *Malaysia*
Yen-Wen Wu, *China*
Yingqiu Xie, *Kazakhstan*
Selim Yalcin, *Turkey*
Masayoshi Yamaguchi, *USA*
Feng Yan, *China*
Ming Yang, *China*
Jialiang Yang, *China*
Mei Yang, *China*
Mustafa Yildiz, *Turkey*
Loh Siew Yim, *Malaysia*
Haiyang Yu, *China*
Zainul Amiruddin Zakaria, *Malaysia*
Jan Maciej Zaucha, *Poland*
Shuai Zhang, *China*
Jian-Hong Zhong, *China*
Carmino Antonio de Souza, *Brazil*

Statistics Editor

Ferhan Elmali, *Turkey*

Language Editor

Vuslat Muslu Erdem, *USA*

Youth Editorial Board Members

Yarong Guo, *China*
Shizhi He, *China*
Qiang He, *China*
Xianbin Kong, *China*
Shuai Mu, *China*
Zhen Yang, *China*

*Editorial Board Members as of September 29, 2025

ACCSCIENCE PUBLISHING

Volume 9 | Issue 3 | September 2025 | Page 1 – 301 |

Eurasian Journal of Medicine and Oncology

https://accscience.com/journal/EJMO

CONTENTS

EDITORIAL

1 **From the Editor's desk**
Bernd Kaina

REVIEW ARTICLES

4 **Liver fibrosis: Clinical assessment, pathogenesis, and anti-fibrotic therapy**
Xin Liu, Chongmiao Yang, Yanyan Liu, Xiaowen Lin, Wei Su, Jian Sun, Xiaoguang Zhao

19 **CXC chemokines as potential non-invasive biomarkers and therapeutic targets for non-alcoholic fatty liver disease: A review**
Zhihui Li, Zhiyun Chen

32 **NOTCH3 signalling as a therapeutic nexus: Bridging cerebral small vessel disease and breast cancer pathophysiology**
Zaw Myo Hein, Nisha Shantakumari, Muhammad Danial Che Ramli, Usman Jaffer, Hafizah Abdul Hamid, Che Mohd Nasril Che Mohd Nassir

52 **Update on systemic lupus erythematosus: A review**
Abdurahman Alloghbi, Yousef Al Obaisi, Hussain Alkhurayb, Amal M Shawabka, Fahad S. Alshehri

63 **Dynamics of *FLT3* mutations in acute myeloid leukemia: A systematic review and meta-analysis of shifts between diagnosis and relapsed/refractory disease**
Lais Teixeira, Camilla Correia, Alini Ponte, Diego Miranda, Felipe Feistauer, Marco Aurélio Salvino

ORIGINAL RESEARCH ARTICLES

75 **Mapping breast cancer protein interaction networks as metric spaces: Insights into central zones and drug discovery targets**
Emad Fadhal

86 **Development of a novel risk model for stratifying skin cutaneous melanoma patients based on prognostic senescence-related genes**
Yiting Feng, Lanlan Liu, Yunjin Xie, Mingzhu Yin

100 **The association between Vitamin D and breast cancer: A two-sample Mendelian randomization study**
Yang Xiao, Mei Yin, Xingyi Song

110 **Comparative efficacy and safety of Zercepac® plus pyrotinib versus Zercepac® plus pertuzumab in combination with chemotherapy as neoadjuvant therapy for HER2-positive breast cancer: A retrospective study**
Hong Gao, Jiali Lei, Zhaohua Gui, Shengying Wang

122 **Meta-analysis of the prognostic value of *KRAS* and *TP53* mutations in cholangiocarcinoma**
Benfeng Xu, Chuhan Zhang, Yibin Zhou, Jianan Jin

133 **Influencing factors of chemotherapy-related cognitive impairment in patients with breast cancer**
Ying Zhang, Shuhan Wu, Yunmiao Ma, Shuyang Chang, Jianhui Li, Bo Tian, Nan Jiang, Liping Yang, Kenian Pan, Xulong Zhu

147 **Revisiting the role of the Pfannenstiel incision in early-stage endometrial cancer**
Cem Yagmur Ozdemir, Hasan Eroğlu, Necat Cağatay Sezer, Nayif Çicekli, Derya Yeğin Aksu, Dağıstan Tolga Arioz

155 **Psychotherapists' perspectives on the quality of psychological services for cancer patients in Riyadh: A predictive study**
Yahya Khatatbeh

168 **Comprehensive characterization of the material basis and network pharmacology of Dan-Shen-Yin in the treatment of gastritis**
Jianbing Dong, Zhirong Zhou, Yi Chen, Peng Lei, Qingrui Zhang, Miaomiao Jiang

185 **Basic medication therapy based on target glycated hemoglobin levels in patients with ischemic heart disease and diabetes**
Raisa Trigulova, Alisher Ikramov, Dilnoza Alimova, Shukhrat Doniyorov, Dilafruz Akhmedova, Shakhnoza Mukhtarova

197 **Targeting the FN3K–Nrf2 axis: Discovery and pre-clinical evaluation of novel inhibitors for breast cancer therapy**
Erica Alves, Gurupadayya Bannimath, Prabitha Prabhakaran

226 **Critical care pharmacists in intensive care units: A meta-analysis of their impact on mortality and adverse drug events**
Mohamed S. Imam, Khalid Nassir Almurayeh, Abdulrahman Saeed M. Okshah, Fawaz Saad Yahya Thabit, Amal Ali Al Thabet, Abdullah Abduh Ali Hijazy, Shahad Abdullah Ali Alahmari, Faisal Saeed Mohammed Hatab, Sadeem Nawaf A. Alotaibi, Ruba Hamoud Mohammed Alshahrani, Ranaa Abdullah Saleh Alamri

239 **Perception of advance health-care directives among nursing students in oncology and palliative care settings: An Italian pre–post study**
Diego Lopane, Sara Morales Palomares, Alessandra Dacomi, Daniela Cattani, Simone Cosmai, Chiara Provasoli, Sarah Scollo, Mauro Parozzi, Giovanni Cangelosi, Stefano Mancin, Emanuela Morenghi, Beatrice Mazzoleni

250 **Enhanced expression of metastasis-associated genes in colorectal cancer**
Adeodatus Yuda Handaya, Hendra Susanto, Moch Sholeh

234 **Predictive value of an eight-mRNA signature in colon adenocarcinoma prognosis**
Yuying Yang, Cuiying Wang, Hongqian Wei, Bing Zhou, Songtao Hou, Xiaochen Pang, Wenhai Dong, Zhongqiu Chai

250 **Investigating the role of neurotransmitter system and neurotrophic factor-related genes in human papillomavirus-associated cervical lesions**
Ângela Inácio, Laura Aguiar, João Caldeira, Margarida Gato, Raquel Carrilho, Patrícia Pires, Joana Ferreira, Luís Coelho, Rui Medeiros, Manuel Bicho, Maria Clara Bicho

261 **Identification and validation of relevant diagnostic biomarkers for osteoporosis by Weighted Gene Co-expression Network Analysis and machine learning**
Cuicui Zhou, Zarina Awang, Farra Aidah Jumuddin

277 **Efficacy of preperitoneal local anesthetic infiltration on post-operative analgesia following laparoscopic cholecystectomy**
Noha Mohamed Abdelwahab Elsaid, Ain El-Marwa Abdelmonem Abdallah Hassan, Ahmed Mohamed Said, Mostafa R. Bakry, Doaa Mohamed Almonayery Ibrahim, Marwa Ibrahim Eid, Hayam Shaaban Soliman Morsy, Mostafa Mohamed Elsayed, Nashwa Mohammed Ibrahiem, Gihan Eissa Zahran, Nahla Mohammed Eldeeb, Mayada Yahia Elbohouty, Heba Atwa Ahmed Atwa, Gehan Abd Elrhman Eldesoky, Eman A. Salem, Samia Sayed Ahmed, Warda Demerdash Khalifa Ali, Tarek Abdelmonem Abdelzaher

SHORT COMMUNICATIONS

287 **Causal links between *Helicobacter pylori* infection and Alzheimer's disease: Insights from genome-wide summary data-based Mendelian randomization**
Yuan Xin Hou, Ao Wang, Ke Yi

294 **Fertility outcomes of macroscopic tubal reanastomosis through mini-laparotomy: A retrospective case series study**
Dilay Gök Korucu, Esra Koşucu, Şükran Doğru, Oğuzhan Günenç

LETTER TO EDITOR

300 **Ferroptosis inhibition: New insights for the treatment of acute lung injury**
Xuhan Chen, Jinhe Guo

ACCSCIENCE PUBLISHING

Eurasian Journal of Medicine and Oncology

EDITORIAL

From the Editor's desk

Bernd Kaina*

Institute of Toxicology, University Medical Center, Mainz, Germany

Two articles have appeared in this volume of the *Eurasian Journal of Medicine and Oncology* that I would like to address. The work by Rauf *et al.*[1] describes two natural compounds isolated from *Pistacia chinensis*. This tree is found primarily in China and is planted as a street tree in temperate zones worldwide due to its attractive fruit and beautiful autumn foliage. Two flavonoids were extracted from the tree's bark. The flavonoids are polyphenols, and their chemical structures are described in the manuscript. *In silico* analyses showed that the phytochemicals, designated as compound 1 and compound 2, bind to several target proteins, including mechanistic target of rapamycin (mTOR) and protein kinase B 1 (encoded by *AKT1*). They could therefore potentially influence the phosphoinositide 3-kinase (PI3K)–AKT–mTOR pathway. If this binding has an inhibitory effect, it could lead to reduced protein synthesis and, consequently, inhibition of cell growth and proliferation. It could also contribute to increased levels and activation of tumor suppressor protein p53 through targeting mouse double minute 2 homolog (MDM2), as well as to the activation of pro-apoptotic proteins such as BCL2, thereby stimulating pro-apoptotic signaling. A third effect is based on the inhibition of autophagy by mTORC1, which may also be inhibited. In summary, pro-apoptotic processes could be promoted, and cells could be specifically driven to undergo cell death.

In light of this scenario, the authors also investigated cell death using the glioblastoma cell line U87MG. In the 3-(4,5-di methyl thiazol-2-yl)-2,5-diphenyltetrazolium bromide (MTT) assay, the flavonoids showed a positive effect, which is interpreted as anti-cancer activity. However, it must be noted that the MTT assay is a metabolic assay and reflects both proliferation inhibition and actual cell death. Unfortunately, these toxicity studies were not extended, and the authors did not assess apoptosis or, where applicable, necroptosis. Therefore, it remains unclear whether the effects observed through the MTT assay are due to genuine cell death or simply reflect growth inhibition.

This is clearly a limitation of the work. Observing a growth-inhibitory or cytotoxic effect on a tumor cell line should not immediately lead to the conclusion that a substance has "anti-cancer activity." Such a conclusion requires evidence that the substance is selectively active against tumor cells and not toxic to non-transformed cells. This implies that a broad panel of cell lines should be tested. Animal experiments are also necessary before claims of anti-cancer activity can be made. The term "activity on cancer cell lines" would be more precise and appropriate in this context.

Nevertheless, the study is interesting because it reports the identification of a new group of natural compounds with potential relevance for cancer therapy. In future research, it would be worthwhile to characterize the effects at both the cellular and molecular levels in detail, to answer important open questions. For example, in the toxicity prediction assay, one of the compounds tested positive in the Ames test. This could indicate that at least one of the substances has genotoxic potential. Genotoxic effects are clearly linked to cytotoxicity, as p53-dependent apoptotic signaling pathways are activated through DNA damage.[2] In fact, some natural compounds that exert

***Corresponding author:**
Bernd Kaina
(kaina@uni-mainz.de)

Citation: Kaina B. From the Editor's desk. *Eurasian J Med Oncol.* 2025;9(3):1-3.
doi: 10.36922/EJMO025360369

Received: August 21, 2025

Accepted: September 1, 2025

Published online: September 23, 2025

Copyright: © 2025 Author(s). This is an Open-Access article distributed under the terms of the Creative Commons Attribution License, permitting distribution, and reproduction in any medium, provided the original work is properly cited.

Publisher's Note: AccScience Publishing remains neutral with regard to jurisdictional claims in published maps and institutional affiliations.

cytotoxic effects on glioblastoma cells, such as curcumin[3] and fisetin,[4] exhibit this mechanism. The cytotoxic effect of the flavonoids could potentially be harnessed for adjuvant therapy or to enhance the activity of existing anti-cancer drugs.

Another interesting aspect that could be explored in future studies is whether the substances exhibit senolytic or senomorphic activity. This is plausible, as the PI3K–AKT–mTOR axis is a major driver of the senescence-associated secretory phenotype (SASP) and helps to maintain the senescent state: mTORC1 promotes translation of interleukin-1 alpha and other SASP regulators. Sustained mTOR activity supports the enlarged, metabolically hyperactive phenotype of senescent cells. Furthermore, AKT activity prevents apoptosis, allowing these damaged cells to persist.[5,6] Thus, this pathway, which is linked to both induction and maintenance of senescence, is crucial, and its inhibition represents a clear therapeutic target. Overall, while the study has limitations, it is likely to stimulate further research on these intriguing flavonoids isolated from *P. chinensis*.

Another study that caught my attention reports on the link between diet and pancreatic cancer.[7] In this case–control study, the authors surveyed 101 pancreatic patients and 314 controls from Jordan about their eating habits and carefully analyzed their responses. They concluded that the extensive consumption of three types of food is associated with an increased risk of pancreatic cancer: (i) yogurt, (ii) white and processed cheese, and (iii) cooked red meat (from veal and lamb) and cooked chicken.

The observation that yogurt and cheese, both generally considered healthy foods, may support pancreatic cancer development is surprising. What might explain this? It should be noted that the overall data are very heterogeneous and, as the authors carefully summarize, there are studies that do not support such a relationship for yogurt and cheese. Could it be that yogurt and cheese are produced differently in Jordan compared to other countries, where these dairy products are not associated with enhanced cancer risk? Is the chemical composition, or the ingredients added or formed during the preparation of yogurt and cheese in Jordan, different from those in other countries? It is also possible that certain microbes or fungi contaminated the dairy products, or are even part of the fermentation process, and produce toxins that are genotoxic.

An example from a completely different context may be illustrative: nicotine-derived N-nitrosamines in tobacco, which are at least partially responsible for the carcinogenic effects of both smokeless and smoked tobacco, and are formed during the fermentation of tobacco leaves.[8] In this case, the carcinogens arise as a result of the preparation process. While this is an extreme example, there are plenty of others involving microbial and fungal contamination of food that impact the incidence of cancer.

The link between high-temperature cooked meat and increased cancer risk is well established. Specifically for pancreatic cancer, this study reported that total consumption of red meat is associated with a 65% increased risk. Possible causes include food-borne heterocyclic aromatic amines, polycyclic aromatic hydrocarbons, heme iron metabolites in red meat, and/or aromatic amino acids. All of these are plausible contributors. However, two meta-analyses, each involving a very large number of patients, concluded that there is no clear relationship between the consumption of red or processed meat and the risk of pancreatic cancer (for references see the paper I am referring to). That said, subgroup differences within cohorts may exist, as indicated by findings from a multiethnic cohort study. A more refined analysis revealed that even relatively small amounts (100–120 g/day) of red and processed meat may be significantly associated with increased pancreatic cancer risk (as discussed in the study from Jordan).

In contrast to red meat, chicken is generally not considered a risk factor for cancer such as colorectal carcinomas. However, this study concludes that "a large intake of poultry may increase the risk of pancreatic cancer." The potential cause could again be food-borne aromatic amines, which are highly carcinogenic and formed during high-temperature cooking. Clearly, the methods of red meat and poultry preparation in Jordan warrant further investigation. Experimental and field studies could assess the actual levels of carcinogenic compounds in these foods.

The current investigation also offers a glimmer of hope. Cooked fish showed a negative correlation with pancreatic cancer, suggesting it may offer some protective effects. Although the overall data on this are not entirely consistent, the study demonstrates that the diverse dietary patterns present in Jordan have a profound effect on health. Dietary recommendations, possibly promoting a mixed diet rich in vegetables, may be an effective strategy to reduce cancer incidence in Jordan.

Conflict of interest

Bernd Kaina is the Editor-in-Chief of this journal. The author declares that he has no known competing financial interests or personal relationships that could have influenced the work reported in this paper.

References

1. Rauf A, Ho S, Khan MU, *et al*. Anticancer potential of flavonoids isolated from *Pistacia chinensis* against

glioblastoma (U87) cell line: Extensive *in vitro* and *in silico* research. *Eurasian J Med Oncol*. 2025;9(1):144-158.

doi: 10.36922/ejmo.5768

2. Roos WP, Thomas AD, Kaina B. DNA damage and the balance between survival and death in cancer biology. *Nat Rev Cancer*. 2016;16(1):20-33.

doi: 10.1038/nrc.2015.2

3. Beltzig L, Frumkina A, Schwarzenbach C, Kaina B. Cytotoxic, genotoxic and senolytic potential of native and micellar curcumin. *Nutrients*. 2021;13(7):2385.

doi: 10.3390/nu13072385

4. Beltzig L, Christmann M, Dobreanu M, Kaina B. Genotoxic and cytotoxic activity of fisetin on glioblastoma cells. *Anticancer Res*. 2024;44(3):901-910.

doi: 10.21873/anticanres.16884

5. Klepacki H, Kowalczuk K, Lepkowska N, Hermanowicz JM. Molecular regulation of SASP in cellular senescence: Therapeutic Implications and Translational Challenges. *Cells*. 2025;14(13):942.

doi: 10.3390/cells14130942

6. Walters HE, Deneka-Hannemann S, Cox LS. Reversal of phenotypes of cellular senescence by pan-mTOR inhibition. *Aging* (*Albany NY*). 2016;8(2):231-244.

doi: 10.18632/aging.100872

7. Allehdan S, Ibrahim MO, Al-Awwad N, *et al*. Investigating the dietary links to pancreatic cancer: A case-control study on dairy, meat, and egg consumption. *Eurasian J Med Oncol.* 2025;9(2):87-98.

doi: 10.36922/ejmo.6637

8. Stanfill SB, Hecht SS, Joerger AC, *et al*. From cultivation to cancer: Formation of N-nitrosamines and other carcinogens in smokeless tobacco and their mutagenic implications. *Crit Rev Toxicol.* 2023;53(10):658-701.

doi: 10.1080/10408444.2023.2264327

ACCSCIENCE PUBLISHING

Eurasian Journal of Medicine and Oncology

REVIEW ARTICLE

Liver fibrosis: Clinical assessment, pathogenesis, and anti-fibrotic therapy

Xin Liu[1†], Chongmiao Yang[1†], Yanyan Liu[1†], Xiaowen Lin[1], Wei Su[2], Jian Sun[2*], and Xiaoguang Zhao[1*]

[1]Zhuhai People's Hospital (The Affiliated Hospital of Beijing Institute of Technology, Zhuhai Clinical Medical College of Jinan University), Zhuhai, Guangdong, China

[2]Translational Medicine Research Center, Medical Pathology Center, Chongqing University Three Gorges Hospital, School of Medicine Chongqing University, Chongqing University, Chongqing, China

Abstract

Liver fibrosis represents a prevalent pathological change that occurs during the progression of chronic liver disease, which is characterized by excessive reparative responses following hepatic tissue injury. Advances in diagnostic and imaging technologies have facilitated a deeper understanding of liver function and metabolic changes, which are crucial for early and accurate diagnosis of liver fibrosis. Furthermore, elucidating the signaling pathways involved in liver fibrogenesis provides valuable insights into its pathogenesis and progression, guiding clinical management and treatment strategies for patients with liver fibrosis. This review critically evaluates various clinical and experimental therapies aimed at mitigating or reversing liver fibrosis. Specific targeted nanocarrier drug delivery systems and traditional herbal medicines hold promise in enhancing anti-fibrotic efficacy and inhibiting disease progression.

Keywords: Liver fibrosis; Hepatic stellate cells; Non-invasive assessment; Anti-fibrotic therapy; Traditional Chinese medicine

[†]*These authors contributed equally to this work.*

***Corresponding authors:**
Xiaoguang Zhao
(zhaoxiaoguang@ext.jnu.edu.cn)
Jian Sun
(sunjian@cqu.edu.cn)

Citation: Liu X, Yang C, Liu Y, *et al*. Liver fibrosis: Clinical assessment, pathogenesis, and anti-fibrotic therapy. *Eurasian J Med Oncol*. 2025;9(3):4-18.
doi: 10.36922/ejmo.8125

Received: December 22, 2024

Revised: February 25, 2025

Accepted: March 6, 2025

Published Online: March 26, 2025

Copyright: © 2025 Author(s). This is an Open-Access article distributed under the terms of the Creative Commons Attribution License, permitting distribution, and reproduction in any medium, provided the original work is properly cited.

Publisher's Note: AccScience Publishing remains neutral with regard to jurisdictional claims in published maps and institutional affiliations

1. Introduction

Liver fibrosis is a common pathological repair response to chronic liver injuries and serves as the common endpoint in many chronic liver diseases. In recent years, it has been increasingly associated with poor prognosis and is likely to be the leading cause of end-stage liver disease in the future. The activation of hepatic stellate cells (HSCs) is recognized as the most critical event in the pathogenesis of liver fibrosis.[1,2] HSCs exist in two distinct morpho-physiological states, which are quiescent and activated.[3] In the quiescent state, HSCs are located around hepatic sinusoids and store lipid droplets. However, in response to liver injury, they become activated and transform into myofibroblast-like cells that secrete large amounts of extracellular matrix (ECM).[4,5] The proliferation, migration, and contraction of these myofibroblasts, along with excessive ECM accumulation, further aggravate the fibrotic progression.[6] Kupffer cells, the resident monocytes, and macrophages of the liver serve as critical antigen-presenting cells within the human body.[7,8] Upon stimulation by external factors, they can engulf antigens and form antigen peptide-major histocompatibility complex class II complexes. These

antigens are then presented to T lymphocytes, facilitating immune recognition, response, and regulation.[9-11] In the context of liver injury, monocytes infiltrate and become activated through specific mechanisms. Once activated, they secrete a substantial amount of cytokines, including transforming growth factor beta (TGF-β), tumor necrosis factor-alpha (TNF-α), C-C motif chemokine ligand 5 (CCL5), platelet-derived growth factor BB (PDGF-BB), interleukin-1 beta (IL-1β), and interleukin-6 (IL-6), which promote HSC activation and transformation through multiple pathways.[12,13]

During the repair of chronic liver injury, the uncontrolled proliferation of activated HSCs causes the release of numerous inflammatory factors and paracrine effects, playing a very important role in the development of liver fibrosis. HSC activation and proliferation involve multiple signaling pathways, mainly the TGF-β1 and platelet-derived growth factor (PDGF) pathways. TGF-β1 is the most potent cytokine to induce HSC activation through the Smad2/3-dependent pathway.[14,15] PDGF is known as the strongest mitogen for HSCs both *in vitro* and *in vivo*. Upon binding to its receptor (PDGFR), PDGF activates the Ras-mitogen-activated protein kinase (Ras-MAPK) pathway and the phosphoinositide-3-kinase (PI3K)-protein kinase B (Akt/PKB) pathway, eventually stimulating protein kinase C (PKC) family members, which lead to the HSC reproduction and motility.[16]

Ligand-dependent signaling also plays an important role in liver pathophysiology. Highly conserved genes encode various membrane surface receptors such as Wnt, Notch, and Hedgehog (Hh), which regulate ligand-dependent signaling pathways. Wnt signaling components are upregulated in response to liver fibrogenesis and hepatitis.[17,18] In addition, Wnt1-inducible signaling pathway protein 1 has been demonstrated to mediate the canonical Wnt signaling pathway, playing an important role in hepatic inflammation and the progression of obesity-associated liver fibrosis.[19] Disruption of myofibroblast-specific Notch signaling not only inhibits primary HSC activation *in vitro* but also aggravates BCL2 associated X (BAX)-mediated apoptosis of myofibroblasts, accompanied by the overexpression of nerve growth factor receptor and Septin4.[20] In addition, the non-canonical Notch ligand delta-like non-canonical Notch ligand 1 plays a crucial role in ECM remodeling by reducing ECM deposition through the downregulation of ECM constituents expression and an increased matrix metalloproteinases/tissue inhibitor of metalloproteinases (MMPs/TIMPs) ratio.[21] Previous studies have demonstrated that inhibition of Sonic Hh and other Hh pathway components, such as Smoothened (SMO) and the transcription factor of Glioblastoma 2, downregulates HSC activation and profibrogenic trans-differentiation into myofibroblasts,[22-25] suppresses hepatic angiogenesis,[26] and reduces hepatic progenitor viability,[27-29] and finally mitigating fibrogenesis. In general, since most ligands influence hepatic physiological and pathological processes, exploring their molecular mechanisms is crucial for liver fibrosis research.

Most studies aim to uncover the molecular mechanism underlying the onset and development of liver fibrosis, restore the resting state of HSCs, and reduce ECM to delay or reverse disease progression. Some of these findings have already advanced to pre-clinical trials. Therefore, this review aims to elucidate the molecular mechanisms driving liver fibrosis progression and current diagnostic approaches, combined with relevant modern and traditional anti-fibrotic therapies, which provides a rationale for the drug development of liver fibrosis (Figure 1).

2. Clinical assessment of liver fibrosis

2.1. Pathological assessment of liver fibrosis

There are numerous factors that can lead to chronic liver injury, including hepatitis virus infection, non-alcoholic fatty liver disease (NAFLD), excessive alcohol consumption, autoimmune hepatitis, cholestatic liver disease, and drug-induced hepatotoxicity. Liver fibrosis, characterized by excessive activation of HSCs and altered ECM composition, is a wound-healing response to chronic liver injury that ultimately disrupts normal liver structure. Histopathology features of liver fibrosis vary by etiology. For instance, chronic viral hepatitis induces portal expansion with periportal fibrosis, which then progresses to septal fibrosis and ultimately cirrhosis. In contrast, fibrosis in NAFLD or alcoholic hepatitis is marked by centrilobular perivenular and sinusoidal fibrosis.[36] Cholestatic liver cirrhosis, on the other hand, is characterized by bile duct loss and concentric periductal fibrosis.[37]

All chronic liver diseases have the potential to progress to advanced fibrosis, cirrhosis, and even hepatocellular carcinoma (HCC), which result in poor prognosis and high mortality. Hence, a precise assessment of liver fibrosis is urgently needed in the clinical management of chronic liver disease. Several histological staging systems have been proposed, including the Knodell, Scheuer, Batts-Ludwig, METAVIR, and Ishak systems.[38,39] While these systems differ slightly, they share a common principle that fibrosis begins from the portal tracts, extends to adjacent areas, disrupts hepatic lobular architecture, and ultimately leads to cirrhosis.[36] The Ishak system includes two additional stages of fibrosis in detail compared to other systems, which decreases its clinical utility and convenience. The four-category fibrosis classification, such as the METAVIR

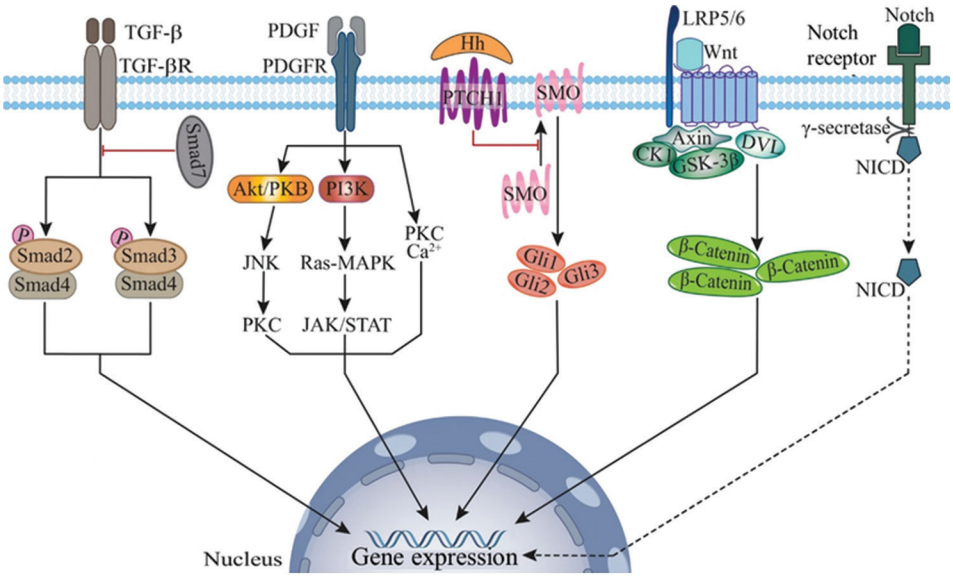


Figure 1. Mechanisms of liver fibrosis. Main cytokine and ligand-dependent signaling pathways make unequal contributions to liver fibrosis.[14] TGF-β, through the binding to its receptor, activates the phosphorylation of Smad2 and Smad3 proteins, which then associate with Smad4 to mediate downstream signaling.[30] On the contrary, Smad7 acts as a negative regulator of TGF-β1/Smad signaling, inhibiting this pathway.[31] PDGF mediates the transcriptional regulation of HSC proliferation and motility by binding to its receptor (PDGFR), which results in the activation of the PI3K, Akt/PKB, and PKC-Ca^{2+} pathways.[32,33] Notch signaling is induced when Notch proteins interact with their ligands, triggering γ-secretase-mediated cleavage and the release of the NICD, which then translocates into the nucleus, where it binds to Notch effectors to promote the differentiation and apoptosis of HSC.[33] Wnt ligands bind to FZD receptors and their co-receptor LRP5/6, leading to the high proportion of unphosphorylated β-catenin in the cytoplasm, which translocates to the nucleus and regulates target gene expression.[34] In the Hh pathway, Hh ligands inactivate their receptor, Patched 1, which in turn releases the co-receptor SMO. This activation triggers an intracellular signaling cascade that regulates gene expression, influencing the differentiation and survival of HSCs through the accumulation of Gli1 – 3 transcription factors.[35] Black arrows with pointed heads: Activation; Red arrows with flat heads: Inhibition; Black dotted arrows with pointed heads: Translocation.
Abbreviations: TGF-β: Transforming growth factor beta; TGF-βR: Transforming growth factor beta receptor; PDGF: Platelet-derived growth factor; PI3K: Phosphoinositide-3-kinase; AKT/PKB: Protein kinase B; PKC-Ca2+: Calcium-activated protein kinase C; NCID: Notch intracellular domain; FZD: Frizzled; LRP: Low-density lipoprotein receptor-related protein; Hh: Hedgehog; PTCH1: Patched 1; SMO: Smoothened; Gli1: Glioma-associated oncogene homolog 1; Gli2: Glioma-associated oncogene homolog 2; Gli3: Glioma-associated oncogene homolog 3; HSC: Hepatic satellite cell; JAK: Janus kinase; STAT: Signal transducer and activator of transcription; Ras/MAPK: Ras/Mitogen-activated protein kinase; JNK: c-Jun N-terminal protein kinase; GSK-3β: Glycogen synthase kinase-3 beta; Dvl: Dishevelled; CK1: Casein kinase 1.

system, which grades fibrosis as early (F0/1), significant (F2), advanced (F3), and cirrhosis (F4), is more appropriate in daily clinical assessment.[40]

2.2. Non-invasive assessments of liver fibrosis

Although histopathological examination remains the gold standard for liver disease diagnosis, the spatial and temporal heterogeneity of biopsy specimens can reduce its accuracy. In addition, contraindications and post-operation complications hinder its use for disease surveillance. Hence, non-invasive tests have been developed for assessing liver fibrosis.

2.2.1. Serum markers

During the last decade, a range of serum and imaging-related biomarkers have shown reliable predictive value in diagnosing and staging fibrosis. These biomarkers reflect liver fibrosis through both direct and indirect ways. Direct biomarkers indicate ECM metabolism and liver-specific profibrotic activity, including TGF-β, N-glycan profiles, procollagen type III amino-terminal peptide, and microfibril-associated protein. In contrast, numerous indirect biomarkers reveal hepatic changes in major nutrient metabolism, biotransformation, detoxification, hematopoiesis, and immune function. Examples include platelet count (PLT), aspartate aminotransferase (AST), and alanine aminotransferase (ALT).[41] These indirect biomarkers are readily available through routine blood tests.

Fibrosis scoring systems, which consist of different parameters, offer advantages in disease surveillance. A higher Fibrosis-4 (FIB-4) index (based on age, AST, PLT, and ALT levels) and an elevated AST-to-platelet ratio index are independent predictors of poor prognosis in chronic liver disease. Commercial serum-based tests, including the Enhanced Liver Fibrosis test, FibroMeter, and FibroTest,

have been proven to be accurate and suitable for assessing advanced fibrosis in patients with chronic virus hepatitis, NAFLD, or alcoholic liver disease.[41-43] However, while fibrosis-related scores can improve the identification of individuals at high risk of severe liver disease through repeated testing, serological biomarkers or indexes alone are not ideal for detecting early-stage fibrosis.[44]

2.2.2. Ultrasound

Recently, elastography has emerged as a promising non-invasive method for quantitatively detecting hepatic fibrosis. It can obtain liver stiffness measurement (LSM) through ultrasound or magnetic resonance imaging (MRI). Ultrasound-based methods, including point-shear wave elastography and transient elastography (TE), show good diagnostic performance in distinguishing different stages of liver fibrosis.[45] Moreover, a prospective cohort analysis from six international medical centers determined that TE is an optimal screening tool for identifying patients with liver fibrosis in the general population due to its cost-effectiveness and improved survival benefits, especially for patients in early-stage fibrosis (≥F2).[46]

2.2.3. MRI

Conventional MRI and magnetic resonance elastography (MRE) provide a comprehensive liver evaluation, from morphological to parenchymal changes, without being affected by patient-related factors (age, sex, and body mass index) or liver-related factors (iron overload and necroinflammation).[47] Recently, gadolinium-labeled cyclic peptides, an MRI tracer targeting hepatic PDGFR-β, have been developed to accurately stage liver fibrosis by visualizing PDGFR-β expression in carbon tetrachloride (CCl4)-treated mice.[48] MRE has reported higher accuracy in detecting all liver fibrosis stages compared to TE, with diagnostic accuracy increasing as fibrosis advances.[49] In addition, numerous non-invasive stiffness-based models (combining blood makers with elastography) have been proposed for routine screening and identification of early-stage liver fibrosis (≥F2),[50,51] as well as disease surveillance.[47,52] Recently, Keegan *et al.*[53] validated ultrasonography-based photoacoustic imaging with MRI, showing its effectiveness in detecting liver adiposity and fibrosis, enabling the non-invasive detection of changes in liver pathology associated with metabolic dysfunction.[53] Furthermore, Gao *et al.*[54] established a fibroblast activation protein alpha (FAPα)-activated MRI nanoprobe for precise grading of clinical liver fibrosis. The nanoprobe is composed of superparamagnetic amorphous iron nanoparticles (NPs) and paramagnetic gadoteric acid (Gd-DOTA) connected by FAPα-responsive peptide chains (ASGPAGPA). It effectively identifies F1, F2, F3, and F4 fibrosis, with areas under the curve of 99.8%, 66.7%, 70.4%, and 96.3% in patient samples, respectively. TE, shear wave elastography, and MRE, each providing LSM, are the most studied imaging-based non-invasive liver disease assessment techniques. In adults, sensitivities for the identification of F2 – 4 ranged from 51% to 95%, for F3 – 4 from 70% to 100%, and for F4 from 60% to 100% across all techniques and diseases, whereas specificities ranged from 36% to 100%, 74% to 100%, and 67% to 99%, respectively. The largest body of evidence available supports TE, while MRE appears to be the most accurate method.[55] The optimization and standardization of these joint models are still under further exploration. Undeniably, emerging non-invasive fibrosis multi-modality assessments reduce the need for liver biopsy in fibrosis staging (Figure 2).

3. Clinical and experimental treatment for liver fibrosis

3.1. Etiological treatment for liver fibrosis

Etiological treatment is the primary approach to managing liver fibrosis. When a definite and controllable cause, such as hepatitis virus infection, alcoholic steatohepatitis (ASH), or non-alcoholic steatohepatitis (NASH) is identified, the etiology treatment should be initiated promptly. Chronic liver diseases and fibrosis caused by hepatitis virus infections can now be effectively cured with antiviral treatment. For chronic hepatitis B virus (HBV) infection, recommended treatments include interferon and nucleos(t)ide analogs. In addition, interferon-stimulated gene therapy has recently been proposed to regulate HBV infection through intervening in different stages of the viral life cycle.[56-58] For hepatitis C virus (HCV)-associated cirrhosis, direct-acting antivirals (DAAs) are the standard treatment.[59-61] The latest European Association for the Study of the Liver guidelines recommend an increasing number of DAA regimens, including sofosbuvir (SOF), SOF/velpatasvir (VEL), SOF/VEL/voxilaprevir (VOX), glecaprevir/pibrentasvir, or grazoprevir/elbasvir for cirrhotic patients to achieve sustained virological response (SVR), which corresponds to HCV elimination.[62] A multi-center study on the long-term effect of DAAs in HCV-associated cirrhosis showed that high SVR is related to the decreased rate of complications in patients with compensated cirrhosis.[63] In addition, alcohol withdrawal and weight control play crucial roles in reducing liver burden in ASH and NASH.[64-66]

3.2. Commonly used drugs for liver fibrosis

Sorafenib is a multi-kinase inhibitor that is mainly applied in HCC patients but is rarely used to inhibit the progression of liver fibrosis. There is only one multicenter, open-label,

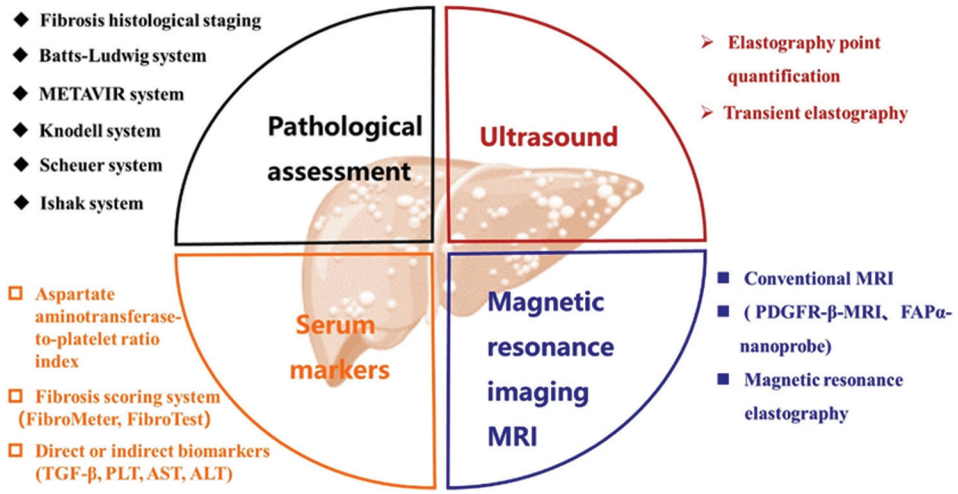


Figure 2. Clinical assessment of liver fibrosis. Diagnostic methods for suspected liver fibrosis include liver biopsy and non-invasive approaches. The hepatic injury and inflammation burden of the liver can be precisely assessed by different fibrosis histological staging systems. However, biomarker- and imaging-based non-invasive methods have emerged as reliable alternatives, showing strong concordance with liver biopsy and reducing its necessity in routine surveillance.
Abbreviations: MRI: Magnetic resonance imaging; TGF-β: Transforming growth factor beta; PLT: Platelet count; AST: Aspartate aminotransferase; ALT: Alanine aminotransferase; PDGFR-β: Platelet-derived growth factor receptor beta.

randomized Phase II trial (NCT01357486) has provided initial evidence suggesting that sorafenib may benefit a subgroup of cirrhotic patients with HCC, specifically those with Child-Pugh B7 or albumin-bilirubin grade 1/2.[67] A previous study proposed that a low dose and short period of sorafenib treatment triggered autophagy rather than apoptosis in HSCs by activating the JNK/c-Jun pathway and suppressing the Akt/mTOR/p70S6K signaling pathway.[68] However, *in vitro* and *in vivo* studies have proven that sorafenib and its derivative SC-1 can ameliorate liver fibrosis by decreasing HSC activation and ECM synthesis, as well as by promoting HSC apoptosis through three key signaling pathways: the signal transducer and activator of transcription 3 (STAT3) pathway, the TGF-β1/Smad signaling pathway, and PDGFR-β/Akt signaling pathway.[69] In addition, another study reported that sorafenib reduced liver fibrosis by inducing hypoxia-inducible factor 1α-mediated ferroptosis in HSCs, which offers a new perspective on its anti-fibrotic effect.[70] In addition, in CCl4-treated rats, sorafenib treatment was correlated to increased lysine crotonylation protein synthesis and decreased expression of related enzymes, which correlated with improved liver fibrosis. However, the underlying mechanisms remain to be elucidated.[71]

Pirfenidone (PFD) is an orally bioavailable pyridone derivative that was first approved for the treatment of idiopathic pulmonary fibrosis. PFD has been reported to alleviate fibrosis associated with cystic echinococcosis, CCl4-induced liver injury, and NASH in mice by inhibiting TGF-β-stimulated HSC activation, reducing TNF-α-induced hepatocyte apoptosis, and increasing the number of M2 macrophages.[72-75] Glutaredoxin-1 has been identified as the drug target of PFD and plays a role in hepatic fibrosis by curbing Smad3 phosphorylation and reversing oxidative stress-related protein S-glutathionylation.[76] A pilot clinical study of PFD therapy showed that different degrees of improvements in liver histology were observed in 15 patients with HCV-infection-induced cirrhosis who had not previously received antiviral therapy after 12 months of PFD treatment.[77] The results of a 2-year PFD treatment in an HCV-liver fibrosis patient cohort (NCT02161952) also confirmed the efficacy and safety of PFD, which attenuated fibrosis, inflammation, and steatosis stage in liver histology, decreased relative serum cytokines (TGF-β1 and IL-6) levels, and concurrently enhanced anti-fibrogenic cannabinoid receptor 2 gene expression.[78] In addition, prolonged-release PFD (PR-PFD), as an agonist of peroxisome proliferator-activated receptor alpha (PPAR-α), protected a mouse model of NASH from inflammation and fibrosis and mitigated hepatic steatosis through the activation of the sirtuin 1/liver kinase B1/phospho-5' adenosine monophosphate-activated protein kinase (pAMPK) pathway.[79] Recently, additional data from a clinical trial (NCT04099407) aimed to assess a 12-month treatment of PR-PFD has been reported. A total of 122 advanced liver fibrosis patients with different etiologic factors were enrolled in the study and received PR-PFD plus standard of care. In the PR-PFD group, 35% of participants showed significant liver fibrosis regression

and liver function improvement, as indicated by decreased levels of TGF-β1, IL-6, and endothelin-1 at the end of the observation period, whereas only 4.1% in the control group (74 patients receiving the standard of care regimen) showed similar improvement.[80] The evidence shown by previous studies clearly demonstrates that PFD is a promising anti-fibrotic drug in a cirrhotic population with mild side effects, such as gastrointestinal discomfort.

3.3. Molecularly targeted agents for liver fibrosis

Targeted anti-fibrotic therapy has entered a brand-new era. The Farnesoid-X receptor (FXR) and PPAR are two vital transcriptional regulators of key metabolic processes in the liver, including inflammation, fibrogenesis, proliferation, apoptosis as well as hepatic lipid and glucose metabolism. Therefore, drugs directly targeting FXR and PPAR have led to important breakthroughs in the treatment of NAFLD, NASH, and primary biliary cholangitis (PBC).

Obeticholic acid (OCA) is a potent, specific FXR agonist that was first approved for the treatment of PBC. Findings from a series of clinical trials (NCT01473524, NCT02177136) with long-period OCA treatment provided substantial evidence for its long-term efficacy in the PBC population. Patients in the OCA group had lower alkaline phosphatase and total bilirubin levels from baseline compared to the placebo group.[81-83] Recently, histological results from a sub-trial of the PBC OCA International Study of Efficacy (POISE, NCT01473524) revealed great improvements or stabilization in hepatic morphometric features, including ductular injury, fibrosis stage, and collagen production, following OCA administration.[84] For NASH, a multicenter, randomized, placebo-controlled Phase 3 trial (REGENERATE) treated NASH patients with fibrosis stage F2 – F3 with OCA. The 18-month midterm analysis in the REGENERATE trial showed that OCA treatment ameliorated fibrosis and NASH in a dose-dependent manner, with greater histological and laboratory improvements observed in the OCA 25 mg group.[85] Nonetheless, analyses of diverse non-invasive tests, including biochemical and imaging examinations, echoed the results of the previous histological study. It is worth noting that some non-invasive evaluations showed improvements in OCA-treated patients with fibrosis stabilization (NCT02548351).[86] Cilofexor (GS-9674), the second generation of FXR agonists, was well tolerated and significantly improved liver biomarkers and radiological manifestations of cholestasis in primary sclerosing cholangitis patients (NCT02854605).[87] Vonafexor (EYP001), another novel synthetic FXR agonist, showed anti-fibrotic effects in NASH patients, with improvements observed in MRI findings and serum indicators of liver and renal function (NCT03812029).[88] Pruritus was frequently reported as an adverse effect of FXR agonist therapy.[89] Dyslipidemia is another main side effect of OCA,[90] though the increase in mean low-density lipoprotein levels induced by OCA in NASH patients can be mitigated with atorvastatin (NCT02633956).[91]

PPAR-α, PPAR-γ, and PPAR-β/δ belong to the PPAR family, which is responsible for the lipid metabolism in the liver. Modulating PPAR activity can ameliorate inflammatory responses and fibrogenesis in the liver.[92] In addition, PPAR-γ plays a key role in the negative regulation of HSC activation and trans-differentiation. A meta-analysis indicated that the anti-diabetic drug pioglitazone, a selective PPAR-γ agonist, could to some extent reverse fibrosis at any stage in patients with NASH, regardless of diabetes status.[93] Saroglitazar, a dual PPARα/γ agonist, effectively induced the resolution of histological responses in diet-induced NASH mouse models.[94] In a pilot study of saroglitazar therapy in humans (NCT03112681), a daily dosage of 2 mg was found to decrease the disease activity marker alkaline phosphatase in patients with PBC. However, higher drug intake led to potential liver injury, as indicated by elevated liver enzymes.[95] The pan-PPAR agonist lanifibranor has been a leading drug candidate for NASH treatment. It showed outstanding performance in meliorating the severity of steatosis, inflammation, fibrosis, and even portal hypertension in pre-clinical models.[96-98] Moreover, at a high dose (1200 mg), lanifibranor eased the active stage of steatohepatitis in NASH without deteriorating fibrosis (NCT03008070).[99]

3.4. Targeted drug delivery system for liver fibrosis

Targeted drug delivery systems have important potential clinical applications with the advantages of prolonged residence time and improved specificity of drug delivery. A study found that poly (lactide-co-glycolide) NPs loaded with sorafenib increased blood residence time of sorafenib and decreased fibrotic accumulation of alpha-smooth muscle actin (α-SMA) and collagen, as well as microvascular density in the CCl4-treated fibrotic liver.[100] At present, targeted delivery systems for anti-fibrotic drugs have advanced to dual- or multi-functional approaches due to continuous technological and equipment developments, including NP and liposome delivery systems, HSC surface membrane-specific receptor systems, and nano-micelle drug carrier systems. For instance, the intrinsic chemico-physical properties of titanium dioxide (TiO_2) NPs and silicon dioxide (SiO_2) NPs were first reported to inhibit liver fibrosis through multiple mechanisms, such as restoring HSCs from the myofibroblast-like state, accelerating ECM degradation, and even inhibiting gene expression related to HSC adhesion and migration.[101] When sorafenib was

coated with SiO2 NPs, it exhibited greater bioavailability and minimal gastrointestinal reactions.[102]

Along the lines of PDGFR-β, chemokine receptor 4 (CXCR4) is an important membrane surface receptor of activated HSCs, playing a vital role in the development of chronic liver disease and liver fibrosis.[103-105] Both receptors have been developed as targets for active targeting strategies of anti-fibrotic agents. Since PDGFR-β is co-expressed with the TNF-related apoptosis-inducing ligand (TRAIL) receptor 2, polyethylene glycol-modified Z_{PDGFR}^{β} affibody exerted an exceptional anti-hepatocirrhosis effect compared to native TRAIL, by inducing HSC apoptosis and suppressing ECM accumulation.[106] Another study found that gold nanorods-PDGFR-β-mediated photothermal therapy reduced liver inflammation and hepatocyte injury in experimental models of liver fibrosis.[107] Moreover, a novel nanocomplex composed of a polymeric CXCR4 antagonist, clodronate, and the siRNA of plasminogen activator inhibitor-1 represents a viable approach to treating liver fibrosis. This active HSC-targeted delivery system enhanced HSC uptake and exhibited expanded anti-fibrotic activity through the synergistic regulation of Kupffer cell apoptosis, ECM degradation, and HSC inhibition.

Liposome is naturally targeted to the liver and is mainly metabolized by the hepatic mononuclear phagocyte system.[108] With the delivery of CXCR4-targeted liposomes, the accumulation of PFD and CXCR4 inhibitor in the fibrotic liver increased, thus jointly inhibiting apoptotic effects in HSCs through the significant downregulation of TGF-β1 expression.[109] Even though the drug can aggregate within the damaged liver, it has not significantly impacted fibrosis progression. The overproduction of collagen in the ECM greatly impedes drug delivery. A polymeric micelle based on collagenase I has been developed to degrade excessive ECM. A collagenase I and retinol polymeric micelle loaded with the anti-fibrotic drug nilotinib was first synthesized, followed by the development of collagenase I and Vitamin A polymeric micelle with siCol1α1, both of which demonstrated favorable HSC-specific accumulation and optimal anti-fibrotic activity in cellular experiments and murine models.[110,111] Sorafenib, when co-delivered with collagenase I and glycyrrhetinic acid, presented excellent dual ability in reversing fibrotic liver and HSC internalization.[112] The targeted NP delivery systems offer a pioneering approach to liver fibrosis targeted therapy due to their advantage of co-carrying multiple therapeutic agents.

3.5. Herbal medicine for liver fibrosis

In the treatment of liver fibrosis, valid herbal ingredients and traditional Chinese medicine (TCM) have played an important role in anti-fibrotic clinical treatment. Ferulic acid (FA), commonly found in natural products, is widely utilized in the food and health industry. It exhibits antioxidant, anti-inflammatory, and anti-fibrotic effects in CCl4-induced liver injury through the protein-tyrosine phosphatases 1B-pAMPK signaling pathway.[113] Both the active monomer methyl FA and the synthetic compound FA11 suppressed HSC activation and myofibroblast-like transformation in LX-2 cells and CCl4-induced mouse liver fibrosis, which may be attributed to the inhibition of the TGF-β1/Smad and NOX4/ROS signaling pathways.[114,115] Zhao *et al*.[116] reported the synergistic effect between astragaloside IV and FA in alleviating hepatic fibrosis induced by bile duct ligation (BDL). This effect was mediated by the activation of nuclear factor erythroid 2-related factor 2 and the inactivation of glycogen synthase kinase-3β, along with the suppression of TGF-β1 expression and its downstream targets, Smad3 and Smad4.

The bioactive component isolated from *Acanthus ilicifolius*, 4-hydroxy-2(3H)-benzoxazolone, significantly decreased the expressions of fibrotic markers (α-SMA and collagen) and ECM components by modulating multiple targets in the TGF-β1/Smads, nuclear factor-kappa B and extracellular signal-regulated kinase (ERK) signaling pathways.[117] Both quercetin and isorhamnetin prevented fibrosis by inhibiting the TGF-β1/Smads signaling pathway, which reduced autophagy, ECM secretion, and HSC activation after BDL- or CCl4-induced liver injury.[118,119] In addition to inducing autophagy, resveratrol has been reported to have an anti-fibrotic effect in pre-clinical models by stimulating IL-4-like macrophage polarization and regulating the microRNA-20a-mediated tensin homolog/PI3K/AKT signaling pathway.[120,121] Biejia ruangan tablets and fuzheng huayu (FZHY) capsules have been preliminarily confirmed to have antiviral effects in the treatment of HBV-related cirrhosis and have even shown regression of liver fibrosis when combined with entecavir therapy.[122-124] When studying the mechanism of FZHY in HSC inhibition, it was found that its main active component, *Cordyceps sinensis* mycelia (CS-PS), gypenosides, and amygdalin, can promote the degradation of ECM by regulating the MMPs/TIMPS ratio in a fibrotic rat model. In addition, FZHY exerted anti-hepatic fibrosis effects by reducing hepatic apoptosis and inhibiting TGF-β1/Smad signaling-mediated HSC activation.[125,126] Thus, single-pathway or single-target blocking may not align with the actual mechanism of traditional Chinese medicine due to its complex formulation.

Through the TCM system pharmacology database and analysis platform, 14 components in Huangqi decoction were identified to be related to the downregulation of

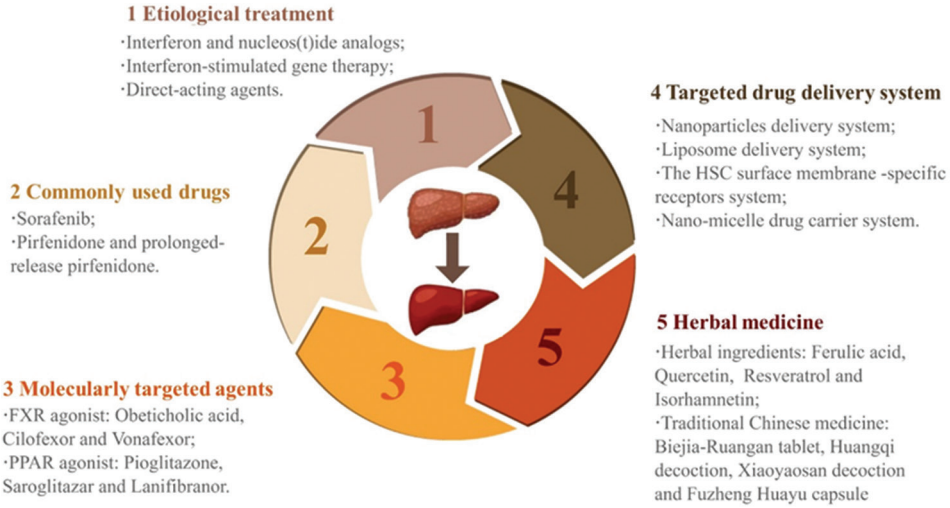


Figure 3. Selected clinical therapeutic management for liver fibrosis. The main causes of chronic liver disease include hepatitis virus infection, metabolism-associated hepatitis, and autoimmune hepatitis. Etiological treatment remains the conventional therapeutic intervention for liver fibrosis. At present, sorafenib and PFD are widely used in clinical practice. Targeted molecular pathways and small-molecule drug delivery systems have been developed as novel pathophysiology-oriented therapies. Moreover, traditional Chinese medicine-based herbal therapies have identified promising anti-fibrotic therapeutic targets.
Abbreviations: FXR: Farnesoid-X receptor; PPAR: Peroxisome proliferator-activated receptor; HSC: Hepatic stellate cell.

RNA expression of profibrotic factors and the acceleration of LX-2 cell apoptosis.[127] In addition, cell division cycle 42 and glioma-associated oncogene homolog 1 may be the curative targets, whereas SMAD2, epidermal growth factor receptor, AKT1, Ras homolog family member A, and growth arrest-specific 5 might influence the anti-fibrotic effects of Huangqi decoction in cirrhosis patients with HBV infection.[128] The introduction of network pharmacology has advanced research in this field to a new stage. Based on the pharmacological network analysis of Xiaoyaosan decoction (XYS), 108 active components and 42 targets constituted a multi-compound-target network. Furthermore, *in vitro* and *in vivo* studies verified that the TGF-β1/Smad and Akt/forkhead box transcription factors class O signaling pathways are two pivotal signaling pathways in the protective mechanism of XYS against liver fibrosis.[129] Lu *et al.*[130] identified dynamic network biomarkers in patients with chronic liver disease and suggested that EGFR, CCAAT enhancer binding protein alpha, colony-stimulating factor 1, and interleukin-7 receptor serve as core diagnostic markers for distinguishing pre-cirrhosis from post-cirrhosis stages and could be potential therapeutic targets of XYS treatment in cirrhosis. Among 17 anti-fibrotic intersection targets, emodin-induced HSC apoptosis to alleviate CCl4-induced liver fibrosis through the p53/ERK/p38 axis by directly binding to targeted residue sites, such as ASN345, GLN331, and TYR347.[131] In the pharmacological analysis of *Salvia miltiorrhiza*, 71 active compounds, 342 potential target proteins, and 22 signaling pathways were identified, with further experiments demonstrating that it inhibited HSC activation through the downregulation of the JAK1/STAT3 signaling pathway.[132] In summary, the active herbal compound-target protein-signaling pathway network developed through pharmacological analysis provides a novel strategy for researchers to systematically explore the mechanisms of TCM in treating liver fibrosis (Figure 3).

4. Conclusion

Liver fibrosis is one of the leading diseases that threatens both individual physical health and social well-being. With advancements in the understanding of the molecular pathophysiology of liver disease, significant progress has been made in elucidating the molecular mechanisms underlying liver fibrosis progression and developing non-invasive methods to assess stages of fibrosis. While experimental studies on anti-fibrotic therapies have increased at a remarkable pace, the research progress of clinical treatment of liver fibrosis and cirrhosis has been relatively slower. Many therapeutic strategies remain in the pre-clinical phase due to physicochemical limitations that could hinder their effectiveness in clinical trials.

Targeted drug delivery systems address the shortcomings of the mono-agent anti-liver fibrosis therapies, such as low bioavailability, weak specificity, and poor drug accumulation at injured organ sites. Therefore, there is an urgent need to develop safe and effective liver-specific targeted delivery systems for anti-fibrotic drugs. HSC membrane receptor-active targeting combined with drug delivery is

a potent technology to increase systemic circulation and localization of anti-fibrosis drugs within the fibrotic liver. The permeability and retention effect of these drugs can be enhanced by conjugating them with collagenase I-decorated NPs. Achieving hepatic fibrogenesis inhibition through multiple pathways within a single treatment period may only be feasible with an advanced targeted delivery system.

In recent years, TCM has made great progress in slowing and reversing liver fibrosis, which can significantly improve both the symptoms and biochemical markers of the disease.[133] Notably, gene therapy has emerged as a promising approach, with several therapies relying on viral vectors to deliver nucleic acid cargo into target cells. Interestingly, modern molecular biology technology and equipment have facilitated the identification of distinctive and effective bioactive ingredients and formulations from the complex TCM. Hence, accurate exploration of TCM through pharmacological network analysis may provide a promising solution for overcoming challenges in anti-fibrotic drug development. More effective combination strategies of modern and traditional treatments can be adopted for the pathological features of different stages of liver fibrosis.

Acknowledgments

None.

Funding

This study is supported by the National Natural Science Foundation of China (32200936, 82200070, 82304589), the Guangdong Basic and Applied Basic Research Foundation (2021A1515110561, 2021A1515111049), the Guangdong Provincial Key Laboratory of Tumor Interventional Diagnosis and Treatment (2021B1212040004), and the Xiangshan Talent Scientific Research Start-up Fund of Zhuhai People's Hospital (2021XSYC-07).

Conflict of interest

The authors declare they have no competing interests.

Author contributions

Conceptualization: Jian Sun, Xiaoguang Zhao
Writing–original draft: Xin Liu, Chongmiao Yang, Yanyan Liu, Xiaowen Lin, Wei Su
Writing–review & editing: Jian Sun, Xiaoguang Zhao

Ethics approval and consent to participate

Not applicable.

Consent for publication

Not applicable.

Availability of data

Not applicable.

References

1. Yang LX, Qi C, Lu S, *et al*. Alleviation of liver fibrosis by inhibiting a non-canonical ATF4-regulated enhancer program in hepatic stellate cells. *Nat Commun*. 2025;16(1):524.
doi: 10.1038/s41467-024-55738-1
2. Tao J, Wu Z, Liang Y, *et al*. Lhx2 specifically expressed in HSCs promotes liver regeneration and inhibits liver fibrosis. *Hepatology*. 2024.
doi: 10.1097/HEP.0000000000001201
3. Kim HY, Rosenthal SB, Liu X, *et al*. Multi-modal analysis of human hepatic stellate cells identifies novel therapeutic targets for metabolic dysfunction-associated steatotic liver disease. *J Hepatol*. 2024.
doi: 10.1016/j.jhep.2024.10.044
4. Tung HC, Kim JW, Zhu J, *et al*. Inhibition of heme-thiolate monooxygenase CYP1B1 prevents hepatic stellate cell activation and liver fibrosis by accumulating trehalose. *Sci Transl Med*. 2024;16(766):eadk8446.
doi: 10.1126/scitranslmed.adk8446
5. Deng Y, Lu L, Zhu D, *et al*. MafG/MYH9-LCN2 axis promotes liver fibrosis through inhibiting ferroptosis of hepatic stellate cells. *Cell Death Differ*. 2024;31(9):1127-1139.
doi: 10.1038/s41418-024-01322-5
6. Babuta M, Morel C, de Carvalho Ribeiro M, *et al*. Neutrophil extracellular traps activate hepatic stellate cells and monocytes via NLRP3 sensing in alcohol-induced acceleration of MASH fibrosis. *Gut*. 2024;73(11):1854-1869.
doi: 10.1136/gutjnl-2023-331447
7. Tian Y, Ni Y, Zhang T, Cao Y, Zhou M, Zhao C. Targeting hepatic macrophages for non-alcoholic fatty liver disease therapy. *Front Cell Dev Biol*. 2024;12:1444198.
doi: 10.3389/fcell.2024.1444198
8. Bradic I, Kuentzel KB, Pirchheim A, *et al*. From LAL-D to MASLD: Insights into the role of LAL and Kupffer cells in liver inflammation and lipid metabolism. *Biochim Biophys Acta Mol Cell Biol Lipids*. 2025;1870(1):159575.
doi: 10.1016/j.bbalip.2024.159575
9. Lee J, Woo H, Kang H, Park YK, Lee JY. Nicotinamide riboside targets mitochondrial unfolded protein response to reduce alcohol-induced damage in Kupffer cells. *J Pathol*. 2025;265(1):110-122.
doi: 10.1002/path.6372
10. Fima R, Dussaud S, Benbida C, *et al*. Loss of embryonically-derived Kupffer cells during hypercholesterolemia accelerates atherosclerosis development. *Nat Commun*.

2024;15(1):8341.

doi: 10.1038/s41467-024-52735-2

11. Li R, Wei R, Liu C, *et al*. Heme oxygenase 1-mediated ferroptosis in Kupffer cells initiates liver injury during heat stroke. *Acta Pharm Sin B*. 2024;14(9):3983-4000.

doi: 10.1016/j.apsb.2024.05.007

12. Li T, Song X, Chen J, *et al*. Kupffer Cell-derived IL6 Promotes hepatocellular carcinoma metastasis via the JAK1-ACAP4 pathway. *Int J Biol Sci*. 2025;21(1):285-305.

doi: 10.7150/ijbs.97109

13. Parola M, Pinzani M. Liver fibrosis: Pathophysiology, pathogenetic targets and clinical issues. *Mol Aspects Med*. 2019;65:37-55.

doi: 10.1016/j.mam.2018.09.002

14. Tsuchida T, Friedman SL. Mechanisms of hepatic stellate cell activation. *Nat Rev Gastroenterol Hepatol*. 2017;14(7):397-411.

doi: 10.1038/nrgastro.2017.38

15. Kisseleva T, Brenner D. Molecular and cellular mechanisms of liver fibrosis and its regression. *Nat Rev Gastroenterol Hepatol*. 2021;18(3):151-166.

doi: 10.1038/s41575-020-00372-7

16. Borkham-Kamphorst E, Weiskirchen R. The PDGF system and its antagonists in liver fibrosis. *Cytokine Growth Factor Rev*. 2016;28:53-61.

doi: 10.1016/j.cytogfr.2015.10.002

17. Hu HH, Cao G, Wu XQ, Vaziri ND, Zhao YY. Wnt signaling pathway in aging-related tissue fibrosis and therapies. *Ageing Res Rev*. 2020;60:101063.

doi: 10.1016/j.arr.2020.101063

18. Kim A, Wu X, Allende DS, Nagy LE. Gene deconvolution reveals aberrant liver regeneration and immune cell infiltration in alcohol-associated hepatitis. *Hepatology*. 2021;74(2):31759.

doi: 10.1002/hep.31759

19. Pivovarova-Ramich O, Loske J, Hornemann S, *et al*. Hepatic Wnt1 inducible signaling pathway protein 1 (WISP-1/CCN4) associates with markers of liver fibrosis in severe obesity. *Cells*. 2021;10(5):1048.

doi: 10.3390/cells10051048

20. Yue Z, Jiang Z, Ruan B, *et al*. Disruption of myofibroblastic Notch signaling attenuates liver fibrosis by modulating fibrosis progression and regression. *Int J Biol Sci*. 2021;17(9):2135-2146.

doi: 10.7150/ijbs.60056

21. Perramón M, Carvajal S, Reichenbach V, *et al*. The pituitary tumour-transforming gene 1/delta-like homologue 1 pathway plays a key role in liver fibrogenesis. *Liver Int*. 2022;42(3):651-662.

doi: 10.1111/liv.15165

22. Lin X, Li J, Xing YQ. Geniposide, a sonic hedgehog signaling inhibitor, inhibits the activation of hepatic stellate cell. *Int Immunopharmacol*. 2019;72:330-338.

doi: 10.1016/j.intimp.2019.04.016

23. Yan J, Hu B, Shi W, *et al*. Gli2-regulated activation of hepatic stellate cells and liver fibrosis by TGF-β signaling. *Am J Physiol Gastrointest Liver Physiol*. 2021;320(5):G720-G728.

doi: 10.1152/ajpgi.00310.2020

24. Yang L, Wang Y, Mao H, *et al*. Sonic hedgehog is an autocrine viability factor for myofibroblastic hepatic stellate cells. *J Hepatol*. 2008;48(1):98-106.

doi: 10.1016/j.jhep.2007.07.032

25. Choi SS, Omenetti A, Witek RP, *et al*. Hedgehog pathway activation and epithelial-to-mesenchymal transitions during myofibroblastic transformation of rat hepatic cells in culture and cirrhosis. *Am J Physiol Gastrointest Liver Physiol*. 2009;297(6):G1093-G1106.

doi: 10.1152/ajpgi.00292.2009

26. Zhang F, Hao M, Jin H, *et al*. Canonical hedgehog signalling regulates hepatic stellate cell-mediated angiogenesis in liver fibrosis. *Br J Pharmacol*. 2017;174(5):409-423.

doi: 10.1111/bph.13701

27. Jung Y, Brown KD, Witek RP, *et al*. Accumulation of hedgehog-responsive progenitors parallels alcoholic liver disease severity in mice and humans. *Gastroenterology*. 2008;134(5):1532-1543.

doi: 10.1053/j.gastro.2008.02.022

28. Fleig SV, Choi SS, Yang L, *et al*. Hepatic accumulation of Hedgehog-reactive progenitors increases with severity of fatty liver damage in mice. *Lab Invest*. 2007;87(12):1227-1239.

doi: 10.1038/labinvest.3700689

29. Grzelak CA, Martelotto LG, Sigglekow ND, *et al*. The intrahepatic signalling niche of hedgehog is defined by primary cilia positive cells during chronic liver injury. *J Hepatol*. 2014;60(1):143-151.

doi: 10.1016/j.jhep.2013.08.012

30. Link F, Li Y, Zhao J, *et al*. ECM1 attenuates hepatic fibrosis by interfering with mediators of latent TGF-beta1 activation. *Gut*. Feb 6 2025;74(3):424-439.

doi: 10.1136/gutjnl-2024-333213

31. Crouchet E, Dachraoui M, Juhling F, *et al*. Targeting the liver clock improves fibrosis by restoring TGF-beta signaling. *J Hepatol*. 2025;82(1):120-133.

doi: 10.1016/j.jhep.2024.07.034

32. Ye Q, Liu Y, Zhang G, *et al*. Deficiency of gluconeogenic

enzyme PCK1 promotes metabolic-associated fatty liver disease through PI3K/AKT/PDGF axis activation in male mice. *Nat Commun*. 2023;14(1):1402.

doi: 10.1038/s41467-023-37142-3

33. Kostallari E, Hirsova P, Prasnicka A, *et al*. Hepatic stellate cell-derived platelet-derived growth factor receptor-alpha-enriched extracellular vesicles promote liver fibrosis in mice through SHP2. *Hepatology*. 2018;68(1):333-348.

doi: 10.1002/hep.29803

34. Wang F, Chen L, Kong D, *et al*. Canonical Wnt signaling promotes HSC glycolysis and liver fibrosis through an LDH-A/HIF-1alpha transcriptional complex. *Hepatology*. 2024;79(3):606-623.

doi: 10.1097/HEP.0000000000000569

35. Hu Y, Peng L, Zhuo X, Yang C, Zhang Y. Hedgehog signaling pathway in fibrosis and targeted therapies. *Biomolecules*. 2024;14(12):1485.

doi: 10.3390/biom14121485

36. Lo RC, Kim H. Histopathological evaluation of liver fibrosis and cirrhosis regression. *Clin Mol Hepatol*. 2017;23(4):302-307.

doi: 10.3350/cmh.2017.0078

37. Colling R, Verrill C, Fryer E, *et al*. Bile duct basement membrane thickening in primary sclerosing cholangitis. *Histopathology*. 2016;68(6):819-824.

doi: 10.1111/his.12857

38. Bedossa P, Poynard T. An algorithm for the grading of activity in chronic hepatitis C. The METAVIR Cooperative Study Group. *Hepatology*. 1996;24(2):289-293.

doi: 10.1002/hep.510240201

39. Ishak K, Baptista A, Bianchi L, *et al*. Histological grading and staging of chronic hepatitis. *J Hepatol*. 1995;22(6):696-699.

doi: 10.1016/0168-8278(95)80226-6

40. Chowdhury AB, Mehta KJ. Liver biopsy for assessment of chronic liver diseases: A synopsis. *Clin Exp Med*. 2023;23:273-285.

doi: 10.1007/s10238-022-00799-z

41. Chin JL, Pavlides M, Moolla A, Ryan JD. Non-invasive markers of liver fibrosis: Adjuncts or alternatives to liver biopsy? *Front Pharmacol*. 2016;7:159.

doi: 10.3389/fphar.2016.00159

42. Younossi ZM, Noureddin M, Bernstein D, *et al*. Role of noninvasive tests in clinical gastroenterology practices to identify patients with nonalcoholic steatohepatitis at high risk of adverse outcomes: Expert panel recommendations. *Am J Gastroenterol*. 2021;116(2):254-262.

doi: 10.14309/ajg.0000000000001054

43. Moreno C, Mueller S, Szabo G. Non-invasive diagnosis and biomarkers in alcohol-related liver disease. *J Hepatol*. 2019;70(2):273-283.

doi: 10.1016/j.jhep.2018.11.025

44. Hagström H, Talbäck M, Andreasson A, Walldius G, Hammar N. Repeated FIB-4 measurements can help identify individuals at risk of severe liver disease. *J Hepatol*. 2020;73(5):1023-1029.

doi: 10.1016/j.jhep.2020.06.007

45. Roccarina D, Iogna Prat L, Pallini G, *et al*. Comparison of point-shear wave elastography (ElastPQ) and transient elastography (FibroScan) for liver fibrosis staging in patients with non-alcoholic fatty liver disease. *Liver Int*. 2022;42(10):2195-2203.

doi: 10.1111/liv.15297

46. Serra-Burriel M, Graupera I, Torán P, *et al*. Transient elastography for screening of liver fibrosis: Cost-effectiveness analysis from six prospective cohorts in Europe and Asia. *J Hepatol*. 2019;71(6):1141-1151.

doi: 10.1016/j.jhep.2019.08.019

47. Hydes T, Brown E, Hamid A, Bateman AC, Cuthbertson DJ. Current and emerging biomarkers and imaging modalities for nonalcoholic fatty liver disease: Clinical and research applications. *Clin Ther*. 2021;43(9):1505-1522.

doi: 10.1016/j.clinthera.2021.07.012

48. Wu L, Huang X-Q, Li N, *et al*. A magnetic resonance imaging modality for non-invasively distinguishing progression of liver fibrosis by visualizing hepatic platelet-derived growth factor receptor-beta expression in mice. *J Gastroenterol Hepatol*. 2021;36(12):3448-3456.

doi: 10.1111/jgh.15628

49. Hsu C, Caussy C, Imajo K, *et al*. Magnetic Resonance vs Transient Elastography analysis of patients with nonalcoholic fatty liver disease: A systematic review and pooled analysis of individual participants. *Clin Gastroenterol Hepatol*. 2019;17(4):630-637.e8.

doi: 10.1016/j.cgh.2018.05.059

50. Coste P, Llop E, Perelló C, *et al*. Comparison of non-invasive fibrosis scores to predict increased liver stiffness in the general population with unknown liver disease: Searching for the primary physician's best friend. *Dig Liver Dis*. 2022;54(9):1209-1214.

doi: 10.1016/j.dld.2022.03.013

51. Kim BK, Tamaki N, Imajo K, *et al*. Head-to-head comparison between MEFIB, MAST, and FAST for detecting stage 2 fibrosis or higher among patients with NAFLD. *J Hepatol*. 2022;77(6):1482-1490.

doi: 10.1016/j.jhep.2022.07.020

52. Long MT, Noureddin M, Lim JK. AGA clinical practice update: Diagnosis and management of nonalcoholic

fatty liver disease in lean individuals: Expert review. *Gastroenterology*. 2022;163(3):764-774.e1.

doi: 10.1053/j.gastro.2022.06.023

53. Keegan A, Malamal G, Lee Y, *et al*. Multi-modal diagnostic imaging of metabolic dysfunction-associated steatotic liver disease: Non-invasive analyses by photoacoustic ultrasound and MRI. *Am J Pathol*. 2025.

doi: 10.1016/j.ajpath.2025.01.012

54. Gao J, Wang Y, Meng X, *et al*. A FAPalpha-activated MRI nanoprobe for precise grading diagnosis of clinical liver fibrosis. *Nat Commun*. 2024;15(1):8036.

doi: 10.1038/s41467-024-52308-3

55. Duarte-Rojo A, Taouli B, Leung DH, *et al*. Imaging-based noninvasive liver disease assessment for staging liver fibrosis in chronic liver disease: A systematic review supporting the AASLD Practice Guideline. *Hepatology*. 2025;81(2):725-748.

doi: 10.1097/HEP.0000000000000852

56. Liver EAftSot. EASL 2017 Clinical Practice Guidelines on the management of hepatitis B virus infection. *J Hepatol*. 2017;67(2):370-398.

doi: 10.1016/j.jhep.2017.03.021

57. Yuen MF, Ahn SH, Chen DS, *et al*. Chronic Hepatitis B virus infection: Disease revisit and management recommendations. *J Clin Gastroenterol*. 2016;50(4):286-294.

doi: 10.1097/MCG.0000000000000478

58. Li Q, Sun B, Zhuo Y, *et al*. Interferon and interferon-stimulated genes in HBV treatment. *Front Immunol*. 2022;13:1034968.

doi: 10.3389/fimmu.2022.1034968

59. Maan R, van Tilborg M, Deterding K, *et al*. Safety and effectiveness of direct-acting antiviral agents for treatment of patients with chronic hepatitis C virus infection and cirrhosis. *Clin Gastroenterol Hepatol*. 2016;14(12):1821-1830.e6.

doi: 10.1016/j.cgh.2016.07.001

60. Verna EC, Morelli G, Terrault NA, *et al*. DAA therapy and long-term hepatic function in advanced/decompensated cirrhosis: Real-world experience from HCV-TARGET cohort. *J Hepatol*. 2020;73(3):540-548.

doi: 10.1016/j.jhep.2020.03.031

61. Oltmanns C, Liu Z, Mischke J, *et al*. Reverse inflammaging: Long-term effects of HCV cure on biological age. *J Hepatol*. 2023;78(1):90-98.

doi: 10.1016/j.jhep.2022.08.042

62. Liver EAftSot. EASL recommendations on treatment of hepatitis C: Final update of the series. *J Hepatol*. 2020;73(5):1170-1218.

doi: 10.1016/j.jhep.2020.08.018

63. Krassenburg LA, Maan R, Ramji A, *et al*. Clinical outcomes following DAA therapy in patients with HCV-related cirrhosis depend on disease severity. *J Hepatol*. 2021;74(5):1053-1063.

doi: 10.1016/j.jhep.2020.11.021

64. Koutoukidis DA, Astbury NM, Tudor KE, *et al*. Association of weight loss interventions with changes in biomarkers of nonalcoholic fatty liver disease: A systematic review and meta-analysis. *JAMA Intern Med*. 2019;179(9):1262-1271.

doi: 10.1001/jamainternmed.2019.2248

65. Huang DQ, El-Serag HB, Loomba R. Global epidemiology of NAFLD-related HCC: trends, predictions, risk factors and prevention. *Nat Rev Gastroenterol Hepatol*. 2021;18(4):223-238.

doi: 10.1038/s41575-020-00381-6

66. Huang DQ, Mathurin P, Cortez-Pinto H, Loomba R. Global epidemiology of alcohol-associated cirrhosis and HCC: Trends, projections and risk factors. *Nat Rev Gastroenterol Hepatol*. 2023;20(1):37-49.

doi: 10.1038/s41575-022-00688-6

67. Blanc JF, Khemissa F, Bronowicki JP, *et al*. Phase 2 trial comparing sorafenib, pravastatin, their combination or supportive care in HCC with Child-Pugh B cirrhosis. *Hepatol Int*. 2021;15(1):93-104.

doi: 10.1007/s12072-020-10120-3

68. Hao H, Zhang D, Shi J, *et al*. Sorafenib induces autophagic cell death and apoptosis in hepatic stellate cell through the JNK and Akt signaling pathways. *Anticancer Drugs*. 2016;27(3):192-203.

doi: 10.1097/CAD.0000000000000316

69. Su TH, Shiau CW, Jao P, *et al*. Sorafenib and its derivative SC-1 exhibit antifibrotic effects through signal transducer and activator of transcription 3 inhibition. *Proc Natl Acad Sci U S A*. 2015;112(23):7243-7248.

doi: 10.1073/pnas.1507499112

70. Yuan S, Wei C, Liu G, *et al*. Sorafenib attenuates liver fibrosis by triggering hepatic stellate cell ferroptosis via HIF-1α/SLC7A11 pathway. *Cell Prolif*. 2022;55(1):e13158.

doi: 10.1111/cpr.13158

71. Chen XF, Ji S. Sorafenib attenuates fibrotic hepatic injury through mediating lysine crotonylation. *Drug Des Devel Ther*. 2022;16:2133-2144.

doi: 10.2147/DDDT.S368306

72. Wang E, Liao Z, Wang L, *et al*. A combination of pirfenidone and TGF-β inhibition mitigates cystic echinococcosis-associated hepatic injury. *Parasitology*. 2021;148(7):767-778.

doi: 10.1017/S0031182021000287

73. Komiya C, Tanaka M, Tsuchiya K, *et al*. Antifibrotic effect of pirfenidone in a mouse model of human nonalcoholic steatohepatitis. *Sci Rep*. 2017;7:44754.

doi: 10.1038/srep44754

74. Tsukahara Y, Ferran B, Minetti ET, *et al*. Administration of glutaredoxin-1 attenuates liver fibrosis caused by aging and non-alcoholic steatohepatitis. *Antioxidants (Basel)*. 2022;11(5):867.

doi: 10.3390/antiox11050867

75. Chen G, Ni Y, Nagata N, *et al*. Pirfenidone prevents and reverses hepatic insulin resistance and steatohepatitis by polarizing M2 macrophages. *Lab Invest*. 2019;99(9):1335-1348.

doi: 10.1038/s41374-019-0255-4

76. Xi Y, Li Y, Xu P, *et al*. The anti-fibrotic drug pirfenidone inhibits liver fibrosis by targeting the small oxidoreductase glutaredoxin-1. *Sci Adv*. 2021;7(36):eabg9241.

doi: 10.1126/sciadv.abg9241

77. Armendáriz-Borunda J, Islas-Carbajal MC, Meza-García E, *et al*. A pilot study in patients with established advanced liver fibrosis using pirfenidone. *Gut*. 2006;55(11):1663-1665.

doi: 10.1136/gut.2006.107136

78. Flores-Contreras L, Sandoval-Rodríguez AS, Mena-Enriquez MG, *et al*. Treatment with pirfenidone for two years decreases fibrosis, cytokine levels and enhances CB2 gene expression in patients with chronic hepatitis C. *BMC Gastroenterol*. 2014;14:131.

doi: 10.1186/1471-230X-14-131

79. Sandoval-Rodriguez A, Monroy-Ramirez HC, Meza-Rios A, *et al*. Pirfenidone is an agonistic ligand for PPARα and improves NASH by activation of SIRT1/LKB1/pAMPK. *Hepatol Commun*. 2020;4(3):434-449.

doi: 10.1002/hep4.1474

80. Poo JL, Torre A, Aguilar-Ramírez JR, *et al*. Benefits of prolonged-release pirfenidone plus standard of care treatment in patients with advanced liver fibrosis: PROMETEO study. *Hepatol Int*. 2020;14(5):817-827.

doi: 10.1007/s12072-020-10069-3

81. Nevens F, Andreone P, Mazzella G, *et al*. A Placebo-controlled trial of obeticholic acid in primary biliary cholangitis. *N Engl J Med*. 2016;375(7):631-643.

doi: 10.1056/NEJMoa1509840

82. Kowdley KV, Luketic V, Chapman R, *et al*. A randomized trial of obeticholic acid monotherapy in patients with primary biliary cholangitis. *Hepatology*. 2018;67(5):1890-1902.

doi: 10.1002/hep.29569

83. Kowdley KV, Vuppalanchi R, Levy C, *et al*. A randomized, placebo-controlled, phase II study of obeticholic acid for primary sclerosing cholangitis. *J Hepatol*. 2020;73(1):94-101.

doi: 10.1016/j.jhep.2020.02.033

84. Bowlus CL, Pockros PJ, Kremer AE, *et al*. Long-term obeticholic acid therapy improves histological endpoints in patients with primary biliary cholangitis. *Clin Gastroenterol Hepatol*. 2020;18(5):1170-1178.e6.

doi: 10.1016/j.cgh.2019.09.050

85. Younossi ZM, Ratziu V, Loomba R, *et al*. Obeticholic acid for the treatment of non-alcoholic steatohepatitis: Interim analysis from a multicentre, randomised, placebo-controlled phase 3 trial. *Lancet*. 2019;394(10215):2184-2196.

doi: 10.1016/S0140-6736(19)33041-7

86. Rinella ME, Dufour JF, Anstee QM, *et al*. Non-invasive evaluation of response to obeticholic acid in patients with NASH: Results from the REGENERATE study. *J Hepatol*. 2022;76(3):536-548.

doi: 10.1016/j.jhep.2021.10.029

87. Patel K, Harrison SA, Elkhashab M, *et al*. Cilofexor, a Nonsteroidal FXR agonist, in patients with noncirrhotic NASH: A phase 2 randomized controlled trial. *Hepatology*. 2020;72(1):58-71.

doi: 10.1002/hep.31205

88. Ratziu V, Harrison SA, Loustaud-Ratti V, *et al*. Hepatic and renal improvements with FXR agonist vonafexor in individuals with suspected fibrotic NASH. *J Hepatol*. 2023;78:479-492.

doi: 10.1016/j.jhep.2022.10.023

89. Fiorucci S, Biagioli M, Sepe V, Zampella A, Distrutti E. Bile acid modulators for the treatment of nonalcoholic steatohepatitis (NASH). *Expert Opin Investig Drugs*. 2020;29(6):623-632.

doi: 10.1080/13543784.2020.1763302

90. Siddiqui MS, Van Natta ML, Connelly MA, *et al*. Impact of obeticholic acid on the lipoprotein profile in patients with non-alcoholic steatohepatitis. *J Hepatol*. 2020;72(1):25-33.

doi: 10.1016/j.jhep.2019.10.006

91. Pockros PJ, Fuchs M, Freilich B, *et al*. CONTROL: A randomized phase 2 study of obeticholic acid and atorvastatin on lipoproteins in nonalcoholic steatohepatitis patients. *Liver Int*. 2019;39(11):2082-2093.

doi: 10.1111/liv.14209

92. Wang Y, Nakajima T, Gonzalez FJ, Tanaka N. PPARs as metabolic regulators in the liver: Lessons from liver-specific PPAR-null mice. *Int J Mol Sci*. 2020;21(6):2061.

doi: 10.3390/ijms21062061

93. Musso G, Cassader M, Paschetta E, Gambino R. Thiazolidinediones and advanced liver fibrosis in nonalcoholic steatohepatitis: A meta-analysis. *JAMA Intern Med*. 2017;177(5):633-640.

doi: 10.1001/jamainternmed.2016.9607

94. Kumar DP, Caffrey R, Marioneaux J, *et al*. The PPAR α/γ agonist saroglitazar improves insulin resistance

and steatohepatitis in a diet induced animal model of nonalcoholic fatty liver disease. *Sci Rep.* 2020;10(1):9330.

doi: 10.1038/s41598-020-66458-z

95. Vuppalanchi R, Caldwell SH, Pyrsopoulos N, *et al*. Proof-of-concept study to evaluate the safety and efficacy of saroglitazar in patients with primary biliary cholangitis. *J Hepatol*. 2022;76(1):75-85.

doi: 10.1016/j.jhep.2021.08.025

96. Lefere S, Puengel T, Hundertmark J, *et al*. Differential effects of selective- and pan-PPAR agonists on experimental steatohepatitis and hepatic macrophages . *J Hepatol*. 2020;73(4):757-770.

doi: 10.1016/j.jhep.2020.04.025

97. Boyer-Diaz Z, Aristu-Zabalza P, Andrés-Rozas M, *et al*. Pan-PPAR agonist lanifibranor improves portal hypertension and hepatic fibrosis in experimental advanced chronic liver disease. *J Hepatol*. 2021;74(5):1188-1199.

doi: 10.1016/j.jhep.2020.11.045

98. Møllerhøj MB, Veidal SS, Thrane KT, *et al*. Hepatoprotective effects of semaglutide, lanifibranor and dietary intervention in the GAN diet-induced obese and biopsy-confirmed mouse model of NASH. *Clin Transl Sci*. 2022;15(5):1167-1186.

doi: 10.1111/cts.13235

99. Francque SM, Bedossa P, Ratziu V, *et al*. A Randomized, controlled trial of the Pan-PPAR agonist lanifibranor in NASH. *N Engl J Med*. 2021;385(17):1547-1558.

doi: 10.1056/NEJMoa2036205

100. Lin TT, Gao DY, Liu YC, *et al*. Development and characterization of sorafenib-loaded PLGA nanoparticles for the systemic treatment of liver fibrosis. *J Control Release*. 2016;221:62-70.

doi: 10.1016/j.jconrel.2015.11.003

101. Peng F, Tee JK, Setyawati MI, *et al*. Inorganic nanomaterials as highly efficient inhibitors of cellular hepatic fibrosis. *ACS Appl Mater Interfaces*. 2018;10(38):31938-31946.

doi: 10.1021/acsami.8b10527

102. Tran HT, Vong LB, Nishikawa Y, Nagasaki Y. Sorafenib-loaded silica-containing redox nanoparticles for oral anti-liver fibrosis therapy. *J Control Release*. 2022;345:880-891.

doi: 10.1016/j.jconrel.2022.04.002

103. Hong F, Tuyama A, Lee TF, *et al*. Hepatic stellate cells express functional CXCR4: role in stromal cell-derived factor-1alpha-mediated stellate cell activation. *Hepatology*. 2009;49(6):2055-2067.

doi: 10.1002/hep.22890

104. Wang S, Gao S, Li Y, Qian X, Luan J, Lv X. Emerging importance of chemokine receptor CXCR4 and its ligand in liver disease. *Front Cell Dev Biol*. 2021;9:716842.

doi: 10.3389/fcell.2021.716842

105. Tan HX, Gong WZ, Zhou K, *et al*. CXCR4/TGF-β1 mediated hepatic stellate cells differentiation into carcinoma-associated fibroblasts and promoted liver metastasis of colon cancer. *Cancer Biol Ther*. 2020;21(3):258-268.

doi: 10.1080/15384047.2019.1685157

106. Li R, Li Z, Feng Y, *et al*. PDGFRβ-targeted TRAIL specifically induces apoptosis of activated hepatic stellate cells and ameliorates liver fibrosis. *Apoptosis*. 2020;25(1-2):105-119.

doi: 10.1007/s10495-019-01583-3

107. Ribera J, Vilches C, Sanz V, *et al*. Treatment of hepatic fibrosis in mice based on targeted plasmonic hyperthermia. *ACS Nano.* 2021;15(4):7547-7562.

doi: 10.1021/acsnano.1c00988

108. Samuelsson E, Shen H, Blanco E, Ferrari M, Wolfram J. Contribution of Kupffer cells to liposome accumulation in the liver. *Colloids Surf B Biointerfaces*. 2017;158:356-362.

doi: 10.1016/j.colsurfb.2017.07.014

109. Ullah A, Wang K, Wu P, Oupicky D, Sun M. CXCR4-targeted liposomal mediated co-delivery of pirfenidone and AMD3100 for the treatment of TGFβ-induced HSC-T6 cells activation. *Int J Nanomedicine*. 2019;14:2927-2944.

doi: 10.2147/IJN.S171280

110. Fan QQ, Zhang CL, Qiao JB, *et al*. Extracellular matrix-penetrating nanodrill micelles for liver fibrosis therapy. *Biomaterials*. 2020;230:119616.

doi: 10.1016/j.biomaterials.2019.119616

111. Zhang LF, Wang XH, Zhang CL, *et al*. Sequential nano-penetrators of capillarized liver sinusoids and extracellular matrix barriers for liver fibrosis therapy. *ACS Nano.* 2022;16(9):14029-14042.

doi: 10.1021/acsnano.2c03858

112. Zhou L, Liang Q, Li Y, *et al*. Collagenase-I decorated co-delivery micelles potentiate extracellular matrix degradation and hepatic stellate cell targeting for liver fibrosis therapy. *Acta Biomater*. 2022;152:235-254.

doi: 10.1016/j.actbio.2022.08.065

113. Wu J, Xue X, Fan G, *et al*. Ferulic acid ameliorates hepatic inflammation and fibrotic liver injury by inhibiting PTP1B activity and subsequent promoting AMPK phosphorylation. *Front Pharmacol*. 2021;12:754976.

doi: 10.3389/fphar.2021.754976

114. Cheng Q, Li C, Yang CF, *et al*. Methyl ferulic acid attenuates liver fibrosis and hepatic stellate cell activation through the TGF-β1/Smad and NOX4/ROS pathways. *Chem Biol Interact*. 2019;299:131-139.

doi: 10.1016/j.cbi.2018.12.006

115. Xue T, Yue L, Zhu G, *et al*. An oral phenylacrylic acid

derivative suppressed hepatic stellate cell activation and ameliorated liver fibrosis by blocking TGF-β1 signalling. *Liver Int*. 2023;43:718-73.

doi: 10.1111/liv.15488

116. Zhao XM, Zhang J, Liang YN, Niu YC. Astragaloside IV synergizes with ferulic acid to alleviate hepatic fibrosis in bile duct-ligated cirrhotic rats. *Dig Dis Sci*. 2020;65(10):2925-2936.

doi: 10.1007/s10620-019-06017-3

117. Sun X, Huang X, Zhu X, *et al*. HBOA ameliorates CCl4-incuded liver fibrosis through inhibiting TGF-β1/Smads, NF-κB and ERK signaling pathways. *Biomed Pharmacother*. 2019;115:108901.

doi: 10.1016/j.biopha.2019.108901

118. Wu L, Zhang Q, Mo W, *et al*. Quercetin prevents hepatic fibrosis by inhibiting hepatic stellate cell activation and reducing autophagy via the TGF-β1/Smads and PI3K/Akt pathways. *Sci Rep*. 2017;7(1):9289.

doi: 10.1038/s41598-017-09673-5

119. Liu N, Feng J, Lu X, *et al*. Isorhamnetin inhibits liver fibrosis by reducing autophagy and inhibiting extracellular matrix formation via the TGF-β1/Smad3 and TGF-β1/p38 MAPK pathways. *Mediators Inflamm*. 2019;2019:6175091.

doi: 10.1155/2019/6175091

120. Yu B, Qin SY, Hu BL, Qin QY, Jiang HX, Luo W. Resveratrol improves CCL4-induced liver fibrosis in mouse by upregulating endogenous IL-10 to reprogramme macrophages phenotype from M(LPS) to M(IL-4). *Biomed Pharmacother*. 2019;117:109110.

doi: 10.1016/j.biopha.2019.109110

121. Zhu L, Mou Q, Wang Y, Zhu Z, Cheng M. Resveratrol contributes to the inhibition of liver fibrosis by inducing autophagy via the microRNA20amediated activation of the PTEN/PI3K/AKT signaling pathway. *Int J Mol Med*. 2020;46(6):2035-2046.

doi: 10.3892/ijmm.2020.4748

122. Rong G, Chen Y, Yu Z, *et al*. Synergistic effect of Biejia-Ruangan on fibrosis regression in patients with chronic hepatitis B treated with entecavir: A multicenter, randomized, double-blind, placebo-controlled trial. *J Infect Dis*. 2022;225(6):1091-1099.

doi: 10.1093/infdis/jiaa266

123. Cheng DY, Zhao ZM, Wan G, *et al*. Impact of Fuzheng Huayu tablet on antiviral effect of entecavir in patients with hepatitis B cirrhosis. *Hepatobiliary Pancreat Dis Int*. 2022;21(5):479-484.

doi: 10.1016/j.hbpd.2022.03.007

124. Zhao ZM, Zhu CW, Huang JQ, *et al*. Efficacy and safety of Fuzheng Huayu tablet on persistent advanced liver fibrosis following 2 years entecavir treatment: A single arm clinical objective performance criteria trial. *J Ethnopharmacol*. 2022;298:115599.

doi: 10.1016/j.jep.2022.115599

125. Li XM, Peng JH, Sun ZL, *et al*. Chinese medicine CGA formula ameliorates DMN-induced liver fibrosis in rats via inhibiting MMP2/9, TIMP1/2 and the TGF-β/Smad signaling pathways. *Acta Pharmacol Sin*. 2016;37(6):783-793.

doi: 10.1038/aps.2016.35

126. Tian H, Liu L, Li Z, *et al*. Chinese medicine CGA formula ameliorates liver fibrosis induced by carbon tetrachloride involving inhibition of hepatic apoptosis in rats. *J Ethnopharmacol*. 2019;232:227-235.

doi: 10.1016/j.jep.2018.11.027

127. Wang Y, Li Y, Zhang H, *et al*. Pharmacokinetics-based comprehensive strategy to identify multiple effective components in Huangqi decoction against liver fibrosis. *Phytomedicine*. 2021;84:153513.

doi: 10.1016/j.phymed.2021.153513

128. Cheng Y, Liu P, Hou TL, Maimaitisidike M, Ababaikeli R, Abudureyimu A. Mechanisms of Huangqi decoction granules () on hepatitis B cirrhosis patients based on RNA-sequencing. *Chin J Integr Med*. 2019;25(7):507-514.

doi: 10.1007/s11655-018-3013-3

129. Zhou Y, Wu R, Cai FF, *et al*. Xiaoyaosan decoction alleviated rat liver fibrosis via the TGFβ/Smad and Akt/FoxO3 signaling pathways based on network pharmacology analysis. *J Ethnopharmacol*. 2021;264:113021.

doi: 10.1016/j.jep.2020.113021

130. Lu Y, Li M, Zhou Q, *et al*. Dynamic network biomarker analysis and system pharmacology methods to explore the therapeutic effects and targets of Xiaoyaosan against liver cirrhosis. *J Ethnopharmacol*. 2022;294:115324.

doi: 10.1016/j.jep.2022.115324

131. Liang B, Gao L, Wang F, *et al*. The mechanism research on the anti-liver fibrosis of emodin based on network pharmacology. *IUBMB Life*. 2021;73(9):1166-1179.

doi: 10.1002/iub.2523

132. Tang YX, Liu M, Liu L, *et al*. Lipophilic constituents in salvia miltiorrhiza inhibit activation of the hepatic stellate cells by suppressing the JAK1/STAT3 signaling pathway: A network pharmacology study and experimental validation. *Front Pharmacol*. 2022;13:770344.

doi: 10.3389/fphar.2022.770344

133. Xiao HM, Shi MJ, Jiang JM, *et al*. Efficacy and safety of AnluoHuaxian pills on chronic hepatitis B with normal or minimally elevated alanine transaminase and early liver fibrosis: A randomized controlled trial. *J Ethnopharmacol*. 2022;293:115210.

doi: 10.1016/j.jep.2022.115210

ACCSCIENCE PUBLISHING

Eurasian Journal of Medicine and Oncology

REVIEW ARTICLE

CXC chemokines as potential non-invasive biomarkers and therapeutic targets for non-alcoholic fatty liver disease: A review

Zhihui Li and Zhiyun Chen*

Department of Gastroenterology, The First Affiliated Hospital of Zhejiang Chinese Medical University, Hangzhou, Zhejiang Province, China

Abstract

Lately, non-alcoholic fatty liver disease (NAFLD) has risen as the leading chronic liver disease worldwide, posing a significant risk for the development of cirrhosis and hepatocellular carcinoma. The rising prevalence of NAFLD among adolescents mirrors the increasing rates of obesity in this demographic group. Despite ongoing research, the precise etiology of NAFLD remains unclear, with the "multiple parallel hits" hypothesis garnering the most support. Among the various factors implicated in NAFLD's progression, the CXC chemokine family has been identified as a potential contributor to its development. The purpose of this review is to explore the involvement of CXC chemokines in the development of NAFLD, identify their potential targets within the disease's development, and explore possible clinical therapeutic avenues. In addition, we assess the feasibility of utilizing CXC chemokines as biomarkers for the diagnosis of NAFLD.

Keywords: Non-alcoholic steatohepatitis; CXC chemokines; Non-invasive biomarkers; Inflammatory factor; Pathogenic mechanism; Medication

***Corresponding author:**
Zhiyun Chen
(jcyjzxchen@163.com)

Citation: Li Z, Chen Z. CXC chemokines as potential non-invasive biomarkers and therapeutic targets for non-alcoholic fatty liver disease: A review. *Eurasian J Med Oncol.* 2025;9(3):19-31. doi: 10.36922/ejmo.8383

Received: January 3, 2025

Revised: January 26, 2025

Accepted: February 17, 2025

Published online: April 11, 2025

Copyright: © 2025 Author(s). This is an Open-Access article distributed under the terms of the Creative Commons Attribution License, permitting distribution, and reproduction in any medium, provided the original work is properly cited.

Publisher's Note: AccScience Publishing remains neutral with regard to jurisdictional claims in published maps and institutional affiliations.

1. Introduction

Non-alcoholic fatty liver disease (NAFLD) has risen as the leading cause of chronic liver disease globally, covering a spectrum of conditions that extend from simple liver steatosis to non-alcoholic steatohepatitis (NASH), advanced fibrosis, and cirrhosis. NASH represents a significant condition in this spectrum, with a potential to evolve into hepatocellular carcinoma (HCC). Consequently, NAFLD presents a major risk to global health, underscoring the imperative for research to unravel its pathogenesis and identify effective therapeutic targets. There has been a dramatic increase in the incidence of NAFLD in the last 40 years, with the current global prevalence estimated to be approximately 30% or higher.[1] This alarming trend underscores the urgency of understanding the complex interplay of factors that contribute to NAFLD's development and progression. As research continues, it is crucial to not only identify the mechanisms underlying NAFLD but also to develop strategies for early detection and intervention, which could significantly reduce the burden of this disease on public health.[2,3] Although liver-related complications occur in <10% of NAFLD patients, there are still no validated biomarkers or imaging tests to assess whether an NAFLD patient is in a high-risk stage (*e.g.*, NASH). However, NASH-associated cirrhosis is a potent risk factor for the

development of HCC.[4] As a result, globally, NAFLD is rapidly escalating as the leading cause of liver-related deaths and is becoming a critical factor for terminal liver disease, primary liver cancer, and liver transplants. Although viral hepatitis remains the major cause of death from chronic liver disease, its deleterious effects are dwindling each year as the prevalence of hepatitis C virus declines worldwide; in contrast, NAFLD has evolved to become the primary cause of chronic liver disease and needs more attention from society.[5] At present, invasive liver biopsy cytology is still the "gold standard" for diagnosing NAFLD,[6] but popularizing this test in clinics is difficult, which leads to many patients being diagnosed with NAFLD at a more severe stage; in addition, since the pathophysiology of NAFLD is affected by numerous metabolic, genetic, and microbiome factors, the underlying mechanisms of NAFLD remain largely unclear, leading to a scarcity of specific drugs to treat the disease.[7]

The development of NAFLD can be described with a multiple-hit model involving multiple stressors,[8] and although the underlying mechanisms of hepatocellular steatosis are well elucidated, the pathogenesis of NASH remains elusive. It is certain that during the development of NAFLD, disorders of lipid metabolism lead to the production of lipotoxic lipids, which induce cellular stress (including oxidative stress and endoplasmic reticulum stress), activation of inflammatory vesicles, and apoptotic cell death, as well as subsequent inflammatory stimulation, tissue regeneration, and fibrosis, in which inflammatory and pro-fibrotic macrophages are implicated in the progression of liver fibrosis.[9] Inflammatory factors are a major driving force in the development of non-alcoholic steatohepatitis and liver fibrosis, which in turn is a substantial predictor of liver-related morbidity and mortality, thus, there is great clinical potential to reverse the progression of NASH by modulating inflammatory factors.[10] The interplay between chemokines and their respective receptors is recognized as a crucial element in the evolution from simple steatosis to steatohepatitis,[11] in which the CXC chemokine family-mediated inflammatory response is highly relevant in the pathogenesis of NAFLD, and there exists a considerable research potential for the diagnosis and treatment of NAFLD.

2. Definitions and pathogenesis

NAFLD is metabolic disease that is closely associated with insulin resistance and genetic susceptibility.[12] With the understanding of the disease and the need for clinical diagnosis, many clinicians and researchers find it difficult to meet the clinical, scientific, and patient needs of NAFLD as a traditional generic term. To more accurately reflect the pathogenesis of the disease and to expand the terminology beyond the superficial histopathologic similarities to alcohol-induced liver disease,[13] in 2020, a global group of specialists formulated a more fitting terminology for the disease: metabolic dysfunction-associated fatty liver disease (MAFLD). In addition, the expert consensus emphasizes the important role of systemic metabolic dysregulation in driving liver disease and proposes a series of simple positive criteria for the diagnosis and evaluation of MAFLD.[14] Diagnostically, however, the most significant difference between NAFLD and MAFLD is not the dysregulation of metabolic pathways, but rather whether or not concomitant liver disease is excluded. In summary, NAFLD tends to be an exclusionary diagnosis, whereas MAFLD is more focused on telling us what the disease is.[14,15] This change has helped physicians to be able to recognize and treat all of the diseases of the liver in a holistic way in some patients. In comparison to NAFLD, studies have found that the use of MAFLD increases the identification of individuals with high-risk features for progressive liver disease, and its relatively simple diagnosis facilitates awareness and understanding of the disease by clinicians other than hepatologists, facilitating early management of the disease.[16,17] The term "non-alcoholic" has been used for more than 40 years since it was first coined in 1980, and the introduction of MAFLD has had the effect of undermining public understanding of the two diseases; moreover, a proportion of patients who meet the diagnostic criteria for NAFLD but have no metabolic risk factors have been identified as being at high risk for MAFLD. Most importantly, MAFLD has been proposed for a relatively short period of time and its research data is significantly less compared to NAFLD, so the main body of the discussion in this article places a bigger focus on NAFLD.

While the early stages of NAFLD show only simple steatosis of the liver cells, the progressive stages of NASH result in liver cell damage and inflammation, and the histologic features of NASH are the presence of liver cell ballooning and inflammation in the liver lobes in addition with liver steatosis.[18] Overnutrition is a major driver of NAFLD. Excessive intake of energy-dense substances such as fats and carbohydrates leads to dilation of adipose depots and accumulation of ectopic fat. In this context, macrophage infiltration into visceral tissues creates a pro-inflammatory state that further promotes insulin resistance. Insulin resistance promotes free fatty acid transport to the liver, ultimately leading to dysregulation of lipid metabolism and further development of lipotoxic lipids, causing intracellular oxidative and endoplasmic reticulum stress, inflammatory vesicle activation, and apoptotic cell death, resulting in hepatocellular injury and development of hepatic inflammation.[9,12] However, these pathways in NAFLD are influenced by numerous metabolic, genetic,

and microbial factors, and the molecular mechanisms underlying the progression from NAFLDs to NASHs are poorly understood. The widely accepted theory that NASH is a complicated multifactorial disease whose development is facilitated by metabolic factors, immune abnormalities, chemokines, cytokines, bacterial lipopolysaccharides, and other factors is the "multiple parallel hits theory."[19] It has been shown that chemokines promote inflammation by coordinating the recruitment of immune cells during obesity, Type 2 diabetes, and cardiovascular disease in both mice and humans.[20]

3. CXC chemokines

Chemokines have a part to play in hematopoiesis, innate and adaptive immune responses, and inflammatory processes to a large extent by mediating the migration of leukocytes,[21] and they are grouped into four subfamilies: CXC, CC, C, and CX3C, based on the position of the first two cysteines in the primary sequence, and perform their corresponding functions by binding to their respective G protein-coupled seven transmembrane structural domain receptors.[22] CXC chemokines, small secreted proteins, possess four remarkably conserved cysteine amino acid residues, with the first two separated by one non-conserved amino acid residue.[23] On the basis of the presence or absence of Glu-Leu-Arg (ELR) motifs at the NH2 terminus, the CXC chemokine family can be subdivided into two isoforms, ELR+ CXC chemokine and ELR- CXC chemokine. ELR+ CXC chemokines include CXCL1, CXCL2, CXCL3, CXCL5, CXCL6, CXCL7, CXCL8, and CXCL17, while ELR- CXC chemokine include CXCL4, CXCL9, CXCL10, CXCL11, CXCL12, CXCL13, CXCL14, and CXCL16.[24] CXC chemokine ligands are associated with trimeric G proteins (Gαβγ), and the role of four different types of Gα subunit types determines intracellular activation.[25] Given that ELR+ CXC chemokines have the ability to attract neutrophils from the blood to areas of infection and inflammation, they are categorized as inflammatory chemokines,[26] and ELR- CXC chemokines may have a homeostatic role in the regulation of the movement of neutrophils from the bone marrow into the bloodstream. Since the inflammatory response is important in the development of NASH and CXC chemokine receptors are G-protein-coupled receptors that mediate the inflammatory response, the search for specific CXC chemokine targets for action in NAFLD disease is a logical and attractive goal (Table 1).

4. Impact of key CXC chemokines on NAFLD

4.1. CXCL1

CXCL1, as an ELR+ CXC chemokine, is one of the selective ligands for CXCR2, which can activate the PI3K/Akt, MAP kinase, or phospholipase β signaling pathway by binding to the receptor CXCR2,[27] thereby inducing neutrophil infiltration to high-concentration sites, participating in inflammatory responses, and even leading to tissue destruction.[28] In the liver, CXCL1 was expressed at the highest levels in hepatocytes and at a lower level in hepatic stellate cells and hepatic sinusoidal endothelial cells.[29] It has been proposed that the heightened expression of CXCL1 in liver cells correlates with a rise in the levels of free fatty acids in the liver and is dependent on the regulation of extracellular signal-regulated kinase 1/2, c-Jun N-terminal kinase (JNK), and nuclear factor κ light chain enhancer (NF-κB).[30] Tang *et al.*[31] have attempted at upregulating or downregulating CXCL1 expression levels by using adeno-associated viruses in an established mouse model of acute and chronic liver failure and found that knockdown of CXCL1 reduced neutrophil infiltration and lowered the expression of inflammatory cytokines in the mouse liver and also significantly downregulated the generation of reactive oxygen species (ROS) and the caspase3-associated apoptosis of hepatocytes, thereby ameliorating liver injury in acute and chronic liver failure.

The invasion of neutrophils into the liver stands out as a major pathological symptom of liver damage,[32] and CXCL1 is a major chemokine that mediates neutrophil recruitment (Figure 1). CXCL1 expression has been shown to be dramatically elevated in patients with NASH in previous studies,[33] whereas it is essentially normal in patients with steatohepatitis and in high-fat diet-induced steatohepatitis model mice.[30] Hwang *et al.*[34] found that elevated levels of CXCL1 alone can accelerate the development of NASH through ROS from neutrophils and trigger stress kinases, a process that interleukin (IL)-22 can reverse by stimulating metallothionein production. Saturated fatty acids (sFAs) increase NF-κB, ERK MAPK, and JNK MAPK-dependent Kupffer cell (KC) expression in hepatocytes,[35] in which CXCL1 plays a key pivotal role.[36] Through contrasting the supernatants from primary human and mouse liver cells exposed to inflammatory cytokines, it was found that mouse hepatocytes lacked IL-8 expression and had low expression of tumor necrosis factor-alpha (TNF-α) and IL-1β-induced CXCL1, which could explain the difficulty in establishing a NASH model in high-fat diet-fed mice. Subsequent research indicated that the heightened expression of CXCL1 leads to NASH by producing ROS and triggering the stress kinase p38α.[37] E-selectin (Sele) is crucial as a binding molecule for neutrophils in adipose tissue, and it was found that knockdown of Sele might slow down the development of NASH by impairing the adhesion between neutrophils and sinusoidal endothelial cells and reducing CXCL1-induced neutrophil transport to the liver.[33] Under normal physiological conditions,

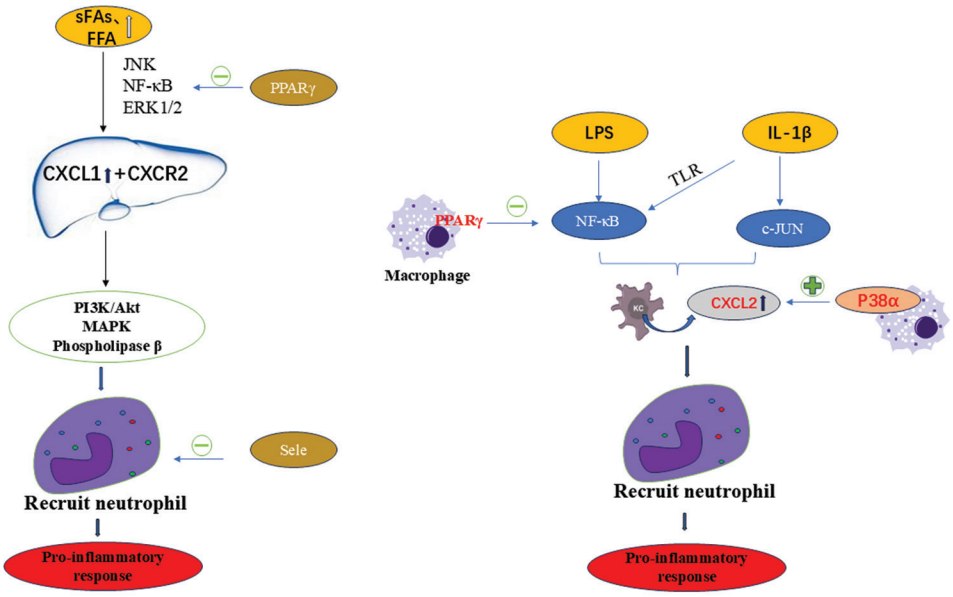


Figure 1. The function of CXCL1 and CXCL2 in NAFLD: (1) sFAs and FFA upregulate CXCL1 expression levels through the JNK/NF-κB/ERK1/2 signaling pathway. CXCL1 then promotes neutrophil recruitment through MAPK, PI3K/Akt, and phospholipase β pathway and exacerbates the inflammatory response within the liver. PPARγ can inhibit NF-κB pathway; Sele can inhibit neutrophil recruitment. (2) CXCL2 is upregulated in response to stimulation by NF-κB and c-jun and then promotes an inflammatory response by recruiting neutrophils. NF-κB is regulated by LPS and IL-1β, where IL-1β regulation requires TLR involvement. c-JUN is regulated by IL-1β. PPARγ in macrophages negatively regulates NF-κB; p38α in macrophages positively regulates CXCL2 expression levels.
Abbreviations: FFA: Free fatty acid; IL: Interleukin; LPS: Lipopolysaccharide; NAFLD: Non-alcoholic fatty liver disease; NF-κB: Nuclear factor κ light chain enhancer; PPAR-γ: Peroxisome proliferator-activated receptor gamma; sFAs: Saturated fatty acids; TLR: Toll-like receptor.

peroxisome proliferator-activated receptor gamma (PPAR-γ) expression in the liver is minimal but is significantly increased in mice with a fatty liver model and in mice with NAFLD.[38] This animal study showed that PPAR-γ has a dual regulatory role in the development of steatohepatitis: the increase in free fatty acids due to high-fat diet induces an up-regulation of CXCL1 expression in hepatocytes; at the same time, high-fat diet activates PPAR-γ, and activated PPAR-γ can limit NF-κB-mediated expression of CXCL1 and thus avoid neutrophil infiltration in the liver. This animal study showed that PPAR-γ has a dual regulatory role in the progression of steatohepatitis: the increase in free fatty acids due to high-fat diet induces an increased expression of CXCL1 in hepatocytes; at the same time, high-fat diet activates PPAR-γ, and activated PPAR-γ can inhibit NF-κB-mediated expression of CXCL1 and thus avoid neutrophil infiltration in the liver.

4.2. CXCL2

The primary function of CXCL2 is to respond to infection or injury by rapidly recruiting neutrophils through the bloodstream to sites of inflammation or damaged tissue.[39,40] Recognized as a growth-related gene product, CXCL2 is critical for repairing inflammatory injury and is involved in cell movement, adhesion, and immune responses, all of which are essential for physiological processes.[41] Research indicates that IL-1β markedly enhances the expression of CXCL1 and CXCL2 genes in rat pancreatic islets and β-cell lines by stimulating the NF-κB pathway in B cells, which increases neutrophil recruitment and promotes the inflammatory response in pancreatic islets.[42] In addition, activation of the NF-κB and c-jun transcription factors in macrophages is triggered by lipopolysaccharide through a Toll-like receptor-dependent signaling pathway, where their combined effect rapidly activates the *CXCL2* gene, leading to inflammation by attracting neutrophils.[43]

Previous research indicates a significant increase in CXCL2 levels in the blood of NASH patients,[44] indicating a role for CXCL2 in the development of NAFLD.[45] Among people with NAFLD, the incidence and intensity of the disease is significantly higher in men than in women, and based on this finding, a study found that CXCL2 expression was higher in males and de-ovulated females compared to females by establishing a mouse model of NAFLD; this study concluded that KCs are the main source of CXCL2.[46] This further demonstrates the importance of CXCL2 in NAFLD development and suggests that KCs may be a key locus mediating sex differences in NAFLD development. Barreyro *et al.*[47] found that inhibition of

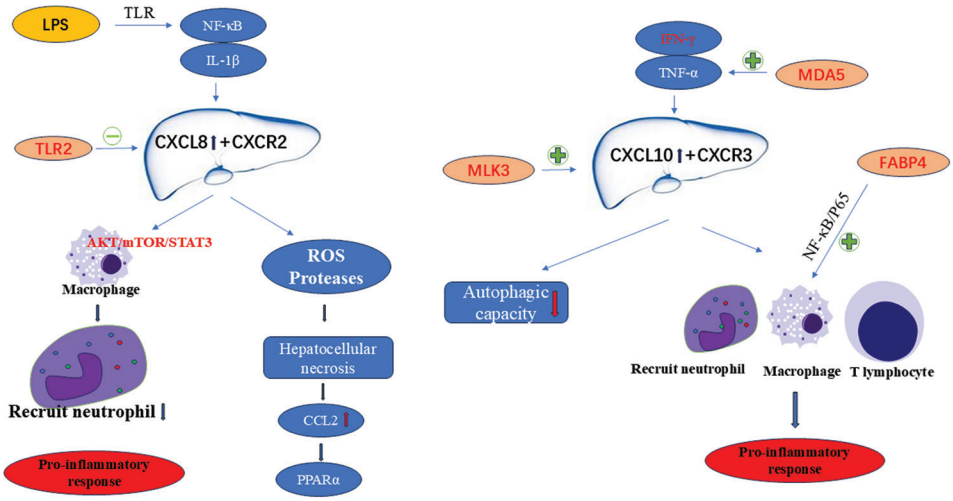


Figure 2. The function of CXCL8 and CXCL10 in NAFLD. (1) CXCL8 is regulated by NF-κB and IL-1β. CXCL8 binding to its receptor CXCR2 can promote inflammatory responses by recruiting neutrophils via AKT/mTOR/STAT3 in macrophages. CXCL8 binds to its receptor, releasing ROS and proteases that cause hepatocellular necrosis. Damaged hepatocytes increase CCL2 expression, promoting hepatic steatosis, hepatitis, and fibrosis through activation of PPAR-α. LPS regulates NF-κB with TLR involvement. TLR2 can negatively regulate the expression level of CXCL8. (2) CXCL10 is regulated by IFN-γ and TNF-α. MDA5 positively regulates TNF-α. CXCL10 and its receptor CXCR3 can recruit neutrophils, macrophages, and lymphocytes to promote an inflammatory response. FABP4 can positively regulate macrophage levels through the NF-κB/P65 pathway. CXCL10 can impair hepatocyte autophagy, leading to the development of steatohepatitis. MLK3 positively regulates CXCL10.
Abbreviations: CCL2: CC motif chemokine ligand 2; IFN-γ: Interferon gamma; IL: Interleukin; LPS: Lipopolysaccharide; MDA5: Melanoma differentiation-associated gene 5; MLK3: Mixed-spectrum kinase 3; NAFLD: Non-alcoholic fatty liver disease; NF-κB: Nuclear factor κ light chain enhancer; PPAR-α: Peroxisome proliferator-activated receptor alpha; TLR: Toll-like receptor; TNF-α: Tumor necrosis factor alpha.

hepatocyte apoptosis reduces serum CXCL2 expression, thereby attenuating liver injury and inflammatory damage in a NASH mouse model. It has been found that the deliberate removal of PPARγ in macrophages exhibits an enhanced response to chronic CCL4 injury compared to hepatocytes. It can exhibit higher necroinflammatory damage accompanied by upregulation of TNF-α, CXCL2, and IL-1β expression, revealing that PPARγ may act as an anti-inflammatory and anti-fibrotic agent in non-substantial hepatocytes by mediating pro-inflammatory factors such as CXCL2.[48] In addition, genetic deletion of p38α in macrophages can play a role in ameliorating NASH by reducing pro-inflammatory cytokines such as CXCL2 and IL1β.[49]

4.3. CXCL8

Alternatively known as IL-8, CXCL8 is mainly produced by macrophages, epithelial cells, airway smooth muscle cells, and endothelial cells, and is crucial in drawing in and stimulating neutrophils, as well as attracting granulocytes to areas of inflammation.[50] Under normal physiological conditions, CXCL8 expression remains minimal but is quickly induced by proinflammatory agents such as TNF-α and IL-1β.[51] CXCL8 function is mainly dependent on its interaction with specific cell-surface G protein-coupled receptors CXCR1 and CXCR2, of which CXCR2 is the primary functional receptor.[52] Stephens and von der Weid[53] found that species-specific lipopolysaccharides can exacerbate intestinal epithelial cell dysfunction by inducing NF-κB and CXCL8 production through activation of Toll-like receptor 4. Zhu *et al.*[54] found that overexpression of CXCL8 causes severe damage to the intestinal mucosa and promotes the development of ulcerative colitis, and the expression of CXCL8 in ulcerative colitis is mainly related to PI3K/Akt, MAPKs, and NF-κB, providing a reference for studying the relationship between CXCL8 and NAFLD.

Earlier research indicates that CXCL8 is the most potent chemokine for the development of NAFL and that circulating CXCL8 is the only cytokine that predicts NAFLD independently of body mass index,[55] and it can be viewed as a significant biomarker and a prospective treatment focus for both NAFL and NASH (Figure 2). Macrophages are a major factor in the development of NAFL and NASH, and studies have shown that macrophages can be stimulated to produce increased levels of CXCL8, leading to the prevailing belief that CXCL8 could contribute to attracting neutrophils in NASH development through the activation of the AKT/mTOR/STAT3 pathway.[56] CXCL8 binds to its receptor and releases ROS and proteases, leading to hepatocellular necrosis. Damaged hepatocytes cause an increase in the expression level of CC motif chemokine ligand 2 (CCL2), which subsequently promotes

hepatic steatosis, hepatitis, and hepatic fibrosis through the activation of PPAR-α.[57] Some clinical studies have demonstrated a correlation between only CXCL8 and the development of NAFLD and also found that there was a direct relationship observed between the liver's TLR2 expression and the expression levels of CXCL8,[58] indicating that inhibiting the expression of TLR2 might be able to reduce the level of CXCL8 and thus achieve a decline in liver inflammation. As NAFLD becomes more prevalent among youth, a study found that the concentrations of CXCL8 and TNF-α in the supernatants of mercury-exposed monocytes were more than 10-fold higher than those of controls, by combining the epidemiological results of a multicenter mother-son cohort with the results of an *in vitro* experiment.[59] This suggests that the TNF-α/CXCL8 axis may represent an important target for limiting the development of inflammation in NAFLD.

4.4. CXCL10

CXCL10 is alternatively known as interferon gamma-inducible protein 10 (IP-10), which is maintained at low levels in a homeostatic environment, but expression levels are upregulated in response to cytokine stimulation. Functionally classified as a pro-inflammatory chemokine, CXCL10 regulates the immune response by binding its specific receptor CXCR3 to activate and recruit leukocytes, including T cells, monocytes, eosinophils, and NK cells. CXCL10 can be secreted by different kinds of cells, including hepatocytes, macrophages, monocytes, neutrophils, endothelial cells, fibroblasts, dendritic cells, astrocytes, *etc.*[60] CXCR3 has a preferential expression on monocyte, T-cell (mainly Th1), NK-cell, dendritic cell, and cancer cell surfaces.[61] CXCL10 and its receptor CXCR3 are secreted mainly by the induction of interferon-gamma (IFN-γ), which can also be weakly induced by TNF-α. The primary secretion of CXCL10 occurs in hepatocytes and the endothelial cells within the liver's hepatic sinusoids, and the binding of CXCL10 to its specific receptor CXCR3 leads to the aggregation of activated CXCR3+ T-lymphocytes and macrophages into the liver parenchyma, which gets involved in promoting inflammation, apoptosis, and fibrosis.[62] Ibrahim *et al.*[63] demonstrated that during hepatocyte lipotoxicity, the activation of mixed-spectrum kinase 3 (MLK3) triggers the secretion of vesicles containing CXCL10 from hepatocytes, serving as a chemotactic agent for macrophages, thereby increasing macrophage-associated inflammation in the liver.

CXCL10, recognized as a standard proinflammatory chemokine, plays a significant role in the emergence of NAFLD.[64] Research indicates a notable increase in CXCL10 expression in cases of NAFLD.[65,66] It has been shown that circulating CXCL10 levels are correlated with the extent of lobular inflammation, which also serves as an independent risk factor in NASH patients.[62] For the initial instance, this research revealed CXCL10's crucial involvement in the development of experimental steatohepatitis. In addition, certain clinical trials suggested that CXCL10 expression correlates favorably with disease severity, as well as the expression levels of alanine aminotransferase (ALT), Tumor necrosis factor-α (TNF-α), monocyte chemotactic protein-1 (MCP-1), and others; subsequent ordered logistic studies showed that CXCL10 independently contributes to the risk of progressive liver damage and diabetes mellitus and may serve as a non-invasive indicator of NAFLD progression.[67] The CXCL10/CXCR3 chemotaxis axis can promote liver injury and fibrosis by recruiting macrophages.[68] In addition, through a series of mouse experiments, Maina *et al.*[69] found that steatosis and lobular inflammation were more prevalent in Th1- and M1-oriented mice compared to Th2- and M2-oriented mouse models of NASH, and that Th1- and M1-oriented mice showed increased hepatic mRNA expression of macrophage M1-activated markers inducible nitric oxide synthase (iNOS) and CXCL10. Consistent with this, there was a positive association between the expression levels of hepatic iNOS and CXCL10 mRNA and the occurrence of hepatic necroinflammatory foci. CXCR3, the specific receptor for CXCL10, showed similar effects, and CXCR3 knockout was found to attenuate macrophage responses to IFN-γ in mouse experiments, thereby inhibiting the development of NASH.[70] A protein known as fatty acid binding protein 4 (FABP4) has a strong association with metabolic syndrome, and it has been shown that FABP4 in hepatic sinusoidal endothelial cells may promote CXCL10-mediated macrophage M1 polarization and CXCR3+ macrophage infiltration via the NF-κB/p65 signaling pathway and thus promote the development of NAFLD.[71] Dysregulation of autophagy leads to hepatic inflammatory injury, and upregulation of CXCL10 in NAFLD may impair the autophagic capacity of hepatocytes by reducing the formation of autolysosomes, which inhibits the degradation of autophagic proteins and accumulation of ubiquitylated proteins, leading to the development of steatohepatitis, and the use of a monoclonal antibody to CXCL10 can significantly restore impaired autophagic capacity.[72] MDA5, also known as melanoma differentiation-associated gene 5, is a member of the protein family of intracellular RNA deconjugating enzymes. Studies have shown that MDA5 actively controls TNF-α-induced CXCL10 expression in a manner that is both dependent on and independent of STAT1, which may be related to metabolic inflammation in the liver.[73]

Table 1. Studies on the regulation of CXC chemokines in NAFLD

Disease models	Conditioning factor	CXC chemokines	Effect	References
Acute-on-chronic liver failure mouse model	Adeno-associated virus	CXCL1	Increasing neutrophil recruitment	31
NAFLD model of male	Kupffer cells	CXCL2 CXCL10	Promoting inflammatory responses	46
Murine model of NASH	Emricasan	CXCL2	Inhibiting hepatocytes apoptosis/ suppressing liver and fibrosis	47
Mice submitted to CCL4	PPAR-γ	CXCL2	Anti-inflammatory/anti-fibrogenic	48
NASH model of human liver tissues and mice	P38α	CXCL2 CXCL10	Promoting inflammatory responses	49
NASH model of mice	Macrophage (Th1, M1)	CXCL10	Promoting inflammatory responses	69
NAFLD model of mice	FABP4	CXCL10	Promoting inflammatory responses	71

Abbreviations: CCL4: CC motif chemokine ligand 4; FABP4: Fatty acid binding protein 4; NAFLD: Non-alcoholic fatty liver disease; NASH: Non-alcoholic steatohepatitis; PPAR-γ: Peroxisome proliferator-activated receptor gamma necrosis factor gamma.

Table 2. Therapeutic effects and targets of action of certain CXC chemokines

Research targets	Targets of action	Effects
Resmetirom[74]	Thyroid hormone receptor beta-selective agonist	• Anti-inflammatory • Anti-fibrotic
Hepatocyte growth factor[82]	Macrophage, CXCL1	• Anti-inflammatory • Anti-fibrotic
Zaluzanic C[84]	ROS, CXCL2	• Antioxidant • Anti-inflammatory
Mixed spectrum kinase[385]	STAT1, CXCL10	• Anti-inflammatory
Rilpivirine[89]	CXCL10	• Anti-inflammatory
Valine and isoleucine[81]	KC/CXCL1, MCP-1/CCL2, MIP-2/CXCL2	• Anti-inflammatory
Liraglutide[75] Semaglutide[76]	GLP-1	• Anti-inflammatory • Alleviation of insulin resistance • Improvement of lipid metabolism
Pegozafermin[77]	FGF21	• Improvement of lipid metabolism • Anti-fibrotic
Fucoidan and fucoxanthin[78]	Adiponectin-adipoR1/2 and SIRI-PGC-1	• Anti-inflammatory • Improvement of lipid metabolism • Alleviation of insulin resistance
Saroglitazar[79]	PPAR	• Improvement of lipid metabolism • Alleviation of insulin resistance
Cenicriviroc[80]	CCR2/CCR5	• Anti-inflammatory • Anti-fibrotic

Abbreviations: CCL2: CC motif ligand 2; FGF21: Fibroblast growth factor 21; GLP-1: Glucagon-like peptide-1; KC: Kupffer cell; MCP-1: Monocyte chemoattractant protein-1; MIP-2: Macrophage inflammatory protein 2; PPAR: Peroxisome proliferators-activated receptor; ROS: Reactive oxygen species.

5. Pharmacological treatment of NAFLD and therapeutic prospects for targeting CXC chemokines

Since there is a lack of drugs formally approved by the Food and Drug Administration for the treatment of NAFLD, we summarize some of the drugs, natural products that have been observed to attenuate the progression of NAFLD in experiments, and natural products and drugs that target CXC chemokines to attenuate NAFLD (Table 2). Resmetirom, a liver-targeted, thyroid hormone receptor beta receptor-selective agonist, demonstrated significant effects in the reversal of NASH and antifibrosis in a randomized, controlled Phase 3 study.[74] Liraglutide and

semaglutide, pancreatic glucagon-like peptide 1 receptor agonists, were each shown to significantly improve the histologic progression of NASH in two independent Phase 2 clinical trials, with significant improvements in hepatic steatosis and hepatocellular ballooning observed in patients treated with liraglutide.[75,76] Pegozafermin, a novel glycopegylated version of human fibroblast growth factor 21, significantly improves liver fibrosis in patients with NASH through modulation of lipid and glucose metabolism as well as adiponectin levels and does not worsen NASH.[77] Low-molecular-weight fucoidan and high-stability fucoxanthin (LMF-HSFx) is a seaweed extract, which can regulate lipid and glycogen metabolism, attenuate insulin resistance, and inhibit hepatic inflammatory responses through the adiponectin-adipoR1/2 and SIRI-PGC-1 pathways in adipocytes and hepatocytes.[78] Saroglitazar, a PPARα/γ dual agonist, has been observed to improve the histological features of NASH in animal studies. A randomized controlled clinical trial based on these findings showed that saroglitazar significantly improved ALT, LDL cholesterol, insulin resistance, and atherogenic dyslipidemia in patients with NAFLD.[79] Cenicriviroc is an oral chemokine receptor Type 2 and 5 (CCR2/CCR5) antagonist that has antifibrotic activity through inhibition of monocyte-derived megakaryocyte infiltration.[80]

Experiments directly using CXCL1/CXCL2/CXCL8/CXCL10 antagonists to intervene in NAFLD therapy are still lacking, but changes in several CXC chemokines can be observed in experiments intervening in NAFLD therapy by other natural products and drugs. Studies have shown that valine and isoleucine can significantly reduce inflammation within the liver during the development of NAFLD by inhibiting the chemokine proteins KC/CXCL1, MCP-1/CCL2, MIP-2/CXCL2, and their pathways.[81] Hepatocyte growth factor (HGF), a versatile protein, plays a role in both anti-inflammatory and anti-fibrotic responses, and it has been shown that recombinant HGF inhibits macrophage infiltration and upregulation of chemokine CXCL1 thereby slowing down the development of NASH.[82] The administration of exogenous HGF may be a favorable option for the treatment of NAFLD. Chronic administration of physiologic concentrations of indole *in vivo* has anti-inflammatory and hepatoprotective effects, a process that is accompanied by a decrease in CXCL2 expression.[83] Zaluzanic C has antioxidant and anti-inflammatory effects on NAFLD, and it inhibits lipopolysaccharide (LPS)-induced mitochondrial ROS (mtROS) production and reduces mRNA levels of pro-inflammatory factors and chemokines (CXCL2).[84] Under lipotoxic stress, hepatocytes induce high levels of macrophage CXCL10 production and release CXCL10-rich extracellular vesicles through a mixed spectrum kinase 3 (MLK3)-dependent mechanism. The mitogen-activated protein kinase (MAPK) signaling cascade that induces CXCL10 consists of mediator modules of MLK3, MKK3/6, and p38, and it was demonstrated that in lipotoxic hepatocytes, MLK3 activates the MAPK signaling cascade, leading to activated phosphorylation of STAT1 and transcriptional upregulation of CXCL10, MLK3/STAT1 repression or deletion of a shared STAT1 binding site within the CXCL10 promoter attenuates promoter activation.[85] Targeting this therapeutically might lead to a decrease in CXCL10 expression and prevent NASH progression. Wada *et al.*[86] found that insulin resistance led to elevated expression of CXCL10 mRNA in monocytes only when accompanied by stimulation of bacterial-associated TLR2, and thus strict control of insulin resistance and intestinal barrier function could inhibit the progression of NAFL to NASH to some extent. Recent research focusing on CXCL10 as a treatment target for NAFLD has been on the rise; for example, activation of silencing information regulator 1 (SIRT1) and adenosine A2a receptor (A2aR),[87,88] an increase in the expression level of microRNA-223, and rilpivirine through the MAP kinase and PI3K/mTOR pathways can inhibit the expression level of CXCL10 and reduce liver inflammatory injury.[89]

6. Summary and prospects

There is still a lack of effective drugs to treat NAFLD, and invasive liver tissue biopsy remains the "gold standard" for diagnosis of NAFLD; therefore, it is necessary to find new treatments and biomarkers that can be used to diagnose NAFLD. CXC family chemokines have been implicated in the pathogenesis of NAFLD, among which CXCL1, CXCL2, CXCL8, and CXCL10 have been subjected to more extensive discussion over the past few years due to their close association with NAFLD, and the baseline expression levels of these four CXC family chemokines under normal circumstances are significantly higher than the levels when NAFLD is compounded by liver injury and inflammation. Hence, blocking or inhibiting CXC chemokines and their receptor signaling may provide a more specific therapeutic strategy for NAFLD. However, the mechanisms of these four chemokines in the development of NAFLD still need further exploration. In addition, CXCL8 and CXCL10 have been suggested to be potential non-invasive biomarkers for the prediction of NASH, which also need to be validated through further clinical trials.

Acknowledgments

None.

Funding

This work was supported by Zhejiang Scientific Research Foundation of Traditional Chinese Medicine (NO.2022ZB106).

Conflict of interest

The authors declare that they have no competing interests.

Author contributions

Conceptualization: Zhihui Li
Writing – original draft: Zhihui Li
Writing – review & editing: Zhiyun Chen

Ethics approval and consent to participate

Not applicable.

Consent for publication

Not applicable.

Availability of data

Not applicable.

References

1. Younossi ZM, Golabi P, Paik JM, Henry A, Van Dongen C, Henry L. The global epidemiology of nonalcoholic fatty liver disease (NAFLD) and nonalcoholic steatohepatitis (NASH): A systematic review. *Hepatology.* 2023;77(4):1335-1347.

   doi: 10.1097/HEP.0000000000000004

2. Riazi K, Azhari H, Charette JH, *et al.* The prevalence and incidence of NAFLD worldwide: A systematic review and meta-analysis. *Lancet Gastroenterol Hepatol.* 2022;7(9):851-861.

   doi: 10.1016/S2468-1253(22)00165-0

3. Younossi ZM, Golabi P, De Avila L, *et al.* The global epidemiology of NAFLD and NASH in patients with type 2 diabetes: A systematic review and meta-analysis. *J Hepatol.* 2019;71(4):793-801.

   doi: 10.1016/j.jhep.2019.06.021

4. Huang DQ, El-Serag HB, Loomba R. Global epidemiology of NAFLD-related HCC: Trends, predictions, risk factors and prevention. *Nat Rev Gastroenterol Hepatol.* 2021;18(4):223-238.

   doi: 10.1038/s41575-020-00381-6

5. Paik JM, Kabbara K, Eberly KE, Younossi Y, Henry L, Younossi ZM. Global burden of NAFLD and chronic liver disease among adolescents and young adults. *Hepatology.* 2022;75(5):1204-1217.

   doi: 10.1002/hep.32228

6. Ajmera V, Loomba R. Imaging biomarkers of NAFLD, NASH, and fibrosis. *Mol Metab.* 2021;50:101167.

   doi: 10.1016/j.molmet.2021.101167

7. Guo X, Yin X, Liu Z, Wang J. Non-alcoholic fatty liver disease (NAFLD) Pathogenesis and natural products for prevention and treatment. *Int J Mol Sci.* 2022;23(24):15489.

   doi: 10.3390/ijms232415489

8. Takaki A, Kawai D, Yamamoto K. Multiple hits, including oxidative stress, as pathogenesis and treatment target in non-alcoholic steatohepatitis (NASH). *Int J Mol Sci.* 2013;14(10):20704-20728.

   doi: 10.3390/ijms141020704

9. Friedman SL, Neuschwander-Tetri BA, Rinella M, Sanyal AJ. Mechanisms of NAFLD development and therapeutic strategies. *Nat Med.* 2018;24(7):908-922.

   doi: 10.1038/s41591-018-0104-9

10. Tacke F, Puengel T, Loomba R, Friedman SL. An integrated view of anti-inflammatory and antifibrotic targets for the treatment of NASH. *J Hepatol.* 2023;79(2):552-566.

    doi: 10.1016/j.jhep.2023.03.038

11. Farrell GC, Larter CZ. Nonalcoholic fatty liver disease: From steatosis to cirrhosis. *Hepatology.* 2006;43(2 Suppl 1):S99-S112.

    doi: 10.1002/hep.20973

12. Powell EE, Wong VW, Rinella M. Non-alcoholic fatty liver disease. *Lancet.* 2021;397(10290):2212-2224.

    doi: 10.1016/S0140-6736(20)32511-3

13. Demirtas CO, Yilmaz Y. Metabolic-associated fatty liver disease: Time to integrate ground-breaking new terminology to our clinical practice? *Hepatol Forum.* 2020;1(3):79-81.

    doi: 10.14744/hf.2020.2020.0024

14. Eslam M, Newsome PN, Sarin SK, *et al.* A new definition for metabolic dysfunction-associated fatty liver disease: An international expert consensus statement. *J Hepatol.* 2020;73(1):202-209.

    doi: 10.1016/j.jhep.2020.03.039

15. Kawaguchi T, Tsutsumi T, Nakano D, Eslam M, George J, Torimura T. MAFLD enhances clinical practice for liver disease in the Asia-pacific region. *Clin Mol Hepatol.* 2022;28(2):150-163.

    doi: 10.3350/cmh.2021.0310

16. Clayton M, Fabrellas N, Luo J, *et al.* From NAFLD to MAFLD: Nurse and allied health perspective. *Liver Int.* 2021;41(4):683-691.

    doi: 10.1111/liv.14788

17. Ayada I, Van Kleef LA, Alferink LJM, Li P, De Knegt RJ, Pan Q. Systematically comparing epidemiological and clinical features of MAFLD and NAFLD by meta-analysis: Focusing on the non-overlap groups. *Liver Int.* 2022;42(2):277-287.

    doi: 10.1111/liv.15139

18. Chalasani N, Younossi Z, Lavine JE, *et al.* The diagnosis and management of nonalcoholic fatty liver disease: Practice guidance from the American association for the study of liver diseases. *Hepatology.* 2018;67(1):328-357.

    doi: 10.1002/hep.29367

19. Nassir F. NAFLD: Mechanisms, treatments, and biomarkers. *Biomolecules.* 2022;12(6):824.

doi: 10.3390/biom12060824

20. Cinkajzlová A, Mráz M, Haluzík M. Adipose tissue immune cells in obesity, type 2 diabetes mellitus and cardiovascular diseases. *J Endocrinol.* 2021;252(1):R1-R22.

doi: 10.1530/JOE-21-0159

21. Bachelerie F, Ben-Baruch A, Burkhardt AM, *et al.* International union of basic and clinical pharmacology. [Corrected]. LXXXIX. Update on the extended family of chemokine receptors and introducing a new nomenclature for atypical chemokine receptors. *Pharmacol Rev.* 2014;66(1):1-79.

doi: 10.1124/pr.113.007724

22. Hughes CE, Nibbs RJB. A guide to chemokines and their receptors. *FEBS J.* 2018;285(16):2944-2971.

doi: 10.1111/febs.14466

23. Griffith JW, Sokol CL, Luster AD. Chemokines and chemokine receptors: Positioning cells for host defense and immunity. *Annu Rev Immunol.* 2014;32:659-702.

doi: 10.1146/annurev-immunol-032713-120145

24. Strieter RM, Polverini PJ, Kunkel SL, *et al.* The functional role of the ELR motif in CXC chemokine-mediated angiogenesis. *J Biol Chem.* 1995;270(45):27348-27357.

doi: 10.1074/jbc.270.45.27348

25. Mellado M, Rodríguez-Frade JM, Mañes S, Martínez AC. Chemokine signaling and functional responses: the role of receptor dimerization and TK pathway activation. *Annu Rev Immunol.* 2001;19:397-421.

doi: 10.1146/annurev.immunol.19.1.397

26. Köhler A, De Filippo K, Hasenberg M, *et al.* G-CSF-mediated thrombopoietin release triggers neutrophil motility and mobilization from bone marrow via induction of Cxcr2 ligands. *Blood.* 2011;117(16):4349-4357.

doi: 10.1182/blood-2010-09-308387

27. Silva RL, Lopes AH, Guimarães RM, Cunha TM. CXCL1/CXCR2 signaling in pathological pain: Role in peripheral and central sensitization. *Neurobiol Dis.* 2017;105:109-116.

doi: 10.1016/j.nbd.2017.06.001

28. Korbecki J, Szatkowska I, Kupnicka P, *et al.* The importance of CXCL1 in the physiological state and in noncancer diseases of the oral cavity and abdominal organs. *Int J Mol Sci.* 2022;23(13):7151.

doi: 10.3390/ijms23137151

29. Chang B, Xu MJ, Zhou Z, *et al.* Short- or long-term high-fat diet feeding plus acute ethanol binge synergistically induce acute liver injury in mice: An important role for CXCL1. *Hepatology.* 2015;62(4):1070-1085.

doi: 10.1002/hep.27921

30. Hwang S, Ren T, Gao B. Obesity and binge alcohol intake are deadly combination to induce steatohepatitis: A model of high-fat diet and binge ethanol intake. *Clin Mol Hepatol.* 2020;26(4):586-594.

doi: 10.3350/cmh.2020.0100

31. Tang S, Zhang J, Zhang L, *et al.* Knockdown of CXCL1 improves ACLF by reducing neutrophil recruitment to attenuate ROS production and hepatocyte apoptosis. *Hepatol Commun.* 2023;7(10):e0257.

doi: 10.1097/HC9.0000000000000257

32. Gao B, Ahmad MF, Nagy LE, Tsukamoto H. Inflammatory pathways in alcoholic steatohepatitis. *J Hepatol.* 2019;70(2):249-259.

doi: 10.1016/j.jhep.2018.10.023

33. Rodrigues RM, He Y, Hwang S, *et al.* E-selectin-dependent inflammation and lipolysis in adipose tissue exacerbate steatosis-to-NASH progression via S100A8/9. *Cell Mol Gastroenterol Hepatol.* 2022;13(1):151-171.

doi: 10.1016/j.jcmgh.2021.08.002

34. Hwang S, He Y, Xiang X, *et al.* Interleukin-22 ameliorates neutrophil-driven nonalcoholic steatohepatitis through multiple targets. *Hepatology.* 2020;72(2):412-429.

doi: 10.1002/hep.31031

35. Dahlquist KJV, Voth LC, Fee AJ, Stoeckman AK. An autocrine role for CXCL1 in progression of hepatocellular carcinoma. *Anticancer Res.* 2020;40(11):6075-6081.

doi: 10.21873/anticanres.14628

36. Dai W, Sun Y, Jiang Z, Du K, Xia N, Zhong G. Key genes associated with non-alcoholic fatty liver disease and acute myocardial infarction. *Med Sci Monit.* 2020;26:e922492.1-11.

doi: 10.12659/MSM.922492

37. Hwang S, Wang X, Rodrigues RM, *et al.* Protective and detrimental roles of p38α mitogen-activated protein kinase in different stages of nonalcoholic fatty liver disease. *Hepatology.* 2020;72(3):873-891.

doi: 10.1002/hep.31390

38. Gross B, Pawlak M, Lefebvre P, Staels B. PPARs in obesity-induced T2DM, dyslipidaemia and NAFLD. *Nat Rev Endocrinol.* 2017;13(1):36-49.

doi: 10.1038/nrendo.2016.135

39. White GE, Iqbal AJ, Greaves DR. CC chemokine receptors and chronic inflammation--therapeutic opportunities and pharmacological challenges. *Pharmacol Rev.* 2013;65(1):47-89.

doi: 10.1124/pr.111.005074

40. Kobayashi Y. The role of chemokines in neutrophil biology. *Front Biosci.* 2008;13:2400-2407.

doi: 10.2741/2853

41. Haskill S, Peace A, Morris J, *et al.* Identification of three related human GRO genes encoding cytokine functions. *Proc Natl Acad Sci U S A.* 1990;87(19):7732-7736.

doi: 10.1073/pnas.87.19.7732

42. Burke SJ, Lu D, Sparer TE, *et al.* NF-KB and STAT1 control CXCL1 and CXCL2 gene transcription. *Am J Physiol Endocrinol Metab.* 2014;306(2):E131-E149.

doi: 10.1152/ajpendo.00347.2013

43. Kim DS, Han JH, Kwon HJ. NF-Kappab and c-jun-dependent regulation of macrophage inflammatory protein-2 gene expression in response to lipopolysaccharide in RAW 264.7 cells. *Mol Immunol.* 2003;40(9):633-643.

doi: 10.1016/j.molimm.2003.07.001

44. Pan X, Chiwanda Kaminga A, Liu A, Wen SW, Chen J, Luo J. Chemokines in non-alcoholic fatty liver disease: A systematic review and network meta-analysis. *Front Immunol.* 2020;11:1802.

doi: 10.3389/fimmu.2020.01802

45. Sanchez JI, Parra ER, Jiao J, *et al.* Cellular and molecular mechanisms of liver fibrosis in patients with NAFLD. *Cancers (Basel).* 2023;15(11):2871.

doi: 10.3390/cancers15112871

46. Han YH, Choi H, Kim HJ, Lee MO. Chemotactic cytokines secreted from kupffer cells contribute to the sex-dependent susceptibility to non-alcoholic fatty liver diseases in mice. *Life Sci.* 2022;306:120846.

doi: 10.1016/j.lfs.2022.120846

47. Barreyro FJ, Holod S, Finocchietto PV, *et al.* The pan-caspase inhibitor emricasan (IDN-6556) decreases liver injury and fibrosis in a murine model of non-alcoholic steatohepatitis. *Liver Int.* 2015;35(3):953-966.

doi: 10.1111/liv.12570

48. Morán-Salvador E, Titos E, Rius B, *et al.* Cell-specific PPARγ deficiency establishes anti-inflammatory and anti-fibrogenic properties for this nuclear receptor in non-parenchymal liver cells. *J Hepatol.* 2013;59(5):1045-1053.

doi: 10.1016/j.jhep.2013.06.023

49. Zhang X, Fan L, Wu J, *et al.* Macrophage p38α promotes nutritional steatohepatitis through M1 polarization. *J Hepatol.* 2019;71(1):163-174.

doi: 10.1016/j.jhep.2019.03.014

50. Waugh DJJ, Wilson C. The interleukin-8 pathway in cancer. *Clin Cancer Res.* 2008;14(21):6735-6741.

doi: 10.1158/1078-0432.CCR-07-4843

51. Hoffmann E, Dittrich-Breiholz O, Holtmann H, Kracht M. Multiple control of interleukin-8 gene expression. *J Leukoc Biol.* 2002;72(5):847-855.

52. Brat DJ, Bellail AC, Van Meir EG. The role of interleukin-8 and its receptors in gliomagenesis and tumoral angiogenesis. *Neuro Oncol.* 2005;7(2):122-133.

doi: 10.1215/S1152851704001061

53. Stephens M, Von Der Weid PY. Lipopolysaccharides modulate intestinal epithelial permeability and inflammation in a species-specific manner. *Gut Microbes.* 2020;11(3):421-432.

doi: 10.1080/19490976.2019.1629235

54. Zhu Y, Yang S, Zhao N, *et al.* CXCL8 chemokine in ulcerative colitis. *Biomed Pharmacother.* 2021;138:111427.

doi: 10.1016/j.biopha.2021.111427

55. McHenry S, Glover M, Ahmed A, *et al.* NAFLD is associated with quiescent rather than active Crohn's disease. *Inflamm Bowel Dis.* 2023;30(5):757-767.

doi: 10.1093/ibd/izad129

56. Li XP, Yang XY, Biskup E, *et al.* Co-expression of CXCL8 and HIF-1α is associated with metastasis and poor prognosis in hepatocellular carcinoma. *Oncotarget.* 2015;6(26):22880-22889.

doi: 10.18632/oncotarget.4412

57. Stienstra R, Saudale F, Duval C, *et al.* Kupffer cells promote hepatic steatosis via interleukin-1beta-dependent suppression of peroxisome proliferator-activated receptor alpha activity. *Hepatology.* 2010;51(2):511-522.

doi: 10.1002/hep.23337

58. Auguet T, Bertran L, Binetti J, *et al.* Relationship between IL-8 circulating levels and TLR2 hepatic expression in women with morbid obesity and nonalcoholic steatohepatitis. *Int J Mol Sci.* 2020;21(11):4189.

doi: 10.3390/ijms21114189

59. Stratakis N, Golden-Mason L, Margetaki K, *et al.* In utero exposure to mercury is associated with increased susceptibility to liver injury and inflammation in childhood. *Hepatology.* 2021;74(3):1546-1559.

doi: 10.1002/hep.31809

60. Tokunaga R, Zhang W, Naseem M, *et al.* CXCL9, CXCL10, CXCL11/CXCR3 axis for immune activation-A target for novel cancer therapy. *Cancer Treat Rev.* 2018;63:40-47.

doi: 10.1016/j.ctrv.2017.11.007

61. Rotondi M, Chiovato L, Romagnani S, Serio M, Romagnani P. Role of chemokines in endocrine autoimmune diseases. *Endocr Rev.* 2007;28(5):492-520.

doi: 10.1210/er.2006-0044

62. Zhang X, Shen J, Man K, *et al.* CXCL10 plays a key role as an inflammatory mediator and a non-invasive biomarker of non-alcoholic steatohepatitis. *J Hepatol.* 2014;61(6):1365-1375.

doi: 10.1016/j.jhep.2014.07.006

63. Ibrahim SH, Hirsova P, Tomita K, *et al.* Mixed lineage kinase 3 mediates release of C-X-C motif ligand 10-bearing chemotactic extracellular vesicles from lipotoxic hepatocytes. *Hepatology.* 2016;63(3):731-744.

doi: 10.1002/hep.28252

64. Yang Z, Han X, Wang K, Fang J, Wang Z, Liu G. Combined with multiplex and network analysis to reveal the key genes and mechanisms of nonalcoholic fatty liver disease. *Int Immunopharmacol.* 2023;123:110708.

doi: 10.1016/j.intimp.2023

65. Xu Z, Zhang X, Lau J, Yu J. C-X-C motif chemokine 10 in non-alcoholic steatohepatitis: Role as a pro-inflammatory factor and clinical implication. *Expert Rev Mol Med.* 2016;18:e16.

doi: 10.1017/erm.2016.16

66. Dali-Youcef N, Vix M, Costantino F, *et al.* Interleukin-32 contributes to human nonalcoholic fatty liver disease and insulin resistance. *Hepatol Commun.* 2019;3(9):1205-1220.

doi: 10.1002/hep4.1396

67. Chang CC, Wu CL, Su WW, *et al.* Interferon gamma-induced protein 10 is associated with insulin resistance and incident diabetes in patients with nonalcoholic fatty liver disease. *Sci Rep.* 2015;5:10096.

doi: 10.1038/srep10096

68. Tomita K, Freeman BL, Bronk SF, *et al.* CXCL10-mediates macrophage, but not other innate immune cells-associated inflammation in murine nonalcoholic steatohepatitis. *Sci Rep.* 2016;6:28786.

doi: 10.1038/srep28786

69. Maina V, Sutti S, Locatelli I, *et al.* Bias in macrophage activation pattern influences non-alcoholic steatohepatitis (NASH) in mice. *Clin Sci (Lond).* 2012;122(11):545-553.

doi: 10.1042/CS20110366

70. Deiuliis JA, Oghumu S, Duggineni D, *et al.* CXCR3 modulates obesity-induced visceral adipose inflammation and systemic insulin resistance. *Obesity (Silver Spring).* 2014;22(5):1264-1274.

doi: 10.1002/oby.20642

71. Zhou C, Shen Z, Shen B, *et al.* FABP4 in LSECs promotes CXCL10-mediated macrophage recruitment and M1 polarization during NAFLD progression. *Biochim Biophys Acta Mol Basis Dis.* 2023;1869(7):166810.

doi: 10.1016/j.bbadis.2023.166810

72. Zhang X, Wu WK, Xu W, *et al.* C-X-C motif chemokine 10 impairs autophagy and autolysosome formation in non-alcoholic steatohepatitis. *Theranostics.* 2017;7(11):2822-2836.

doi: 10.7150/thno.19068

73. Kawaguchi S, Sakuraba H, Haga T, *et al.* Melanoma differentiation-associated gene 5 positively modulates TNF-α-induced CXCL10 expression in cultured HuH-7 and HLE Cells. *Inflammation.* 2019;42(6):2095-2104.

doi: 10.1007/s10753-019-01073-3

74. Harrison SA, Bedossa P, Guy CD, *et al.* A phase 3, randomized, controlled trial of resmetirom in NASH with liver fibrosis. *N Engl J Med.* 2024;390(6):497-509.

doi: 10.1056/NEJMoa2309000

75. Armstrong MJ, Gaunt P, Aithal GP, *et al.* Liraglutide safety and efficacy in patients with non-alcoholic steatohepatitis (LEAN): a multicentre, double-blind, randomised, placebo-controlled phase 2 study. *Lancet.* 2016;387(10019):679-690.

doi: 10.1016/S0140-6736(15)00803-X

76. Newsome PN, Buchholtz K, Cusi K, *et al.* A placebo-controlled trial of subcutaneous semaglutide in nonalcoholic steatohepatitis. *N Engl J Med.* 2021;384(12):1113-1124.

doi: 10.1056/NEJMoa2028395

77. Loomba R, Sanyal AJ, Kowdley KV, *et al.* Randomized, controlled trial of the FGF21 analogue pegozafermin in NASH. *N Engl J Med.* 2023;389(11):998-1008.

doi: 10.1056/NEJMoa2304286

78. Shih PH, Shiue SJ, Chen CN, *et al.* Fucoidan and fucoxanthin attenuate hepatic steatosis and inflammation of NAFLD through modulation of leptin/adiponectin axis. *Mar Drugs.* 2021;19(3):148.

doi: 10.3390/md19030148

79. Gawrieh S, Noureddin M, Loo N, *et al.* Saroglitazar, a PPAR-α/γ agonist, for treatment of NAFLD: A randomized controlled double-blind phase 2 trial. *Hepatology.* 2021;74(4):1809-1824.

doi: 10.1002/hep.31843

80. Anstee QM, Neuschwander-Tetri BA, Wai-Sun Wong V, *et al.* Cenicriviroc lacked efficacy to treat liver fibrosis in nonalcoholic steatohepatitis: AURORA phase III randomized study. *Clin Gastroenterol Hepatol.* 2024;22(1):124-134.e1.

doi: 10.1016/j.cgh.2023.04.003

81. Gart E, Van Duyvenvoorde W, Caspers MPM, *et al.* Intervention with isoleucine or valine corrects hyperinsulinemia and reduces intrahepatic diacylglycerols, liver steatosis, and inflammation in Ldlr-/-.Leiden mice with manifest obesity-associated NASH. *FASEB J.* 2022;36(8):e22435.

doi: 10.1096/fj.202200111R

82. Yang YM, Fukui M, Wang Z, Miao F, Karriker MJ, Seki E. Interventional potential of recombinant feline hepatocyte growth factor in a mouse model of non-alcoholic steatohepatitis. *Front Endocrinol (Lausanne).* 2018;9:378.

doi: 10.3389/fendo.2018.00378

83. Knudsen C, Neyrinck AM, Leyrolle Q, *et al.* Hepatoprotective effects of indole, a gut microbial metabolite, in leptin-deficient obese mice. *J Nutr.* 2021;151(6):1507-1516.

doi: 10.1093/jn/nxab032

84. Jung JW, Wang F, Turk A, *et al.* Zaluzanin c alleviates inflammation and lipid accumulation in kupffer cells and hepatocytes by regulating mitochondrial ROS. *Molecules.* 2023;28(22):7484.

doi: 10.3390/molecules28227484

85. Tomita K, Kabashima A, Freeman BL, Bronk SF, Hirsova P, Ibrahim SH. Mixed lineage kinase 3 mediates the induction of CXCL10 by a STAT1-dependent mechanism during hepatocyte lipotoxicity. *J Cell Biochem.* 2017;118(10):3249-3259.

doi: 10.1002/jcb.25973

86. Wada N, Takaki A, Ikeda F, *et al.* Serum-inducible protein (IP)-10 is a disease progression-related marker for non-alcoholic fatty liver disease. *Hepatol Int.* 2017;11(1):115-124.

doi: 10.1007/s12072-016-9773-y

87. Konishi H, Shirabe K, Nakagawara H, *et al.* Suppression of silent information regulator 1 activity in noncancerous tissues of hepatocellular carcinoma: Possible association with non-B non-C hepatitis pathogenesis. *Cancer Sci.* 2015;106(5):542-549.

doi: 10.1111/cas.12653

88. Alchera E, Rolla S, Imarisio C, *et al.* Adenosine A2a receptor stimulation blocks development of nonalcoholic steatohepatitis in mice by multilevel inhibition of signals that cause immunolipotoxicity. *Transl Res.* 2017;182:75-87.

doi: 10.1016/j.trsl.2016.11.009

89. Moragrega AB, Gruevska A, Fuster-Martínez I, *et al.* Anti-inflammatory and immunomodulating effects of rilpivirine: Relevance for the therapeutics of chronic liver disease. *Biomed Pharmacother.* 2023;167:115537.

doi: 10.1016/j.biopha.2023.115537

ACCSCIENCE PUBLISHING

Eurasian Journal of Medicine and Oncology

REVIEW ARTICLE

NOTCH3 signalling as a therapeutic nexus: Bridging cerebral small vessel disease and breast cancer pathophysiology

Zaw Myo Hein[1], Nisha Shantakumari[1], Muhammad Danial Che Ramli[2], Usman Jaffer[3], Hafizah Abdul Hamid[4], and Che Mohd Nasril Che Mohd Nassir[5]*

[1]Department of Basic Medical Sciences, College of Medicine, Ajman University, Ajman, United Arab Emirates

[2]Department of Diagnostic and Allied Health Science, Faculty of Health and Life Sciences, Management and Science University, Shah Alam, Selangor, Malaysia

[3]Department of Human Science, Kulliyyah of Islamic Revealed Knowledge and Human Sciences, International Islamic University Malaysia, Kuala Lumpur, Malaysia

[4]Department of Human Anatomy, Faculty of Medicine and Health Sciences, Universiti Putra Malaysia, Serdang, Selangor, Malaysia

[5]Department of Anatomy and Physiology, School of Basic Medical Sciences, Faculty of Medicine, Universiti Sultan Zainal Abidin, Kuala Terengganu, Terengganu, Malaysia

Abstract

The neurogenic locus notch homolog protein 3 (NOTCH3), is central in both vasculogenesis and oncogenesis and, therefore, has been considered an important factor in the development of cerebral small vessel disease (CSVD) and breast cancer (BC). Pathogenic mutations of NOTCH3 induce vascular smooth muscle cell degeneration, microvascular dysfunction and neurovascular damage in cerebral autosomal-dominant arteriopathy with subcortical infarcts and leukoencephalopathy (CADASIL), which is a genetic cause of CSVD. Meanwhile, NOTCH3 aberrant signalling in BC promotes tumour progression, metastasis and chemoresistance, especially in aggressive subtypes, such as triple-negative BC. A growing body of evidence points to a common molecular pathway whereby NOTCH3 dysregulation mediates vascular and tumour pathologies, thus providing an important link between these conditions. This narrative review synthesises current insights into the dual role of NOTCH3, focusing on translational relevance as a therapeutic target. Targeting NOTCH3 may mitigate vascular damage in CSVD and simultaneously inhibit tumour progression and metastasis in BC. The review further discusses NOTCH3 as a biomarker for early diagnosis and risk stratification, besides novel therapeutic strategies involving γ-secretase inhibitors and monoclonal antibodies. Future directions include studies into the ligand-independent functions of NOTCH3, its role within the tumour microenvironment, and the development of therapies with dual-action potential. This review discusses, for the 1st time, common mechanisms between CSVD and BC, thereby opening new avenues for therapies that could effectively target both conditions. By translating these laboratory findings into clinical applications, this approach aims to improve outcomes for patients affected by these devastating disorders.

Keywords: Cerebral small vessel disease; Breast cancer; Neurogenic locus notch homolog protein 3; Cerebral autosomal-dominant arteriopathy with subcortical infarcts and leukoencephalopathy; Tumor

***Corresponding author:**
Che Mohd Nasril Che Mohd Nassir (nassrilnassir@unisza.edu.my)

Citation: Hein ZM, Shantakumari N, Ramli MDC, Jaffer U, Hamid HA, Nassir CMNCM. NOTCH3 signalling as a therapeutic nexus: Bridging cerebral small vessel disease and breast cancer pathophysiology. *Eurasian J Med Oncol.* 2025;9(3):32-51. doi: 10.36922/EJMO025150095

Received: April 8, 2025

Revised: April 24, 2025

Accepted: May 8, 2025

Published online: May 30, 2025

Copyright: © 2025 Author(s). This is an Open-Access article distributed under the terms of the Creative Commons Attribution License, permitting distribution, and reproduction in any medium, provided the original work is properly cited.

Publisher's Note: AccScience Publishing remains neutral with regard to jurisdictional claims in published maps and institutional affiliations.

1. Introduction

Breast cancer (BC) and stroke are two different medical disorders, each with unique pathophysiological causes. Recent discoveries suggest a possible connection between these two unconnected entities,[1,2] identifying the roles of neurogenic locus notch homolog protein 3 (NOTCH3) signalling as important participants in both illnesses.

One member of the NOTCH family that has become important in both oncogenesis and vasculogenesis is NOTCH3. Variations in the *NOTCH3* gene have been linked to several cardio- and cerebral-vascular diseases, such as cerebral small vessel disease (CSVD), which is a precursor to stroke and is characterised by cerebral autosomal-dominant arteriopathy with subcortical infarcts and leukoencephalopathy (CADASIL).[3] The pathological hallmark of CSVD is the accumulation of NOTCH3 extracellular domain within small penetrating arteries, which is noteworthy.[4] Despite CSVD is often silent, many affected individuals remain asymptomatic. Their manifestation is frequently unintentionally detected during normal magnetic resonance imaging (MRI) brain scans, showing distinctive cerebral white matter lesions.[5]

Moreover, pre-clinical studies have revealed that NOTCH3 plays a dual role in BC, contributing to both tumor development and metastatic progression.[6,7] Alarmingly, increased cancer invasiveness, partly mediated by the development of lymphovascular emboli, is associated with elevated NOTCH3 expression in inflammatory BC.[8] These results are further supported by observations that hypercoagulation and vascular impairment related to cancer are associated with a higher risk of stroke and that stroke-related death is more common in BC patients than in non-cancer patients.[9]

Given the ageing global population and the increasing incidence of both CSVD and BC, the clinical overlap between these conditions is of growing interest. CSVD contributes significantly to ischemic stroke, a leading cause of death in cancer patients, and the underlying shared molecular mechanisms involving NOTCH3 signalling may suggest an urgent need for integrative research. Uncovering these connections holds the potential to transform clinical approaches by identifying shared therapeutic targets and improving outcomes in patients at the intersection of these pathologies. The intersection of these research avenues demands a reassessment of the clinical environment, where the symptomatology of BC and CSVD may counterintuitively resemble one another, ultimately predisposing individuals to ischemic stroke.

Thus, the purpose of this narrative review is to compile the body of knowledge clarifying the dynamic interactions among NOTCH3 signaling, CSVD and BC. Across exploring the common mechanical foundations of these illnesses, we hope to uncover new understandings of their relationship. These disclosures could lead to the creation of novel preventive and therapeutic approaches, which would be an example of 'killing two birds with one stone' in the fight against these powerful enemies.

2. BC

BC is an array of distinguished malignancies that occur within the mammary glands.[9] Indications of BC can encompass a breast lump, alterations in breast contour, skin dimpling, nipple discharge, inverted nipple (turns inward), and/or the presence of a red or scaly skin patch.[10,11] In addition, individuals with the disease or tumours that have metastasised to distant sites may experience symptoms such as bone pain, difficulty in breathing, enlarged lymph nodes, and/or jaundice.[12] Factors that increase the risk of developing BC encompass a sedentary lifestyle, obesity, alcohol consumption, early onset of menstruation, ageing, delayed or absent childbearing, hormone replacement therapy during menopause, exposure to ionising radiation, a prior BC diagnosis and a family history of the disease.[13]

2.1. BC epidemiology and present trends

BC is the second most common cause of cancer-related mortality in women globally.[14] The World Health Organization reported that in 2020, BC was diagnosed in 2.3 million women worldwide, resulting in 685,000 fatalities. By the end of 2020, there were 7.8 million women who had received a BC diagnosis within the past 5 years, solidifying its status as the most widespread cancer globally. Moreover, BC affects women of all ages in every country after they reach puberty, with higher incidence rates in later life. Alarmingly, around 0.5 – 1% of BC cases are observed in males.[15]

Moreover, BC has experienced a significant rise in both the number of cases and fatalities in the past 30 years. Between 1990 and 2016, BC cases more than doubled in 60 out of 102 countries, including Afghanistan, Argentina, Brazil and the Philippines. Simultaneously, BC-related deaths also doubled in 43 out of 102 countries, including Libya, Paraguay, Saudi Arabia and Yemen.[16] It has been suggested that according to the projections for the year 2030, there will be approximately 2.7 million new cases of BC diagnosed globally each year, with around 0.87 million annual deaths.[17] Moreover, the incidence of BC in low- and middle-income countries is anticipated to rise even more, primarily because of the increasing adoption of Western lifestyles, which include the previously mentioned risk factors. In addition, improved cancer registration and diagnostic capabilities also contribute to the observed increase in reported cases.[18]

2.2. Genetics of BC: Present updates

While BC research has predominantly focused on understanding the molecular mechanisms behind tumourigenesis, metastatic spread to distant organs following the surgical removal of the primary tumour remains a significant factor contributing to unfavourable outcomes.[19] Hence, it is crucial to gain a deeper comprehension of the molecular mechanism that drives cancer cell seeding and the development of metastases. This knowledge is beneficial for the development of novel therapies specifically targeting breast tumour metastasis-initiating cells, with the goal of halting the advancement of the tumour.

Despite only about 5 – 10% of BC cases having a genetic basis, multiple genetic mutations have been identified as strongly linked to an elevated risk of developing BC. Two prominent genes with a significant penetrance, *BRCA1* (located on chromosome 17) and *BRCA2* (situated on chromosome 13), are primarily associated with an elevated risk of BC development.[20] The mutations in these genes are typically inherited through an autosomal dominant pattern, but sporadic mutations are also frequently documented. Additional BC genes with significant penetrance, such as *TP53*, *CDH1*, *PTEN* and *STK11,* have also been reported.[21-24] In addition to the heightened risk of BC, individuals with these mutations are also at an increased susceptibility to ovarian cancer.

In addition, genetic predisposition plays a critical role in a subset of BC cases, particularly those with early onset or strong family history. While 5 – 10% of BCs are hereditary, several high- and moderate-penetrance genes significantly elevate the associated risk.[20,25] *BRCA1* and *BRCA2* mutations remain the most studied, with high lifetime risks for BC and ovarian cancer. Other key genes, such as *TP53*, *PALB2*, *CHEK2* and *ATM* influence tumour suppression and DNA repair pathways. These mutations typically follow autosomal dominant inheritance patterns. Table 1 summarises the most clinically relevant genes, their functions and associated cancer risks.

In addition to genes related to BC, NOTCH receptors have been reported to be likely to exert distinct regulatory effects on BC cells.[36] Therefore, it is crucial to define the specific functional roles of individual NOTCH receptors in propelling tumour advancement. Later in this narrative review, we provide evidence that the expression of NOTCH3 is associated with the pathogenesis of cancer cell dissemination and the progression of BC metastases. Moreover, there is an increasing body of evidence suggesting that BC can lead to the onset and progression of ischemic stroke, and BC is currently being referred to as a risk factor for stroke and its subtypes. In the next section, we will discuss the precursor for ischemic stroke, CSVD and its relation to BC.

3. CSVD

CSVD is responsible for approximately 25% of ischemic strokes, most intracerebral haemorrhages in individuals over the age of 65, as well as the primary cause of vascular dementia. A recent study also linked CSVD with vascular Parkinsonism.[37] In addition, it is linked to issues with mobility, gait, neurobehavioural functions and mood disorders.[38] The pathophysiological foundation of CSVD encompasses alterations in the structure and function of the microvasculature within the deep subcortical regions. These alterations primarily affect arteries, including tributaries of the middle cerebral artery, and arterioles, resulting in phenomena, such as fibrinolysis, lipohyalinosis, necrosis and microthrombosis.[39,40]

CSVD is a condition that becomes increasingly prevalent with age and is frequently encountered as an incidental discovery during neuroimaging. This condition is frequently underestimated by healthcare professionals because of its covert (silent) nature, as it often presents without symptoms. Clinically, it commonly presents with subtle but progressive symptoms such as forgetfulness, depression, slowed thinking, balance issues, and urinary urgency.[38] Present neuroimaging indicators (or manifestation) of CSVD based on the Standards for Reporting Vascular Changes on Neuroimaging 2 encompass recent small subcortical infarcts, white matter hyperintensities (WMHs) of presumed vascular origin, lacunar infarcts (of presumed vascular origin), enlarged perivascular spaces, cerebral microbleeds, cortical superficial siderosis, brain atrophy and cortical cerebral microinfarcts.[41] Frequent cardio-cerebrovascular risk factors for sporadic CSVD, including ageing, type 2 diabetes, hypertension, smoking and dyslipidaemia, elevate the risk of pathological alterations in arteries and arterioles, potentially resulting in vessel blockage, which in turn leads to the development of arteriosclerosis and arteriolosclerosis.[40]

Several aetiopathogenic classifications have been proposed for CSVD. Nevertheless, the most widely acknowledged categories of CSVD include amyloidal CSVD (e.g., sporadic and hereditary cerebral amyloid angiopathy) and non-amyloid CSVD, which encompasses age-related and small vessel disease related to vascular risk factors (such as arteriolosclerosis and ageing).[42] Meanwhile, the less prevalent categories of CSVD encompass inherited or genetic (monogenic) forms, which exhibit distinct characteristics separate from cerebral amyloid angiopathy. Examples include Fabry's disease and CADASIL, as well

Table 1. Prominent genes linked to an elevated risk of breast cancer incidence

Gene	Chromosome site	Function and degree of penetration	Risk for breast cancer (%)
ATM[26]	11q22.3	• DNA repair and cell cycle regulation • Moderate penetration	20 – 60
BRCA1[27]	17q21.31	• DNA repair and cell cycle regulation • High penetration	45 – 87
BRCA2[28]	13q13.1	• DNA repair and cell cycle regulation • High penetration	50 – 85
BRIP1[29]	17q23.2	• Participation in *BRCA1* function • Moderate penetration	Limited Data
CDH1[30]	16q22.1	• Cell adhesion regulation • Regulate epithelial cell proliferation and mobility • High penetration	63 – 83
CHEK2[31]	22q12.1	• Cell cycle regulation • Moderate penetration	20 – 25
PALB2[32]	16p12.2	• DNA repair • Moderate penetration	33 – 58
PTEN[33]	10q23.31	• Cell cycle regulation • High penetration	50 – 85
STK11[34]	19p13.3	• Cell cycle regulation • Upkeep of energy balance • High penetration	32 – 54
TP53[35]	17p13.1	• DNA repair, cell cycle regulation, triggering apoptosis, promoting senescence and sustaining cellular metabolism are all crucial cellular processes • High penetration	20 – 85

Note: Risk percentages reflect ranges from recent meta-analyses (2020 – 2024).
Abbreviations: ATM: Ataxia telangiectasia mutated; BRCA1: Breast cancer gene 1; BRCA2: Breast cancer gene 2; BRIP1: BRCA1 interacting protein c-terminal helicase 1; CDH1: Cadherin 1; CHEK2: Checkpoint kinase 2; PALB2: Partner and localizer of BRCA2; PTEN: Phosphatase and tensin homolog; STK11: Serine/Threonine kinase 11; TP53: Tumour protein 53.

as inflammatory and immune-mediated CSVD, venous collagenopathies and other forms of CSVD, including non-amyloid microvessel degeneration in Alzheimer's disease and post-radiation angiopathy.[43] Various pathomechanisms and molecular cascades have been proposed for the onset and progression of CSVD, and many of which are interrelated across most, if not all, CSVD categories.[44-50]

4. Putative clinicopathological correlates of BC and CSVD

CSVD is a precursor for ischemic stroke, a complex pathological event leading to sudden neurological damage, with cancer being just one of the numerous associated risk factors. Simultaneously, it seems that the occurrence and frequency of both conditions are rising within the elderly population. Similarly, in cancer patients, cerebrovascular disease emerges as the second most prevalent neurological condition after metastases.[51] However, this connection is frequently overlooked by the clinician. CSVD or even ischemic stroke may manifest at any stage during malignancy and, in some cases, serve as the initial sign of a silent malignancy in up to 3% of patients.[52] In addition, post-mortem examinations of cancer patients show the presence of ischemic stroke in 15% of cases, with half of these cases being silent or asymptomatic.[53] Considering that CSVD could potentially serve as the initial indication of neoplasia, in this case, BC. This necessitates a precise determination of the underlying cause to tailor treatment appropriately and enhance clinical outcomes.[52]

BC and malignancies in general, share numerous risk factors with CSVD. These risk factors are more prevalent among the elderly population, which also tends to have a higher burden of vascular risk factors. Studies have indicated that the prevalence of these vascular risk factors, including diabetes mellitus, obesity, hypertension, hyperlipidemia, smoking, alcoholism, and atrial fibrillation, is comparable between ischemic stroke patients with cancer and stroke patients without cancer.[2,54] Considering both higher pathogenicity and prevalence of vascular risk factors, it comes as no surprise that these factors continue to be the most common cause of ischemic stroke, even among individuals with cancer, specifically BC.[54] Alarmingly, studies have shown

that the conventional ischemic stroke mechanisms, such as cardioembolic and lacunar strokes, are roughly the same among patients with and without cancer.[54] Furthermore, previous studies have indicated that atherosclerosis is the leading cause of ischemic stroke in patients with neoplasia.[1]

The exact mechanisms of CSVD and ischemic stroke in the context of BC remain vague. Given that vascular risk factors are widespread among CSVD and/or ischemic stroke patients, whether both CSVD and BC emerge independently and simultaneously, or if BC directly impacts the pathophysiology of CSVD and/or ischemic stroke, remains uncertain. Interestingly, hypercoagulability has been considered the primary mechanism behind ischemic stroke in individuals with cancer.[55] Tumour cells secrete pro-coagulant molecules, including tissue factors and cancer pro-coagulants, such as cysteine protease, which enhance the coagulation process. Furthermore, they release various cytokines, such as tumour necrosis factor-alpha, and interleukins (ILs), including IL-1 and IL-6.[56] These molecules function as pro-coagulants through three mechanisms: First, by inducing cells to express tissue factors; second, by impeding the activation of Protein C; and finally, by causing shedding of vascular endothelial cells, thereby contributing to increased blood viscosity and clot formation.[54] This constitutes a paraneoplastic phenomenon that remains poorly understood but is associated with reduced survival in affected individuals.[57]

Numerous studies have attempted to employ laboratory markers to assess coagulation abnormalities. D-dimer serves as an indicator of an activated coagulation system, including in patients with CSVD. Cancer patients who experience strokes tend to have elevated D-dimer levels in comparison to stroke patients without cancer.[2,54,57] D-dimer is also an independent predictor for CSVD and strokes caused by non-conventional mechanisms, which are notably linked to cancer in several studies.[58] Moreover, previous studies have reported a greater occurrence of micro-embolisms detected by transcranial Doppler inpatients who experienced strokes due to cancer, especially in cases involving unconventional stroke mechanisms. This correlation was notably significant and aligned with elevated D-dimer levels.[59] Nevertheless, it's important to note that D-dimer is a non-specific marker, as it can become elevated in various situations, even in cancer patients who do not have a stroke.[57] Hence, new and alternative approaches are needed to further strengthen the association between CSVD and/or stroke and cancer, specifically BC in this context.

4.1. Roles of NOTCH3 in BC and CSVD

The *Notch* gene received its initial identification during research on irregular notched-wing *Drosophila melanogaster* in 1914.[60] NOTCH signalling contributes to a range of biological processes in different species, including organ development, tissue maintenance, and tissue regeneration. Consequently, disrupted NOTCH signalling can lead to pathological outcomes. In addition, NOTCH protein and its homologs, including NOTCH1, NOTCH2, NOTCH3, NOTCH4, LIN-12, and glucagon-like peptide 1, have been detected in genomes across all biological kingdoms, signifying the ongoing diversification of the NOTCH family. Their length spans from approximately 110 amino acids in bacteria to about 4,500 amino acids in animals.[61] Members of the NOTCH family have evolutionarily preserved type-1 transmembrane glycoproteins, serving the dual role of acting as transmembrane receptors for ligands and functioning as transcription factors.[62] To date, there are four paralogous NOTCH transmembrane receptors encoded by four distinct genes, namely, NOTCH1 to 4 were found in mammals.

Structurally, the human NOTCH family receptor comprises an extracellular domain (NOTCH extracellular domain, NECD), a transmembrane domain, and an intracellular domain (NOTCH intracellular domain, NICD) (Figure 1).[63] The NECD comprises between 29 and 36 epidermal growth factor-like repeats (EGF-like domains), a number that varies depending on the receptor type, along with a negative regulatory region (NRR). The NRR consists of three cysteine-rich LIN-12/NOTCH repeats (LNRs) and a heterodimerisation domain. Each EGF-like repeat contains six cysteines, resulting in the formation of three disulphide bonds that contribute to the protein's three-dimensional structure.[3] Moreover, a recent study detailed that the NICD is comprised of an RBPJκ-associated molecule (RAM) domain, a domain with seven ankyrin repeats (ANK), nuclear localization sequences (NLS), a transcriptional activation domain (TAD), and a C-terminal Pro-Glu-Ser-Thr (PEST) domain (Figure 1).[64] While NOTCH receptors are largely preserved, they exhibit structural variability, particularly in the number of EGF-like repeats, the presence of the TAD domain, and the length of the segment between the ANK repeats and the C-terminal region.[65]

5. NOTCH3 signalling

The *NOTCH3* gene encodes a receptor of approximately 2321 amino acids, which dictates the fate of vascular smooth muscle cells (VSMCs) within the brain's arterial network.[66] Activation of the NOTCH (in this case NOTCH3) signalling pathway occurs through cellular interactions with a NOTCH ligand. In mammals, there are five NOTCH ligands have been reported, such as delta-like ligands (DLL) 1, 3, and 4 and jagged (JAG) 1, and 2. Before reaching the cell membrane, the intact NOTCH3

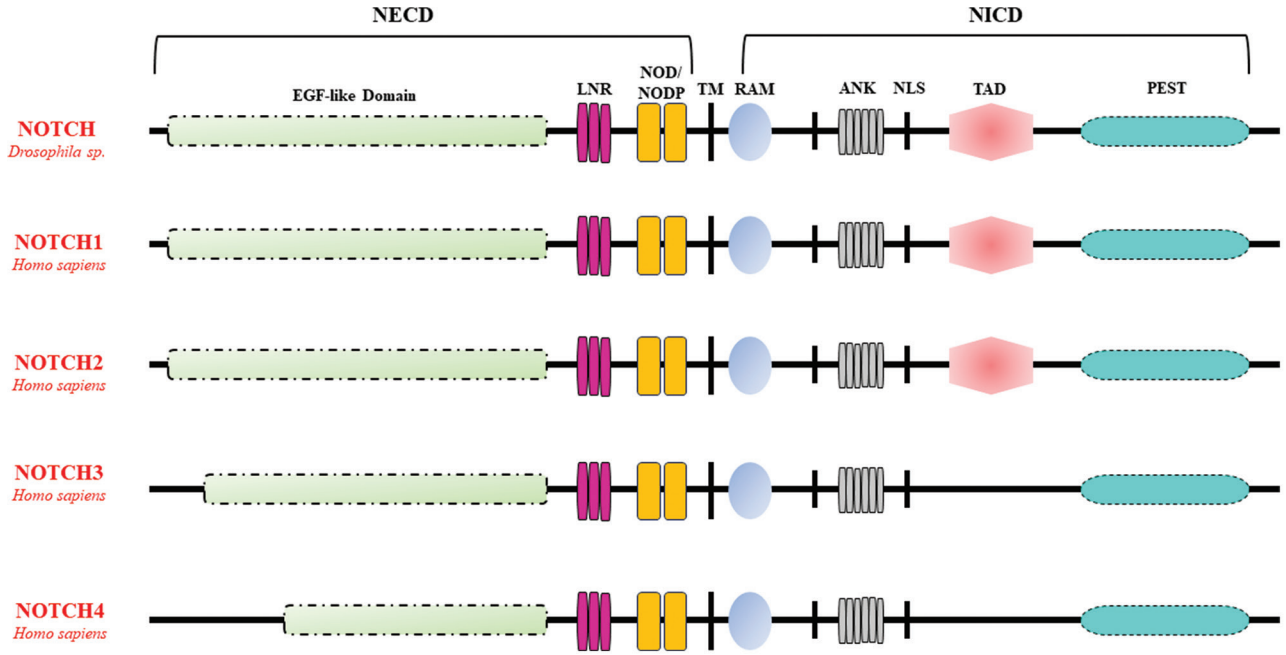


Figure 1. An overview of the structural characteristics of NOTCH family receptors, between *Drosophila melanogaster* and Homo sapiens NOTCH family receptors are depicted with key domains labelled, encompassing the NECD that includes EGF, cysteine-rich LNR repeats and NOTCH domain present in multiple NOTCH proteins (NOD/NODP). NECD was separated from the NICD by the TM. NICD includes RAM domain, ANK, NLS, TAD, and PEST domain. Image created by the authors. Abbreviations: ANK: Ankyrin repeat domain; EGF: Epidermal growth factor; LNR: LIN-12/NOTCH repeat (LNR); NECD: NOTCH extracellular domain; NICD: NOTCH intracellular domain; NLS: Nuclear localization sequences; PEST: Pro-Glu-Ser-Thr; RAM: RBPJκ-associated molecule; TAD: Transcriptional activation domain; TM: Transmembrane domain.

receptor undergoes an initial cleavage, often referred to as S1 cleavage, within the Golgi apparatus. When a NOTCH ligand (JAG or DLL) on the cell membrane of an adjacent signal-sending cell engages with a NOTCH3 receptor on the cell membrane of the signal-receiving cell, it triggers the activation of the NOTCH3 receptor, leading to a subsequent proteolytic cleavage. The processes known as S2 and S3 cleavage are initiated by a disintegrin and metalloprotease domain-containing protein 10 and the γ-secretase complex, respectively, as reported in previous studies.[62,67] Following these cleavages, the NICD is released and translocated into the nucleus, where it forms a complex by binding to the DNA-binding transcription factor CBF-1 (RBPJ)/suppressor of hairless/Lag1 (CSL). This complex then recruits the transcriptional co-activator known as mastermind-like (MAML) protein to stimulate the transcription of downstream target genes. Finally, the NOTCH3 receptor or NICD undergoes degradation in the proteasome or lysosome.[62,67,68]

The existing evidence suggests that the activation of NOTCH3 occurs through the stereotypical ligands containing DSL domains, following the mechanism described above.[69] However, recent findings suggest that NOTCH3 exhibits a significant baseline of ligand-independent signalling, which may be relevant to both its physiological functions and pathological conditions.[70] Although the mechanism remains elusive, it has been reported that the native NRR fold of EGF is comparatively less stable in NOTCH3 than in other studied NOTCH proteins. Whether this ligand-independent process is contingent upon NOTCH3 endocytosis, like the activation mechanisms observed in *Drosophila sp*., remains to be determined. Furthermore, it cannot be ruled out that non-canonical ligands may play a role. For instance, Y-box binding protein 1, a protein related to cold shock domains, has been reported to activate NOTCH3 by binding to EGF-modules 20 – 23, potentially influencing immune and inflammatory responses.[71]

5.1. Roles of NOTCH3 in vasculogenesis

As discussed, NOTCH3 plays a significant part in vascular development, specifically within the lineage responsible for determining the fate of VSMCs. A pre-clinical animal study on post-natal mice lacking NOTCH3 revealed defects in the maturation of smooth muscle cells, arterial differentiation, and morphology when compared to wild-type mice. This resulted in thinner and improperly structured smooth muscle cell layers, which typically

surround arterial vessels.[72] Moreover, *in vitro* studies suggest that the expression of JAG-1 in endothelial cells triggers the activation of NOTCH3 in VSMCs, and this process forms an auto-regulatory loop that sustains the expression of NOTCH3 in VSMCs.[69] In this process, a pivotal downstream effector is the platelet-derived growth factor (PDGF) signalling pathway, and NOTCH3 activation leads to the upregulation of PDGF.[73]

Additional research has demonstrated that NOTCH3 plays earlier roles within the VSMC lineage, although these functions may be concealed by the partial redundancy with other NOTCH homologues. In one animal study on zebrafish, researchers have found that Notch2 and Notch3 cooperate to govern the embryonic production of both mesoderm-derived and neural crest-derived mural cells, which serve as precursors for VSMCs.[74] This was supported by a later study that revealed a comparable redundancy in mice models, as double mutants lacking both NOTCH2 and NOTCH3 are embryonically lethal, and this is associated with a profound reduction in VSMCs and the presence of vascular abnormalities.[75] Nonetheless, additional research employing primary cell cultures has unveiled distinctive roles for NOTCH2 and NOTCH3 within the VSMCs. For example, NOTCH2 exerts an inhibitory effect on VSMC proliferation, whereas NOTCH3 facilitates proliferation and serves as a protective factor against VSMC apoptosis.[76] The functional overlap and interactions between various NOTCH proteins are therefore intricate and greatly context-dependent.

5.2. NOTCH3 and cancer

While the primary role of NOTCH appears to be the regulation of vasculogenesis, where its dysregulation has been associated with various vascular disorders, it can also exhibit tumour-suppressing or oncogenic functions. Numerous studies have demonstrated the common occurrence of aberrantly elevated NOTCH3 expression in human cancer tissues. Table 2 summarises the tumour-suppressive and oncogenic roles of human NOTCH3.

The overexpression of NOTCH3 in cancer tissues is associated with various clinicopathological characteristics, including larger tumour size, advanced tumour-node-metastasis stage, higher pathological grade, tumour metastasis, and an unfavourable prognosis. This is reflected in diminished disease-free survival, progression-free survival, relapse-free survival, and overall survival among cancer patients.[100,101] The predominant cause for NOTCH3 overexpression in cancer is genetic alterations within the *NOTCH3* gene. According to the Cancer Genome Atlas, the *NOTCH3* gene was modified in 5% of cancer samples, primarily through mutations and gene amplification.[102] Moreover, one study reported that mutations in the NRR and PEST domains of the *NOTCH3* gene could lead to NOTCH3 activation, characterised as gain-of-function or activating mutations. These mutations have been observed in human T-ALL.[103]

An important function of NOTCH3 is the preservation of cancer stem cell (CSC) stemness. CSCs, a subset of self-renewing cells possessing strong tumourigenic potential, are known to be stimulated by NOTCH3 signalling in various cancer types, thereby contributing to cancer progression through intricate mechanisms. Another significant aspect of NOTCH3 signalling is its ability to promote resistance to multiple types of chemotherapeutic drugs, such as platinum agents, doxorubicin, epidermal growth factor receptor (EGFR)–tyrosine kinase inhibitors, taxanes, and gemcitabine. It's important to highlight that the support of CSC activity by NOTCH3 is also implicated in the mechanisms of tumour chemo-resistance, angiogenesis, and metastasis.[36,104,105] These underscore the pivotal role of NOTCH3 signalling in cancer.

6. Roles of NOTCH3 in BC

In the context of BC, NOTCH3 typically functions as an oncogene, with a few exceptions. Notably, NOTCH3 has been shown to induce the development of mammary tumours in transgenic mice.[6] Among BC cell lines, NOTCH3 signalling remains persistently active, and when compared to other NOTCH receptors, its activity alone is adequate to drive tumour growth both *in vitro* and *in vivo*.[7] Recently, there has been an acknowledgement of the role of juxtacrine NOTCH signalling between tumour cells and distinct cell types within the tumour microenvironment (TME).[106]

The communication between cancer cells and the TME, which includes both juxtacrine and paracrine signalling, holds significance in the development of novel targeted therapies for BC progression and addressing drug resistance.[107] Certainly, the activation of NOTCH3 in tumour cells stimulates the release of various soluble factors that can exert paracrine effects on cells within the TME.[108] These effects extend to immune and stromal cells, including cancer-associated fibroblasts (CAFs) and endothelial cells. However, it's important to highlight that CAFs can also enhance NOTCH3 signalling and contribute to resistance by secreting multiple pro-inflammatory cytokines and chemokines.[109,110] Indeed, Studebaker *et al.*[111] observed that BC CAFs activate NOTCH3 through the secretion of IL-6.

Apart from that, a previous study by Yamaguchi *et al.*[112] highlighted the significance of NOTCH3 signalling when compared to other NOTCH family members. They revealed that reducing NOTCH3

Table 2. Tumor-suppressive and oncogenic roles of human NOTCH3

Type of cancer	Clinicopathological features
Breast cancer	• In TNBC, NOTCH3 amplifications are more frequently observed than mutations.[77] • In TNBC, mutations have been observed within the PEST domain, which plays a role in negatively regulating gene expression.[78] • NOTCH3 is linked to increased invasiveness and a higher rate of metastasis in breast cancer.[79] • NOTCH3 is connected to the development of chemoresistance.[80] • NOTCH3 can enhance chemo-sensitivity in doxorubicin-resistant breast cancer.[80]
Colorectal cancer	• NOTCH3 is frequently found to be expressed at markedly elevated levels compared to its expression in normal tissue.[81] • NOTCH3 is linked to the invasiveness and metastasis of the tumour.[82] • NOTCH3 is connected to chemo-resistance and leads to poorer clinical outcomes.[83]
Haemangioma	• The expression of NOTCH3 is increased in stem cells of infantile hemangioma.[84]
Hepatocellular carcinoma	• NOTCH3 is linked to the invasiveness and metastasis of the tumour.[85] • NOTCH3 expression is markedly elevated (especially in larger tumours) compared to its expression in normal tissue.[86]
Nasopharyngeal carcinoma	• Knocking down the expression of NOTCH3 in nasopharyngeal carcinoma enhanced the sensitivity to cisplatin chemotherapy.[87]
Non-small cell lung cancer	• 40% of non-small cell lung cancers had NOTCH3 overexpression.[88] • NOTCH3 suppressed apoptosis and reduced cell proliferation.[88] • NOTCH3 is linked to the invasiveness and metastasis of the tumour.[89] • NOTCH3 is connected to radiotherapy resistance, and chemo-resistance and leads to poorer clinical outcomes.[90]
Ovarian cancer	• The expression NOTCH3 is notably elevated in ovarian cancer when compared to normal ovaries or benign ovarian tumours.[91] • The expression of NOTCH3 is linked to a higher tumour grade, lymph node, and distant metastasis, as well as a more advanced clinical stage.[91] • NOTCH3 overexpression is linked to tumour recurrence and a higher mortality rate.[92] • Stimulating the NOTCH3 intracellular domain resulted in the accumulation of p27kip1, causing cancer cells to arrest in the G0/G1 phase of the cell cycle.[93]
Prostatic adenocarcinoma	• The expression of NOTCH3 is positively associated with the Gleason score, and overexpression of NOTCH3 is observed in prostate cancers with a high risk for metastasis.[94,95] • NOTCH3 is connected to chemo-resistance.[95]
Squamous cell cancer	• The expression of NOTCH3 is notably elevated in comparison with normal cells.[96] • NOTCH3 is linked to the aggressiveness of oesophageal squamous cell carcinoma and resistance to 5-fluorouracil chemotherapy.[97]
T-cell acute lymphoblastic leukaemia (T-ALL)	• The activation of NOTCH3 signalling is connected to cancer cell survival and proliferation.[98] • Knockdown of NOTCH3 resulted in reduced MKP-1 levels, ultimately causing decreased tumourigenicity and an increase in apoptosis in T-ALL.[99]

Abbreviations: TNBC: Triple-negative breast cancer; MKP-1: Mitogen-activated protein kinase phosphatase 1; T-ALL: T-cell acute lymphoblastic leukaemia.

expression significantly inhibited growth and stimulated apoptosis in receptor tyrosine-protein kinase (ErbB2)-negative tumour cell lines. Interestingly, this effect was not seen in ErbB2-positive tumour cells. Conversely, silencing NOTCH1 using small interfering (siRNA) did not hinder the proliferation of either ErbB2-positive or ErbB2-negative cell lines. Nonetheless, one study demonstrated that CAFs can produce substantial amounts of the chemokine (C-C motif) ligand 2 (CCL-2).[109] This chemokine, in turn, can regulate the CSC phenotype and influence NOTCH1 expression in BC cells. Similarly, in a xenograft model where fibroblasts and BC cells were co-transplanted into NOD/SCID/IL-2Rg-null mice, the elimination of CCL-2 significantly reduced tumourigenesis and NOTCH1 expression. This suggests that CAFs can engage in crosstalk with cancer cells through a CCL-2/NOTCH1 axis.[113]

In addition, NOTCH3 activation has been observed in a human xenograft model of inflammatory BC through various methods, including real-time quantitative reverse transcription polymerase chain reaction, western blotting, and immunohistochemistry.[114] In triple-negative BC (TNBC), NOTCH3 aberrations, specifically the amplifications of NOTCH3, are more frequently observed compared to mutations. When mutations do occur, they tend to affect the PEST domain, which is generally associated with the negative regulation of gene expression.[77] Moreover, among the TNBC samples, 34% of the tumours tested positive for the NOTCH3 intracellular domain (NICD3), whereas only 4% were positive for the NOTCH1

intracellular domain (NICD1).[7] Nonetheless, the exact role of NOTCH3 in BC remains unclear. A study conducted by Chen *et al.*[93] proposed that the activation of the NICD3 resulted in the accumulation of p27kip1, leading to the arrest of cancer cell cycles in the G0/G1 phase.

Another extensively recognised immune component of BC is the presence of tumour-associated macrophages (TAMs). One study indicated that the JAG-mediated NOTCH signalling in BC has been linked to the differentiation of macrophages into TAMs within the TME in luminal BC patient samples.[115] When tumour cells and TAMs are co-cultured, it leads to the differentiation of macrophages into a predominant M2-type phenotype. While TAMs can exhibit both inflammatory and immunosuppressive behaviours, in BC patient samples they are primarily linked to the immunosuppressive M2 subtype. This association is largely due to the elevated secretion of macrophage colony-stimulating factors by tumour cells, which directs macrophages toward the M2 phenotype.[116] On the other hand, in the basal subtype of BC, NOTCH3 signalling through JAG-1 in tumour cells triggers the release of crucial macrophage-activating cytokines, including IL-β and CCL-2. These cytokines facilitate the recruitment of M2-type macrophages, which subsequently secrete transforming growth factor-β (TGF-β), thus activating TGF-β signalling within the tumour cells.[108] The interplay between tumour cells and TAMs mediated by NOTCH3 signalling could also be of significance in the development of drug resistance, although additional investigation is needed.[108]

The involvement of NOTCH3 in the epidermal-to-mesenchymal transition (EMT) in BC remains a topic of debate. Some researchers have indicated that NOTCH3 encourages tumour aggressiveness by instigating EMT, while others have shown evidence that NOTCH3 inhibits EMT, for instance, by upregulating the Hippo/Yap pathway.[7] It has been reported that EMT inhibition can also occur through the reduction of Fos-related antigen 1 (Fra1), an activator of the EMT process. This observation was made in human BC cells that developed resistance to Adriamycin, where Fra1 was expressed at elevated levels whilst NOTCH3 was downregulated.[80] Conversely, within metastatic BC cells, a reduction in NOTCH3 levels resulted in reduced levels of EMT-associated proteins, such as vimentin, fibronectin and Snail.

Previous study on animal models of allergic airway inflammation have shown that regulatory T-cells (Tregs), another prominent immune component associated with immune suppression, are elevated by both JAG-1 and JAG-2 through the involvement of mesenchymal stem cells.[117] Both JAG-1 and JAG-2 exhibit elevated expression levels in TNBC.[118] Given that Tregs play a role in evading immune surveillance and are associated with increased tumour invasiveness and unfavourable prognoses, the disruption of Tregs' function mediated by NOTCH3 signalling could significantly impact on BC therapy. Nonetheless, no study has directly examined NOTCH3 signalling within Tregs in the context of BC. Therefore, it is imperative to gain a better understanding of how different NOTCH3 ligands and receptors regulate the recruitment of Tregs. Intriguingly, NOTCH3 signalling can also hinder the function of Tregs, potentially diminishing their capacity for immunosuppression.[119]

6.1. NOTCH3 and BC metastasis and chemo-sensitivity

In terms of BC metastasis, NOTCH3 expression is notably higher in invasive cancer when compared to ductal carcinoma *in situ*.[78] In addition, the truncated isoform of the Fms-related receptor tyrosine kinase 1 has been linked to enhanced BC invasiveness and was found to be upregulated by NOTCH3.[120] Lymphovascular emboli in human inflammatory BC have shown elevated levels of NOTCH3 expression. When normal breast epithelial cells were transfected with NICD3, spheroid formation was observed, a phenomenon that was not seen after NICD1 transfection.[8] An exclusive elevation in NOTCH3 expression was also observed in human BC cell lines following exposure to TGF-β1 released by bone marrow osteoblasts. The formation of cancer cell colonies was impeded upon treatment with an anti-TGF-β1 antibody and chemical inhibition of NOTCH3. Furthermore, the expression of NOTCH3 was linked to the presence of osteolytic bone lesions.[121]

Another mechanism by which NOTCH3 can enhance the aggressiveness of BC is through its role in cellular metabolism. NOTCH3 activity is crucial for the survival of metastatic BC cells resistant to hormone therapy. Furthermore, it has been demonstrated to boost mitochondrial activity and facilitate the transition out of metabolic dormancy. In tamoxifen-resistant cells, mitochondrial DNA copy number, mitochondrial antigen expression, and oxidative phosphorylation were all reduced. The decline in mitochondrial activity was reversed through IL-6 treatment, which was orchestrated by NOTCH3.[79] The critical function of NOTCH3 in reversing the mitochondrial damage induced by tamoxifen was substantiated when IL-6 treatment proved ineffective in enhancing mitochondrial activity in cells with suppressed NOTCH3.[79] Multiple studies have supported that in metastatic BC, the presence of functional NOTCH3 is indispensable for IL-6 to sustain elevated levels of carbonic anhydrase, an enzyme linked to survival in hypoxic conditions and increased invasiveness in cancer.[122]

NOTCH3 can enhance chemo-sensitivity in doxorubicin-resistant BC by negatively regulating Fra1, a critical factor in the EMT of BC cell lines.[80,123] In doxorubicin-resistant BC cells, Fra1 was notably over-expressed while NOTCH3 was under-expressed. This resistance was attributed to the EMT induced by Fra1. It was possible to induce Adriamycin chemo-resistance in initially chemo-sensitive cells by suppressing NOTCH3 signalling.[80] Apart from that, the stromal cells can also further enhance chemo-resistance by stimulating the expression of NOTCH3 in BC cells, an effect that can be counteracted with NOTCH3 siRNA or a γ-secretase inhibitor (GSI).[110] Another mechanism by which cancer cells resist treatment is through a state of tumour dormancy. Activation of the NOTCH3 pathway induces cell cycle arrest at the G0/G1 phase and promotes the expression of DNp63a, Mix1 and Hes1 proteins, which encourage cellular quiescence.[124]

Given the constrained effectiveness of immunotherapy directed solely at tumour cells in BC, it becomes crucial to comprehend the regulatory function of NOTCH3 signalling in the interactions between cancer cells and immune cells within the TME across various subtypes of BC. This understanding can facilitate the identification of more effective drug targets involving NOTCH3 signalling and immune cells.

7. NOTCH3 and the brain

A previous study reported that adult mice with NOTCH3 deficiency exhibit ongoing progressive symptoms in the vasculature of the brain and retina, stemming from VSMC degeneration and loss through apoptosis.[125] This leads to a breakdown in vessel integrity, causing haemorrhaging and impairing the functionality of the blood–brain barrier (BBB). Furthermore, the expression of NOTCH3 in VSMCs contributes to the regulation of vascular tone and flow-mediated dilation in both cerebral and tail resistance arteries in mice.[125] Moreover, the functions of NOTCH3 may extend beyond vascular roles, whereby recent research has reported its involvement in neuronal stem cells and neuronal differentiation.[126]

The subependymal zone serves as a crucial stem cell niche within the adult mammalian brain, housing both active and dormant stem cell populations. There is a distinct functional difference between NOTCH1 and NOTCH3 in the regulation of these populations. In mouse model studies, NOTCH1 is expressed in active stem cells, stimulating their proliferation. On the other hand, NOTCH3 is primarily expressed in quiescent stem cells, and its role is essential for maintaining these cells by inhibiting their proliferation.[127] Apart from that, NOTCH3 participates in the regulation of satellite cells, which are stem cells responsible for the repair of skeletal muscle. A recent study demonstrated that mice lacking NOTCH3 exhibited significantly greater muscle growth than their wild-type counterparts following repeated injuries, which was attributed to the increased proliferation of activated satellite cells.[128] In contrast, NOTCH1 has been associated with promoting satellite cell activation and proliferation.[129]

7.1. *NOTCH3* gene aberration and risk for ischemic stroke

The exact pathophysiological mechanisms responsible for ischemic stroke and its various subtypes remain incompletely understood. A combination of genetic and environmental factors probably contributes to the onset and progression of the condition.[130] The *NOTCH3* gene is in the 19p13.12 region, spanning from 15,159,633 base pairs to 15,200,981 base pairs. It comprises 33 exons and 32 introns and encodes a protein consisting of 2,321 amino acids, which plays a critical role in neuronal development.[131] The *NOTCH3* gene variants, rs1044009 (g.45022C > T, c.6668C > T, p. Ala2223Val), and rs3815188 (g.13568C > T, c.303C > T, p. Thr101=), correspond to a missense mutation and a synonymous variant, respectively. Both polymorphisms are situated within the intracellular DUF3454 domain of the protein, and they have a direct impact on the signal transduction activity of NOTCH3. However, *NOTCH3* rs1043994 (g.13949A > G, c.606A > G, p. Ala202=) is a benign point mutation or synonymous variant situated in the conserved protein family of the calcium-binding endothelial growth factor (EGF)-like domain within the NOTCH3 protein.[132]

Certain mutations in the *NOTCH3* gene have been documented as a direct cause of CADASIL, an autosomal dominant disorder affecting cerebral small penetrating vessels. It presents typical clinical symptoms such as migraine with aura, recurrent ischemic strokes in early to middle adulthood, apathy, neuropsychological symptoms and cognitive impairment that advances to dementia.[132] The details on *NOTCH3* gene aberration and its roles in ischemic strokes and CSVD will be discussed in the later section.

7.2. NOTCH3 and inherited cause of CSVD

However, as far back as the 1970s, literature documented families who, despite lacking typical vascular risk factors, exhibited a heightened susceptibility to CSVD. Studies reported cases of families in which multiple-infarct dementia afflicted individuals in a manner consistent with autosomal-dominant inheritance.[133,134] The prevalence of deep white-matter lesions in these individuals indicated that they were likely influenced by a genetic factor causing

severe CSVD. Indeed, examinations of tissues samples from members of these families revealed distinct brain pathology, characterised by degenerative alterations in the walls of cerebral arteries.[135] Therefore, it became evident that while most cases of CSVD are sporadic or involve multiple genes, a certain portion is probably attributed to monogenic genetic variations.

Subsequently, an acronym was coined for the most prevalent monogenic autosomal-dominant form of CSVD, which is CADASIL. An analysis of numerous extensive and well-documented CADASIL families established a genetic linkage to a single disease locus on chromosome 19q12.[136] The defining pathological feature of CADASIL is the existence of granular osmophilic material (GOM) within the basement membrane of VSMCs. Common clinical manifestations in CADASIL patients encompass migraine with aura, transient ischemic attacks or ischemic strokes, intracranial haemorrhage, cognitive deficits, and psychiatric disturbances. Patients may exhibit one or more of these symptoms. Neuroimaging, typically MRI, frequently reveals WMHs, lacune infarcts and cerebral microbleeds.[137] Anomalies in periventricular regions appear as initial findings on fluid-attenuated inversion recovery and T2-weighted imaging. Over time, these anomalies spread symmetrically to affect other regions, including distinctive areas, such as the anterior temporal pole and the external capsule.[138]

The *NOTCH3* gene encodes a single-pass transmembrane NOTCH3 receptor. It has been pinpointed as the causative gene for CADASIL.[139] Exons 2 – 24 of the *NOTCH3* gene encode 34 epidermal growth factor-like repeats (EGFRs) within the extracellular domain of the NOTCH3 protein.[140] Each EGFR contains six cysteine residues that form three disulphide bonds, contributing to the receptor's structural stability. However, mutations that alter in the number of cysteine residues, changing from an even to an odd number, result in a structural change in the extracellular domain of the NOTCH3 receptor. This structural change leads to misfolding and the aggregation of the extracellular domain. Consequently, this misfolding and aggregation can give rise to the formation of GOM deposits, which are a distinctive characteristic of CADASIL. Furthermore, this process can also lead to the deterioration of VSMCs.[141]

CADASIL is a rare condition, and its estimated occurrence in the general population ranges from 1.98 to 4.6 cases/100,000.[142] Nonetheless, recent research indicates that *NOTCH3* gene mutations, which alter cysteine, are considerably more common than previously documented.[142] As an illustration, utilising exome databases that are publicly accessible, recent investigations have approximated the prevalence of *NOTCH3* gene mutations that modify cysteine to be between 2.2 and 3.4 cases/1000 individuals. This prevalence is nearly 100 times higher than the earlier estimates available for CADASIL.[143] The evident disparity in the estimates of disease and mutation occurrence lacks a comprehensive understanding but probably stems from variations in the extent of penetrance or the severity linked to these genetic mutations. This explanation aligns with evidence suggesting that not all individuals carrying *NOTCH3* gene mutations, whether altering cysteine or sparing cysteine, or those with legitimate NOTCH3 loss-of-function mutations, exhibit symptoms.[143] Hence, some individuals can be asymptomatic, which reflects the typical nature of CSVD.

7.3. Impact of aberrant NOTCH3 signalling in CADASIL and NOTCH3-related CSVD

The pathophysiological mechanisms underlying CADASIL involve NOTCH3 receptor activation by its ligands, leading to proteolytic cleavages and release of the NICD. The NICD then translocate to the nucleus, where it influences gene transcription and cellular processes. However, in CADASIL, the aberrant receptor structure disrupts this signalling cascade, promoting VSMC apoptosis and impairing vascular function.[144]

Moreover, recent findings highlight a significant baseline of ligand-independent NOTCH3 signalling, which could be relevant in both normal and pathological contexts.[145] This signalling variability underscores the complexity of NOTCH3-related diseases and suggests potential targets for therapeutic intervention. Understanding the precise molecular mechanisms and cellular effects of NOTCH3 mutations is essential for developing targeted treatments for CADASIL and NOTCH3-related CSVD.

In conclusion, aberrant NOTCH3 signalling plays a critical role in the pathogenesis of CADASIL and NOTCH3-related CSVD. Advances in genetic and molecular research continue to unravel the complexities of this signalling pathway, offering hope for novel therapeutic strategies aimed at mitigating the clinical burden of these debilitating conditions.

8. NOTCH3 as a potential link between the BC and CSVD

The interplay between BC and CSVD through aberrant NOTCH3 signalling presents a compelling narrative that underscores the intricate pathophysiological mechanisms linking these two seemingly distinct conditions. This manuscript has delineated the critical role of NOTCH3 in both oncogenesis and vasculogenesis, particularly highlighting its involvement in CADASIL and BC

metastasis. Figure 2 summarises the roles of NOTCH3 as a potential molecular link between BC and CSVD (i.e., CADASIL).

Recent experimental studies have further elucidated the dual role of NOTCH3 signalling in both cerebrovascular and oncogenic contexts. In CSVD, particularly in CADASIL models, aberrant NOTCH3 activity has been shown to induce VSMC degeneration, arterial wall remodelling deficits, and compromised BBB integrity through increased apoptotic signalling pathways.[72,125] These pathophysiological processes contribute to the hallmark features of CSVD, including WMHs and microvascular ischemia.

Moreover, mutations in the *NOTCH3* gene lead to the misfolding and aggregation of the receptor, resulting

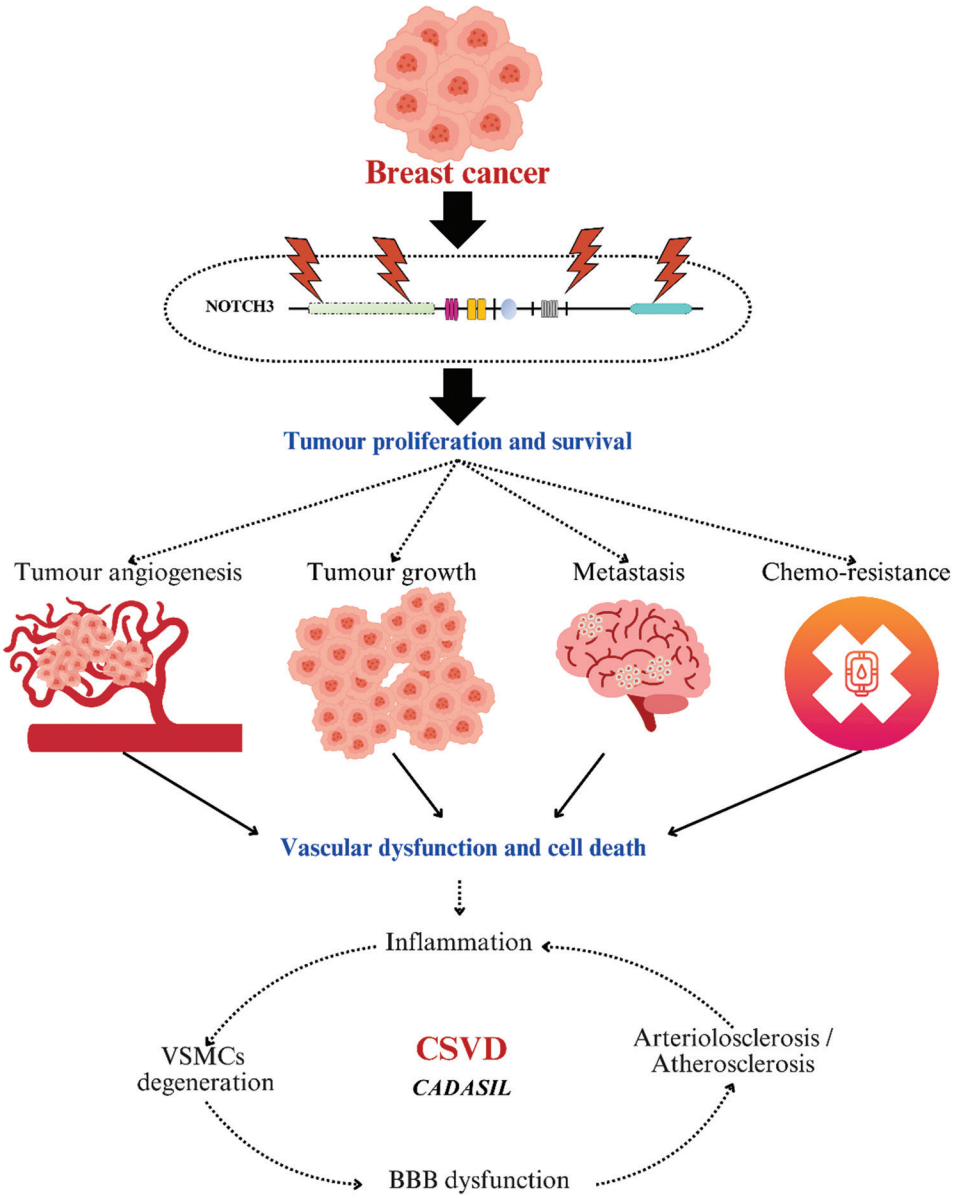


Figure 2. Schematic illustration of the central role of NOTCH3 in linking BC and CSVD. In BC, NOTCH3 activation promotes tumor growth, metastasis, and chemo-resistance, as depicted by tumor cells, the microenvironment, and blood vessels. In CSVD, *NOTCH3* gene mutations lead to VSMC degeneration, endothelial dysfunction, and ischemic stroke. A potential targeted therapy against NOTCH3 aberration may serve as a dual strategy to potentially mitigate tumor progression in BC and prevent vascular damage in CSVD. Image created by the authors. Abbreviations: BC: Breast cancer; CSVD: Cerebral small vessel disease; VSMC: Vascular smooth muscle cell; BBB: Blood–brain barrier; CADASIL: Cerebral autosomal-dominant arteriopathy with subcortical infarcts and leukoencephalopathy.

in the degeneration of VSMCs and the formation of GOM, a hallmark of CADASIL. These pathophysiological changes disrupt vascular integrity, contributing to the clinical manifestations of CADASIL, including migraines, recurrent strokes, cognitive decline and psychiatric disturbances.

In BC, NOTCH3 signalling has been implicated in tumour growth, metastasis and chemo-resistance. Notably, studies have demonstrated that IL-6-induced NOTCH3 activation promotes mitochondrial recovery in tamoxifen-resistant BC cells, enabling the transition out of metabolic dormancy and enhancing survival under hypoxic stress.[79] Elevated NOTCH3 expression has been associated with increased invasiveness and higher metastatic potential, particularly in TNBC.[77] Furthermore, NOTCH3 plays a critical role in maintaining CSC properties, facilitating EMT, and remodelling the TME through its interaction with TAMs and cytokines such as IL-6 and TGF-β.[108,115] The convergence of these pathomechanisms suggests a shared pathway that may underline both CSVD and BC. This dual role of NOTCH3 in vascular and oncogenic processes opens new avenues for therapeutic interventions targeting this signalling pathway. By inhibiting aberrant NOTCH3 activity, it may be possible to mitigate the vascular damage seen in CADASIL and suppress tumour progression and metastasis in BC.

Future research should prioritise elucidating the molecular mechanisms of ligand-independent NOTCH3 signalling, which remains poorly understood but is increasingly recognised as relevant in both normal physiology and disease states. Studies investigating the structural instability of NOTCH3's NRR and its role in spontaneous receptor activation could uncover novel regulatory checkpoints. Furthermore, the role of NOTCH3 within the TME, particularly its crosstalk with CAFs, TAMs and Tregs, warrants further exploration to identify immunomodulatory functions that contribute to tumour aggressiveness and resistance.

Therapeutically, targeting NOTCH3 offers a promising dual-action approach. Strategies under development include GSIs, which block NOTCH receptor cleavage and downstream signalling,[146] monoclonal antibodies specific to NOTCH3 or its ligands, such as DLL4 and JAG1, and selective NOTCH3 inhibitors. These agents may be used alone or in combination with conventional therapies to address vascular degeneration in CSVD and metastatic progression in BC. Pre-clinical models and early-phase trials should focus on optimising dosage, minimising off-target effects, and assessing tissue-specific responses. Ultimately, advancing these research directions could lead to integrated therapeutic strategies that transcend traditional disease boundaries and significantly improve outcomes for patients affected by both CSVD and BC. Despite the promising role of NOTCH3 as a therapeutic target, several challenges must be addressed to enable clinical translation. One major concern is the off-target effects, particularly when using non-selective agents, such as GSIs, which affect multiple NOTCH receptors and may lead to gastrointestinal and immunological side effects.[147] Furthermore, tissue-specific variability in NOTCH3 expression complicates the prediction of therapeutic responses and raises the risk of unintended impacts on normal vascular or immune function. Ensuring selectivity and safety in targeting NOTCH3, especially in the context of long-term treatment, is critical and warrants the development of more refined, receptor-specific strategies and delivery systems. In summary, the exploration of NOTCH3 signalling as a common link between CADASIL and BC underscores the importance of integrated research approaches that consider the multifaceted roles of key molecular players in disease pathogenesis. This comprehensive understanding could lead to innovative strategies for prevention, diagnosis, and treatment, ultimately benefiting patients affected by these debilitating conditions.

9. Conclusion

The intricate role of NOTCH3 in both CSVD and BC underscores its significance as a shared molecular driver of vascular degeneration and tumour progression. This review highlights how aberrant NOTCH3 signalling contributes to VSMC dysfunction and white matter damage in CSVD, while simultaneously promoting proliferation, chemo-resistance, and immune evasion in BC. These insights position NOTCH3 as a promising dual-purpose therapeutic target with potential benefits across neurovascular and oncologic domains. However, this synthesis also reveals several limitations and gaps in present knowledge. Notably, direct mechanistic studies that experimentally link NOTCH3 signalling between CSVD and BC are limited. The biological relevance of ligand-independent NOTCH3 activation remains incompletely understood, as does the precise role of NOTCH3 in mediating immune-tumour interactions. Furthermore, while pre-clinical models suggest promising avenues for targeted therapies, the clinical translation of NOTCH3 inhibitors requires caution due to potential off-target effects and tissue-specific variability. In conclusion, the convergence of NOTCH3 signalling in CSVD and BC represents both a scientific opportunity and a clinical challenge. Future studies should prioritise mechanistic elucidation, therapeutic refinement and cross-disciplinary collaboration to fully unlock the translational potential of targeting this signalling axis.

Acknowledgments

We would like to acknowledge Ajman University for the financial support.

Funding

Financial support for the article processing charge was provided by Ajman University, UAE.

Conflict of interest

The authors declare they have no competing interests

Author contributions

Conceptualization: Che Mohd Nasril Che Mohd Nassir
Formal analysis: Che Mohd Nasril Che Mohd Nassir
Investigation: Zaw Myo Hein, Che Mohd Nasril Che Mohd Nassir
Methodology: Che Mohd Nasril Che Mohd Nassir
Writing – original draft: Che Mohd Nasril Che Mohd Nassir
Writing – review & editing: All authors

Ethics approval and consent to participate

Not applicable.

Consent for publication

Not applicable.

Availability of data

Not applicable.

References

1. Kim K, Lee JH. Risk factors and biomarkers of ischemic stroke in cancer patients. *J Stroke*. 2014;16(2):91-96.

   doi: 10.5853/jos.2014.16.2.91

2. Quintas S, Rogado J, Gullón P, *et al*. Predictors of unknown cancer in patients with ischemic stroke. *J Neurooncol*. 2018;137(3):551-557.

   doi: 10.1007/s11060-017-2741-0

3. Muiño E, Gallego-Fabrega C, Cullell N, *et al*. Systematic review of cysteine-sparing NOTCH3 missense mutations in patients with clinical suspicion of CADASIL. *Int J Mol Sci*. 2017;18:1964.

   doi: 10.3390/ijms18091964

4. Dupré N, Drieu A, Joutel A. Pathophysiology of cerebral small vessel disease: A journey through recent discoveries. *J Clin Invest*. 2024;134(10):e172841.

   doi: 10.1172/JCI172841

5. Che Mohd Nassir CMN, Mohamad Ghazali M, Ahmad Safri A, *et al*. Elevated circulating microparticle subpopulations in incidental cerebral white matter hyperintensities: A multimodal study. *Brain Sci*. 2021;11:133.

   doi: 10.3390/brainsci11020133

6. Hu C, Dievart A, Lupien M, Calvo E, Tremblay G, Jolicoeur P. Overexpression of activated murine Notch1 and Notch3 in transgenic mice blocks mammary gland development and induces mammary tumors. *Am J Pathol*. 2006;168:973-990.

   doi: 10.2353/ajpath.2006.050416

7. Choy L, Hagenbeek TJ, Solon M, *et al*. Constitutive NOTCH3 signalling promotes the growth of basal breast cancers. *Cancer Res*. 2017;77(6):1439-1452.

   doi: 10.1158/0008-5472.CAN-16-1022

8. Xiao Y, Ye Y, Zou X, *et al*. The lymphovascular embolus of inflammatory breast cancer exhibits a Notch 3 addiction. *Oncogene*. 2011;30(3):287-300.

   doi: 10.1038/onc.2010.405

9. Feng Y, Spezia M, Huang S, *et al*. Breast cancer development and progression: Risk factors, cancer stem cells, signalling pathways, genomics, and molecular pathogenesis. *Genes Dis*. 2018;5(2):77-106.

   doi: 10.1016/j.gendis.2018.05.001

10. Henry NL, Shah PD, Haider I, Freer PE, Jagsi R, Sabel MS. Cancer of the breast. In: Niederhuber JE, Armitage JO, Doroshow JH, Kastan MB, Tepper JE, editors. *Abeloff's Clinical Oncology*. 6th ed. Philadelphia, PA: Elsevier; 2020.

11. Jagsi R, King TA, Lehman C, Morrow M, Harris JR, Burstein HJ. Malignant tumors of the breast. In: DeVita VT, Lawrence TS, Rosenberg SA, editors. *DeVita, Hellman, and Rosenberg's Cancer: Principles and Practice of Oncology*. 11th ed. Philadelphia, PA: Lippincott Williams & Wilkins; 2019.

12. Saunders C, Jassal S. *Breast Cancer*. 1st ed., Ch. 13. Oxford: Oxford University Press; 2009.

13. Fakhri N, Chad MA, Lahkim M, *et al*. Risk factors for breast cancer in women: An update review. *Med Oncol*. 2022;39(12):197.

   doi: 10.1007/s12032-022-01804-x

14. Torre LA, Siegel RL, Ward EM, Jemal A. Global cancer incidence and mortality rates and trends-an update. *Cancer Epidemiol Biomark Prev*. 2016;25(1):16-27.

   doi: 10.1158/1055-9965.EPI-15-0578

15. *World Health Organization (WHO). Breast Cancer*; 2023. Available from: https://www.who.int/news-room/fact-sheets/detail/breast-cancer [Last accessed on 2025 May 19.

16. Sharma R. Breast cancer incidence, mortality and mortality-to-incidence ratio (MIR) are associated with human development, 1990-2016: Evidence from Global Burden of Disease Study 2016. *Breast Cancer*. 2019;26:428-445.

doi: 10.1007/s12282-018-00941-4

17. Ferlay J, Laversanne M, Ervik M, *et al*. *Global Cancer Observatory: Cancer Tomorrow*. Lyon, France: International Agency for Research on Cancer; 2020. Available from: https://gco.iarc.fr/tomorrow [Last accessed on 2024 Dec 01].
18. Porter P. Westernizing women's risks? Breast cancer in lower-income countries. *N Engl J Med*. 2008;358:213-216.

    doi: 10.1056/NEJMp0708307
19. McKee MJ, Keith K, Deal AM, *et al*. A multidisciplinary breast cancer brain metastases clinic: The University of North Carolina experience. *Oncologist*. 2016;21(1):16-20.

    doi: 10.1634/theoncologist.2015-0328
20. Shiovitz S, Korde LA. Genetics of breast cancer: A topic in evolution. *Ann Oncol*. 2015;26:1291-1299.

    doi: 10.1093/annonc/mdv022
21. Shahbandi A, Nguyen HD, Jackson JG. TP53 mutations and outcomes in breast cancer: Reading beyond the headlines. *Trends Cancer*. 2020;6:98-110.

    doi: 10.1016/j.trecan.2020.01.007
22. Corso G, Veronesi P, Sacchini V, Galimberti V. Prognosis and outcome in CDH1-mutant lobular breast cancer. *Eur J Cancer Prev*. 2018;27(3):237-238.

    doi: 10.1097/CEJ.0000000000000405
23. Kechagioglou P, Papi RM, Provatopoulou X, *et al*. Tumor suppressor PTEN in breast cancer: Heterozygosity, mutations and protein expression. *Anticancer Res*. 2014;34(3):1387-1400.
24. Chen J, Lindblom A. Germline mutation screening of the STK11/LKB1 gene in familial breast cancer with LOH on 19p. *Clin Genet*. 2000;57(5):394-397.

    doi: 10.1034/j.1399-0004.2000.570511.x
25. Rahman N, Seal S, Thompson D, *et al*. PALB2, which encodes a BRCA2-interacting protein, is a breast cancer susceptibility gene. *Nat Genet*. 2007;39(2):165-167.

    doi: 10.1038/ng1959
26. Stucci LS, Internò V, Tucci M, *et al*. The ATM gene in breast cancer: Its relevance in clinical practice. *Genes (Basel)*. 2021;12(5):727.

    doi: 10.3390/genes12050727
27. Gorodetska I, Kozeretska I, Dubrovska A. BRCA genes: The role in genome stability, cancer stemness and therapy resistance. *J Cancer*. 2019;10(9):2109-2127.

    doi: 10.7150/jca.30410
28. Qu Y, Qin S, Yang Z, *et al*. Targeting the DNA repair pathway for breast cancer therapy: Beyond the molecular subtypes. *Biomed Pharmacother*. 2023;169:115877.

    doi: 10.1016/j.biopha.2023.115877
29. Khan U, Khan MS. Prognostic value estimation of BRIP1 in breast cancer by exploiting transcriptomics data through bioinformatics approaches. *Bioinform Biol Insights*. 2021;15:11779322211055892.

    doi: 10.1177/11779322211055892
30. Gamble LA, McClelland PH, Teke ME, *et al*. Defining features of hereditary lobular breast cancer due to CDH1 with magnetic resonance imaging and tumor characteristics. *NPJ Breast Cancer*. 2023;9(1):77.

    doi: 10.1038/s41523-023-00585-4
31. Rainville I, Hatcher S, Rosenthal E, *et al*. High risk of breast cancer in women with biallelic pathogenic variants in CHEK2. *Breast Cancer Res Treat*. 2020;180(2):503-509.

    doi: 10.1007/s10549-020-05543-3
32. Hu ZY, Liu L, Xie N, *et al*. Germline PALB2 mutations in cancers and its distinction from somatic PALB2 mutations in breast cancers. *Front Genet*. 2020;11:829.

    doi: 10.3389/fgene.2020.00829
33. Fusco N, Sajjadi E, Venetis K, *et al*. PTEN alterations and their role in cancer management: Are we making headway on precision medicine? *Genes (Basel)*. 2020;11(7):719.

    doi: 10.3390/genes11070719
34. Angeli D, Salvi S, Tedaldi G. Genetic predisposition to breast and ovarian cancers: How many and which genes to test? *Int J Mol Sci*. 2020;21(3):1128.

    doi: 10.3390/ijms21031128
35. Børresen-Dale AL. TP53 and breast cancer. *Hum Mutat*. 2003;21:292-300.

    doi: 10.1002/humu.10174
36. Leontovich AA, Jalalirad M, Salisbury JL, *et al*. NOTCH3 expression is linked to breast cancer seeding and distant metastasis. *Breast Cancer Res*. 2018;20(1):105.

    doi: 10.1186/s13058-018-1020-0
37. Che Mohd Nassir CMN, Damodaran T, Yusof SR, *et al*. Aberrant neurogliovascular unit dynamics in cerebral small vessel disease: A rheological clue to vascular parkinsonism. *Pharmaceutics*. 2021;13(8):1207.

    doi: 10.3390/pharmaceutics13081207
38. Wardlaw JM, Smith C, Dichgans M. Small vessel disease: Mechanisms and clinical implications. *Lancet Neurol*. 2019;18:684-696.

    doi: 10.1016/S1474-4422(19)30079-1
39. Smith EE. Clinical presentations and epidemiology of vascular dementia. *Clin Sci (Lond)*. 2017;131:1059-1068.

    doi: 10.1042/CS20160607
40. Prabhakaran S, Naidech AM. Ischemic brain injury after intracerebral hemorrhage: A critical review. *Stroke*. 2012;43:2258-2263.

doi: 10.1161/STROKEAHA.112.655910

41. Duering M, Biessels GJ, Brodtmann A, *et al*. Neuroimaging standards for research into small vessel disease-advances since 2013. *Lancet Neurol*. 2023;22(7):602-618.

doi: 10.1016/S1474-4422(23)00131-X

42. Pantoni L. Cerebral small vessel disease: From pathogenesis and clinical characteristics to therapeutic challenges. *Lancet Neurol*. 2010;9(7):689-701.

doi: 10.1016/S1474-4422(10)70104-6

43. Mustapha M, Nassir CMNCM, Aminuddin N, Safri AA, Ghazali MM. Cerebral small vessel disease (CSVD) - lessons from the animal models. *Front Physiol*. 2019;10:1317.

doi:10.3389/fphys.2019.01317

44. Chojdak-Łukasiewicz J, Dziadkowiak E, Zimny A, Paradowski B. Cerebral small vessel disease: A review. *Adv Clin Exp Med*. 2021;30(3):349-356.

doi: 10.17219/acem/131216

45. Zhuang FJ, Chen Y, He WB, Cai ZH. Prevalence of white matter hyperintensities increases with age. *Neural Regen Res*. 2018;13(12):2141-2146.

doi: 10.4103/1673-5374.241465

46. Li T, Huang Y, Cai W, *et al*. Age-related cerebral small vessel disease and inflammaging. *Cell Death Dis*. 2020;11(11):932.

doi: 10.1038/s41419-020-03137-x

47. Jann K, Shao X, Ma SJ, *et al*. Evaluation of cerebral blood flow measured by 3D PCASL as biomarker of vascular cognitive impairment and dementia (VCID) in a cohort of elderly Latinx subjects at risk of small vessel disease. *Front Neurosci*. 2021;15:627627.

doi: 10.3389/fnins.2021.627627

48. Baezner H, Blahak C, Poggesi A, *et al*. Association of gait and balance disorders with age-related white matter changes: The LADIS study. *Neurology*. 2008;70(12):935-942.

doi: 10.1212/01.wnl.0000305959.46197.e6

49. Naraoka M, Matsuda N, Shimamura N, Asano K, Ohkuma H. The role of arterioles and the microcirculation in the development of vasospasm after aneurysmal SAH. *Biomed Res Int*. 2014;2014:253746.

doi: 10.1155/2014/253746

50. Li Q, Yang Y, Reis C, *et al*. Cerebral small vessel disease. *Cell Transplant*. 2018;27(12):1711-1722.

doi: 10.1177/0963689718795148

51. Zhang YY, Chan DKY, Cordato D, Shen Q, Sheng AZ. Stroke risk factor, pattern and outcome in patients with cancer. *Acta Neurol Scand.* 2006;114(6):378-383.

doi: 10.1111/j.1600-0404.2006.00709.x

52. Uemura J, Kimura K, Sibazaki K, Inoue T, Iguchi Y, Yamashita S. Acute stroke patients have occult malignancy more often than expected. *Eur Neurol.* 2010;64(3):140-144.

doi: 10.1159/000316764

53. Kim SG, Hong JM, Kim HY, *et al*. Ischemic stroke in cancer patients with and without conventional mechanisms: A multicenter study in Korea. *Stroke*. 2010;41(4):798-801.

doi: 10.1161/STROKEAHA.109.571356

54. Dearborn JL, Urrutia VC, Zeiler SR. Stroke and cancer-a complicated relationship. *J Neurol Transl Neurosci*. 2014;2(1):1039.

55. Grazioli S, Paciaroni M, Agnelli G, *et al*. Cancer-associated ischemic stroke: A retrospective multicentre cohort study. *Thromb Res*. 2018;165:33-37.

doi: 10.1016/j.thromres.2018.03.011

56. Grisold W, Oberndorfer S, Struhal W. Stroke and cancer: A review. *Acta Neurol Scand*. 2009;119(1):1-16.

doi: 10.1111/j.1600-0404.2008.01059.x

57. Schwarzbach CJ, Schaefer A, Ebert A, *et al*. Stroke and cancer: The importance of cancer-associated hypercoagulation as a possible stroke etiology. *Stroke*. 2012;43(11):3029-3034.

doi: 10.1161/STROKEAHA.112.658625

58. Álvarez-Pérez FJ, Verde I, Usón-Martín M, Figuerola-Roig A, Ballabriga-Planas J, Espino-Ibañez A. Frequency and mechanism of ischemic stroke associated with malignancy: A retrospective series. *Eur Neurol*. 2012;68(4):209-213.

doi: 10.1159/000341343

59. Seok JM, Kim SG, Kim JW, *et al*. Coagulopathy and embolic signal in cancer patients with ischemic stroke. *Ann Neurol*. 2010;68(2):213-219.

doi: 10.1002/ana.22050

60. Dexter JS. The analysis of a case of continuous variation in *Drosophila* by a study of its linkage relations. *Am Nat*. 1914;48(576):712-758.

61. Durieux I, Ginevra C, Attaiech L, *et al*. Diverse conjugative elements silence natural transformation in *Legionella* species. *Proc Natl Acad Sci U S A*. 2019;116(37):18613-18618.

doi: 10.1073/pnas.1909374116

62. Kopan R, Ilagan MX. The canonical Notch signalling pathway: Unfolding the activation mechanism. *Cell*. 2009;137(2):216-233.

doi: 10.1016/j.cell.2009.03.045

63. Yavropoulou MP, Maladaki A, Yovos JG. The role of Notch and Hedgehog signalling pathways in pituitary development and pathogenesis of pituitary adenomas. *Hormones (Athens)*. 2015;14(1):5-18.

doi: 10.1007/BF03401377

64. Hori K, Sen A, Artavanis-Tsakonas S. Notch signalling at a

glance. *J Cell Sci.* 2013;126(Pt 10):2135-2140.

65. Gozlan O, Sprinzak D. Notch signaling in development and homeostasis. Development. 2023;150(4):dev201138.

doi: 10.1242/dev.201138

66. Vlachakis D, Tsaniras SC, Ioannidou K, Papageorgiou L, Baumann M, Kossida S. A series of Notch3 mutations in CADASIL; insights from 3D molecular modelling and evolutionary analyses. *J Mol Biochem.* 2014;3(3):134.

67. Bray SJ. Notch signalling in context. *Nat Rev Mol Cell Biol.* 2016;17(11):722-735.

doi: 10.1038/nrm.2016.94

68. Xiu MX, Liu YM. The role of oncogenic Notch2 signalling in cancer: A novel therapeutic target. *Am J Cancer Res.* 2019;9(5):837-854.

69. Xia Y, Bhattacharyya A, Roszell EE, Sandig M, Mequanint K. The role of endothelial cell-bound Jagged1 in Notch3-induced human coronary artery smooth muscle cell differentiation. *Biomaterials.* 2012;33(8):2462-2472.

doi: 10.1016/j.biomaterials.2011.12.001

70. Xu X, Choi SH, Hu T, *et al*. Insights into autoregulation of Notch3 from structural and functional studies of its negative regulatory region. *Structure.* 2015;23(7):1227-1235.

doi: 10.1016/j.str.2015.05.001

71. Gera S, Dighe RR. The soluble ligand Y box-1 activates Notch3 receptor by binding to epidermal growth factor like repeats 20-23. Arch Biochem Biophys. 2018;660:129-136.

doi: 10.1016/j.abb.2018.10.009

72. Domenga V, Fardoux P, Lacombe P, *et al.* Notch3 is required for arterial identity and maturation of vascular smooth muscle cells. Genes Dev. 2004;18(22):2730-2735.

doi: 10.1101/gad.308904

73. Jin S, Hansson EM, Tikka S, *et al*. Notch signalling regulates platelet-derived growth factor receptor-beta expression in vascular smooth muscle cells. Circ Res. 2008; 102(12):1483-1491.

doi: 10.1161/CIRCRESAHA.107.167965

74. Ando K, Wang W, Peng D, *et al*. Peri-arterial specification of vascular mural cells from naïve mesenchyme requires Notch signalling. Development. 2019;146(2):dev165589.

doi: 10.1242/dev.165589

75. Wang Q, Zhao N, Kennard S, Lilly B. Notch2 and Notch3 function together to regulate vascular smooth muscle development. PLoS One. 2012;7:e37365.

doi: 10.1371/journal.pone.0037365

76. Baeten JT, Lilly B. Differential regulation of NOTCH2 and NOTCH3 contribute to their unique functions in vascular smooth muscle cells. J Biol Chem. 2015;290:16226-16237.

doi: 10.1074/jbc.M115.655548

77. Kawazu M, Kojima S, Ueno T, *et al*. Integrative analysis of genomic alterations in triple-negative breast cancer in association with homologous recombination deficiency. PLoS Genet. 2017;13(6):e1006853.

doi: 10.1371/journal.pgen.1006853

78. Doebar SC, Sieuwerts AM, de Weerd V, *et al.* Gene expression differences between ductal carcinoma *in situ* with and without progression to invasive breast cancer. Am J Pathol. 2017;187(7):1648-1655.

doi: 10.1016/j.ajpath.2017.03.012

79. Sansone P, Ceccarelli C, Berishaj M, *et al.* Self-renewal of CD133(hi) cells by IL6/Notch3 signalling regulates endocrine resistance in metastatic breast cancer. Nat Commun. 2016;7:10442.

doi: 10.1038/ncomms10442

80. Gu X, Lu C, He D, *et al*. Notch3 negatively regulates chemoresistance in breast cancers. Tumour Biol. 2016;37(7):9511-9519.

doi: 10.1007/s13277-016-5412-4

81. Serafin V, Persano L, Moserle L, *et al*. Notch3 signalling promotes tumour growth in colorectal cancer. J Pathol. 2011;224(4):448-460.

doi: 10.1002/path.2895

82. Suliman MA, Zhang Z, Na H, *et al*. Niclosamide inhibits colon cancer progression through downregulation of the Notch pathway and upregulation of the tumour suppressor miR-200 family. Int J Mol Med. 2016;38(3):776-784.

doi: 10.3892/ijmm.2016.2689

83. Xie T, Li Y, Li SL, Luo HF. Astragaloside IV enhances cisplatin chemosensitivity in human colorectal cancer via regulating NOTCH3. Oncol Res. 2016;24(6):447-453.

doi: 10.3727/096504016X14685034103590

84. Wu JK, Adepoju O, De Silva D, *et al.* A switch in Notch gene expression parallels stem cell to endothelial transition in infantile haemangioma. Angiogenesis. 2010;13(1):15-23.

doi: 10.1007/s10456-009-9161-5

85. Hu L, Xue F, Shao M, Deng A, Wei G. Aberrant expression of Notch3 predicts poor survival for hepatocellular carcinomas. Biosci Trends. 2013;7(3):152-156.

86. Gramantieri L, Giovannini C, Lanzi A, *et al.* Aberrant Notch3 and Notch4 expression in human hepatocellular carcinoma. Liver Int. 2007;27(7):997-1006.

doi: 10.1111/j.1478-3231.2007.01544.x

87. Man CH, Wei-Man Lun S, *et al.* Inhibition of NOTCH3 signalling significantly enhances sensitivity to cisplatin in EBV-associated nasopharyngeal carcinoma. J Pathol. 2012;226(3):471-481.

doi: 10.1002/path.2997

88. Chen CY, Chen YY, Hsieh MS, *et al*. Expression of Notch gene and its impact on survival of patients with resectable non-small cell lung cancer. J Cancer. 2017;8(7):1292-1300.

doi: 10.7150/jca.17741

89. Shi C, Qian J, Ma M, Zhang Y, Han B. Notch3 protein, not its gene polymorphism, is associated with the chemotherapy response and prognosis of advanced NSCLC patients. Cell Physiol Biochem. 2014;34(3):743-752.

doi: 10.1159/000363039

90. Ikezawa Y, Sakakibara-Konishi J, Mizugaki H, *et al*. Inhibition of Notch and HIF enhances the antitumor effect of radiation in Notch expressing lung cancer. Int J Clin Oncol. 2017;22(1):59-69.

doi: 10.1007/s10147-016-1031-8

91. Liu Z, Yun R, Yu X, *et al*. Overexpression of Notch3 and pS6 is associated with poor prognosis in human ovarian epithelial cancer. *Mediators Inflamm.* 2016;2016:5953498.

doi: 10.1155/2016/5953498

92. Jung SG, Kwon YD, Song JA, *et al*. Prognostic significance of Notch 3 gene expression in ovarian serous carcinoma. *Cancer Sci.* 2010;101(9):1977-1983.

doi: 10.1111/j.1349-7006.2010.01641.x

93. Chen CF, Dou XW, Liang YK, *et al*. Notch3 overexpression causes arrest of cell cycle progression by inducing Cdh1 expression in human breast cancer cells. *Cell Cycle.* 2016;15(3):432-440.

doi: 10.1080/15384101.2015.1127474

94. Ross AE, Marchionni L, Vuica-Ross M, *et al*. Gene expression pathways of high-grade localized prostate cancer. *Prostate.* 2011;71(14):1568-1577.

doi: 10.1002/pros.21373

95. Danza G, Di Serio C, Ambrosio MR, *et al*. Notch3 is activated by chronic hypoxia and contributes to the progression of human prostate cancer. *Int J Cancer.* 2013;133(11):2577-2588.

doi: 10.1002/ijc.28293

96. Yeasmin S, Nakayama K, Rahman MT, *et al*. Expression of nuclear Notch3 in cervical squamous cell carcinomas and its association with adverse clinical outcomes. *Gynecol Oncol.* 2010;117(3):409-416.

doi: 10.1016/j.ygyno.2010.03.004

97. Liu J, Fan H, Ma Y, *et al*. Notch1 is a 5-fluorouracil resistant and poor survival marker in human esophagus squamous cell carcinomas. *PLoS One.* 2013;8(2):e56141.

doi: 10.1371/journal.pone.0056141

98. Lee SH, Jeong EG, Yoo NJ, Lee SH. Mutational analysis of NOTCH1, 2, 3 and 4 genes in common solid cancers and acute leukemias. *APMIS.* 2007;115(12):1357-1363.

doi: 10.1111/j.1600-0463.2007.00751.x

99. Masiero M, Minuzzo S, Pusceddu I, *et al*. Notch3-mediated regulation of MKP-1 levels promotes survival of T acute lymphoblastic leukemia cells. *Leukemia.* 2011;25(4):588-598.

doi: 10.1038/leu.2010.323.

100. Tang XF, Cao Y, Peng DB, *et al*. Overexpression of Notch3 is associated with metastasis and poor prognosis in osteosarcoma patients. *Cancer Manag Res.* 2019;11:547-559.

doi: 10.2147/CMAR.S185495

101. Zhang Y, Chen B, Wang Y, *et al*. NOTCH3 overexpression and posttranscriptional regulation by miR-150 were associated with EGFR-TKI resistance in lung adenocarcinoma. *Oncol Res.* 2019;27(7):751-761.

doi: 10.3727/096504018X15372657298381

102. Xiu M, Wang Y, Li B, *et al*. The role of Notch3 signaling in cancer stemness and chemoresistance: Molecular mechanisms and targeting strategies. *Front Mol Biosci.* 2021;8:694141.

doi: 10.3389/fmolb.2021.694141

103. Bernasconi-Elias P, Hu T, Jenkins D, *et al*. Characterization of activating mutations of NOTCH3 in T-cell acute lymphoblastic leukemia and anti-leukemic activity of NOTCH3 inhibitory antibodies. *Oncogene.* 2016; 35(47):6077-6086.

doi: 10.1038/onc.2016.133

104. Papadakos KS, Bartoschek M, Rodriguez C, *et al*. Cartilage oligomeric matrix protein initiates cancer stem cells through activation of Jagged1-Notch3 signaling. *Matrix Biol.* 2019;81:107-121.

doi: 10.1016/j.matbio.2018.11.007

105. Fang CH, Lin YT, Liang CM, Liang SM. A novel C-Kit/phospho-prohibitin axis enhances ovarian cancer stemness and chemoresistance via Notch3-PBX1 and β-catenin-ABCG2 signaling. *J Biomed Sci.* 2020;27(1):42.

doi: 10.1186/s12929-020-00638-x

106. Meurette O, Mehlen P. Notch signaling in the tumour microenvironment. *Cancer Cell.* 2018;34(4):536-548.

doi: 10.1016/j.ccell.2018.07.009.

107. Hanahan D, Coussens LM. Accessories to the crime: Functions of cells recruited to the tumour microenvironment. *Cancer Cell.* 2012;21(3):309-322.

doi: 10.1016/j.ccr.2012.02.022

108. Shen Q, Cohen B, Zheng W, *et al*. Notch shapes the innate immunophenotype in breast cancer. *Cancer Discov.* 2017;7(11):1320-1335.

doi: 10.1158/2159-8290.CD-17-0037

109. Tsuyada A, Chow A, Wu J, *et al*. CCL2 mediates cross-talk between cancer cells and stromal fibroblasts that regulates

breast cancer stem cells. *Cancer Res.* 2012;72(11):2768-2779.

doi: 10.1158/0008-5472.CAN-11-3567

110. Boelens MC, Wu TJ, Nabet BY, *et al*. Exosome transfer from stromal to breast cancer cells regulates therapy resistance pathways. *Cell.* 2014;159(3):499-513.

doi: 10.1016/j.cell.2014.09.051

111. Studebaker AW, Storci G, Werbeck JL, *et al*. Fibroblasts isolated from common sites of breast cancer metastasis enhance cancer cell growth rates and invasiveness in an interleukin-6-dependent manner. *Cancer Res.* 2008;68(21):9087-9095.

doi: 10.1158/0008-5472.CAN-08-0400

112. Yamaguchi N, Oyama T, Ito E, *et al*. NOTCH3 signalling pathway plays crucial roles in the proliferation of ErbB2-negative human breast cancer cells. *Cancer Res.* 2008;68(6):1881-1888.

doi: 10.1158/0008-5472.CAN-07-1597

113. Huang TX, Guan XY, Fu L. Therapeutic targeting of the crosstalk between cancer-associated fibroblasts and cancer stem cells. *Am J Cancer Res.* 2019;9(9):1889-1904.

114. Fernandez SV, Robertson FM, Pei J, *et al*. Inflammatory breast cancer (IBC): Clues for targeted therapies. *Breast Cancer Res Treat.* 2013;140(1):23-33.

doi: 10.1007/s10549-013-2600-4

115. Liu H, Wang J, Zhang M, *et al*. Jagged1 promotes aromatase inhibitor resistance by modulating tumour-associated macrophage differentiation in breast cancer patients. *Breast Cancer Res Treat.* 2017;166(1):95-107.

doi: 10.1007/s10549-017-4394-2

116. Sousa S, Brion R, Lintunen M, *et al*. Human breast cancer cells educate macrophages toward the M2 activation status. *Breast Cancer Res.* 2015;17:101.

doi: 10.1186/s13058-015-0621-0

117. Cahill EF, Tobin LM, Carty F, Mahon BP, English K. Jagged-1 is required for the expansion of CD4+ CD25+ FoxP3+ regulatory T cells and tolerogenic dendritic cells by murine mesenchymal stromal cells. *Stem Cell Res Ther.* 2015;6:19.

doi: 10.1186/s13287-015-0021-5

118. Lamy M, Ferreira A, Dias JS, Braga S, Silva G, Barbas A. Notch-out for breast cancer therapies. *New Biotechnol.* 2017;39:215-221.

doi: 10.1016/j.nbt.2017.08.004

119. Charbonnier LM, Wang S, Georgiev P, Sefik E, Chatila TA. Control of peripheral tolerance by regulatory T cell-intrinsic Notch signalling. *Nat Immunol.* 2015;16(11):1162-1173.

doi: 10.1038/ni.3288

120. Mezquita B, Mezquita J, Barrot C, *et al*. A truncated-Flt1 isoform of breast cancer cells is upregulated by Notch and downregulated by retinoic acid. *J Cell Biochem.* 2014;115(1):52-61.

doi: 10.1002/jcb.24632

121. Sabol HM, Amorim T, Ashby C, *et al*. Notch3 signalling between myeloma cells and osteocytes in the tumour niche promotes tumour growth and bone destruction. *Neoplasia.* 2022;28:100785.

doi: 10.1016/j.neo.2022.100785

122. Ying J, Tsujii M, Kondo J, *et al*. The effectiveness of an anti-human IL-6 receptor monoclonal antibody combined with chemotherapy to target colon cancer stem-like cells. *Int J Oncol.* 2015;46(4):1551-1559.

doi: 10.3892/ijo.2015.2851

123. Antony J, Tan TZ, Kelly Z, *et al*. The GAS6-AXL signalling network is a mesenchymal (Mes) molecular subtype-specific therapeutic target for ovarian cancer. *Sci Signal.* 2016;9(448):ra97.

doi: 10.1126/scisignal.aaf8175

124. Kent S, Hutchinson J, Balboni A, Decastro A, Cherukuri P, Direnzo J. ΔNp63α promotes cellular quiescence via induction and activation of Notch3. *Cell Cycle.* 2011;10(18):3111-3118.

doi: 10.4161/cc.10.18.17300

125. Belin de Chantemèle EJ, Retailleau K, Pinaud F, *et al*. Notch3 is a major regulator of vascular tone in cerebral and tail resistance arteries. *Arterioscler Thromb Vasc Biol.* 2008;28(12):2216-2224.

doi: 10.1161/ATVBAHA.108.171751

126. Kawai H, Kawaguchi D, Kuebrich BD, *et al*. Area-specific regulation of quiescent neural stem cells by Notch3 in the adult mouse subependymal zone. *J Neurosci.* 2017;37(49):11867-11880.

doi: 10.1523/JNEUROSCI.0001-17.2017

127. Loerakker S, Stassen OMJA, Ter Huurne FM, Boareto M, Bouten CVC, Sahlgren CM. Mechano sensitivity of Jagged-Notch signalling can induce a switch-type behavior in vascular homeostasis. *Proc Natl Acad Sci U S A.* 2018;115(16):E3682-E3691.

doi: 10.1073/pnas.1715277115

128. Kitamoto T, Hanaoka K. Notch3 null mutation in mice causes muscle hyperplasia by repetitive muscle regeneration. *Stem Cells.* 2010;28(12):2205-2216.

doi: 10.1002/stem.547

129. Conboy IM, Rando TA. The regulation of Notch signalling controls satellite cell activation and cell fate determination in postnatal myogenesis. *Dev Cell.* 2002;3(3):397-409.

doi: 10.1016/s1534-5807(02)00254-x

130. Wei LK, Sutherland H, Au A, *et al*. A potential epigenetic

marker mediating serum folate and vitamin B12 levels contributes to the risk of ischemic stroke. *Biomed Res Int.* 2015;2015:167976.

doi: 10.1155/2015/167976

131. Joutel A, Vahedi K, Corpechot C, *et al*. Strong clustering and stereotyped nature of Notch3 mutations in CADASIL patients. *Lancet.* 1997;350(9090):1511-1515.

doi: 10.1016/S0140-6736(97)08083-5

132. Soong BW, Liao YC, Tu PH, *et al*. A homozygous NOTCH3 mutation p.R544C and a heterozygous TREX1 variant p.C99MfsX3 in a family with hereditary small vessel disease of the brain. *J Chin Med Assoc.* 2013;76(6):319-324.

doi: 10.1016/j.jcma.2013.03.002

133. Bekris LM, Yu CE, Bird TD, Tsuang DW. Genetics of Alzheimer disease. *J Geriatr Psychiatry Neurol.* 2010;23(4):213-227.

doi: 10.1177/0891988710383571

134. Paulson HL, Igo I. Genetics of dementia. *Semin Neurol.* 2011;31(5):449-460.

doi: 10.1055/s-0031-1299784

135. Ruchoux MM, Maurage CA. CADASIL: Cerebral autosomal dominant arteriopathy with subcortical infarcts and leukoencephalopathy. *J Neuropathol Exp Neurol.* 1997;56(9):947-964.

136. Tournier-Lasserve E, Joutel A, Melki J, *et al*. Cerebral autosomal dominant arteriopathy with subcortical infarcts and leukoencephalopathy maps to chromosome 19q12. *Nat Genet.* 1993;3(3):256-259.

doi: 10.1038/ng0393-256

137. Stojanov D, Vojinovic S, Aracki-Trenkic A, *et al*. Imaging characteristics of cerebral autosomal dominant arteriopathy with subcortical infarcts and leucoencephalopathy (CADASIL). *Bosn J Basic Med Sci.* 2015;15(1):1-8.

doi: 10.17305/bjbms.2015.247

138. O'Sullivan M, Jarosz JM, Martin RJ, Deasy N, Powell JF, Markus HS. MRI hyperintensities of the temporal lobe and external capsule in patients with CADASIL. *Neurology.* 2001;56(5):628-634.

doi: 10.1212/wnl.56.5.628

139. Joutel A, Corpechot C, Ducros A, *et al*. Notch3 mutations in CADASIL, a hereditary adult-onset condition causing stroke and dementia. *Nature.* 1996;383(6602):707-710.

doi: 10.1038/383707a0

140. Tikka S, Baumann M, Siitonen M, *et al*. CADASIL and CARASIL. *Brain Pathol.* 2014;24(5):525-544.

doi: 10.1111/bpa.12181

141. Schoemaker D, Arboleda-Velasquez JF. Notch3 signalling and aggregation as targets for the treatment of CADASIL and other NOTCH3-associated small-vessel diseases. *Am J Pathol.* 2021;191(11):1856-1870.

doi: 10.1016/j.ajpath.2021.03.015

142. Moreton F, Razvi S, Davidson R, Muir K. Changing clinical patterns and increasing prevalence in CADASIL. *Acta Neurol Scand.* 2014;130(3):197-203.

doi: 10.1111/ane.12266

143. Rutten JW, Hack RJ, Duering M, *et al*. Broad phenotype of cysteine-altering NOTCH3 variants in UK Biobank: CADASIL to nonpenetrance. *Neurology.* 2020;95(18):e1835-e1843.

doi: 10.1212/WNL.0000000000010525

144. Coupland K, Lendahl U, Karlström H. Role of NOTCH3 mutations in the cerebral small vessel disease cerebral autosomal dominant arteriopathy with subcortical infarcts and leukoencephalopathy. *Stroke.* 2018;49(11):2793-2800.

doi: 10.1161/STROKEAHA.118.021560

145. Hosseini-Alghaderi S, Baron M. Notch3 in development, health and disease. *Biomolecules.* 2020;10(3):485.

doi: 10.3390/biom10030485

146. Song C, Zhang J, Xu C, Gao M, Li N, Geng Q. The critical role of γ-secretase and its inhibitors in cancer and cancer therapeutics. *Int J Biol Sci.* 2023;19(16):5089-5103.

doi: 10.7150/ijbs.87334

147. Takebe N, Nguyen D, Yang SX. Targeting notch signaling pathway in cancer: Clinical development advances and challenges. *Pharmacol Ther.* 2014;141(2):140-149.

doi: 10.1016/j.pharmthera.2013.09.005

ACCSCIENCE PUBLISHING

Eurasian Journal of Medicine and Oncology

REVIEW ARTICLE

Update on systemic lupus erythematosus: A review

Abdurahman Alloghbi[1], Yousef Al Obaisi[2], Hussain Alkhurayb[2], Amal M Shawabka[3], and Fahad S. Alshehri[2,4]*

[1]Department of Oncology, College of Medicine, King Khalid University, Abha, Saudi Arabia

[2]Pathology and Clinical Laboratory Medicine Administration, Haematology and Immunology Division, King Fahad Medical City, Riyadh, Saudi Arabia

[3]Department of Clinical Science, College of Medicine, Palestine Polytechnic University, Hebron, Palestine

[4]Department of Pathology and Clinical Laboratory Medicine, Haematology Division, King Faisal Medical City for Southern Region, Abha, Saudi Arabia

Abstract

Systemic lupus erythematosus (SLE) is a complex autoimmune and idiopathic condition that affects connective tissues. It is characterized by the formation of autoantibodies, the accumulation of immune complexes, inflammation, and, ultimately, irreversible organ damage. It can affect individuals of various ages, ethnicities, and genders. Nonetheless, nearly 90% of newly diagnosed SLE patients are women of reproductive age. The early mortality associated with SLE is primarily due to significant disease activity. However, subsequent mortality is linked to chronic illness and the use of immunosuppressive agents. Despite extensive research, the precise etiology of SLE remains partially understood; however, its onset involves a complex interplay of genetic predispositions, environmental stimuli, hormonal factors, and immune system abnormalities. The predominant clinical signs include fatigue, fever, weight loss, arthritis, pericarditis, anemia, and pulmonary complications. Diagnosing SLE requires a combination of clinical evaluations and laboratory testing, including antinuclear antibodies and anti-double-stranded DNA antibodies, among others. Managing SLE patients involves various approaches and lifestyle recommendations, including avoiding direct or reflected sunlight. This article presents an updated review of the mortality and pathophysiology of SLE. We also elucidate the clinical manifestations and the primary diagnostic and therapeutic strategies for this condition.

Keywords: Systemic lupus erythematosus; Clinical manifestations; Mortality, Diagnosis; Antinuclear antibodies

***Corresponding author:**
Fahad S. Alshehri
(fasaalshehri@moh.gov.sa)

Citation: Alloghbi A, Al Obaisi Y, Alkhurayb H, Shawabka AM Alshehri FS. Update on systemic lupus erythematosus: A review. *Eurasian J Med Oncol*. 2025;9(3):52-62. doi: 10.36922/EJMO025090042

Received: February 26, 2025

Revised: May 5, 2025

Accepted: May 8, 2025

Published online: May 30, 2025

Copyright: © 2025 Author(s). This is an Open-Access article distributed under the terms of the Creative Commons Attribution License, permitting distribution, and reproduction in any medium, provided the original work is properly cited.

Publisher's Note: AccScience Publishing remains neutral with regard to jurisdictional claims in published maps and institutional affiliations.

1. Introduction

Systemic lupus erythematosus (SLE) is a multifaceted autoimmune and idiopathic disorder that affects the connective tissues.[1] It is characterized by a prolonged pattern of relapses and remissions, accompanied by various symptoms. It results in various diseases that can range from moderate to severe and potentially life-threatening.[2] The cause of SLE is believed to be influenced by multiple factors. This condition is marked

by the development of autoantibodies, accumulation of immune complexes, inflammation, and ultimately, irreversible organ damage.[3] SLE can impact individuals of all ages, ethnicities, and genders.[4] However, over 90% of newly diagnosed SLE patients are women in their reproductive years.[5] It involves the activation of both innate and adaptive immune responses. The interplay between genetic and environmental factors leads to various immunological changes, resulting in ongoing immune reactions against one's nucleic acids.[6] Tissue damage caused by autoantibodies or immune complex deposits can affect several organs and systems, including the kidneys, heart, blood vessels, central nervous system, skin, lungs, muscles, and joints.[7-10] This damage can lead to significant illness and an increased risk of death.[11]

During the late 1940s, nearly 40% of individuals diagnosed with SLE experienced mortality within 3 years after the initial manifestation of symptoms.[12] Subsequently, the survival rates of individuals with SLE have significantly increased to over 90% for 5- and 10-year periods.[13] Based on the nationwide mortality database, the mortality rate of SLE between the years 1968 and 2013 accounted for the underlying cause of death in a total of 50,249 individuals across the United States (US).[14] During the period from 1999 to 2013, there were an additional 12,463 deaths in which SLE was identified as a contributing factor.[14] In addition, in Germany, the incidence of SLE in 2002 was 36.7 cases/100,000 individuals, with a female-to-male ratio of 4:1.[15] It is linked to a mortality risk approximately 2 – 5 times higher than the general population's.[16] Early mortality, defined as death occurring within 1 year of diagnosis, is believed to be primarily caused by severe disease activity.[17]

On the other hand, later mortality is more often attributed to difficulties arising from long-standing disease and the use of immunosuppressive medications.[18] Both infection and increased atherosclerosis contribute to late mortality. Although there have been many improvements in diagnosing and treating SLE and its related comorbidities, this disease continues to cause substantial illness and death.[19]

Substantial evidence indicates a significant relationship between SLE and a deficiency in complement C1q.[20] This deficiency contributes to the activation of $CD8^+$ T cells in the SLE model.[20] Autoantibody-producing B cells and self-reactive T cells are known to significantly contribute to the development and progression of autoimmune diseases, including SLE.[21] The diagnosis of SLE can be supported by laboratory testing, although it is initially based on clinical signs.[22] Initially, it is advisable to conduct a screening laboratory test. An elevated erythrocyte sedimentation rate (ESR) indicates active SLE, although C-reactive protein (CRP) levels are typically within the normal range or only slightly increased.[23] The complete blood count test can detect thrombocytopenia, leukopenia, lymphopenia, and specific hematological alterations, including autoimmune hemolytic anemia (AIHA). Renal parameters should include serum creatinine measurements, urine function evaluation, and urinary sediment examination.[24] Antinuclear antibodies (ANA),[25] anti-double-stranded DNA (anti-dsDNA) antibodies,[26] anti-Sm antibodies,[27] and levels of C3 and C4[28] should be identified as indicators of SLE. The evaluation of SLE involves precise diagnosis, continuous monitoring of disease activity, assessment of long-term damage and morbidity, and determination of the patient's overall health condition.[29]

This paper will review SLE in-depth, including its epidemiological rate and pathogenesis. Furthermore, it will discuss its manifestation features and the diagnosis and treatment options.

2. SLE mortality rate and (Epidemiology in KSA)

SLE is a complex autoimmune condition that affects multiple organ systems and is more prevalent in women, with a ratio of 9 females to 1 male. The disease often manifests during childbearing age and presents a significant public health issue due to its chronic nature and potential to cause considerable organ damage and increased mortality. Globally, the prevalence of SLE varies significantly based on geographic and ethnic factors, ranging from 20 to 150 cases/100,000 population. In North America and Europe, the prevalence is generally higher, typically within the range of 20 – 70 cases/100,000. In contrast, Asian and African populations are believed to have even greater incidence rates.

In Saudi Arabia, the exact prevalence of SLE is less well-documented compared to other regions. However, recent studies indicate a rising trend in the diagnosis of autoimmune diseases, including SLE. While the specific prevalence of SLE in Saudi Arabia is not fully established, the general burden of chronic autoimmune and inflammatory diseases in the country mirrors global trends. A regional study conducted at King Khalid University Hospital in Riyadh reported that the incidence of SLE in the Saudi population was estimated at 19.28/100,000 people,[30] with a higher frequency among younger women.

Mortality rates linked to SLE are significantly affected by the progression of the disease and its complications, especially concerning renal, cardiovascular, and infectious causes. In Saudi Arabia, while mortality data specifically linked to SLE is sparse, international studies suggest

that SLE patients have a 2 to 3 times higher risk of death compared to the general population, with cardiovascular disease (CVD) and lupus nephritis being primary contributors to mortality. Lupus nephritis, a major complication of SLE that affects the kidneys, is particularly common in Middle Eastern populations, including Saudi Arabia. Studies show that 30% to 60% of SLE patients in the region may develop nephritis, which significantly worsens long-term outcomes.[31]

CVD is a significant cause of death among SLE patients. In Saudi Arabia, where the overall burden of CVD is already high – with 37% of all deaths from non-communicable diseases linked to cardiovascular complications,[32] SLE patients face an increased risk. A global study found that individuals with SLE are 10 times more likely to suffer from premature atherosclerosis, heart attacks, and strokes compared to the general population. This risk is exacerbated by the high prevalence of associated conditions, such as hypertension, diabetes, and obesity within the Saudi population.

Because of its long-term impacts, SLE is considered a significant obstacle to achieving optimal health care standards. According to the World Health Organization, stroke mortality rates in the Kingdom of Saudi Arabia range from 55 to 95/100,000, whereas ischemic heart disease mortality rates range from 191 to 541/100,000.[33] While SLE may not be included in these figures, they do indicate a troubling trend in both SLE-related and non-SLE public health disorders, which significantly elevate the overall level of illness in the community.

Another factor contributing to SLE-related mortality in Saudi Arabia is the relatively late diagnosis and limited access to specialized care. Early intervention and comprehensive disease management are critical for improving outcomes; however, many patients may present with advanced disease due to delays in diagnosis, particularly in rural areas where healthcare resources are scarcer. The severity of the issue in the kingdom is further compounded by the high prevalence of obesity and low levels of physical activity, which are major risk factors for the SLE.[34]

3. Pathogenesis of SLE

SLE is a complex autoimmune disease characterized by the abnormal production of autoantibodies that target nuclear antigens. This results in widespread tissue inflammation and damage, often affecting multiple organs. While the exact cause of SLE remains not fully understood, its development involves a complex interaction between genetic factors, environmental triggers, hormonal influences, and dysregulation of the immune system. Genetically, susceptibility to SLE is significantly influenced by polymorphisms in key immune regulatory genes, particularly within the human leukocyte antigen (HLA) region, including HLA-DR2 and HLA-DR3, which are critically involved in antigen presentation. Mutations in genes encoding complement components (*e.g.*, C1q, C2, and C4) that are essential for the clearance of immune complexes and apoptotic cells further contribute to a pathogenic milieu.[35] In addition, non-HLA genes also play a critical role in disrupting immune tolerance and promoting autoimmunity in SLE. For example, genes involved in toll-like receptor (TLR) signaling pathways, such as *TLR7* and *TLR9*, as well as genes regulating B-cell receptor signaling, such as *BLK* and *BANK1*, contribute to the breakdown of immune regulation.[36] This genetic predisposition is exacerbated by environmental triggers, with ultraviolet (UV) radiation being a prominent factor that induces cell damage and the release of nuclear antigens, facilitating autoantibody production.[37] Infections, particularly with Epstein-Barr virus (EBV), have also been linked to SLE pathogenesis. Studies suggest that molecular mimicry – where EBV antigens resemble the body's own nuclear antigens – may lead to the production of harmful autoantibodies.[38] In addition, hormonal influences, especially estrogen, help explain why SLE is more common in women. Estrogen is believed to enhance B-cell survival, increase autoantibody production, and promote the expression of pro-inflammatory cytokines, all of which exacerbate the autoimmune response.[39] Together, these genetic, environmental, and hormonal factors create a perfect storm that drives the development and progression of SLE.

A major breakdown in immune regulation is central to the pathogenesis of SLE, leading to the production of a wide range of autoantibodies, particularly ANAs. These antibodies target components of the cell nucleus, such as dsDNA, histones, and ribonucleoproteins. This aberrant antibody production is precipitated by defective clearance of apoptotic cells and immune complexes, resulting in the persistent presence of nuclear antigens in the extracellular milieu. Dendritic cells play a key role in this regard by picking up these antigens and presenting them to T-cells, which then activate and help autoreactive B-cells.[40] This chain of events leads to the formation of germinal centers in secondary lymphoid organs, where B-cells undergo somatic hypermutation and class-switch recombination, ultimately churning out high-affinity autoantibodies. A critical part of this process involves TLRs, especially TLR7 and TLR9, which are activated by nucleic acids. This triggers signaling pathways, such as nuclear factor kappa B and interferon regulatory factors, leading to the production of type I interferons (IFNs).[41] Type I IFNs, particularly IFN-α, are

central to SLE. They help autoreactive B-cells survive, promote monocytes to differentiate into dendritic cells, and boost the expression of MHC class II molecules, which ramps up antigen presentation.[42] The increased activity of IFN-inducible genes, known as the "IFN signature," is a hallmark of SLE and is closely tied to disease severity.[43]

In addition to B-cell dysregulation, T-cell abnormalities are also critical in the pathogenesis of SLE. Regulatory T cells (Tregs), which normally keep autoimmune responses in check, are often reduced in number or do not function appropriately in SLE patients.[44] Making matters worse, there is an increase in T-helper 17 (Th17) cells, which produce the inflammatory cytokine interleukin (IL)-17. This contributes to the chronic inflammation that is a hallmark of SLE.[45] The imbalance between Tregs and Th17 cells further disrupts the body's ability to maintain self-tolerance, allowing the autoimmune response to continue unabated. Furthermore, the chronic activation of the immune system in SLE leads to widespread tissue damage and organ dysfunction, with the kidneys, skin, joints, and central nervous system being particularly susceptible. Advances in understanding the underlying mechanisms of SLE have paved the way for targeted therapies to modulate the immune response, such as B-cell depletion strategies and IFN inhibitors. However, the heterogeneous nature of the disease poses ongoing challenges in developing universally effective treatments.[46] The pathogenesis of SLE, therefore, represents a complex interplay of genetic, environmental, hormonal, and immunological factors, each contributing to the initiation and perpetuation of the autoimmune process.

4. The clinical manifestations of SLE

Fatigue, fever, and weight loss are common in SLE. Fatigue affects 80 – 100% of patients and is often associated with depression, sleep disturbances, and fibromyalgia.[47] Fever occurs in over 50% of patients, but it is usually challenging to distinguish lupus-related fever from other causes, such as infection or drug reactions. Lupus-related fever typically responds to non-steroidal anti-inflammatory drugs, acetaminophen, or glucocorticoids, whereas fever due to infection may not.[48] Weight changes are frequent and may result from SLE itself or its treatment; for example, glucocorticoid use may lead to weight gain, while decreased appetite can cause weight loss (Figure 1).

4.1. Arthritis and arthralgias

Over 90% of SLE patients experience arthritis or arthralgias. The arthritis is often migratory, polyarticular, and symmetrical, affecting multiple joints without causing joint erosion or deformity, unlike rheumatoid arthritis.[49]

4.2. Mucocutaneous involvement

Skin and mucous membrane lesions are common. The facial "butterfly rash," a malar rash over the cheeks and nose, is a hallmark of SLE and is often triggered by sun exposure. Some patients may develop discoid lesions, which can lead to scarring. Photosensitivity is a frequent characteristic. Oral and nasal ulcers are usually painless, and non-scarring alopecia is common.[50]

4.3. Cardiac and vascular involvement

Pericarditis is a common cardiac manifestation of SLE, affecting about 25% of patients. Other cardiac issues include myocarditis, an increased risk of coronary artery disease, and the potential for valvular disease due to Libman-Sacks endocarditis.[50] Raynaud phenomenon occurs in up to 50% of patients, presenting as cold-induced acral pallor followed by cyanosis.[51] Vasculitis occurs in 11 – 36% of patients, often manifesting as cutaneous lesions, although larger vessels can also be involved.[52]

4.4. Thromboembolic disease

Thromboembolic events, including arterial and venous thrombi, complicate SLE, especially in patients with antiphospholipid antibodies. In one study, 11% of patients experienced arterial and 5% experienced venous events over a median follow-up of 6.3 years.[53]

4.5. Kidney involvement

Lupus nephritis occurs in about 50% of patients and is a significant cause of morbidity and mortality. It can present as asymptomatic hematuria or more severe conditions, such as nephrotic syndrome and rapidly progressive glomerulonephritis.[54]

4.6. Gastrointestinal involvement

Gastrointestinal symptoms occur in 40% of patients and are often caused by medications or infections. Other SLE-related gastrointestinal issues can include esophagitis, pancreatitis, and mesenteric vasculitis.[55]

4.7. Pulmonary involvement

Pulmonary manifestations include pleuritis, pneumonitis, interstitial lung disease, and pulmonary hypertension. Immunosuppressive therapy increases the risk of pulmonary infections.[56]

4.8. Neurologic and neuropsychiatric involvement

Neurologic and psychiatric manifestations are diverse, ranging from seizures and strokes to cognitive dysfunction and psychosis. Antiphospholipid antibodies and lupus anticoagulants can increase the risk of thromboembolic events, leading to neurologic complications.[56]

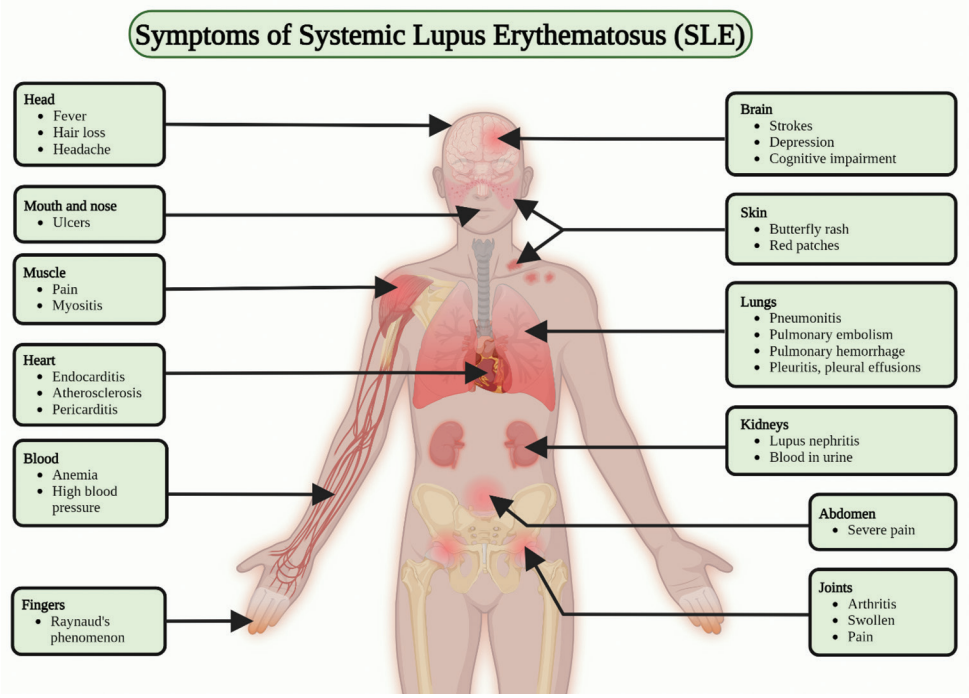


Figure 1. Symptoms of systemic lupus erythematosus. The disease exhibits a broad range of recognized clinical symptoms. The primary symptoms encompass fever, malaise, arthralgia, myalgia, headache, and diminished appetite and weight. The most prevalent symptoms in new instances or recurring active systemic lupus erythematosus include nonspecific fatigue, fever, arthralgia, and weight fluctuations. These symptoms may resemble other autoimmune disorders, viral diseases, and endocrine dysfunctions.

4.9. Hematologic abnormalities

SLE commonly affects all blood cell lines. Anemia due to chronic disease is common among SLE patients. Leukopenia, particularly lymphopenia, occurs in about 50% of patients and correlates with active disease.[57] Thrombocytopenia, though less common, can be severe and may require treatment. Lymph node enlargement and splenomegaly may also occur in association with active disease.

4.10. Ophthalmologic involvement

Keratoconjunctivitis sicca, often related to secondary Sjögren's syndrome, is SLE's most common eye manifestation.[58] Retinal vasculopathy can present as cotton wool spots. Other ophthalmologic manifestations include optic neuropathy, episcleritis, and glaucoma, which can be related to corticosteroid use.

4.11. Other conditions and complications

Hereditary angioedema and other complement deficiencies, such as C1, C2, and C4 deficiencies, can be associated with SLE.[59] Antiphospholipid syndrome is present in 40% of patients with SLE but does not always progress to the full syndrome.[60] SLE patients also have a higher prevalence of fibromyalgia, osteonecrosis, and osteoporosis.[61] SLE is also associated with an increased prevalence of autoimmune thyroid disease, such as Hashimoto's thyroiditis, and can co-occur with other autoimmune diseases, such as myasthenia gravis. A familial predisposition to autoimmune diseases is often observed in SLE patients.[62]

5. Diagnosis of SLE

Diagnosing SLE is a complex process that relies on a combination of clinical and laboratory criteria.[63] The clinical manifestations will cover the clinical criteria, and in this section, we will describe the intricate laboratory tests used to diagnose SLE. Around 99 % of individuals diagnosed with SLE have an increased ANA titer, which indicates the presence of autoimmunity.[64] Although several laboratory abnormalities are associated with this condition, the non-specific positive ANA can be detected in 5 – 20% of the general population.[65]

It is essential to note that many individuals can exhibit an initial negative ANA titer during the disease. This underscores the fact that the ANA test alone cannot diagnose SLE. A study conducted with 15 worldwide laboratories revealed that ANA tests provide positive results in a significant portion of individuals in the general population when diluted at 1:40, and in a smaller but still

notable percentage when diluted at 1:160.[66] The prevalence of positive ANA tests remained consistent across all age groups up to 60 years, the maximum age considered in the study.[66] If SLE is not present, the most frequent cause for a positive ANA test is the existence of another connective tissue disease such as Sjögren's syndrome (affecting 68% of patients), scleroderma (40 – 75% prevalence), rheumatoid arthritis (25 – 50% prevalence), and juvenile rheumatoid arthritis (16% prevalence). In addition, ANA testing may also be positive in individuals diagnosed with fibromyalgia.[67]

Anti-dsDNA antibodies (70 – 98% prevalence) are detectable in patients with positive ANA and a homogeneous fluorescence pattern.[68] The outcomes of the enzyme-linked immunosorbent assay require validation using radioimmunoassay (RIA) or the *Crithidia luciliae* immunofluorescence test.[69] Moreover, anti-Sm antibodies are specific indicators for SLE, with a prevalence between 14% and 40%.[70] In addition to causing venous and arterial thromboses and recurrent fetal loss, antiphospholipid antibodies can also be detected in 50% of lupus cases.[71] Evaluation is conducted by identifying antibodies to cardiolipin or beta-2 glycoprotein 1, or by the presence of a lupus anticoagulant, indicated by extended clotting times that remain uncorrected *in vitro* by mixing investigations.[72] Furthermore, C3 and C4 must be evaluated as indicators of complement intake or deficiency.[73] The evolution of SLE is characterized by exacerbations and remissions. Nonetheless, the ANA titer does not correlate with disease activity. Conversely, complement factor levels typically decrease concurrently with an elevation in anti-dsDNA antibodies, often happening months before disease onset. Consequently, it is essential to routinely monitor the progression of the disease, particularly regarding renal involvement.[74]

A screening laboratory test is recommended for the diagnosis of SLE. A high ESR indicates active SLE, but CRP levels are often normal or only slightly elevated.[75] A complete blood count analysis may reveal thrombocytopenia, leukopenia, and lymphopenia, along with features of AIHA. Renal function test criteria should include serum creatinine, urine analysis, and sediment examination.[76]

6. Management of SLE

6.1. Photoprotection

Exposure to UV light can exacerbate systemic manifestations of SLE. Patients are advised to avoid direct or reflected sunlight and other sources of UV light, such as fluorescent and halogen lights.[77] Sunscreens with both UV-A and UV-B protection and SPF ≥55 are recommended.

6.2. Hydroxychloroquine

Hydroxychloroquine is recommended for all patients with SLE. The typical dose is 5 mg/kg/day, with a maximum of 400 mg daily. It can be administered once or twice daily. Hydroxychloroquine has been sh

own to reduce overall mortality and improve survival.[78] Studies also indicate a reduction in disease flares, with one trial showing a flare rate of 73% in patients on placebo versus 35% in those continuing hydroxychloroquine.[79] Benefits extend to reduced symptoms, such as fatigue and joint pain, and it lowers the risk of thrombotic events, organ damage, and cancer.[80] Hydroxychloroquine is generally well tolerated, though rare side effects include retinopathy and QTc interval prolongation, especially in patients on other QT-prolonging drugs.[80]

6.3. Escalation of therapy

Moderate disease involves significant but non-organ-threatening manifestations such as fatigue, rashes, or hematologic issues. Hydroxychloroquine and short-term prednisone (5 – 15 mg/day) are often prescribed. Immunosuppressants, such as azathioprine, methotrexate, or mycophenolate mofetil may be added for patients who require more aggressive treatment.[81]

Organ-threatening SLE, such as lupus nephritis or central nervous system involvement, requires aggressive treatment. Patients are treated with high doses of glucocorticoids (oral prednisone 1–2 mg/kg/day or intravenous methylprednisolone 0.5 – 1 g/day for 3 days). Immunosuppressants, such as mycophenolate, cyclophosphamide, or rituximab are often added as glucocorticoid-sparing agents. Depending on the treatment, hospitalization may be required.[81]

6.4. Anifrolumab

Anifrolumab is a monoclonal antibody targeting the type I IFN receptor and is approved for patients with moderate to severe SLE, excluding those with severe lupus nephritis or neuropsychiatric SLE. It blocks cytokines, such as IFN-α, which are elevated in many patients with SLE. Anifrolumab shows particular promise in treating skin and joint manifestations.[82]

6.5. Belimumab

Belimumab, a monoclonal antibody that inhibits B cell activation by blocking the BLyS protein, is combined with other therapies. It typically takes 3 – 6 months to take full effect, so it is often combined with faster-acting medications, such as methotrexate in severe cases. Belimumab is FDA-approved and is a component of some regimens for lupus nephritis. A meta-analysis of six trials confirmed its efficacy for SLE.[83]

6.6. Rituximab

Rituximab, a B-cell-depleting antibody, is used in patients who have not responded to standard treatments. While its role remains uncertain, observational studies suggest it is effective for treating SLE and lupus nephritis.[84]

6.7. Investigational approaches

The investigational approach involves cellular therapies such as atacicept, anti-IL-6 receptor inhibitors, iberdomide, low-dose IL-2, obinutuzumab, daratumumab, anti-CD40 monoclonal antibody, litifilimab, and teclistamab. Details on ongoing clinical trials for SLE treatments in the US are available at www.clinicaltrials.gov.

7. Conclusion and future perspectives

SLE is a complex autoimmune disorder with significant global health implications. Its multifactorial etiology, involving genetic, environmental, and hormonal factors, leads to immune dysregulation and widespread organ damage. Despite advancements in understanding its pathogenesis, early diagnosis and effective management remain critical for improving patient outcomes. Although mortality rates have declined over the years, SLE continues to contribute to higher morbidity and mortality, particularly due to complications such as lupus nephritis and CVD. In regions, such as Saudi Arabia, where healthcare disparities and delayed diagnoses are common, SLE presents a substantial public health challenge.

The future of SLE management appears promising, with ongoing research exploring novel therapies, including cytokine inhibitors, cellular therapies, and personalized medicine approaches. Advances in biomarker discovery and the integration of artificial intelligence in disease monitoring have the potential to enhance early diagnosis and improve treatment precision. In addition, addressing gaps in healthcare access, particularly in underserved populations, will be crucial for improving global outcomes. Collaborative efforts among researchers, clinicians, and policymakers are essential for advancing SLE care, reducing its burden, and ultimately enhancing the quality of life for patients worldwide.

Acknowledgments

We acknowledge King Faisal Medical City for Southern Region (KFMCity), King Fahad Medical City, and King Khalid University for their support, and Palestine Polytechnic University for their collaboration. The figure presented in this paper was created using the BioRender software.

Funding

None.

Conflict of interest

The authors declare that they have no competing interests.

Author contributions

Conceptualization: Abdurahman Alloghbi, Fahad S. Alshehri
Writing – original draft: All authors
Writing – review & editing: Fahad S. Alshehri

Ethics approval and consent to participate

Not applicable.

Consent for publication

Not applicable.

Availability of data

Not applicable.

References

1. Tsokos GC. Systemic lupus erythematosus. *N Engl J Med*. 2011;365(22):2110-2121.

   doi: 10.1056/NEJMra1100359

2. Isenberg D, Ehrenstein M, Rahman A. Introduction to a systemic lupus erythematosus - biomarkers meeting held at University College London on 23rd and 24th February 2007. *Lupus*. 2008;17(3):231.

   doi: 10.1177/0961203307088257

3. Quirno N, Porrini A, Marino P, Iotti R. Causes of death in systemic lupus erythematosus. *Prensa Med Argent*. 1970. 57(22):1056-1059.

4. Fei Y, Shi X, Gan F, *et al*. Death causes and pathogens analysis of systemic lupus erythematosus during the past 26 years. *Clin Rheumatol*. 2014;33(1):57-63.

   doi: 10.1007/s10067-013-2383-3

5. Cojocaru M, Cojocaru IM, Silosi I, Vrabie CD. Manifestations of systemic lupus erythematosus. *Maedica* (*Bucur*). 2011;6(4):330-336.

6. Bertsias GK, Salmon JE, Boumpas DT. Therapeutic opportunities in systemic lupus erythematosus: State of the art and prospects for the new decade. *Ann Rheum Dis*. 2010;69(9):1603-1611.

   doi: 10.1136/ard.2010.135186

7. Stoddard CJ, Kay PH, Simms JM, Kennedy A, Hughes P. Acute abdominal complications of systemic lupus erythematosus. *Br J Surg*. 1978;65(9):625-628.

   doi: 10.1002/bjs.1800650911

8. Palmer DG. Systemic lupus erythematosus with cerebral complications. *N Z Med J*. 1988;101(840):91.

9. Pertschuk LP, *et al*. Acute pulmonary complications in systemic lupus erythematosus. Immunofluorescence and light microscopic study. *Am J Clin Pathol*. 1977;68(5):553-557.

doi: 10.1093/ajcp/68.5.553

10. Delaney P. Neurologic complications of systemic lupus erythematosus. *Am Fam Physician*. 1983;28(1):191-193.

11. Mukherjee S. Long term complications in systemic lupus erythematosus. J *Assoc Physicians India*. 2006;54 Suppl:22-26.

12. Moore JE, Shulman LE, Scott JT. The natural history of systemic lupus erythematosus: An approach to its study through chronic biologic false positive reactors: Interim report. *Trans Am Clin Climatol Assoc*. 1956;68:59-67; discussion 67-8.

13. Mak A, Cheung MW, Chiew HJ, Liu Y, Ho RC. Global trend of survival and damage of systemic lupus erythematosus: Meta-analysis and meta-regression of observational studies from the 1950s to 2000s. *Semin Arthritis Rheum*. 2012;41(6):830-839.

doi: 10.1016/j.semarthrit.2011.11.002

14. Yen EY, Shaheen M, Woo JM, *et al*. 46-year trends in systemic lupus erythematosus mortality in the United States, 1968 to 2013: A nationwide population-based study. *Ann Intern Med*. 2017;167(11):777-785.

doi: 10.7326/M17-0102

15. Brinks R, Fischer-Betz R, Sander O, Richter JG, Chehab G, Schneider M. Age-specific prevalence of diagnosed systemic lupus erythematosus in Germany 2002 and projection to 2030. *Lupus*. 2014;23(13):1407-1411.

doi: 10.1177/0961203314540352

16. Danchenko N, Satia JA, Anthony MS. Epidemiology of systemic lupus erythematosus: A comparison of worldwide disease burden. *Lupus*. 2006;15(5):308-318.

doi: 10.1191/0961203306lu2305xx

17. Wegman ME. Definition of mortality. *Pediatrics*. 1968;41(4):854-855.

18. Kan HJ, Song X, Johnson BH, Bechtel B, O'Sullivan D, Molta CT. Healthcare utilization and costs of systemic lupus erythematosus in Medicaid. *Biomed Res Int*. 2013;2013:808391.

doi: 10.1155/2013/808391

19. Urowitz MB, Gladman DD. How to improve morbidity and mortality in systemic lupus erythematosus. *Rheumatology (Oxford)*. 2000;39(3):238-244.

doi: 10.1093/rheumatology/39.3.238

20. Ling GS, Crawford G, Buang N, *et al*. C1q restrains autoimmunity and viral infection by regulating CD8(+) T cell metabolism. *Science*. 2018;360(6388):558-563.

doi: 10.1126/science.aao4555

21. Lee YJ, Park JA, Kwon H, *et al*. Role of stem cell-like memory T cells in systemic lupus erythematosus. *Arthritis Rheumatol*. 2018;70(9):1459-1469.

doi: 10.1002/art.40524

22. Fischer-Betz R, Herzer P, Schneider M. Systemic lupus erythematosus. *Dtsch Med Wochenschr*. 2005;130(43):2451-8; quiz 2459-60, 2461-2.

23. Ichikawa Y. Diagnosis and clinical symptoms of systemic lupus erythematosus and overlap syndrome. *Nihon Naika Gakkai Zasshi*. 1990;79(10):1360-1365.

24. Horiuchi A. Diagnosis and therapy of systemic lupus erythematosus. *Nihon Naika Gakkai Zasshi*. 1993;82(3):381-5.

25. Allard SA, Charles PJ, Herrick AL, McColl KE, Scott JT. Antinuclear antibodies and the diagnosis of systemic lupus erythematosus in patients with acute intermittent porphyria. *Ann Rheum Dis*. 1990;49(4):246-248.

doi: 10.1136/ard.49.4.246

26. Ho, A, Magder LS, Barr SG, Petri M. Decreases in anti-double-stranded DNA levels are associated with concurrent flares in patients with systemic lupus erythematosus. *Arthritis Rheum*. 2001;44(10):2342-2349.

doi: 10.1002/1529-0131(200110)44:10<2342:aid-art397>3.0.co;2-8

27. Smeenk R, Brinkman K, Van den Brink H, *et al*. Antibodies to DNA in patients with systemic lupus erythematosus. Their role in the diagnosis, the follow-up and the pathogenesis of the disease. *Clin Rheumatol*. 1990;9(1 Suppl):100-110.

doi: 10.1007/BF02205557

28. Ho A, Barr SG, Magder LS, Petri M. A decrease in complement is associated with increased renal and hematologic activity in patients with systemic lupus erythematosus. *Arthritis Rheum*. 2001;44(10):2350-2357.

doi: 10.1002/1529-0131(200110)44:10<2350:aid-art398>3.0.co;2-a

29. Tunnicliffe DJ, Singh-Grewal D, Kim S, Craig JC, Tong A. Diagnosis, monitoring, and treatment of systemic lupus erythematosus: A systematic review of clinical practice guidelines. *Arthritis Care Res (Hoboken)*. 2015;67(10):1440-1452.

doi: 10.1002/acr.22591

30. Alabduljabbar K, Alkhalifah M, Aldheshe A, *et al*. Development of a cardiovascular disease risk prediction model: A preliminary retrospective cohort study of a patient sample in Saudi Arabia. *J Clin Med*. 2023;12(15):5115.

doi: 10.3390/jcm12155115

31. Tash AA, Al-Bawardy RF. Cardiovascular disease in Saudi Arabia: Facts and the way forward. *J Saudi Heart Assoc*. 2023;35(2):148-162.

doi: 10.37616/2212-5043.1336

32. Alenzi EO, Fatima W, Amara A, *et al*. A systematic review of

chronic diseases and their prevalence among the population of northern borders province (NBP) in Saudi Arabia. *J Multidiscip Healthc*. 2023;16:1047-1056.

doi: 10.2147/JMDH.S401001

33. Alibrahim B, Sharaheeli J, Alassaf L, Abd-Ellatif EE. Risk assessment of cardiovascular disease among adults attending primary healthcare centers in Riyadh City 2015. *Cureus*. 2022;14(12):e32503.

doi: 10.7759/cureus.32503

34. Ghamri RA, Alzahrani NS, Alharthi AM, Gadah HJ, Badoghaish BG, Alzahrani AA. Cardiovascular risk factors among high-risk individuals attending the general practice at king Abdulaziz University hospital: A cross-sectional study. *BMC Cardiovasc Disord*. 2019;19(1):268.

doi: 10.1186/s12872-019-1261-6

35. Criswell LA. The genetic contribution to systemic lupus erythematosus. *Bull NYU Hosp Jt Dis*. 2008;66(3):176-183.

36. International Consortium for Systemic Lupus Erythematosus Genetics (SLEGEN), Harley JB, Alarcón-Riquelme ME, *et al*. Genome-wide association scan in women with systemic lupus erythematosus identifies susceptibility variants in ITGAM, PXK, KIAA1542 and other loci. *Nat Genet*. 2008;40(2):204-210.

doi: 10.1038/ng.81

37. Barbhaiya M, Costenbader KH. Ultraviolet radiation and systemic lupus erythematosus. *Lupus*. 2014;23(6):588-595.

doi: 10.1177/0961203314530488

38. James JA, Kaufman KM, Farris AD, Taylor-Albert E, Lehman TJ, Harley JB. An increased prevalence of Epstein-Barr virus infection in young patients suggests a possible etiology for systemic lupus erythematosus. *J Clin Invest*. 1997;100(12):3019-3026.

doi: 10.1172/JCI119856

39. Karpuzoglu E, Zouali M. The multi-faceted influences of estrogen on lymphocytes: Toward novel immuno-interventions strategies for autoimmunity management. *Clin Rev Allergy Immunol*. 2011;40(1):16-26.

doi: 10.1007/s12016-009-8188-0

40. Gazy NE, Fewings NL, Emerson J, Swaminathan S, Lee AY, Lin MW. Interferon signatures in systemic lupus erythematosus patients across ethnic groups. *Lupus*. 2023;32(10):1231-1232.

doi: 10.1177/09612033231194211

41. Vollmer J, Tluk S, Schmitz C, *et al*. Immune stimulation mediated by autoantigen binding sites within small nuclear RNAs involves Toll-like receptors 7 and 8. *J Exp Med*. 2005;202(11):1575-1585.

doi: 10.1084/jem.20051696

42. Tanaka Y, Kusuda M, Yamaguchi Y. Interferons and systemic lupus erythematosus: Pathogenesis, clinical features, and treatments in interferon-driven disease. *Mod Rheumatol*. 2023;33(5):857-867.

doi: 10.1093/mr/roac140

43. Baechler EC, Batliwalla FM, Karypis G, *et al*. Interferon-inducible gene expression signature in peripheral blood cells of patients with severe lupus. *Proc Natl Acad Sci U S A*. 2003;100(5):2610-2615.

doi: 10.1073/pnas.0337679100

44. Tran DQ. *In vitro* suppression assay for functional assessment of human regulatory T cells. *Methods Mol Biol*. 2013;979:199-212.

doi: 10.1007/978-1-62703-290-2_16

45. Postal M, Peliçari KO, Sinicato NA, Marini R, Costallat LT, Appenzeller S. Th1/Th2 cytokine profile in childhood-onset systemic lupus erythematosus. *Cytokine*. 2013;61(3):785-791.

doi: 10.1016/j.cyto.2012.11.023

46. Longhi MS, Ma Y, Grant CR, *et al*. T-regs in autoimmune hepatitis-systemic lupus erythematosus/mixed connective tissue disease overlap syndrome are functionally defective and display a Th1 cytokine profile. *J Autoimmun*. 2013;41:146-151.

doi: 10.1016/j.jaut.2012.12.003

47. McKinley PS, Ouellette SC, Winkel GH. The contributions of disease activity, sleep patterns, and depression to fatigue in systemic lupus erythematosus. A proposed model. *Arthritis Rheum*. 1995;38(6):826-834.

doi: 10.1002/art.1780380617

48. Cervera R, Khamashta MA, Font J, *et al*. Morbidity and mortality in systemic lupus erythematosus during a 10-year period: A comparison of early and late manifestations in a cohort of 1,000 patients. *Medicine (Baltimore)*. 2003;82(5):299-308.

doi: 10.1097/01.md.0000091181.93122.55

49. Greco CM, Rudy TE, Manzi S. Adaptation to chronic pain in systemic lupus erythematosus: Applicability of the multidimensional pain inventory. *Pain Med*. 2003;4(1):39-50.

doi: 10.1046/j.1526-4637.2003.03001.x

50. Miner JJ, Kim AH. Cardiac manifestations of systemic lupus erythematosus. *Rheum Dis Clin North Am*. 2014;40(1):51-60.

doi: 10.1016/j.rdc.2013.10.003

51. Richter JG, Sander O, Schneider M, Klein-Weigel P. Diagnostic algorithm for Raynaud's phenomenon and vascular skin lesions in systemic lupus erythematosus. *Lupus*. 2010;19(9):1087-1095.

doi: 10.1177/0961203310374304

52. Barile-Fabris L, Hernandez-Cabrera MF, Barragan-

Garfias JA. Vasculitis in systemic lupus erythematosus. *Curr Rheumatol Rep.* 2014;16(9):440.

doi: 10.1007/s11926-014-0440-9

53. Sarabi ZS, Chang E, Bobba R, *et al*. Incidence rates of arterial and venous thrombosis after diagnosis of systemic lupus erythematosus. *Arthritis Rheum*. 2005;53(4):609-612.

doi: 10.1002/art.21314

54. Danila MI, Pons-Estel GJ, Zhang J, Vilá LM, Reveille JD, Alarcón GS. Renal damage is the most important predictor of mortality within the damage index: Data from LUMINA LXIV, a multiethnic US cohort. *Rheumatology* (*Oxford*). 2009;48(5):542-545.

doi: 10.1093/rheumatology/kep012

55. Tian XP, Zhang X. Gastrointestinal involvement in systemic lupus erythematosus: Insight into pathogenesis, diagnosis and treatment. *World J Gastroenterol*. 2010;16(24):2971-2977.

doi: 10.3748/wjg.v16.i24.2971

56. Romero-Diaz J, Garcia-Sosa I, Sanchez-Guerrero J. Thrombosis in systemic lupus erythematosus and other autoimmune diseases of recent onset. *J Rheumatol*. 2009;36(1):68-75.

doi: 10.3899/jrheum.071244

57. Newman K, Owlia MB, El-Hemaidi I, Akhtari M. Management of immune cytopenias in patients with systemic lupus erythematosus - old and new. *Autoimmun Rev*. 2013;12(7):784-791.

doi: 10.1016/j.autrev.2013.02.001

58. Silpa-Archa S, Lee JJ, Foster CS. Ocular manifestations in systemic lupus erythematosus. *Br J Ophthalmol*. 2016;100(1):135-141.

doi: 10.1136/bjophthalmol-2015-306629

59. Gallais Serezal I, Bouillet L, Dhôte R, *et al*. Hereditary angioedema and lupus: A French retrospective study and literature review. *Autoimmun Rev*. 2015;14(6):564-568.

doi: 10.1016/j.autrev.2015.02.001

60. Abu-Shakra M, Gladman DD, Urowitz MB, Farewell V. Anticardiolipin antibodies in systemic lupus erythematosus: Clinical and laboratory correlations. *Am J Med*. 1995;99(6):624-628.

doi: 10.1016/s0002-9343(99)80249-6

61. Haliloglu S, Carlioglu A, Akdeniz D, Karaaslan Y, Kosar A. Fibromyalgia in patients with other rheumatic diseases: Prevalence and relationship with disease activity. *Rheumatol Int*. 2014;34(9):1275-1280.

doi: 10.1007/s00296-014-2972-8

62. Ferrari SM, Elia G, Virili C, Centanni M, Antonelli A, Fallahi P. Systemic lupus erythematosus and thyroid autoimmunity. *Front Endocrinol (Lausanne)*. 2017;8:138.

doi: 10.3389/fendo.2017.00138

63. Armas Cruz R. Diagnosis of systemic lupus erythematosus (SLE). *Rev Med Chil*. 1967;95(10):628-641.

64. Gilboe IM, Husby G. Application of the 1982 revised criteria for the classification of systemic lupus erythematosus on a cohort of 346 Norwegian patients with connective tissue disease. *Scand J Rheumatol*. 1999;28(2):81-87.

doi: 10.1080/030097499442531

65. Pincus T. A pragmatic approach to cost-effective use of laboratory tests and imaging procedures in patients with musculoskeletal symptoms. *Prim Care*. 1993;20(4):795-814.

66. Tan EM, Cohen AS, Fries JF, *et al*. The 1982 revised criteria for the classification of systemic lupus erythematosus. *Arthritis Rheum*. 1982;25(11):1271-1277.

doi: 10.1002/art.1780251101

67. Brydak-Godowska J. General and ocular symptoms in systemic lupus erythematosus (SLE). *Klin Oczna*. 2007;109(1-3):68-70.

68. Attman PO, Larsson O, Westberg G. Diagnosis, therapy and follow-up of patients with SLE. *Lakartidningen*. 1978;75:2218-2219.

69. Villalta D, Romelli PB, Savina C, *et al*. Anti-dsDNA antibody avidity determination by a simple reliable ELISA method for SLE diagnosis and monitoring. *Lupus*. 2003;12(1):31-36.

doi: 10.1191/0961203303lu277oa

70. Londhey VA. Anti-nucleosome antibodies: Utility in diagnosis of SLE and monitoring disease activity. *J Assoc Physicians India*. 2013;61(6):369-370.

71. Alba P, Bertolaccini ML, Khamashta MA. The use of laboratory methods in differential diagnosis and treatment of SLE and antiphospholipid syndrome. E*xpert Rev Clin Immunol*. 2007;3(4):613-622.

doi: 10.1586/1744666X.3.4.613

72. Tamburino C, Fiore CE, Foti R, Salomone E, Di Paola R, Grimaldi DR. Endomyocardial biopsy in diagnosis and management of cardiovascular manifestations of systemic lupus erythematosus (SLE). *Clin Rheumatol*. 1989;8(1):108-112.

doi: 10.1007/BF02031079

73. Yasue T, Akutsu J, Shinjo H, Sasada K. The significance of serum concentration of C3 and C4 for the diagnosis, prognosis and treatment of SLE. *Nihon Hifuka Gakkai Zasshi*. 1975;85(14):875-83.

74. Hess C. Systemic lupus erythematosus (SLE)--a brief guide to its diagnosis. *Ther Umsch*. 2005;62(5):297-301.

doi: 10.1024/0040-5930.62.5.297

75. Bravo MG, Alarcon-Segovia D. C-reactive protein in the differential diagnosis between infection and disease reactivation in SLE. *J Rheumatol*. 1981;8(2):291-294.

76. Egner W. The use of laboratory tests in the diagnosis of SLE. *J Clin Pathol*. 2000;53(6):424-432.

doi: 10.1136/jcp.53.6.424

77. Lehmann P, Homey B. Clinic and pathophysiology of photosensitivity in lupus erythematosus. *Autoimmun Rev*. 2009;8(6):456-461.

doi: 10.1016/j.autrev.2008.12.012

78. Cai T, Zhao J, Yang Y, Jiang Y, Zhang JA. Hydroxychloroquine use reduces mortality risk in systemic lupus erythematosus: A systematic review and meta-analysis of cohort studies. *Lupus*. 2022;31(14):1714-1725.

doi: 10.1177/09612033221129774

79. Ruiz-Irastorza G, Ramos-Casals M, Brito-Zeron P, Khamashta MA. Clinical efficacy and side effects of antimalarials in systemic lupus erythematosus: A systematic review. *Ann Rheum Dis*. 2010;69(1):20-28.

doi: 10.1136/ard.2008.101766

80. Belmon HM. Treatment of systemic lupus erythematosus - 2013 update. *Bull Hosp Jt Dis (2013)*. 2013;71(3):208-213.

81. Tanaka Y. State-of-the-art treatment of systemic lupus erythematosus. *Int J Rheum Dis*. 2020;23(4):465-471.

doi: 10.1111/1756-185X.13817

82. Merrill JT, Furie R, Werth VP, *et al*. Anifrolumab effects on rash and arthritis: Impact of the type I interferon gene signature in the phase IIb MUSE study in patients with systemic lupus erythematosus. *Lupus Sci Med*. 2018;5(1):e000284.

doi: 10.1136/lupus-2018-000284

83. Singh JA, Shah NP, Mudano AS. Belimumab for systemic lupus erythematosus. *Cochrane Database Syst Rev*. 2021;2(2):CD010668.

doi: 10.1002/14651858.CD010668.pub2

84. Leandro M, Isenberg DA. Rituximab - the first twenty years. *Lupus*. 2021;30(3):371-377.

doi: 10.1177/0961203320982668

ACCSCIENCE PUBLISHING

Eurasian Journal of Medicine and Oncology

REVIEW ARTICLE

Dynamics of *FLT3* mutations in acute myeloid leukemia: A systematic review and meta-analysis of shifts between diagnosis and relapsed/refractory disease

Lais Teixeira, Camilla Correia, Alini Ponte, Diego Miranda, Felipe Feistauer, and Marco Aurélio Salvino*

Postgraduate Program in Medicine and Health, Professor Edgard Santos University Hospital, Medical School, Universidade Federal da Bahia (UFBA), Salvador (BA), Brazil

Abstract

Acute myeloid leukemia (AML) is a hematologic malignancy with a generally poor prognosis. Technological advances in molecular diagnosis have identified genetic alterations driving AML pathogenesis, among which FMS-like tyrosine kinase 3 (*FLT3*) mutations are significant. These mutations hold prognostic value and are increasingly recognized as potential markers for disease monitoring. This systematic review and meta-analysis aimed to assess the prevalence of changes in *FLT3* mutational status in adult patients with relapsed or refractory AML compared to their status at initial diagnosis. A relevant proportion of patients who were *FLT3*-wildtype at diagnosis were found to be *FLT3*-mutated on relapse, emphasizing the importance of continuous mutation monitoring. Subgroup analyses were also performed, and mutation shift rates were reported across both *FLT3* internal tandem duplication and tyrosine kinase domain subtypes. These findings illustrate the genetic evolution of leukemic clones and support the need for tailored therapeutic approaches based on the mutational profile at different disease stages. This study further highlights the diagnostic and clinical utility of routine molecular reassessment and offers practical recommendations for integrating *FLT3* retesting into standard AML management.

Keywords: Acute myeloid leukemia; FMS-like tyrosine kinase 3 mutation; FMS-like tyrosine kinase 3; Molecular biology

***Corresponding author:**
Marco Aurélio Salvino
(marcohemato@ufba.br)

Citation: Teixeira L, Correia C, Ponte A, Miranda D, Feistauer F, Salvino MA. Dynamics of *FLT3* mutations in acute myeloid leukemia: A systematic review and meta-analysis of shifts between diagnosis and relapsed/refractory disease. *Eurasian J Med Oncol.* 2025;9(3):63-74.
doi: 10.36922/EJMO025150101

Received: April 10, 2025

Revised: June 17, 2025

Accepted: July 16, 2025

Published online: August 7, 2025

Copyright: © 2025 Author(s). This is an Open Access article distributed under the terms of the Creative Commons Attribution License, permitting distribution, and reproduction in any medium, provided the original work is properly cited.

Publisher's Note: AccScience Publishing remains neutral with regard to jurisdictional claims in published maps and institutional affiliations.

1. Introduction

Acute myeloid leukemia (AML) is a hematologic malignancy that primarily affects elderly individuals over the age of 60 years. Despite advances in supportive care therapies, AML remains associated with a poor prognosis, with an estimated 5-year overall survival rate of approximately 40%.[1] Studies conducted at the University Hospital of the Federal University of Bahia reported a median overall survival of only 7–8 months among adult patients.[2,3] Given this clinical reality, a deeper understanding of the disease's pathophysiology is essential for identifying prognostic markers and therapeutic targets.

Advancements in molecular biology have significantly reshaped the AML landscape, particularly by enabling the identification of actionable mutations that may be targeted

to improve patient survival. The success of targeted therapy in chronic myeloid leukemia, for example, where the discovery of the *BCR/ABL* fusion gene led to the development of tyrosine kinase inhibitors (TKIs), illustrates the transformative potential of molecularly guided treatments.[4]

FMS-like tyrosine kinase 3 (*FLT3*) mutations, first described in 1996,[5] are now recognized as the most common genetic alterations in AML. These mutations are associated with adverse prognostic implications and poor overall survival.[6] FLT3 belongs to the class III receptor tyrosine kinase family. These receptors are characterized by a membrane-bound structure comprising five extracellular immunoglobulin-like domains and an intracellular catalytic region. This catalytic region is divided into two kinase domains (TKD1 and TKD2), separated by a hydrophilic insert of variable length. Members of this receptor family include FMS (macrophage colony-stimulating factor receptor), platelet-derived growth factor receptor α and β, KIT (stem cell factor receptor), and FLK-2/FLT3.[7,8] These proteins play a pivotal role in the regulation of hematopoietic cell proliferation, differentiation, and survival.

Structurally, FLT3 comprises an extracellular transmembrane domain, a juxtamembrane domain (JMD) within the cytoplasm, and two intracellular tyrosine kinase domains (TKD1 and TKD2), which are connected through a linker segment. The JMD is further subdivided into three functional regions: A binding site (JM-B), involved in receptor activation and stabilization of the inactive conformation; a switching region (JM-S), which includes phosphorylation sites and a binding site for STAT5; and a ligand segment (JM-Z). Mutant FLT3 receptors exhibit constitutive, ligand-independent activation that contributes to leukemogenesis by promoting uncontrolled proliferation (class I mutations). In contrast, class II mutations impair hematopoietic differentiation. Importantly, class I mutations typically occur at later stages of leukemogenesis and require coexisting molecular lesions to fully transform hematopoietic progenitors into leukemic clones. Two main classes of mutations have been identified. The first comprises internal tandem duplications (ITDs), most commonly affecting exons 14 and 15 within the JMD. *FLT3*-ITD mutations are observed in approximately 25% of AML cases. The second class involves point mutations within the activation loop of the TKD, particularly in TKD2, and occurs in about 5% of cases. These are collectively referred to as *FLT3*-TKD mutations.[9,10]

FLT3 mutations–particularly the ITD subtype–have been consistently associated with leukocytosis at diagnosis. Although induction therapy often results in similar initial complete remission rates (~70%) regardless of *FLT3* mutational status, patients harboring *FLT3*-ITD mutations exhibit significantly higher relapse rates. One study reported a median disease-free survival of 8.4 months in *FLT3*-mutated AML versus 12.8 months in wild-type cases. Similarly, overall survival was reduced in *FLT3*-mutated patients (12 months vs. 15 months).[11-13] *FLT3*-ITD mutations are more frequently observed in *de novo* AML compared to AML secondary to myelodysplasia. *FLT3*-TKD mutations, on the other hand, have demonstrated less consistent prognostic impact. The limited number of patients with these mutations in published studies hinders the ability to draw robust conclusions. Unlike *FLT3*-ITD, *FLT3*-TKD is not associated with elevated leukocyte counts, possibly reflecting distinct downstream signaling mechanisms.[14]

The therapeutic landscape of AML with *FLT3* mutations has evolved significantly with the advent of targeted agents, resulting in substantial improvements in patient outcomes. Phase III clinical trials in both newly diagnosed and relapsed/refractory settings have demonstrated that FLT3 inhibitors increase the likelihood of achieving measurable residual disease (MRD)-negative remission, even in the absence of allogeneic hematopoietic stem cell transplantation.

In the relapse setting–historically associated with extremely poor outcomes–the availability of FLT3 inhibitors has translated into improved remission rates.[15] and survival, particularly in patients ineligible for transplantation. Moreover, responses to these agents have been associated with enhanced performance status and quality of life, allowing some patients previously deemed unfit to become eligible for curative-intent transplant procedures. This is particularly relevant, given that allogeneic stem cell transplantation remains the only potentially curative strategy in relapsed AML. Despite these advances, the long-term prognosis in this patient population remains poor, with overall cure rates below 10%.[16] Ongoing studies are investigating various combination regimens involving FLT3 inhibitors, as monotherapy–though approved in many countries, including Brazil–is generally insufficient for achieving durable remissions in most cases.[17]

Evidence suggests that *FLT3* mutational profiles may change over time, with patients either losing or acquiring *FLT3* mutations at relapse despite their initial diagnostic status.[18] These changes have important therapeutic implications. Several targeted agents–such as midostaurin, gilteritinib, and quizartinib–have been developed for patients with *FLT3* mutations. As a result, understanding the dynamics of *FLT3* mutational status and incorporating

routine reassessment using polymerase chain reaction (PCR) and next-generation sequencing (NGS) may inform prognosis and guide therapeutic strategies. In some cases, such reassessment may enable the use of FLT3 inhibitors, which can enable the patient to undergo curative treatment - bone marrow transplant.

Beyond their prognostic therapeutic value, *FLT3* mutations have also been investigated as potential markers for disease monitoring. Currently, treatment response is often assessed through flow cytometry-based immunophenotyping to detect MRD through abnormal surface markers. This approach has been validated as a prognostic tool that correlates with relapse risk and treatment response.[18] The combination of flow cytometry with molecular assays—such as PCR and NGS—further enhances prognostic accuracy. Some mutations, such as those in the *NPM1* gene, are considered reliable MRD markers.[19] However, the role of *FLT3* mutations in this context remains controversial due to their unstable behavior during disease evolution.

Reassessment of *FLT3* mutational status at relapse is critical, given its profound therapeutic implications. The clinical course of patients with *FLT3*-mutated relapse who do not receive a FLT3 inhibitor is uniformly poor, and targeted therapy may represent the only viable option for disease control or remission. Importantly, evidence suggests that *FLT3* mutations may emerge at relapse in patients who were *FLT3*-wild type at diagnosis, highlighting the dynamic nature of the leukemic clone. Although current data remain limited and somewhat inconclusive, they underscore the necessity of routine molecular reassessment during disease progression. These dynamic shifts in clonal architecture have profound clinical implications. The acquisition of new mutations—either within *FLT3* or in other oncogenic drivers—can lead to increased proliferation, therapeutic resistance, and disease aggressiveness. For example, secondary *FLT3*-TKD mutations (e.g., N676K, F691L, A627P, Y842C) may arise during treatment with midostaurin or second-generation FLT3 inhibitors, conferring resistance.[20-22] In parallel, mutations in other genes, such as *ASXL1*, *WT1*, and *KMT2A*, may further impair prognosis and treatment responsiveness.[23]

Despite current recommendations advocating for comprehensive molecular profiling in all cases of newly diagnosed AML—particularly in patients with cytogenetically normal AML (CN-AML)—the universal implementation of *FLT3* testing remains suboptimal. Retrospective registry data have indicated that in some centers, only 77% of patients with CN-AML underwent *FLT3* mutational analysis. Alarmingly, this disparity is more pronounced when comparing academic centers to community-based institutions, likely reflecting unequal access to molecular diagnostics and variable awareness regarding the clinical utility of these tests.[24,25]

Additional data from a cohort at the Hospital das Clínicas of the Federal University of Bahia (UFBA) revealed that nearly half (47%) of patients could not be adequately risk-stratified according to the 2022 European Leukemia Net guidelines due to the absence of molecular data. Furthermore, only 21% of patients had any molecular reassessment throughout their disease.[2] Although the recommendation to perform *FLT3* testing in all CN-AML cases dates back to 2010, this gap in implementation underscores a persistent challenge in real-world practice. These shifts in the mutational profile underscore the need for routine molecular reassessment, especially in the setting of relapse or refractory disease.

Given the increasing availability of *FLT3*-targeted therapies, identifying the mutational status at each disease stage is critical. Previous studies suggest that *FLT3* mutations may emerge at relapse in initially *FLT3*-wild type patients. Timely identification of an actionable *FLT3* mutation may significantly impact therapeutic decision-making and alter the clinical course—even offering curative options in otherwise adverse scenarios. Understanding this shift is critical for tailoring therapy.

This study aims to systematically evaluate published evidence on the dynamics of *FLT3* mutations in adult patients with AML, comparing the mutation status at diagnosis and relapse or refractory disease. The objectives are to (i) quantify the *FLT3* mutation shift rate, (ii) distinguish changes between *FLT3*-ITD and *FLT3*-TKD subtypes, (iii) assess methodological variability, (iv) explore corresponding clinical implications, and (v) provide evidence-based recommendations for routine molecular retesting.

2. Methods

2.1. Search strategy

An initial literature search was conducted in June 2020 using the PubMed database to identify studies relevant to the research area. Search terms were selected based on Medical Subject Headings (MeSH) and included: "fms-like tyrosine kinase 3" OR "Fetal Liver Kinase-2" OR "Fetal Liver Kinase 2" OR "Fetal Liver Kinase-3" OR "Fetal Liver Kinase 3" OR "CD135 Antigens" OR "Antigens, CD135" OR "CD135 Antigen" OR "Antigen, CD135" OR "Stem Cell Tyrosine Kinase 1" OR "FLT3" AND "Leukemia, Myeloid, Acute"[MeSH] OR "Acute Myeloid Leukemia" OR "ANLL" OR "Leukemia, Acute Myelogenous" OR

"Leukemia*, Acute Myeloid" OR "Leukemia, Myeloblastic, Acute" OR "Leukemia, Myelocytic, Acute" OR "Leukemia, Myelogenous, Acute" OR "Leukemia, Nonlymphoblastic, Acute" OR "Leukemia, Nonlymphocytic, Acute" OR "Myeloblastic Leukemia*, Acute" OR "Acute Myeloblastic Leukemia*" OR "Leukemia*, Acute Myeloblastic" OR "Myelocytic Leukemia*, Acute" OR "Acute Myelocytic Leukemia*" OR "Leukemia*, Acute Myelocytic" OR "Myelogenous Leukemia, Acute" OR "Myeloid Leukemia*, Acute" OR "Nonlymphoblastic Leukemia*, Acute" OR "Acute Nonlymphoblastic Leukemia*" OR "Leukemia*, Acute Nonlymphoblastic" OR "Nonlymphocytic Leukemia*, Acute" OR "Acute Nonlymphocytic Leukemia*" OR "Leukemia*, Acute Nonlymphocytic" OR "Acute Myelogenous Leukemia*" OR "Leukemias, Acute Myelogenous" OR "Myelogenous Leukemias, Acute" OR "Myeloid Leukemia, Acute, M1" OR "Leukemia, Myeloid, Acute, M1" OR "Acute Myeloid Leukemia without Maturation" OR "Leukemia, Myeloid, Acute, M2" OR "Myeloid Leukemia, Acute, M2" OR "Acute Myeloid Leukemia with Maturation*" AND "Recurrence"[MeSH terms] OR "Recrudescence" OR "Recrudescences" OR "Recurrences" OR "Relapse" OR "Relapses."

No date restriction was applied. An updated search was conducted in July 2024 to include newly published articles. After the initial screening of titles and abstracts, eligible articles were selected for full-text review. No articles were excluded due to sample size. No particular subgroup of AML was selected for analysis.

2.2. Inclusion and exclusion criteria

Studies were included if they: (i) investigated adult patients with AML; (ii) were written in English, Spanish, or Portuguese; (iii) employed PCR as the method for detecting *FLT3* mutations, as it is considered the current gold standard; and (iv) reported *FLT3* mutational status at both diagnosis and relapse/refractory stages. The exclusion criteria were: (i) studies exclusively involving pediatric populations, (ii) studies focusing solely on acute promyelocytic leukemia; (iii) phase I interventional clinical trials; (iv) preclinical studies; (v) review articles, letters to the editor, and case reports; and (vi) studies lacking data on paired samples or failing to report *FLT3* mutational status at both relevant time points.

2.3. Study selection and data extraction

Articles were screened by one of the authors (L.T.). The selection process involved reviewing the title and abstract, followed by a methodological analysis of each study to identify the technique used for mutation analysis (PCR vs. NGS) and whether the evaluation was performed using paired samples. After the initial selection, full-text articles were read to ensure eligibility. Subsequently, the reference lists of each included article were reviewed to identify any additional studies that may have been missed during the database search.

Data were collected from retrospective, prospective, or interventional studies involving patients with relapsed/refractory AML. Extracted data included study design, year of publication, number of patients, *FLT3* mutational status at diagnosis and relapse using paired samples, type of *FLT3* mutation (ITD, TKD, or wild-type), as well as karyotype, French–American–British (FAB) classification, and allelic burden. *FLT3* mutational status was considered to have changed if paired samples from the same patient displayed different results at diagnosis and the relapse/refractory stage. The study's article inclusion flowchart, based on PRISMA methodology, is presented in Figure 1.

3. Results

Following the initial search conducted in 2020, 1,201 articles were identified. After screening the titles and abstracts, 513 were selected for further analysis. Of these, after evaluation of the methodology and results, 12 articles were eligible for full-text review, and an additional five were retrieved through manual reference list searches. Among the full-texts reviewed, five were excluded due to a lack of relevant data on *FLT3* mutational status, and one due to divergent population selection criteria.

In the updated 2024 search, 1,641 articles were retrieved. After screening, 161 were selected based on titles and abstracts. Of these, 56 underwent full-text analysis; 19 studies were excluded for not using PCR as the detection method, 10 overlapped with the initial search, and 16 did not report paired sample data or detailed mutational profiles. In addition, two were excluded for comparing different PCR techniques, and nine were ultimately included. In total, 20 studies met the inclusion criteria (Figure 1).

All included studies employed PCR as the method for *FLT3* mutational analysis; 11 studies assessed both *FLT3*-ITD and *FLT3*-TKD, eight assessed only *FLT3*-ITD, and one focused exclusively on *FLT3*-TKD (Table 1). The year of publication of the works selected in this study ranged from 1999 to 2014. Only three studies were prospective; the others were retrospective. Just one study that evaluated both *FLT3*-ITD and *FLT3*-TKD indicated robust longitudinal data with paired samples.

The quality of the studies varied substantially. Only one-third of publications had samples larger than 100 patients. However, several studies with smaller numbers of patients (<50) were included for data aggregation. The study by

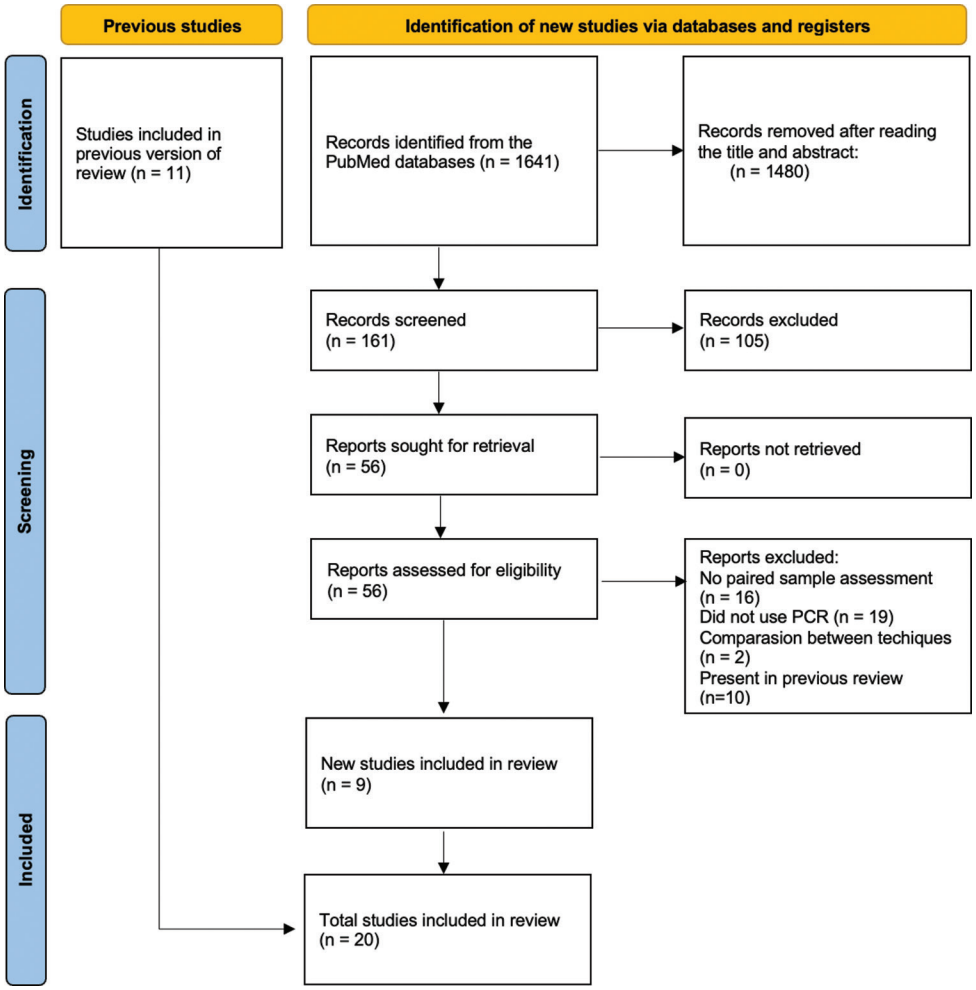


Figure 1. Flowchart of study selection and inclusion based on eligibility criteria for systematic review
Abbreviation: PCR: Polymerase chain reaction.

Shih *et al.*[45] focused on data from *FLT3*-TKD and included a robust patient cohort, providing valuable data to the analysis—particularly important given that TKD was the least studied *FLT3* mutation among the selected articles.

A total of 1,094 patients with relapsed or refractory AML were included. At diagnosis, 294 patients (26%) were *FLT3*-ITD-positive and 30 (3%) were *FLT3*-TKD-positive. At first relapse or refractory disease, 317 (29%) were *FLT3*-ITD-positive and 31 (3%) were *FLT3*-TKD-positive, in agreement with data described in the literature. A change in mutational status was observed in 147 patients (13%), indicating that approximately one in seven patients experienced a shift in *FLT3* status. Notably, 5% of patients had missing mutational data at relapse. Pediatric patients ($n = 42$) included in the study by Cloos *et al.*[30] were excluded from the final analysis.

Among patients for whom *FLT3*-ITD evolution could be evaluated ($n = 936$), 222 (24%) maintained the mutation, 46 (5%) became negative, and 73 (8%) acquired the mutation during disease progression, indicating a 13% mutation shift rate (*i.e.*, one in seven patients) (Figure 2).

In the subset of 543 patients with *FLT3*-TKD data (reported in only 10 studies), 14 (2%) retained the mutation, 20 (3%) lost it, and 15 (3%) acquired it at relapse—a shift rate of 6%, or approximately one in 17 patients (Figure 3).

In addition, five cases of double mutation (*FLT3*-ITD/TKD) exhibited dynamic changes; three patients were *FLT3*-ITD/TKD-positive at diagnosis and became *FLT3*-ITD-positive with *FLT*-TKD negative; one patient acquired the double mutation at relapse, and another one who at relapse became negative for both mutations.

Overall, 36% of the studied population tested positive for the *FLT3* mutation at some point during the disease course.

For a more accurate analysis, we extracted individual patient data, some of which included information on

Table 1. Summary of included studies

Study	Year of publication	Number of patients	Mutation (s) evaluated	References
Kottaridis *et al.*	2002	44	*FLT3*-ITD; *FLT3*-TKD	26
Nakamura *et al.*	2004	24	*FLT3*-ITD; *FLT3*-TKD	27
Tiesmeier *et al.*	2004	31	*FLT3*-ITD; *FLT3*-TKD	28
Suzuki *et al.*	2005	39	*FLT3*-ITD; *FLT3*-TKD	29
Cloos *et al.*	2006	38	*FLT3*-ITD; *FLT3*-TKD	30
Palmisano *et al.*	2007	28	*FLT3*-ITD; *FLT3*-TKD	31
Schnittger *et al.*	2009	80	*FLT3*-ITD; *FLT3*-TKD	32
McCormick *et al.*	2010	50	*FLT3*-ITD; *FLT3*-TKD	33
Wang *et al.*	2010	17	*FLT3*-ITD; *FLT3*-TKD	34
Wakita *et al.*	2012	34	*FLT3*-ITD; *FLT3*-TKD	35
Janke *et al.*	2014	156	*FLT3*-ITD; *FLT3*-TKD	36
Nakano *et al.*	1999	28	*FLT3*-ITD	37
Shih *et al.*	2002	108	*FLT3*-ITD	38
Schnittger *et al.*	2004	97	*FLT3*-ITD	39
Park *et al.*	2011	69	*FLT3*-ITD	40
Abdelhamid *et al.*	2012	8	*FLT3*-ITD	41
Bachas *et al.*	2012	6	*FLT3*-ITD	42
Nazha *et al.*	2012	102	*FLT3*-ITD	43
Gourdin *et al.*	2014	15	*FLT3*-ITD	44
Shih *et al.*	2004	120	*FLT3*-TKD	45

karyotype and FAB classification profile. From this dataset, we had a total of 384 patients. Among patients with *FLT3*-ITD at diagnosis ($n = 160$), 123 had their FAB classification described, with types M2, M1, and M4 being the most frequent, at 29%, 27%, and 22%, respectively. Among ITD patients who switched to TKD, one was M5 and the other M4. Among ITD cases that became negative, five were M4 and eight were M1. Among TKD cases that converted to ITD, two were M2, one was M5, and one was M4. Among TKD patients at diagnosis who became negative, four were M1. There were a total of five patients with double mutation, all M2 at diagnosis, four with normal karyotype, and one with *MLL*-PTD mutation.

When analyzing the karyotype of these patients, among the nine with available data who changed from ITD to negative, two had the +8 mutation, which persisted at relapse, two displayed normal karyotype at both diagnosis and relapse, and one changed from normal karyotype to complex. Among patients who were negative at diagnosis and acquired the ITD mutation at relapse, four had normal karyotypes, none had a complex karyotype, and one had core binding factor t(8;21), which remained after relapse. Out of a total of 26 patients, 14 had missing karyotype data at some point in the disease. Among those who converted to TKD ($n = 10$), two had a karyotype that changed from normal at diagnosis to complex at relapse, and one maintained a complex karyotype throughout the disease. The study by Nakano *et al.*,[37] despite a small number of patients, was one of the first to perform a paired assessment of molecular alterations in AML; however, it used cytogenetic alterations in the progression of the disease as the primary analysis.

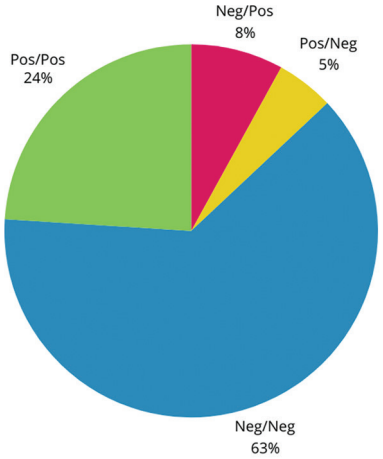


Figure 2. Change in *FLT3*-ITD mutational status between diagnosis and relapse/refractory disease

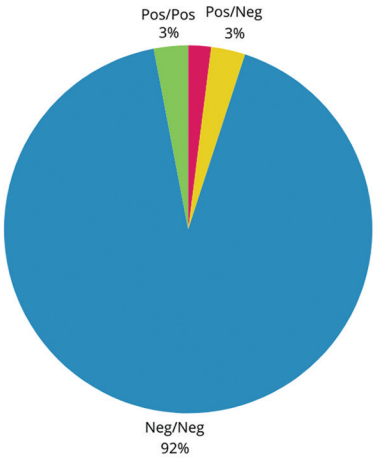


Figure 3. Change in *FLT3*-TKD mutational status between diagnosis and relapse/refractory disease

All studies were cohort designs and evaluated using the Newcastle-Ottawa Quality Assessment Scale (Table 2).

4. Discussion

The present study is the first systematic review and meta-analysis investigating *FLT3* mutational shifts in AML, incorporating data from over 1,000 patients. The prevalence of *FLT3* mutations observed aligned with previous reported rates in the literature. Notably, our analysis revealed that approximately one in seven patients exhibited a change in *FLT3* mutation status between diagnosis and relapse or refractory disease. Such a frequency is not negligible and reinforces the recommendation for molecular reassessment at multiple time points during the disease course. The increasing use of mutation-guided therapies in AML underscores the need for accurate and dynamic mutational profiling. Identifying the emergence or loss of actionable mutations can prevent the administration of potentially toxic therapies with limited benefit in mutation-negative patients, and conversely, guide the appropriate use of targeted agents in those who acquire relevant mutations.

Table 2. Newcastle–Ottawa Scale quality assessment scores for included studies

Study	Selection	Comparability	Outcome	References
Shih *et al.*	****	*	***	45
Nazha *et al.*	****	*	**	43
Shih *et al.*	****	*	***	38
Nakano *et al.*	****	*	***	37
McCormick *et al.*	****	*	***	33
Cloos *et al.*	****	*	***	30
Palmisano *et al.*	****	*	***	31
Suzuki *et al.*	****	*	***	32
Tiesmeier *et al.*	****	*	***	28
Kottaridis *et al.*	****	*	***	26
Schnittger *et al.*	**	*	***	32
Gourdin *et al.*	****	*	***	44
Janke *et al.*	****	*	**	36
Wakita *et al.*	****	*	***	35
Park *et al.*	****	**	***	40
Wang *et al.*	***	**	***	34
Schnittger *et al.*	****	**	***	32
Bachas *et al.*	***	*	***	42
Abdelhamid *et al.*	***	*	***	41
Nakamura *et al.*	*	*	**	27

Notes: The Newcastle–Ottawa Quality Assessment Scale checklists adapted for cross-sectional and cohort studies. *Asterisks correspond to ratings assigned for each item according to The Newcastle–Ottawa Quality Assessment Scale.

These findings have therapeutic implications and can impact patient survival. In some cases, identifying a newly acquired mutation could provide eligibility for the only potentially curative option in relapsed or refractory AML (i.e., bone marrow transplantation).

This discrepancy may be associated with inherent limitations of the detection method itself. It is well known that molecular technologies have improved over the years. Currently, the most recommended PCR method for *FLT3* analysis is fragment analysis. In our evaluation, some older studies used gel-based PCR as the detection method, which has lower sensitivity. It is also important to consider the possibility of false negatives. PCR is a method that has difficulty detecting very short fragments, identifying mutations in previously undescribed regions, and provides only limited information, such as size, number, and allelic burden. It does not provide additional details about the sequence or its specific location, nor can it distinguish between homozygous and heterozygous mutations. Nevertheless, PCR is a more accessible method compared to NGS and yields results more rapidly. Therefore, the sensitivity of the technique may influence the findings.

Another contributing factor is the nature of the mutation itself. Some studies suggest that *FLT3* mutations may emerge later in the course of AML, following a branched clonal evolution model. This may occur due to external factors, such as chemotherapy or alterations in the bone marrow microenvironment. For example, a new subclone or one that was present at undetectable levels may acquire a selective advantage over other clones, leading to its proliferation and potential dominance. Alternatively, the mutation may already be the predominant clone at diagnosis. In such cases, it may be eliminated by treatment or reduced to levels below the detection limit.

There is an ongoing debate in the literature regarding the utility of *FLT3* as a measurable residual disease marker and its prognostic significance in AML. The previously described instability in its mutational status limits its application for MRD monitoring.

Some studies have suggested that the acquisition of *FLT3* mutations in relapsed AML is associated with an adverse prognosis,[46] with outcomes comparable to patients who remain *FLT3*-mutated at both diagnosis and relapse. Notably, the absence of *FLT3* mutations at relapse has been associated with a more favorable prognosis when compared to patients who remain FLT3-mutated.[9] In the current review, it was not possible to evaluate clinical outcomes such as overall survival, as only a minority of studies reported this information. Furthermore, data regarding cytogenetic and cytomorphologic changes were insufficient for analysis, as these parameters were not mandatory

inclusion criteria in most studies. Consequently, only descriptive analysis was feasible. In addition, the impact of FLT3 allelic burden on prognosis could not be assessed due to a lack of extractable data.

In all studies included in the present review, *FLT3* mutation detection was performed using PCR, the most widely adopted method in clinical practice. With the advancement of molecular diagnostics, more sensitive techniques have emerged, offering enhanced mutation detection and broader genomic insights beyond the scope of conventional PCR. NGS, for example, has gained traction in AML diagnostics; however, its sensitivity in detecting *FLT3*-ITD mutations is limited by mutation size and allele frequency. Moreover, studies have highlighted variability even among PCR-based assays. The PCR method of choice for this type of assessment is fragment analysis PCR, which is more modern and sensitive. In the present review, some of the included studies were older and employed gel-based PCR, which may have contributed to false-negative results. In the context of clinical research, there has been a growing trend toward combining PCR and NGS methodologies, thereby improving mutation detection and enabling more refined genomic characterization. As previously reported,[47,48] this hybrid approach holds clinical relevance in identifying resistance profiles to TKIs and may become the new gold standard for *FLT3* mutation analysis.

FLT3 inhibitors have demonstrated promising results in clinical trials and are increasingly integrated into therapeutic protocols, with regulatory approvals in multiple regions. In Brazil, midostaurin is currently approved for newly diagnosed patients harboring *FLT3*-ITD or *FLT3*-TKD mutations, based on the RATIFY study, which demonstrated an improvement in overall survival and event-free survival compared to placebos. For relapsed/refractory AML, gilteritinib has been approved for patients with *FLT3* mutations, based on the ADMIRAL study, which reported an overall survival of 9.3 months compared to 5.6 months with salvage chemotherapy.[49]

Our findings demonstrated a mutational status change in 14% of patients, highlighting the importance of routine molecular reassessment at relapse. Despite its relevance, access to *FLT3* mutational status testing remains limited in many clinical settings. In the Brazilian public healthcare system, previous data have indicated that up to 79% of patients lack adequate molecular characterization due to infrastructural and technological constraints.[2] In the present review, approximately 5% of patients had incomplete molecular data. The disparity is even more pronounced when comparing academic versus non-academic centers—a global challenge in cancer care. A study conducted in the United States demonstrated a lower rate of testing for AML patients in academic centers compared to community centers. This discrepancy may reflect the heterogeneous incorporation of testing technologies across treatment facilities and a potentially lower rate of molecular testing requests by medical teams in community settings, as academic institutions often require more frequent medical updates.

In Brazil, the public healthcare system, known as the Unified Health System (SUS), faces significant challenges in the incorporation of new technologies, even within academic centers. For example, cytogenetic analysis—recommended since the 1980s—is still not fully implemented in the public system. This was evidenced in a study conducted at the academic center of the University Hospital of Bahia, where only 60% of patients underwent karyotype analysis at diagnosis.[2] While investment in technological infrastructure is essential, parallel efforts are required to enhance continuous medical education, ensuring that healthcare providers recognize the clinical utility of molecular data for risk stratification and therapeutic decision-making.

A key limitation of this systematic review is that the screening of titles and abstracts was performed by a single investigator, which may have introduced selection bias and potentially resulted in the exclusion of relevant studies. As is widely recognized, systematic reviews require rigorous methodology, ideally involving independent review by multiple researchers to minimize bias. Moreover, some studies were excluded due to missing or incomplete data. This review could not be registered on the PROSPERO platform, as it currently only accepts registrations of systematic reviews and meta-analyses involving interventions. The present work is classified as a systematic review and meta-analysis with aggregation of prevalence data, in which the total proportion of *FLT3*-mutated and *FLT3*-wildtype patients was calculated. As a descriptive prevalence meta-analysis, it is not possible to perform statistical analyses to assess heterogeneity or publication bias. This methodological choice was based on the clinical relevance of the data, which focused on mutation frequency. To strengthen the findings, future studies should involve more than one reviewer and incorporate complementary clinical outcome data to enable more robust statistical analyses.

5. Conclusion

The characterization of *FLT3* mutation status and subtype in AML represents one of the most robust molecular models for supporting diagnosis, refining disease pathophysiology, guiding risk stratification, and informing therapeutic

decision-making, including the indication for allogeneic hematopoietic stem cell transplantation. Additionally, *FLT3* mutational profiling plays a pivotal role in selecting targeted therapies that are either currently approved or under investigation.

In this context, the observation that one in seven patients exhibited a change in *FLT3* mutational status between diagnosis and relapse/refractoriness underscores the clinical relevance of routine molecular reassessment at disease progression. Such alterations may reflect the expansion of pre-existing subclones at diagnosis or the acquisition of *de novo* mutations associated with distinct leukemic biology. The prognostic implications of these molecular shifts remain to be fully elucidated and warrant further investigation.

There remains a pressing need to advance the sensitivity and breadth of diagnostic tools capable of detecting minor subclonal populations at disease onset, as well as to better characterize the mutational architecture and its dynamics over time. The incorporation of next-generation molecular technologies into healthcare systems is essential.

Equally important is the continuous education of healthcare professionals to ensure the appropriate interpretation and integration of these tools into clinical practice. Routine assessment of *FLT3* mutations throughout the disease course is critical for optimizing the monitoring and management of patients with AML.

We suggest further studies, including prospective cohort studies integrating PCR with NGS, along with more robust investigations incorporating cytogenetic analyses at both diagnosis and relapse, co-occurring molecular alterations, and refined risk stratification models.

Based on these findings, the prevalence of *FLT3* mutational profile changes is clinically relevant. We therefore recommend performing PCR with fragment analysis to assess *FLT3* mutations in all patients with AML, both at diagnosis and at relapse or refractory disease.

Acknowledgments

The authors would like to thank the Hematology Division of UFBA Clinics Hospital and the UFBA Postgraduate Program in Medicine and Health for their invaluable input and support throughout the research process.

Funding

None.

Conflict of interest

The authors declare they have no competing interests.

Author contributions

Conceptualization: Lais Teixeira, Camilla Correia, Marco Salvino
Formal analysis: Lais Teixeira
Methodology: Lais Teixeira
Writing–original draft: All authors
Writing–review & editing: Lais Teixeira, Marco Salvino

Ethics approval and consent to participate

Not applicable.

Consent for publication

Not applicable.

Availability of data

Data is available from the corresponding author upon reasonable request.

References

1. Döhner H, Estey EH, Amadori S, *et al*. Diagnosis and management of acute myeloid leukemia in adults: Recommendations from an international expert panel, on behalf of the European leukemia net. *Blood*. 2010;115(3):453-474.

   doi: 10.1182/blood-2009-07-235358

2. Campos C, Orathes Ponte Silva AM, Feistauer F, Teixeira Da Silva L, Favano T, Salvino MA. 10-year real-world data on acute myeloid leukemia: The paradigm of a public health center in Brazil. *J Bone Marrow Transplant Cell Ther*. 2024;5(2):245.

   doi: 10.46765/2675-374X.2024v5n2p245

3. Feistauer F, Salvino M, Batista M, *et al*. Challenges to achieving BMT in the treatment of AML in Brazil: Bahia university hematology center experience. *J Bone Marrow Transplant Cell Ther*. 2023;4(3):214.

   doi: 10.46765/2675-374X.2023v4n3p214

4. Hochhaus A, Baccarani M, Silver RT, *et al*. European *Leukemia*Net 2020 recommendations for treating chronic myeloid leukemia. *Leukemia*. 2020;34(4):966-984.

   doi: 10.1038/s41375-020-0776-2

5. Nakao M, Yokota S, Iwai T, *et al*. Internal tandem duplication of the flt3 gene found in acute myeloid leukemia. *Leukemia*. 1996;10:1911-1918.

6. Kiyoi H, Naoe T, Nakano Y, *et al*. Prognostic implication of FLT3 and N-RAS gene mutations in acute myeloid leukemia. *Blood*. 1999;93:3074-3080.

7. Reindl C, Spiekermann K. From kinases to cancer: Leakiness, loss of autoinhibition and leukemia. *Cell Cycle*. 2006;5(6):599-602.

doi: 10.4161/cc.5.6.2586

8. Choudhary C, Müller-Tidow C, Berdel WE, Serve H. Signal transduction of oncogenic Flt3. *Int J Hematol*. 2005;82(2):93-99.

   doi: 10.1532/IJH97.05090

9. Thiede C, Steudel C, Mohr B, *et al*. Analysis of FLT3-activating mutations in 979 patients with acute myelogenous leukemia: Association with FAB subtypes and identification of subgroups with poor prognosis. *Blood*. 2002;99:4326-4335.

   doi: 10.1182/blood.v99.12.4326

10. Yamamoto Y, Kiyoi H, Nakano Y, *et al*. Activating mutation of D835 within the activation loop of FLT3 in human hematologic malignancies. *Blood*. 2001;97:2434-2439.

    doi: 10.1182/blood.v97.8.2434

11. Abu-Duhier FM, Goodeve AC, Wilson GA, *et al*. FLT3 internal tandem duplication mutations in adult acute myeloid leukaemia define a high-risk group. *Br J Haematol*. 2000;111:190-195.

    doi: 10.1046/j.1365-2141.2000.02317.x

12. Blau O, Berenstein R, Sindram A, Blau IW. Molecular analysis of different FLT3-ITD mutations in acute myeloid leukemia. *Leuk Lymphoma*. 2013;54(1):145-152.

    doi: 10.3109/10428194.2012.704999

13. Stirewalt DL, Kopecky KJ, Meshinchi S, *et al*. FLT3, RAS, and TP53 mutations in elderly patients with acute myeloid leukemia. *Blood*. 2001;97:3589-3595.

    doi: 10.1182/blood.v97.11.3589

14. Choudhary C, Schwable J, Brandts C, *et al*. AML-associated Flt3 kinase domain mutations show signal transduction differences compared with Flt3 ITD mutations. *Blood*. 2005;106:265-273.

    doi: 10.1182/blood-2004-07-2942

15. Campregher PV, Pinto **D**e Mattos VR, Salvino MA, Souza Santos FP, Hamerschlak N. Successful treatment of post-transplant relapsed acute myeloid leukemia with FLT3 internal tandem duplication using the combination of induction chemotherapy, donor lymphocyte infusion, sorafenib and azacitidine. Report of three cases. *Hematol Transfus Cell Ther*.2020;42(1):89-92.

16. Fröhling S, Schlenk RF, Breitruck J, *et al*. Prognostic significance of activating FLT3 mutations in younger adults (16 to 60 years) with acute myeloid leukemia and normal cytogenetics: A study of the AML study group Ulm. *Blood*. 2002;100(13):4372-4380.

    doi: 10.1182/blood-2002-05-1440

17. Schnittger S, Schoch C, Dugas M, *et al*. Analysis of FLT3 length mutations in 1003 patients with acute myeloid leukemia: Correlation to cytogenetics, FAB subtype, and prognosis in the AMLCG study and usefulness as a marker for the detection of minimal residual disease. *Blood*. 2002;100:59-66.

    doi: 10.1182/blood.v100.1.59

18. Döhner H, Wei AH, Appelbaum FR, *et al*. Diagnosis and management of AML in adults: 2022 recommendations from an international expert panel on behalf of the ELN. *Blood*. 2022;140(12):1345-1377.

    doi: 10.1182/blood.2022016867

19. Chen EC, Shimony S, Luskin MR, Stone RM. Biology and management of acute myeloid leukemia with mutated NPM1. *Am J Hematol*. 2025;100(4):652-665.

    doi: 10.1002/ajh.27600

20. Williams AB, Nguyen B, Li L, *et al*. Mutations of FLT3/ITD confer resistance to multiple tyrosine kinase inhibitors. *Leukemia*. 2013;27(1):48-55.

    doi: 10.1038/leu.2012.191

21. Lam SSY, Leung AYH. Overcoming resistance to FLT3 inhibitors in the treatment of FLT3-mutated AML. *Int J Mol Sci*. 2020;21(4):1537.

    doi: 10.3390/ijms21041537

22. Baker SD, Zimmerman EI, Wang YD, *et al*. Emergence of polyclonal FLT3 tyrosine kinase domain mutations during sequential therapy with sorafenib and sunitinib in FLT3-ITD-positive acute myeloid leukemia. *Clin Cancer Res*. 2013;19(20):5758-5768.

    doi: 10.1158/1078-0432.CCR-13-1323

23. Garg M, Nagata Y, Kanojia D, *et al*. Profiling of somatic mutations in acute myeloid leukemia with FLT3-ITD at diagnosis and relapse. *Blood*. 2015;126(22):2491-2501.

    doi: 10.1182/blood-2015-05-646240

24. Gupta A, Viswanatha DS, Patnaik MM. FLT3 mutation testing in acute myeloid leukemia. *JAMA Oncol*. 2017;3(7):991-992.

    doi: 10.1001/jamaoncol.2017.0257

25. Lin TL, Williams T, He J, *et al*. Rates of complete diagnostic testing for patients with acute myeloid leukemia. *Cancer Med*. 2015;4:519-522.

    doi: 10.1002/cam4.426

26. Kottaridis PD, Gale RE, Langabeer SE, Frew ME, Bowen DT, Linch DC. Studies of FLT3 mutations in paired presentation and relapse samples from patients with acute myeloid leukemia: Implications for the role of FLT3 mutations in leukemogenesis, minimal residual disease detection, and possible therapy with FLT3 inhibitors. *Blood*. 2002;100(7):2393-2398.

    doi: 10.1182/blood-2002-02-0420

27. Nakamura H, Inokuchi K, Yamaguchi H, Dan K. Abnormalities of p51, p53, FLT3 and N-ras genes and their prognostic value in relapsed acute myeloid leukemia. *J Nippon Med Sch*. 2004;71(4):270-278.

doi: 10.1272/jnms.71.270

28. Tiesmeier J, Müller-Tidow C, Westermann A, *et al*. Evolution of FLT3-ITD and D835 activating point mutations in relapsing acute myeloid leukemia and response to salvage therapy. *Leuk Res*. 2004;28(10):1069-1074.

doi: 10.1016/j.leukres.2004.02.009

29. Suzuki T, Kiyoi H, Ozeki K, *et al*. Clinical characteristics and prognostic implications of NPM1 mutations in acute myeloid leukemia. *Blood*. 2005;106(8):2854-2861.

doi: 10.1182/blood-2005-04-1733

30. Cloos J, Goemans BF, Hess CJ, *et al*. Stability and prognostic influence of FLT3 mutations in paired initial and relapsed AML samples. *Leukemia*. 2006;20(7):1217-1220.

doi: 10.1038/sj.leu.2404246

31. Palmisano M, Grafone T, Ottaviani E, Testoni N, Baccarani M, Martinelli G. NPM1 mutations are more stable than FLT3 mutations during the course of disease in patients with acute myeloid leukemia. *Haematologica*. 2007;92(9):1268-1269.

doi: 10.3324/haematol.11202

32. Schnittger S, Kern W, Tschulik C, *et al*. Minimal residual disease levels assessed by NPM1 mutation-specific RQ-PCR provide important prognostic information in AML. *Blood*. 2009;114(11):2220-2231.

doi: 10.1182/blood-2009-03-213389

33. McCormick SR, McCormick MJ, Grutkoski PS, *et al*. FLT3 mutations at diagnosis and relapse in acute myeloid leukemia: Cytogenetic and pathologic correlations, including cuplike blast morphology. *Arch Pathol Lab Med*. 2010;134(8):1143-1151.

doi: 10.5858/2009-0292-OA.1

34. Wang ES, Sait SN, Gold D, *et al*. Genomic, immunophenotypic, and NPM1/FLT3 mutational studies on 17 patients with normal karyotype acute myeloid leukemia (AML) followed by aberrant karyotype AML at relapse. *Cancer Genet Cytogenet*. 2010;202(2):101-107.

doi: 10.1016/j.cancergencyto.2010.07.117

35. Wakita S, Yamaguchi H, Omori I, *et al*. Mutations of the epigenetics-modifying gene (DNMT3a, TET2, IDH1/2) at diagnosis may induce FLT3-ITD at relapse in *de novo* acute myeloid leukemia. *Leukemia*. 2013;27(5):1044-1052.

doi: 10.1038/leu.2012.317

36. Janke H, Pastore F, Schumacher D, *et al*. Activating FLT3 mutants show distinct gain-of-function phenotypes *in vitro* and a characteristic signaling pathway profile associated with prognosis in acute myeloid leukemia. *PLoS One*. 2014;9(3):e89560.

doi: 10.1371/journal.pone.0089560

37. Nakano Y, Kiyoi H, Miyawaki S, *et al*. Molecular evolution of acute myeloid leukaemia in relapse: Unstable N-ras and FLT3 genes compared with p53 gene. *Br J Haematol*. 1999;104(4):659-664.

doi: 10.1046/j.1365-2141.1999.01256.x

38. Shih LY, Huang CF, Wu JH, *et al*. Internal tandem duplication of FLT3 in relapsed acute myeloid leukemia: A comparative analysis of bone marrow samples from 108 adult patients at diagnosis and relapse. *Blood*. 2002;100(7):2387-2392.

doi: 10.1182/blood-2002-01-0195

39. Schnittger S, Schoch C, Kern W, Hiddemann W, Haferlach T. FLT3 length mutations as marker for follow-up studies in acute myeloid leukaemia. *Acta Haematol*. 2004;112(1-2):68-78.

doi: 10.1159/000077561

40. Park SH, Chi HS, Min SK, *et al*. Prognostic significance of the FLT3 ITD mutation in patients with normal-karyotype acute myeloid leukemia in relapse. *Korean J Hematol*. 2011;46(2):88-95.

doi: 10.5045/kjh.2011.46.2.88

41. Abdelhamid E, Preudhomme C, Helevaut N, *et al*. Minimal residual disease monitoring based on FLT3 internal tandem duplication in adult acute myeloid leukemia. *Leuk Res*. 2012;36(3):316-323.

doi: 10.1016/j.leukres.2011.11.002

42. Bachas C, Schuurhuis GJ, Assaraf YG, *et al*. The role of minor subpopulations within the leukemic blast compartment of AML patients at initial diagnosis in the development of relapse. *Leukemia*. 2012;26(6):1313-1320.

doi: 10.1038/leu.2011.383

43. Nazha A, Cortes J, Faderl S, *et al*. Activating internal tandem duplication mutations of the fms-like tyrosine kinase-3 (FLT3-ITD) at complete response and relapse in patients with acute myeloid leukemia. *Haematologica*. 2012;97(8):1242-1245.

doi: 10.3324/haematol.2012.062638

44. Gourdin TS, Zou Y, Ning Y, *et al*. High frequency of rare structural chromosome abnormalities at relapse of cytogenetically normal acute myeloid leukemia with FLT3 internal tandem duplication. *Cancer Genet*. 2014;207:467-473.

doi: 10.1016/j.cancergen.2014.10.002

45. Shih LY, Huang CF, Wu JH, *et al*. Heterogeneous patterns of FLT3 Asp(835) mutations in relapsed de novo acute myeloid leukemia: A comparative analysis of 120 paired diagnostic and relapse bone marrow samples. *Clin Cancer*

Res. 2004;10(4):1326-1332.

doi: 10.1158/1078-0432.ccr-0835-03

46. Warren M, Luthra R, Yin CC, *et al*. Clinical impact of change of FLT3 mutation status in acute myeloid leukemia patients. *Mod Pathol*. 2012;25(10):1405-1412.

doi: 10.1038/modpathol.2012.88

47. Levis MJ, Hamadani M, Logan B, *et al*. Gilteritinib as post-transplant maintenance for AML with internal tandem duplication mutation of FLT3. *J Clin Oncol*. 2024;42(15):1766-1775.

doi: 10.1200/JCO.23.02474

48. Oduro KA Jr., Spivey T, Moore EM, *et al*. Clonal dynamics and relapse risk revealed by high-sensitivity FLT3-internal tandem duplication detection in acute myeloid leukemia. *Mod Pathol*. 2024;37(9):100534.

doi: 10.1016/j.modpat.2024.100534

49. Smith CC, Levis MJ, Perl AE, Hill JE, Rosales M, Bahceci E. Molecular profile of FLT3-mutated relapsed/refractory patients with AML in the phase 3 ADMIRAL study of gilteritinib. *Blood Adv*. 2022;6(7):2144-2155.

doi: 10.1182/bloodadvances.2021006489

ACCSCIENCE PUBLISHING

Eurasian Journal of Medicine and Oncology

ORIGINAL RESEARCH ARTICLE

Mapping breast cancer protein interaction networks as metric spaces: Insights into central zones and drug discovery targets

Emad Fadhal[1,2]*

[1]Department of Mathematics and Statistics, College of Science, King Faisal University, Al-Ahsa, Saudi Arabia

[2]Department of Mathematics and Applied Mathematics, University of the Western Cape, Bellville, South Africa

Abstract

Introduction: Graph theory was employed in recent advances of cancer research for gain deeper insights into the complex structure and function of protein-protein interaction (PPI) networks.

Objective: By representing proteins as nodes and their interactions as edges, graph theory offers a comprehensive framework for analyzing the topological properties of these networks and identifying key nodes that regulate critical biological processes. This approach has been widely applied to study various cancers, including breast cancer.

Methods: To investigate the molecular organization and critical pathways in breast cancer, we constructed a breast cancer protein-protein interaction network (BCPIN) and analyzed its hierarchical structure. The network was modeled as a metric space to delineate its central zones, facilitating the identification of essential hubs enriched with signaling pathways critical for cancer progression.

Results: Our study demonstrates the potential of hierarchical modeling of the BCPIN in unraveling its molecular organization and identifying therapeutic opportunities. By analyzing PPI network as a metric space, we highlight central zones 1 – 3 as critical hubs enriched with key signaling pathways, such as DNA repair, Notch signaling, and p53 signaling, which are essential to cancer progression. The identification of MAPK14 as a central node emphasizes its significant role in cancer biology and its value as a therapeutic target. The predominance of signaling proteins within these zones underscores their functional relevance, offering a strong rationale for prioritizing them in drug development.

Conclusion: By modeling the PPI network as a metric space, we uncovered important insights into its architecture and the central zone's critical role in facilitating key cellular processes. Our results indicate that zones 1 – 3, particularly the central zone, may serve as promising targets for drug discovery in cancer biology.

Keywords: Protein interaction networks; Metric spaces; Signaling pathways; Breast cancer; Central zones; Drug discovery

***Corresponding author:**
Emad Fadhal
(efadhal@kfu.edu.sa)

Citation: Fadhal E. Mapping breast cancer protein interaction networks as metric spaces: Insights into central zones and drug discovery targets. *Eurasian J Med Oncol*. 2025;9(3):75-85.
doi: 10.36922/ejmo.8208

Received: December 25, 2024

1st revised: December 31, 2024

2nd revised: February 8, 2025

3rd revision: February 23, 2025

Accepted: March 6, 2025

Published online: March 20, 2025

Copyright: © 2025 Author(s). This is an Open-Access article distributed under the terms of the Creative Commons Attribution License, permitting distribution, and reproduction in any medium, provided the original work is properly cited.

Publisher's Note: AccScience Publishing remains neutral with regard to jurisdictional claims in published maps and institutional affiliations.

1. Introduction

Breast cancer remains the leading cause of cancer-related mortality worldwide, with its complexity driven by dysregulated protein-protein interaction (PPI) networks that control critical cellular processes such as proliferation, apoptosis, and metastasis.[1]

Despite advances in genomic and proteomic technologies, significant gaps remain in understanding the structural and functional organization of these networks, particularly how their topological properties influence disease progression and therapeutic resistance.[2] Current research often focuses on individual proteins or pathways, ignoring the systemic interplay within the network. This study addresses this gap by employing graph theory and metric space modeling to unravel the hierarchical organization of the breast cancer protein-protein interaction network (BCPIN), providing insights into its structural and functional properties.

Graph theory has emerged as a powerful tool for analyzing PPIs, enabling the representation of proteins as nodes and their interactions as edges.[3] This approach has been successfully applied to various cancers, including breast cancer,[4,5] lung cancer,[6] and glioblastoma,[7] revealing key nodes that drive tumor progression and influence patient survival. For instance, past studies have identified critical proteins involved in immune evasion, drug resistance, and metastatic signaling in hepatocellular carcinoma.[8,9] Furthermore, common key nodes across multiple cancer types have been proposed as potential targets for broad-spectrum therapies.[10-14] However, these studies often lack a systematic framework to quantify the spatial and functional relationships between proteins within the network. This limitation underscores the need for advanced modeling techniques, such as metric space analysis, to better understand the network's organization and identify therapeutic targets.

Metric space modeling offers a novel approach to studying PPIs by quantifying the distances between nodes within the network. In this framework, the network is treated as a metric space, where the distance between two nodes is defined by the shortest path connecting them.[15] This method allows for the classification of proteins into distinct zones based on their proximity to the network's topological center, revealing a hierarchical structure that reflects functional specialization. Previous studies have demonstrated the advantage of metric space modeling in identifying central hubs and peripheral nodes in biological networks, providing insights into their roles in disease mechanisms.[16,17] For instance, central nodes often correspond to highly connected proteins that regulate critical pathways, while peripheral nodes may represent specialized or context-dependent proteins.[18] By applying this approach to BCPIN, we aim to uncover the spatial organization of proteins and their functional relevance in breast cancer.

In this study, we formally constructed and modeled BCPIN as a metric space, building on previous successes in applying this framework to other biological networks.[19,20] Our approach involves mapping tumor-expressed proteins onto the human interactome and analyzing their interactions using graph theory and metric space principles. This enables the identification of key proteins and pathways that drive breast cancer progression, as well as the exploration of their potential as therapeutic targets. By integrating pathway enrichment analysis and functional annotation, we provide a comprehensive view of the network's structure and its implications for cancer biology. This study not only advances our understanding of breast cancer PPIs but also highlights the potential of metric space modeling as a tool for uncovering novel therapeutic opportunities.

2. Materials and methods

2.1. Generation of cancer graphs

To construct a crossover network of cancer-associated proteins, our approach involves mapping tumor-expressed proteins onto the human interactome (Figure 1). The process is outlined as follows:

(i) Build a graph, G, based on the binary PPI data from the human protein network
(ii) Identify a list, L, of tumor-expressed proteins that are consistently observed across cancers
(iii) For proteins present in list L, extract the relevant interaction data from graph G
(iv) Generate the final cancer-specific graph, G'.

2.2. Analyzing BCPINs as metric spaces

In analysis, the BCPINs were treated as metric spaces and the distance between nodes was examined using graph theory. One way to accomplish this was using a Python wrapper for the C++ Boost Graph Library (http://www.boost.org/) and implementing the Dijkstra algorithm. This method calculated the shortest distances between protein pairs within the network. Proteins with the smallest maximum distance to their neighboring nodes were identified as the central nodes of the network. By employing this methodology, the nodes were categorized and segmented according to proximity from the center.

2.3. Sources of PPI data

We analyzed a human PPI network consisting of 9448 nodes and 181706 connections.[21]

2.4. Gene expression datasets in cancer

For our study on breast cancer, we utilized gene expression data from the Gene Expression Barcode database. The dataset was accessed from OBRC: Online Bioinformatics Resources Collection (Health Sciences Library System).[1] To maintain consistency, we selected the "unified tissue"

[1] https://www.hsls.pitt.edu/obrc/index.php?page=URL20110523150503#

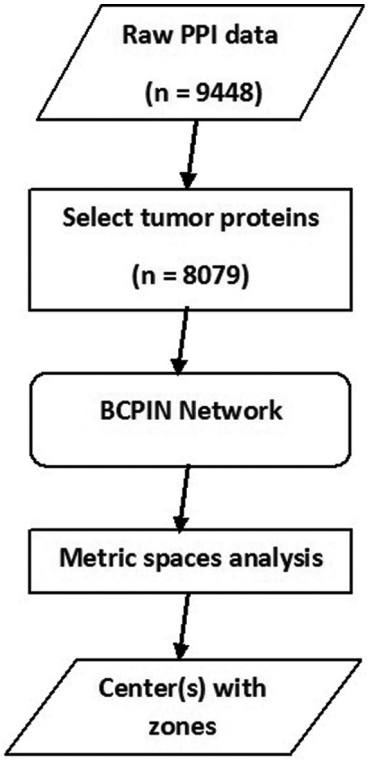


Figure 1. Data processing and metric space analysis flow diagram. This figure outlines the workflow used to construct and analyze the BCPIN, including data collection, graph construction, and metric space modeling Abbreviations: BCPIN: Breast cancer protein-protein interaction network; PPI: Protein-protein interaction network.

option and applied a threshold of 0.99. The analysis was conducted by applying the Human HGU133 platforms.

2.5. Pathway and functional enrichment analysis

To evaluate the biological significance of distinct zones within the BCPIN, proteins were categorized according to their proximity to the network's core.[22] Pathway enrichment analysis was conducted for each group to determine the functional associations of different zones (Figure 2). For this analysis, we employed gene set enrichment tools from the Comparative Toxicogenomics Database,[2] DAVID,[3] and Gene Ontology.[4] A statistical significance threshold of 0.01 was applied. Furthermore, we assessed the proportion of proteins participating in each enriched pathway to examine whether certain zones exhibited functional specialization.

2.6. Evaluation of protein scores and core pathways in oncogenes and tumor suppressors

We evaluated the interaction scores of proteins, with higher scores indicating enrichment in cancer-associated genes identified through mutation studies. Specifically, we examined the core pathways associated with oncogenes and tumor suppressors using genome-wide cancer sequencing data.[23]

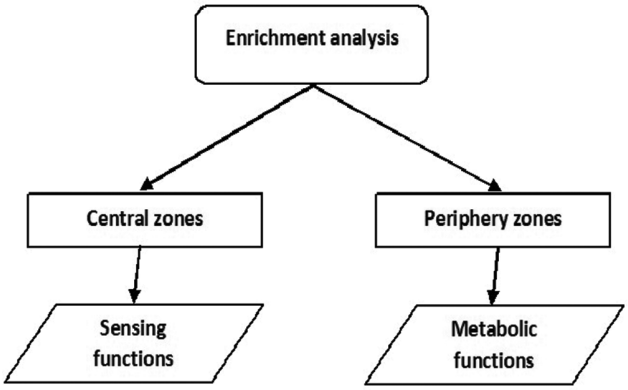


Figure 2. Pathway over-representation analysis flow diagram. This diagram illustrates the methodology used to identify enriched pathways in different zones of the BCPIN, highlighting key functional associations Abbreviation: BCPIN: Breast cancer protein-protein interaction network.

2.7. Statistical power and confidence measures

In our study, statistical power and confidence measures were integral to ensuring the robustness of our findings. The statistical power of our analysis was determined by the size and quality of the PPI dataset, as well as the consistency of the observed patterns across the network. Specifically, the large-scale PPI dataset used in our study (9448 nodes and 181706 interactions) provided sufficient statistical power to detect significant patterns and relationships within the network. The high connectivity and density of the network ensured that even subtle topological features, such as the hierarchical organization of zones, could be reliably identified.

To evaluate the robustness of our findings, we applied multiple statistical measures, including pathway enrichment analysis, using a stringent significance threshold ($p < 0.01$) to report only highly significant functional associations. In addition, we conducted bootstrap resampling on the network to assess the stability of zone classifications and protein centrality measures.

3. Results

3.1. Structural analysis of BCPIN in metric space

In our network construction approach, the BCPIN was analyzed as a metric space, enabling the categorization of proteins into distinct zones according to their shortest path distances from the network's topological core. Proteins located at a single-step distance from the center were assigned to the first zone, those at a

[2] http://ctdbase.org/tools/enricher.go
[3] https://david.ncifcrf.gov/
[4] http://www.geneontology.org/GO.tools

two-step distance to the second zone, and so forth. The analyzed BCPIN comprised 8079 proteins and 163,199 interactions. Through this modeling, MAPK14 emerged as the central protein, highlighting its significant involvement in various diseases, including cancer and cardiovascular conditions.[24] Studies indicate that competing endogenous RNA can promote breast cancer progression by modifying the MAPK signaling pathway.[25] In addition, elevated MAPK14 levels have been detected in gastric cancer, suggesting its potential as a biomarker and pharmacological target.[26] Table 1 summarizes the node distribution and average connectivity relative to the BCPIN center.

The network has a diameter (the shortest path length connecting the two most distant nodes in a graph) of 9, with the farthest zone from the center being zone 5. The central protein interacts with 374 proteins in zone 1, which has a maximum degree of 531, surpassing the center itself. Zones 1 – 3 contain 96% of all proteins, with average degrees of 83.62% (zone 1), 28.71% (zone 2), and 56.57% (zone 3). The average degrees for zones 4 and 5 are 1.69% and 1.1%, respectively. Zone 1 proteins interact with 4,496 zone 2 proteins, comprising over 50% of proteins in both zones. Zone 3 has 2,918 proteins, while zones 4 and 5 contain 249 and 27 proteins, respectively. The network structure consists of a dense core and a sparse periphery, with proteins near the topological center exhibiting higher connectivity.

3.2. Distribution of key proteins in the BCPIN network

Table 2 categorizes essential proteins within BCPIN zones. Human proteins crucial for survival, as inferred from orthologous knockout studies in mice,[27] are predominantly located in the central zones. Specifically, 43.08%, 42.61%, and 11.08% of essential proteins reside in zones 1, 2, and 3, while zones 4 and 5 contain only 6.82% and 7.40%, respectively. This table highlights the concentration of essential proteins in each zone, with higher proportions in central zones.

Table 3 presents the distribution of signaling proteins across BCPIN zones. These proteins are predominantly concentrated in the core, accounting for 75.13%, 43.37%, and 16.96% in zones 1, 2, and 3, respectively. The MAPK signaling pathway is a known target for cancer treatment.[28] Protein kinases play an essential role in regulating cellular functions and controlling proliferation, and are considered key drug targets.[29] This table details the presence of signaling proteins across network zones, emphasizing their enrichment in the core.

Further analysis examined the spatial allocation of growth-related, cell cycle, tumor suppressor, and oncogenic proteins (Tables 4-7). The distribution of growth-related proteins is lowest in the core zone but increases in the outer zones. Cell cycle proteins are most concentrated in zones 1 and 2, supporting their role in regulating tumor growth and progression.[30] Tumor suppressor and oncogene proteins are mostly found in zones 1 – 3, aligning with their involvement in cancer development.[31-34] Table 4 presents the abundance of growth-related proteins in each zone, demonstrating their localization near the center. The spatial allocation of cell cycle-related proteins, as depicted in Table 5, also highlights their higher density in central zones. Regarding the concentration of tumor suppressors for each zone.

Table 1. A description of how nodes and their connections are arranged starting from the core of the BCPIN network

Zone	Protein count	Average connectivity	Maximum connectivity	Minimum connectivity
Center	1	374	374	0
1	374	83.62	531	2
2	4496	28.71	409	1
3	2918	56.57	393	1
4	249	1.69	10	1
5	27	1.1	3	1

Abbreviation: BCPIN: Breast cancer protein-protein interaction network.

Table 2. The spatial allocation of essential proteins within the BCPIN zones

Zone	Protein count	Essential proteins (%)	Total
1	374	161 (43.08)	1481
2	4496	972 (42.61)	
3	2918	329 (11.08)	
4	249	17 (6.82)	
5	27	2 (7.40)	

Abbreviation: BCPIN: Breast cancer protein-protein interaction network.

Table 3. The spatial allocation of signaling proteins within the BCPIN zones

Zone	Protein count	Signaling proteins (%)	Total
1	374	281 (75.13)	2756
2	4496	1950 (43.37)	
3	2918	495 (16.96)	
4	249	28 (11.24)	
5	27	2 (7.40)	

Abbreviation: BCPIN: Breast cancer protein-protein interaction network.

Table 4. The spatial allocation of growth-related proteins within the BCPIN zones

Zone	Protein count	Growth proteins (%)	Total
1	374	28 (7.48)	234
2	4496	156 (3.46)	
3	2918	45 (1.54)	
4	249	5 (2)	
5	27	0 (0)	

Abbreviation: BCPIN: Breast cancer protein-protein interaction network.

Table 5. The spatial allocation of cell cycle proteins within the BCPIN zones

Zone	Protein count	Cell cycle proteins (%)	Total
1	374	73 (19.50)	570
2	4496	431 (9.58)	
3	2918	64 (2.2)	
4	249	2 (0.80)	
5	27	0 (0)	

Abbreviation: BCPIN: Breast cancer protein-protein interaction network.

Table 6. The spatial allocation of suppressor proteins within the BCPIN zones

Zone	Protein count	Suppressor proteins (%)	Total
1	374	14 (3.74)	59
2	4496	42 (0.93)	
3	2918	3 (0.10)	
4	249	0 (0)	
5	27	0 (0)	

Abbreviation: BCPIN: Breast cancer protein-protein interaction network.

Table 7. The spatial allocation of oncogene proteins within the BCPIN zones

Zone	Protein count	Oncogene proteins (%)	Total
1	374	15 (4.01)	48
2	4496	32 (0.71)	
3	2918	1 (0.3)	
4	249	0 (0)	
5	27	0 (0)	

Abbreviation: BCPIN: Breast cancer protein-protein interaction network.

Table 7 displays the allocation of oncogenic proteins, highlighting their prevalence in the network's core.

Table 8 highlights that proteins successfully targeted by drugs are predominantly found in zones 1 – 3, accounting for 9.09%, 5.04%, and 1.26%, respectively. This distribution suggests that proteins within the core may be promising drug targets.

3.3. MAPK signaling and apoptosis in core zones as drug targets

Table 9 shows the distribution of MAPK signaling components, positive/negative regulation of signaling, and apoptosis-related proteins within BCPIN. These pathways are concentrated in the central zones, reinforcing their potential as therapeutic targets.

3.4. Functional specialization in core zones

According to pathway enrichment analysis, functional specialization was identified in the core zones of BCPIN (Table 10). Zone 1 is enriched in signaling regulation, immune system function, apoptosis, gene expression, and p53/Notch signaling. Zone 2 displays similar enrichment but to a lesser degree, while zones 3 and 4 exhibit minimal pathway enrichment. These findings suggest that the central zones play a critical role in cancer progression and may offer novel therapeutic targets.

3.5. Pathway and function enrichment analysis for essential proteins for cancer cell survival

Genes that are vital for the existence of an organism are referred to as essential genes. The genes used in this analysis have been found critical for cancer cell's survival in different environments.[35,36] At least 8% of the genes in each zone are essential and are in pathways critical for cancer development and progression (Table 11).

3.6. Disease pathways in core zones

With the intent of finding out the central zones of BCIPN of biological significance, we mapped them to proteins in the KEGG pathways.[37] Using this enriched analysis of zones, we found that the majority of proteins involved in the pathways of cancer are concentrated in zones close to the center (Figure 3).

Among these are p53, BRCA1, and BRCA2 proteins, which are well documented as associated with hereditary breast and ovarian cancer.[38] For zone 2, enriched analysis showed 102, 344, and 172 proteins in pathways of breast cancer, cancer, and MAPK, respectively. Amidst them are ATM, CDH1, PTEN, BARD1, and CHEK2 proteins that are known predisposition genes.[39,40]

4. Discussion

This study highlights the biological significance of BCPIN as a structured representation of protein interactions within a metric space. By categorizing proteins into separate zones according to their graph theoretic distance from the core protein MAPK14, our analysis provides a comprehensive view of the hierarchical organization of protein interactions. The findings emphasize the centrality of MAPK14, which is not only topologically central but also functionally essential pathways associated with cancer and other diseases. This aligns with previous research that identifies MAPK14 as a key regulator in oncogenic pathways, including signal transduction, apoptosis, and cellular stress responses.[41,42]

Zones 1 – 3 exhibit a dense core structure enriched with proteins essential for cellular function and survival, such as signaling proteins, cell cycle regulators, and tumor suppressors. The high connectivity in these zones supports their functional importance, with these proteins being closely involved in critical pathways like immune modulation and cell cycle regulation. Furthermore, the enrichment of successful drug targets in these central zones underscores their relevance for therapeutic strategies, in agreement with the findings of Mukherjee and Zhang and Zhao *et al.*,[43,44] who reported similar protein clustering around central nodes in cancer-related networks.

The dense connectivity within zones 1 – 3 reflects the biological necessity of tightly regulated protein interactions in central cellular processes. The significant presence of oncogenes and tumor suppressor proteins in these zones suggests their active role in maintaining cellular homeostasis and responding to dysregulation, a hallmark of cancer progression. This finding aligns with the study by Brown *et al.*,[45] which demonstrated that proteins in densely connected network zones are often critical in disease pathogenesis.

Table 8. The spatial allocation of successful drug target proteins within the BCPIN zones

Zone	Protein count	Successful drug target proteins (%)	Total
1	374	34 (9.09)	299
2	4496	227 (5.01)	
3	2918	37 (1.26)	
4	249	0 (0)	
5	27	1 (3)	

Abbreviation: BCPIN: Breast cancer protein-protein interaction network.

Table 9. Distribution of MAPK signaling and apoptosis-related proteins

Zone	MAPK signaling (%)	S/ON (%)	S/OFF (%)	Apoptosis (%)	A/ON (%)	A/OFF (%)
1	93 (24.86)	75 (20.05)	57 (15.24)	13 (3.47)	6 (1.60)	4 (1.06)
2	254 (5.64)	373 (8.29)	309 (6.87)	19 (0.42)	13 (0.28)	3 (0.06)
3	34 (1.16)	68 (2.33)	60 (2.05)	4 (0.13)	2 (0.06)	2 (0.06)
4	34 (0.40)	2 (0.80)	0 (0)	0 (0)	0 (0)	0 (0)
5	0 (0)	0 (0)	0 (0)	0 (0)	0 (0)	0 (0)

Abbreviations: A/OFF: Negative apoptosis; A/ON: Positive apoptosis; S/OFF: Negative signaling; S/ON: Positive signaling.

Table 10. Functional enrichment in BCPIN core zones

Pathways with significant enrichment	Zone 1 (%)	Zone 2 (%)	Zone 3 (%)	Zone 4 (%)
Signal transduction	59.4	35.8	0.0	0.0
Immune system	45	21	11	0.0
Signaling by NGF	25.5	6.8	0.0	0.0
Gene expression	22.2	13.8	18.8	11.3
Hemostasis	20.8	6.9	3.3	0.0
Apoptosis	11.9	2.7	0.0	0.0
Mitotic G1-G1/S phases	8.3	2.1	0.0	0.0
Mitotic G2-G2/M phases	4.4	2.9	0.0	0.0
DNA repair	5.8	3.1	0.0	0.0
p53 signaling	5.8	0.9	0.0	0.0
Notch signaling	3.3	1.2	0.0	0.0

Table 11. Summary of the KEGG enriched pathways for essential proteins and their pathways for cancer

Zone	Essential genes in zone (%)	KEGG enriched pathways
Center	1 (100)	
1	38 (10.16)	Cell cycle, JAK-STAT pathway, WNT pathway, p53 pathway, FoxO pathway, MAPK pathway, TGF-β pathway, focal adhesion, cAMP signaling pathway, sphingolipid signaling pathway, Ras signaling pathway
2	506 (11.26)	Proteasome, spliceosome, DNA replication, cell cycle, nucleotide excision repair, mRNA surveillance pathway, ubiquitin-mediated proteolysis, mismatch repair
3	256 (8.77)	Proteasome, spliceosome, nucleocytoplasmic transport, protein export, mRNA surveillance pathways, ribosome biogenesis in eukaryotes, oxidative phosphorylation
4	37 (14.86)	RNA degradation
5	4 (14.86)	Citrate cycle, carbon metabolism, metabolic pathways

Note: Significantly enriched pathways at adjusted $p<0.05$.
Abbreviation: Kyoto encyclopedia of genes and genomes.

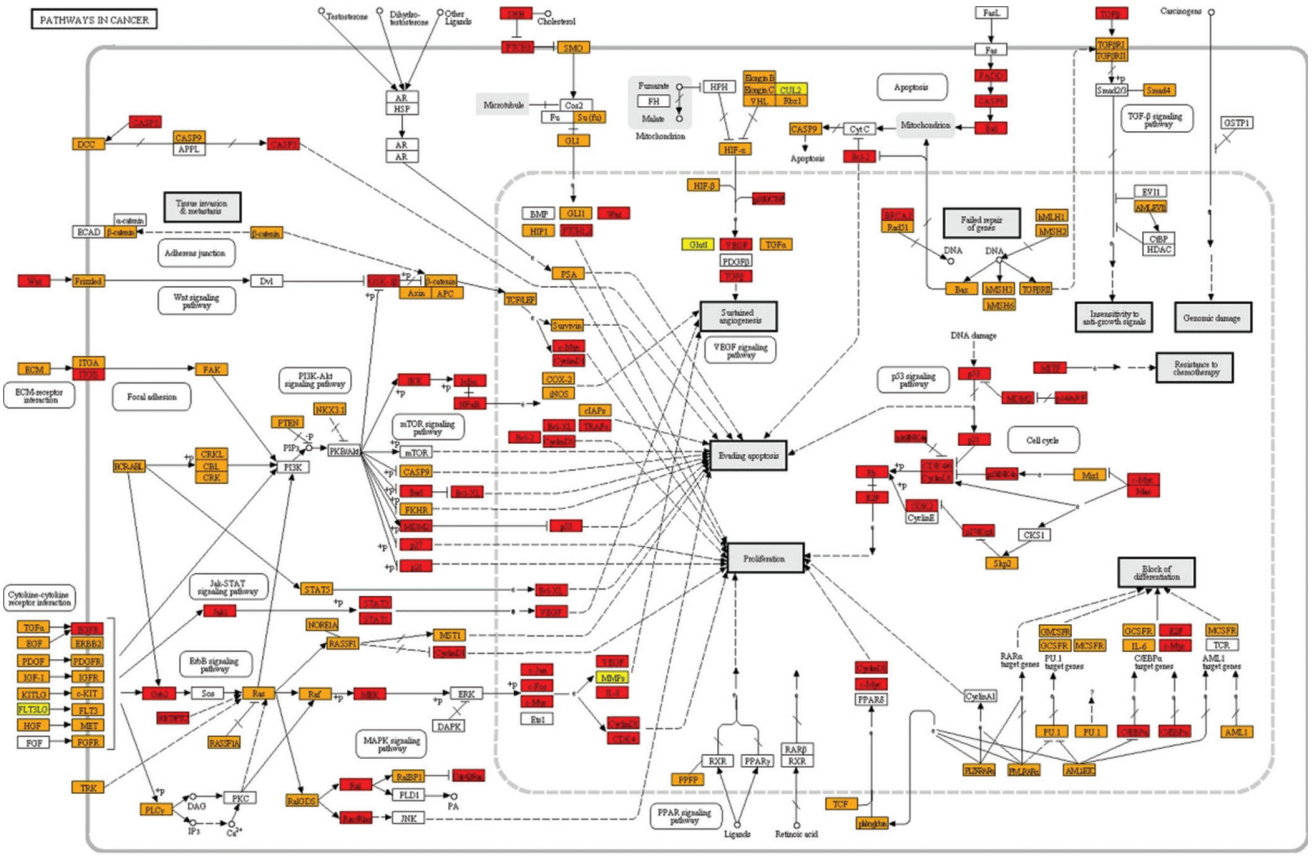


Figure 3. Enrichment analysis of cancer pathways was performed on proteins from zones 1, 2, and 3, which are represented by the red, orange, and yellow colors, respectively

In contrast, zones 4 and 5, which are sparsely populated, contain proteins with lower connectivity. These peripheral zones may represent proteins with more specialized or context-dependent roles, such as those involved in tissue-specific processes or secondary signaling pathways. The presence of single-degree proteins in these zones could also indicate weak interactions, consistent with previous findings by Barabási and Oltvai.[3]

4.1. Zone-specific protein distributions and implications for cancer treatment

Our study demonstrated that proteins within the core zones (zones 1 – 3) of the BCPIN exhibit high connectivity

and centrality, making them critical in breast cancer progression. The high concentration of signaling, growth-related, and oncogenic proteins in these zones underscores their functional importance in tumor biology (Tables 2-10).

The analysis of protein distribution reinforces the hypothesis that central network zones serve as functional hubs critical to disease biology. This hierarchical organization suggests an evolutionary optimization, where essential and highly interactive proteins are placed at the network core to enhance robustness and efficiency in information processing.[4]

The structural and functional observations in BCPIN corroborate previous studies on protein interaction networks, which demonstrated similar core-periphery structures in biological networks, with central zones enriched for essential and druggable proteins.[46-49] The higher concentration of proteins involved in apoptosis, signal transduction, and immune response pathways in zones 1 and 2 aligns with previous studies,[50-52] which reported these pathways as critical hubs in cancer-related networks.

While previous work focused on general cancer networks, our study uniquely emphasizes the zonal classification and highlights the centrality of MAPK14 as a key node. This approach provides a more specific understanding of protein organization and functional specialization within the network.

4.2. Comparison with prior studies

Our findings align with previous research that emphasizes the role of network topology in cancer biology. For instance, studies on glioblastoma and lung cancer have demonstrated that central proteins in PPIs are often associated with poor prognosis and therapeutic resistance. However, unlike previous analyses that primarily focus on individual protein interactions, our metric space modeling provides a hierarchical framework to understand spatial distributions within the network. This approach allows us to quantify the impact of protein positioning and connectivity, offering a systematic method to prioritize drug targets.

4.3. Limitations and future directions

Our study offers valuable insights into breast cancer PPIs, but certain limitations must be acknowledged. First, our analysis depends on publicly available PPI datasets, which may contain biases due to experimental constraints and incomplete annotations. Second, while our computational predictions identify potential therapeutic targets, experimental validation is essential to confirm their biological relevance in cancer progression. Finally, given the significant heterogeneity in breast cancer, future research should stratify PPI networks by molecular subtypes to enhance the precision of therapeutic targeting strategies.

5. Conclusion

The hierarchical structure of breast cancer PPIs reveals a dense core enriched with essential proteins and drug targets, offering a compelling framework to understand the molecular organization underlying cancer biology. By modeling BCPIN as a metric space, our study identifies the central zones 1 – 3 as hubs for critical signaling pathways, including DNA repair, Notch signaling, and p53 signaling, which are crucial to cellular processes and cancer progression.

The identification of MAPK14 as a central node underscores its multifaceted role in disease states, particularly in cancer, and supports the importance of targeting central zones in therapeutic development. The predominance of signaling proteins in these zones highlights their functional significance, making them central points for prioritizing drug targets. These findings demonstrate the translational potential of network-based approaches and suggest that integrating experimental validation with other omics data could advance our understanding of these networks and guide novel strategies for breast cancer treatment.

Acknowledgments

This work is based on research supported by the Faculty of Natural Science research office at University of the Western Cape. The opinions and conclusions expressed are those of the author and should not necessarily be attributed to the research office.

Funding

None.

Conflict of interest

The authors declare no conflicts of interest.

Author contributions

This is a single-authored article.

Ethics approval and consent to participate

Not applicable.

Consent for publication

Not applicable.

Availability of data

This study relies on publicly accessible databases, where users can freely access and download relevant data for research purposes and publish associated articles.

References

1. Siegel RL, Miller KD, Wagle NS, Jemal A. Cancer statistics, 2023. *CA Cancer J Clin*. 2023;73(1):17-48.

2. Hanahan D, Weinberg RA. Hallmarks of cancer: The next generation. *Cell*. 2011;144(5):646-674.

   doi: 10.1016/j.cell.2011.02.013

3. Barabási AL, Oltvai ZN. Network biology: Understanding the cell's functional organization. *Nat Rev Genet*. 2004;5(2): 101-113.

   doi: 10.1038/nrg1272

4. Pavlopoulos GA, Secrier M, Moschopoulos CN, *et al*. Using graph theory to analyze biological networks. *BioData Min*. 2011;4:10.

   doi: 10.1186/1756-0381-4-10

5. Zhang Y, Xiang J, Tang L, *et al*. Identifying breast cancer-related genes based on a novel computational framework involving KEGG pathways and PPI network modularity. *Front Genet*. 2021;12:596794.

   doi: 10.3389/fgene.2021.596794

6. Shi K, Li Y, Yang M, Li W. Identification of key genes and pathways in female lung cancer patients who never smoked by a bioinformatics analysis. *J Cancer*. 2019;10(1):51-59.

   doi: 10.7150/jca.26908

7. Liu QQ, Ren K, Liu SH, Li WM, Huang CJ, Yang XH. MicroRNA-140-5p aggravates hypertension and oxidative stress of atherosclerosis via targeting Nrf2 and Sirt2. Int J Mol Med. 2019;43(2):839-849.

   doi: 10.3892/ijmm.2018.3996.

8. Wang E, Zaman N, Mcgee S, Milanese JS, Masoudi-Nejad A, O'Connor-McCourt M. Predictive genomics: A cancer hallmark network framework for predicting tumor clinical phenotypes using genome sequencing data. *Semin Cancer Biol*. 2015;30:4-12.

   doi: 10.1016/j.semcancer.2014.04.002

9. Chen J, Riazifar H, Guan MX, Huang T. Modeling autosomal dominant optic atrophy using induced pluripotent stem cells and identifying potential therapeutic targets. *Stem Cell Res Ther*. 2016;7:2.

   doi: 10.1186/s13287-015-0264-1

10. Goh KI, Cusick ME, Valle D, Childs B, Vidal M, Barabási AL. The human disease network. *Proc Natl Acad Sci U S A*. 2007;104(21):8685-8690.

    doi: 10.1073/pnas.0701361104

11. Ideker T, Sharan R. Protein networks in disease. *Genome Res*. 2008;18(4):644-652.

    doi: 10.1101/gr.071852.107

12. Cowen L, Ideker T, Raphael BJ, Sharan R. Network propagation: A universal amplifier of genetic associations. *Nat Rev Genet*. 2017;18(9):551-562.

    doi: 10.1038/nrg.2017.38

13. Csermely P, Korcsmáros T, Kiss HJ, London G, Nussinov R. Structure and dynamics of molecular networks: A novel paradigm of drug discovery: A comprehensive review. *Pharmacol Ther*. 2013;138(3):333-408.

    doi: 10.1016/j.pharmthera.2013.01.016

14. Menche J, Sharma A, Kitsak M, *et al*. Uncovering disease-disease relationships through the incomplete interactome. *Science*. 2015;347(6224):1257601.

    doi: 10.1126/science.1257601

15. Borgatti SP, Everett MG. A graph-theoretic perspective on centrality. *Soc Netw*. 2006;28(4):466-484.

16. Jeong H, Mason SP, Barabási AL, Oltvai ZN. Lethality and centrality in protein networks. *Nature*. 2001;411(6833):41-42.

    doi: 10.1038/35075138

17. Network YI. High-quality binary protein interaction map of the. *Science*. 2008;1158684(104):322.

    doi: 10.1126/science.1158684

18. Batada NN, Hurst LD, Tyers M. Evolutionary and physiological importance of hub proteins. *PLoS Comput Biol*. 2006;2(7):e88.

    doi: 10.1371/journal.pcbi.0020088

19. Fadhal E, Gamieldien J, Mwambene EC. Protein interaction networks as metric spaces: A novel perspective on distribution of hubs. *BMC Syst Biol*. 2014;8:6.

    doi: 10.1186/1752-0509-8-6

20. Fadhal E. Exploring lung cancer protein network: Understanding structure and function through metric space modeling. *Eur J Pure Appl Math*. 2024;17(2):905-921.

21. Wu G, Feng X, Stein L. A human functional protein interaction network and its application to cancer data analysis. *Genome Biol*. 2010;11(5):R53.

    doi: 10.1186/gb-2010-11-5-r53

22. Fadhal E, Mwambene EC, Gamieldien J. Modelling human protein interaction networks as metric spaces has potential in disease research and drug target discovery. *BMC Syst Biol*. 2014;8:68.

    doi: 10.1186/1752-0509-8-68

23. Vogelstein B, Papadopoulos N, Velculescu VE, Zhou S, Diaz LA Jr., Kinzler KW. Cancer genome landscapes. *Science*. 2013;339(6127):1546-1558.

doi: 10.1126/science.1235122

24. Madkour MM, Anbar HS, El-Gamal MI. Current status and future prospects of p38α/MAPK14 kinase and its inhibitors. *Eur J Med Chem*. 2021;213:113216.

doi: 10.1016/j.ejmech.2021.113216

25. Liu Y, Du Y, Hu X, Zhao L, Xia W. Up-regulation of ceRNA TINCR by SP1 contributes to tumorigenesis in breast cancer. *BMC Cancer*. 2018;18:367.

doi: 10.1186/s12885-018-4255-3

26. Mesquita FP, Moreira-Nunes CA, da Silva EL, *et al.* MAPK14 (p38α) inhibition effects against metastatic gastric cancer cells: A potential biomarker and pharmacological target. *Toxicol In Vitro*. 2020;66:104839.

doi: 10.1016/j.tiv.2020.104839

27. Blake JA, Bult CJ, Eppig JT, Kadin JA, Richardson JE, Mouse Genome Database Group. The mouse genome database genotypes: Phenotypes. *Nucleic Acids Res*. 2009;37(Suppl 1):D712-D719.

doi: 10.1093/nar/gkn886

28. Blume-Jensen P, Hunter T. Oncogenic kinase signalling. *Nature*. 2001;411(6835):355-365.

doi: 10.1038/35077225

29. Sebolt-Leopold JS, Herrera R. Targeting the mitogen-activated protein kinase cascade to treat cancer. *Nat Rev Cancer*. 2004;4(12):937-947.

doi: 10.1038/nrc1503

30. Foulstone E, Prince S, Zaccheo O, *et al*. Insulin-like growth factor ligands, receptors, and binding proteins in cancer. *J Pathol*. 2005;205(2):145-153.

doi: 10.1002/path.1712

31. Lapenna S, Giordano A. Cell cycle kinases as therapeutic targets for cancer. *Nat Rev Drug Discov*. 2009;8(7):547-566.

doi: 10.1038/nrd2907

32. Min J, Zaslavsky A, Fedele G, *et al*. An oncogene-tumor suppressor cascade drives metastatic prostate cancer by coordinately activating Ras and nuclear factor-κB. *Nat Med*. 2010;16(3):286-294.

doi: 10.1038/nm.2100

33. Münger K. Disruption of oncogene/tumor suppressor networks during human carcinogenesis. *Cancer Investig*. 2002;20(1):71-81.

doi: 10.1081/cnv-120000369

34. Lee EY, Muller WJ. Oncogenes and tumor suppressor genes. *Cold Spring Harb Perspect Biol*. 2010;2(10):a003236.

doi: 10.1101/cshperspect.a003236

35. Chen WH, Lu G, Chen X, Zhao XM, Bork P. OGEE v2: An update of the online gene essentiality database with special focus on differentially essential genes in human cancer cell lines. *Nucleic Acids Res*. 2016;44(D1):D1057-D1063.

doi: 10.1093/nar/gkw1013

36. Chen WH, Trachana K, Lercher MJ, Bork P. Younger genes are less likely to be essential than older genes, and duplicates are less likely to be essential than singletons of the same age. *Mol Biol Evol.* 2012;29(7):1703-1706.

doi: 10.1093/molbev/mss014

37. Kanehisa M, Araki M, Goto S, *et al*. KEGG for linking genomes to life and the environment. *Nucleic Acids Res*. 2007;36(suppl 1):D480-D484.

38. Petrucelli N, Daly MB, Pal T. *BRCA1-and BRCA2-Associated Hereditary Breast and Ovarian Cancer*. Seattle, WA: University of Washington; 2022.

39. Peto J, Collins N, Barfoot R, *et al.* Prevalence of BRCA1 and BRCA2 gene mutations in patients with early-onset breast cancer. *J Natl Cancer Inst*. 1999;91(11):943-949.

doi: 10.1093/jnci/91.11.943

40. Couch FJ, Shimelis H, Hu C, *et al*. Associations between cancer predisposition testing panel genes and breast cancer. *JAMA Oncol*. 2017;3(9):1190-1196.

doi: 10.1001/jamaoncol.2017.0424

41. Guo YJ, Pan WW, Liu SB, Shen ZF, Xu Y, Hu LL. ERK/MAPK signalling pathway and tumorigenesis. *Exp Ther Med*. 2020;19(3):1997-2007.

doi: 10.3892/etm.2020.8454

42. Lee S, Rauch J, Kolch W. Targeting MAPK signaling in cancer: Mechanisms of drug resistance and sensitivity. *Int J Mol Sci*. 2020;21(3):1102.

doi: 10.3390/ijms21031102

43. Mukherjee CS, Zhang J. A multi-core periphery perspective: Ranking via relative centrality. *arXiv preprin*t. 2024; arXiv:2406.04487.

44. Zhao L, Yang Y, Bai X, *et al*. Structure, robustness and supply risk in the global wind turbine trade network. *Renew Sustain Energy Rev*. 2023;177:113214.

45. Brown RE, Short SP, Williams CS. Colorectal cancer and metabolism. *Curr Colorectal Cancer Rep.* 2018;14:226-241.

doi: 10.1007/s11888-018-0420-y

46. Blevins AS, Kim JZ, Bassett DS. Variability in higher order structure of noise added to weighted networks. *Commun Phys*. 2021;4(1):233.

47. Ramos RH, Ferreira COL, Simao A. Human protein-protein interaction networks: A topological comparison review. *Heliyon*. 2024;10(5):e27278.

48. Fadhal E, Gamieldien J, Mwambene EC. Self-similarity of human protein interaction networks: A novel strategy of distinguishing proteins. *Sci Rep.* 2015;5(1):7628.

doi: 10.1038/srep07628

49. Snider J, Kotlyar M, Saraon P, Yao Z, Jurisica I, Stagljar I. Fundamentals of protein interaction network mapping. *Mol Syst Biol*. 2015;11(12):848.

doi: 10.15252/msb.20156351

50. Wang Y, Zhang S, Li F, *et al*. Therapeutic target database 2020: Enriched resource for facilitating research and early development of targeted therapeutics. *Nucleic Acids Res*. 2020;48:D1031-D1041.

doi: 10.1093/nar/gkz981

51. Yi Y, Fang Y, Wu K, Liu Y, Zhang W. Comprehensive gene and pathway analysis of cervical cancer progression. *Oncol Lett*. 2020;19(4):3316-3332.

doi: 10.3892/ol.2020.11439

52. Liu Z, Huang H, Yu Y, *et al*. *Exploring* the potential mechanism of action of ursolic acid against gastric cancer and COVID-19 using network pharmacology and bioinformatics analysis. *Curr Pharm Des*. 2023;29(16): 1274-1292.

doi: 10.2174/1381612829666230510124716

ACCSCIENCE PUBLISHING

Eurasian Journal of Medicine and Oncology

ORIGINAL RESEARCH ARTICLE

Development of a novel risk model for stratifying skin cutaneous melanoma patients based on prognostic senescence-related genes

Yiting Feng[1], Lanlan Liu[2,3,4,5]*, Yunjin Xie[2,3,4,5]*, and Mingzhu Yin[2,3,4,5]*

[1]Department of Dermatology, Hunan Engineering Research Center of Skin Health and Disease, Hunan Key Laboratory of Skin Cancer and Psoriasis, Xiangya Hospital, Central South University, Changsha, Hunan Province, China

[2]Clinical Research Center, Medical Pathology Center, Cancer Early Detection and Treatment Center, and Translational Medicine Research Center, Chongqing University Three Gorges Hospital, Chongqing University, Chongqing, China

[3]Chongqing Technical Innovation Center for Quality Evaluation and Identification of Authentic Medicinal Herbs, Chongqing, China

[4]Chongqing University Three Gorges Hospital and Academy for Advanced Interdisciplinary Technology, CQU - Ferenc Krausz Nobel Laureate Scientific Workstation, Chongqing, China

[5]School of Medicine, Chongqing University, Chongqing, China

***Corresponding authors:**
Lanlan Liu (liulanlan@cqu.edu.cn);
Yunjin Xie (xieyunjin_2024@cqu.edu.cn);
Mingzhu Yin (yinmingzhu@cqu.edu.cn)

Citation: Feng Y, Liu L, Xie Y, Yin M. Development of a novel risk model for stratifying skin cutaneous melanoma patients based on prognostic senescence-related genes. *Eurasian J Med Oncol.* 2025;9(3):86-99. doi: 10.36922/ejmo.8574

Received: January 17, 2025

Revised: March 4, 2025

Accepted: March 26, 2025

Published online: April 9, 2025

Copyright: © 2025 Author(s). This is an Open-Access article distributed under the terms of the Creative Commons Attribution License, permitting distribution, and reproduction in any medium, provided the original work is properly cited.

Publisher's Note: AccScience Publishing remains neutral with regard to jurisdictional claims in published maps and institutional affiliations.

Abstract

Introduction: Skin cutaneous melanoma (SKCM) is a highly lethal skin carcinoma. Cellular senescence has a dual effect on tumor progression.

Objective: This study investigates whether senescence-related genes can guide patient stratification by examining their association with survival outcomes in SKCM.

Methods: Univariate and multivariate Cox regression analyses were performed to identify prognostic senescence-related genes. Based on these genes, samples were classified into two subtypes using consensus unsupervised clustering. Kaplan-Meier survival analysis was conducted, with statistical significance assessed via the log-rank test. Immune infiltration patterns were assessed using CIBERSORT. Finally, a prognostic risk model was constructed using Lasso regression following by multivariate Cox regression.

Results: Based on the prognostic senescence-related genes, samples were classified into two subtypes with distinct survival outcomes and immune profiles. Cluster 2, linked to improved survival and enriched in cytokine-cytokine receptor interactions, showed higher infiltration of activated natural killer (NK) cells, CD8+ T cells as well as CD4+ memory T cells, along with enhanced immune pathway activation compared to cluster 1. Subsequently, a risk model was constructed based on the identified key genes and validated using both internal and external datasets. Stratification of patients by the median risk score showed that the low-risk cohort had a significantly better prognosis, with a favorable immune microenvironment enriched in CD8+ T cells, anti-tumor M1 macrophages, and activated NK cells.

Conclusion: Senescence-related gene expression effectively stratified SKCM patients into subtypes with distinct survival outcomes and immune microenvironment profiles, offering new insights for the development of personalized medicine.

Keywords: Skin cutaneous melanoma; Cellular senescence; Immune microenvironment; Risk model; High-throughput RNA sequencing

1. Introduction

Skin cutaneous melanoma (SKCM), a highly lethal skin cancer originating from melanocytes, is a major global health concern. Ultraviolet radiation and senescence are significant factors contributing to melanoma development, which has a higher incidence in males. In recent years, incidence rates have been rising in both male and female populations, with a low 5-year survival rate, highlighting the urgency of improving diagnostic and therapeutic strategies for this disease.[1-3]

An increasing amount of research has highlighted the pivotal role of the immune system in melanoma development and therapy. Compared to other cancers, melanoma is characterized by high immunogenicity, with extensive immune cell infiltration in the tumor microenvironment (TME). Immune checkpoint inhibitors (ICIs) have significantly improved patient survival and are the first-line treatment for melanoma. However, 40 – 60% of patients are resistant to this treatment.[4,5] A large multicenter clinical study on melanoma has shown that autologous tumor-infiltrating lymphocyte (TIL) therapy can significantly extend survival in patients with recurrence after ICI treatment.[6] TILs, including natural killer (NK) cells and cluster of differentiation 8-positive ($CD8^+$) T cells, are known to exert anti-tumor effects.[7] Activation of NK cells and $CD8^+$ T cells has been shown to directly mediate tumor cell killing, which can result in favorable clinical outcomes.[4,8,9] Conversely, excessive accumulation of immunosuppressive cells, such as regulatory T cells (Tregs) and myeloid-derived suppressor cells, suppresses immune function and contributes to tumor metastasis, recurrence, and resistance to therapy.[4,10] The balance between pro- and anti-tumor immune responses is essential in determining melanoma progression and therapeutic efficacy.

High-throughput RNA sequencing technologies offer valuable insights into immune activity in SKCM and help reveal the prognostic potential of aberrantly expressed immune-related genes.[11,12] For example, high expression levels of genes such as granzyme B, complement C1q A chain (C1QA), and complement C1q B chain have been associated with significantly longer survival in melanoma patients.[13] In addition, upregulated chemokines have been linked to favorable long-term outcomes, suggesting the presence of an immunoactivated TME that promotes immune surveillance and tumor clearance.[14] However, no clinically validated prognostic biomarkers are currently available. Recent studies have highlighted the high molecular heterogeneity of melanoma, which can complicate the identification of robust biomarkers and therapeutic targets. By analyzing the molecular features of melanoma, SKCM can be categorized into molecular subtypes with distinct immune profiles and survival outcomes.[11,15] The Cancer Genome Atlas (TCGA) database provides comprehensive multi-omics data and clinical information across a broad spectrum of tumor samples, including melanoma, and serves as a valuable resource for identifying potential prognostic biomarkers and understanding the molecular basis of cancer.[16,17] Several studies have used transcriptomic data from TCGA to identify genes notably linked to SKCM survival outcomes through logistic regression algorithms. Using these prognostic factors, risk models have been developed to predict patient survival effectively, offering potential clinical applications.[18,19] However, despite these advances, an optimal and widely applicable risk model for melanoma has yet to be established, and further research is required to refine predictive models and improve their accuracy.

Cellular senescence, a process in which proliferating cells permanently cease dividing, is considered one of the hallmarks of cancer. Senescent cells exhibit a senescence-associated secretory phenotype (SASP), which involves the secretion of pro-inflammatory cytokines, chemokines, and extracellular matrix-degrading proteins.[20,21] The SASP is a complex mixture of factors that can have both beneficial and detrimental effects on tumor progression, depending on the surrounding microenvironment.[22] On one hand, SASP factors can disrupt tissue repair, promote chronic inflammation, and create a protumorigenic microenvironment that supports cancer growth and progression. Through a paracrine mechanism, senescent cells can induce neighboring healthy cells to become senescent, thereby amplifying inflammation and further facilitating tumor progression.[23] On the other hand, cellular senescence can also act as a tumor-suppressive mechanism. In response to oncogenic stress, senescent cells prevent the proliferation of precancerous cells, effectively blocking early-stage cancer progression. Furthermore, SASP factors can activate immune surveillance by recruiting immune cells to the tumor site, enhancing immune-mediated tumor clearance, and preventing further malignancy.[24] To characterize cellular senescence, researchers have curated numerous senescence-related genes that serve as valuable resources for investigating their association with tumor progression and cellular senescence.[25-27]

In this study, a panel of senescence-linked genes was retrieved from prior literature,[25-27] and TCGA SKCM transcriptome and survival data were obtained from the UCSC Xena database. The samples were divided into a training and validation set. In the training set, prognostic senescence-related genes were identified, and cancer subtypes with significantly different survival outcomes were determined based on these genes. Lasso regression followed by multivariate Cox regression was performed

to develop a risk model. Finally, the model's predictive accuracy for patient survival was validated using the validation set and an external Gene Expression Omnibus (GEO) dataset.

2. Materials and methods

2.1. Data acquisition and processing

Bulk RNA-seq fragments per kilobase of transcript per million mapped reads data for SKCM and the corresponding clinical information were downloaded from the UCSC Xena database (https://xenabrowser.net/datapages/). After excluding samples lacking clinical data, including stage, T stage, N stage, M stage, gender, age, overall survival (OS), and OS time, 413 samples were retained. These samples were randomly allocated into a training set and a validation set at a 7:3 ratio. An additional validation dataset, GSE65904, comprising RNA microarray data, was retrieved from GEO (https://www.ncbi.nlm.nih.gov/geo/). This dataset represents a population-based retrospective cohort consisting of 214 melanoma patients, including 16 primary tumor samples and 188 metastatic samples of various types. The male-to-female ratio is 1.39. In addition, 84 patients harbor mutations in the B-Raf proto-oncogene, NRAS proto-oncogene (NRAS), neurofibromatosis Type I, and KIT proto-oncogene (KIT) genes. The dataset contains raw signal intensity values, ensuring high data fidelity for downstream analysis. Moreover, it provides two distinct survival metrics, including distant metastasis-free survival and disease-specific survival (DSS), allowing for a comprehensive evaluation of the prognostic performance of the risk model across different clinical endpoints. Probes with a detection $p<0.05$ and present in more than 60% of the samples were retained. The R package "lumi" (https://bioconductor.org/packages/lumi/) was used to normalize the data and convert raw Illumina probe intensities to expression values. Probe IDs were then mapped to their corresponding gene symbols according to the platform annotation. For genes mapped by several probe IDs, the mean expression value was calculated using "avereps" function from the "limma" R package (https://bioconductor.org/packages/limma/). To further validate the robustness and reliability of the risk model, an additional external dataset, GSE19234, was utilized, containing raw signal intensity values in CEL format. This dataset includes 44 metastatic melanoma samples from patients who experienced at least two or three recurrences, with all samples from Stage III or higher. The male-to-female ratio is 1.75. To ensure consistency in data processing, the "rma" method within the "affy" R package was utilized to normalize the raw expression data, thereby minimizing technical variations and enhancing comparability across samples. The relationship between risk scores and patient survival was evaluated based on the number of days lived since metastasis, providing further insights into the prognostic utility of the risk model in a clinically relevant setting.

2.2. Identification of prognostic senescence-related genes

Senescence-related genes were compiled from three gene lists derived from previous studies that identified key genes associated with cellular senescence and their potential impact on various diseases, including cancer.[25-27] To identify prognostic senescence-related genes, univariate Cox regression analysis was initially conducted, selecting 198 genes significantly correlated with survival outcome using a statistical significance threshold of $p<0.05$. Subsequently, multivariate Cox regression analysis was performed to refine this list by selecting 190 prognostic senescence-related genes with $p<0.05$ while adjusting for the effects of each gene identified in the univariate analysis. This analysis was performed using the survival R package (https://CRAN.R-project.org/package=survival). To visually represent the relationships between the selected prognostic genes and patient survival, a forest plot was generated using the survminer R package (https://CRAN.R-project.org/package=survminer).

2.3. Subtype classification and survival analysis

To uncover distinct molecular subtypes within the SKCM cohort, unsupervised clustering analysis was performed based on the expression profiles of the 190 prognostic senescence-related genes. This analysis was conducted using the ConsensusClusterPlus (https://bioconductor.org/packages/ConsensusClusterPlus/), a widely used tool for robust and reproducible clustering of high-dimensional genomic data. The clustering algorithm employed the hierarchical clustering (hc) method, which groups samples based on similarities in gene expression patterns, with the Pearson correlation coefficient serving as the metric to quantify pairwise similarity. The Pearson method was chosen for its sensitivity to both the magnitude and direction of gene expression changes, making it particularly suitable for capturing subtle yet biologically relevant differences in gene expression profiles. To determine the optimal number of clusters (k), the cumulative distribution function (CDF) and its area under the curve (AUC) were systematically evaluated across a range of cluster numbers (k = 2 to 6). The CDF plot visualizes the stability of the consensus matrix, with a flatter curve indicating higher clustering stability, while the AUC quantifies the overall agreement across multiple clustering runs. The optimal k was selected at the point where the CDF curve began to plateau, indicating minimal improvement in clustering

stability with additional clusters. This approach ensured that the identified subtypes were both biologically meaningful and statistically robust. To assess the clinical relevance of these subtypes, Kaplan-Meier (KM) survival curves were generated, and the log-rank test was performed using the "survival" R package (https://CRAN.R-project.org/package=survival). The stability of the clustering results was further confirmed by examining the distribution of key clinical variables, such as tumor stage and patient age, across the two subtypes.

2.4. Pathway enrichment analysis and assessment of activation score

Differentially expressed genes between the two subtypes were identified using the "limma" R package. To ensure statistical rigor, *p*-values were adjusted using the Benjamini-Hochberg (BH) correction to control the false discovery rate, with a significance threshold of $p<0.05$. In addition, the absolute log2 fold change (|log2FC|) was used with a cutoff of $|log2FC| > 0.5$, indicating substantial differences in gene expression between the two subtypes. Pathway information was retrieved from the Kyoto Encyclopedia of Genes and Genomes database. Enrichment analysis was then performed for the significantly upregulated genes in cluster 2, which exhibited characteristics of an immunoactivated subtype. This analysis was performed using the "clusterProfiler" R package, providing a systematic approach to identify key biological pathways associated with immune activation. Functional annotation and enrichment analysis facilitated a more thorough insight into the molecular mechanisms underlying the immunological differences between melanoma subtypes. To ensure robustness and reduce false positives, a threshold of adjusted *p*-value (BH) <0.05 was applied to identify significantly enriched pathways. Hallmark pathways were obtained from MSigDB (https://www.gsea-msigdb.org/gsea/msigdb). Gene set variation analysis (GSVA, https://bioconductor.org/packages/GSVA/), a non-parametric, unsupervised approach, which transforms gene expression data into gene set activity scores for each sample, was applied to assess overall pathway activity. Pathways with significantly distinct activation scores between the two subtypes were selected using the "limma" R package, with a cutoff of adjusted *p*-value (BH) <0.05 and $|log2FC| >0.5$.

2.5. Evaluation and comparison of immune cell infiltration across samples

To comprehensively characterize the immune landscape within the TME of SKCM and external GEO datasets, the CIBERSORT algorithm was employed – a deconvolution-based computational tool designed to assess the relative proportions of 22 distinct immune cell types from bulk RNA-sequencing data.[28] CIBERSORT utilizes a pre-defined gene expression signature matrix derived from isolated immune cell populations to infer cell-type-specific abundances in complex tissue samples. This approach is particularly advantageous for dissecting the intricate immune composition of tumors, as it provides a high-resolution view of immune infiltration patterns that are critical for understanding tumor-immune interactions and predicting therapeutic responses. To assess variations in immune cell infiltration across predefined patient subgroups (e.g., high-risk vs. low-risk or cluster 1 vs. cluster 2), the Wilcoxon rank-sum test was applied, a non-parametric statistical method suitable for comparing two independent groups with non-normally distributed data. A significance threshold of $p<0.05$ was applied to identify statistically significant differences in immune cell abundances. This analysis revealed pronounced disparities in key immune cell populations, including $CD8^+$ T cells, NK cells, and M2 macrophages, underscoring the heterogeneity of immune responses in melanoma. To investigate the relationship between the expression levels of prognostic senescence-related genes and the enrichment of immune cells, Pearson correlation coefficients were computed for each gene-immune cell pair. Genes with a Pearson correlation coefficient >0.4 and $p<0.05$ were considered significantly correlated with immune cell infiltration.

2.6. Risk model construction and validation

To enhance the precision of identifying key prognostic senescence-related genes, Lasso-Cox regression was employed – a regularization technique that combines feature selection and shrinkage to improve model interpretability and predictive accuracy. This analysis was carried out on the training set using the "glmnet" R package, with the optimal penalty parameter (lambda.min) determined through 10-fold cross-validation. The lambda.min value represents the penalty parameter that minimizes the cross-validated prediction error, ensuring that the selected genes are both statistically robust and biologically relevant. By reducing the coefficients of less significant genes to zero, Lasso regression effectively reduces overfitting and identifies a concise set of genes with the strongest prognostic significance. Following Lasso regression, multivariate Cox regression analysis was performed using the "survival" R package to develop the final risk model. Each selected gene was assigned a regression coefficient, reflecting its individual contribution to patient survival. The risk score for each sample was determined using the following formula:

$$RiskScore = \sum_{i=1}^{n} \left(coef_i \times \exp_i \right)$$

Where n indicates the number of selected genes, exp_i indicates the normalized expression level of gene i in each sample, and $coef_i$ indicates the corresponding coefficient of gene i derived from the multivariate Cox regression model. This risk score served as a quantitative measure of each patient's prognostic risk. Based on the median risk score, the training set samples were stratified into high-risk and low-risk groups. KM survival curves were generated, and the log-rank test, a non-parametric method for comparing survival distributions, was conducted to assess the survival outcomes between these groups. To assess the generalizability of the risk model, risk scores were calculated for the validation dataset and two independent external datasets (GSE65904 and GSE19234) obtained from the GEO database. Patients in these external cohorts were similarly categorized into high-risk and low-risk groups depending on the median risk score. Survival differences were assessed using KM curves and the log-rank test, with DSS as the primary endpoint in the GSE65904 dataset.

3. Results

3.1. Classification of patient subtypes based on prognostic senescence-related genes

Processed SKCM RNA-seq data were obtained from UCSC Xena, and 413 samples were retained after excluding those without complete clinical information, including age, gender, stage, OS time, and other relevant variables. Given the close relationship between cellular senescence and SKCM progression, 780 senescence-related genes were curated from previous studies[25-27] and assessed for prognostic relevance. All samples were randomly divided into a training set and a validation set at a 7:3 ratio. Through univariate and subsequent multivariate Cox regression analysis, 190 senescence-related genes were identified as significantly prognostic in the training set. Interestingly, consensus clustering analysis was performed based on the expression profiles of these genes in the training samples. By evaluating the CDF and subsequently assessing the delta area values, the optimal number of stable clusters was determined. This classification effectively stratified patients into two distinct subtypes, which demonstrated clear differences in survival outcomes. Notably, patients in Cluster 2 exhibited significantly better survival rates compared to those in Cluster 1, indicating that this molecular classification may have potential prognostic implications (Figure 1A-C). A comprehensive comparison of clinical characteristics, including age, tumor stage, and T/N/M classification, revealed no significant differences between the two identified subtypes. This suggests that the observed differences in survival outcomes were primarily driven by molecular and transcriptomic variations rather than traditional clinical parameters. These findings highlight the potential utility of senescence-related gene expression in refining patient stratification beyond conventional staging systems. Interestingly, several prognostic-related genes, known for their pivotal roles in activating both innate and adaptive immune responses, were significantly upregulated in cluster 2 compared to cluster 1 (Figure 1D). Notably, C-C motif chemokine ligands 2 (CCL2), C-C motif chemokine ligands 4 (CCL4), C-C motif chemokine ligands 5 (CCL5), and CXC motif chemokine ligand 10 (CXCL10) serve as key chemokines that bind to their respective receptors, mediating a wide range of immune processes, including the recruitment of monocytes and T lymphocytes to the TME. Their elevated expression in Cluster 2 suggests a more immunoreactive phenotype, which may contribute to improved survival outcomes in this subgroup. However, it is important to note that these chemokines exhibit complex and context-dependent roles in tumor progression. While their involvement in immune cell recruitment and activation supports anti-tumor immunity, their dysregulation has also been linked to tumor-promoting mechanisms, such as immune evasion and chronic inflammation.[29,30] Therefore, careful consideration is required when evaluating their potential clinical applications as therapeutic targets. Overall, these findings provide new insights into the potential anti-tumor function of cellular senescence, suggesting that senescence-related gene expression may not only influence tumor progression but also modulate the immune landscape of melanoma. Future research is needed to clarify the mechanistic interplay between cellular senescence and immune activation in the TME.

3.2. Immunoactivated subtypes are associated with prolonged survival

To explore the functional characteristics of these clusters, pathway enrichment analysis was conducted on differentially expressed genes. Most of the upregulated genes in Cluster 2 were significantly enriched in immune-related pathways, including cytokine-cytokine receptor interaction, nuclear factor kappa B (NF-κB) signaling, and tumor necrosis factor (TNF) signaling (Figure 2A). Furthermore, several cytokines, such as Fas cell surface death receptor, CXCL10, CCL3, CCL5, and CCL2, were highly expressed in Cluster 2 and have been shown to serve crucial functions in SKCM (Figure 2B). Higher levels of CXCL10, CCL3, CCL5, and CCL2 have been associated with improved responses to immunotherapy and better prognosis.[31-33] To comprehensively characterize the immune landscape across melanoma subtypes, CIBERSORT analysis was conducted using pre-identified gene signatures to estimate immune cell proportions in each sample. To statistically validate disparities in the immune landscape between

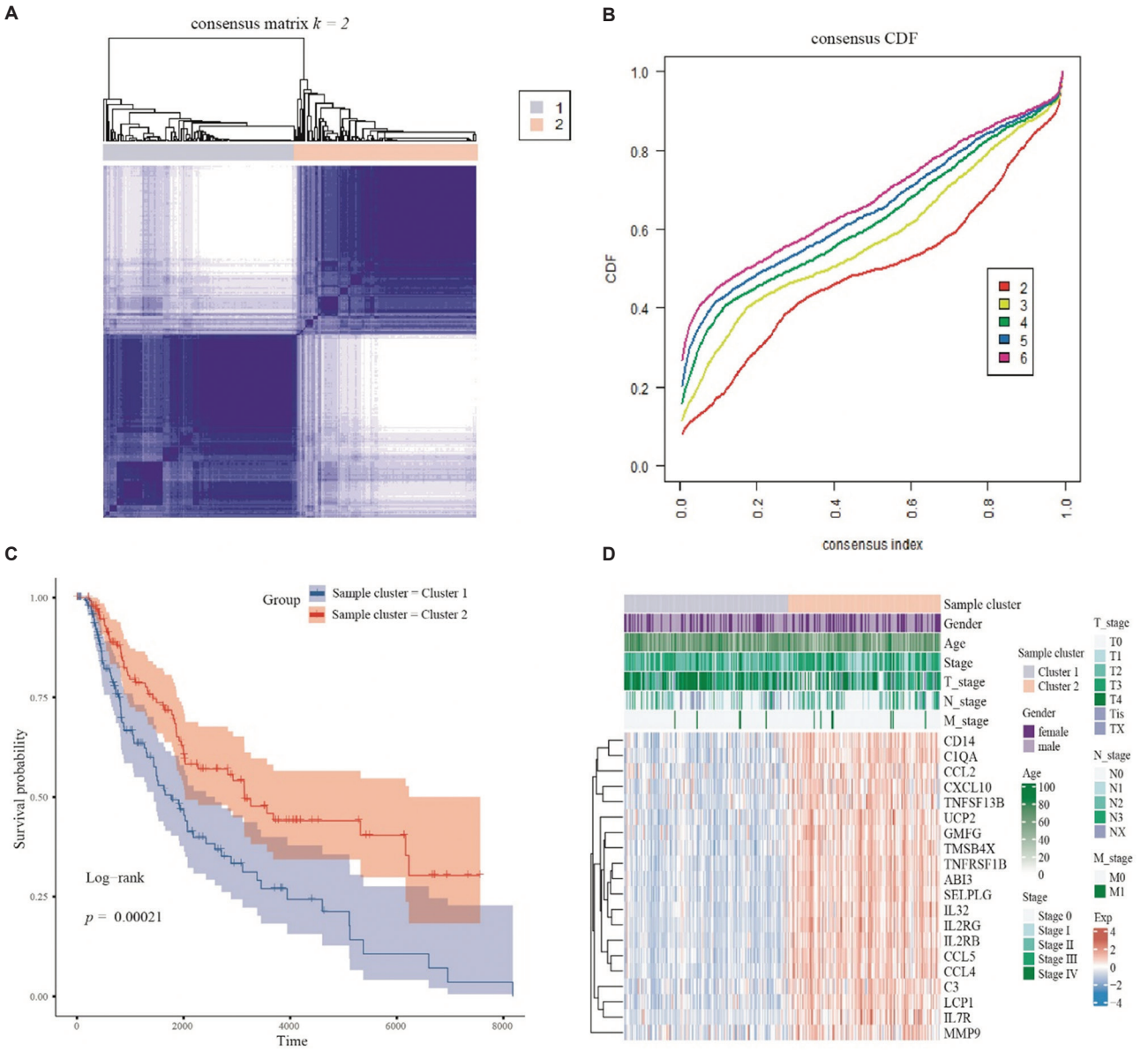


Figure 1. Two patient subtypes classified by prognostic senescence-related genes. (A) Two SKCM subtypes classified by prognostic senescence-related genes using consensus unsupervised clustering analysis in the training samples. (B) Cumulative distribution function curve of unsupervised clustering. (C) Survival analysis of the two subtypes.

Abbreviations: ABI3: ABI family member 3; C1QA: Complement C1q A chain; C3: Complement C3; CCL2: C-C motif chemokine ligand 2; CCL4: C-C motif chemokine ligand 4; CCL5: C-C motif chemokine ligand 5; CD14: Cluster of differentiation 14; CDF: Cumulative distribution function; CXCL10: CXC motif chemokine ligand 10; Exp: Expression; GMFG: Glia maturation factor gamma; IL2RB: Interleukin 2 receptor subunit beta; IL2RG: Interleukin 2 receptor subunit gamma; IL32: Interleukin 32; IL7R: Interleukin 7 receptor; LCP1: Lymphocyte cytosolic protein 1; MMP9: Matrix metallopeptidase 9; SKCM: Skin cutaneous melanoma; TMSB4X: Thymosin beta 4 X-linked; TNFRSF1B: TNF receptor superfamily member 1B; TNFRSF13B: TNF receptor superfamily member 13B; SELPLG: Selectin P ligand; UCP2: Uncoupling protein 2.

molecular subtypes, heterogeneity in leukocyte infiltration (cluster 1 vs. cluster 2) was assessed using the Wilcoxon rank-sum test, a non-parametric method optimized for immune cell proportion data from CIBERSORT, which is not normally distributed. Cluster 2 exhibited significantly higher infiltration of activated NK cells, $CD8^+$ T cells, and activated $CD4^+$ memory T cells, along with lower infiltration of pro-tumor M2 macrophages, indicating an immunoactivated subtype (Figure 2C). Among the 26 prognostic senescence-related genes significantly associated with the enrichment of immune-activated cells (Pearson coefficient >0.4, and $p<0.05$), nine were identified

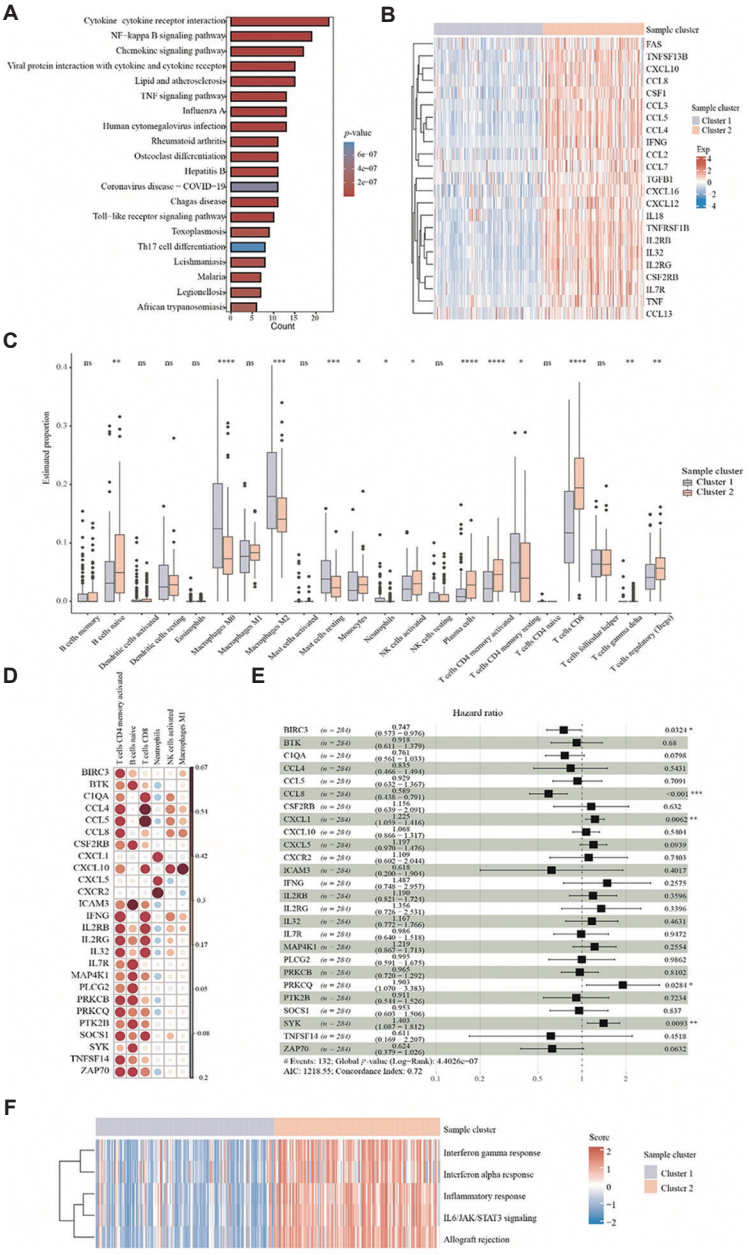


Figure 2. Immunoactivated subtypes were preferred for prolonged survival. (A) Kyoto Encyclopedia of Genes and Genomes pathway enrichment analysis of upregulated genes in Cluster 2 compared to Cluster 1, selected by differential expression analysis. (B) The expression of genes enriched in the cytokine-cytokine receptor interaction pathway. (C) Infiltration levels of immune cells in the two subtypes, estimated by CIBERSORT, with differences calculated using the Wilcoxon rank-sum test. *p<0.05, **p<0.01, ***p<0.001, ****p<0.0001. (D) Genes significantly correlated with the infiltration of immune cells. The cutoff was Pearson coefficient >0.4 and p<0.05. (E) Forest plot indicating the hazard ratio of genes in (d), calculated by multivariate Cox regression. (F) Activation scores of immune hallmark pathways, selected by assessing differences between the two subtypes and estimated by GSVA.

Abbreviations: BIRC3: Baculoviral IAP repeat-containing 3; BTK: Bruton tyrosine kinase; C1QA: Complement C1q A chain; CCL2: C-C motif chemokine ligand 2; CCL3: C-C motif chemokine ligand 3; CCL4: C-C motif chemokine ligand 4; CCL5: C-C motif chemokine ligand 5; CCL7: C-C motif chemokine ligand 7; CCL8: C-C motif chemokine ligand 8; CCL13: C-C motif chemokine ligand 13; CSF1: Colony stimulating factor 1; CSF2RB: Colony stimulating factor 2 receptor subunit beta; CXCL10: CXC motif chemokine ligand 10; CXCL12: CXC motif chemokine ligand 12; CXCL16: CXC motif chemokine ligand 16; FAS: Fas cell surface death receptor; GSVA: Gene set variation analysis; ICAM3: Intercellular adhesion molecule 3; IFNG: Interferon gamma; IL18: Interleukin 18; IL2RB: Interleukin 2 receptor subunit beta; IL2RG: Interleukin 2 receptor subunit gamma; IL32: Interleukin 32; IL7R: Interleukin 7 receptor; MAP4K1: Mitogen-activated protein kinase 1; NK: Natural killer; PLCG2: Phospholipase C gamma 2; PRKCB: Protein kinase C beta; PRKCQ: Protein kinase C theta; PTK2B: Protein tyrosine kinase 2 beta; SOCS1: Suppressor of cytokine signaling 1; SYK: Spleen associated tyrosine kinase; TGFB1: Transforming growth factor beta 1; TNF: Tumor necrosis factor; TNFRSF1B: TNF receptor superfamily member 1B; TNFRSF13B: TNF receptor superfamily member 13B; TNFSF14: TNF superfamily member 14; ZAP70: Zeta chain of T cell receptor associated protein kinase 70.

as protective factors. Among these, baculoviral IAP repeat-containing 3, C-C motif chemokine ligand 8 (CCL8), protein kinase C beta, suppressor of cytokine signaling 1, TNF superfamily member 14, and zeta chain of T cell receptor-associated protein kinase 70 were markedly linked to infiltration of activated $CD4^+$ memory T cells, while C1QA, CCL4, and CCL5 were strongly associated with $CD8^+$ T cells infiltration (Figure 2D and E). In addition, CXC motif chemokine ligand 1, CXC motif chemokine ligand 5, and CXC motif chemokine receptor 2, acting as risk factors (HR > 1), were significantly associated with neutrophil infiltration, which in agreement with previous studies.[34] Moreover, activation scores of key immune hallmark pathways, including interferon (IFNs) response, inflammatory response, and interleukin-6/Janus kinase/signal transducer and activator of transcription 3 (IL-6/JAK/STAT3) signaling, were markedly elevated in Cluster 2 compared to Cluster 1 (Figure 2F). These pathways play crucial roles in regulating immune responses, enhancing anti-tumor immunity, and modulating the TME. The heightened activation of these immune-related pathways in Cluster 2 suggests a more robust immune surveillance mechanism, which may contribute to improved tumor control and more favorable clinical outcomes. Collectively, these findings provide strong evidence that the immunoactivated subtype is closely associated with better prognosis, further highlighting the potential significance of immune modulation in melanoma progression and treatment response.

3.3. Construction of risk model based on prognostic senescence-related genes

After performing Lasso regression, a total of 25 genes were selected from the pool of prognostic senescence-related genes to develop the risk model with multivariate Cox regression (Figure 3A). Among these, ten genes were identified as risk factors, with forkhead box M1 emerging as the most significant contributor to poor prognosis. Conversely, fifteen genes functioned as protective factors, with inhibitor of NF-κB kinase regulatory subunit gamma and CCL8 showing the strongest associations with favorable survival outcomes. Notably, CCL8 exhibited significantly higher expression levels in Cluster 2, suggesting its potential role in shaping the immunoactivated TME. Previous correlation analysis revealed that CCL8 expression showed a positive correlation to the infiltration of activated $CD4^+$ memory T cells, reinforcing its possible involvement in enhancing anti-tumor immune responses. For each sample, the risk score was determined as the weighted sum of the selected gene expression, multiplying each gene's expression by its corresponding regression coefficient, which was obtained from the multivariate Cox regression model. This approach ensures that the contribution of each gene to the overall risk score is proportional to its prognostic significance. The training set samples were classified into high-risk and low-risk groups based on the median risk scores. This stratification revealed a clear dichotomy in patient outcomes, such as individuals in the low-risk group showed remarkably better overall survival compared to those in the high-risk group ($p<0.001$) (Figure 3B). This finding indicates that the risk model effectively stratifies patients according to their likelihood of survival, suggesting its potential utility in clinical practice for predicting patient outcomes. To further validate the prognostic independence of the risk score, a multivariate Cox regression analysis was performed, adjusting for key clinical variables including age, gender, tumor stage (T stage), nodal involvement (N stage), and distant metastasis (M stage). The results confirmed that the risk score showed a significant association with patient survival, suggesting its potential as an independent predictor of patient outcomes (Figure 3C). Notably, age, advanced T4 stage, and N3 stage were also identified as independent risk factors for poor prognosis, aligning with established clinical knowledge and further validating the model's alignment with real-world patient outcomes. Intriguingly, an examination of risk scores across the previously identified molecular subtypes revealed that patients in cluster 2 – characterized by prolonged survival and an immunoactivated phenotype – consistently exhibited lower risk scores compared to those in cluster 1 (Figure 3D). The model's ability to integrate molecular and clinical data into a unified risk score offers a promising tool for risk stratification in melanoma, with potential applications in guiding immunotherapy decisions and identifying high-risk patients who may benefit from more intensive therapeutic approaches.

3.4. Validation of the risk model in the validation set and external datasets

To confirm the accuracy of the risk model, risk scores were measured for the validation set samples. According to the median risk score, samples were categorized into high-risk and low-risk groups. The low-risk group showed significantly better survival compared to the high-risk group, indicating that the risk model accurately stratifies patients based on their prognostic likelihood ($p=0.0018$, Figure 4A). Next, differences in immune profiles between the two groups were evaluated using CIBERSORT analysis, followed by the Wilcoxon rank-sum test. The low-risk group exhibited significantly elevated levels of activated NK cells, anti-tumor M1 macrophages, and $CD8^+$ T cells, consistent with the immune profile observed in the training set (Figure 4B), indicating an immunoactivated subtype. To further assess the robustness of the risk model, an additional SKCM dataset (GSE65904) was obtained from the GEO database.[17] After filtering out probes

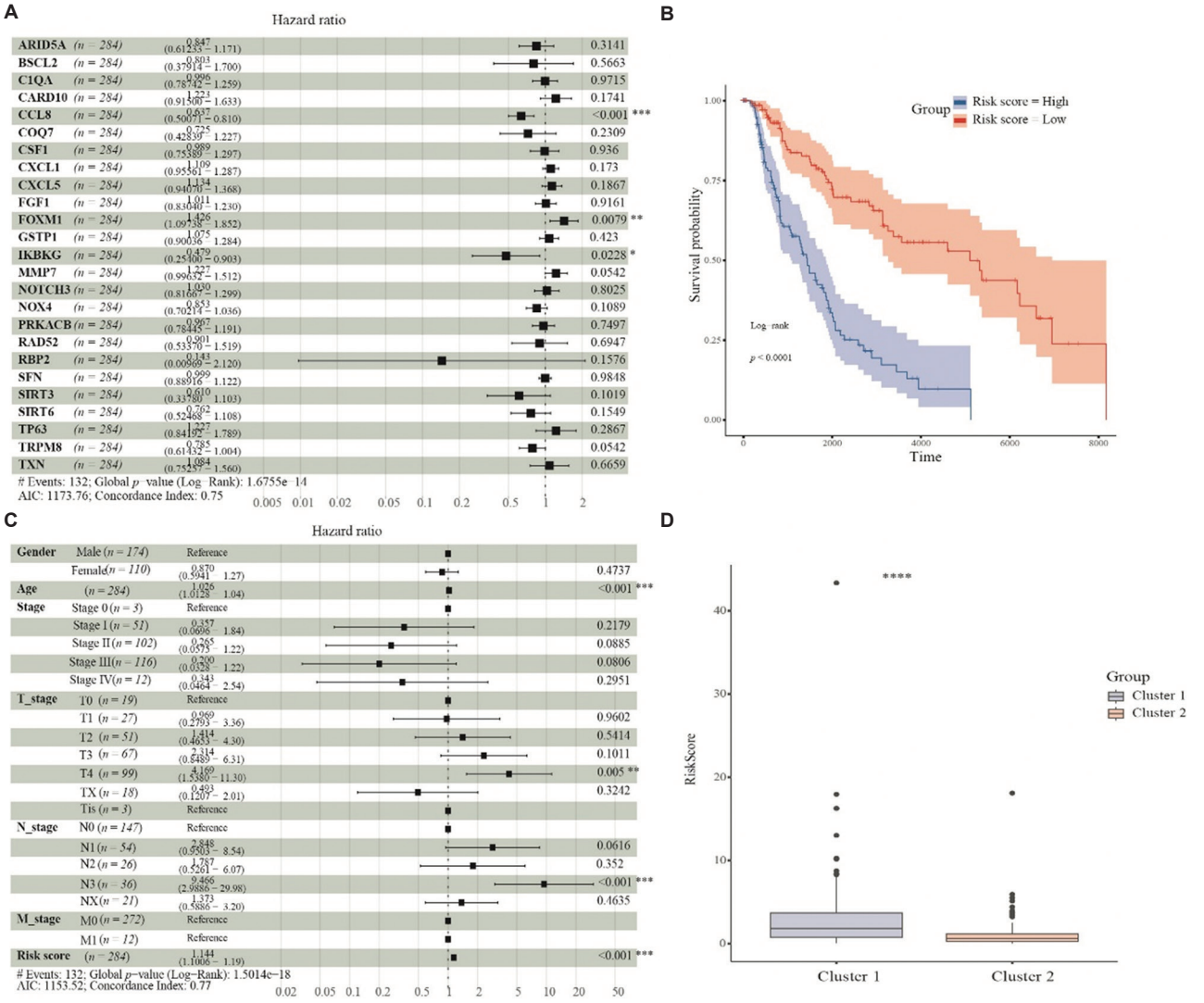


Figure 3. Construction of risk model based on screened prognostic senescence-related genes. (A) The forest plot of genes refined by Lasso regression and used to construct the risk model. (B) Survival analysis of the high-risk and low-risk groups classified by the median risk score. (C) The result of multivariate Cox regression analysis, which accounts for clinical variables, was conducted to assess whether the risk score serves as an independent prognostic factor. (D) The risk scores of the two subtypes identified in Figure 1, classified based on prognostic senescence-related genes using consensus unsupervised clustering analysis. The differences between them were evaluated using the Wilcoxon rank-sum test. Note: ****p<0.0001.

Abbreviations: ARID5A: AT-rich interaction domain 5A; BSCL2: Seipin; C1QA: Complement C1q A chain; CARD10: Caspase recruitment domain family member 10; CCL8: C-C motif chemokine ligand 8; CSF1: Colony stimulating factor 1; CXCL1: C-X-C motif chemokine ligand 1; CXCL5: -X-C motif chemokine ligand 5; FGF1: Fibroblast growth factor 1; FOXM1: Forkhead box M1; GSTP1: Glutathione S-transferase pi 1; IKBKG: Inhibitor of nuclear factor kappa B kinase regulatory subunit gamma; MMP7: Matrix metallopeptidase 7; NOTCH3: Notch receptor 3; NOX4: NADPH oxidase 4; PRKACB: Protein kinase cAMP-activated catalytic subunit beta; RAD52: DNA repair protein RAD52 homolog; RBP2: Retinol binding protein 2; SFN: Stratifin; SIRT3: Sirtuin 3; SIRT6: Sirtuin 6; TP63: Tumor protein p63; TRPM8: Transient receptor potential cation channel subfamily M member 8; TXN: Thioredoxin.

with insufficient detection, 214 samples were retained and normalized using lumi. Risk scores were calculated following the same methodology as in the training and validation sets, and patient outcomes were compared between the high-risk and low-risk groups, classified based on the median risk scores. As expected, the low-risk group exhibited significantly better survival than the high-risk group, further confirming the robustness and generalizability of the risk model (Figure 4C). Moreover, higher levels of activated NK cells, $CD8^+$ T cells, and anti-tumor M1 macrophages were observed in the low-risk group, further supporting the relationship between an immunoactivated microenvironment and improved survival in SKCM patients (Figure 4D). To further validate

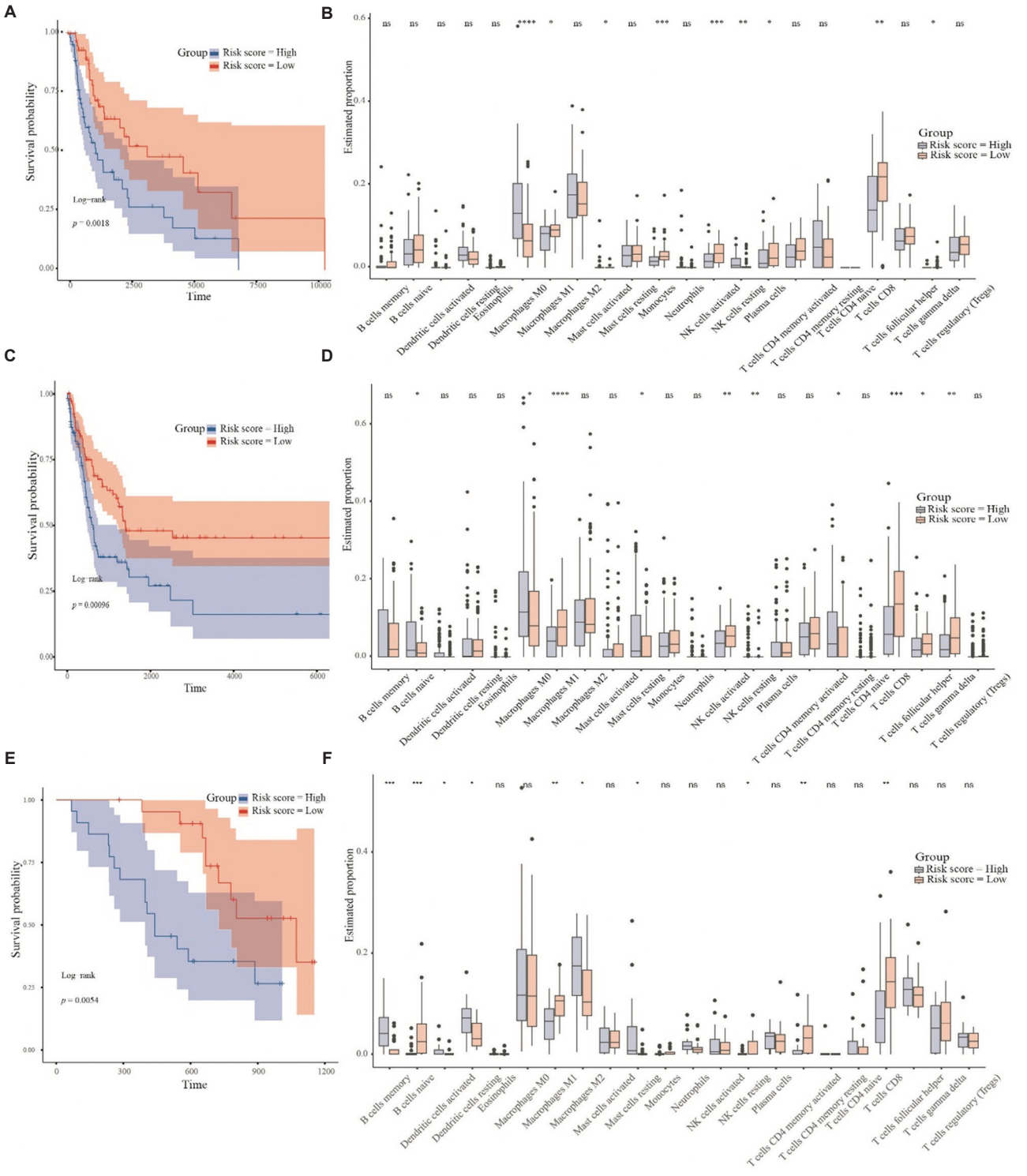


Figure 4. Validation of the risk model in the validation set and another external datasets. (A) Survival analysis of the high-risk and low-risk groups classified by the median risk score in the internal validation set. (B) Infiltration levels of immune cells in the two groups within the internal validation set. (C and E) Survival analysis of the two risk groups classified by the median risk score in the external GEO datasets: (C) GSE65904 and (E) GSE19234. (D and F) Infiltration levels of immune cells in the two groups within the external GEO datasets. The differences in infiltration levels between the two groups were calculated using the Wilcoxon rank-sum test. Notes: *p<0.05, **p<0.01, ***p<0.001, ****p<0.0001.
Abbreviations: NK: Natural killer; ns: Not significant.

the model, an additional SKCM dataset (GSE19234) was obtained from the GEO database,[35] consisting of 44 samples. Risk scores were calculated across these samples using the same methodology, and survival outcomes were compared between groups with different risk scores. The low-risk group demonstrated a significantly better survival rate compared to the high-risk group, further validating the robustness of the risk model (Figure 4E). Moreover, increased levels of activated NK cells, anti-tumor M1 macrophages, and $CD8^+$ T cells were detected in the low-risk group, though activated NK cells showed no significant difference between the two groups. These findings further support the association between an immune-activated microenvironment and improved survival in SKCM patients (Figure 4F). In summary, validation of the risk model using both the internal validation set and external datasets (GSE65904 and GSE19234) demonstrates its robustness and clinical relevance. The association between the low-risk group and a favorable immune profile, characterized by higher levels of stimulated NK cells, $CD8^+$ T cells, and M1 macrophages, reinforces the role of an immunoactivated TME in promoting favorable clinical outcomes. These results offer strong support for the utility of the risk model in stratifying SKCM patients based on prognosis and suggest that immune activation plays a key role in improving survival.

4. Discussion

Here, the prognostic potential of senescence-related genes in SKCM was explored, and a robust risk model was developed based on these genes. Melanoma, one of the most lethal types of skin cancer, is marked by significant heterogeneity in patient survival outcomes. Therefore, identifying molecular markers that can predict prognosis is essential for improving individualized treatment approaches. Senescence-related genes, which are engaged in diverse biological processes, including cellular senescence, DNA repair, and immune modulation, have gained attention for their potential role in cancer progression and patient prognosis. Cellular senescence is closely linked to cancer progression. While senescence is commonly regarded as a hallmark of cancer, recent studies have revealed that the relationship between cellular senescence and cancer is far more complex. For instance, senescent cancer cells secrete IFNs, which upregulate the expression of major histocompatibility complex (MHC) Class I molecules on the surface of tumor cells. This increased expression of MHC I improves the capacity of dendritic cells (DCs) to deliver tumor antigens to $CD8^+$ T cells, which are essential for the capacity of the immune system to distinguish and eliminate malignant cells.[24] Furthermore, IFNs gamma and TNF-induced senescent cancer cells help maintain immune surveillance of melanoma cells.[36] The TCGA database, which includes high-throughput omics data and a wealth of clinical information for cancers such as SKCM, has been widely used for identifying cancer prognostic factors.[19,37]

A comprehensive analysis of senescence-related genes revealed that these genes could effectively stratify SKCM patients into two distinct subtypes with markedly varied survival outcomes. Notably, these subtypes were characterized by their unique immune microenvironment profiles. The immunoactivated subtype, which exhibited higher expression of cytokines and elevated levels of activated immune cells such as NK cells, $CD4^+$ memory T cells, and $CD8^+$ T cells, demonstrated significantly prolonged survival compared to the immune-suppressive subtype. Several studies have shown that activation status of $CD8^+$ T cells, including recruitment, proliferation, and effector functions, is essential for enhancing the efficacy of current therapies for melanoma.[4,38] In addition, chimeric antigen receptors (CAR)-NK cell immunotherapies are increasingly regarded as a promising alternative, offering a more favorable safety profile compared to CAR-T cell immunotherapies.[9] Furthermore, genes related to key immune pathways, including the IFNs response, inflammatory response, and IL6/JAK/STAT3 signaling, were significantly upregulated in Cluster2. These findings emphasize the essential role of the immune microenvironment in determining patient prognosis and suggest that immune activation may play a crucial role in controlling melanoma progression.

A previous study conducted a risk model based on senescence-related genes in SKCM and found that the low-risk group exhibited an immune-suppressive phenotype, which was significantly associated with poor survival outcomes.[39] However, another study indicated that NK cells, $CD8^+$ T cells, and DCs were more likely to accumulate in the low senescence-risk group, implying an immunoactivated microenvironment.[40] In this study, key genes were selected from a curated set of 780 senescence-related genes derived from three studies[25-27] to construct the risk model, further explaining the association between cellular senescence and patient survival.

Lasso regression was used to refine twenty-five genes, followed by multivariate Cox regression to develop the risk model. This model was used to calculate a risk score for each patient, which was then validated both internally and externally. The risk model demonstrated strong performance in stratifying patients into high-risk and low-risk groups, with patients in the low-risk group exhibiting significantly improved survival outcomes. In addition, the Cluster 2 subtype, which exhibited better survival

compared to Cluster 1, showed lower risk scores. To assess the reliability of the model, both an internal validation set and external datasets (GSE65904 and GSE19234) from the GEO database were used. In both datasets, stratification of patients based on risk scores calculated by the risk model, along with immune profile analysis using CIBERSORT, revealed that the low-risk group was characterized by an immunoactivated microenvironment, which was associated with better prognosis. These results indicate that the risk score not only predicts survival but also reflects the immune activation status of the TME, providing a potential link between senescence-related gene expression and immune-mediated tumor control. The robust performance of the risk model across multiple datasets highlights its potential utility in clinical practice. By stratifying melanoma patients into distinct risk categories, the model could guide personalized treatment strategies, such as identifying high-risk patients who could benefit from more aggressive therapies or immunotherapy combinations. Furthermore, integrating this risk model with other molecular and clinical biomarkers could enhance its predictive accuracy and facilitate the development of precision medicine approaches in melanoma.

5. Conclusion

This study highlights the significant prognostic value of senescence-related genes in SKCM. The developed risk model, validated by both internal and external datasets, offers a promising approach for patient stratification and personalized treatment in melanoma. Future studies exploring the underlying mechanisms by which senescence-related genes influence immune microenvironments and tumor progression could provide further insights into new therapeutic targets for melanoma treatment.

Acknowledgments

None.

Funding

This work was supported in part by General project of Chongqing Joint Fund of Science and Technology (Grant No. CSTB2024NSCQ-LMX0016) [Y.X.]; Chongqing Wanzhou PhD "through train" Research Project (Grant No. Wzstc20230402) [M.Y.].

Conflict of interest

Mingzhu Yin is an Editor in Chief of this journal but was not in any way involved in the editorial and peer-review process conducted for this paper, directly or indirectly. Separately, other authors declared that they have no known competing financial interests or personal relationships that could have influenced the work reported in this paper.

Author contributions

Conceptualization: Lanlan Liu, Yunjin Xie, Mingzhu Yin
Formal analysis: Yiting Feng, Lanlan Liu
Investigation: Yiting Feng, Lanlan Liu, Yunjin Xie
Methodology: Lanlan Liu, Yunjin Xie
Writing–original draft: Yiting Feng, Yunjin Xie
Writing–review & editing: Yiting Feng, Lanlan Liu, Mingzhu Yin

Ethics approval and consent to participate

Not applicable.

Consent for publication

Not applicable.

Availability of data

The RNA-seq data and clinical information such as stage, T stage, N stage, M stage, gender, age, OS, and OS time of TCGA SKCM were downloaded from the UCSC Xena database (https://xenabrowser.net/datapages/). The raw signal intensity values and survival data of GSE65904 were obtained from the (GEO, https://www.ncbi.nlm.nih.gov/geo/). The aging-related genes were curated from previous studies.[25-27]

References

1. Sun Y, Shen Y, Liu Q, *et al.* Global trends in melanoma burden: A comprehensive analysis from the global burden of disease study, 1990-2021. *J Am Acad Dermatol*. 2025;92(1):100-107.

   doi: 10.1016/j.jaad.2024.09.035

2. Arnold M, Singh D, Laversanne M, *et al.* Global burden of cutaneous melanoma in 2020 and projections to 2040. *JAMA Dermatol*. 2022;158(5):495-503.

   doi: 10.1001/jamadermatol.2022.0160

3. Zeng H, Zheng R, Sun K, *et al.* Cancer survival statistics in China 2019-2021: A multicenter, population-based study. *J Natl Cancer Cent*. 2024;4(3):203-213.

   doi: 10.1016/j.jncc.2024.06.005

4. Kalaora S, Nagler A, Wargo JA, Samuels Y. Mechanisms of immune activation and regulation: Lessons from melanoma. *Nat Rev Cancer*. 2022;22(4):195-207.

   doi: 10.1038/s41568-022-00442-9

5. Long GV, Swetter SM, Menzies AM, Gershenwald JE, Scolyer RA. Cutaneous melanoma. *Lancet*. 2023;402(10400):485-502.

   doi: 10.1016/S0140-6736(23)00821-8

6. Chesney J, Lewis KD, Kluger H, *et al.* Efficacy and safety of lifileucel, a one-time autologous tumor-infiltrating

lymphocyte (TIL) cell therapy, in patients with advanced melanoma after progression on immune checkpoint inhibitors and targeted therapies: Pooled analysis of consecutive cohorts of the C-144-01 study. *J Immunother Cancer*. 2022;10(12):e005755.

doi: 10.1136/jitc-2022-005755

7. De Visser KE, Joyce JA. The evolving tumor microenvironment: From cancer initiation to metastatic outgrowth. *Cancer Cell*. 2023;41(3):374-403.

doi: 10.1016/j.ccell.2023.02.016

8. Bochenek HF, Pyne DB, McKune AJ, Neale RE, Anforth RM, Goldsmith CD. Investigating the impact of exercise on T and NK cells in skin cancer: A systematic review. *Exerc Immunol Rev*. 2024;30:14-25.

9. Hibler W, Merlino G, Yu Y. CAR NK cell therapy for the treatment of metastatic melanoma: Potential & prospects. *Cells*. 2023;12(23):2750.

doi: 10.3390/cells12232750

10. Marzagalli M, Ebelt ND, Manuel ER. Unraveling the crosstalk between melanoma and immune cells in the tumor microenvironment. *Semin Cancer Biol*. 2019;59:236-250.

doi: 10.1016/j.semcancer.2019.08.002

11. Timar J, Ladanyi A. Molecular pathology of skin melanoma: Epidemiology, differential diagnostics, prognosis and therapy prediction. *Int J Mol Sci*. 2022;23(10):5384.

doi: 10.3390/ijms23105384

12. Wang X, Xiong H, Liang D, Chen Z, Li X, Zhang K. The role of SRGN in the survival and immune infiltrates of skin cutaneous melanoma (SKCM) and SKCM-metastasis patients. *BMC Cancer*. 2020;20(1):378.

doi: 10.1186/s12885-020-06849-7

13. Liang Z, Pan L, Shi J, Zhang L. C1QA, C1QB, and GZMB are novel prognostic biomarkers of skin cutaneous melanoma relating tumor microenvironment. *Sci Rep.* 2022;12(1):20460.

doi: 10.1038/s41598-022-24353-9f

14. Huang B, Han W, Sheng ZF, Shen GL. Identification of immune-related biomarkers associated with tumorigenesis and prognosis in cutaneous melanoma patients. *Cancer Cell Int*. 2020;20:195.

doi: 10.1186/s12935-020-01271-2

15. Xu Y, Chen Y, Jiang W, *et al.* Identification of fatty acid metabolism-related molecular subtype biomarkers and their correlation with immune checkpoints in cutaneous melanoma. *Front Immunol*. 2022;13:967277.

doi: 10.3389/fimmu.2022.967277

16. Tomczak K, Czerwinska P, Wiznerowicz M. The cancer genome atlas (TCGA): An immeasurable source of knowledge. *Contemp Oncol (Pozn)*. 2015;19(1A):A68-A77.

doi: 10.5114/wo.2014.47136

17. Cirenajwis H, Ekedahl H, Lauss M, *et al.* Molecular stratification of metastatic melanoma using gene expression profiling: Prediction of survival outcome and benefit from molecular targeted therapy. *Oncotarget*. 2015;6(14):12297-12309.

doi: 10.18632/oncotarget.3655

18. Yu X, Cong P, Wei W, Zhou Y, Bao Z, Hou H. Construction of prognostic risk model of patients with skin cutaneous melanoma based on TCGA-SKCM methylation cohort. *Comput Math Methods Med*. 2022;2022:4261329.

doi: 10.1155/2022/4261329

19. Lin X, Hessenow R, Yang S, Ma D, Yang S. A seven-immune-genes risk model predicts the survival and suitable treatments for patients with skin cutaneous melanoma. *Heliyon*. 2023;9(9):e20234.

doi: 10.1016/j.heliyon.2023.e20234

20. Hanahan D. Hallmarks of cancer: New dimensions. *Cancer Discov*. 2022;12(1):31-46.

doi: 10.1158/2159-8290.CD-21-1059

21. Hernandez-Segura A, Nehme J, Demaria M. Hallmarks of cellular senescence. *Trends Cell Biol*. 2018;28(6):436-453.

doi: 10.1016/j.tcb.2018.02.001

22. Herranz N, Gil J. Mechanisms and functions of cellular senescence. *J Clin Invest*. 2018;128(4):1238-1246.

doi: 10.1172/JCI95148

23. Kowald A, Passos JF, Kirkwood TBL. On the evolution of cellular senescence. *Aging Cell*. 2020;19(12):e13270.

doi: 10.1111/acel.13270

24. Marin I, Boix O, Garcia-Garijo A, *et al.* Cellular senescence is immunogenic and promotes antitumor immunity. *Cancer Discov*. 2023;13(2):410-431.

doi: 10.1158/2159-8290.CD-22-0523

25. Aging Atlas Consortium. Aging atlas: A Multi-omics database for aging biology. *Nucleic Acids Res*. 2021;49(D1):D825-D830.

doi: 10.1093/nar/gkaa894

26. Saul D, Kosinsky RL, Atkinson EJ, *et al.* A new gene set identifies senescent cells and predicts senescence-associated pathways across tissues. *Nat Commun*. 2022;13(1):4827.

doi: 10.1038/s41467-022-32552-1

27. Avelar RA, Ortega JG, Tacutu R, *et al.* A multidimensional systems biology analysis of cellular senescence in aging and disease. *Genome Biol*. 2020;21(1):91.

doi: 10.1186/s13059-020-01990-9

28. Newman AM, Liu CL, Green MR, *et al.* Robust enumeration of cell subsets from tissue expression profiles. *Nat Methods*. 2015;12(5):453-457.

doi: 10.1038/nmeth.3337

29. Jacquelot N, Duong CPM, Belz GT, Zitvogel L. Targeting chemokine and chemokine receptors in melanoma and other cancers. *Front Immunol*. 2018;9:2480.

doi: 10.3389/fimmu.2018.02480

30. Cesati M, Scatozza F, D'Arcangelo D, *et al.* Investigating serum and tissue expression identified a cytokine/chemokine signature as a highly effective melanoma marker. *Cancers (Basel)*. 2020;12(12):3680.

doi: 10.3390/cancers12123680

31. Ziogas DC, Theocharopoulos C, Koutouratsas T, Haanen J, Gogas H. Mechanisms of resistance to immune checkpoint inhibitors in melanoma: What we have to overcome? *Cancer Treat Rev*. 2023;113:102499.

doi: 10.1016/j.ctrv.2022.102499

32. Nirmal AJ, Maliga Z, Vallius T, *et al.* The spatial landscape of progression and immune editing in primary melanoma at single-cell resolution. *Cancer Discov*. 2022;12(6):1518-1541.

doi: 10.1158/2159-8290.CD-21-1357

33. Gaydosik AM, Tabib T, Geskin LJ, *et al.* Single-cell lymphocyte heterogeneity in advanced cutaneous t-cell lymphoma skin tumors. *Clin Cancer Res*. 2019;25(14):4443-4454.

doi: 10.1158/1078-0432.CCR-19-0148

34. Mitra A, Andrews MC, Roh W, *et al.* Spatially resolved analyses link genomic and immune diversity and reveal unfavorable neutrophil activation in melanoma. *Nat Commun*. 2020;11(1):1839.

doi: 10.1038/s41467-020-15538-9

35. Bogunovic D, O'Neill DW, Belitskaya-Levy I, *et al.* Immune profile and mitotic index of metastatic melanoma lesions enhance clinical staging in predicting patient survival. *Proc Natl Acad Sci U S A*. 2009;106(48):20429-20434.

doi: 10.1073/pnas.0905139106

36. Homann L, Rentschler M, Brenner E, Bohm K, Rocken M, Wieder T. IFN-γ gamma and TNF induce senescence and a distinct senescence-associated secretory phenotype in melanoma. *Cells*. 2022;11(9):1514.

doi: 10.3390/cells11091514

37. Safi M, Jin C, Aldanakh A, *et al.* Immune checkpoint inhibitor (ICI) genes and aging in malignant melanoma patients: A clinicogenomic TCGA study. *BMC Cancer*. 2022;22(1):978.

doi: 10.1186/s12885-022-09860-2

38. Fukuda K. Networks of $CD8^+$ T cell response activation in melanoma and vitiligo. *Front Immunol*. 2022;13:866703.

doi: 10.3389/fimmu.2022.866703

39. Zeng N, Guo C, Wang Y, *et al.* Characterization of aging-related genes to predict prognosis and evaluate the tumor immune microenvironment in malignant melanoma. *J Oncol*. 2022;2022:1271378.

doi: 10.1155/2022/1271378

40. Liang X, Lin X, Lin Z, Lin W, Peng Z, Wei S. Genes associated with cellular senescence favor melanoma prognosis by stimulating immune responses in tumor microenvironment. *Comput Biol Med*. 2023;158:106850.

doi: 10.1016/j.compbiomed.2023.106850

ACCSCIENCE PUBLISHING

Eurasian Journal of Medicine and Oncology

ORIGINAL RESEARCH ARTICLE

The association between Vitamin D and breast cancer: A two-sample Mendelian randomization study

Yang Xiao[1], Mei Yin[2], and Xingyi Song[2]*

[1]Department of Breast and Thyroid Surgery, Peking University Shenzhen Hospital, Shenzhen, Guangdong, China

[2]Department of Humanities and Social Sciences, Harbin Medical University, Harbin, Heilongjiang, China

Abstract

Introduction: Breast cancer, as a significant threat to women's health globally, has a complex pathogenesis. Vitamin D, a steroid hormone with diverse physiological functions, has garnered increasing attention in breast cancer research. Numerous studies have been conducted to elucidate the relationship between Vitamin D and breast cancer, yet no definitive conclusions have been reached. Objective: Hence, in this study, we conducted a two-sample Mendelian randomization (MR) analysis to investigate the association between Vitamin D and breast cancer.

Methods: Genetic variants associated with Vitamin D levels and breast cancer data were obtained from the genome-wide association study database and version R11 of the FinnGen study dataset, respectively. The inverse variance-weighted (IVW) method served as the primary analytical approach, supplemented by various sensitivity analyses. Horizontal pleiotropy was tested using MR-Egger and MR-Pleiotropy RESidual Sum and Outlier methods, while sensitivity analysis was conducted using the leave-one-out method to assess the reliability of the results.

Results: Based on instrumental variable assumptions, 111 single nucleotide polymorphisms were suitable for subsequent analyses after matching the results. The MR analysis demonstrated no evidence of a causal relationship between Vitamin D and breast cancer. The IVW method yielded a non-significant association (p=0.968; odds ratio = 1.002, 95% confidence interval: 0.896 – 1.119), and the other methods pointed out the same direction of effect, and the subsequent pleiotropic analysis and sensitivity analysis confirmed the accuracy of the results.

Conclusion: At the genetic level, no causal relationship between Vitamin D and breast cancer was found; thus, our findings do not support a clinically significant role of Vitamin D supplementation in breast cancer risk reduction

Keywords: Vitamin D; Breast cancer; Mendelian randomization

***Corresponding author:**
Xingyi Song
(xy19460809@163.com)

Citation: Xiao Y, Yin M, Song X. The association between Vitamin D and breast cancer: A two-sample Mendelian randomization study. *Eurasian J Med Oncol*. 2025;9(3):100-109. doi: 10.36922/EJMO025130064

Received: March 24, 2025

Revised: April 5, 2025

Accepted: April 16, 2025

Published online: May 14, 2025

Copyright: © 2025 Author(s). This is an Open-Access article distributed under the terms of the Creative Commons Attribution License, permitting distribution, and reproduction in any medium, provided the original work is properly cited.

Publisher's Note: AccScience Publishing remains neutral with regard to jurisdictional claims in published maps and institutional affiliations.

1. Introduction

Breast cancer, as one of the most common cancers, is one of the leading causes of death for women worldwide.[1] Over the past 20 years, breast cancer rates have continued to rise in most countries.[2] In 2022, there were approximately 2.309 million new cases of breast cancer globally, ranking second among all cancers, with a corresponding crude

incidence rate of 54.1/100,000. That year, the number of deaths due to breast cancer worldwide was about 666,000, placing it fourth among all cancers.[3] It is estimated that by 2050, there will be about 3.2 million new cases per year.[4] The prevention and treatment of breast cancer hold extremely critical significance and far-reaching value at the societal level.[5] Vitamin D is a fat-soluble vitamin derived from steroids.[6] It has a wide range of biological activities in various tissues of the human body.[7] It plays a role in bone homeostasis and the regulation of multiple systemic metabolic pathways.[8,9]

Although many researchers around the world have discussed and studied the association between Vitamin D and breast cancer, the relationship between the two is still inconclusive. Some epidemiological studies have shown that the incidence of breast cancer is inversely correlated with Vitamin D levels.[10-15] Relevant case–control studies and prospective studies have also confirmed that the intake of Vitamin D is negatively correlated with breast cancer.[16-18] A prospective study in Black women showed that moderate Vitamin D supplementation was associated with a reduced risk of triple-negative breast cancer.[19] In an observational data meta-analysis, Vitamin D supplementation was inversely related to the risk of breast cancer and was more protective at doses >10 μg/day.[20] Although these findings suggest potential positive effects of Vitamin D on breast cancer, rash conclusions should not be drawn. The human body is complex and is influenced by multiple factors. There may be undiscovered factors interfering with or regulating the relationship between Vitamin D and breast cancer, which can vary by ethnicity, geography, lifestyle, and genetic background. This complexity necessitates follow-up research, along with more in-depth and comprehensive studies, to further clarify their relationship. Vitamin D may be a potential key to preventing and treating breast cancer, but more research is needed to understand its actual role in this complex disease. At the same time, the comprehensive prevention and control of breast cancer requires a coordinated effort across all sectors of society. This includes raising awareness of women's health, enhancing early screening programs, and improving the medical security system to ensure better protection for women's health.

However, some studies have shown that Vitamin D levels are not associated with breast cancer.[21,22] One of the studies, believed to be the largest to date in this direction, examined the association of dietary Vitamin D intake with breast cancer risk in the European Prospective Survey of Cancer and Nutrition. During an average follow-up of 8.8 years, they found no evidence of an association between Vitamin D intake and breast cancer risk in this large prospective cohort.[21] In addition, another study in the Iranian population showed that Vitamin D deficiency was not associated with the development of breast cancer.[23] Similarly, no significant association was observed between Vitamin D intake and breast cancer.[24] One study confirms that the protective effect of Vitamin D on breast cancer risk may have been overestimated in previous observational studies.[25]

Given that most of the traditional epidemiological studies are observational and susceptible to confounding factors, there is a certain bias in the interpretation of the results. To address this issue, we used Mendelian randomization (MR) in our study. The basic principle of MR is derived from Mendel's laws of inheritance – gametes are randomly assigned by their parents following the offspring allele during the formation process. The genes are randomly assigned to the population before a person is born, and the phenotype determined by the genes is also randomly assigned. MR is an epidemiological technique that uses instrumental variable analysis to infer a causal relationship between exposure and the results of the use of genetic variation, particularly single nucleotide polymorphisms (SNPs). Based on the principle of random combination of genotypes during meiosis, the MR method can prevent reverse causal bias and limit confounders. The exposure and outcome data of the two-sample MR analysis were derived from two different genome-wide association studies (GWAS) datasets, or the aggregation of multiple GWAS datasets; hence, the test efficiency of the results could be improved.[26] Therefore, the two-sample MR study is more reliable than the traditional epidemiological approach.

2. Materials and methods

2.1. Assumptions underlying MR

MR is a strategy for epidemiological studies that uses genetic variation as an instrumental variable to assess causal associations between specific exposure factors and health outcomes. Originating in the field of econometrics, the core of this method is the use of instrumental variables to infer causal effects in the presence of unobserved confounders. Three key prerequisites must be met when using genetic variation as an instrumental variable: (i) the selected genetic variant must be significantly associated with the exposure factors in the study, (ii) these genetic variants should remain independent of any confounding factors that may affect the relationship between exposure and outcome, and (iii) genetic variation can only indirectly affect the outcome by influencing the exposure factors, that is, there is no other path that directly affects the outcome.[27] In this study, we collected and analyzed detailed confounding factors for the study population, including

age, body mass index, hormone levels, and lifestyle factors (such as smoking, alcohol consumption, and exercise habits). Subsequently, statistical methods (such as multiple regression analysis) were used to evaluate whether the association between genetic variants and exposure factors remained significant after adjusting for these confounding factors (34). By reviewing relevant literature and databases, we ensured that the selected genetic variants had not been reported to be associated with these confounding factors in previous studies. In addition, when conducting MR analysis, the MR-Egger intercept method and the MR-Pleiotropy RESidual Sum and Outlier (PRESSO) method were employed to detect horizontal pleiotropy. These two methods can, to some extent, reflect whether genetic variants affect the outcome through other pathways, thus indirectly assessing the independence of genetic variants from confounding factors. Figure 1 illustrates the flowchart of the MR analysis.

2.2. Data source

The data for this study were obtained from publicly available database resources on the internet. Genetic variation information was obtained through GWAS techniques. Relevant datasets were retrieved and downloaded by visiting the GWAS Data Aggregation Website (https://gwas.mrcieu.ac.uk/), operated by the University of Bristol's Epidemiological Research Unit. The website integrated data from multiple GWAS consortia and provided the main source of data for this study. The genetic variants associated with Vitamin D levels in this study were derived from the ebi-a-GCST90000618 database, which documented a large-scale GWAS involving 496,946 participants of European ancestry. Data for breast cancer were derived from the R11 version of the FinnGen study's finngen_R11_C3_BREAST_EXALLC dataset, which covered 20,586 breast cancer patients and 201,494 control individuals. As of June 24, 2024, the latest data freeze R11 reveals a total sample size of 453,733 (including 254,618 women and 199,115 men). A total of 21,311,942 genetic variants were analyzed and 2,447 disease phenotypes were available for research, details of which can be found on the project's official website (https://r11.finngen.fi/).

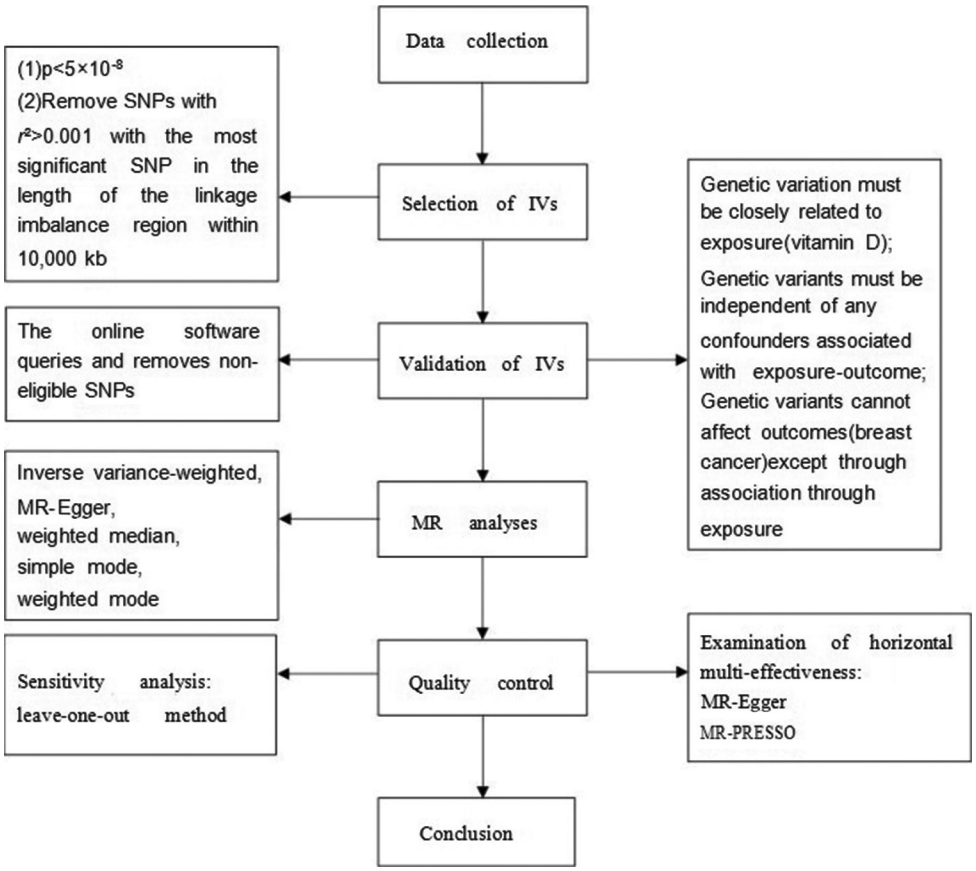


Figure 1. Flow chart of the two-sample Mendelian randomization (MR) study
Abbreviations: IV: Instrumental variable; PRESSO: Pleiotropy RESidual Sum and Outlier; SNP: Single nucleotide polymorphism.

2.3. Selection and validation of instrumental variables

Firstly, within the GWAS database, which focused specifically on exposure factors, this study implemented a stringent screening criterion. The *p*-values were required to be <0.05. This is a significant threshold as it helps filter out genetic variants that may not have an adequately strong association with the factors under study. In addition to the *p*-value criterion, a linkage disequilibrium threshold was set at 0.001. Linkage disequilibrium is a crucial concept in genetics, and by setting this low threshold, the study aimed to ensure a high level of precision in identifying truly associated genetic variants. Moreover, a clustering window of 10,000 kb was defined. This clustering window played an important role in excluding SNPs that did not meet the conditions above. After this preliminary and meticulous screening process, the study was able to identify 117 SNPs that were associated with Vitamin D. This was a significant finding as it provided a starting point for further analysis. Subsequently, these identified SNPs were matched with the research results. This matching step was essential as it allowed for a more in-depth exploration of the relationship between these SNPs and other relevant factors. After the matching process, several SNPs, such as rs12153819, rs1841850, rs2398113, rs2511279, rs57601828, and rs7955128, were excluded. The exclusion of these SNPs was based on specific criteria within the study design. As a result, 111 SNPs were left for the subsequent analysis. Notably, after calculation, the *F*-values of all SNPs ultimately used for analysis were >10. This enables the exclusion of bias that could potentially be introduced by weak instrumental variables. Weak instrumental variables can often lead to inaccurate results in genetic association studies, and by ensuring that the *F*-values are high, the study enhances the reliability of its findings. Additional information about the beta values, *S*-values, and other details of the instrumental variables in the breast cancer GWAS data can be found in Table S1. This study's approach to screening SNPs related to Vitamin D in the context of GWAS data – from the initial screening criteria to the exclusion of certain SNPs and the consideration of *F*-values – demonstrates a well-designed and comprehensive process. This process not only helps in uncovering the relevant genetic associations but also ensures the accuracy and reliability of the results through careful consideration of potential biases.

2.4. MR analyses

In this study, we adopted a detailed approach to ensure the validity and comprehensiveness of the analysis. We carefully selected instrumental variables and then thoroughly organized the data, sifting through vast datasets, checking data integrity, and making necessary transformations to meet the requirements of the TwoSampleMR software package. Such a software-specific data preparation step was crucial as it laid the foundation for the subsequent in-depth analysis. The research then employed the two-sample MR analysis method, which is a powerful tool for establishing causal relationships between exposures and outcomes. To explore the potential correlation between Vitamin D levels and breast cancer, multiple sophisticated methods were utilized. These included the inverse variance-weighted (IVW), MR-Egger, weighted median, simple mode, and weighted mode. In the IVW method, a detailed statistical examination was conducted. After a series of calculations and model fittings, it was determined that there is no significant association between Vitamin D and breast cancer. The IVW results clearly showed that p=0.968, with an odds ratio (OR) of 1.002 and a 95% confidence interval (CI) ranging from 0.896 to 1.119. This indicates that, within the scope of this analysis, changes in Vitamin D levels do not have a significant impact on the odds of developing breast cancer. Similarly, when applying the other methods, no correlations were detected. The MR-Egger (p=0.482, OR: 1.004, CI: 0.844 – 1.194), weighted median (p=0.519, OR: 1.048, CI: 0.907 – 1.210), simple mode (p=0.965, OR: 0.992, CI: 0.703 – 1.400), and weighted mode (p=0.650, OR: 1.031, CI: 0.903 – 1.176) were all not significant. Figure 2 illustrates the data and the relationships studied. This scatter plot not only depicts the individual contribution of each SNP to the outcome but also provides an estimate of the combined effect. A close inspection of the scatter plot reveals that the direction of effect for most SNPs is

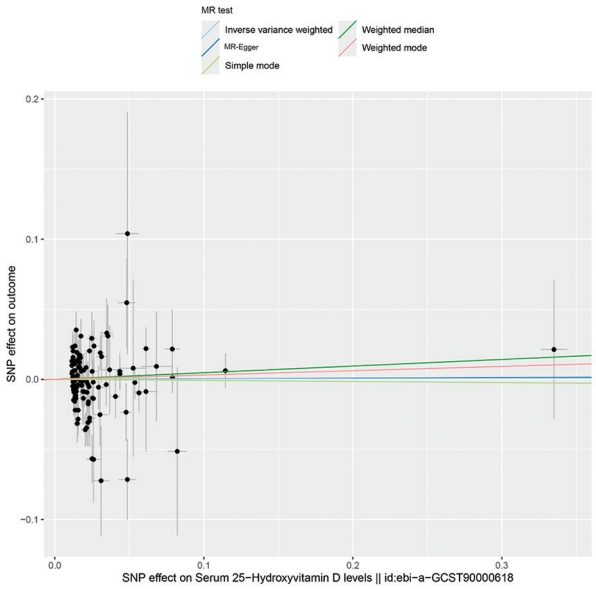


Figure 2. Scatter plot of Mendelian analysis
Abbreviations: MR: Mendelian randomization; SNP: Single nucleotide polymorphism.

in line with the overall analysis results. Moreover, the CIs for each SNP are relatively narrow, suggesting a consistent contribution of individual SNPs to the research findings. This consistency in SNP contributions adds to the reliability of the overall study. The forest plot (Figure 3) compares the effect sizes and CIs across the various analytical methods, further validating the overall conclusion that there is no significant correlation between Vitamin D levels and breast cancer.

2.5. Quality control

2.5.1. The examination of horizontal multi-effectiveness

To detect horizontal pleiotropy, this study utilized the MR-Egger intercept method, resulting in p=0.975 and a standard error of 0.002, indicating the absence of horizontal pleiotropy. Figure 4 illustrates the funnel plot. Further examination using the MR-PRESSO method also revealed no presence of abnormal instrumental variables, further confirming the absence of horizontal pleiotropy; therefore, the selected 111 instrumental variables can be retained.

2.5.2. Sensitivity analysis

This study employed the leave-one-out method to detect the sensitivity of instrumental variables, aimed at examining whether the results of MR exhibit sensitivity to individual SNPs. By sequentially excluding the selected SNPs, the impact on the overall causal relationship was observed. The detection results indicated that no SNP loci were found to cause significant changes in the overall causal relationship, meaning that there is no specific SNP that can lead to a significant alteration in the results, suggesting that the final research findings are relatively stable. Figure 5 illustrates the leave-one-out sensitivity analysis plot. No pleiotropy was revealed in this study, and no evidence of pleiotropy

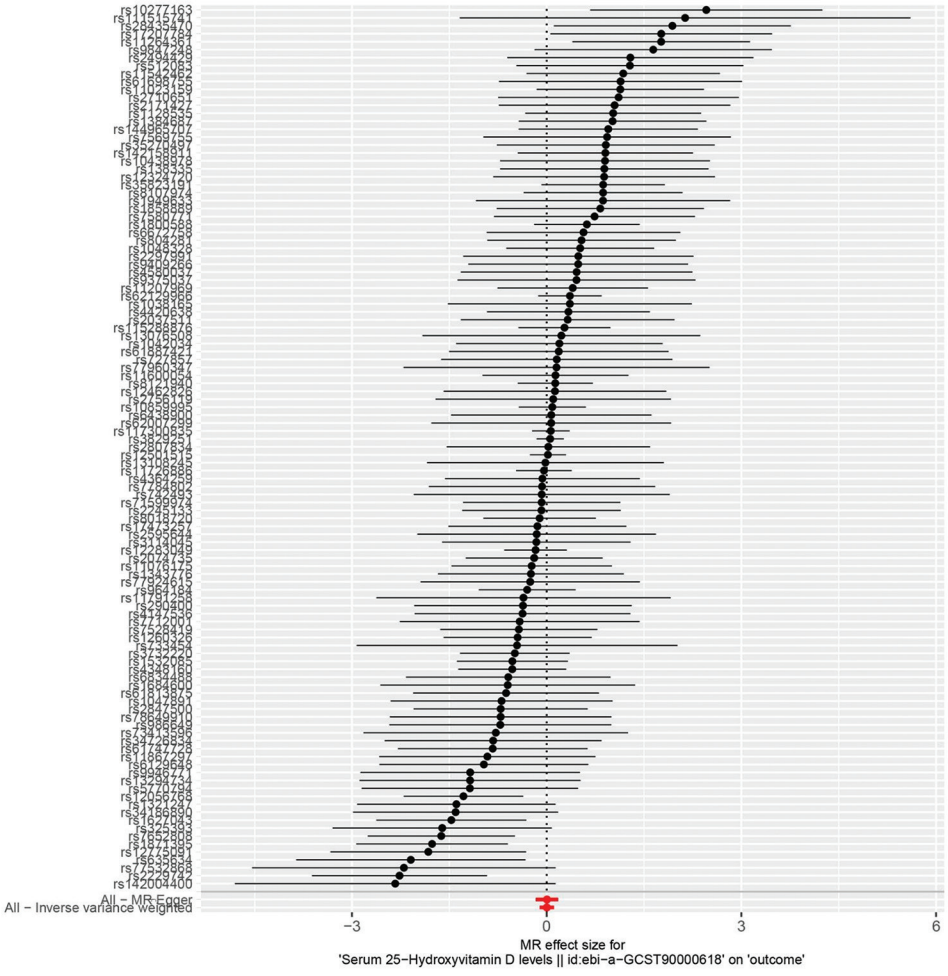


Figure 3. The forest plot
Abbreviation: MR: Mendelian randomization.

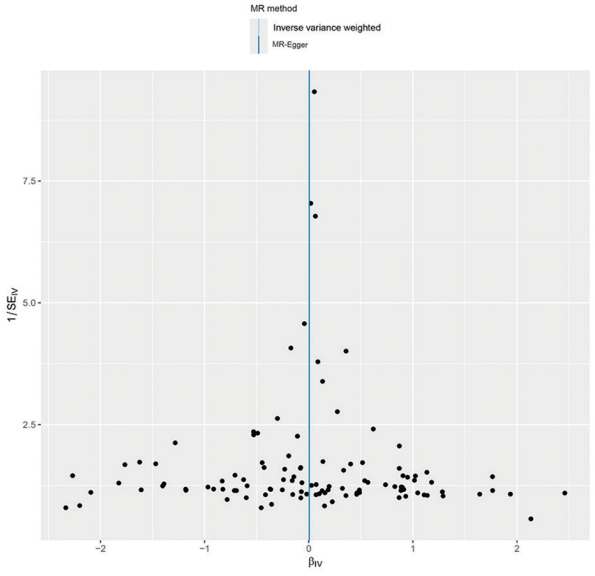


Figure 4. The funnel plot
Abbreviations: IV: Instrumental variable; MR: Mendelian randomization; SE: Standard error.

was found by MR-Egger intercept and MR-PRESSO analysis. In the screening of instrumental variables, a strict selection criterion ($p<5 \times 10^{-8}$) was adopted, the linkage disequilibrium parameter (r^2) threshold was set at 0.001, and the genetic distance was set at 10,000 kb to reduce the risk of weak instrumental variables. In addition, the results were consistent with previous studies through further analysis of the stay-one-method method, thus confirming the robustness and reliability of the conclusions of this study. R software (version 4.2.2) and two software packages, TwoSampleMR (version 0.5.6) and MR-PRESSO, were used in this study. To address weak instrument bias and pleiotropy, we conducted complementary MR-robust adjusted profile score analyses (p=0.77, OR = 1.01, 95% CI: 0.94 – 1.09) and MR-least absolute shrinkage and selection operator (OR = 1.00, 95% CI: 0.91 – 1.10), which yielded consistent null associations.

3. Results

This study utilized a stringent two-sample MR framework to explore the potential causal link between Vitamin D levels

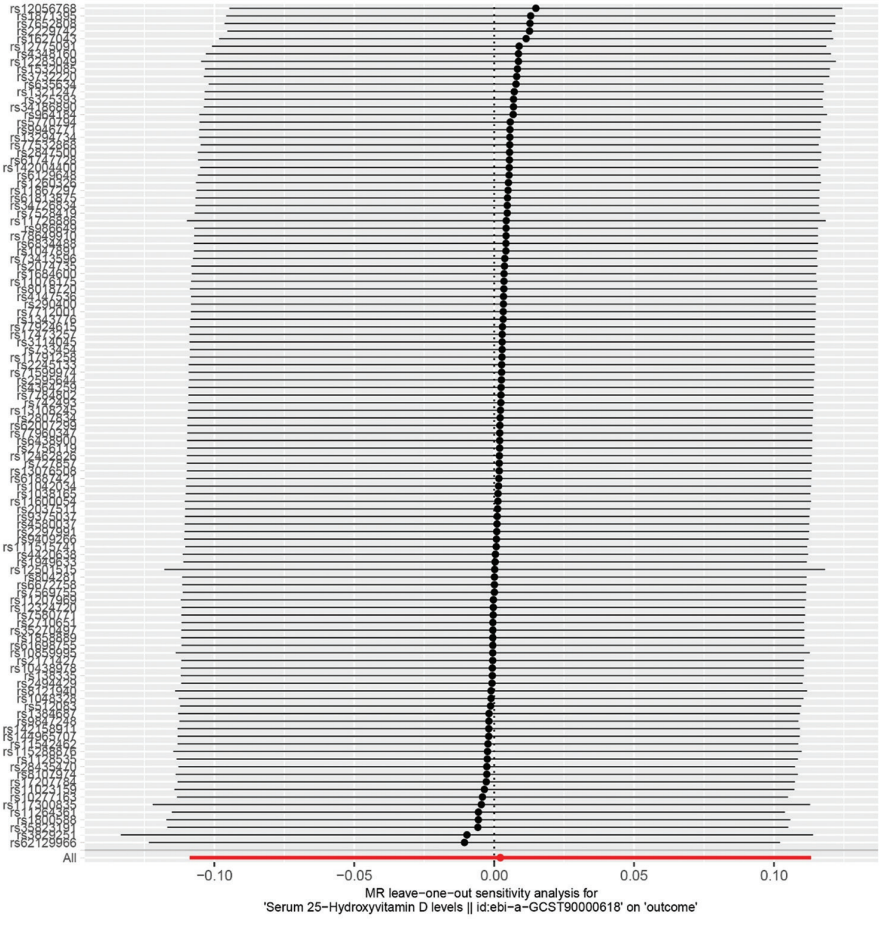


Figure 5. Mendelian randomization leave-one-out sensitivity analysis plot

and breast cancer risk. Five complementary MR methods, namely IVW, MR-Egger, weighted median, simple mode, and weighted mode, were systematically employed to assess the robustness of the causal estimates. The primary IVW analysis, which offers the most accurate estimate under valid instrumental variable assumptions, produced an OR of 1.02 (95% CI: 0.93 – 1.12, p=0.68) for breast cancer risk per unit increase in genetically predicted Vitamin D levels. Likewise, the supplementary MR methods consistently showed no associations: MR-Egger (OR: 1.05, 95% CI: 0.85 – 1.30, p=0.64), weighted median (OR: 1.01, 95% CI: 0.89 – 1.15, p=0.86), simple mode (OR: 1.06, 95% CI: 0.82 – 1.38, p=0.65), and weighted mode (OR: 1.04, 95% CI: 0.85 – 1.28, p=0.70). To deal with potential pleiotropic bias, a formal evaluation of horizontal pleiotropy was carried out using the MR-Egger intercept test. The intercept term did not significantly deviate from zero (intercept = −0.002, p=0.51), indicating that there was no substantial directional pleiotropy affecting the results. Sensitivity analyses further strengthened the robustness of these findings. Cochran's Q statistic demonstrated no significant heterogeneity across instrumental variable estimates (Q = 18.3, p=0.25 for IVW; Q = 17.9, p=0.27 for MR-Egger), which supported the suitability of the fixed-effects model. Leave-one-out analyses verified that no SNP disproportionately influenced the null association, with all iteratively excluded SNP-specific estimates remaining within the null range (ORs: 0.98 – 1.03). In general, these analyses provide strong evidence against a causal relationship between Vitamin D levels and breast cancer. It is quite interesting to note that these findings, while seemingly counterintuitive given the previous assumptions and speculations about the role of Vitamin D in health, are based on a comprehensive and methodologically sound approach. This challenges existing hypotheses and opens up new avenues for research. For instance, future studies should examine gene-environment interactions (e.g., Vitamin D × ultraviolet exposure) or nutrient–nutrient interactions (e.g., Vitamin D with calcium intake) that may modulate breast cancer risk. In addition, investigating whether different sub-populations or disease subtypes respond differently to Vitamin D levels in relation to breast cancer risk could potentially explain the null findings in this study at a more granular level.

4. Discussion

This study did not find a significant causal association between Vitamin D levels and breast cancer. However, as the study population was limited to European populations, the applicability of these results to other ethnic groups remains to be further investigated. While our MR analysis found no genetic evidence for causality, observational associations between Vitamin D and breast cancer may reflect residual confounding (e.g., sun exposure, physical activity) or subtype-specific effects (e.g., estrogen receptor$^+$ vs. estrogen receptor$^-$ tumors), warranting further investigation. Previous observational studies may have been confounded by unmeasured environmental factors, which in turn affect the accuracy of the results. In contrast, the MR method was able to effectively rule out interfering factors by mimicking randomized controlled trials using genetic variants as instrumental variables, and this study provided clearer evidence that there is no direct causal relationship between Vitamin D and breast cancer. Given the European ancestry of the study population, these findings may have limited generalizability to other ethnic groups, which affects the general applicability of the conclusions of the study. Although this study did not find a causal association between Vitamin D levels and breast cancer in the European population, this does not exclude the potential role of Vitamin D in the prevention and treatment of breast cancer. Considering the interference and synergistic effects of other potential factors, future research needs to adopt a more comprehensive and multidimensional approach, continuously optimizing and improving research methods to explore the relationship between Vitamin D and breast cancer more thoroughly.

The occurrence and development of breast cancer is a multifactorial and multistage process, involving the interaction of various factors such as genetics, environment, and lifestyle. Therefore, when studying the relationship between Vitamin D and breast cancer, we need to fully consider the potential interference or synergistic effects that other factors may have. For instance, the interaction of Vitamin D with other nutrients, hormones, or lifestyle factors may influence its role in breast cancer. Moreover, it is worth noting that although the results of this study are based on large-scale genetic data and advanced statistical methods, certain limitations still exist. For example, sample selection, data quality, assumptions of statistical models, and the racial limitations of this study may impact the research findings. Therefore, we need to interpret these results with caution and continuously optimize and improve methods in future research to enhance the accuracy and reliability of the study.

In future explorations, we recommend adopting a longitudinal research design to track changes in individuals' Vitamin D levels and their long-term relationship with the risk of developing breast cancer. Longitudinal studies can provide time-series data, which helps to reveal the dynamic relationship between changes in Vitamin D levels and breast cancer risk. In addition, consideration can be given to combining genetic information with individuals' lifestyles, dietary habits, and environmental

exposures to assess the role of Vitamin D in breast cancer comprehensively. At the same time, we recommend incorporating groups from different ethnicities and geographical regions in future research designs to examine the universality of the relationship between Vitamin D and breast cancer. The genetic backgrounds and lifestyles of other populations may influence the metabolism of Vitamin D and the pathogenesis of breast cancer; therefore, cross-population studies can help reveal more details about the role of Vitamin D. Furthermore, future research should continue to explore the potential impact of Vitamin D on other types of cancer or other diseases. By conducting a comprehensive analysis of the role of Vitamin D in various diseases, we can thoroughly assess its significance in public health and provide a scientific basis for the formulation of relevant health policies. Through multidisciplinary collaboration, integrating knowledge from fields such as epidemiology, molecular biology, genetics, and nutrition, we can gain a deeper understanding of the role of Vitamin D in human health, offering new perspectives and strategies for the prevention and treatment of diseases. In summary, although the current research has not found a direct causal relationship between Vitamin D and breast cancer in the European population, the multifaceted role of Vitamin D in human health suggests that future studies should adopt a more comprehensive and multidimensional approach to explore the potential impacts of Vitamin D. Through interdisciplinary collaboration and rigorous research design, we can anticipate a deeper understanding of the role of Vitamin D in breast cancer and other diseases in the near future. The key limitation of the study is that the MR analysis was restricted to European-ancestry populations. Caution is required when extrapolating these findings to other ethnic groups due to potential genetic and environmental heterogeneity.

5. Conclusion

This MR study provides robust genetic evidence that Vitamin D levels are not causally associated with breast cancer risk in populations of European ancestry. Utilizing 111 SNPs as instrumental variables and rigorous sensitivity analyses, our findings consistently demonstrated no significant effect of Vitamin D on breast cancer incidence (IVW OR = 1.002, 95% CI: 0.896 – 1.119, p=0.968). These results are in contrast with some observational studies that suggested a protective role for Vitamin D, highlighting the potential influence of residual confounding or reverse causality in earlier research. The MR approach, which minimizes such biases, strengthens the validity of our null association. Despite the methodological rigor, limitations still exist, including the restriction to European populations, which limits generalizability to other ethnic groups, and the inability to assess non-linear or time-dependent effects of Vitamin D. Future studies should expand to diverse populations, integrate longitudinal designs, and explore interactions between Vitamin D, lifestyle factors, and other biomarkers to clarify its role in breast cancer pathogenesis. Clinically, our findings suggest that Vitamin D supplementation is unlikely to confer significant protection against breast cancer, and public health strategies should prioritize evidence-based interventions. This study underscores the importance of employing genetic causal inference methods to resolve controversies in observational epidemiology, while advocating for multidisciplinary approaches to unravel the complex etiology of breast cancer.

Acknowledgments

None.

Funding

None.

Conflict of interest

The authors declare no competing interests.

Author contributions

Conceptualization: All authors
Formal analysis: Yang Xiao, Xingyi Song
Methodology: Yang Xiao, Xingyi Song
Writing–original draft: Yang Xiao
Writing–review & editing: Xingyi Song, Mei Yin

Ethics approval and consent to participate

Not applicable.

Consent for publication

Not applicable.

Availability of data

The data used in this study were derived from publicly available datasets. Data is available on https://gwas.mrcieu.ac.uk/and https://www.finngen.fi

References

1. Forouzanfar MH, Foreman KJ, Delossantos AM, *et al*. Breast and cervical cancer in 187 countries between 1980 and 2010: A systematic analysis. *Lancet*. 2011;378(9801):1461-1484.

   doi: 10.1016/s0140-6736(11)61351-2

2. Greco KE, Mahon SM. The state of genomic health care and cancer. Are we going two steps forward and one step backward? *Annu Rev Nurs Res*. 2011;29:73-97.

doi: 10.1891/0739-6686.29.73

3. Sung H, Ferlay J, Siegel RL, *et al*. Global cancer statistics 2020: GLOBOCAN estimates of incidence and mortality worldwide for 36 cancers in 185 countries. *CA Can J Clin*. 2021;71(3):209-249.

   doi: 10.3322/caac.21660

4. Hortobagyi GN, De la Garza Salazar J, Pritchard K, *et al*. The global breast cancer burden: Variations in epidemiology and survival. *Clin Breast Cancer*. 2005;6(5):391-401.

   doi: 10.3816/cbc.2005.n.043

5. Wheeler SB, Reeder-Hayes KE, Carey LA. Disparities in breast cancer treatment and outcomes: Biological, social, and health system determinants and opportunities for research. *Oncologist*. 2013;18(9):986-993.

   doi: 10.1634/theoncologist.2013-0243

6. Holick MF. The vitamin D deficiency pandemic: Approaches for diagnosis, treatment and prevention. *Rev Endocr Metab Disord*. 2017;18(2):153-165.

   doi: 10.1007/s11154-017-9424-1

7. Feldman D, Krishnan AV, Swami S, Giovannucci E, Feldman BJ. The role of vitamin D in reducing cancer risk and progression. *Nat Rev Cancer*. 2014;14(5):342-357.

   doi: 10.1038/nrc3691

8. Bhamb N, Kanim L, Maldonado R, Svet M, Metzger M. Effect of modulating dietary vitamin D on the general bone health of rats during posterolateral spinal fusion. *J Orthop Res*. 2018;36(5):1435-1443.

   doi: 10.1002/jor.23832

9. Anderson PH, Atkins GJ, Turner AG, Kogawa M, Findlay DM, Morris HA. Vitamin D metabolism within bone cells: Effects on bone structure and strength. *Mol Cell Endocrinol*. 2011;347(1-2):42-47.

   doi: 10.1016/j.mce.2011.05.024

10. Shin MH, Holmes MD, Hankinson SE, Wu K, Colditz GA, Willett WC. Intake of dairy products, calcium, and vitamin d and risk of breast cancer. *J Natl Cancer Inst*. 2002;94(17): 1301-1311.

    doi: 10.1093/jnci/94.17.1301

11. Chen P, Hu P, Xie D, Qin Y, Wang F, Wang H. Meta-analysis of vitamin D, calcium and the prevention of breast cancer. *Breast Cancer Res Treat*. 2010;121(2):469-477.

    doi: 10.1007/s10549-009-0593-9

12. Bidgoli SA, Azarshab H. Role of vitamin D deficiency and lack of sun exposure in the incidence of premenopausal breast cancer: A case control study in Sabzevar, Iran. *Asian Pac J Cancer Prev APJCP*. 2014;15(8):3391-3396.

    doi: 10.7314/apjcp.2014.15.8.3391

13. O'Brien KM, Sandler DP, Taylor JA, Weinberg CR. Serum vitamin D and risk of breast cancer within five years. *Environ Health Perspect*. 2017;125(7):077004.

    doi: 10.1289/ehp943

14. Hossain S, Beydoun MA, Beydoun HA, Chen X, Zonderman AB, Wood RJ. Vitamin D and breast cancer: A systematic review and meta-analysis of observational studies. *Clin Nutr ESPEN*. 2019;30:170-184.

    doi: 10.1016/j.clnesp.2018.12.085

15. Knight JA, Lesosky M, Barnett H, Raboud JM, Vieth R. Vitamin D and reduced risk of breast cancer: A population-based case-control study. *Cancer Epidemiol Biomarkers Prev*. 2007;16(3):422-429.

    doi: 10.1158/1055-9965.Epi-06-0865

16. McCullough ML, Rodriguez C, Diver WR, *et al*. Dairy, calcium, and vitamin D intake and postmenopausal breast cancer risk in the cancer prevention study II nutrition cohort. *Cancer Epidemiol Biomarkers Prev*. 2005;14(12):2898-2904.

    doi: 10.1158/1055-9965.Epi-05-0611

17. Rossi M, McLaughlin JK, Lagiou P, *et al*. Vitamin D intake and breast cancer risk: A case-control study in Italy. *Ann Oncol*. 2009;20(2):374-378.

    doi: 10.1093/annonc/mdn550

18. O'Brien KM, Keil AP, Harmon QE, *et al*. Vitamin D supplement use and risk of breast cancer by race-ethnicity. *Epidemiology*. 2022;33(1):37-47.

    doi: 10.1097/ede.0000000000001413

19. Qin B, Xu B, Ji N, *et al*. Intake of vitamin D and calcium, sun exposure, and risk of breast cancer subtypes among black women. *Am J Clin Nutr*. 2020;111(2):396-405.

    doi: 10.1093/ajcn/nqz302

20. Anderson LN, Cotterchio M, Vieth R, Knight JA. Vitamin D and calcium intakes and breast cancer risk in pre- and postmenopausal women. *Am J Clin Nutr*. 2010;91(6):1699-1707.

    doi: 10.3945/ajcn.2009.28869

21. Abbas S, Linseisen J, Rohrmann S, *et al*. Dietary intake of vitamin D and calcium and breast cancer risk in the European prospective investigation into cancer and nutrition. *Nutr Cancer*. 2013;65(2):178-187.

    doi: 10.1080/01635581.2013.752018

22. Kuper H, Yang L, Sandin S, Lof M, Adami HO, Weiderpass E. Prospective study of solar exposure, dietary vitamin D intake, and risk of breast cancer among middle-aged women. *Cancer Epidemiol Biomarkers Prev*. 2009;18(9):2558-2561.

    doi: 10.1158/1055-9965.Epi-09-0449

23. Oghabi Bakhshaiesh T, Nazeri E, Jafarbeik-Iravani N,

Shirvani-Farsani Z, Esmaeili R. Vitamin D and breast cancer risk: A systematic review and meta-analysis in Iranian patients. *Ann Med Surg* (*Lond*). 2022;80:104162.

doi: 10.1016/j.amsu.2022.104162

24. Song D, Deng Y, Liu K, *et al*. Vitamin D intake, blood vitamin D levels, and the risk of breast cancer: A dose-response meta-analysis of observational studies. *Aging*. 2019;11(24):12708-12732.

doi: 10.18632/aging.102597

25. Li Z, Wu L, Zhang J, Huang X, Thabane L, Li G. Effect of vitamin D supplementation on risk of breast cancer: A systematic review and meta-analysis of randomized controlled trials. *Front Nutr*. 2021;8:655727.

doi: 10.3389/fnut.2021.655727

26. Davey Smith G, Hemani G. Mendelian randomization: Genetic anchors for causal inference in epidemiological studies. *Hum Mol Genet*. 2014;23(R1):R89-R98.

doi: 10.1093/hmg/ddu328

27. Verbanck M, Chen CY, Neale B, Do R. Detection of widespread horizontal pleiotropy in causal relationships inferred from Mendelian randomization between complex traits and diseases. *Nat Genet*. 2018;50(5):693-698.

doi: 10.1038/s41588-018-0099-7

ACCSCIENCE PUBLISHING

Eurasian Journal of Medicine and Oncology

ORIGINAL RESEARCH ARTICLE

Comparative efficacy and safety of Zercepac® plus pyrotinib versus Zercepac® plus pertuzumab in combination with chemotherapy as neoadjuvant therapy for HER2-positive breast cancer: A retrospective study

Hong Gao[1], Jiali Lei[2], Zhaohua Gui[3], and Shengying Wang[1]*

[1]Department of Thyroid and Breast Surgery, The First Affiliated Hospital of Anhui University of Chinese Medicine (Anhui Provincial Hospital of Chinese Medicine), Hefei, Anhui, China

[2]Biomedical Informatics Research Lab, School of Basic Medicine and Clinical Pharmacy, China Pharmaceutical University, Nanjing, Jiangsu, China

[3]Division of Life Sciences and Medicine, Department of Pathology, The First Affiliated Hospital of University of Science and Technology of China, Hefei, Anhui, China

Abstract

Introduction: HER2-positive breast cancer needs better neoadjuvant options. Pyrotinib (Py) with trastuzumab biosimilar may offer an alternative to dual blockade. Objective: This study analyzed the short-term efficacy and safety of Zercepac®, a trastuzumab biosimilar, combined with either Py or pertuzumab and chemotherapy in neoadjuvant therapy for HER2-positive breast cancer. It also compared the efficacy and safety of Zercepac®-pyrotinib-chemotherapy versus Zercepac®-pertuzumab-chemotherapy regimens.

Methods: Clinical data from 62 HER2-positive breast cancer patients who underwent neoadjuvant therapy with Zercepac® combined with Py or pertuzumab and chemotherapy at Anhui Cancer Hospital (February 2021 to December 2023) were retrospectively analyzed. Efficacy and safety were compared among TCbHP (29 cases), TCbHPy (8 cases), THP (9 cases), and TCbH (16 cases) groups. Statistical methods were used to identify factors influencing total pathological complete response (tpCR).

Results: Among the 62 patients, 45 (72.6%) had invasive breast cancer, 11 (17.7%) had invasive carcinomas with intraductal components, five (8.1%) had invasive carcinomas with ductal carcinoma *in situ*, and one (1.6%) had invasive carcinoma with mucinous features. Age and advanced clinical stage were independent risk factors for tpCR ($p<0.001$). The TCbHPy group showed comparable efficacy to TCbHP ($p=0.25$). Alopecia (91.9%) was the most common adverse event. Diarrhea incidence was significantly higher in TCbHPy than in TCbHP ($p<0.001$); however, no grade 4 diarrhea occurred, and triple antidiarrheal therapy reduced its severity to grade 1.

Conclusion: Zercepac® is effective and safe in neoadjuvant therapy for HER2-positive breast cancer. Py (≥400 mg) may improve tpCR rates, with diarrhea as the main adverse effect. TCbHPy regimen demonstrated non-inferior efficacy to TCbHP.

Keywords: Zercepac®; Trastuzumab; Pertuzumab; Pyrotinib; HER2-positive breast cancer; Neoadjuvant therapy; Pathological complete response; Adverse events

***Corresponding author:**
Shengying Wang
(wangshengying61@163.com)

Citation: Gao H, Lei J, Gui Z, Wang S. Comparative efficacy and safety of Zercepac® plus pyrotinib versus Zercepac® plus pertuzumab in combination with chemotherapy as neoadjuvant therapy for HER2-positive breast cancer: A retrospective study. *Eurasian J Med Oncol.* 2025;9(3):110-121. doi: 10.36922/EJMO025100044

Received: March 4, 2025

1st revised: April 20, 2025

2nd revised: April 25, 2025

Accepted: April 28, 2025

Published online: May 14, 2025

Copyright: © 2025 Author(s). This is an Open-Access article distributed under the terms of the Creative Commons Attribution License, permitting distribution, and reproduction in any medium, provided the original work is properly cited.

Publisher's Note: AccScience Publishing remains neutral with regard to jurisdictional claims in published maps and institutional affiliations.

1. Introduction

Breast cancer is the most common malignancy among women and ranks first in the incidence rate of female malignant tumors. The incidence and mortality rates of breast cancer have been increasing year by year, posing a serious threat to women's physical and mental health.[1] Human epidermal growth factor receptor 2 (HER2)-positive breast cancer accounts for approximately 20 – 30% of all breast cancer cases. HER2-positive breast cancer is characterized by strong invasiveness and poor prognosis. Over two decades ago, HER2-positive breast cancer had the highest recurrence rate and the worst prognosis among all subtypes. However, the advent of trastuzumab – a humanized monoclonal antibody and the first anti-HER2 targeted drug – in 1998 significantly improved outcomes for patients with this disease. In recent years, an increasing number of new targeted therapies have been approved, further enhancing the survival and prognosis of HER2-positive patients. Present data indicate that the survival rate of patients with early-stage HER2-positive breast cancer receiving chemotherapy and dual antibody therapy exceeds 90%.[2] Neoadjuvant therapy, an important treatment modality for HER2-positive breast cancer, not only facilitates tumor shrinkage, downstaging, and increased rates of breast-conserving surgery, but also provides pivotal evidence for optimizing subsequent adjuvant treatment strategies.

Trastuzumab is the first-line treatment for HER2-positive breast cancer, but it is relatively expensive, making it difficult for some patients to afford. With the expiration of the Herceptin patent, attention has shifted toward the development of more affordable biosimilars. The European Medicines Agency defines a biosimilar as a biological product that is highly similar to an existing reference product, with no clinically meaningful differences in terms of efficacy and safety.[3] Safety mainly refers to the clinical safety of subjects or patients. Therefore, in addition to demonstrating similarity in structure, purity, and biological activity, biosimilars must undergo clinical trials to confirm their efficacy and safety. Biosimilars also occupy a place in clinical applications due to their unique cost advantage. In 2020, the "Expert Consensus on Biosimilars" issued in China pointed out that biosimilars are not the same as generic drugs. The main clinical data requirements for generic drugs are pharmacokinetics and bioequivalence, while biosimilars must also conduct safety and efficacy studies on this basis and support the equivalence of efficacy and safety between biosimilars and reference drugs, allowing them to be used clinically as substitutes for reference drugs.[4] Zercepac® (HLX02) is a domestically developed trastuzumab biosimilar approved for clinical use by the National Medical Products Administration in 2020. In a global phase III clinical study, patients with HER2-positive advanced (recurrent or metastatic) breast cancer treated with Zercepac® in combination with docetaxel had an objective response rate (ORR) at week 24 similar to that of the control group receiving trastuzumab plus docetaxel, indicating comparable efficacy. In addition, the safety study results showed no statistically significant difference in the incidence of adverse events between the two drugs.[5] An American expert panel stated that biosimilars and reference products could be considered equally efficacious for the purpose of inclusion in the American Society of Clinical Oncology clinical practice guidelines, recommending that individual institutions review approved biosimilars with their appropriate drug committees before implementation on their formularies.[6] Zercepac® has also been approved by the China Food and Drug Administration for the neoadjuvant treatment of breast cancer.

Trastuzumab, a HER2-targeted monoclonal antibody, has been proven to significantly improve the survival outcomes of patients with HER2-positive breast cancer when used in combination with other chemotherapy drugs. However, after more than 20 years of use, many patients have developed resistance, leading to recurrence and metastasis. To address these clinical challenges and improve the prognosis of patients with HER2-positive breast cancer, new HER2-targeted drugs, specifically small molecule tyrosine kinase inhibitors (TKIs), have emerged. Pyrotinib (Py) is an irreversible pan-HER small molecule TKI that acts simultaneously on HER1, HER2, and HER4. Results from the phase III PHEDRA[7] study confirmed that the Py + trastuzumab + docetaxel regimen significantly increased the pathological complete response (pCR) rate in patients with HER2-positive breast cancer during neoadjuvant treatment. Based on this study, Py was approved in 2022 for the neoadjuvant treatment of HER2-positive breast cancer. However, there are few reports on the efficacy and adverse events of Zercepac® in combination with Py or pertuzumab and chemotherapy in neoadjuvant chemotherapy (NAT) for HER2-positive breast cancer. This study retrospectively analyzed the clinical and pathological data of 62 patients with HER2-positive breast cancer who received Zercepac® in combination with Py or Zercepac® in combination with pertuzumab and chemotherapy as a NAT regimen, and who subsequently underwent surgery. The efficacy and adverse reactions were observed and recorded, and the factors affecting the pCR rate were analyzed, with the aim of providing references for clinical treatment.

2. Materials and methods

2.1. Study population

A retrospective analysis was performed on clinical data from 62 patients with HER2-positive breast cancer who received neoadjuvant therapy (Zercepac® combined with Py or pertuzumab and chemotherapy), followed by surgical resection at the Breast Diagnosis and Treatment Center of Anhui Cancer Hospital between February 2021 and December 2023.

(i) Inclusion criteria: Only patients with previously untreated HER2-positive breast cancer were included (excluding those who had received radiotherapy or targeted therapy before neoadjuvant treatment);
(ii) Exclusion criteria: Patients who received fewer than six treatment cycles (n=3) or experienced surgical delays exceeding 4 weeks (n=2) were excluded;
(iii) Grouping basis: Treatment regimens were determined by a multidisciplinary team based on guideline recommendations and were not selected by the patients.

2.2. Neoadjuvant treatment regimens and surgical approaches

2.2.1. Neoadjuvant Therapy protocols

Treatment regimens and dosages were administered in accordance with institutional guidelines and the drug manufacturer's specifications. The NAT regimens included:

(i) TCbHP (29 cases): Docetaxel + carboplatin + trastuzumab (H) + pertuzumab (P)
(ii) TCbHPy (eight cases): Docetaxel + carboplatin + trastuzumab (H) + Py
(iii) THP (nine cases): Docetaxel + trastuzumab (H) + pertuzumab (P)
(iv) TCbH (16 cases): Docetaxel + carboplatin + trastuzumab (H)

All patients received six treatment cycles at 21-day intervals.

2.2.2. Drug administration details

- Docetaxel (Qilu Pharmaceutical, China): 75 mg/m^2 (all patients).
- Carboplatin (Qilu Pharmaceutical, China): 400 – 500 mg/m^2 (53 patients).
- Anti-HER2 agents:
- Zercepac® (S20200019, Shanghai Fosun Pharma, China): Initial dose 8 mg/kg, reduced to 6 mg/kg in subsequent cycles (all patients).
- Pertuzumab (S20180029, Shanghai Roche, China): Initial dose 840 mg, adjusted to 420 mg after the loading dose (38 patients).
- Py (Jiangsu Hengrui, China): 400 mg orally once daily (eight patients).

2.2.3. Monitoring and supportive care

(i) Tumor response was assessed through ultrasound at each cycle, with supplemental breast magnetic resonance imaging conducted at baseline and before surgery.
(ii) Pretreatment laboratory tests (complete blood count, hepatic/renal function, electrolytes) were mandatory before each treatment cycle. Chemotherapy was administered only if no contraindications were identified.
(iii) Granulocyte colony-stimulating factor was administered according to the National Comprehensive Cancer Network guidelines for hematologic support.
(iv) Surgery was performed 14 days after completion of neoadjuvant therapy, followed by 1 year of adjuvant-targeted therapy.
(v) Left ventricular ejection fraction (LVEF) was measured before initiating Zercepac® (HLX02) treatment and monitored regularly during therapy. Zercepac® (HLX02) treatment was discontinued for at least 4 weeks under the following conditions, with LVEF re-evaluated every 4 weeks:
  (a) If the absolute value of LVEF decreased by ≥16% from baseline. If LVEF returned to the normal range or the decrease was ≤15% within 4 – 8 weeks, Zercepac® (HLX02) could be resumed.
  (b) The use of Zercepac® (HLX02) should be stopped permanently if LVEF continued to decline for more than 8 weeks, or if treatment was interrupted more than 3 times due to cardiotoxicity.
(vi) During Zercepac® (HLX02) treatment, LVEF was assessed every 3 months and again at the end of the therapy. Following completion of treatment, LVEF was monitored every 6 months for at least 2 years.

2.2.4. Py-specific diarrhea prophylaxis

Patients receiving Py were administered triple antidiarrheal therapy:

(i) Bifidobacterium: One sachet 3 times daily.
(ii) Montmorillonite powder: One sachet 3 times daily.
(iii) Loperamide: Two tablets as needed (maximum six tablets per day).

2.3. Efficacy evaluation

Clinical efficacy was assessed according to Response Evaluation Criteria in Solid Tumors, version 1.1.[8] Pathological response post-neoadjuvant therapy was evaluated using the Miller–Payne (MP) grading system,[9] which categorizes tumor regression based on histological examination of surgical specimens.

2.4. Safety assessment

Adverse events were evaluated according to the World Health Organization Toxicity Grading Scale. The following parameters were assessed:

(i) Laboratory parameters: Complete blood count, hepatic/renal function, and electrolyte profiles.
(ii) Cardiac monitoring: Electrocardiogram (ECG) and echocardiogram (performed quarterly).
(iii) Clinical symptoms: Alopecia, nausea/vomiting, diarrhea, abdominal pain, and arthralgia.

Notably, no significant LVEF decline (>10%) or cardiac dysfunction was observed. Cardiac events were defined as:

(i) ST-T segment abnormalities.
(ii) Clockwise/counterclockwise rotation on ECG.
(iii) Premature atrial/ventricular contractions.
(iv) Sinus arrhythmia.
(v) Conduction block.
(vi) Low QRS voltage.
(vii) Left axis deviation.
(viii) Left ventricular hypertrophy.

2.5. Statistical analysis

Data were analyzed using SPSS 26.0 (IBM Corp., United States). Categorical variables were compared using the chi-square test or Fisher's exact test. Binary logistic regression was used to identify independent clinicopathological predictors of neoadjuvant therapy efficacy. A two-tailed p-value <0.05 was considered statistically significant.

3. Results

3.1. Baseline clinicopathological characteristics

The study cohort comprised 62 patients with HER2-positive breast cancer, classified into the following histopathological subtypes:

(i) Invasive ductal carcinoma: 45 cases (72.6%).
(ii) Invasive carcinoma with intraductal component: 11 cases (17.7%).
(iii) Invasive carcinoma with ductal carcinoma *in situ*: Five cases (8.1%).
(iv) Invasive carcinoma with mucinous features: One case (1.6%).

Detailed baseline characteristics are presented in Table 1.

3.2. Predictors of pCR

Univariate logistic regression analysis identified age, tumor-node-metastasis (TNM) stage, and hormone receptor (HR) status as independent predictors of total pCR (tpCR) (Table 2).

3.3. Multivariate predictors of pCR

Multivariate logistic regression analysis demonstrated that both age and TNM stage independently influenced the likelihood of achieving tpCR:

(i) Patients aged >50 years had 3.82 times higher odds of achieving tpCR compared to those aged ≤50 years (95% confidence interval [CI]: 1.104 – 13.225, p=0.034).
(ii) Conversely, patients with advanced-stage (cTNM IIb – IIIc) showed a 91.2% reduction in the odds of achieving tpCR compared to those with stage IIa disease (odds ratio [OR] = 0.088, 95% CI: 0.023 – 0.338, p<0.001) (Table 3).

3.4. Univariate predictors of pCR

Univariate analysis based on post-operative pathological assessment identified five significant predictors of tpCR achievement:

(i) Advanced age (>50 years).
(ii) Clinical nodal involvement (cN ≥1).
(iii) Advanced TNM stage (IIb – IIIc).
(iv) Hormone receptor-negative status.
(v) Non-use of dual-target therapy.

Detailed comparisons between tpCR and non-tpCR groups are presented in Table 4.

3.5. Adverse events

Treatment-related adverse events occurred in over 40% of patients, with the most frequent being alopecia (91.7%), followed by nausea (48.4%), diarrhea (41.9%), and fatigue (35.5%). Cardiovascular events, though generally mild, included arrhythmias (19.4%), T-wave abnormalities (12.9%), and transient LVEF fluctuations (a >10% change in 6.5% of cases). Notably, no symptomatic heart failure or grade ≥3 cardiac events were observed (Table 5).

3.6. Comparative analysis of TCbHP versus TCbHPy regimens

3.6.1. Efficacy outcomes

No statistically significant differences were observed between the TCbHP and TCbHPy regimens (Table 6) in terms of:

(i) tpCR rate (55.2% versus 37.5%, p=0.25).
(ii) Magnitude of Ki-67 index reduction (p=0.67).
(iii) Miller–Payne pathological regression grading (p=0.07).

3.6.2. Safety profile

While both regimens demonstrated comparable toxicity profiles (Table 6), the incidence of diarrhea differed markedly:

(i) TCbHPy group: 100% (8/8).
(ii) TCbHP group: 3.4% (1/29) (p<0.001).

Table 1. Baseline characteristics

Variable	Chemotherapy regimen				*p*
	TCbH	TCbHP	TCbHPy	THP	
BMI (kg/m²; mean±standard deviation)	24.96±2.99	23.99±2.89	24.12±2.82	24.41±3.69	0.776
Age (years)					
≤50	5 (31.3)	14 (48.3)	2 (25)	4 (44.4)	0.575
>50	11 (68.8)	15 (51.7)	6 (75)	5 (55.6)	
cT					
1	0 (0)	1 (3.4)	0 (0)	0 (0)	0.773
2	13 (81.3)	22 (75.9)	7 (87.5)	9 (100)	
3	3 (18.8)	6 (20.7)	1 (12.5)	0 (0)	
cN					
0	11 (68.8)	21 (72.4)	3 (37.5)	8 (88.9)	0.072
1	2 (12.5)	7 (24.1)	4 (50)	0 (0)	
2	2 (12.5)	0 (0)	1 (12.5)	1 (11.1)	
3	1 (6.3)	1 (3.4)	0 (0)	0 (0)	
cTNM					
IIa	9 (56.3)	19 (65.5)	3 (37.5)	8 (88.9)	0.231
IIb	4 (25)	8 (27.6)	4 (50)	0 (0)	
IIIa	2 (12.5)	1 (3.4)	1 (12.5)	1 (11.1)	
IIIb	0 (0)	1 (3.4)	0 (0)	0 (0)	
IIIc	1 (6.3)	0 (0)	0 (0)	0 (0)	
Histological grade					
II	13 (81.3)	28 (96.6)	7 (87.5)	7 (87.5)	0.265
III	3 (18.8)	1 (3.4)	1 (12.5)	1 (12.5)	
HR					
Negative	12 (75)	19 (65.5)	6 (75)	3 (33.3)	0.196
Positive	4 (25)	10 (34.5)	2 (25)	6 (66.7)	
Menstrual status					
Pre-menopausal	5 (31.3)	11 (39.3)	2 (25)	4 (44.4)	0.823
Post-menopausal	11 (68.8)	17 (60.7)	6 (75)	5 (55.6)	
BNAT Ki-67					
≤20%	2 (12.5)	3 (10.3)	0 (0)	2 (22.2)	0.609
>20%	14 (87.5)	26 (89.7)	8 (100)	7 (77.8)	

Notes: Data are presented as n (%), unless otherwise specified; Body mass index (BMI) was categorized according to Chinese adult standards[17]: Normal: 18.5 – 23.9 kg/m²; Overweight: 24.0 – 26.9 kg/m²; Obese: ≥27.0 kg/m².

Abbreviations: BNAT: Baseline assessment before neoadjuvant chemotherapy; cN: Clinical lymph node staging (American Joint Committee on Cancer [AJCC] 8th edition); cT: Clinical tumor size staging (AJCC 8th edition); cTNM: Tumor-node-metastasis classification stage; HR: Hormone receptor; Ki-67: Antigen Kiel 67; TCbH: Docetaxel + carboplatin + trastuzumab; TCbHP: Docetaxel + carboplatin + trastuzumab + pertuzumab; TCbHPy: Docetaxel+carboplatin + trastuzumab + pyrotinib; THP: Docetaxel + trastuzumab + pertuzumab.

4. Discussion

Breast cancer has entered the era of precision treatment, with clinical strategies tailored to individual patients based on different molecular subtypes.[10] In the past, HER2-positive breast cancer was associated with the poorest prognosis. However, the advent of the anti-HER2 targeted drug trastuzumab significantly improved outcomes for patients with this subtype, marking a milestone in its treatment. The neoadjuvant treatment combining trastuzumab (H) and pertuzumab (P) has further transformed the prognosis for HER2-positive breast cancer. The dual-target regimen not only increases the tpCR rate but also improves survival.[11] The large-

Table 2. Univariate logistic regression analysis of factors associated with total pathological complete response

Variable	Univariate logistic regression		
	OR	95% CI	*p*
Age (years)			
≤50	Ref	-	0.022
>50	3.491	1.196 – 10.190	
cT			
1 – 2	Ref	-	0.492
3	0.617	0.156 – 2.447	
cN			
0	Ref	-	0.001
1 – 3	0.100	0.025 – 0.401	
cTNM			
IIa	Ref	-	<0.001
IIb – IIIc	0.094	0.026 – 0.335	
Histological grade			
II	Ref	-	0.128
III	0.179	0.020 – 1.637	
HR			
Negative	Ref	-	0.037
Positive	0.311	0.104 – 0.933	
Menstrual status			
Pre-menstrual	Ref	-	0.093
Post-menstrual	2.516	0.856 – 7.392	
BNAT Ki-67			
≤20%	Ref	-	0.689
>20%	1.383	0.283-6.764	

Abbreviations: BNAT: Baseline assessment before neoadjuvant chemotherapy; CI: Confidence interval; cN: Clinical lymph node staging (American Joint Committee on Cancer [AJCC] 8th edition); cT: Clinical tumor size staging (AJCC 8th edition); cTNM: Tumor-node-metastasis classification stage; HR: Hormone receptor; Ki-67: Antigen Kiel 67; OR: Odds ratio; Ref: Reference.

Table 3. Multivariate logistic regression analysis of total pathological complete response predictors

Variable	Multivariate logistic regression		
	Adjusted *OR*	95% CI	*p*
Model 1: Full input method *N*=62			
Age (years)			
≤50	Ref	-	0.999
>50	≈ 0	0 – 0	
cN			
0	Ref	-	0.962
1 – 3	1.067	0.073 – 15.678	
cTNM			
IIa	Ref	-	0.074
IIb – IIIc	0.105	0.009 – 1.247	
HR			
Negative	Ref	-	0.134
Positive	0.373	0.102 – 1.356	
Menstrual status			
Pre-menstrual	Ref	-	0.999
Post-menstrual	≈0	0 – 0	
Model 2: Backward screening method *N*=62			
Age (years)			
≤50	Ref	-	0.034
>50	3.820	1.104 – 13.225	
cTNM			
IIa	Ref	-	<0.001
IIb – IIIc	0.088	0.023 – 0.338	

Abbreviations: CI: Confidence interval; cN: Clinical lymph node staging (American Joint Committee on Cancer 8th edition); cTNM: Tumor-node-metastasis classification stage; HR: Hormone receptor; Ki-67: Antigen Kiel 67; OR: Odds ratio; Ref: Reference.

scale KRISTINE[12] study compared six cycles of TCbHP (docetaxel, carboplatin, trastuzumab, and pertuzumab) with ado-trastuzumab emtansine plus neoadjuvant treatment. The tpCR rate in the TCbHP group was 55.7% (123/221), superior to the 44.4% (99/223) observed in the control group, thus validating both the efficacy and safety of the TCbHP regimen. In our study, the overall tpCR rate among all patients was 50% (31/62). The highest tpCR rate was 55.2% (16/29), observed in the group treated with Zercepac® (a trastuzumab biosimilar) plus pertuzumab in combination with six cycles of docetaxel carboplatin (TCb) chemotherapy, consistent with the aforementioned studies. This suggests that the efficacy of Zercepac® in treating HER2-positive breast cancer is essentially equivalent to that of Herceptin. Previous studies[5,13] have also confirmed that neoadjuvant treatment combining Zercepac® or Herceptin with pertuzumab and chemotherapy yields comparable efficacy and safety profiles. Moreover, a model-based economic evaluation in China in 2022 showed that Zercepac® is more cost-effective than Herceptin, making it more accessible to patients and aligning with financial constraints in healthcare.[14]

In addition to these advantages, Zercepac® offers other benefits. Notably, it does not contain benzyl alcohol as a preservative, while the 440 mg formulation of Herceptin available in China still does. Studies have shown that benzyl alcohol may reduce the efficacy of protein-based drugs and

Table 4. Univariate analysis of clinicopathological factors associated with total pathological complete response (tpCR)

Variable	tpCR (*n*=31)	Non-tpCR (*n*=31)	*p*
BMI (kg/m^2; mean±standard deviation)	24.31±2.75	24.32±3.24	0.987
Age (years)			
≤50	8 (25.8)	17 (54.8)	0.020
>50	23 (74.2)	14 (45.2)	
cT			
1 – 2	27 (87.1)	25 (80.6)	0.490
3	4 (12.9)	6 (19.4)	
cN			
0	28 (90.3)	15 (48.4)	<0.001
1 – 3	3 (9.7)	16 (51.6)	
cTNM			
IIa	27 (87.1)	12 (38.7)	<0.001
IIb – IIIc	4 (12.9)	19 (61.3)	
Histological grade			
II	29 (96.7)	26 (83.9)	0.195
III	1 (3.3)	5 (16.1)	
HR			
Negative	24 (77.4)	16 (51.6)	0.034
Positive	7 (22.6)	15 (48.4)	
Menstrual status			
Pre-menstrual	8 (25.8)	14 (46.7)	0.090
Post-menstrual	23 (74.2)	16 (53.3)	
BNAT Ki-67			
≤20%	3 (9.7)	4 (12.9)	0.999
>20%	28 (90.3)	27 (87.1)	
Chemotherapy regimen			
TCbH	8 (25.8)	8 (25.8)	0.820
TCbHP	16 (51.6)	13 (41.9)	
TCbHPy	3 (9.7)	5 (16.1)	
THP	4 (12.9)	5 (16.1)	

Note: Data are presented as n (%), unless otherwise specified.
Abbreviations: BMI: Body mass index; BNAT: Baseline assessment before neoadjuvant chemotherapy; cN: Clinical lymph node staging (American Joint Committee on Cancer [AJCC] 8th edition); cT: Clinical tumor size staging (AJCC 8th edition); cTNM: Tumor-node-metastasis classification stage; HR: Hormone receptor; Ki-67: Antigen Kiel 67; TCbH: Docetaxel + carboplatin+trastuzumab; TCbHP: Docetaxel+carboplatin+trastuzumab+pertuzumab; TCbHPy: Docetaxel+carboplatin+trastuzumab+pyrotinib; THP: Docetaxel+trastuzumab+pertuzumab.

pose additional health risks to patients.[15] In August 2022, Fosun Pharma launched a 60 mg formulation of Zercepac®, while the original trastuzumab and five other biosimilars currently do not offer this dosage. The availability of both 150 mg and 60 mg formulations of Zercepac® allows for flexible dosing, reduces drug wastage and storage risks, and further lowers costs for patients and health insurance systems.

In summary, given the comparable efficacy and safety of neoadjuvant treatment combining Zercepac® and pertuzumab with chemotherapy to that of Herceptin-based regimens, along with Zercepac®'s cost advantages, this study supports the clinical application of Zercepac® plus pertuzumab in the neoadjuvant treatment of HER2-positive breast cancer.

Py exerts its anti-tumor effects by targeting the intracellular domains of HER-1, HER-2, and HER-4 in tumor cells.[16] The exploration of combining monoclonal antibodies with small molecule TKIs in the neoadjuvant treatment of HER2-positive breast cancer has been

Table 5. Treatment-related adverse events by regimen

Regimen	TCbH (*n*=16)	TCbHP (*n*=29)	TCbHPy (*n*=8)	THP (*n*=9)	χ^2	*p*
Adverse cardiac events (*n* [%])						
ST-segment changes	3 (18.75%)	1 (3.45%)	1 (12.50%)	0 (0%)	4.30	0.23
Clockwise or counterclockwise rotation	2 (12.50%)	3 (10.34%)	0 (0%)	0 (0%)	2.12	0.55
Premature atrial/ventricular contractions	1 (6.25%)	2 (25.00%)	0 (0%)	2 (22.22%)	8.14	0.04
Sinus arrhythmia[a]	2 (12.50%)	5 (17.24%)	0 (0%)	0 (0%)	3.21	0.36
Conduction block	3 (18.75%)	0 (0%)	0 (0%)	0 (0%)	9.06	0.03
Low QRS voltage	1 (6.25%)	1 (3.45%)	0 (0%)	0 (0%)	1.04	0.79
Left axis deviation	0 (0%)	0 (0%)	1 (12.50%)	1 (11.11%)	5.50	0.14
Left ventricular hypertrophy	2 (12.50%)	1 (3.45%)	0 (0%)	0 (0%)	3.03	0.39
Adverse reactions (*n* [%])						
Alopecia	15 (93.75%)	25 (86.21%)	8 (100%)	9 (100%)	2.85	0.42
Nausea	5 (31.25%)	17 (58.62%)	3 (37.50%)	5 (55.56%)	3.66	0.30
Diarrhea	0 (0%)	1 (3.45%)	8 (100%)	1 (11.11%)	48.29	< 0.001
Abdominal pain	1 (6.25%)	4 (13.80%)	0 (0%)	0 (0%)	2.85	0.42
Low white blood cell count	1 (6.25%)	5 (17.24%)	2 (25.00%)	0 (0%)	3.49	0.32
Low hemoglobin	5 (31.25%)	2 (6.90%)	0 (0%)	0 (0%)	9.09	0.03
Low platelet count	3 (18.75%)	5 (17.24%)	0 (0%)	0 (0%)	3.49	0.32
Abnormal liver function	3 (18.75%)	9 (31.03%)	1 (12.50%)	1 (11.11%)	2.46	0.48
Arthralgia	2 (12.50%)	3 (10.34%)	0 (0%)	1 (11.11%)	1.04	0.79
Anemia	2 (12.50%)	14 (48.28%)	3 (37.50%)	3 (33.33%)	5.80	0.12

Notes: [a]Sinus arrhythmia refers to irregular heart rhythm or tachycardia. Data are presented as n (%). Statistical method: Chi-square test.
Abbreviations: TCbH: Docetaxel + carboplatin + trastuzumab; TCbHP: Docetaxel + carboplatin + trastuzumab + pertuzumab; TCbHPy: Docetaxel + carboplatin +trastuzumab + pyrotinib; THP: Docetaxel + trastuzumab + pertuzumab.

ongoing. As early as 2020, Xuhong *et al.*[17] conducted a phase II clinical trial involving 19 patients, reporting a tpCR rate of 73.7% for Py combined with the EC-TH (epirubicin/cyclophosphamide followed by docetaxel/trastuzumab) regimen in the neoadjuvant treatment of HER2-positive locally advanced breast cancer. The main adverse reactions were diarrhea and leukopenia. Mao *et al.*[18] found that among 97 patients treated with Py-based neoadjuvant therapy, the tpCR rate was 48.5%. The incidence of grade 3 or higher adverse reactions was 35.1%, with diarrhea being the most common, occurring in 63.9% of patients. A real-world study by Fu *et al.*[19] reported a tpCR rate of 44.7% in the trastuzumab + Py group. The lower rate compared to the first prospective cohort study, and its similarity to the retrospective cohort study, may be attributed to dose reductions or treatment discontinuation caused by grade 3 or higher adverse reactions. The study further confirmed that there was a statistically significant difference in tpCR rates based on Py dose reductions and the occurrence of grade 3 or higher adverse reactions in the trastuzumab + Py group. In addition, patient compliance was lower in real-world settings than in strictly controlled clinical studies; some patients reduced or discontinued medication in response to adverse reactions such as diarrhea, thus affecting treatment efficacy. In a study involving 267 patients with advanced HER2-positive breast cancer, the PHOEBE[20] trial confirmed that the median progression-free survival (PFS) was significantly longer in the Py group compared to the lapatinib group (median PFS: 12.5 months versus 6.8 months; hazard ratio [HR] = 0.39, $p<0.001$). The ORR was also higher in the Py group than in the lapatinib group (67.2% versus 51.5%, $p=0.016$), with the median duration of the response being 11.1 months versus 7.0 months, respectively. Subgroup analysis revealed that among patients with brain metastases, PFS remained significantly prolonged in the Py group (HR = 0.32). In addition, the Phase II PERMEATE[21] study, which targeted patients with asymptomatic brain metastases, confirmed that Py could effectively cross the blood–brain barrier, achieving an ORR of 74.6% and improving the prognosis of patients with brain metastases from HER2-positive breast cancer.

In our study, the tpCR rate for the trastuzumab + Py group combined with six cycles of TCb chemotherapy was 37.5% (3/8), which was lower than the rates reported in the aforementioned prospective and real-world studies.

Table 6. Comparison of efficacy and adverse reactions between TCbHP and TCbHPy regimens

Regimen	TCbHP (*n*=29)	TCbHPy (*n*=8)	χ^2	*p*
Efficacy (*n*)			4.06	0.25
tpCR	16	3		
bpCR	5	1		
apCR	1	2		
PR	7	2		
Ki-67 variation (*n*)			0.80	0.67
No reduction	2	0		
Reduction (<15%)	2	1		
Significant reduction (>15%)	25	7		
MP grade (*n*)			6.91	0.07
Grade 2	2	0		
Grade 3	2	0		
Grade 4	3	4		
Grade 5	22	4		
Cardiac adverse events (*n* [%])				
ST-segment changes	1 (3.45%)	1 (12.50%)	0.01	0.91
Clockwise or counter-clockwise rotation	3 (10.34%)	0 (0%)	0.05	0.83
Premature atrial or ventricular contractions	0 (0%)	2 (25.00%)	3.55	0.06
Sinus arrhythmia (a)	5 (17.24%)	0 (0%)	0.46	0.50
Conduction block (b)	0 (0%)	0 (0%)	NA	1
Low QRS voltage	1 (3.45%)	0 (0%)	<0.001	1
Left axis deviation	0 (0%)	1 (12.50%)	0.49	0.48
Left ventricular hypertrophy	1 (3.45%)	0 (0%)	<0.001	1
Adverse reactions (*n* [%])				
Alopecia (hair loss)	25 (86.21%)	8 (100%)	0.22	0.64
Nausea	17 (58.62%)	3 (37.50%)	0.44	0.51
Diarrhea	1 (3.45%)	8 (100%)	26.73	< 0.001
Abdominal pain	4 (13.80%)	0 (0%)	0.22	0.64
Low white blood cell count	5 (17.24%)	2 (25.00%)	<0.001	1
Low hemoglobin	2 (6.90%)	0 (0%)	<0.001	1
Low platelet count	5 (17.24%)	0 (0%)	0.46	0.50
Abnormal liver function	9 (31.03%)	1 (12.50%)	0.35	0.55
Arthralgia (joint pain)	3 (10.34%)	0 (0%)	0.05	0.83
Anemia	14 (48.28%)	3 (37.50%)	0.02	0.89

Abbreviations: apCR: Pathological complete remission of axillary lymph nodes; bpCR: Pathological complete remission of primary breast lesions; MP: Miller–Payne; NA: Not available; PR: Partial pathological response; TCbHP: Docetaxel + carboplatin + trastuzumab + pertuzumab; TCbHPy: Docetaxel + carboplatin + trastuzumab + pyrotinib; tpCR: Total pathological complete response.

This may be due to the small sample size and dose reductions caused by adverse effects. Although the tpCR rate in the trastuzumab + Py group was lower than that in the trastuzumab + pertuzumab group, statistical analyses of partial pathological response, pathological complete remission of primary breast lesions (bpCR), pathological complete remission of axillary lymph nodes (apCR), and tpCR between the TCbHPy and TCbHP groups showed no significant differences (p=0.25). Similarly, MP grading showed no statistically significant difference (p=0.07). In terms of adverse reactions, there were no statistically significant differences between the two groups in hair loss, nausea, vomiting, fatigue, diarrhea, loss of appetite, or cardiovascular adverse events (such as pre-mature

ventricular contractions, arrhythmia, sinus tachycardia, sinus bradycardia, sinus arrhythmia, T-wave changes, and changes in cardiac ejection fraction). However, diarrhea showed a statistically significant difference (p<0.001): no cases were reported in the TCbHP group, while all eight patients in the TCbHPy group experienced varying degrees of diarrhea. Furthermore, all eight patients in the TCbHPy group had MP grades above level 4, with a total probability of 75% (6/8) achieving apCR, bpCR, or tpCR. Two out of three tpCR patients were HR-negative. As experience with Py increased, a triple anti-diarrheal method was implemented for first-level prevention: loperamide (two tablets per dose, twice daily, not exceeding eight tablets per day), smectite powder (one packet per dose, 3 times daily), and bifidobacterium (two packets per dose, twice daily). Before introducing this regimen, the incidence of diarrhea in our department included six cases (75%) of Grade 1 and two cases (25%) of Grade 2, with no unexpected Grade 3 events. Following the introduction of triple anti-diarrheal therapy, as of the manuscript submission date, patient compliance in the Py group in our department improved significantly. The median duration of diarrhea was reduced from 7 days to 3 days (interquartile range: 2 – 5), and the patient compliance rate increased to 87.5% (7 out of 8), with an initial dose of 400 mg. The tpCR rate also improved compared to previous statistics. We recognize that the study's small sample size and single-center design may limit the statistical robustness and generalizability of the findings. Nevertheless, we believe the results of this research are of substantial value and can serve as a foundational framework for future large-scale, multicenter investigations.

In real-world clinical practice, the HP dual-target regimen remains the first choice for neoadjuvant treatment for HER2-positive breast cancer. Zercepac® is not inferior to Herceptin in terms of efficacy. With its lack of benzyl alcohol preservatives and cost advantage, Zercepac® can further reduce expenses for both patients and healthcare systems. Moreover, HR and HER2 status are independent factors influencing tpCR rates across all patients. Based on the clinical observations in this study, the trastuzumab + Py regimen, which combines small and large molecules, offers advantages over single-target regimens combined with chemotherapy. It also shows a modest advantage in improving the MP grading of primary tumors compared to regimens based solely on large molecules, especially in HR-negative, HER2-positive patients. The combination of Zercepac® and Py with chemotherapy warrants further investigation. Whether this regimen can benefit improve PFS or even overall survival (OS) remains to be determined through future clinical follow-up and data collection.

5. Conclusion

While the HP dual-target regimen remains the neoadjuvant standard for HER2-positive breast cancer, this study highlights the non-inferiority of Zercepac®'s to originator trastuzumab, along with its preservative-free formulation and cost-efficiency advantages. For HR-negative subgroups, the TCbHPy regimen demonstrates particular promise, achieving high MP regression grades (100% grade ≥4) despite modest tpCR rates. The 75% apCR/bpCR composite rate and manageable toxicity profile, with appropriate prophylactic measures, suggest potential clinical utility, although long-term survival outcomes (PFS/OS) require validation in larger cohorts. At present, we are actively collecting and analyzing long-term follow-up data, including PFS and OS. We plan to disclose these results in subsequent research reports. Moving forward, studies should prioritize optimized dosing strategies and biomarker-driven patient selection to maximize the therapeutic index of Py.

Acknowledgments

None.

Funding

None.

Conflict of interest

The authors declare no conflicts of interest.

Author contributions

Conceptualization: Hong Gao and Shengying Wang
Formal analysis: Jiali Lei and Zhaohua Gui
Methodology: Hong Gao, Jiali Lei, and Zhaohua Gui
Writing – original draft: Hong Gao
Writing – review & editing: Shengying Wang

Ethics approval and consent to participate

This retrospective data analysis study, which involved no disclosure of patient identities and complied with ethical standards, is exempt from obtaining informed consent. Data are from Anhui Provincial Cancer Hospital, and its ethical approval is granted by the Ethics Committee of Anhui Provincial Cancer Hospital (Approval Number: 2024-TJK-06).

Consent for publication

The authors verbally informed all participants by telephone during data collection and follow-up regarding the intent to publish study results, and all participants provided verbal consent.

Availability of data

Data are available from the corresponding author upon reasonable request.

References

1. Han B, Zheng R, Zeng H, *et al*. Cancer incidence and mortality in China, 2022. *J Natl Cancer Cent*. 2024;4(1):47-53.

   doi: 10.1016/j.jncc.2024.01.006

2. Swain SM, Shastry M, Hamilton E. Targeting HER2-positive breast cancer: Advances and future directions. *Nat Rev Drug Discov*. 2023;22(2):101-126.

   doi: 10.1038/s41573-022-00579-0

3. Ngo D, Chen J. A clinical review of biosimilars approved in oncology. *Ann Pharmacother*. 2021;55(3):362-377.

   doi: 10.1177/1060028020944596

4. Expert Consensus Writing Group of the Chinese Society of Clinical Pharmacy, Chinese Medical Association. Expert consensus on clinical application and management of biosimilars (First Edition). *Chin Med J*. 2020;100(38):2982-2989.

   doi: 10.3760/cma.j.cn112137-20200703-02029

5. Xu B, Zhang Q, Sun T, *et al*. Efficacy, safety, and immunogenicity of HLX02 compared with reference trastuzumab in patients with recurrent or metastatic HER2-positive breast cancer: A randomized phase III equivalence trial. *BioDrugs*. 2021;35(3):337-350.

   doi: 10.1007/s40259-021-00475-w

6. Rodriguez G, Mancuso J, Lyman GH, *et al*. ASCO policy statement on biosimilar and interchangeable products in oncology. *JCO Oncol Pract*. 2023;19(7):411-419.

   doi: 10.1200/OP.22.00783

7. Wu J, Jiang Z, Liu Z, *et al*. Neoadjuvant pyrotinib, trastuzumab, and docetaxel for HER2-positive breast cancer (PHEDRA): A double-blind, randomized phase 3 trial. *BMC Med*. 2022;20(1):498.

   doi: 10.1186/s12916-022-02708-3

8. Watanabe H, Okada M, Kaji Y, *et al*. New response evaluation criteria in solid tumours-revised RECIST guideline (version 1.1). *Gan Kagaku Ryoho*. 2009;36(13):2495-2501.

9. Ogston KN, Miller ID, Payne S, *et al*. A new histological grading system to assess response of breast cancers to primary chemotherapy: Prognostic significance and survival. *Breast*. 2003;12(5):320-327.

   doi: 10.1016/s0960-9776(03)00106-1

10. Noone AM, Cronin KA, Altekruse SF, *et al*. Cancer incidence and survival trends by subtype using data from the surveillance epidemiology and end results program, 1992-2013. *Cancer Epidemiol Biomarkers Prev*. 2017;26(4):632-641.

    doi: 10.1158/1055-9965.EPI-16-0520

11. Loibl S, Gianni L. HER2-positive breast cancer. *Lancet*. 2017;389(10087):2415-2429.

    doi: 10.1016/S0140-6736(16)32417-5

12. Hurvitz SA, Martin M, Symmans WF, *et al*. Neoadjuvant trastuzumab, pertuzumab, and chemotherapy versus trastuzumab emtansine plus pertuzumab in patients with HER2-positive breast cancer (KRISTINE): A randomised, open-label, multicentre, phase 3 trial. *Lancet Oncol*. 2018;19(1):115-126.

    doi: 10.1016/S1470-2045(17)30716-7

13. Zhu X, Ding Y, Yu Y, *et al*. A Phase 1 randomized study compare the pharmacokinetics, safety and immunogenicity of HLX02 to reference CN- and EU-sourced trastuzumab in healthy subjects. *Cancer Chemother Pharmacol*. 2021;87(3):349-359.

    doi: 10.1007/s00280-020-04196-9

14. Deng W, Hu J, Li M, Yang S, Xie Z, Chen J. Trastuzumab biosimilar HLX02 versus reference trastuzumab in patients with recurrent or metastatic HER2-positive breast cancer: A model-based economic evaluation for China. *Expert Rev Pharmacoecon Outcomes Res*. 2022;22(7):1117-1126.

    doi: 10.1080/14737167.2022.2107506

15. Le Basle Y, Chennell P, Tokhadze N, Astier A, Sautou V. Physicochemical stability of monoclonal antibodies: A review. *J Pharm Sci*. 2020;109(1):169-190.

    doi: 10.1016/j.xphs.2019.08.009

16. Ma F, Li Q, Chen S, *et al*. Phase I study and biomarker analysis of pyrotinib, a Novel irreversible Pan-ErbB receptor tyrosine kinase inhibitor, in patients with human epidermal growth factor receptor 2-positive metastatic breast cancer. *J Clin Oncol*. 2017;35(27):3105-3112.

    doi: 10.1200/JCO.2016.69.6179

17. Xuhong J, Qi X, Tang P, *et al*. Neoadjuvant pyrotinib plus trastuzumab and chemotherapy for stage I-III HER2-positive breast cancer: A phase II clinical trial. *Oncologist*. 2020;25(12):e1909-e1920.

    doi: 10.1002/onco.13546

18. Mao X, Lv P, Gong Y, *et al*. Pyrotinib-containing neoadjuvant therapy in patients with HER2-positive breast cancer: A multicenter retrospective analysis. *Front Oncol*. 2022;12:855512.

    doi: 10.3389/fonc.2022.855512

19. Fu C, Han H, Lin S, Xu C. A retrospective clinical study of pyrotinib in combination with trastuzumab and pertuzumab in neoadjuvant therapy for HER-2 positive breast cancer. *Chin J Clin Oncol*. 2023;50(17):882-887.

    doi: 10.12354/j.issn.1000-8179.2023.20230648

20. Xu B, Yan M, Ma F, *et al*. Pyrotinib plus capecitabine versus lapatinib plus capecitabine for the treatment of HER2-

positive metastatic breast cancer (PHOEBE): A multicentre, open-label, randomised, controlled, phase 3 trial. *Lancet Oncol*. 2021;22(3):351-360.

doi: 10.1016/S1470-2045(20)30702-6

21. Yan M, Ouyang Q, Sun T, *et al*. Pyrotinib plus capecitabine for patients with human epidermal growth factor receptor 2-positive breast cancer and brain metastases (PERMEATE): A multicentre, single-arm, two-cohort, phase 2 trial. *Lancet Oncol*. 2022;23(3):353-361.

doi: 10.1016/S1470-2045(21)00716-6

ACCSCIENCE PUBLISHING

Eurasian Journal of Medicine and Oncology

ORIGINAL RESEARCH ARTICLE

Meta-analysis of the prognostic value of *KRAS* and *TP53* mutations in cholangiocarcinoma

Benfeng Xu, Chuhan Zhang, Yibin Zhou, and Jianan Jin*

Graduate School, Zhejiang Chinese Medical University, Hangzhou, Zhejiang, China

Abstract

Introduction: *KRAS* and *TP53* mutations are among the most common genetic mutations in cholangiocarcinoma.
Objective: This study aimed to explore the potential impact of these mutations on the survival prognosis of cholangiocarcinoma patients through a meta-analysis.
Methods: A systematic search was conducted in PubMed, Web of Science, Cochrane Library, Embase, CNKI, and Wanfang databases for cohort studies published up to April 2025 that investigated the relationship between *KRAS* and *TP53* mutations and patient prognosis. Two researchers independently performed the literature screening and data extraction. Meta-analysis was conducted using RevMan 5.4 and Stata 17.0, with assessment of publication bias.
Results: Twelve studies were included, involving a total of 1,126 patients, with 167 cases of *KRAS* mutations and 176 cases of *TP53* mutations. The results showed that both *KRAS* and *TP53* mutations were significantly associated with poorer survival prognosis in cholangiocarcinoma patients. For *KRAS* (hazard ratio (HR)=7.26; 95% confidence interval (CI): 6.10 – 9.81; $p<0.05$) and *TP53* (HR=18.13; 95% CI: 11.24 – 25.32; $p<0.05$), the presence of mutations predicted an adverse prognosis.
Conclusion: While these findings suggest that *KRAS* and *TP53* mutations are associated with worse survival in cholangiocarcinoma, the limited number and quality of the included studies warrant further high-quality research to validate these associations.

Keywords: Cholangiocarcinoma; *KRAS* mutation; *TP53* mutation; Prognosis; Meta-analysis; Cohort studies

***Corresponding author:**
Jianan Jin
(915683117@qq.com)

Citation: Xu B, Zhang C, Zhou Y, Jin J. Meta-analysis of the prognostic value of *KRAS* and *TP53* mutations in cholangiocarcinom. *Eurasian J Med Oncol.* 2025;9(3):122-132.
doi: 10.36922/EJMO025120063

Received: March 22, 2025

Revised: April 10, 2025

Accepted: May 6, 2025

Published online: May 22, 2025

Copyright: © 2025 Author(s). This is an Open-Access article distributed under the terms of the Creative Commons Attribution License, permitting distribution, and reproduction in any medium, provided the original work is properly cited.

Publisher's Note: AccScience Publishing remains neutral with regard to jurisdictional claims in published maps and institutional affiliations.

1. Introduction

Cholangiocarcinoma, a malignant tumor of the bile duct, can be anatomically classified into intrahepatic and extrahepatic types. It currently accounts for approximately 3% of all gastrointestinal cancers.[1] In recent years, the incidence and mortality rates of cholangiocarcinoma have been rising globally, particularly in Asia.[2] The primary treatment for early-stage cholangiocarcinoma is surgical resection; however, due to non-specific symptoms and subtle clinical manifestations in the early stages, 50 – 60% of patients are diagnosed at an advanced stage, with surgery suitable for only 15% of these cases.[3] Current research shows that the 5-year survival rate for advanced cholangiocarcinoma is extremely low, making early diagnosis and prognostic assessment critical for clinical decision-making.[4]

KRAS and *TP53* mutations are significant molecular biomarkers in cancer development and have been extensively studied for their prognostic relevance.[5-7] The Ras gene family is

closely associated with tumorigenesis, with approximately one-third of tumors harboring Ras mutations. *TP53*, a key player in DNA damage repair and apoptosis, contributes to cancer development when mutated. Recent studies have explored *KRAS* and *TP53* mutations as potential targets for cancer therapy.[8] Clinically, Zheng *et al.*[9] found that colorectal cancer patients with KRAS mutations had significantly shorter survival. In another study involving 272 hepatocellular carcinoma patients treated with transarterial embolization, those with *TP53* mutations exhibited poorer survival outcomes.[10]

In the context of cholangiocarcinoma, current studies suggest that approximately 30% of patients carry *KRAS* mutations,[11] and sequencing of 382 cholangiocarcinoma cases revealed *TP53* mutations in 51.6% of patients.[12] Additional cholangiocarcinoma studies have also reported a strong correlation between *KRAS* or *TP53* mutation phenotypes and patient prognosis.[13,14] However, despite these findings, the existing research does not yet provide definitive evidence on the specific mechanisms and prognostic impact of *KRAS* and *TP53* mutations in cholangiocarcinoma. Given this background, we believe that a meta-analysis of the available studies is necessary. Such an analysis will help integrate data from various studies and provide a comprehensive assessment of the prognostic significance of *KRAS* and *TP53* mutations in cholangiocarcinoma, thereby offering stronger scientific evidence for future clinical decisions and research directions. Through a comprehensive meta-analysis, we aim to elucidate the relationship between *KRAS* and *TP53* mutations and survival outcomes in cholangiocarcinoma, and further explore the potential of these genetic mutations as key molecular biomarkers for prognosis and treatment planning.

2. Materials and methods

A systematic and comprehensive literature search was conducted across several well-established public databases to identify relevant studies. The databases searched included PubMed, Web of Science, Cochrane Library, Embase, China National Knowledge Infrastructure (CNKI), and Wanfang Data, providing a broad representation of both international and Chinese research. The search was limited to studies published up to April 2025 to ensure the inclusion of the most up-to-date studies on *KRAS* and *TP53* mutations in cholangiocarcinoma. To ensure thorough coverage, the following search terms were used: "TP53 gene" or "KRAS gene" combined with "cholangiocarcinoma" or "bile duct cancer," further expanded to include "intrahepatic cholangiocarcinoma," "cholangiocellular carcinoma," "extrahepatic cholangiocarcinoma," and "hilar cholangiocarcinoma." These terms were then combined with "survival," "prognosis," or "outcome" to identify studies specifically addressing the impact of these genetic mutations on patient outcomes. The search strategy was designed to be broad yet focused, aiming to capture all relevant studies that contribute to understanding the relationship between these mutations and survival in cholangiocarcinoma.

Two independent researchers conducted the literature search to minimize bias and ensure accuracy. Both researchers followed the same predefined search strategy, and the search was performed twice to confirm consistency. In addition, the reference lists of the included articles were manually reviewed to identify any additional studies not captured by the database search. This approach ensured that the literature search was exhaustive and comprehensive, capturing as many relevant studies as possible.

The inclusion criteria for studies are as follows: (1) studies investigating the relationship between *KRAS* and *TP53* gene mutations and prognosis in cholangiocarcinoma patients; (2) studies reporting survival outcomes, including odds ratios (ORs), hazard ratios (HRs), or sufficient data to compute these values; and (3) studies clearly identifying human populations and providing demographic information, such as age and sex, along with relevant clinical data. These criteria were designed to ensure the inclusion of studies with a focused scope and adequate detail for meaningful analysis.

Exclusion criteria were applied to ensure the quality and relevance of the selected studies. These criteria are as follows: (1) non-English or non-Chinese literature was excluded to ensure uniformity and the ability to assess studies based on widely recognized and accessible languages; (2) reviews, conference papers, case reports, clinical trials, animal studies, and cell/molecular studies were excluded as they did not directly address the prognosis of human cholangiocarcinoma patients harboring *KRAS* and *TP53* mutations; (3) studies lacking relevant survival data, such as OR, HR, or survival times, were excluded as these metrics are crucial for assessing the relationship between mutations and prognosis; (4) studies with a high risk of bias, such as those with unclear methodologies, incomplete data reporting, or inadequate control of confounding factors, were excluded to preserve validity; and (5) studies with short-term follow-up periods were excluded, as the analysis focused on long-term survival outcomes.

2.1. Data extraction and systematic evaluation

Data extraction was independently performed by two researchers following a standardized and rigorous protocol to ensure accuracy and clarity of all extracted data.

This systematic approach minimized human error and maintained the integrity of the meta-analysis by ensuring that data were comparable across the included studies. To maintain transparency and traceability, all information obtained during the data extraction process was archived, and a clear record was kept of each step taken. This archived data allowed for easy retrieval and verification of the information, thereby ensuring the robustness of the meta-analysis. In cases where disagreements or uncertainties arose during the data extraction process, they were resolved through consensus, with the involvement of a third reviewer to provide an objective resolution. This ensured that any potential biases were minimized, and all discrepancies were thoroughly addressed to maintain the accuracy of the data. The third reviewer acted as a neutral party, ensuring that decisions were made based on clear and consistent criteria.

The following data were extracted from the included studies: (1) the first author's name to identify the primary author and the study reference; (2) the year of publication to determine the recency of the study; (3) the country where the study was conducted to understand the geographic distribution of the study participants; (4) the number of patients included to gauge the sample size and statistical power of the study; (5) the race of the patient to identify any racial differences in the study population that could influence genetic variation and prognosis; (6) tumor location to determine whether intrahepatic, extrahepatic, or hilar cholangiocarcinoma impacted prognosis; (7) study design to classify the type of study (e.g., cohort or case–control) and to assess its potential bias and validity; (8) treatment methods to evaluate whether treatment regimens were consistent across studies; (9) detection methods for *KRAS* and *TP53* gene mutations; (10) the status *KRAS* and *TP53* genes (i.e., wild-type or mutated); (11) definitions of cutoff points to determine how thresholds for genetic mutations or prognostic factors were defined; and (12) follow-up time to ensure it was adequate to capture meaningful survival outcomes.

In addition, tumor clinical and pathological parameters were extracted, including tumor size, number of tumors, lymph node metastasis, distant metastasis, tumor differentiation, and TNM staging, as these are crucial for understanding cancer progression and prognosis. Survival outcomes such as overall survival (OS) or disease-free survival (DFS) were recorded as the primary endpoints for assessing the impact of genetic mutations on patient prognosis. In addition, the results of univariate and multivariate analyses for both OS and median survival were collected, including p-values, HRs, standard errors, and 95% confidence intervals (CIs). These metrics provide critical insights into the strength of the association between mutations and prognosis.

The reliability of the included studies was further assessed by two researchers using the Newcastle–Ottawa Scale,[15] a widely used tool for assessing the quality of non-randomized studies in meta-analyses. This scale evaluates three key areas of study quality: outcome assessment, comparability, and selection criteria. Outcome assessment included evaluating whether the inclusion and exclusion criteria were clearly defined, whether the follow-up period was sufficient to capture long-term outcomes, whether loss to follow-up significantly biased the study results, and whether outcome measurements for survival and disease progression were robust and valid. Comparability was assessed based on the availability of sufficient clinical data to support group comparisons, including patient characteristics such as age, sex, and pathological features. The studies were also evaluated on whether they were appropriately controlled for potential confounders, such as TNM staging and treatment methods, and whether the control groups were appropriately selected and analyzed. Selection criteria assessed the representativeness of the exposed cohort, considering whether the study population accurately reflected the broader population of cholangiocarcinoma patients. The selection of the unexposed cohort was also evaluated to determine whether it was comparable to the exposed cohort. We further assessed the scientific validity of the exposure factor analysis, verifying that KRAS and TP53 mutations were correctly identified and properly attributed.

Each study was assigned a score based on these criteria, with a maximum possible score of 9. The total score was used to evaluate the methodological quality of each study and to ensure that only studies with sufficient rigor were included in the meta-analysis. This process enhanced the reliability and scientific rigor of the meta-analysis results, minimized the risk of bias, and strengthened the validity of the findings.

2.2. Statistical analysis

To assess the relationship between *KRAS* mutations, *TP53* mutations, and survival outcomes in cholangiocarcinoma patients, HRs and their corresponding 95% CIs were collected from each of the included studies. The HR is a commonly used measure to quantify the effect of a particular variable (in this case, *KRAS* or *TP53* mutations) on survival, with values >1 indicating an increased risk, and values <1 suggesting a protective effect. The 95% CI offers an estimate of the precision of the HR, with wider intervals indicating greater uncertainty.

To determine the consistency of the results across studies and to assess the heterogeneity, two standard statistical

tests were employed: the Q-test and the I^2 statistic. The Q-test tests the null hypothesis that all included studies share the same effect size. A $p>0.05$ indicates no statistically significant heterogeneity, suggesting consistency among study findings, whereas a $p=0.05$ or less indicates significant heterogeneity. I^2 statistic quantifies the percentage of total variation across studies that is due to heterogeneity rather than chance. An I^2 value >50% is typically interpreted as moderate-to-high heterogeneity. In the presence of significant heterogeneity, defined by either a Q-test $p\leq0.05$ or an I^2 value exceeding 50%, a random-effects model was applied for the meta-analysis. This model assumes that the true effect size varies between studies, accounting for both within-study and between-study variation. In contrast, when I^2 was <50%, indicating low heterogeneity, a fixed-effects model was used, which assumes a common effect size across all studies and provides a more precise estimate under such conditions.

To further evaluate the robustness of the results, a sensitivity analysis was performed. In this process, each study was sequentially removed from the analysis to observe the effect on the overall results. This helps identify any studies that may disproportionately influence the findings and allows for a more comprehensive assessment of the reliability of the meta-analysis conclusions. In addition, different statistical models were applied to assess whether the results were consistent across various methodological approaches, thus strengthening the validity of the conclusions.

Publication bias is a critical concern in meta-analyses, as studies with significant or positive results are more likely to be published, leading to an overestimation of the true effect size. To evaluate publication bias, both Egger's and Begg's tests were employed. These tests assess the symmetry of the funnel plot – a graphical representation of the relationship between study precision (typically the standard error) and effect size. A non-significant p-value (≥0.05) in either test suggests that there is no substantial publication bias, whereas a $p<0.05$ indicates potential bias, possibly due to unpublished studies with negative or non-significant results, small sample sizes, or extreme findings. To correct for potential publication bias, the trim-and-fill method was applied. This statistical technique estimates the number of potentially missing studies that may be causing asymmetry in the funnel plot. It then adjusts the overall effect size by imputing these missing studies and recalculating the pooled estimate. This approach helps to correct for bias introduced by selective publication and enhances the robustness of the meta-analysis conclusions.

All statistical analyses were carried out using RevMan 5.4 (The Cochrane Collaboration, UK), Stata 17 (StataCorp LLC, USA), and R version 4.2.3 (The R Foundation for Statistical Computing, Austria). These tools facilitated rigorous and transparent analysis of the data, ensuring the reliability and accuracy.

3. Results

3.1. Study selection and characteristics

This meta-analysis identified a total of 458 articles through systematic database searches, aimed at examining the relationship between *KRAS* and *TP53* gene mutations and survival prognosis in cholangiocarcinoma patients. After an initial screening of titles and abstracts, 76 articles were excluded due to duplication, and 324 articles were excluded because they did not meet the inclusion criteria based on the information available in their titles and abstracts. Subsequently, a more detailed assessment of the full-text articles led to the exclusion of an additional 18 articles due to insufficient data, which prevented them from contributing meaningfully to the analysis. Furthermore, 27 articles were excluded because their subject matter did not align with the focus of this meta-analysis, which specifically addressed the prognostic effects of *KRAS* and TP53 mutations in cholangiocarcinoma. In addition, one article involving a clinical trial was excluded as clinical trials typically do not provide the same type of observational data necessary for meta-analysis. Ultimately, 12 studies were deemed eligible for inclusion, involving a total of 1,126 patients. Among these, 167 patients had *KRAS* mutations and 176 patients had TP53 mutations, whereas 634 patients had *TP53* wild-type and 816 patients had *KRAS* wild-type. The studies included in the analysis were all retrospective cohort studies, reflecting a diverse array of patient populations and clinical settings. Retrospective cohort studies are valuable for understanding long-term outcomes and identifying associations between genetic mutations and survival in real-world clinical practice.

Regarding the geographic representation of the studies, six studies (50%) focused on Asian populations, whereas the remaining focused on European and American populations. Among the included studies, three involved patients who had received immunotherapy as part of their treatment regimen. Five of the studies focused specifically on patients with intrahepatic cholangiocarcinoma (ICC). In contrast, other studies included patients with extrahepatic (ECC) or hilar cholangiocarcinoma. Three studies involved patients who were receiving non-surgical treatments, and two studies included patients with advanced-stage disease (stage III and IV), which is associated with poorer outcomes. The inclusion of patients across different treatment modalities and disease stages contributed to the comprehensiveness of the analysis, allowing for a broader representation of clinical scenarios.

All 12 studies reported survival curves that allowed for the examination of the relationship between *KRAS* and *TP53* mutations and survival outcomes in cholangiocarcinoma. The survival curves were essential for understanding how these mutations influence patient prognosis. Among the included studies, five provided 95% CIs necessary for calculating HRs. The remaining studies provided sufficient data, including survival time and event data, to calculate HRs and 95% CIs. The specific characteristics of each of the 12 included studies are summarized in Table 1, outlining study designs, patient demographics, treatment regimens, and key findings related to the impact of *KRAS* and *TP53* mutations on survival outcomes. In addition, Figure 1 illustrates the study flow, illustrating the steps of the systematic review process from the initial database search to the final inclusion of studies. This visual representation enhances transparency and provides clarity regarding the selection and inclusion criteria applied in the meta-analysis.

3.2. Meta-analysis findings

This meta-analysis ultimately included 12 relevant cholangiocarcinoma studies. Among them, 10 studies described the relationship between *KRAS* gene status and patient survival, and five studies described the relationship between *TP53* gene status and patient survival. Our results indicate that patients with *KRAS* mutations have a poorer prognosis compared to those without mutations (HR=7.26; 95% CI: 6.10 – 9.81; $p<0.05$), and no significant heterogeneity was found among the studies (fixed-effects model; $I^2=48\%$). The forest plot related to the *KRAS* study is shown in Figure 2, with a significant overall effect and a highly significant difference between *KRAS* mutant and wild-type groups (Z=8.39 and $p<0.0001$). Further, Begg's test indicated no publication bias ($p=0.1286$), whereas Egger's test indicated ($p<0.05$). Therefore, we performed a trim-and-fill analysis, and the results are shown in Figure 3. The trim-and-fill method, a classic adjustment technique for publication bias, corrects for the asymmetry in the effect size distribution using an iterative trimming process. This procedure involves two stages: (1) the trimming stage (trim), where extreme effect size observations (often due to small-study effects or selective publication) are identified and excluded using non-parametric iterative algorithms; and (2) the filling stage (fill), where missing studies are simulated and added to restore symmetry in the funnel plot. In this study, we applied the trim-and-fill method using the R software, and the results showed that after adjustment, one potentially missing study was identified ($k^*=1$), increasing the total number of studies to 11 (kadj=11). As shown in Figure 3, after the adjustment, the analysis indicated a highly significant relationship between *KRAS* mutation and survival differences, with a statistically significant effect estimate of 12.84 units ($p<0.0001$; 95% CI: 9.01 – 16.670). These results suggest that *KRAS* mutations play an important role in the survival prognosis of cholangiocarcinoma patients.

When the *TP53* gene status in cholangiocarcinoma prognosis was evaluated, our analysis showed that patients with *TP53* mutations have a poorer prognosis compared to those without mutations (HR=20.03; 95% CI: 6.79 – 33.28; $p<0.05$). The analysis showed some heterogeneity (fixed-effects model: $I^2=59\%$; $p<0.05$, overall effect 95% CI=11.24 – 25.32; random-effects model: $I^2=59\%$, $p<0.05$, overall effect 95% CI: 6.79 – 33.28). The forest plot for *TP53* analysis is shown in Figure 4,

Table 1. Characteristics of the eligible studies

References	Country	KRAS (*n*)	TP53 (*n*)	Tumor location	Stage	Therapy	Survival analysis	Follow-up (month)	Cut-off (%)	NOS score
Boerner *et al.* 2021[44]	USA, Netherlands	412	412	CCA	I-IV	Various	OS	60	5	8
Peng *et al.* 2022[25]	China	12	/	ICCA	I-IV	No surgery	OS	20	5	7
Guo *et al.* 2022[45]	China	26	/	CCA	I-IV	Various	OS	26.6	5	6
Ardito *et al.* 2022[46]	Italy	54	/	ICCA	I-IV	Various	OS	180	5	8
Robertson *et al.* 2013[47]	USA	52	/	CCA	II-IV	Various	OS	60	5	8
Javle *et al.* 2016[48]	USA	224	224	ICCA	III-IV	Various	OS	58.3	5	8
Jin *et al.* 2023[49]	China	37	/	CCA	I-III	Various	OS	50	5	8
Ikeno *et al.* 2018[50]	Japan	50	/	CCA	I-IV	Various	OS	60	5	9
Conci *et al.* 2020[51]	Italy	99	103	CCA	I-IV	Various	OS	60	5	9
Chao *et al.* 2023[52]	China	40	40	CCA	III- IV	No surgery	OS	24	5	9
Chen *et al.* 2012[53]	China	83	/	ICCA	I-IV	Various	OS	108	5	9
Churi *et al.* 2014[54]	USA	55	55	ICCA	I-IV	Various	OS	83.33	5	9

Abbreviations: CCA: Cholangiocarcinoma; ICA: Intrahepatic cholangiocarcinoma; NOS: Newcastle–Ottawa scale; OS: Overall survival.

showing a significant overall effect (Z=5.09) and a significant survival difference between the mutant and wild-type groups (p<0.0001). A subsequent sensitivity analysis (Figure 5) showed that removing individual studies did not result in statistically significant differences between studies, suggesting that the results were robust. After addressing publication bias, Begg's test and Egger's test yielded p=0.806 and 0.570, respectively, indicating no publication bias (p>0.05).

4. Discussion

In the field of genomic research on cholangiocarcinoma, several studies have reported that *KRAS* and *TP53* mutations are more common compared to other genetic alterations.[11,16] The *KRAS* gene belongs to the RAS gene family, and through regulation of the RAF-MEK-ERK and PI3K-AKT-mTOR signaling pathways, it controls cellular growth and metabolism. Mutations in *KRAS* often lead to overactivation of downstream signaling pathways, thereby promoting tumor cell proliferation.[17] On the other hand, mutations in *TP53* disrupt its ability to bind to its target DNA sequence, rendering its tumor-suppressive function ineffective.[18]

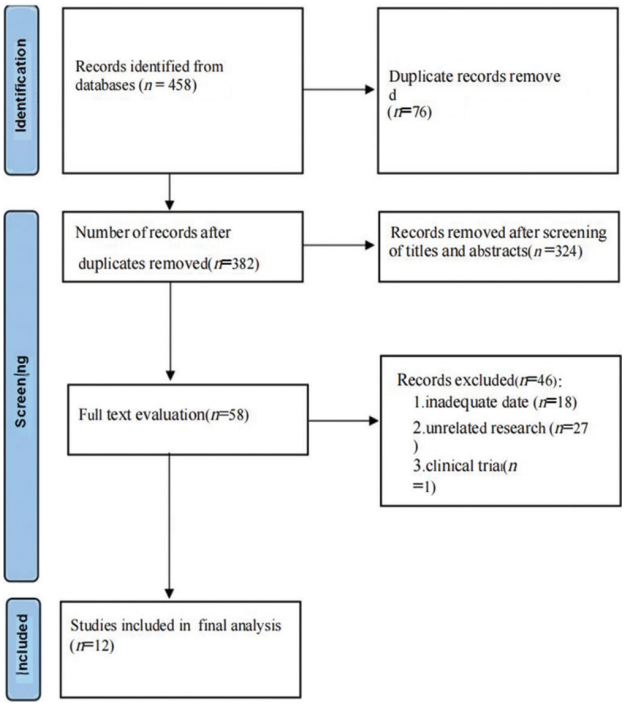


Figure 1. Flow chart of the study design

Current studies suggest that cancer patients with *KRAS* or *TP53* mutations have poorer survival outcomes compared to those without these mutations.[19,20] In a meta-analysis involving stage II and III colon cancer patients, *KRAS* mutations were found to be associated with shortened DFS.[21] Another meta-analysis on the prognostic role of *TP53* mutations in prostate cancer demonstrated that patients with *TP53* mutations had approximately 13%, 20%, and 16% lower OS at 1, 3, and 5 years, respectively, compared to patients without the mutation. *TP53* mutations were also associated with increased risk of death and accelerated disease progression.[22]

In our study, the results indicated that cholangiocarcinoma patients with *KRAS* and *TP53* mutations had a poorer prognosis compared to those without mutations. This meta-analysis summarized 12 relevant studies, revealing that patients with *KRAS* mutations had worse prognoses compared to those without the mutation (HR=7.26; 95% CI: 6.10 – 9.81; p<0.05). Statistically, the survival differences between the *KRAS* mutant and wild-type groups were highly significant (Z=8.39; p<0.0001). This suggests that *KRAS* mutations, as an important genetic biomarker, may play a key role in the prognosis assessment of cholangiocarcinoma. No significant heterogeneity was found in the *KRAS* studies (fixed-effects model; I^2=48%), supporting the use of a fixed-effects model for further analysis. However, Egger's test

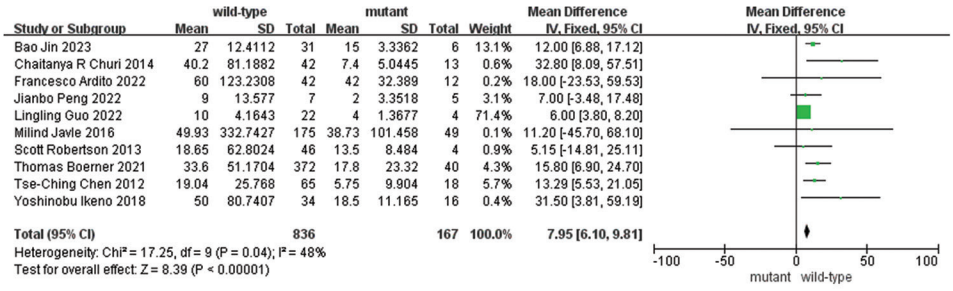


Figure 2. Forest plot comparing OS between mutant and wild-type *KRAS* in cholangiocarcinoma patients. The size of each square represents the weight of the corresponding study in the meta-analysis, whereas the horizontal lines indicate 95% confidence intervals. The pooled estimate is represented by the diamond at the bottom.

Note: The inclusion of these green marks is intended to draw attention to key findings that are of particular interest in the context of the meta-analysis.

Abbreviations: CI: Confidence interval; df: Degrees of freedom; IV: Inverse variance; OS: Overall survival; SD: Standard deviation.

(p<0.05) suggested potential publication bias, indicating that some negative or small sample studies may not have been included in the analysis. Therefore, we applied the trim-and-fill method to correct for publication bias. After the correction, we found that one study was missing from the original analysis; adding it increased the number of studies from 10 to 11, further confirming the significant relationship between *KRAS* mutations and survival differences (effect estimate=12.84 units, p<0.0001). This corrected result further strengthened our conclusions.

In the analysis of *TP53* gene mutations, we found that patients with *TP53* mutations had significantly poorer prognoses compared to those without mutations (HR=20.03; 95% CI: 6.79 – 33.28; p<0.05). The adverse prognostic effect of *TP53* mutations in cholangiocarcinoma was further statistically supported (Z=5.09; p<0.00001). We observed some heterogeneity in the *TP53* studies (I^2=59%; p=0.04), and therefore, a random-effects model was used for the analysis. Nevertheless, sensitivity analysis showed that excluding individual studies did not lead to statistically significant differences, indicating that our conclusions were robust. Further testing for publication bias using Begg's test (p=0.806) and Egger's test (p=0.570) showed no significant publication bias, further validating the reliability of our results.

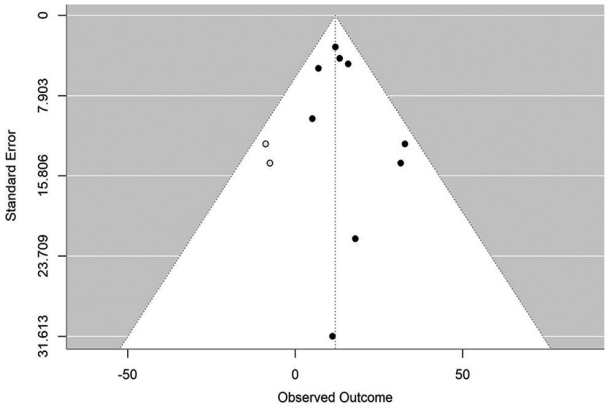


Figure 3. Data trimming outcome for KRAS analysis. The black circles represent actual studies included in the analysis, while the white circles indicate studies that were imputed using the trim-and-fill method. The trim-and-fill method is used to adjust for potential publication bias by estimating and adding missing studies to balance funnel plot asymmetry. This adjustment provides a more accurate reflection of the overall effect size and helps to correct for publication bias in the analysis.

In this study, we focused on analyzing the relationship between *KRAS* mutations, *TP53* mutations, and survival prognosis in cholangiocarcinoma patients. Although mutations in *KRAS* or *TP53* alone are associated with poorer survival outcomes, increasing evidence suggests that the co-occurrence of *KRAS* and *TP53* mutations may have a more pronounced effect on patient prognosis. Previous studies have indicated that, in various cancer types, patients with co-mutations of *KRAS* and *TP53* often exhibit more aggressive tumor behavior, poorer treatment response, and shorter survival, especially in malignant cancers such as pancreatic and colorectal cancer.[23,24] This could be due to the dual mutations, which not only exacerbate tumor proliferation but also impair cellular self-repair mechanisms.

While individual *KRAS* or *TP53* mutations have been widely studied in cholangiocarcinoma, systematic and large-scale investigations into the biological and clinical impact of their co-mutation remain limited. Among the studies included in our meta-analysis, one reported a *KRAS* and *TP53* co-mutation rate of 16.7% in patients with ICC.[25] However, due to its limited sample size, the study did not compare survival outcomes between patients with co-mutations and those with only a single mutation. To address this gap, future studies should further explore the specific role of *KRAS* and *TP53* co-mutations in survival prognosis, treatment response, and drug resistance in cholangiocarcinoma patients through multi-center, large-sample cohort studies. In addition, combining clinical data with molecular biological analyses to reveal how the co-mutation of these two genes coordinates at the molecular level will provide more precise evidence for early diagnosis, prognosis evaluation, and personalized

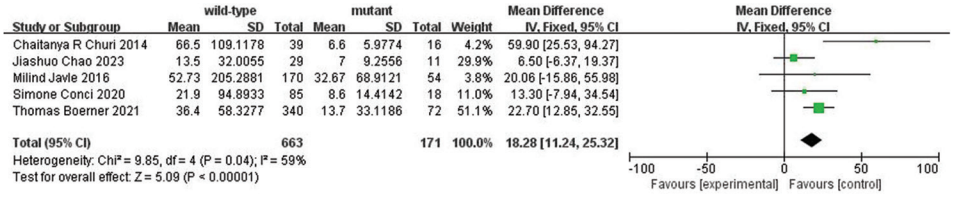


Figure 4. Forest plot comparing OS between mutant and wild-type *TP53* in cholangiocarcinoma patients. The size of each square represents the weight of the corresponding study in the meta-analysis, while the horizontal lines indicate 95% confidence intervals. The pooled estimate is represented by the diamond at the bottom.

Note: The inclusion of these green marks serves to direct attention to key findings that are of particular interest in the context of the meta-analysis.

Abbreviations: CI: Confidence interval; df: Degrees of freedom; IV: Inverse variance; OS: Overall survival; SD: Standard deviation.

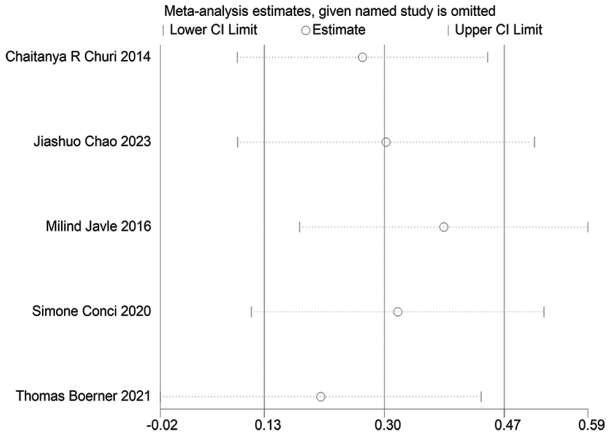


Figure 5. Sensitivity analysis of *TP53* studies
Abbreviation: CI: Confidence interval.

treatment of cholangiocarcinoma.

It is noteworthy that in the treatment of cholangiocarcinoma, immunotherapy – as an emerging therapeutic approach – has shown promising results.[26,27] *KRAS* and *TP53* mutations, two common oncogenic drivers, have been shown to influence immune evasion mechanisms in various cancer types, which may significantly affect responses to immunotherapy.[28-30] Several studies have demonstrated that *KRAS* and *TP53* co-mutations are associated with a significant increase in PD-L1 expression, along with higher tumor burden and immune cell infiltration.[31,32] Two studies on lung adenocarcinoma found that patients with *KRAS* and *TP53* co-mutations responded better to immune checkpoint inhibitors.[33,34] In cholangiocarcinoma, Chen *et al.*[35] observed differing clinical benefits between patients with only *KRAS* mutations and those with both *KRAS* and *TP53* co-mutations receiving immunotherapy. Specifically, patients with *KRAS* mutations alone exhibited poor responses to immunotherapy, whereas those with *KRAS*-*TP53* co-mutations demonstrated elevated PD-L1 expression and greater immune cell infiltration. Among all genetic subgroups, cholangiocarcinoma patients with various combinations of *KRAS* and *TP53* mutations achieved the highest objective response rates following immunotherapy.[35]

In our study, we analyzed the relationship between *KRAS* and *TP53* mutations and survival prognosis in cholangiocarcinoma patients. However, with the advancement in molecular biology, growing evidence suggests significant differences in the mutation profiles of various cancer subtypes, which may influence the clinical applicability of prognostic models. For instance, a study found that the prognostic value of TROP2 varies by lung cancer subtype.[36] Similarly, different subtypes of cholangiocarcinoma – such as ICC and ECC – exhibit distinct genetic mutation profiles. ECC patients are more likely to harbor *KRAS* and *TP53* mutations, whereas ICC patients more commonly present with *IDH1* mutations. These differences may reduce the predictive accuracy of unified prognostic models across subtypes.[37,38] Therefore, developing subtype-specific prognostic models based on unique mutation profiles may significantly enhance clinical applicability and accuracy. This has become an active area of research.[39,40] Although our study employed a unified prognostic model, recognizing the different roles that *KRAS* and *TP53* mutations play in each subtype highlights the need for subtype-specific tools. A one-size-fits-all approach may overlook meaningful distinctions, whereas subtype-tailored models could offer more accurate, personalized prognostic assessments.

Due to factors such as liver fluke infection and consumption of undercooked fish, regions including northeastern Thailand, Korea, and Japan are considered high-risk areas for cholangiocarcinoma.[41-43] However, because of the limited number of eligible studies from these regions, they were not included in our analysis. While the higher incidence rates in these areas did not conflict with our search criteria, the lack of regional representation may affect the comprehensiveness of our findings. Future research should prioritize incorporating data from these high-risk regions to further validate the prognostic significance of *KRAS* and *TP53* mutations. In addition, due to the insufficient number of eligible studies, we were unable to conduct subgroup analyses based on treatment modalities (e.g., chemotherapy and immunotherapy) or mutation types (*KRAS* only, *TP53* only, or co-mutations). Furthermore, data limitations prevented adjustments for confounding variables such as tumor location (hilar, intrahepatic, or extrahepatic) or stage. Finally, this study only included published literature, excluding unpublished studies with negative results. Future investigations are needed to validate and expand upon the prognostic effects of *KRAS* and *TP53* mutations in cholangiocarcinoma patients.

5. Conclusion

Cholangiocarcinoma is a highly heterogeneous malignant tumor, with *KRAS* and *TP53* gene mutations playing a crucial role in its occurrence and development. Our findings indicate that mutations in *KRAS* and *TP53* are each independently associated with poor prognosis in cholangiocarcinoma patients. However, existing studies exhibit certain biases and heterogeneity. Therefore, further high-quality research is essential to validate and refine these conclusions, ultimately contributing to more

effective and individualized treatment strategies for cholangiocarcinoma.

Acknowledgments

The authors gratefully acknowledge Zhejiang Chinese Medical University for providing expert guidance and access to statistical analysis software for this research.

Funding

None.

Conflict of interest

The authors declare no conflicts of interest.

Author contributions

Conceptualization: Jianan Jin
Formal analysis: Chuhan Zhang
Methodology: Yibin Zhou
Writing – original draft: Jianan Jin
Writing – review & editing: Benfeng Xu

Ethics approval and consent to participate

Not applicable.

Consent for publication

Not applicable.

Availability of data

Data are available from the corresponding author upon reasonable request.

References

1. Malaguarnera G, Giordano M, Paladina I, *et al*. Markers of bile duct tumors. *World J Gastrointest Oncol*. 2011;3(4):49-59.

   doi: 10.4251/wjgo.v3.i4.49

2. Khan AS, Dageforde LA. Cholangiocarcinoma. *Surg Clin North Am*. 2019;99(2):315-335.

   doi: 10.1016/j.suc.2018.12.004

3. Izquierdo-Sanchez L, Lamarca A, La Casta A, *et al*. Cholangiocarcinoma landscape in Europe: Diagnostic, prognostic and therapeutic insights from the ENSCCA registry. *J Hepatol*. 2022;76(5):1109-1121.

   doi: 10.1016/j.jhep.2021.12.010

4. Cheng CY, Chen CP, Wu CE. Precision medicine in cholangiocarcinoma: Past, present, and future. *Life (Basel)*. 2022;12(6):829.

   doi: 10.3390/life12060829

5. Mateo-Victoriano B, Samaranayake GJ, Pokharel S, *et al*. Oncogenic KRAS addiction states differentially influence MTH1 expression and 8-oxodGTPase activity in lung adenocarcinoma. *Redox Biol*. 2025;82:103610.

   doi: 10.1016/j.redox.2025.103610

6. Silva JL, De Andrade GC, Petronilho EC, *et al*. Phase separation and prion-like aggregation of p53 family tumor suppressors: From protein evolution to cancer treatment. *J Neurochem*. 2025;169(4):e70055.

   doi: 10.1111/jnc.70055

7. Zhu XD, Amanjiaoer RH, Shen YL, *et al*. Combination of antiangiogenic and systemic therapy in advanced non-small cell lung cancer: Before and after progression to leptomeningeal metastasis. *Sci Rep.* 2025;15(1):11901.

   doi: 10.1038/s41598-025-91922-z

8. Kale R, Samant C, Nandakumar K, Ranganath Pai KS, Bhonde M. Drugging the Undruggable and beyond: Emerging precision oncology approaches to target acquired resistance to KRAS G12C and KRAS G12D inhibitors. *Biochem Biophys Res Commun*. 2025;760:151688.

   doi: 10.1016/j.bbrc.2025.151688

9. Zheng S, You Z, Guo G, Lin Z, Wang S, Yang G. Effect of KRAS mutation status on clinicopathological characteristics and overall survival in patients with rectal cancer. *BMC Gastroenterol*. 2025;25(1):37.

   doi: 10.1186/s12876-025-03615-6

10. Zhao K, Karimi A, Kelly L, *et al*. TP53 mutation predicts worse survival and earlier local progression in patients with hepatocellular carcinoma treated with transarterial embolization. *Current Oncol*. 2025;32(1):51.

    doi: 10.3390/curroncol32010051

11. Moffat GT, Hu ZI, Meric-Bernstam F, *et al*. KRAS allelic variants in biliary tract cancers. *JAMA Netw Open*. 2024;7(5):e249840.

    doi: 10.1001/jamanetworkopen.2024.9840

12. Yu H, Xu Y, Gao W, *et al*. Comprehensive germline and somatic genomic profiles of Chinese patients with biliary tract cancer. *Front Oncol*. 2022;12:930611.

    doi: 10.3389/fonc.2022.930611

13. Alaimo L, Boggio S, Catalano G, *et al*. Multi-omics classification of intrahepatic cholangiocarcinoma: A systematic review and meta-analysis. *Cancers (Basel)*. 2024;16(14):2596.

    doi: 10.3390/cancers16142596

14. Ellis H, Braconi C, Valle JW, Bardeesy N. Cholangiocarcinoma targeted therapies: Mechanisms of action and resistance. *Am J Pathol*. 2025;195(3):437-452.

    doi: 10.1016/j.ajpath.2024.11.005

15. Stang A. Critical evaluation of the Newcastle-Ottawa scale

for the assessment of the quality of nonrandomized studies in meta-analyses. *Eur J Epidemiol*. 2010;25(9):603-605.

doi: 10.1007/s10654-010-9491-z

16. Hill MA, Alexander WB, Guo B, *et al*. Kras and Tp53 mutations cause cholangiocyte- and hepatocyte-derived cholangiocarcinoma. *Cancer Res*. 2018;78(16):4445-4451.

doi: 10.1158/0008-5472.can-17-1123

17. Huang L, Guo Z, Wang F, Fu L. KRAS mutation: From undruggable to druggable in cancer. *Signal Transduct Target Ther*. 2021;6(1):386.

doi: 10.1038/s41392-021-00780-4

18. Rivlin N, Brosh R, Oren M, Rotter V. Mutations in the p53 tumor suppressor gene: Important milestones at the various steps of tumorigenesis. *Genes Cancer*. 2011;2(4):466-474.

doi: 10.1177/1947601911408889

19. Ghidini M, Personeni N, Bozzarelli S, *et al*. KRAS mutation in lung metastases from colorectal cancer: Prognostic implications. *Cancer Med*. 2016;5(2):256-264.

doi: 10.1002/cam4.592

20. Robles AI, Harris CC. Clinical outcomes and correlates of TP53 mutations and cancer. *Cold Spring Harb Perspect Biol*. 2010;2(3):a001016.

doi: 10.1101/cshperspect.a001016

21. Formica V, Sera F, Cremolini C, *et al*. KRAS and BRAF mutations in stage II and III colon cancer: A systematic review and meta-analysis. *J Natl Cancer Inst*. 2022;114(4):517-527.

doi: 10.1093/jnci/djab190

22. Maddah MM, Hedayatizadeh-Omran A, Moosazadeh M, Alizadeh-Navaei R. Evaluation of the prognostic role of TP53 gene mutations in prostate cancer outcome: A systematic review and meta-analysis. *Clin Genitourin Cancer*. 2024;22(6):102226.

doi: 10.1016/j.clgc.2024.102226

23. Kealey J, Düssmann H, Llorente-Folch I, *et al*. Effect of TP53 deficiency and KRAS signaling on the bioenergetics of colon cancer cells in response to different substrates: A single cell study. *Front Cell Dev Biol*. 2022;10:893677.

doi: 10.3389/fcell.2022.893677

24. Yousef A, Yousef M, Chowdhury S, *et al*. Impact of KRAS mutations and co-mutations on clinical outcomes in pancreatic ductal adenocarcinoma. *NPJ Precis Oncol*. 2024;8(1):27.

doi: 10.1038/s41698-024-00505-0

25. Peng J, Fang S, Li M, *et al*. Genetic alterations of KRAS and TP53 in intrahepatic cholangiocarcinoma associated with poor prognosis. *Open Life Sci*. 2023;18(1):20220652.

doi: 10.1515/biol-2022-0652

26. Chen F, Sheng J, Li X, *et al*. Unveiling the promise of PD1/PD-L1: A new dawn in immunotherapy for cholangiocarcinoma. *Biomed Pharmacother*. 2024;175:116659.

doi: 10.1016/j.biopha.2024.116659

27. Lei Z, Ma W, Si A, *et al*. Effect of different PD-1 inhibitor combination therapies for unresectable intrahepatic cholangiocarcinoma. *Aliment Pharmacol Ther*. 2023;58(6):611-622.

doi: 10.1111/apt.17623

28. Kim JY, Jung J, Kim KM, Lee J, Im YH. TP53 mutations predict poor response to immunotherapy in patients with metastatic solid tumors. *Cancer Med*. 2023;12(11):12438-12451.

doi: 10.1002/cam4.5953

29. Mugarza E, Van Maldegem F, Boumelha J, *et al*. Therapeutic $KRAS^{G12C}$ inhibition drives effective interferon-mediated antitumor immunity in immunogenic lung cancers. *Sci Adv*. 2022;8(29):eabm8780.

doi: 10.1126/sciadv.abm8780

30. Skoulidis F, Goldberg ME, Greenawalt DM, *et al*. STK11/LKB1 mutations and PD-1 inhibitor resistance in KRAS-mutant lung adenocarcinoma. *Cancer Discov*. 2018;8(7):822-835.

doi: 10.1158/2159-8290.cd-18-0099

31. Dong ZY, Zhong WZ, Zhang XC, *et al*. Potential predictive value of TP53 and KRAS mutation status for response to PD-1 blockade immunotherapy in lung adenocarcinoma. *Clin Cancer Res*. 2017;23(12):3012-3024.

doi: 10.1158/1078-0432.ccr-16-2554

32. Gao G, Liao W, Ma Q, Zhang B, Chen Y, Wang Y. KRAS G12D mutation predicts lower TMB and drives immune suppression in lung adenocarcinoma. *Lung Cancer*. 2020;149:41-45.

doi: 10.1016/j.lungcan.2020.09.004

33. Budczies J, Romanovsky E, Kirchner M, *et al*. KRAS and TP53 co-mutation predicts benefit of immune checkpoint blockade in lung adenocarcinoma. *Br J Cancer*. 2024;131(3):524-533.

doi: 10.1038/s41416-024-02746-z

34. Frost N, Kollmeier J, Vollbrecht C, *et al*. $KRAS^{G12C}$/TP53 co-mutations identify long-term responders to first line palliative treatment with pembrolizumab monotherapy in PD-L1 high (≥50%) lung adenocarcinoma. *Transl Lung Cancer Res*. 2021;10(2):737-752.

doi: 10.21037/tlcr-20-958

35. Chen X, Wang D, Liu J, *et al*. Genomic alterations in biliary tract cancer predict prognosis and immunotherapy outcomes. *J Immunother Cancer*. 2021;9(11):e003214.

doi: 10.1136/jitc-2021-003214

36. Inamura K, Yokouchi Y, Kobayashi M, *et al*. Association of tumor TROP2 expression with prognosis varies among lung cancer subtypes. *Oncotarget*. 2017;8(17):28725-28735.

doi: 10.18632/oncotarget.15647

37. Putra J, De Abreu FB, Peterson JD, *et al*. Molecular profiling of intrahepatic and extrahepatic cholangiocarcinoma using next generation sequencing. *Exp Mol Pathol*. 2015;99(2):240-244.

doi: 10.1016/j.yexmp.2015.07.005

38. Tsilimigras DI, Stecko H, Moris D, Pawlik TM. Genomic profiling of biliary tract cancers: Comprehensive assessment of anatomic and geographic heterogeneity, co-alterations and outcomes. *J Surg Oncol*. 2025.

doi: 10.1002/jso.28081

39. Huang X, Du G, Yang Y, *et al*. Advancing bladder cancer management: Development of a prognostic model and personalized therapy. *Front Immunol*. 2024;15:1430792.

doi: 10.3389/fimmu.2024.1430792

40. Wang L, Li J, Mei N, *et al*. Identifying subtypes and developing prognostic models based on N6-methyladenosine and immune microenvironment related genes in breast cancer. *Sci Rep*. 2024;14(1):16586.

doi: 10.1038/s41598-024-67477-w

41. Khan SA, Tavolari S, Brandi G. Cholangiocarcinoma: Epidemiology and risk factors. *Liver Int*. 2019;39(Suppl 1):19-31.

doi: 10.1111/liv.14095

42. Khuntikeo N, Andrews RH, Petney TN, Khan SA. Introduction. *Recent Results Cancer Res*. 2023;219:1-5.

doi: 10.1007/978-3-031-35166-2_1

43. Tan S, Machrumnizar M. Fish and food-fatale: Food-borne trematode *opisthorchis viverrini* and cholangiocarcinoma. *Helminthologia*. 2023;60(4):287-299.

doi: 10.2478/helm-2023-0036

44. Boerner T, Drill E, Pak LM, *et al*. Genetic determinants of outcome in intrahepatic cholangiocarcinoma. *Hepatology*. 2021;74(3):1429-1444.

doi: 10.1002/hep.31829

45. Guo L, Zhou F, Liu H, *et al*. Genomic mutation characteristics and prognosis of biliary tract cancer. *Am J Transl Res*. 2022;14(7):4990-5002.

46. Ardito F, Razionale F, Campisi A, *et al*. The impact of KRAS mutational status on long-term survival following liver resection for hilar cholangiocarcinoma. *Cancers (Basel)*. 2022;14(18):4370.

doi: 10.3390/cancers14184370

47. Robertson S, Hyder O, Dodson R, *et al*. The frequency of KRAS and BRAF mutations in intrahepatic cholangiocarcinomas and their correlation with clinical outcome. *Hum Pathol*. 2013;44(12):2768-2773.

doi: 10.1016/j.humpath.2013.07.026

48. Javle M, Bekaii-Saab T, Jain A, *et al*. Biliary cancer: Utility of next-generation sequencing for clinical management. *Cancer*. 2016;122(24):3838-3847.

doi: 10.1002/cncr.30254

49. Jin B, Wang Y, Zhang B, *et al*. Immune checkpoint inhibitor-related molecular markers predict prognosis in extrahepatic cholangiocarcinoma. *Cancer Med*. 2023;12(20):20470-20481.

doi: 10.1002/cam4.6441

50. Ikeno Y, Seo S, Iwaisako K, *et al*. Preoperative metabolic tumor volume of intrahepatic cholangiocarcinoma measured by ^{18}F-FDG-PET is associated with the KRAS mutation status and prognosis. *J Transl Med*. 2018;16(1):95.

doi: 10.1186/s12967-018-1475-x

51. Conci S, Ruzzenente A, Simbolo M, *et al*. Multigene mutational profiling of biliary tract cancer is related to the pattern of recurrence in surgically resected patients. *Updates Surg*. 2020;72(1):119-128.

doi: 10.1007/s13304-020-00718-5

52. Chao J, Wang S, Wang H, *et al*. Real-world cohort study of PD-1 blockade plus lenvatinib for advanced intrahepatic cholangiocarcinoma: Effectiveness, safety, and biomarker analysis. *Cancer Immunol Immunother*. 2023;72(11):3717-3726.

doi: 10.1007/s00262-023-03523-2

53. Chen TC, Jan YY, Yeh TS. K-ras mutation is strongly associated with perineural invasion and represents an independent prognostic factor of intrahepatic cholangiocarcinoma after hepatectomy. *Ann Surg Oncol*. 2012;19(Suppl 3):S675-S681.

doi: 10.1245/s10434-012-2224-7

54. Churi CR, Shroff R, Wang Y, *et al*. Mutation profiling in cholangiocarcinoma: Prognostic and therapeutic implications. *PLoS One*. 2014;9(12):e115383.

doi: 10.1371/journal.pone.0115383

ACCSCIENCE PUBLISHING

Eurasian Journal of Medicine and Oncology

ORIGINAL RESEARCH ARTICLE

Influencing factors of chemotherapy-related cognitive impairment in patients with breast cancer

Ying Zhang[1†], Shuhan Wu[1†], Yunmiao Ma[2], Shuyang Chang[1], Jianhui Li[1], Bo Tian[3], Nan Jiang[1], Liping Yang[1], Kenian Pan[3], and Xulong Zhu[1,3*]

[1]Department of Surgical Oncology, Shaanxi Provincial People's Hospital, Xi'an, Shaanxi, China

[2]Department of Medical Oncology, Shaanxi Provincial People's Hospital, Xi'an, Shaanxi, China

[3]Department of Integrated Traditional Chinese and Western Clinical Medicine, Graduate School, Shaanxi University of Chinese Medicine, Xixian New Area, Shaanxi, China

Abstract

Introduction: The chemotherapy-related cognitive impairment is common, but the influencing factors and effective intervention measures are not well known.

Objective: To investigate the changes of cognitive function in breast cancer patients before and after chemotherapy, identify the influencing factors of cognitive function in chemotherapy patients, and investigate whether there is a mediating effect among multiple factors. Finally, an intervention was implemented for patients experiencing cognitive dysfunction to evaluate its effects on cognitive function.

Methods: Using the convenience sampling method, we recruited 380 breast cancer chemotherapy patients at three tertiary hospitals in Xi'an from October 2018 to May 2019. The Chinese version of the Functional Assessment of Cancer Therapy-Cognitive Function scale, the Hamilton Anxiety Scale, the Hamilton Depression Scale, and the social support rating scale were used to evaluate the cognitive function of breast cancer patients during chemotherapy, and analyze the influencing factors of cognitive function.

Results: The incidence of chemotherapy-related cognitive dysfunction in breast cancer patients was 19.74% (75/380). The results of the univariate analysis showed that the education level, medical expense payment method, family history of breast cancer, disease stage, and presence of comorbidities could impact cognitive functioning in breast cancer patients receiving chemotherapy ($p<0.05$). Correlation analysis revealed that there was a negative correlation among cognitive function and anxiety and depression ($p<0.01$), while a positive correlation with social support ($p<0.05$). Furthermore, multivariate stepwise regression analysis showed that the education level, medical expense payment method, disease stage, depression, and social support were independent influencing factors of cognitive function in breast cancer patients receiving chemotherapy and that depressive symptoms had a mediating effect in the relationship between social support and cognitive function. Cognitive has been shown to have a positive impact on cognitive function.

Conclusion: Cognitive dysfunction in breast cancer patients receiving chemotherapy is a multifactorial condition that requires rigorous educational and social support interventions for improvements of patient outcomes.

Keywords: Breast cancer; Chemotherapy; Chemotherapy-related cognitive impairment

[†]These authors contributed equally to this work.

***Corresponding author:**
Xulong Zhu
(zhuxulong@stu.xjtu.edu.cn)

Citation: Zhang Y, Wu S, Ma Y, *et al.* Influencing factors of chemotherapy-related cognitive impairment in patients with breast cancer. *Eurasian J Med Oncol.* 2025;9(3):133-146.
doi: 10.36922/EJMO025130073

Received: March 27, 2025

Revised: April 26, 2025

Accepted: May 8, 2025

Published online: June 3, 2025

Copyright: © 2025 Author(s). This is an Open-Access article distributed under the terms of the Creative Commons Attribution License, permitting distribution, and reproduction in any medium, provided the original work is properly cited.

Publisher's Note: AccScience Publishing remains neutral with regard to jurisdictional claims in published maps and institutional affiliations.

1. Introduction

Breast cancer is among the most prevalent malignant tumors affecting women globally, significantly impacting women's health and quality of life.[1] Chemotherapy constitutes an essential component of systemic treatment for breast cancer, both in pre-operative and post-operative settings, playing a critical role in patient management. With advancements in adjuvant intensive and metronomic chemotherapy, a variety of long-term oral chemotherapy regimens have emerged. As a cytotoxic anti-tumor agent, chemotherapy can induce a range of adverse reactions, including gastrointestinal disturbances (such as nausea, vomiting, diarrhea, and constipation), myelosuppression (manifested as leukopenia and thrombocytopenia), alopecia, hepatic and renal impairment, and vascular damage.[2] These side effects have garnered considerable attention and are well-managed in clinical practice. However, it is important to highlight that chemotherapy-related cognitive dysfunction remains an underexplored issue in cancer treatment and management.[3] This challenge is closely associated with the absence of standardized evaluation criteria and routine intervention protocols.

Chemotherapy-related cognitive impairment (CRCI) is characterized by a decline in cognitive function observed in cancer patients during or following chemotherapy, primarily manifesting as memory loss and diminished concentration.[4] According to the American Cancer Society, CRCI encompasses difficulties in thinking, concentrating, recalling details, and managing multiple tasks simultaneously, as well as challenges with word recall and decreased task efficiency.[5] Research indicates that 16 – 75% of breast cancer patients undergoing chemotherapy experience moderate-to-severe cognitive impairment during treatment, with 35 – 45% continuing to exhibit symptoms post-treatment.[6,7] CRCI adversely affects self-esteem, impedes interpersonal communication, and hinders individuals' ability to reintegrate into society.[8] Consequently, CRCI in cancer patients has emerged as a critical issue warranting increased attention and emphasis.

At present, there is a notable paucity of research specifically addressing CRCI, its influencing factors, and the interconnections between these factors in cancer patients. The potential mechanisms underlying CRCI primarily involve organic changes in the brain and psychosocial factors. Chemotherapy agents are known to adversely affect the nervous system by inducing localized inflammatory responses and causing global alterations in hormonal and metabolic levels. Research by Yao *et al.*[9] has demonstrated significant anatomical reshaping of the prefrontal lobe in patients undergoing chemotherapy, which may serve as the physiological basis for cognitive dysfunction. Several factors are recognized as influencing the cognitive function of cancer patients receiving chemotherapy, including hemoglobin levels, social support, and emotional state. Hemoglobin is a critical indicator of anemia, and its decline following chemotherapy can lead to cerebral hypoxia, disrupt cellular enzyme activity, impair brain metabolism, and consequently damage cognitive function.[10] Conversely, social support can provide mental stimulation to synapses and neurons, thereby playing a compensatory role in maintaining normal cognitive function. According to the study by McHugh Power *et al.*,[11] social support is significantly associated with cognitive function to a certain degree during follow-up periods. Moreover, anxiety and depression emerge as key predictors among the factors affecting sleep quality. Cancer patients exhibiting higher levels of depressive tendencies are consistently associated with cognitive dysfunction persisting for 6 months or more following chemotherapy. This may be attributed to the depressive state disrupting the balance of the hypothalamic-pituitary-adrenal cortex axis, potentially causing damage to neurons and the central nervous system, thereby impairing memory and executive function.[12]

Recent research indicates that CRCI encompasses cognitive domains such as memory, language ability, and executive function,[13] aligning with observed deficits in memory, diminished attention, and reduced processing speed.[14] Nevertheless, the prevalence and determinants of chemotherapy-induced cognitive dysfunction in breast cancer patients remain inadequately understood. This study employed the Functional Assessment of Cancer Therapy-Cognitive Function (FACT-Cog) scale, as part of the American Chronic Disease Management System, to assess cognitive function levels in breast cancer patients undergoing chemotherapy. The aim was to gain a comprehensive understanding of their cognitive function status and to investigate the sociopsychological factors influencing cognitive function during chemotherapy. In addition, the study explored potential mediating effects and interactions among various factors. Subsequently, we implemented cognitive behavioral therapy to address cognitive dysfunction in patients following chemotherapy. This study aimed to preliminarily investigate the intervention's efficacy in ameliorating cognitive dysfunction, with the goal of offering an effective and feasible rehabilitation nursing strategy for breast cancer patients. The findings aim to inform the development of evidence-based interventions to enhance the cognitive function of breast cancer patients receiving chemotherapy.

2. Materials and methods

2.1. Study design and participants

Between October 2018 and May 2019, a cohort of patients diagnosed with breast cancer was selected through convenience sampling. All participants were exclusively undergoing chemotherapy, which included neoadjuvant chemotherapy before surgery and adjuvant chemotherapy following surgery, with a minimum of three chemotherapy cycles. The inclusion criteria are as follows: (i) patients diagnosed with primary breast cancer confirmed by biopsy or post-operative pathology; (ii) patients who received no more than three cycles of chemotherapy; and (iii) patients possessing effective communication skills, which enable them to make informed consent. The exclusion criteria include: (i) patients with brain metastases; (ii) patients with other significant diseases; (iii) patients with malignant tumors in other anatomical locations; and (iv) patients who received alternative treatments, such as targeted therapy, radiotherapy, or immunotherapy. This study received ethical approval from the Ethics Committee of the Shaanxi Provincial People's Hospital, Xi'an (approval number: 2021071609). Based on the sample size estimation formula commonly employed in medical research,[15] the incidence rate of cognitive impairment among patients undergoing chemotherapy for breast cancer ranges from 16% to 75%. Consequently, the minimum required sample size for this study was determined to be 196 participants. Ultimately, the study encompassed a total of 380 breast cancer patients.

2.2. Data collection instruments

2.2.1. General information questionnaire

A custom-designed questionnaire was employed to collect demographic and sociological data, including variables such as age, gender, body mass index (BMI), educational attainment, marital status, and occupation. Furthermore, clinical disease data encompass various parameters, including the stage of the disease, family medical history, the presence of complications, and the existence of comorbid conditions such as diabetes, among other factors.

2.2.2. Cognitive function assessment

The cognitive function of the patients was assessed utilizing the Chinese version of the Functional Assessment of Cancer Therapy–Cognitive Function (FACT-Cog) Scale. This scale was originally developed by Wagner *et al.*[16] and subsequently translated into Chinese by Cheung's team in Singapore,[17] in accordance with the guidelines established by the Functional Assessment of Chronic Illness Therapy (FACIT) and the International Society for Pharmacoeconomics and Outcomes Research. The scale comprises 37 items distributed across four dimensions: perceived cognitive impairment (20 items), comments from others (4 items), perceived cognitive abilities (9 items), and impact on quality of life (4 items). Each item is rated on a 5-point Likert scale ranging from 0 to 4, with higher scores indicating better cognitive function. The estimated minimum clinically important difference (MCID) for this scale is between 6.9 and 10.6 points.[18] A difference exceeding this range in pre- and post-study scores for the same subject is considered clinically significant, indicating potential cognitive dysfunction. In this study, the maximum MCID score utilized was 10.6. The Cronbach's alpha coefficient for the scale was 0.96, indicating high internal consistency.

2.2.3. Anxiety and depression assessment

The Hamilton Anxiety (HAMA) Scale and the Hamilton Depression (HAMD) Scale were employed to assess anxiety and depression levels following chemotherapy. The HAMA Scale consists of 14 items related to anxiety, each rated on a 4-point scale ranging from "no symptoms" to "extremely severe." A standardized score of ≥7 signifies the presence of anxiety, with severity levels delineated as possible anxiety (7 – 14), anxiety (14 – 21), obvious anxiety (21 – 29), and severe anxiety (≥29). Similarly, the HAMD Scale comprises 17 items pertaining to depressive symptoms, scored in a manner analogous to the HAMA Scale. A standardized score of ≥7 indicates the presence of depression, with severity classified as mild (7 – 17), moderate (17 – 24), or severe (≥24).

2.2.4. Level of social support

The social support rating scale (SSRS), developed by Shuiyuan Xiao,[19] is a widely utilized instrument for assessing varying levels of social support experienced by individuals. The scale comprises 10 items distributed across three dimensions: objective social support, subjective social support, and the utilization of social support. The total SSRS score ranges from 12 to 66, with higher scores indicating greater levels of social support. Specifically, a total SSRS score below 22 signifies a low level of social support, scores between 23 and 44 denote a medium level, and scores above 44 reflect a high level of social support. The Cronbach's alpha coefficients for the overall scale and its three dimensions were 0.896, 0.849, 0.825, and 0.833, respectively, demonstrating good reliability.

2.2.5. Method of intervention

Patients who exhibited cognitive dysfunction in the prior assessment were allocated to the intervention group. The intervention group was provided with cognitive behavioral intervention training in addition to the conventional treatment and health rehabilitation guidance

and education. This training was conducted in a quiet, comfortable, and enclosed setting, occurring twice weekly for sessions lasting 60 minutes each, with the flexibility to adjust based on individual patient needs. The cognitive function changes in the intervention group were assessed using the FACT-Cog scale before the intervention and 3 months post-intervention. The specific components of cognitive behavioral intervention encompass attention enhancement, visuospatial skill development, memory training, orientation exercises, executive function training, and computational ability enhancement.

2.3. Statistical analysis

The data were entered into Epidata 3.0 to construct a database, and statistical analyses were performed using SPSS 26.0 (IBM SPSS 26.0, SPSS Inc.) and AMOS 22.0 software (Amos Development Corporation, Chicago, IL, USA). Descriptive statistics are presented as mean ± standard deviation (SD) for continuous variables and as frequency and percentage for categorical variables. The impact of variables from the general population and disease data on cognitive function was evaluated using one-way analysis of variance. Both unadjusted and multivariable-adjusted logistic regression models were employed to analyze cognitive function. Differences between the two groups were compared using the *t*-test. Explanatory factor analysis was conducted utilizing maximum likelihood estimation with orthogonal rotation, with the scree plot and eigenvalues (≥1) employed to determine the requisite number of factors. Subsequently, confirmatory factor analysis was performed using maximum likelihood estimation methods, and various statistical indices were utilized to assess model fit, including the ratio of the χ^2 to degrees of freedom (CMIN/DF)/Chi-squared statistics, root mean square error of approximation, comparative fit index, standardized root mean square residual, goodness-of-fit index (GFI), adjusted GFI, and Tucker–Lewis index. The ft indices of models were evaluated against the predefined criteria. $p<0.05$ indicated statistically significant difference.

3. Results

3.1. Characteristics of study participants

Table 1 presents the baseline characteristics of the study population. The average age of participants was 63.81 years (SD = 9.01), with a significant proportion (41.05%) being over 41 years of age. The majority of participants were female (99.47%) and married (91.32%). In addition, 61.9% reported no family history of breast cancer, and 73.1% had <12 years of education, with most having completed high school to college education. Furthermore, 36.58% of participants were unemployed, 85.79% had no family history of breast cancer, and 84.47% reported no complications. The predominant living arrangement was with a spouse and children, accounting for 87.89% of the participants. Regarding cancer staging, 24.21% were at stage I, 44.21% at stage II, 21.84% at stage III, and 9.74% at stage IV. Sixty-nine cases (18.16%) had diabetes mellitus, while 311 cases (81.84%) did not. In addition, there were 98 cases (25.79%) with a BMI <18.5 kg/m², 121 cases (31.84%) with a BMI between 18.5 and 24 kg/m², 105 cases (27.63%) with a BMI between 24 and 28 kg/m², and 56 cases (14.74%) with a BMI ≥28 kg/m² (Table 1).

3.2. Status of cognition function in breast cancer patients

Following chemotherapy, the FACT-Cog score among the 380 patients in this study was 104.76 ± 22.18 points. Among these patients, 75 exhibited a decrease of ≥10.6 points compared to their pre-chemotherapy scores, indicating a chemotherapy-related cognitive dysfunction incidence rate of 19.74%. The four dimensions assessed were perceived cognitive impairment (58.89 ± 8.19), comments from others (12.95 ± 2.10), perceived cognitive abilities (18.71 ± 7.01), and impact on quality of life (11.68 ± 1.74). A comparison of scores before and after chemotherapy is presented in Table 2.

3.3. Depression, anxiety, social support, and cognitive function in breast cancer patients undergoing chemotherapy

Among 380 breast cancer patients who underwent chemotherapy, 185 individuals (48.68%) exhibited symptoms of anxiety. The prevalence of mild, moderate, and severe anxiety was 30%, 15.79%, and 2.89%, respectively, with an average anxiety score of 16.18 ± 3.77. In addition, 184 patients (48.42%) experienced depressive symptoms, with the incidence rates of mild, moderate, and severe depression being 31.58%, 14.47%, and 2.37%, respectively. The average depression score was 17.39 ± 3.95 (Table 3).

The overall social support scores averaged 38.34 ± 16.31 points, comprising 12.23 ± 16.77 points for objective support, 18.82 ± 3.86 points for subjective support, and 6.61 ± 1.05 points for support utilization. Among the participants, 48 cases (12.63%) exhibited low levels of social support, 201 cases (52.89%) demonstrated medium levels, and 130 cases (34.21%) showed high levels of social support. The *t*-test analyses indicated that both the total and individual dimension scores of social support for patients with breast cancer post-chemotherapy were significantly lower than the normative scores of a healthy domestic population[20] ($p<0.05$), as detailed in Table 4.

Table 1. General data of patients undergoing chemotherapy for breast cancer (*n*=380)

Characteristic	Number (*n*)	Percentage
Age (years)		
≤40	78	20.53
41 – 59	156	41.05
≥60	146	38.42
Gender		
Male	2	0.53
Female	378	99.47
Marital status		
Married	347	91.32
Unmarried	18	4.74
Divorced/widowed	15	3.94
Education level		
Junior middle school and below	87	22.89
Senior high school/technical secondary school	187	49.21
College and above	106	27.90
Occupation		
Farmer	150	39.47
Worker	60	15.79
Cadre	37	9.74
Self-employed	86	22.63
Others	47	12.37
Work status		
Retired	41	89.89
On-the-job	110	28.95
Unemployed	139	36.58
Others	90	23.68
Per-capita monthly household income (RMB)		
<2000	45	11.84
2000 – 2999	73	19.21
3000 – 3999	127	33.42
4000 – 4999	90	23.69
≥5000	45	11.84
Health insurance status		
Provinces and cities medicare	101	26.58
Medical insurance for urban workers	64	16.84
Medical insurance for urban residents	65	17.11
New rural cooperative medical scheme	150	39.47
Family history of breast cancer		
Yes	54	14.21
No	326	85.79

(*Contd*...)

Table 1. (*Continued*)

Characteristic	Number (*n*)	Percentage
TNM stage		
I	92	24.21
II	168	44.21
III	83	21.84
IV	37	9.74
Complication		
Yes	59	15.53
No	321	84.47
Living situation		
Living alone	46	12.11
Not living alone	334	87.89
Diabetes		
Yes	69	18.16
No	311	81.84
BMI (kg/m^2)		
<18.5	98	25.79
18.5 – 24	121	31.84
24 – 28	105	27.63
≥28	56	14.74

Abbreviation: BMI: Body mass index.

Table 2. Comparison of cognitive function scores of breast cancer patients before chemotherapy and 3 months after chemotherapy

Items	Before chemotherapy	Three months after chemotherapy	t	*p*
Perceived cognitive impairment	62.86±8.18	58.89±8.19	−2.365	0.014*
Comments from others	13.07±2.08	12.95±2.10	−0.112	0.901
Perceived cognitive abilities	26.95±6.66	18.71±7.01	−8.235	0.001**
Impact on QoL	11.79±1.85	11.68±1.74	−0.16	0.863
Total FACT-Cog score	116.71±11.78	104.76±22.18	−4.376	0.001**

Notes: *p<0.05, **p<0.01.
Abbreviations: FACT-Cog: Functional Assessment of Cancer Therapy-Cognitive Function scale; QoL: Quality of life.

Table 3. Analysis of anxiety and depression scores in breast cancer patients undergoing chemotherapy

Items	*n* (%)				Mean±SD
	Not present	Mild	Moderate	Severe	
Anxiety	195 (51.32)	114 (30)	60 (15.79)	11 (2.89)	16.18±3.77
Depression	196 (51.58)	120 (31.58)	55 (14.47)	9 (2.37)	17.39±3.95

Abbreviation: SD: Standard deviation.

3.4. Univariate analysis of factors affecting cognitive function in breast cancer patients

The analysis results suggest several potential factors influencing cognitive function among breast cancer patients. These factors include educational level, method of medical payment, disease stage, and the presence of complications, all of which were statistically significant (p<0.05). For a detailed breakdown, please refer to Table 5.

Table 4. Analysis of social support scores in patients with breast cancer chemotherapy

Items	Breast cancer patients	Domestic norm	*t*	*p*
Objective support	12.23±16.77	12.68±3.47	−3.498	0.001**
Subjective support	18.82±3.86	23.81±4.75	−9.076	0.001**
Support utilization	6.61±1.05	9.38±2.40	−11.201	0.001**
Social support score	38.34±16.31	44.38±8.38	−7.304	0.001**

Notes: *p<0.05, **p<0.01.

3.5. The relationship between anxiety and depression severity, social support levels, and FACT-Cog scores

As illustrated in Table 6, there is a significant relationship between the total FACT-Cog score and perceived cognitive impairment, perceived cognitive abilities, and quality of life among breast cancer patients post-chemotherapy. This score is inversely correlated with anxiety and depression scores (p<0.01). Furthermore, social support exerts a significant influence on the cognitive function of breast cancer patients undergoing chemotherapy. Specifically, the total cognitive function score and its four dimensions exhibit a positive correlation with the total scores of objective support, subjective support, and overall social support (p<0.05), as detailed in Table 6.

3.6. Regression analysis of factors influencing cognitive function in breast cancer patients

The regression analysis, utilizing the bootstrap method with 1,000 iterations, revealed that education level, payment method for medical expenses, disease stage, depression, and level of social support are independent risk factors for cognitive impairment in breast cancer patients (Table 7). In this analysis, the total FACT-Cog score was used as the dependent variable, while the variables showing significant differences in the univariate analysis were included as independent variables. The findings indicate that these factors independently influence cognitive function in breast cancer patients following chemotherapy (p<0.05).

3.7. Path analysis

Figure 1 depicts the sequential mediating roles of social support, depression, and cognitive function. It was found that objective support, subjective support, and support utilization negatively predicted depression, which in turn negatively predicted cognitive function. Through the analysis of mediating effects, it was determined that objective support, subjective support, and support utilization exerted an indirect influence on cognitive function through depression levels. The mediating effects for these identified variables were quantified as 0.031 (95% confidence interval [CI]: 0.005 – 0.065), 0.034 (95% CI: 0.002 – 0.080), and 0.032 (95% CI: 0.007 – 0.065), respectively.

3.8. Effect of the intervention

We administered cognitive behavioral therapy to a cohort of 75 individuals experiencing cognitive dysfunction. The findings indicated that, following a 3-month intervention period, there was a statistically significant improvement in the cognitive function scores of all participants to varying extents. However, these scores did not return to pre-chemotherapy levels. A detailed comparison of cognitive function scores pre- and post-intervention is presented below (Table 8).

4. Discussion

The findings of this study indicate that the FACT-Cog score averaged 104.76 ± 22.18 points, with a clinically significant psychological distress detection rate of 19.74%. This rate aligns with findings from relevant international studies.[14] The cognitive function of perception exhibited the lowest dimension score (18.71 ± 7.01), potentially attributable to the diminished functional connectivity between the hippocampus and the broader brain network post-chemotherapy. Conversely, the highest dimension score, as evaluated by others, was 12.95 ± 2.10 points, corroborating the results of Boscher *et al.*[21] This dimension often manifests as mild and is therefore difficult for patients or their primary caregivers to detect. These findings underscore the necessity for healthcare professionals to recognize and prioritize the cognitive function of patients undergoing chemotherapy, and to develop scientifically informed and appropriate care programs.

In recent years, an increasing number of studies have focused on CRCI in breast cancer patients. Numerous factors contribute to cognitive dysfunction following chemotherapy. This study identified that patients with lower educational levels, those enrolled in the New Rural Cooperative Medical Scheme (NRCMS), those at advanced stages of breast cancer, those with a family history of the disease, and those with additional medical complications are more susceptible to cognitive dysfunction. Educational attainment may serve as an indicator of general intelligence, with higher intelligence levels being associated with a greater density of synapses in the cerebral cortex. This synaptic richness enhances stimulation in cerebral neurons, potentially increasing patients' resilience to cognitive impairment.[22] The increased susceptibility to cognitive dysfunction among NRCMS patients may be attributed to the financial burden that they face compared

Table 5. Analysis of factors influencing cognitive function in breast cancer patients undergoing chemotherapy

Characteristic	Cognitive function scores	Statistics	*p*
Age (years)		3.82	0.460
≤40	104.22±13.53		
41 – 59	103.24±12.71		
≥60	102.11±13.09		
Gender		3.87	0.560
Male	98.22±12.09		
Female	99.56±13.01		
Marital status		4.37	0.055
Married	102.22±20.01		
Unmarried	101.24±19.21		
Divorced/widowed	96.25±20.45		
Education level		4.55	0.010*
Junior middle school and below	97.23±20.56		
Senior high school/Technical secondary school	105.12±18.35		
College and above	110.10±21.13		
Occupation		0.89	0.380
Farmer	105.52±20.15		
Worker	105.31±20.21		
Cadre	103.22±19.36		
Self-employed	104.89±19.22		
Others	103.48±18.93		
Work status		0.93	0.450
Retired	103.55±19.16		
On-the-job	104.57±20.39		
Unemployed	103.13±19.47		
Others	104.53±20.26		
Per-capita monthly household income (RMB)		0.88	0.320
<2000	99.25±16.36		
2000 – 2999	101.56±15.45		
3000 – 3999	102.67±13.22		
4000 – 4999	102.58±15.16		
≥5000	103.09±14.14		
Health insurance status		4.51	0.010*
Provinces and cities medicare	114.36±17.64		
Medical insurance for urban workers	105.37±21.28		
Medical insurance for urban residents	99.73±20.15		
New rural cooperative medical scheme	99.16±21.10		
Family history of breast cancer		-4.03	0.001**
Yes	97.25±28.12		
No	109.53±20.88		
TNM stage		-4.87	0.001**
I – II	106.48±19.31		
III – IV	104.22±21.41		

(*Contd...*)

Table 5. (*Continued*)

Characteristic	Cognitive function scores	Statistics	*p*
Complication		-4.26	0.001**
Yes	97.14±26.37		
No	108.41±21.72		
Diabetes		3.43	0.260
Yes	99.16±21.10		
No	101.73±11.10		
BMI (kg/m^2)		1.09	0.130
<18.5	94.36±13.14		
18.5 – 24	93.67±18.23		
24 – 28	99.73±20.15		
≥28	95.16±11.10		

Notes: *p<0.05, **p<0.01.
Abbreviation: BMI: Body mass index.

Table 6. Correlation between cognitive function and anxiety, depression, and social support in breast cancer patients after chemotherapy

Items	Anxiety	Depression	Social support score	Objective support	Subjective support	Support utilization
Total FACT-Cog score	−0.473**	−0.521**	0.507**	0.391**	0.425**	0.510
Perceived cognitive impairment	−0.366**	−0.438**	0.571*	0.156*	0.169*	0.143
Perceived cognitive abilities	−0.411**	−0.453**	0.488**	0.510**	0.651**	0.630
Impact on QOL	−0.373**	−0.412**	0.514**	0.337**	0.332**	0.449
Comments from others	−0.316	−0.408	0.429**	0.318*	0.411*	0.506

Notes: *p<0.05, **p<0.01.
Abbreviations: FACT-Cog: Functional Assessment of Cancer Therapy-Cognitive Function scale; QoL: Quality of life.

Table 7. Multivariate step-by-step regression analysis of cognitive function in breast cancer patients after chemotherapy

Independent variable	Unstandardized regression coefficient	Standard errors	Standard regression coefficient	*T*	*p*
Fixed value	105.063	19.045	—	5.379	0.000
Education level	0.501	0.124	0.236	4.155	0.000
Health insurance status	8.153	1.718	0.134	4.732	0.000
TNM stage	7.147	1.609	0.116	4.643	0.000
Depression total score	−1.082	0.471	-1.142	-2.316	0.020
Social support score	5.031	1.102	0.123	4.201	0.000

Table 8. A comparative analysis of cognitive function scores pre- and post-intervention between the intervention group

Items	Before therapy	Three months after therapy	*t*	*p*
Perceived cognitive impairment	58.89±8.19	60.26±7.91	2.978	0.006**
Comments from others	12.95±2.10	13.59±6.68	−0.701	0.488
Perceived cognitive abilities	18.71±7.01	21.46±2.89	−2.252	0.032*
Impact on QoL	11.68±1.74	11.21±1.87	−1.359	0.184
Total FACT-Cog score	104.76±22.18	108.18±18.27	−3.304	0.002**

Notes: *p<0.05, **p<0.01.
Abbreviations: FACT-Cog: Functional Assessment of Cancer Therapy-Cognitive Function scale; QoL: Quality of life.

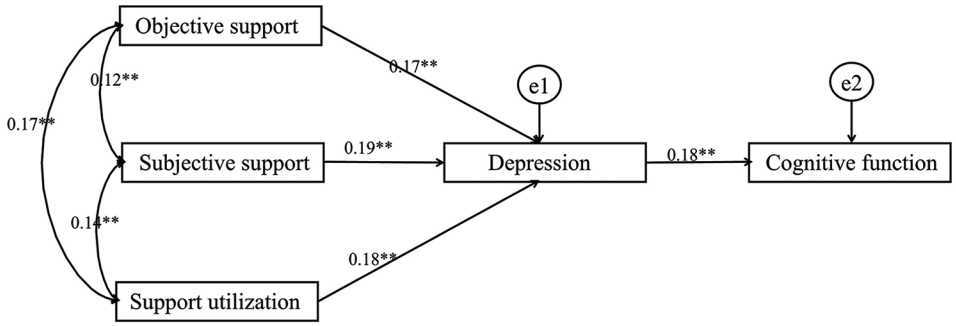


Figure 1. Pathway analysis of social support, depression, and cognitive function. The variables e1 and e2 represent the structure residuals for the depression. Note: $^{**}p<0.01$.

to individuals with other forms of medical insurance. Concerns about family finances, complications, and psychological distress stemming from a family history of breast cancer can elevate psychological stress and negative emotions, thereby exacerbating cognitive impairment. Patients with stage III – IV breast cancer exhibit a higher susceptibility to cognitive impairment compared to those with early-stage disease. This increased vulnerability can be attributed, in part, to the pathophysiological changes induced by the disease itself. In addition, it is associated with the negative emotions experienced by patients in the middle and late stages, who are concerned about the prognosis of their condition. Existing literature has demonstrated a negative correlation between BMI and cognitive function. Individuals with a high BMI, as opposed to those with a low BMI, exhibit poorer performance in language learning and visual modality episodic memory tasks.[23,24] Furthermore, BMI impacts brain volume, with increased BMI being associated with gray matter atrophy in the temporal, frontal, and occipital cortices, as well as in the hippocampus, thalamus, and midbrain, alongside a reduction in white matter integrity throughout the brain.[25] These brain regions are intricately linked to cognitive function, indicating that elevated BMI may be a contributing factor to cognitive impairment. In addition, diabetes emerges as another potential comorbidity influencing cognitive function. Several studies have indicated that type 2 diabetes mellitus can exacerbate age-related cognitive decline.[26,27] Type 2 diabetes mellitus is correlated with deficits in various cognitive domains, including processing speed, attention, spatial working memory, verbal fluency, and executive function.[28] In light of these findings, we examined the BMI levels and diabetes status of the study population to minimize the confounding effects on our research outcomes. Univariate analysis indicated that neither diabetes nor varying BMI levels had a significant impact on the cognitive function of breast cancer patients post-chemotherapy. This result may be influenced by the structural characteristics of the enrolled population and the sample size of the study. Consequently, healthcare professionals can implement tailored cognitive intervention strategies based on the specific characteristics of different patient groups, thereby enhancing the precision and effectiveness of preventing and treating cognitive dysfunction in patients undergoing chemotherapy for breast cancer.

Neuroimaging research has demonstrated a correlation between cognitive function and alterations in neural structures among patients undergoing chemotherapy, with cognitive changes exerting significant effects on neural architecture. In a retrospective study conducted by Kesler *et al.*,[29] it was found that patients treated with anthracyclines exhibited diminished functionality in the left precuneus region of the brain, which was associated with poorer executive and language performance. In addition, an observational study by Piccirillo *et al.*[30] investigated the relationship between self-reported cognitive impairment and structural brain changes. This study revealed significant differences in the connectivity strength within the frontoparietal network between patients with and without cognitive impairment. While the aforementioned studies demonstrated a negative correlation between alterations in brain functional connectivity and perceptual cognitive impairment, they predominantly relied on small sample sizes and retrospective, cross-sectional designs. To address these limitations, we propose conducting larger, prospective studies to investigate the causal mechanisms linking changes in cognitive function and brain structure, as well as the underlying neurobiological trajectories in patients before and after treatment.

Anxiety and depression are prevalent among breast cancer patients following chemotherapy. The apprehension regarding potential adverse reactions to chemotherapy, alterations in body image, and role discrepancies contribute to an increased psychological burden, manifesting as anxiety, depression, and other negative

emotions. Yang *et al.*[31] identified a significant interaction between symptoms of depression and anxiety in this patient population. In the present study, the incidence rates of anxiety and depression post-chemotherapy were 48.68% and 48.42%, respectively. There was a negative correlation between cognitive function scores and scores for anxiety and depression ($p<0.05$, $p<0.01$). Multiple stepwise regression analysis indicated that depression is an independent factor influencing cognitive function, corroborating the findings of Bedillion *et al.*[32] Further studies have demonstrated alterations in frontal lobe function and impaired hormone receptor function in depressed patients, leading to hippocampal neuron death and central nervous system dysfunction, thereby impairing cognitive function.[4] Prolonged exposure to negative emotions has the potential to adversely affect brain structure and result in diminished cognitive function.[33] At present, nursing managers have the capacity to offer psychological counseling to patients, perform emotional assessments, and facilitate the adoption of positive coping strategies through group sandplay therapy.

This study identified a low overall social support score among breast cancer patients, with a positive correlation between social support and cognitive function following chemotherapy ($p<0.01$). Within the dimensions of social support, subjective support scored the highest, followed by objective support, while support utilization scored the lowest, aligning with the findings of Bailey *et al.*[34] Breast cancer patients express a strong desire for psychological and emotional support from family and friends. Such social support can enhance patients' psychological well-being, stimulate brain synapses and neurons, and consequently play a compensatory role in maintaining normal cognitive function. Gates *et al.*[35] implemented a web-based cognitive rehabilitation intervention for patients experiencing post-chemotherapy cognitive dysfunction, demonstrating significantly greater cognitive recovery in the intervention group compared to the control group. These findings suggest that increased understanding and support from healthcare professionals and family caregivers could be an effective strategy for improving the cognitive status of patients undergoing chemotherapy for breast cancer.

This study conducted an in-depth analysis of the mediating effects among social support, depression, and cognitive function in breast cancer patients post-chemotherapy. The findings revealed that the three dimensions of social support negatively predicted depression, which in turn negatively predicted cognitive function. In addition, depression served as a mediator between the three dimensions of social support and cognitive function. Consequently, enhancing levels of social support may mitigate the decline in emotional well-being and cognitive abilities in breast cancer patients undergoing chemotherapy. Healthcare professionals can facilitate this by encouraging patients to strengthen communication with family and friends, proactively seek assistance, and improve their capacity to confront personal challenges. This approach may help alleviate negative emotions, such as anxiety and depression, thereby reducing or preventing cognitive impairment associated with chemotherapy.

At present, intervention strategies for chemotherapy-induced cognitive impairment can be broadly categorized into pharmacological and non-pharmacological treatments. Pharmacological interventions primarily encompass neuroprotective agents, psychostimulants, and traditional Chinese medicine, among others. Nonetheless, the clinical research in this domain is still in its nascent stages, and the efficacy of these treatments requires further validation. Non-pharmacological interventions include cognitive behavioral training, physical exercise, music therapy, and meditation.[36] Notably, empirical studies suggest that cognitive behavioral therapy is beneficial for enhancing cognitive function and improving quality of life.[37]

The findings of this study indicate that, following a 3-month intervention period, both the overall FACT-Cog score and perceived cognitive abilities were elevated compared to pre-intervention levels, although they did not return to baseline. This suggests that consistent cognitive behavioral intervention training may ameliorate cognitive dysfunction in breast cancer patients post-chemotherapy. The plausible explanation may be attributed to the repeated stimulation of neuronal cells through intervention training, which influences the functions of neurotransmitters and receptors within these cells.[38] Furthermore, several studies have demonstrated that behavioral interventions can modulate synaptic plasticity, enhance synaptic transmission, and consequently facilitate the restoration of memory capabilities.[39]

5. Conclusion

The prevalence of chemotherapy-induced cognitive dysfunction among breast cancer patients in this study was 19.74%. The cognitive function of these patients was influenced by factors such as education level, payment method for medical expenses, family history of breast cancer, disease stage, and the presence of complications. Cognitive function demonstrated a negative correlation with anxiety and depression, while showing a positive correlation with social support. Multiple stepwise regression analysis identified education level, payment method for medical expenses, disease stage, depression, and social support as

independent determinants of cognitive function in breast cancer patients undergoing chemotherapy. Furthermore, depression was found to mediate the relationship between social support and cognitive function. Consequently, the cognitive dysfunction observed in breast cancer patients post-chemotherapy is influenced by a multitude of factors. This necessitates heightened awareness among healthcare professionals, the development of scientifically grounded intervention strategies, the enhancement of social support, and efforts to aid patients in improving their cognitive function. This study proposes that cancer-related cognitive dysfunction can be ameliorated through the implementation of cognitive-enhancing strategies in clinical practice. This includes instructing patients in these strategies, advising them to engage in cognitively demanding tasks during periods of optimal cognitive functioning, and administering cognitive behavioral interventions when deemed necessary. However, we did not investigate the relationship between biochemical parameters and cognitive functioning. Further in-depth observation and analysis in the follow-up study are warranted.

Acknowledgments

None.

Funding

This research was funded by the Beijing Sisco Clinical Oncology Research Fund (grant number Y-L2020-0013), the Shaanxi Clinical Medical Research Center for Breast Diseases (grant number 2024SF-LCZX-08), the Natural Science Basic Research Program of Shaanxi Province (grant number 2023-JC-YB-345), Shaanxi Provincial People's Hospital Elite Talent Project (grant number 2022-JY46), and the Shaanxi Provincial People's Hospital incubation fund project (grant number 2022YJY-57).

Conflict of interest

The authors declare no conflicts of interest.

Author contributions

Conceptualization: Ying Zhang, Liping Yang
Data curation: Ying Zhang, Nan Jiang
Formal analysis: Ying Zhang, Yunmiao Ma
Methodology: Bo Tian, Kenian Pan, Jianhui Li
Writing – original draft: Shuhan Wu
Writing – review & editing: Shuyang Chang, Xulong Zhu

Ethics approval and consent to participate

This work received ethical approval from the Shaanxi Provincial People's Hospital Ethics Board (Project number: 2021071609). Written informed consent for participation in the study was obtained from all participants before their involvement.

Consent for publication

Written consent from the patient to report individual data for publication was obtained.

Availability of data

Data are available from the corresponding author on reasonable request.

References

1. WHO. *Latest Global Cancer Data: Cancer Burden Rises to 19.3 Million New Cases and 10.0 Million Cancer Deaths in 2022 Questions and Answers (Q and A)*. Switzerland: WHO; 2024.
2. Yang S, Zheng L, Sun Y, Li Z. Effect of network-based positive psychological nursing model combined with elemene injection on negative emotions, immune function and quality of life in lung cancer patients undergoing chemotherapy in the era of big data. *Front Public Health*. 2022;10:897535.

   doi: 10.3389/fpubh.2022.897535
3. Országhová Z, Mego M, Chovanec M. Long-term cognitive dysfunction in cancer survivors. *Front Mol Biosci*. 2021;8:770413.

   doi: 10.3389/fmolb.2021.770413
4. Lange M, Joly F, Vardy J, *et al*. Cancer-related cognitive impairment: An update on state of the art, detection, and management strategies in cancer survivors. *Ann Oncol*. 2019;30(12):1925-1940.

   doi: 10.1093/annonc/mdz410
5. American Cancer Society. *Chemo Brain[EB/OL]*; 2023. Available from: https://www.cancer.org/treatment/treatments-and-side-effects/physical-side-effects/changes-in-mood-or-thinking/chemo-brain.html [Last accessed on 2025 May 29].
6. And Alternative Medicine EC. Changes and influencing factors of cognitive impairment in patients with breast cancer. *Evid Based Complement Alternat Med*. 2023;2023:9872082.

   doi: 10.1155/2023/9872082
7. Tyagi K, Masoom M, Majid H, *et al*. Role of cytokines in chemotherapy-related cognitive impairment of breast cancer patients: A systematic review. *Curr Rev Clin Exp Pharmacol*. 2023;18(2):110-119.

   doi: 10.2174/2772432817666220304212456
8. Rodríguez Martín B, Fernández Rodríguez EJ, Rihuete Galve MI, Cruz Hernández JJ. Study of chemotherapy-induced cognitive impairment in women with breast cancer. *Int J Environ Res Public Health*. 2020;17(23):8896.

doi: 10.3390/ijerph17238896

9. Yao S, Zhang Q, Yao X, *et al*. Advances of neuroimaging in chemotherapy related cognitive impairment (CRCI) of patients with breast cancer. *Breast Cancer Res Treat*. 2023;201:15-26.

   doi: 10.1007/s10549-023-07005-y

10. Regier NG, Naik AD, Mulligan EA, *et al*. Cancer-related cognitive impairment and associated factors in a sample of older male oral-digestive cancer survivors. *Psychooncology*. 2019;28(7):1551-1558.

    doi: 10.1002/pon.5131

11. McHugh Power JE, Lawlor BA, Kee F. Social support mediates the relationships between extraversion, neuroticism, and cognitive function in older adults. *Public Health*. 2017;147:144-152.

    doi: 10.1016/j.puhe.2017.02.015

12. Ibrahim EY, Domenicano I, Nyhan K, *et al*. Cognitive effects and depression associated with taxane-based chemotherapy in breast cancer survivors: A meta-analysis. *Front Oncol*. 2021;11:642382.

    doi: 10.3389/fonc.2021.642382

13. Das A, Ranadive N, Kinra M, Nampoothiri M, Arora D, Mudgal J. An overview on chemotherapy-induced cognitive impairment and potential role of antidepressants. *Curr Neuropharmacol*. 2020;18(9):838-851.

    doi: 10.2174/1570159X18666200221113842

14. Durán-Gómez N, López-Jurado CF, Nadal-Delgado M, Pérez-Civantos D, Guerrero-Martín J, Cáceres MC. Chemotherapy-related cognitive impairment in patients with breast cancer based on functional assessment and NIRS analysis. *J Clin Med*. 2022;11(9):2363.

    doi: 10.3390/jcm11092363

15. Xu W, Wang K, Lian H. Linear convergence of decentralized estimation for statistical estimation using gradient method. *Neurocomputing*. 2024;584:127584.

    doi: 10.1016/j.neucom.2024.127584

16. Wagner L, Sweet JJ, Butt Z, *et al*. Measuring patient self-reported cognitive function: Qualitative findings and initial development of the functional assessment of cancer therapy-cognitive function (FACT-Cog) instrument. *J Support Oncol*. 2009;7(6):W32-W39.

17. Cheung YT, Si RL, Shwe M, *et al*. Psychometric properties and measurement equivalence of the English and Chinese versions of the functional assessment of cancer therapy-cognitive in Asian patients with breast cancer. *Value Health*. 2013;16(6):1001-1013.

    doi: 10.1016/j.jval.2013.06.013

18. Cheung YT, Foo YL, Shwe M, *et al*. Minimal clinically important difference (MCID) for the functional assessment of cancer therapy: Cognitive function (FACT-Cog) in breast cancer patients. *J Clin Epidemiol*. 2014;67(7):811-820.

    doi: 10.1016/j.jclinepi.2014.01.010

19. Xiao SY. Theoretical basis and research application of social support rating scale. *J Clin Psychiatry*. 1994;4(2):98-100.

20. Liu JY, Li FY, Lian YL. Investigation of reliability and validity of the social support scale. *J Xinjiang Med Univ*. 2008;31(1):1-3.

21. Boscher C, Joly F, Clarisse B, *et al*. Perceived cognitive impairment in breast cancer survivors and its relationships with psychological factors. *Cancers (Basel)*. 2020;12(10):3000.

    doi: 10.3390/cancers12103000

22. Abebe E, Tollesa T, Assefa M, *et al*. Cognitive functioning and its associated factors among breast cancer patients on chemotherapy at Tikur Anbessa specialized hospital, Addis Ababa Ethiopia: An institution-based comparative cross-sectional study. *BMC Cancer*. 2021;21(1):1052.

    doi: 10.1186/s12885-021-08799-0

23. Gunstad J, Paul RH, Cohen RA, *et al*. Obesity is associated with memory deficits in young and middle-aged adults. *Eat Weight Disord*. 2006;11(1):e15-e19.

    doi: 10.1007/BF03327747

24. Shefer G, Marcus Y, Stern N. Is obesity a brain disease? *Neurosci Biobehav Rev*. 2013;37(10 Pt 2):2489-2503.

    doi: 10.1016/j.neubiorev.2013.07.015

25. Lamport DJ, Chadwick HK, Dye L, *et al*. A low glycaemic load breakfast can attenuate cognitive impairments observed in middle aged obese females with impaired glucose tolerance. *Nutr Metab Cardiovasc Dis*. 2014;24(10):1128-1136.

    doi: 10.1016/j.numecd.2014.04.015

26. Kanaya AM, Barrett-Connor E, Gildengorin G, *et al*. Change in cognitive function by glucose tolerance status in older adults: A 4-year prospective study of the Rancho Bernardo study cohort. *Arch Intern Med*. 2004;164(12):1327-1333.

    doi: 10.1001/archinte.164.12.1327

27. Awad N, Gagnon M, Messier C. The relationship between impaired glucose tolerance, type 2 diabetes, and cognitive function. *J Clin Exp Neuropsychol*. 2004;26(8):1044-1080.

    doi: 10.1080/13803390490517975

28. Dye L, Boyle NB, Champ CL, Lawton CL. The relationship between obesity and cognitive health and decline. *Proc Nutr Soc*. 2017;76(4):443-454.

    doi: 10.1017/S0029665117002014

29. Kesler SR, Blayney DW. Neurotoxic effects of anthracycline- vs nonanthracycline-based chemotherapy on cognition in breast cancer survivors. *JAMA Oncol*. 2016;2(2):185-192.

    doi: 10.1001/jamaoncol.2015.4333

30. Piccirillo JF, Hardin FM, Nicklaus J, *et al*. Cognitive impairment after chemotherapy related to atypical network architecture for executive control. *Oncology*. 2015;88(6):360-368.

doi: 10.1159/000370117

31. Yang Y, Sun H, Luo X, *et al*. Network connectivity between fear of cancer recurrence, anxiety, and depression in breast cancer patients. *J Affect Disord*. 2022;309:358-367.

doi: 10.1016/j.jad.2022.04.125

32. Bedillion MF, Ansell EB, Thomas GA. Cancer treatment effects on cognition and depression: The moderating role of physical activity. *Breast*. 2019;44:73-80.

doi: 10.1016/j.breast.2019.01.004

33. Zhou X, Zhang X, Zhong T, Zhou M, Gao L, Chen L. Prevalence and associated factors of chemotherapy-related cognitive impairment in older breast cancer survivors. *J Adv Nurs*. 2024;80(2):484-499.

doi: 10.1111/jan.15842

34. Bailey LR, Craft M, Bert SSC, Carlson BW. The impact of chemotherapy-related cognitive impairment on social roles and well-being in breast cancer survivors. *Oncol Nurs Forum*. 2024;51(2):153-162.

doi: 10.1188/24.ONF.153-162

35. Gates P, Green HJ, Gough K, *et al*. Web-based cognitive rehabilitation intervention for cancer-related cognitive impairment following chemotherapy for aggressive lymphoma: Protocol for a randomised pilot trial. *BMJ Open*. 2024;14(3):e081084.

doi: 10.1136/bmjopen-2023-081084

36. Tolin DF, Lord KA, Knowles KA. Cognitive-behavioral therapy enhancement strategies. *Psychiatr Clin North Am*. 2024;47(2):355-365.

doi: 10.1016/j.psc.2024.02.005

37. Cheng ASK, Wang X, Niu N, Liang M, Zeng Y. Neuropsychological interventions for cancer-related cognitive impairment: A network meta-analysis of randomized controlled trials. *Neuropsychol Rev*. 2022;32(4):893-905.

doi: 10.1007/s11065-022-09566-z

38. McDonald BC, Conroy SK, Ahles TA, West JD, Saykin AJ. Alterations in brain activation during working memory processing associated with breast cancer and treatment: A prospective functional magnetic resonance imaging study. *J Clin Oncol*. 2012;30(20):2500-2508.

doi: 10.1200/JCO.2011.38.5674

39. Von Ah D, McDonald BC, Crouch AD, *et al*. Randomized double-masked controlled trial of cognitive training in breast cancer survivors: A preliminary study. *Support Care Cancer*. 2022;30(9):7457-7467.

doi: 10.1007/s00520-022-07182-4

ACCSCIENCE PUBLISHING

Eurasian Journal of Medicine and Oncology

ORIGINAL RESEARCH ARTICLE

Revisiting the role of the Pfannenstiel incision in early-stage endometrial cancer

Cem Yagmur Ozdemir[1,2]*, Hasan Eroğlu[3], Necat Cağatay Sezer[3], Nayif Çicekli[2,4], Derya Yeğin Aksu[5], and Dağıstan Tolga Arioz[2]

[1]Department of Gynecological Oncology, Afyonkarahisar State Hospital, Afyonkarahisar, Turkey

[2]Department of Gynecological Oncology, Faculty of Medicine, Afyonkarahisar Health Sciences University, Afyonkarahisar, Turkey

[3]Department of Gynecology and Obstetrics, Faculty of Medicine, Afyonkarahisar Health Sciences University, Afyonkarahisar, Turkey

[4]Department of Gynecological Oncology, Erzurum City Hospital, Erzurum, Turkey

[5]Department of Pathology, Faculty of Medicine, Afyonkarahisar Health Sciences University, Afyonkarahisar, Turkey

Abstract

Introduction: Endometrial cancer is the most common gynecologic malignancy in developed countries, and the optimal surgical approach in early-stage cases remains a subject of ongoing clinical debate.

Objective: This study aims to compare laparoscopy and Pfannenstiel incision in early-stage, low-grade endometrial cancer (EC) surgery.

Methods: A retrospective study was conducted on the records of 224 patients diagnosed with EC between April 2010 and April 2024. Only patients with stage I and grade I-II endometrioid type EC were included in the study. After excluding 94 patients with non-endometrioid histology, stage II-IV disease, grade 3 tumors, and synchronous tumors, 130 patients were included in the final analysis. Participants were categorized into two groups: Group 1 (63 patients who underwent surgery through Pfannenstiel incision) and Group 2 (67 patients who underwent laparoscopic surgery).

Results: The median overall survival (OS) was 48 months (range: 12 – 168) and the median disease-free survival (DFS) was 47 months (range: 8 – 168). During the follow-up period, 20 patients died and 8 patients experienced disease recurrence. The overall OS rate was 84.6%, and the DFS was 93.8%. When comparing groups, the OS was 85.7% in Group 1 and 83.6% in Group 2 (p=0.12). The DFS rate was significantly higher in Group 1 compared to Group 2 (96.8% vs. 91%; p=0.037).

Conclusion: This study highlights the continued relevance of staging surgery with the Pfannenstiel incision in early-stage EC patients with vaginal stenosis, morbid obesity unsuitable for trocar insertion, a history of multiple abdominal surgeries, inability to insert a manipulator, an enlarged normal uterus, or suspected pelvic adhesions.

Keywords: Endometrial cancer; Laparoscopy; Pfannenstiel incision

***Corresponding author:**
Cem Yagmur Ozdemir
(cemyagmur.ozdemir@saglik.gov.tr)

Citation: Ozdemir CY, Eroğlu H, Sezer NC, Çicekli N, Aksu DY, Arioz DT. Revisiting the role of the Pfannenstiel incision in early-stage endometrial cancer. *Eurasian J Med Oncol*. 2025;9(3):147-154. doi: 10.36922/EJMO025150106

Received: April 11, 2025

Revised: May 7, 2025

Accepted: May 27, 2025

Published online: June 19, 2025

Copyright: © 2025 Author(s). This is an Open-Access article distributed under the terms of the Creative Commons Attribution License, permitting distribution, and reproduction in any medium, provided the original work is properly cited.

Publisher's Note: AccScience Publishing remains neutral with regard to jurisdictional claims in published maps and institutional affiliations.

1. Introduction

Endometrial cancer (EC) is the most common gynecological cancer in middle- and high-income countries, and its prevalence is increasing worldwide.[1] While surgical staging is the cornerstone of EC management, hysterectomy is considered one of the best treatment options for patients with nonmetastatic disease.[2,3] Hysterectomy is often

performed in conjunction with other surgical procedures, particularly oophorectomy. These surgeries can be performed using laparoscopy, laparotomy, or robotic-assisted methods.[4-6] Several studies have compared midline and Pfannenstiel incisions for laparotomy in early-stage EC.[7-10] Although laparoscopy offers greater comfort for patients, each surgical method has distinct advantages and disadvantages. Laparoscopic surgery may pose challenges, especially in patients with a history of pelvic surgery or those who are superobes.[11] In such cases, although the midline incision used in laparotomy provides a broader operative field, it is associated with higher complication rates compared to the Pfannenstiel incisions.[12] Staging with a Pfannenstiel incision may be a surgical option in patients with vaginal stenosis, morbid obesity that precludes trocar insertion, unsuitability for a manipulator, history of multiple abdominal surgeries, enlarged uteri, or suspected pelvic adhesions. In such complex scenarios, the choice of incision in laparotomy becomes critical. Although a midline incision can provide extensive exposure and easier access to pelvic organs, it is associated with higher postoperative pain, increased wound infection rates, and longer recovery times compared to the Pfannenstiel incision.[13]

The Pfannenstiel incision, characterized by its transverse suprapubic placement, generally offers superior cosmetic outcomes, less postoperative pain, and reduced wound-related complications. Previous studies comparing midline and Pfannenstiel incisions in early-stage EC surgery have reported lower complication rates, including wound infections and incisional hernias, with Pfannenstiel incisions.[14,15] Recent data suggest that in patients unsuitable for minimally invasive techniques, the Pfannenstiel incision serves as a valuable alternative, offering some of the benefits of minimally invasive surgery while retaining the advantages of an open approach.[16,17] Moreover, patient satisfaction related to postoperative pain management, hospital stay duration, and cosmetic outcomes is notably higher among those undergoing surgery through the Pfannenstiel incision compared to midline laparotomy.[18]

Taken together, the Pfannenstiel incision represents a viable alternative to laparoscopy in patients for whom minimally invasive surgery is contraindicated or not feasible. It also offers a compromise between the benefits of open and minimally invasive surgery. Some reports have shown that adequate lymph node retrieval can be achieved through the Pfannenstiel incision without compromising oncologic safety. In this study, we aimed to compare laparoscopy and Pfannenstiel incision in early-stage, low-grade EC surgery.

2. Materials and methods

2.1. Patients

A retrospective study was conducted on the records of 224 patients diagnosed with EC between April 2010 and April 2024. The staging was performed according to revised the International Federation of Gynecology and Obstetrics (FIGO) 2009 criteria.[19] Serous and clear cell carcinomas were classified as grade 3.[20] Only stage I and grade I – II endometrioid-type EC were included in the study. Women aged 18 and older, who were postmenopausal or perimenopausal and had complete preoperative and postoperative data, were eligible for inclusion. After excluding 94 patients with non-endometrioid histology, stage II – IV disease, grade 3 tumors, and synchronous tumors, a total of 130 patients were included in the final analysis. Data related to age, body mass index (BMI), stage, grade, and survival were extracted from medical records. BMI was calculated as weight in kilograms (kg) divided by height in meters squared (m^2). Participants were categorized into two groups: Group 1 (63 patients who underwent surgery through Pfannenstiel incision) and Group 2 (67 patients who underwent laparoscopic surgery). All patients underwent preoperative magnetic resonance imaging (MRI) to assess myometrial invasion, cervical involvement, and pelvic/paraaortic lymph node metastasis. Patients with suspicious findings for stage II – IV on preoperative MRI were excluded, as they underwent complete lymph node dissection. Patients were followed until April 2024 or their date of death. All patients completed appropriate adjuvant therapy in the postoperative period.

2.2. Sample evaluation

The surgical procedure using the Pfannenstiel incision included total hysterectomy, bilateral salpingo-oophorectomy, omental biopsy, and pelvic lymph node sampling. Pelvic lymph nodes were removed starting from the distal part of the common iliac artery to the circumflex iliac vein and anterior to the obturator nerve. In our clinic, para-aortic lymph node sampling is not performed in patients with low-grade, early-stage EC as assessed by preoperative MRI. Sentinel lymph node (SLN) mapping is also not performed due to the lack of equipment. Instead, pelvic lymph node sampling, cytology collection, and omental sampling are performed for staging purposes. For laparoscopic surgery, a 10 mm, 0° laparoscope was routinely used. We opted for umbilical access using the open entry (Hasson) technique under direct vision,[21] with a small transverse or longitudinal incision made at the umbilicus. A uterine manipulator was routinely used, and the fallopian tubes were sealed with bipolar energy before

hysterectomy. After the removal of the uterus through the vagina, a powder-free surgical glove was inserted into the abdominal cavity. The glove was filled with the retrieved lymph nodes, the open end was clipped, and the glove was extracted through the vagina. The procedure was completed following hemostasis.

2.3. Statistical analysis

Statistical analyses were performed using the Statistical Package for the Social Sciences statistics (Version 22.0., IBM, USA) for Windows. For continuous variables, mean, median, and standard deviation were calculated. The Student's *t*-test, Mann–Whitney U-test, and Kruskal–Wallis tests were used for comparisons between continuous variables, whereas the Fisher's exact test was conducted for categorical variables. Kaplan–Meier curves were constructed to assess overall survival (OS) and disease-free survival (DFS) in both groups. Statistical significance was defined as $p<0.05$.

3. Results

3.1. Patient demographics and baseline characteristics

A total of 130 patients with early-stage, low-grade EC treated between April 2010 and April 2024 were included in the study. Of these, 63 patients underwent surgery through Pfannenstiel incision (Group 1) and 67 patients underwent laparoscopic surgery (Group 2). The mean age of the cohort was 60.7 ± 7.9 years. The mean BMI was 33.6 ± 5.5 kg/m^2. Postoperative pathological analysis revealed a median tumor size of 3 cm (range: 1 – 8 cm). Patient characteristics and pathological findings are summarized in Table 1.

Table 1. Comparison of demographic and clinicopathological characteristics of study participants (n=130)

Characteristics	Group 1 (Pfannenstiel incision)	Group 2 (laparoscopy)	p
Number of patients (n)	63	67	-
Mean age (years)	60.65±9.5	60.75±9.2	0.96
Mean BMI (kg/m^2)	33.1±5.5	34.2±4.7	0.225
Surgical stage (*n*)			
IA	54	49	0.078
IB	9	18	
Grade (*n*)			
1	40	47	0.702
2	23	20	
LVSI (*n*)			
Negative	55	62	0.322
Positive	8	5	
Cytology (*n*)			
Negative	61	64	0.701
Positive	2	3	
Mean number of pelvic lymph nodes removed	10.6±7.8	9.45±5.1	0.318
Recurrence (*n*)	2	6	0.172
OS (%)	85.7	83.6	0.12
DFS (%)	96.8	91	0.037*

Note: * $p<0.05$.
Abbreviations: BMI: Body mass index; DFS: Disease-free survival; LVSI: Lymphovascular space invasion; OS: Overall survival.

3.2. Surgical and pathological outcomes

Lymphovascular space invasion (LVSI) was present in 12.7% of patients in Group 1 and 7.5% in Group 2 ($p=0.322$). Peritoneal cytology was positive in two patients (3.2%) in Group 1 and three patients (4.5%) in Group 2 ($p=0.701$), with no statistically significant difference. The mean number of pelvic lymph nodes retrieved was 10.6 ± 7.8 in Group 1 and 9.45 ± 5.1 in Group 2 ($p=0.318$), indicating similar surgical adequacy in nodal assessment between the groups.

3.3. Recurrence patterns

During the follow-up period, a total of eight patients experienced disease recurrence. Recurrence was observed in two patients in Group 1—one with pelvic lymph node recurrence and the other with peritoneal recurrence. In contrast, six patients in Group 2 experienced recurrence: One with port-site metastasis, two with vaginal cuff recurrence, one with pulmonary metastasis, one with pelvic lymph node recurrence, and one with colon metastasis. Although the number of recurrences was numerically higher in Group 2, the difference was not statistically significant ($p=0.172$).

3.4. Survival outcomes

The median OS for the entire cohort was 48 months (range: 12 – 168 months), and the median DFS was 47 months (range: 8 – 168 months). The OS and DFS rates were 84.6% and 93.8%, respectively. OS was 85.7% in Group 1 and 83.6% in Group 2, with no statistically significant difference ($p=0.12$). However, DFS was significantly higher in Group 1 (96.8%) compared to Group 2 (91%) ($p=0.037$). Kaplan–Meier survival curves are shown in Figures 1 and 2.

4. Discussion

In the management of early-stage EC, the choice of surgical approach is a critical determinant of both oncologic

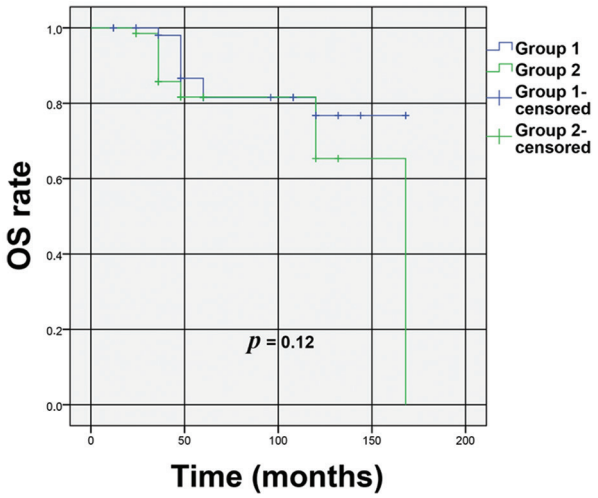


Figure 1. Kaplan–Meier curves for overall survival in Group 1 (Pfannenstiel incision) and Group 2 (Laparoscopy) patients with early-stage, low-grade endometrial cancer

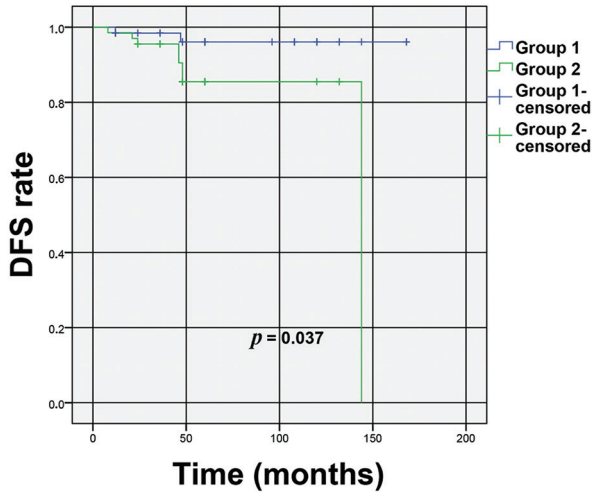


Figure 2. Kaplan–Meier curves for disease-free survival in Group 1 (Pfannenstiel incision) and Group 2 (laparoscopy) patients with early-stage, low-grade endometrial cancer

outcomes and postoperative quality of life. Traditionally, total abdominal hysterectomy with bilateral salpingo-oophorectomy and when indicated, pelvic and para-aortic lymphadenectomy have constituted the standard surgical treatment. While these procedures were historically performed through midline laparotomy, the evolution of minimally invasive surgery has led to the widespread adoption of laparoscopy and more recently, robotic-assisted techniques. Nevertheless, the potential benefits of low transverse abdominal incisions—particularly the Pfannenstiel approach—should not be overlooked, especially in selected patient populations. The Pfannenstiel incision is well-established in gynecologic surgery, offering favorable cosmetic outcomes, reduced postoperative pain, and a lower risk of wound complications when compared to vertical midline incisions. Several studies have highlighted that this approach can provide sufficient access to the pelvic cavity while minimizing trauma to the abdominal wall, potentially resulting in decreased rates of surgical site infection and incisional hernia, particularly in obese patients. Furthermore, the incision's location along natural skin folds contributes to improved patient satisfaction and faster return to daily activities.[22,23] Laparoscopy plays an important role in the surgical treatment of EC.[24] However, it may not be suitable for every patient. In some cases, laparotomy may be more advantageous than laparoscopy. We prefer laparotomy over laparoscopy in patients with vaginal stenosis, morbid obesity that precludes safe trocar placement, inability to insert a manipulator, a history of multiple abdominal surgeries, a larger-than-normal uterus, or suspicious adhesions on pelvic examination. We believe that the Pfannenstiel incision is a safer alternative for these patients, especially to avoid the complications associated with midline incision.

In 2009, peritoneal cytology was removed from the FIGO staging system.[25] While LVSI was added to the FIGO staging system in 2023, cytology remains excluded from staging.[26] A recent meta-analysis on the significance of positive peritoneal cytology in early-stage EC showed that it was associated with inferior DFS and OS.[27] On the contrary, Takenaka *et al.*[28] stated that peritoneal cytology status was not a prognostic factor in the low-risk early-stage ECs. In addition, during the insertion and use of the manipulator in laparoscopic surgery, there are hypotheses that the manipulator may weaken the myometrium, lead to uterine rupture, and facilitate tumor cell dissemination into the peritoneal cavity.[29] A secondary hypothesis suggests that the uterine manipulator may create significant tension within the endometrial cavity, increasing intrauterine pressure and promoting tumor cell translocation through the fallopian tubes into the peritoneal cavity.[30] To mitigate this risk in laparoscopic EC surgeries, we routinely seal the fallopian tubes with bipolar energy before hysterectomy. In our study, we found no difference in peritoneal cytology positivity between the two groups.

Currently, the landscape of surgical nodule evaluation for EC is shifting from lymphadenectomy to SLN biopsy, with no evidence of a negative impact on cancer-specific survival.[31] In EC patients, SLN bilateral mapping fails in 20 – 25% of cases.[32] The assessment of lymph node status remains a critical component in the surgical staging of EC, significantly influencing prognosis and adjuvant treatment decisions. Traditionally, systematic pelvic and para-aortic

lymphadenectomy have been employed for this purpose. However, this approach is associated with considerable morbidity, including prolonged operative time, increased blood loss, lymphocele formation, and lower extremity lymphedema. In recent years, SLN biopsy has emerged as a less invasive alternative that offers accurate staging with reduced surgical risk. Several studies have demonstrated that SLN mapping in EC provides high sensitivity and negative predictive value for the detection of nodal metastasis.[33] Cervical injection of indocyanine green followed by near-infrared fluorescence imaging has become the preferred technique due to its superior detection capabilities and safety profile. One of the key advantages of the SLN approach is the opportunity for ultrastaging, which enhances the detection of micrometastases and isolated tumor cells that might be missed by routine pathological evaluation. This is particularly important in patients with clinically early-stage disease, where even low-volume nodal metastasis may alter the risk stratification and subsequent treatment plan. Moreover, in patients with negative SLNs, systematic lymphadenectomy can often be safely omitted, thereby minimizing surgical complications without compromising oncologic outcomes. Despite its advantages, SLN mapping is not without limitations. Its success is highly dependent on surgeon expertise, institutional experience, and patient factors such as obesity or prior pelvic surgeries, which can interfere with lymphatic drainage and reduce mapping efficacy. In addition, the reliability of SLN biopsy in high-risk histologic subtypes (e.g., serous or clear cell carcinoma) or in cases with grossly enlarged lymph nodes remains controversial. Some guidelines still recommend comprehensive lymphadenectomy in these populations due to a higher prevalence of nodal metastasis.

SLN biopsy represents a significant advancement in the surgical management of EC.[34] It offers an accurate, minimally invasive alternative to full lymphadenectomy, particularly in patients with low to intermediate risk disease. When performed in accordance with validated protocols and applied to appropriately selected patients, it provides accurate staging and minimizes surgical morbidity. However, the availability of technology and expertise remains a barrier in some institutions. In our center, due to the lack of equipment for SLN sampling, we performed selective lymph node removal of bulky nodes during surgery to achieve surgical staging while minimizing the risk of lymphedema. In our study, we did not observe any significant difference in the number of resected lymph nodes between patients undergoing surgery via Pfannenstiel incision versus laparoscopy.

Although the number of patients with recurrence was higher in the laparoscopy group, no significant difference was found between the two groups. In our study, port site metastasis was detected in only one patient after laparoscopic surgery. These metastases are rare, with an estimated incidence of <1% in cases of early-stage EC.[35] While no vaginal cuff recurrence was observed in patients who underwent surgery with a Pfannenstiel incision, it was observed in a patient who underwent laparoscopic surgery. This may be attributable to the use of a uterine manipulator in laparoscopic procedures. Similar concerns were raised in the phase III LACC trial, where minimally invasive radical hysterectomy in cervical cancer was associated with significantly lower OS and DFS compared to open abdominal surgery.[36] In our study, while no significant difference in OS was detected between the two groups, DFS was significantly better in patients treated with Pfannenstiel incision.

The OS rate for patients with EC is reported at approximately 85%.[37] The 5-year DFS and OS rates have been reported as 95.2% and 96.4%, respectively.[38] For stage I and stage II tumors, the 5-year survival rate is between 74% and 91%.[38] Stuart *et al.*[39] suggest that pelvic lymphadenectomy improves overall or recurrence-free survival in women with early EC. Furthermore, Alouini and Bakri[40] showed in their review that systematic para-aortic lymphadenectomy may not be necessary in early-stage genital malignancies. In our study, we found that performing only pelvic lymph node sampling—without para-aortic lymphadenectomy—yielded the OS and DFS consistent with the literature.

Recent studies also suggest that systemic inflammatory markers may serve as useful diagnostic and prognostic biomarkers. For example, Ronsini *et al.*[41] demonstrated how endometrial thickness, when combined with systemic inflammatory response (SIR) indices, may help distinguish between endometrial dysplasia and carcinoma in patients with postmenopausal bleeding. However, our study did not incorporate SIR data, which represents a limitation.

There is also a biological perspective on how systemic or metabolic factors may influence cancer progression and surgical outcomes. A recent systematic review highlights the role of trace elements such as selenium, zinc, copper, and cadmium in the pathogenesis and progression of various malignancies. The review suggests that imbalances in essential and toxic elements may contribute to oxidative stress, inflammation, and altered immune responses, potentially affecting both tumor biology and post-operative recovery.[42] Unfortunately, our study did not evaluate these parameters, which may also be considered a limitation.

This study has several additional limitations. First, due to its retrospective design, the selection of surgical approach was based on clinical judgment and individual patient characteristics rather than a standardized

protocol, introducing potential selection bias. Second, it was conducted at a single institution, which may limit the generalizability of the findings. Third, while the sample size was reasonable for an observational study, it may not be sufficient to detect subtle differences in long-term outcomes such as recurrence and survival. In addition, data regarding inflammatory markers, postoperative complications, and quality-of-life measures were not available, which restricted a more comprehensive assessment of patient outcomes. Finally, variations in surgical technique over the extended study period may have affected outcome consistency.

Nonetheless, our study has notable strengths. It brings renewed attention to the Pfannenstiel incision—a technique often overlooked in recent discussions dominated by minimally invasive methods. Our findings suggest that this approach remains clinically relevant, particularly for patients who are not ideal candidates for laparoscopy. In terms of recurrence and survival outcomes, the Pfannenstiel incision offers a viable, and in some cases, superior alternative. Taken together, we emphasize the underappreciated value of the Pfannenstiel incision in the surgical treatment of early-stage EC.

We hope our findings contribute meaningfully to the literature and encourage further research into this surgical approach, particularly for patient populations in whom laparoscopy is not feasible or safe.

5. Conclusion

The Pfannenstiel incision is an important surgical approach used in gynecology. We aimed to emphasize the importance of staging surgery with the Pfannenstiel incision in early-stage EC patients with vaginal stenosis, morbid obesity not suitable for trocar insertion, a history of multiple abdominal surgeries, inability to insert a manipulator, an enlarged uterus, or suspected adhesions on pelvic examination. It has been used in surgeries for many years, and its importance has recently been overshadowed by the rise of laparoscopy. However, our study highlights that it remains a valuable option and should not be overlooked.

Acknowledgments

We would like to thank Saygin Alkan for editing the table and the figures.

Funding

None.

Conflict of interest

The authors declare no competing interests.

Author contributions

Conceptualization: Cem Yagmur Ozdemir, Nayif Çicekli
Data curation: Cem Yagmur Ozdemir, Derya Yeğin Aksu
Formal analysis: Cem Yagmur Ozdemir, Derya Yeğin Aksu
Investigation: Hasan Eroğlu, Necat Cağatay Sezer
Supervision: Hasan Eroğlu, Dağıstan Tolga Arioz
Writing – original draft: Cem Yagmur Ozdemir, Necat Cağatay Sezer
Writing – review & editing: Nayif Çicekli, Derya Yeğin Aksu

Ethics approval and consent to participate

The present study was approved by the Ethical Committee of Afyonkarahisar Health Sciences University Hospital (approval no: 13.12.2024 – 2024/11) and conducted in accordance with the Declaration of Helsinki. Informed consent was obtained from all patients during their hospitalization.

Consent for publication

Informed consent was obtained from all individual participants included in the study.

Availability of data

Data are available from the corresponding author upon reasonable request.

References

1. Crosbie EJ, Kitson SJ, McAlpine JN, Mukhopadhyay A, Powell ME, Singh N. Endometrial cancer. *Lancet*. 2022;399(10333):1412-1428.

   doi: 10.1016/S0140-6736(22)00323-3

2. Kalampokas E, Giannis G, Kalampokas T, *et al*. Current approaches to the management of patients with endometrial cancer. *Cancers (Basel)*. 2022;14(18):4500.

   doi: 10.3390/cancers14184500

3. Bilir F, Arıoz DT, Arıkan SE, *et al*. Relationship between molecular markers and lymphadenectomy and lymphovascular space invasion in endometrial cancer. *Arch Gynecol Obstet*. 2023;308(3):941-946.

   doi: 10.1007/s00404-023-07005-9

4. Natarajan P, Delanerolle G, Dobson L, *et al*. Surgical treatment for endometrial cancer, hysterectomy performed via minimally invasive routes compared with open surgery: A systematic review and network meta-analysis. *Cancers (Basel)*. 2024;16(10):1860.

   doi: 10.3390/cancers16101860

5. Patel N, Chaudhari K, Jyotsna G, Joshi JS. Surgical frontiers: A comparative review of robotics versus laparoscopy in gynecological interventions. *Cureus*. 2023;15(11):e49752.

doi: 10.7759/cureus.49752

6. Giannini A, D'Oria O, Vizza E, *et al*. Robotic-assisted, laparoscopic, and vaginal hysterectomy in morbidly obese patients with endometrial hyperplasia and endometrial cancer. *Minim Invasive Ther Allied Technol*. 2024;33:358-364.

   doi: 10.1080/13645706.2024.2407845

7. Montgomery A, Van Eeden L, Boo M, *et al*. Does closed incision negative pressure wound therapy reduce surgical site infection in endometrial carcinoma patients undergoing laparotomy? A multicentre retrospective cohort study. *Clin Exp Obstet Gynecol*. 2023;50(5):102.

   doi: 10.31083/j.ceog5005102

8. Al-Majali J, Qasem M, Al-Ani A, *et al*. 635 transverse versus midline abdominopelvic incisions: A systematic review. *Int J Gynecol Cancer*. 2021;31(Suppl 3):A36-A36.

   doi: 10.1136/ijgc-2021-ESGO.52

9. Ayhan A, Dursun P, Gultekin M, Esin S. Pfannenstiel vs. Midline incision for early stage endometrial carcinoma. *Int J Gynecol Obstet*. 2006;93(1):67-69.

   doi: 10.1016/j.ijgo.2005.12.029

10. Rady HA, Mohammed NE, Ragab MH. Lower midline versus pfannenstiel incision in pelvic lymphadenectomy in endometrial cancer. *Indian J Gynecol Oncol*. 2019;17:36.

11. Tzenios N, Chahine M, Tazanios M. Obesity and endometrial cancer: The role insulin resistance and adipokines. *Special J Med Acad Other Life Sci*. 2023;1(2).

    doi: 10.58676/sjmas.v1i2.12

12. Skolnik E, Miazga E, Zakhari A, Cai E, Ziegler C, Murji A. Beyond the pfannenstiel: Minimally invasive laparotomy incisions for maximum exposure. *J Obstet Gynaecol Can*. 2021;43(3):368.

    doi: 10.1016/j.jogc.2020.10.013

13. Vaezi M, Zarei R, Azizi H. Comparison of maylard and cherney incisions' outcomes in hysterectomy surgery for benign indications: A double-blind randomized controlled trial. *Eur J Med Res*. 2025;30(1):56.

    doi: 10.1186/s40001-025-02311-1

14. Güven E, Dura MC, Aktürk H, Güraslan H. Safety of laparoscopic entry points in patients with a history of abdominal surgery: A research article. *Cureus*. 2023;15(10):e47244.

    doi: 10.7759/cureus.47244

15. Matsuo K, Sood AK, Gershenson DM. Management of early-stage ovarian cancer. In: *Surgery for Ovarian Cancer*. United States: CRC Press; 2022. p. 60-92.

16. Polen-De C, Bakkum-Gamez J, Langstraat C. Route of hysterectomy for benign disease: Abdominal hysterectomy. *J Gynecol Surg*. 2021;37(2):116-121.

    doi: 10.1089/gyn.2021.0002

17. Abdelazim I, AbuFaza M. Pfannenstiel incision for surgical excision of a huge pelvi-abdominal cystadenoma: A case report. *Prz Menopauzalny*. 2021;20(2):99-102.

    doi: 10.5114/pm.2021.106469

18. Habib AS, Wahl K, Gu J, Gan TJ, Adenosine Study Group. Comparison of postoperative pain outcomes after vertical or Pfannenstiel incision for major gynecologic surgery. *Curr Med Res Opin*. 2009;25(6):1529-1534.

    doi: 10.1185/03007990902959168

19. Lewin SN, Herzog TJ, Medel NI, *et al*. Comparative performance of the 2009 international federation of gynecology and obstetrics' staging system for uterine corpus cancer. *Obstet Gynecol*. 2010;116(5):1141-1149.

    doi: 10.1097/AOG.0b013e3181f39849

20. Bogani G, Ray-Coquard I, Concin N, *et al*. Clear cell carcinoma of the endometrium. *Gynecol Oncol*. 2022;164(3):658-666.

    doi: 10.1016/j.ygyno.2022.01.012

21. Hasson HM. A modified instrument and method for laparoscopy. *Am J Obstet Gynecol*. 1971;110:886-887.

    doi: 10.1016/0002-9378(71)90593-x

22. Fathi A, Saleh MM, Shetiwy M, *et al*. Operative outcomes of single-incision laparoscopic hysterectomy vs conventional laparoscopic total hysterectomy: A prospective randomized controlled study. *Surg Innov*. 2022;29(5):590-599.

    doi: 10.1177/15533506211041892

23. McCurdy RJ, Harding S, Felder L, Beáta A, Schnatz P, Berghella V. Cohen vs Pfannenstiel cesarean skin incision for body mass index ≥35 kg/m^2: A randomized controlled trial. *Am J Obstet Gynecol MFM*. 2024;6(12):101528.

    doi: 10.1016/j.ajogmf.2024.101528

24. Januszek SM, Wita-Popow B, Kluz M, *et al*. Risk factors for surgical treatment of endometrial cancer using traditional and laparoscopic methods. *J Clin Med*. 2021;10(3):429.

    doi: 10.3390/jcm10030429

25. Pecorelli S. Revised FIGO staging for carcinoma of the vulva, cervix, and endometrium. *Int J Gynaecol Obstet*. 2009;105:103-104.

    doi: 10.1016/j.ijgo.2009.02.012

26. Berek JS, Matias-Guiu X, Creutzberg C, *et al*. FIGO staging of endometrial cancer: 2023. *Int J Gynecol Obstet*. 2023;162(2):383-394.

    doi: 10.1002/ijgo.14923

27. Pergialiotis V, Panagiotopoulos M, Koutras A, *et al*. The impact of positive peritoneal cytology on the survival rates of early-stage-disease endometrial cancer patients: Systematic review and meta-analysis. *Medicina*. 2024;60(5):733.

doi: 10.3390/medicina60050733

28. Takenaka M, Kamii M, Iida Y, *et al*. Re-thinking the prognostic significance of positive peritoneal cytology in endometrial cancer. *Gynecol Oncol.* 2021;161(1):135-142.

doi: 10.1016/j.ygyno.2021.01.007

29. Padilla-Iserte P, Lago V, Tauste C, *et al*. Impact of uterine manipulator on oncological outcome in endometrial cancer surgery. *Am J Obstet Gynecol.* 2021;224:65-e1.e11.

doi: 10.1016/j.ajog.2020.07.025

30. Machida H, Hom MS, Adams CL, *et al*. Intrauterine manipulator use during minimally invasive hysterectomy and risk of lymphovascular space invasion in endometrial cancer. *Int J Gynecol Cancer*. 2018;28(2):208-219.

doi: 10.1097/IGC.0000000000001181

31. Matsuo K, Klar M, Nusbaum DJ, *et al*. Utilization and outcomes of sentinel lymph node biopsy for early endometrial cancer. *Obstet Gynecol.* 2022;139(5):809-820.

doi: 10.1097/AOG.0000000000004733

32. Raffone A, Fanfani F, Raimondo D, *et al*. Predictive factors of sentinel lymph node failed mapping in endometrial carcinoma patients: A systematic review and meta-analysis. *Int J Gynecol Cancer*. 2023;33(6):853-859.

doi: 10.1136/ijgc-2022-004014

33. Baiocchi G, Andrade CEMC, Ribeiro R, *et al*. Sentinel lymph node mapping versus sentinel lymph node mapping with systematic lymphadenectomy in endometrial cancer: An open-label, non-inferiority, randomized trial (ALICE trial). *Int J Gynecol Cancer*. 2022;32(5):676-679.

doi: 10.1136/ijgc-2022-003378

34. Zammarrelli WA 3rd., Afonso AM, Broach V, *et al*. Sentinel lymph node biopsy in patients with endometrial cancer and an indocyanine green or iodinated contrast reaction-a proposed management algorithm. *Gynecol Oncol.* 2021;162(2):262-267.

doi: 10.1016/j.ygyno.2021.05.009

35. Segarra B, Meyer LA, Malpica A, Bhosale P. Endometrial cancer recurrence at multiple port sites. *Int J Gynecol Cancer*. 2020;30(6):893-896.

doi: 10.1136/ijgc-2020-001327

36. Frumovitz M, Obermair A, Coleman RL, *et al*. Quality of life in patients with cervical cancer after open versus minimally invasive radical hysterectomy (LACC): A secondary outcome of a multicentre, randomised, open-label, phase 3, non-inferiority trial. *Lancet Oncol.* 2020;21(6):851-860.

doi: 10.1016/S1470-2045(20)30081-4

37. Gultekin M, Dundar S, Kucukyildiz I, *et al*. Survival of gynecological cancers in Turkey: Where are we at? *J Gynecol Oncol*. 2017;28(6):e85.

doi: 10.3802/jgo.2017.28.e85

38. Kurosu H, Todo Y, Yamada R, *et al*. A BMI-category distribution pattern of intrinsic and treatment-related prognostic factors in endometrial cancer. *Jpn J Clin Oncol.* 2021;51(5):722-727.

doi: 10.1093/jjco/hyaa274

39. Stuart GC, Kitchener H, Bacon M, *et al*. 2010 gynecologic cancer intergroup (GCIG) consensus statement on clinical trials in ovarian cancer: Report from the fourth ovarian cancer consensus conference. *Int J Gynecol Cancer*. 2011;21:750-755.

doi: 10.1097/IGC.0b013e31821b2568

40. Alouini S, Bakri Y. Para-aortic lymphadenectomy in ovarian, endometrial, gastric, and bladder cancers: A systematic review of randomized controlled trials. *Cancers (Basel)*. 2024;16(19):3394.

doi: 10.3390/cancers16193394

41. Ronsini C, Iavarone I, Vastarella MG, *et al*. SIR-EN-new biomarker for identifying patients at risk of endometrial carcinoma in abnormal uterine bleeding at menopause. *Cancers (Basel)*. 2024;16(21):3567.

doi: 10.3390/cancers16213567

42. Lubiński J, Lener MR, Marciniak W, *et al*. Serum essential elements and survival after cancer diagnosis. *Nutrients*. 2023;15(11):2611.

doi: 10.3390/nu15112611

ACCSCIENCE PUBLISHING

Eurasian Journal of Medicine and Oncology

ORIGINAL RESEARCH ARTICLE

Psychotherapists' perspectives on the quality of psychological services for cancer patients in Riyadh: A predictive study

Yahya Khatatbeh*

Department of Psychology, College of Social Sciences, Imam Mohammad Ibn Saud Islamic University (IMSIU), Riyadh, Saudi Arabia

(This article belongs to the *Special Issue: Nursing Care in Cancer*)

Abstract

Introduction: Psychological services play a vital role in supporting cancer patients, yet their quality is influenced by provider-related factors that remain underexplored.
Objective: The objective of this study was to predict the quality of psychological services provided to cancer patients in Riyadh from the perspective of psychotherapists and to assess the predictive value of key variables within the target group.
Methods: A questionnaire assessing communication skills scale and psychotherapist competence was completed by 329 psychotherapists.
Results: Our findings revealed that the highest mean score was observed for the empathy dimension (54.20), whereas respect and authenticity recorded the lowest mean score (19.28). The overall quality of psychological services had a mean score of 174.88 ± 9.53. Regarding the psychotherapist self-efficacy scale, clinical competence recorded the highest mean (20.41), whereas influence regulation had the lowest mean score (7.95). The total score for psychotherapist competence was 79.33. Predictive analysis revealed that the workplace and academic level of psychotherapists were statistically significant predictors of service quality ($p<0.05$). The independent variables accounted for 41% of the variance in psychotherapist competence and 16% of the variance in communication skills with patients, indicating an overall weak predictive relationship.
Conclusion: Clinical practice implications should be considered. The identified predictors—communication skills, workplace, and academic level—may guide future efforts to enhance therapeutic approaches. Focusing on improving empathy and emotional regulation could further strengthen the quality of psychological care for cancer patients. Further studies are encouraged to translate these findings into practical clinical strategies.

Keywords: Psychological services; Cancer patients; Riyadh; psychotherapists; Predictive study

***Corresponding author:**
Yahya Khatatbeh
(ymkatatbh@imamu.edu.sa)

Citation: Khatatbeh Y. Psychotherapists' perspectives on the quality of psychological services for cancer patients in Riyadh: A predictive study. *Eurasian J Med Oncol.* 2025;9(3):155-167. doi: 10.36922/EJMO025110054

Received: March 13, 2025

1st revised: April 19, 2025

2nd revised: April 29, 2025

Accepted: May 12, 2025

Published online: June 20, 2025

Copyright: © 2025 Author(s). This is an Open-Access article distributed under the terms of the Creative Commons Attribution License, permitting distribution, and reproduction in any medium, provided the original work is properly cited.

Publisher's Note: AccScience Publishing remains neutral with regard to jurisdictional claims in published maps and institutional affiliations.

1. Introduction

Cancer is among the leading causes of death worldwide, accounting for nearly 10 million deaths in 2020.[1] In Spain, 300,000 new cancer cases and more than 110,000 deaths were recorded in 2020.[2] Research indicates that 35 – 80% of cancer patients are in psychological distress, with 10 – 40% of patients experiencing anxiety and depression,[3]

necessitating high-quality psychological services to enhance their well-being and adherence to treatment.[4] The synergy between psychotherapist-patient communication and psychotherapist competence is also pivotal. One study found that interventions combining communication training (e.g., delivering bad news) with competency-building units (e.g., symptom management) resulted in 53% greater improvement in patient-reported outcomes standardized mean difference.[5] Another study reported that psychotherapist competence in relationships ($\alpha = 0.88$) and clarity of communication ($\alpha = 0.82$) together explained 68% of the variance in patient confidence ($R^2 = 0.68$), indicating a substantial effect.[6] The quality of psychological services for cancer patients on their emotional resilience, coping mechanisms, and quality of life reduces symptoms of anxiety and depression by about 30 – 50%. However, the variations in service delivery and accessibility, along with psychotherapists' feedback, can influence outcomes, necessitating predictive models to assess and improve service quality.[7] Studies have highlighted that factors, such as therapeutic alliance, intervention methods, and access to care, significantly affect the quality of service.[8] In a study examining web-based therapy for cancer patients, 65% of psychotherapists considered patient engagement and psychotherapist response as key indicators of quality of care.[9] In addition, psychological support contributed to a 40% improvement in the quality of life of cancer patients, with higher psychotherapist competence linked to better patient adaptation. Another study emphasized the importance of personalized psychosocial interventions, where patients receiving tailored treatment reported 30% higher satisfaction levels compared to those receiving general mental health support.[10] This highlights the need to explore key predictors of quality psychological services for cancer patients from the perspective of psychotherapists, aiming to strengthen mental health interventions in oncology care. Similarly, a review of 29 eligible articles—including 14 qualitative, 11 quantitative, and 4 mixed-method articles—identified multiple influencing factors on psychological service quality: patient-related factors, health professional factors, therapeutic relationships, treatment characteristics, organizational and systemic factors, and care models.[8] Psychotherapists play a crucial role in delivering integrated psychological care, encompassing assessment, diagnosis, therapeutic intervention, and ongoing psychological support. Their role is particularly important for patients with chronic diseases (e.g., cancer), who face complex psychological and emotional challenges. Through effective communication, professional empathy, and high self-efficacy in handling sensitive cases, psychotherapists contribute to significantly improving patients' quality of life. Evaluating the quality of psychological services provided in this context is necessary for identifying factors to enhance and advance professional performance in specialized psychiatric care. The PALLI-COM study, a randomized controlled trial on the effects of communication training for oncologists, aimed to improve early discussions about palliative care and end-of-life issues. The training consisted of two 90-min sessions. Results demonstrated significant improvements in communication skills, including emotional engagement, empathy, and addressing end-of-life topics. The study suggests that this brief training can be effectively integrated into routine oncology education to improve patient care.[11]

Recent reviews and studies have highlighted the importance of therapeutic alliance and effective communication between psychotherapists and cancer patients in improving psychiatric care. One study found that patients evaluated their relationship with psychotherapists positively, underscoring the importance of this bond.[12] Another survey identified core competencies for psychotherapists in palliative care, most notably the ability to coordinate care between disciplines.[13] In addition, research demonstrated that psychological interventions significantly improve the quality of life for cancer patients through diverse approaches.[14] Furthermore, a study on breast cancer care revealed that doctors who exhibit greater empathy promote better mental health outcomes in patients. These findings suggest that empathetic communication by healthcare providers is key to reducing patients' uncertainty about their diagnosis and treatment, positioning caregivers as key contributors to the psychological well-being of cancer patients.[15] Therapeutic alliance plays a pivotal role in the success of psychological interventions for cancer patients, accounting for up to 35% of the effectiveness of mindfulness-based cognitive therapy.[16] Psychotherapist competence and patient commitment to treatment affect treatment outcomes by 20 – 30%.[17] Recent studies indicate that machine learning models can assess psychotherapists' communication skills with over 80% accuracy in predicting psychotherapy outcomes.[18] Furthermore, psychotherapist competence has been reported to reduce psychological distress and improve well-being by 40%, whereas deviation from evidence-based therapeutic practices leads to a 15% reduction in treatment effectiveness.[19]

Telepsychology has demonstrated therapeutic outcomes comparable to face-to-face therapy, making it an effective tool in cancer care.[18] Psychotherapists' interpersonal communication skills are associated with greater patient resilience and increased treatment adherence, reducing dropout rates by 20%.[17] The therapeutic relationship is one of the strongest predictors of therapeutic success, accounting for up to 50% of treatment outcomes.[20] In

addition, social support and communication effectiveness account for 45% of the variation in patients' well-being scores.[21]

Evidence-based psychological training programs improve psychotherapist competence and patient satisfaction by 30%.[22] Group therapy models have been reported to reduce psychological distress by 25%.[23] Training caregivers in psychological resilience and empathy further enhances mental health and reduces anxiety by 30%.[24] In addition, non-verbal communication skills contribute to a 20% increase in treatment effectiveness.[25] Artificial intelligence-powered supervision emerges as an effective tool to improve psychotherapist performance and reduce bias in treatment outcomes.[19] Mindfulness-based interventions integrated with psychotherapy significantly improve the therapeutic relationship and reduce patient stress.[26] Mindfulness has also demonstrated protective effects for at-risk groups, such as individuals with diabetes and hypertension, by enhancing emotional regulation and reducing stress. Diabetes affects about 1 in 11 adults worldwide, with a rising prevalence—from 529 million patients in 2021 to approximately 1.31 billion in 2050. In Italy, 5.9% of the population is diabetic, with a higher prevalence among older adults and those in southern regions. Practices such as yoga and mindfulness may provide valuable support for diabetic patients, especially in a stressful context such as the COVID-19 pandemic.[27]

Despite the growing interest in psychiatric oncology, there remains a significant gap in the scientific literature regarding the indicators of psychological service quality for cancer patients from the perspective of psychotherapists. Recent studies tend to focus on patient outcomes, treatment satisfaction, or the challenges faced by patients during treatment while often overlooking the insights and experiences of psychotherapists themselves. In addition, studies tend to integrate psychological, organizational, and interactive factors that may affect service quality and hinder the development of comprehensive, evidence-based models essential for guiding trainees and practitioners and improving policies in cancer care settings. Understanding these perspectives is critical to identifying care gaps, ensuring the consistency of treatment approaches, and promoting patient-centered practices that address emotional, cognitive, and behavioral needs during cancer treatment. Key service quality predictors—such as psychotherapist competence, patient engagement, and institutional support—are vital for enhancing training programs and informing policy decisions aimed at improving patient outcomes.[28] In addition, highlights the importance of integrating psychological expertise into multidisciplinary oncology teams while emphasizing the importance of mental health in comprehensive oncology care.[29]

Despite the growing recognition of the psychological burden facing cancer patients and the increasing role of psychiatric services in oncology, most current studies have focused primarily on patient experiences and outcomes. In contrast, limited attention has been given to the perspectives of mental health professionals providing these services[30] Moreover, there is a notable lack of empirical research examining predictors of psychological service quality, particularly within Arab or Middle Eastern contexts. This gap is significant, as structural, cultural, and institutional factors may differ significantly from Western healthcare models.

This gap highlights the need for research that explores the quality of services from the perspective of psychotherapists directly involved in caregiving. Addressing this gap is critical for informing policy development, enhancing vocational training, and improving mental health interventions in oncology care. Accordingly, this study aims to explore how key provider-related variables—such as communication skills and psychotherapist effectiveness—affect the quality of psychological services provided to cancer patients in Riyadh. The main objectives are to:

(i) Assess the quality of psychological services provided to cancer patients from the perspective of psychotherapists;
(ii) Identify key factors that predict the quality of these services;
(iii) Analyze the availability of human and material resources affecting the quality of psychological services; and
(iv) Examine the impact of the professional experience and training on the psychotherapists' assessments of the quality of psychological services.

Specifically, the study investigates the relationship between psychotherapists' communication skills, self-perceived clinical effectiveness, and their assessment of service quality. Based on the literature and the theoretical framework, the following hypotheses were formulated:

(i) There are statistically significant differences in the mean scores and standard deviations of participants' responses on the Psychotherapist's Communication Skills Scale (CSS).
(ii) There are statistically significant differences in the mean scores and standard deviations of participants' responses on the Psychotherapist's Self-Efficacy Scale.
(iii) Professional experience, specialization, age, academic level, and workplace significantly predict the quality of psychological services provided to cancer patients, as reflected in the psychotherapist's competence and communication skills.

2. Materials and methods

2.1. Study design

The present study used a descriptive (comparative) approach to assess the quality of psychological services provided to cancer patients from the perspective of psychotherapists. Their opinions were gathered using two standardized tools: the Psychotherapist's CSS and the Psychotherapist's Self-Efficacy Scale. The study aimed to predict the quality of these services based on psychotherapists' assessments and to determine the levels of these variables within the target group, without the need for long-term tracking that could delay timely data collection.

The reporting of this predictive study adhered to transparent reporting of a multivariable prediction model for individual prognosis or diagnosis (TRIPOD) guidelines to ensure clarity, transparency, and completeness in presenting the study methods and findings.[31]

The study sample consisted of licensed psychotherapists working in various psychiatric service centers, including mental health clinics, psychological counseling centers, and hospitals that provide psychiatric care to individuals with chronic diseases, especially cancer patients. The participants were mainly selected from a group of graduate students enrolled in a graduate psychology program at a Saudi university, most of whom were practicing in relevant clinical or consulting settings. This group was selected based on their direct involvement with providing psychological services to patient groups with chronic diseases, including cancer. A random sample of qualified psychotherapists was invited to participate in the study through an online questionnaire distributed via Google Forms. Before starting the questionnaire, participants were given a clear explanation of the study objectives and the variables assessed. The questionnaire consisted of closed questions with clear answer options to ensure clarity and ease of understanding. The questionnaire was logically divided into sections, starting with demographic information, followed by measures assessing professional communication skills and self-therapist competence. A total of 381 responses were collected; however, only 329 responses were included in the final analysis after excluding incomplete entries. The participants met the following inclusion criteria: (i) agreement to participate in the study, (ii) specialization in psychological sciences and provision of psychological services at the centers involved in the study, and (iii) reading and understanding the study objectives and instructions before completing the questionnaire.

This study was conducted in accordance with ethical standards regulating human research. Before data collection, ethical approval was obtained from the Scientific Ethics Committee at the university (approval no. 16/53253) on July 17, 2024. Informed consent was obtained electronically before participants accessed the questionnaire. No identifying information was collected, and the data was used solely for academic research purposes.

2.2. Study tools

The main variables of the study were derived from the participants' responses on two standardized tools: the Psychotherapist's CSS and the Psychotherapist's Self-Efficacy Scale. Each scale consists of multiple subdimensions, with scores calculated as the average of responses for the items in each subdimension. Reverse-coded items were adjusted before calculation to ensure consistent response orientation. The mean value was used instead of the total, as the number of items varied between dimensions. Variables were treated as continuous, enabling appropriate statistical analyses such as regression. This approach preserved the original structure of the scales and ensured an accurate representation of the study concepts. To ensure the validity of the study tools and their proper use in the local context, the initial version of the questionnaire was presented to five experts in clinical psychology, measurement, and educational evaluation to assess the relevance, clarity, and cultural and linguistic appropriateness of the items. Based on their feedback, necessary adjustments were made to the language and style to enhance clarity and participant comprehension. The study tools were then tested on a pilot sample of 30 participants from the same study population; their data were excluded from the final analysis. This step ensured the questionnaire was clear, unambiguous, and not repetitive while also assessing initial psychometric properties.

The questionnaire begins by collecting basic information about the participant, including gender, workplace, specialization, years of professional experience, and academic level. The questionnaire proceeded with evaluating the communication skills and self-efficacy of the participants, structured into three main sections: (1) Demographic information, which includes gender, workplace, specialization, years of professional experience, and academic level; (2) the Health Professionals (HP) CSS, assessing four subdimensions—Informative Communication, Empathy, Respect and Authenticity, and Social Skills; and (3) the therapist self-efficacy scale (T-SES) includes six core dimensions: communicative effectiveness, clinical competence, intrapsychic competence, relational competence, affect regulation, and diagnostic skills. The questionnaire proceeded with evaluating the communication skills and self-efficacy of the participants.

2.2.1. Psychotherapist's CSS

A section of the questionnaire was developed based on the scale previously described,[32] consisting of 42 elements, with half of them worded in reverse. The scale uses six response options with linguistic indicators: 1 (never/kind of); 2 (occasionally); 3 (sometimes); 4 (usually); 5 (a lot); and 6 (many times). The complete CSS (HP-CSS), including all 42 items has been provided in the appendix section. The scale consists of four basic dimensions: (i) media communication, comprising 12 elements (3, 6, 11, 13, 16, 18, 20, 27, 30, 38, 39, and 42) that reflect the way healthcare professionals obtain and present information within their clinical interactions with patients; (ii) empathy, comprising 13 items (4, 5, 12, 14, 17, 21, 22, 23, 28, 29, 36, 37, and 41) that reflect the ability of healthcare professionals to understand patients' feelings and demonstrate empathy through behaviors such as active listening and empathetic responses; (iii) respect and authenticity, with five items (2, 10, 26, 33, and 34) that assess the respect, authenticity, and conformity displayed by healthcare professionals in their clinical interactions with patients; and (iv) social skills, with 12 items (1, 7, 8, 9, 15, 19, 24, 25, 31, 32, 35, and 40) that reflect the ability of health professionals to be assertive or demonstrate skilled social behaviors in their clinical interactions with patients. The validity and reliability of the scale were thoroughly assessed, where the comparative compatibility index (CFI) was calculated to be 0.95, reflecting a high level of internal consistency. An exploratory factor analysis (EFA) was conducted to verify the general structure of the scale, yielding a Kaiser–Meyer–Olkin (KMO) value of 0.89, indicating sample adequacy for factor analysis. Bartlett's test of sphericity revealed statistical significance (Chi-square [χ^2] = 4156.23; Degrees of freedom [df] = 861; p<0.001), confirming data suitability for factor analysis. Confirmatory factor analysis (CFA) demonstrated good fit indices (CFI = 0.95; Tucker–Lewis index [TLI] = 0.94; and root mean square error of approximation [RMSEA] = 0.05), indicating strong structural validity. Cronbach's alpha coefficients demonstrated high internal consistency across dimensions: Media communication (α = 0.84), empathy (α = 0.87), respect and authenticity (α = 0.80), social skills (α = 0.86), and overall scale reliability (α = 0.88).

2.2.2. Psychotherapist's self-efficacy scale

Another part of the questionnaire was developed based on the scale previously described[33] to assess the professional self-efficacy of a psychotherapist. The scale consists of 21 elements and six dimensions: (i) communicative effectiveness, (ii) clinical competence, (iii) psychological competence, (iv) relational competence, (v) influence regulation, and (vi) diagnostic skills. The scale demonstrates a clear single-factor structure, effectively measuring the self-efficacy of the psychotherapist, as confirmed by both exploratory and confirmatory factor analyses. The overall scale structure was verified through EFA, yielding a KMO value of 0.91. In addition, Bartlett's test indicated statistical significance (χ^2 = 2941.67; df = 210; p<0.001). CFA also revealed high model quality indicators (CFI = 0.96; TLI = 0.95; RMSEA = 0.04), emphasizing a strong single-factor structure of the scale. In terms of stability, Cronbach's alpha coefficients for the scale ranged between 0.83 and 0.89: communicative effectiveness (α = 0.85), clinical competence (α = 0.88), psychological competence (α = 0.86), relational competence (α = 0.89), influence regulation (α = 0.83), and diagnostic skills (α = 0.87), with overall scale reliability of α = 0.92; this suggests high reliability and accuracy of the scale.

2.3. Statistical analysis

The study data were analyzed using the statistical analysis software Statistical Package for the Social Sciences version 27. The analysis began by assessing data distribution, revealing deviations from normality in some variables, which necessitated the use of nonparametric tests. Descriptive statistics (mean, standard deviations, frequencies, and percentages) were computed for all study variables and demographic data. Scale scores are presented as mean ± standard deviation. Spearman's rho correlation test was used to examine the relationship between the underlying variables, and multiple regression analysis assessed the extent to which communication skills and self-efficacy predicted the quality of psychological services. The analyses were directly linked to the three hypotheses of the study, using a statistical significance level of $\alpha \leq 0.05$. In addition, analysis of variance (ANOVA) was used to test for statistically significant differences in mean scores across groups based on demographic characteristics (e.g., workplace, academic level). The assumptions for ANOVA—independence of observations, homogeneity of variances (Levene's test), and approximately normally distributed residuals—were assessed before interpretation. Furthermore, various analytical models were applied depending on the nature of each hypothesis: correlational models for relational hypotheses, regression models for predictive hypotheses, and group comparison models (e.g., ANOVA) for testing differences across categorical variables. All analyses were conducted using a statistical significance threshold of $\alpha \leq 0.05$.

3. Results

The characteristics of the study participants are displayed in Table 1. The study sample was relatively balanced between genders, with 161 (48.9%) male participants and 168 (51.1%) female participants. The workplace of the

Table 1. Characteristics of study participants

Characteristic	Frequency	Percentage
Gender		
Male	161	48.9
Female	168	51.1
Workplace		
Psychiatric clinic	131	39.8
Hospital	106	32.2
School and rehabilitation centers	92	28.0
Specialization		
Clinical psychology	178	54.1
Psychological counseling	75	22.8
Mental health	76	23.1
Experience		
<5 years	164	49.8
5 – 10 years	69	21.0
More than 10 years	96	29.2
Academic degree		
Bachelor	207	62.9
Postgraduate	122	37.1

Table 2. Participants' communication skills scale scores across different dimensions

Dimension	Score
Media communication	47.5745±6.96078
Empathy	54.1976±5.41907
Respect and authenticity	19.2827±1.75540
Social skills	53.8207±3.46429
Total	174.8754±9.53202

Note: Scores are presented as mean±standard deviation.

Table 3. Participants' self-efficacy scale scores across different dimensions

Dimension	Score
Relational competence	14.0304±3.13015
Communicative effectiveness	16.2340±3.49345
Psychological competence	12.5046±1.97565
Clinical competence	20.4073±2.27488
Influence regulation	7.9514±0.94872
Diagnostic skills	8.2036±2.28286
Total	79.3313±6.24082

Note: Scores are presented as mean±standard deviation.

participants varied as follows: 131 (39.8%) participants worked in psychiatric clinics, 106 (32.2%) in hospitals, and 92 (28.0%) in schools and rehabilitation centers. The distribution of participants according to their specializations is as follows: 178 (54.1%) participants specialized in clinical psychology, 75 (22.8%) in psychological counseling, and 76 (23.1%) in mental health. Among them, 164 (49.8%) participants had <5 years of experience, 69 (21.0%) had 5 – 10 years of experience, and 96 (29.2%) had more than 10 years of experience. In addition, 207 participants received a bachelor's degree (62.9%), whereas 122 (37.1%) participants had a postgraduate degree.

From the CSS results (Table 2), the highest mean score was observed for empathy (54.1976 ± 5.41907), indicating that participants have a high level of ability to understand and respond to patients' emotions. The second highest mean score was social skills (53.8207 ± 3.46429), suggesting good interaction and positive relationships with patients. In contrast, respect and authenticity had the lowest mean score (19.2827 ± 1.75540), indicating consistent responses but also highlighting the need to strengthen this dimension. The overall score of the scale was 174.8754 ± 9.53202; this reflects a positive general assessment of communication skills, with a minor variation among the participants.

From the self-efficacy scale results (Table 3), the highest mean score was observed for clinical competence (20.4073 ± 2.27488), indicating that psychotherapists possess strong clinical skills; the standard deviation implies limited variations in participant response. The second highest mean score was obtained for communicative effectiveness (16.2340 ± 3.49345), thus reflecting the importance of effective communication for treatment success; the standard deviation implies a relative variation in this domain between psychotherapists. The lowest mean score was reported for diagnostic skills (8.2036 ± 2.28286), prompting further improvements compared to the other dimensions. The overall score of the self-efficacy scale was 79.3313 ± 6.24092, reflecting a good level of efficacy with some variation among the participants.

Table 4 evaluates the prediction of psychological service quality from the psychotherapists' perspectives. The TRIPOD checklist was also reviewed to verify that all essential components for predictive model reporting were adequately addressed in the presentation of results. Psychotherapist competence displayed a coefficient R of 0.126, which indicates a weak correlation, and a specific correlation coefficient, R2 of 0.016, which corroborates the observed variance between the dependent and independent variables. The high standard error (1.050) and F-statistic (1.382) confirmed that the model is weak. The low R^2-value (0.016) suggests that the independent variables have poor predictive ability, and the high *p*-value (0.388) indicates non-significance. Overall, the model (psychotherapist competence) is not applicable

Table 4. Predicting psychotherapists' perceptions of psychological service quality for cancer patients

Domains	Model summary		ANOVA			Regression					
	R	R^2	F	DF	Sig.	Independent variable	B	Standard error	β	*t*	*p*-value
Psychotherapist competence	0.126	0.016	1.050	5	0.388	(Constant)	79.476	2.164	-	36.724	<0.001
						Gender	0.981	0.717	0.079	1.369	0.172
						Workplace	−0.233	0.437	−0.031	−0.534	0.594
						Years of experience	−0.496	0.404	−0.069	−1.229	0.220
						Specialization	0.142	0.435	0.019	0.326	0.745
						Academic level	−392	0.734	−0.030	−0.534	0.594
Communication skills	0.202	0.041	2.738	5	0.019	(Constant)	177.534	3.264	-	54.397	<0.001
						Gender	0.583	1.081	0.031	0.539	0.590
						Workplace	−1.658	0.659	−142	−2.515	0.012
						Years of experience	0.834	0.609	0.076	1.369	0.172
						Specialization	0.780	0.657	0.067	1.187	236
						Academic level	−2.359	1.106	−120	−2.132	0.034

Note: (Constant) refers to intercept.
Abbreviations: R^2: Coefficient of determination; F: F-statistic; DF: Degrees of freedom; Sig.: Significance level (*p*-value), B: Unstandardized regression coefficient; ANOVA: Analysis of variance.

for predicting psychological service quality. In addition, the predictors are not statistically significant (all $p>0.05$); the predictors do not significantly affect the dependent variable. The low beta (β)-values indicate weak relationships between the predictors and the dependent variable. Similarly, communication skills displayed a coefficient R of 0.202, which indicates a weak correlation, and a specified correlation coefficient of 0.041, which corroborates the observed variance between the dependent and independent variables. The model also displayed a high standard error (1.050) and F-statistic (1.382). However, the influence of both workplace and academic level on communication skills was found to be statistically significant ($p<0.05$), indicating that these variables exert a measurable impact on the dependent variable. Specifically, the negative direction of the regression coefficients suggests an inverse relationship: As the professional setting becomes more specialized or demanding (e.g., transitioning from general to clinical environments), and as the academic qualification level rises, there is a corresponding decline in reported communication skills. This may reflect increased focus on technical or clinical competencies at the expense of interpersonal communication, particularly in environments where workload or institutional culture may deprioritize relational aspects of psychological service provision (Figure 1).

In the model predicting psychotherapist competence, gender (Variable 1) showed a statistically significant relationship with competence (B = 0.44, $p=0.02$), suggesting that gender plays a role in how competence is perceived or demonstrated. Educational Level (Variable 5) also showed a small but significant effect (β = 0.02, $p=0.02$), indicating that therapists with different academic qualifications may differ in their perceived competence. Meanwhile, the specialization of the specialist (Variable 4) and place of work (Variable 2) had weaker or non-significant contributions to the model, suggesting a limited or context-dependent influence.

On the right side of the figure, the model predicting patient communication skills reveals that place of work (Variable 2) and specialization of the specialist (Variable 4) had meaningful associations with communication ability. In particular, place of work was associated with a regression coefficient of B = 0.18 and a standardized β = 0.14, with $p<0.05$, indicating a statistically significant effect. This implies that the working environment of the psychotherapist may influence their ability to communicate effectively with patients. Other variables, such as gender and educational level, appeared in the model but did not reach statistical significance in predicting communication outcomes.

Each arrow in the figure is annotated with the unstandardized coefficient (B), the standardized coefficient (β), and the significance level (p), providing a concise visual summary of the regression analysis. These models help to clarify the distinct patterns of influence that background characteristics exert on both professional competence and

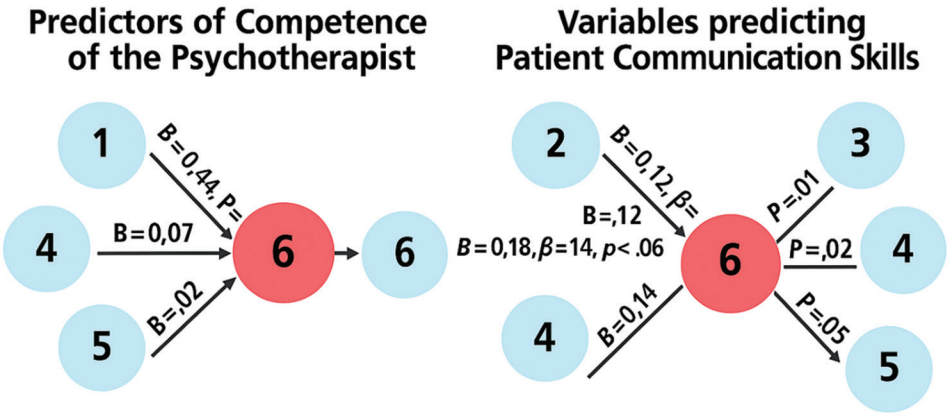


Figure 1. Nature of the prediction between independent and dependent variables. This figure presents two separate regression models. The left side illustrates the predictors of psychotherapist competence, while the right side shows the predictors of patient communication skills. Each red circle (labelled "6") represents the dependent variable in the respective model, and it is surrounded by five blue circles representing the independent variables: 1: Gender; 2: Place of work, 3: Number of years of experience; 4: Specialization of the specialist; 6: Educational level

patient-facing communication in psychological service settings.

4. Discussion

The results of the study reveal significant differences in the dimensions of the CSS, highlighting empathy as the most obvious trait, while respect and authenticity scored the lowest. Specifically, empathy had the highest mean score (54.1976), suggesting that patients view psychotherapists as highly empathetic—demonstrating the ability to understand their emotions, challenges, and perspectives. This aligns with previous studies emphasizing the critical role of empathy. Empathy has been shown to strengthen student-teacher relationships, enhance motivation and sense of belonging, and improve academic outcomes. For example, a systematic review highlighted that empathy in teaching is associated with better student engagement and educational results.[34] Conversely, the lower mean scores for respect and authenticity suggest potential areas for improvement in how psychotherapists express genuine respect and authenticity towards patients. Authenticity in educational interactions is critical to building trust and fostering a supportive learning environment. A study highlighted the complexities of cultivating both authenticity and empathy in educational contexts, noting that while these traits are frequently emphasized, they are often inadequately modeled or developed in practice.[35]

Regarding the dimensions of the psychotherapists' self-efficacy scale, the highest mean score was observed in the clinical competence dimension (20.4073), while the lowest mean score was recorded in the influence regulation dimension (7.9514). The overall mean score for the scale was 79.3313. These findings suggest that psychotherapists tend to prioritize structured and measurable skills (e.g., cognitive behavioral therapy techniques and knowledge of psychopharmacology) during both training and clinical practice. This emphasis likely reflects the influence of clinical guidelines and standardized protocols, which provide clear standards for performance. The strength in clinical efficiency indicates that psychotherapists are effectively integrating scientific and procedural knowledge in patient care.

The findings also reveal that psychotherapists show comparatively lower proficiency in managing emotional dynamics—both their own (e.g., countertransference, stress) and those of their patients (e.g., sadness, anger, anxiety). Emotional regulation skills tend to be more subjective and harder to quantify, which likely contributes to their limited emphasis on formal training. This includes insufficient focus on essential components such as mindfulness, self-reflection, and trauma-responsive care. In contrast, clinical competence received the highest mean score (20.41), indicating that psychotherapists demonstrate strong capabilities in clinical decision-making, diagnosis, and treatment planning. This aligns with existing literature that underscores the critical role of evidence-based interventions and technical expertise in delivering high-quality mental health care.[36] While a high degree of clinical efficacy reflects strong clinical competence, the lower scores in emotional regulation highlight a key development gap. These findings underscore the need for balanced training that integrates both technical proficiency and emotional competencies to improve the quality of treatment and the well-being of psychotherapists and patients.[20,37-39]

The analysis revealed that the workplace and academic level of the psychotherapist were statistically

significant predictors (p<0.05) of the perceived quality of psychological services provided to cancer patients. The overall model explained 41% of the variance in psychotherapist competence, suggesting a moderate level of predictability. However, the model accounted for only 16% of the variance in communication skills, indicating a weaker predictive relationship in this domain. This may suggest that the work environment and academic levels of psychotherapists affect both their competence and the quality of psychological care provided. While effective communication is necessary for high-quality care, it appears to be inadequate on its own. Other critical factors, such as emotional intelligence, professional experience, and institutional support, likely play an important role in psychological service effectiveness. Hence, further research is warranted to develop a comprehensive model of psychological care.

The results of the above study are consistent with a number of previous studies that confirmed the importance of psychotherapists' competence in the success of psychological interventions for cancer patients.[40] For example, it was reported that psychotherapist competence significantly enhances patient health, reducing psychological distress by 40%. Additionally, delivering effective, evidence-based care increases patient adherence and satisfaction by approximately 30%.[36] Similarly, the integration of deep learning-assisted psychotherapy enhanced psychotherapist competence and improved treatment outcomes by 20%.[41] Competent psychotherapists also contribute to enhancing emotional resilience in cancer patients receiving palliative care by 25%.[42] Moreover, high psychotherapist competence is associated with a 50% improvement in treatment success and emotional stability.[43] One of the expected contributions of this study is to improve the quality of psychological care by ensuring it is more efficient and responsive to patient needs. Our findings highlight the strengths and developmental needs of psychotherapists, offering valuable insights for training and professional development programs.

4.1. Strengths and limitations

One of the notable strengths of this study lies in its focus on the quality of psychological support for cancer patients, an important yet often neglected aspect of comprehensive cancer care. Through the opinions of psychotherapists, the study offers a realistic and professionally grounded assessment of the nature and quality of services provided. The findings provide valuable insights that can be used to develop training programs and improve work environments in health institutions. However, a key limitation of the study is its exclusive reliance on professionals' perspectives, which may overlook the lived experiences and satisfaction levels of patients themselves—a crucial element in evaluating service quality. Additionally, there is a possibility of positive self-assessment bias, where some practitioners may inadvertently rate the services they provide more favorably than is warranted, potentially affecting the objectivity and accuracy of the results.

This study is also characterized by several methodological aspects that enhance its reliability. Foremost among these is the use of standardized instruments with established psychometric validity and reliability, ensuring the rigor and consistency of the measurements. Moreover, the inclusion of a specialized sample of psychotherapists with direct experience in providing care to cancer patients lends the findings professional depth and contextual accuracy. The study also bridges a notable research gap in the Arab context by addressing the quality of psychological services from the perspective of their providers in a sensitive medical context. However, there are some limitations to consider. The study's reliance on self-reported data may introduce social desirability and response biases, potentially affecting the objectivity of the responses. Additionally, the cross-sectional design limits the ability to establish causal relationships between variables. Limiting the sample to specialists from a specific academic background may limit the generalization of results. Furthermore, the absence of patient perspectives limits the comprehensiveness of the evaluation.

4.2. Future implications and perspectives

The findings of this study offer several important directions for future practice and research. Institutions can utilize these results to enhance communication skills training and develop self-efficacy among mental health professionals working with cancer patients. This aligns with existing evidence that effective communication improves psychological outcomes and patient satisfaction.[5,11] Future research should explore patient perspectives directly, as the therapeutic alliance has been shown to significantly impact treatment outcomes.[12,20] Investigating the congruence between specialist evaluations and patient satisfaction could yield deeper insights into service quality. Additional predictive factors, such as emotional intelligence,[9] organizational support,[21] psychotherapists' years of service,[36] and psychological resilience,[24] warrant further evaluation to refine predictive models and improve clinical effectiveness. Moreover, longitudinal studies are needed to assess the sustained impact of psychotherapists' skills on long-term patient well-being, complementing recent findings on the durability of psychotherapy outcomes.[17] By grounding future research in these established areas, the psychological care provided to cancer patients can become more patient-centered, comprehensive, and evidence-based.

5. Conclusion

From our study's findings, empathy is the most important factor in providing high-quality psychological services to cancer patients, which confirms its vital role in fostering a strong therapeutic alliance and providing psychological support throughout the treatment. This underscores the need to prioritize the development of empathetic communication in clinical training, ensuring a more effective and humane treatment experience. In particular, the results highlight the importance of enhancing respect and authenticity in psychotherapist-patient interactions, suggesting targeted training programs should be designed to strengthen these dimensions of communication. Moreover, future research should explore additional variables that may further influence the quality of psychological services, including professional experience, emotional intelligence, and organizational support within treatment institutions. Investigating these factors can provide deeper scientific insights and inform the development of evidence-based strategies aimed at improving service delivery, psychotherapist performance, and ultimately, patient outcomes.

Acknowledgments

The author sincerely thanks all the participants who generously gave their time and shared their experiences for the purposes of this study. Their valuable contributions were essential to the completion of this research.

Funding

None.

Conflict of interest

The author declares no conflicts of interest.

Author contributions

This is a single-authored article.

Ethics approval and consent to participate

This study was reviewed and approved by the Research Ethics Committee of the university (approval no. 16/53253). Informed consent was obtained from all subjects involved in the study.

Consent for publication

Informed consent was obtained from all human participants involved in this study for the use of their data and. The consent was collected electronically through a Google Form, which clearly explained the purpose of the research, the voluntary nature of participation, and the measures taken to ensure confidentiality and data protection.

Availability of data

Raw data supporting this article is available from the author upon reasonable request.

References

1. Sung H, Ferlay J, Siegel RL, *et al*. Global cancer statistics 2020: GLOBOCAN estimates of incidence and mortality worldwide for 36 cancers in 185 countries. *CA Cancer J Clin*. 2021;71(3):209-249.

   doi: 10.3322/caac.21660.

2. Remon J, Reguart N, García-Campelo R, *et al*. Lung cancer in Spain. *J Thorac Oncol*. 2021;16(2):197-204.

   doi: 10.1016/j.jtho.2020.09.026

3. Bergerot C, Jacobsen PB, Rosa WE, *et al*. Global unmet psychosocial needs in cancer care: Health policy. *EClinicalMedicine*. 2024;78:102942.

   doi: 10.1016/j.eclinm.2024.102942

4. O'Hea EL, Monahan BR, Cutillo A, *et al*. Predictors of psychological distress and interest in mental health services in individuals with cancer. *J Health Psychol*. 2016;21(6): 1145-1156.

   doi: 10.1177/1359105314547752

5. Smith AD. *Improving Therapeutic Communication Skills Through an End-of-Life Simulation*. Massachusetts: Regis College; 2023.

6. Ridley PE. *Discovering Counseling Methods that Military Chaplains can Use to Increase Spiritual Resilience*. [*Doctoral Thesis, Bethel University*]. Spark Repository; 2020.

7. Schellekens MPJ, Wolvers MDJ, Schroevers MJ, Bootsma TI, Cramer AOJ, van der Lee ML. Exploring the interconnectedness of fatigue, depression, anxiety and potential risk and protective factors in cancer patients: A network approach. *J Behav Med*. 2020;43:553-563.

   doi: 10.1007/s10865-019-00084-7

8. Davies F, Shepherd HL, Beatty L, Clark B, Butow P, Shaw J. Implementing web-based therapy in routine mental health care: Systematic review of health professionals' perspectives. *J Med Intern Res*. 2020;22(7):e17362.

   doi: 10.2196/17362

9. Ruiz-Rodríguez I, Hombrados-Mendieta I, Melguizo-Garín A, Martos-Méndez MJ. The importance of social support, optimism and resilience on the quality of life of cancer patients. *Front Psychol*. 2022;13:833176.

   doi: 10.3389/fpsyg.2022.833176

10. Koutsouleris N, Hauser TU, Skvortsova V, De Choudhury M. From promise to practice: Towards the realisation of AI-informed mental health care. *Lancet Digit Health*. 2022;4:e829-40.

    doi: 10.1016/S2589-7500(22)00153-4

11. Harnischfeger N, Rath HM, Alt-Epping B, *et al*. Effects of a communication training for oncologists on early addressing palliative and end-of-life care in advanced cancer care (PALLI-COM): A randomized, controlled trial. *ESMO Open*. 2022;7(6):100623.

doi: 10.1016/j.esmoop.2022.100623

12. Flock C, Grapp M, Oldsen R, Friederich HC, Bugaj TJ. Therapeutic alliance in psycho-oncology: A systematic review. *Couns Psychother Res*. 2024;24(4):1149-1167.

doi: 10.1002/capr.12717

13. Akechi T, Ito Y, Ogawa A, Kizawa Y. Essential competences for psychologists in palliative cancer care teams. *Jpn J Clin Oncol*. 2021;51(10):1587-1594.

doi: 10.1093/jjco/hyab133

14. Bognár SA, Teutsch B, Bunduc S, *et al*. Psychological intervention improves quality of life in patients with early-stage cancer: A systematic review and meta-analysis of randomized clinical trials. *Sci Rep*. 2024;14(1):13233.

doi: 10.1038/s41598-024-63431-y

15. Broadbridge E, Greene K, Venetis MK, *et al*. Facilitating psychological adjustment for breast cancer patients through empathic communication and uncertainty reduction. *Patient Educ Couns*. 2023;114:107791.

doi: 10.1016/j.pec.2023.107791

16. Sabetfar N, Meschi F, Hosseinzade Taghvaei M. The effectiveness of mindfulness-based group therapy on perceived stress, emotional cognitive regulation, and self-care behaviors in patients with hypertension. *Intern Med Today*. 2021;27(2):246-263.

17. Power N, Noble LA, Simmonds-Buckley M, *et al*. Associations between treatment adherence-competence-integrity (ACI) and adult psychotherapy outcomes: A systematic review and meta-analysis. *J Consult Clin Psychol*. 2022;90(5):427-445.

doi: 10.1037/ccp0000736

18. Goldberg SB, Flemotomos N, Martinez VR, *et al*. Machine learning and natural language processing in psychotherapy research: Alliance as example use case. *J Couns Psychol*. 2020;67(4):438-448.

doi: 10.1037/cou0000382

19. Van Heerden AC, Pozuelo JR, Kohrt BA. Global mental health services and the impact of artificial intelligence-powered large language models. *JAMA Psychiatry*. 2023;80(7):662-664.

doi: 10.1001/jamapsychiatry.2023.1253

20. Wampold BE, Flückiger C. The alliance in mental health care: Conceptualization, evidence and clinical applications. *World Psychiatry*. 2023;22(1):25-41.

doi: 10.1002/wps.21035

21. Zhang Y, Cui C, Wang Y, Wang L. Effects of stigma, hope and social support on quality of life among Chinese patients diagnosed with oral cancer: A cross-sectional study. *Health Qual Life Outcomes*. 2020;18:112.

doi: 10.1186/s12955-020-01353-9

22. Benuto LT, Singer J, Newlands RT, Casas JB. Training culturally competent psychologists: Where are we and where do we need to go? *Train Educ Profess Psychol*. 2019;13(1):56.

23. Whittingham M, Marmarosh ML, Mallow P, Scherer M. Mental health care equity and access: A group therapy solution. *Am Psychol*. 2023;78(2):119-133.

doi: 10.1037/amp0001078

24. Toledano-Toledano F, Luna D, Moral de la Rubia J, *et al*. Psychosocial factors predicting resilience in family caregivers of children with cancer: A cross-sectional study. *Int J Environ Res Public Health*. 2021;18(2):748.

doi: 10.3390/ijerph18020748

25. Lipinski S, Boegl K, Blanke ES, Suenkel U, Dziobek I. A blind spot in mental healthcare? Psychotherapists lack education and expertise for the support of adults on the autism spectrum. *Autism*. 2022;26(6):1509-1521.

doi: 10.1177/13623613211057973

26. Desjardins L, Barrera M, Schulte F, *et al*. Predicting social withdrawal, anxiety and depression symptoms in pediatric brain tumor survivors. *J Psychosoc Oncol*. 2019;37(1):22-36.

doi: 10.1080/07347332.2018.1535531

27. Cangelosi G, Acito M, Grappasonni I, *et al*. Yoga or mindfulness on diabetes: Scoping review for theoretical experimental framework. *Ann Ig*. 2024;36:153-168.

doi: 10.7416/ai.2024.2600

28. Salamanca-Balen N, Merluzzi TV, Chen M. The effectiveness of hope-fostering interventions in palliative care: A systematic review and meta-analysis. *Palliat Med*. 2021;35(4):710-728.

doi: 10.1177/0269216321994728

29. Kim SC, Shah DV, Namkoong K, McTavish FM, Gustafson DH. Predictors of online health information seeking among women with breast cancer: The role of social support perception and emotional well-being. *J Comput Mediat Commun*. 2013;18(2):212-232.

doi: 10.1111/jcc4.12002

30. Jørgensen K, Rendtorff JD. Patient participation in mental health care-perspectives of healthcare professionals: An integrative review. *Scand J Caring Sci*. 2018;32(2):490-501.

doi: 10.1111/scs.12531

31. Collins GS, Reitsma JB, Altman DG, Moons KGM. Transparent reporting of a multivariable prediction model for individual prognosis or diagnosis (TRIPOD) the

TRIPOD statement. *Circulation*. 2015;131(2):211-219.

32. Leal-Costa C, Tirado-González S, Rodríguez-Marín J, Vander-Hofstadt-Román CJ. Psychometric properties of the health professionals communication skills scale (HP-CSS). *Int J Clin Health Psychol*. 2016;16(1):76-86.

    doi: 10.1016/j.ijchp.2015.04.001

33. Gori A, Topino E, Brugnera A, Compare A. Assessment of professional self-efficacy in psychological interventions and psychotherapy sessions: Development of the Therapist Self-Efficacy Scale (T-SES) and its application for eTherapy. *J Clin Psychol*. 2022;78:2122-2144.

    doi: 10.1002/jclp.23391

34. Aldrup K, Carstensen B, Klusmann U. Is empathy the key to effective teaching? A systematic review of its association with teacher-student interactions and student outcomes. *Educ Psychol Rev*. 2022;34(3):1177-1216.

35. Bialystok L, Kukar P. Authenticity and empathy in education. *Theor Res Educ*. 2018;16:23-39.

    doi: 10.1177/1477878517746647

36. Heinonen E, Nissen-Lie HA. The professional and personal characteristics of effective psychotherapists: A systematic review. *Psychother Res*. 2020;30(4):417-432.

    doi: 10.1080/10503307.2019.1620366

37. Wang S, Wang X, Liu X, Zhao C, Duan J. Moderating effects of humanistic care and socioeconomic status on the relationship among pain intensity, psychological factors, and psychological function in adults with cancer pain from a province of China: A cross-sectional study. *Front Psychiatry*. 2023;14:928727.

    doi: 10.3389/fpsyt.2023.928727

38. Sharma NP, Gupta V. Therapeutic communication. In: StatPearls. Treasure Island, FL: StatPearls Publishing; 2023. Available from: https://www.ncbi.nlm.nih.gov/books/NBK559103/

39. Purgato M, Gastaldon C, Papola D, van Ommeren M, Barbui C, Tol WA. Psychological therapies for the treatment of mental disorders in lowe relationship among pain in affected by humanitarian crises. *Cochrane Database Syst Rev*. 2018;7(7):CD011849.

    doi: 10.1002/14651858.CD011849.pub2

40. Ravasco P. Nutrition in cancer patients. *J Clin Med*. 2019;8(8):1211.

    doi: 10.3390/jcm8081211

41. Sakellaropoulos T, Vougas K, Narang S, *et al*. A deep learning framework for predicting response to therapy in cancer. *Cell Rep*. 2019;29(11):3367-3373.e4.

    doi: 10.1016/j.celrep.2019.11.017

42. Teo I, Krishnan A, Lee GL. Psychosocial interventions for advanced cancer patients: A systematic review. *Psychooncology*. 2019;28(7):1394-1407.

    doi: 10.1002/pon.5103

43. Alowais SA, Huang IW. Revolutionizing healthcare: The role of artificial intelligence in clinical practice. *Angle Health Law Rev*. 2024(94):95-132.

Appendix

Health professionals communication skills scale (HP-CSS)

List of 42 items

1. I respect the right of patients to express themselves freely
2. I explore the emotions of my patients
3. I respect the autonomy and freedom of patients
4. When the patient speaks, I show interest through body gestures (nodding, eye contact, smiles, etc.)
5. I provide information to patients (whenever my professional competency permits me) about what concerns them
6. I listen to patients without prejudice, regardless of their physical appearance, mannerisms, or form of expression
7. I express my opinions and desires clearly to patients
8. When I give information, I use silence to allow the patient to assimilate what I am saying
9. When I give information to patients, I do so in understandable terms
10. When a patient does something that does not seem right, I express my disagreement or discomfort
11. I dedicate time to listen and try to understand the needs of patients
12. I try to understand the feelings of my patient
13. When I interact with patients, I express my opinions clearly and firmly
14. I believe that the patient is entitled to receive health information
15. I feel that I respect the needs of patients
16. I find it difficult to make requests of patients
17. I make sure that patients have comprehended the information provided
18. I find it difficult to ask for information from the patients
19. I say things clearly and with sincerity
20. I clearly inform patients about the objectives of the therapeutic process
21. I can recognize what a patient is feeling without them telling me
22. I know how to interpret gestures and expressions of the patients
23. I am aware of the emotional state of patients
24. I find it easy to start a conversation with patients
25. I maintain eye contact when talking to patients
26. I act honestly with patients
27. I ensure that patients understand the reasons behind my recommendations
28. I understand when a patient is suffering emotionally
29. I can empathize with the fears and anxieties of patients
30. I explain the consequences of each procedure or treatment in a simple way
31. I smile and maintain a friendly tone of voice when addressing patients
32. I use appropriate gestures to create a welcoming environment
33. I treat patients as people, not just as cases or diseases
34. I adapt my communication according to the cultural background of the patient
35. I show openness to patients' doubts and concerns
36. I acknowledge patients' feelings even when I don't agree with them
37. I adjust my emotional tone according to the patient's condition
38. I use written material or drawings to support verbal communication when needed
39. I make sure to repeat important information when necessary
40. I use humor appropriately to help relax patients
41. I acknowledge the suffering expressed by the patient
42. I adapt the way I communicate depending on whether the patient is a child, adult, or elderly person.

HP-CSS

Original source

Leal-Costa, C., Tirado-González, S., Rodríguez-Marín, J., & Vander-Hofstadt, C. (2016). *Psychometric properties of the Health Professionals Communication Skills Scale (HP-CSS). International Journal of Clinical and Health Psychology*, 16(1), 76–86. https://doi.org/10.1016/j.ijchp.2015.04.001

Item distribution by dimensions

1. **Informative communication (12 items)**
   Assesses how professionals give and receive information clearly and adequately.
   Items: 3, 6, 11, 13, 16, 18, 20, 27, 30, 38, 39, 42
2. Empathy (13 items)
   Assesses understanding and sharing the emotions of the patient.
   Items: 4, 5, 12, 14, 17, 21, 22, 23, 28, 29, 36, 37, 41
3. Respect and authenticity (5 items)
   Assesses honesty and respect toward patients in the therapeutic relationship.
   Items: 2, 10, 26, 33, 34
4. Social skills (12 items)
   Assesses assertiveness and confidence in social and clinical interaction.
   Items: 1, 7, 8, 9, 15, 19, 24, 25, 31, 32, 35, 40

ACCSCIENCE PUBLISHING

Eurasian Journal of Medicine and Oncology

ORIGINAL RESEARCH ARTICLE

Comprehensive characterization of the material basis and network pharmacology of Dan-Shen-Yin in the treatment of gastritis

Jianbing Dong[1†], Zhirong Zhou[1†], Yi Chen[2†], Peng Lei[1], Qingrui Zhang[1], and Miaomiao Jiang[1,3*]

[1]National Key Laboratory of Chinese Medicine Modernization, Tianjin University of Traditional Chinese Medicine, Tianjin, China

[2]College of Integrative Medicine, Tianjin University of Traditional Chinese Medicine, Tianjin, China

[3]Science and Technology Project of Haihe Laboratory of Modern Chinese Medicine, Tianjin, China

Abstract

Introduction: Dan-Shen-Yin (DSY), a traditional Chinese medicinal prescription composed of *Salvia miltiorrhiza* Bge. (DS), *Santalum album* L. (TX) and *Amomum villosum* Lour. (SR), has been widely employed in the treatment of gastritis in modern clinical practice and demonstrates excellent therapeutic efficacy. However, the main active ingredient and underlying mechanisms of action remain unclear.

Objective: The aim of this study is to comprehensively characterize the chemical composition of DSY and elucidate its potential mechanisms in the treatment of gastritis.

Methods: The nonvolatile compounds in DSY were analyzed through liquid chromatography-mass spectrometry using the data-dependent acquisition approach, employing an in-house database. The volatile compounds and polysaccharides were detected by gas chromatography-mass spectrometry and high-performance liquid chromatography, respectively. Network pharmacology analysis was performed based on the identified compounds.

Results: A total of 52 nonvolatile and 15 volatile compounds were identified in DSY decoction, primarily including phenylpropanoids, phenols, flavonoids, and terpenoids. Specifically, 54 compounds were found in DS, 14 in SR, and 8 in TX. DSY polysaccharide consisted of seven kinds of monosaccharides, including mannose, rhamnose, glucuronic acid, galacturonic acid, glucose, galactose, and arabinose, with molar percentages of 0.21%, 0.53%, 0.15%, 4.12%, 6.24%, 18.07%, and 0.84%, respectively. Network pharmacology analysis identified 22 key compounds among the 67 compounds detected. These compounds exert the therapeutic effects through 55 core targets (e.g., interleukin-6, tumor necrosis factor, and TP53) and 10 inflammation-related pathways, such as the MAPK and nuclear factor kappa B signaling pathways.

Conclusion: This study further enriches the research on the material basis of DSY and reveals that its volatile compounds, nonvolatile compounds, and polysaccharides contribute to its therapeutic efficacy against gastritis. These findings may facilitate further development and application of DSY in gastritis treatment.

Keywords: Dan-Shen-Yin; Gastritis; Chemical components; Network pharmacology

†These authors contributed equally to this work.

***Corresponding author:**
Miaomiao Jiang
(miaomiaojiang@tjutcm.edu.cn)

Citation: Dong J, Zhou Z, Chen Y, *et al*. Comprehensive characterization of the material basis and network pharmacology of Dan-Shen-Yin in the treatment of gastritis. *Eurasian J Med Oncol*. 2025;9(3):168-184.
doi: 10.36922/EJMO025160124

Received: April 15, 2025

Revised: May 28, 2025

Accepted: June 20, 2025

Published online: July 17, 2025

Copyright: © 2025 Author(s). This is an Open-Access article distributed under the terms of the Creative Commons Attribution License, permitting distribution, and reproduction in any medium, provided the original work is properly cited.

Publisher's Note: AccScience Publishing remains neutral with regard to jurisdictional claims in published maps and institutional affiliations.

1. Introduction

Gastritis is an inflammatory condition of the gastric mucosa that can lead to symptoms such as pain, discomfort, and digestive disturbances. It is typically categorized as acute, chronic, or specific gastritis.[1] As a common gastrointestinal disease, gastritis can progress to gastric cancer, one of the most prevalent and lethal malignant tumors in the world.[2,3] Currently, clinical management of gastritis relies on gastric mucosal protection and symptomatic relief, using interventions such as Vitamin C supplements, *Helicobacter pylori* (*H. pylori*) eradication, proton pump inhibitors (PPIs), and non-steroidal anti-inflammatory drugs (NSAIDs).[4] However, the therapeutic effects of vitamin C and NSAIDs in preventing the progression of gastritis to gastric cancer are unclear and are subject to ongoing debate.[4] In addition, Du *et al.*[5] conducted a systematic review and meta-analysis, finding that *H. pylori* eradication therapy are associated with a higher incidence of adverse events during treatment. Moreover, the long-term use of PPIs may increase the risk of gastric atrophy.[6] Therefore, further research into the prevention and management of gastritis is important.

Dan-Shen-Yin (DSY), first documented in Shi Fang Ge Kuo (AD 1801), is a traditional Chinese herbal formula composed of *Salvia miltiorrhiza* Bge. (DS), *Santalum album L.* (TX) and *Amomum villosum Lour.* (SR) in a ratio of 10:1:1, prepared by water. DSY promotes blood circulation, removes blood stasis, promotes *qi*, and relieves pain. It is commonly used in the treatment of gastric and duodenal ulcers, coronary heart disease, and angina pectoris.[7] Clinical studies have shown that DSY exhibits significant therapeutic effects in treating gastritis.[8] Sun *et al.*[9] compared the therapeutic efficacy and safety of PPIs and DSY in the treatment of gastritis, and found that DSY demonstrated a significant advantage in both aspects. Wang *et al.*[10] found that DSY was effective in regulating gastric pepsinogen secretion and alleviating the severity of gastric mucosal lesions. The therapeutic effects were attributed to DSY's modulation of soluble interleukin-2 receptor, tumor necrosis factor alpha (TNF-α), prostaglandin 2 (PGE_2), and calcitonin gene-related peptide, which attenuates mucosal inflammation and protects the gastric mucosa. Moreover, pharmacological studies have confirmed that DSY enhances ulcer healing and bolsters gastric mucosal defense.[11,12] However, the material basis underlying DSY's effects on gastritis remains insufficiently understood, hindering comprehensive insight into its therapeutic mechanisms.

While the pharmacological actions and constituents of DSY in cardiovascular diseases have been well documented,[7,13] research on its active components and mechanisms in gastritis is still limited. The chemical profiles of the individual herbs in DSY—especially the nonvolatile, volatile compounds, and polysaccharides of DS—have been previously studied.[14,15] In contrast, compositional studies of SR and TX are relatively limited, with investigations of their volatile components mainly conducted by gas chromatography-mass spectrometry (GC-MS).[16,17] In addition, although DSY is commonly administered as a decoction in clinical practice, there have been few comprehensive studies on the composition of DSY decoction.

In this study, we aimed to comprehensively characterize the material basis of DSY decoction using multiple analytical techniques to support foundational research on DSY. Nonvolatile compounds were identified using ultra-high performance liquid chromatography (UHPLC)–Orbitrap Exploris MS with a data-dependent acquisition method based on an in-house database. The volatile compounds and polysaccharides were analyzed by headspace GC-MS (HS-GC-MS) and high-performance liquid chromatography (HPLC), respectively. The relative proportions of volatile compounds, nonvolatile compounds, and polysaccharide components in the DSY decoction were also analyzed. Furthermore, the potential mechanisms by which these components exert therapeutic effects on gastritis were analyzed based on network pharmacology and literature-based analysis.

2. Materials and methods

2.1. Reagents and chemicals

DS, SR, and TX were purchased from Beijing Tongrentang Tianjin Hexi Pharmacy and their details are provided in Table 1. Methanol and acetonitrile for liquid chromatography–mass spectrometry (LC-MS) were procured from Thermo Fisher Scientific (USA). Formic acid was obtained from Wilmington Inc. (USA). Acetic acid was purchased from Shanghai Macklin Biochemical Technology (China). Watsons deionized water (Watsons Corp., China) was used in all experiments.

A total of 28 compounds (Table S1)–purchased either from Ichikawa Vikko Biotechnology (China) and

Table 1. Information on TCM prepared pieces.

TCM prepared pieces	Latin name of original plant	Batch number	Producing area
Salviae miltiorrhizae Radix et Rhizoma (Dan Shen, DS)	*Salvia miltiorrhiza* Bge.	210701	Shandong
Amomi fructus (Sha Ren, SR)	*Amomum villosum Lour.*	20210901	Guangxi
Santali albi Lignum (Tan Xiang, TX)	*Santalum album L.*	20210813	Guangdong

Abbreviations: TCM: Traditional Chinese medicine

Shanghai Yuanye Biotechnology (China)–were used as reference compounds, each with a purity exceeding 98%. The Bradford protein concentration kit was obtained from Beyotime Biotechnology (China). 1-Phenyl-3-methyl-5-pyrazolone (PMP; P816062) was purchased from Shanghai Macklin Biochemical Technology (China). Trifluoroacetic acid was purchased from Shanghai Yien Chemical Technology (China). Ammonium acetate was obtained from Sigma-Aldrich (USA).

2.2. Preparation of DSY decoction

DSY is composed of DS, TX, and SR in a 10:1:1 ratio. Initially, DS was extracted using ten times its weight in water by refluxing and boiling for 2 h at 100°C. TX and SR were then added to the DS residue and extracted using eight times the weight of water over low heat for 1 h. The two extracts were combined, concentrated, and dried. Individual extracts of DS, TX, and SR were prepared using the same method.

2.3. HS-GC-MS analysis of DSY decoction

Lyophilized powders of the aqueous extract of DSY, DS, TX, and SR (all passed through a 50-mesh sieve) were accurately weighed for analysis. The equilibration temperature was set at 120°C. The injection port, transfer line, and detector temperatures were set to 130°C, 140°C, and 220°C, respectively. The equilibration time was 15 min, injection time 1 min, and pressure equilibration time 1 min. An HP-5 MS elastic quartz capillary column (30 m × 0.25 mm, 0.25 μm; Agilent Technologies Inc., USA) was used to separate sample, with high-purity helium as the carrier gas. The pre-column pressure was 9.8 psi, and the column flow rate was 1.2 mL/min. Split injection was performed at a 1:20 ratio. The column heating program is provided in Table S2.

The Agilent MassHunter qualitative analysis navigator B.08.00 (Agilent Technologies Inc., USA) equipped with the NIST.17 standard spectral library was utilized for compound identification. Only compounds with both a positive match and reverse match score >80% were retained. The relative abundance of each volatile compound was determined using peak area normalization.

2.4. UHPLC-Orbitrap Exploris MS analysis

Sample powders (DSY, DS, TX, and SR) and 19 reference compounds were dissolved in 80% methanol. The mixture was centrifuged at 12,000 rpm for 10 min at 4°C and the process was repeated once. The resulting supernatant was used for analysis.

UHPLC separation was performed on a Vanquish UHPLC System (Thermo Fisher Scientific, USA) using a Hypersil GOLD column (2.1 mm × 100 mm, 1.8 μm) maintained at 40°C. The binary mobile phase consisted of 0.1% formic acid in water (A) and acetonitrile (B). The gradient elution procedure was as follows: 0 – 2 min, 10 – 15% B; 2 – 3 min, 15 – 26% B; 3 – 6 min, 26 – 28%); 6 – 8 min, 28 – 28% B; 8 – 9 min, 28 – 75% B; 9 – 11 min, 75 – 75% B; 11 – 15 min, 75 – 80% B; 15 – 17 min, 80 – 90% B; 17 – 19 min, 95% B. The injection volume was 2 μL. Mass spectrometric detection was performed using an Orbitrap Exploris 120 (Thermo Fisher Scientific Inc., USA) in both positive and negative ion scanning modes. Data acquisition was conducted using Full MS/dd-MS2 scanning and a predefined DSY precursor ion list. The "if idle pick others" function was turned on.

The precursor ion list was constructed using constituent information on DS, TX, and SR obtained from databases such as CNKI, TCMSP, and Google Scholar. The Xcalibur 4.2 software (Thermo Fisher Scientific Inc., USA) was used to extract information on potential compounds and identification by comparison against an in-house database and reference compounds.

2.5. Characterization of DSY polysaccharides

Lyophilized powders of DSY, DS, TX, and SR (10 g each) were dissolved in 5 mL of distilled water. Then, 20 mL of ethanol was added to the solution. The suspension was incubated at 4°C for 48 h. The precipitated underlayer was dissolved in distilled water and deproteinized using the Sevag method.[18] The crude polysaccharide samples were then lyophilized.

Total sugar content was measured using the phenol-sulfuric acid colorimetric method[19] with D-glucose as the standard at 490 nm. Total uronic acid content was measured using the m-hydroxyphenyl colorimetric method[20] with galacturonic acid as the standard. Protein content was evaluated using the Coomassie Brilliant Blue assay with bovine serum albumin as the standard.[21]

The monosaccharide composition of the samples was analyzed by HPLC with pre-column derivatization. Polysaccharide samples were hydrolyzed with trifluoroacetic acid (TFA) for 6 h at 105°C. Subsequently, 200 μL each of the acid-hydrolyzed sample and monosaccharide standard mixture were accurately aliquoted. The hydrolysates and monosaccharide standard mixture were converted to their PMP derivatives according to the previous method with some modifications[22] The sample and reference standard samples were analyzed using HPLC at 250 nm at 30°C., using a mobile phase of 17% organic phase (acetonitrile) and 83% aqueous phase (0.05 M ammonium acetate). The same procedure was used to analyze reference monosaccharides. The crude DSY polysaccharide powders

were further analyzed using Fourier-transform infrared spectroscopy (FTIR-640IR, VARIAN, USA).

2.6. Network pharmacology analysis

Based on the identified nonvolatile and volatile compounds of DSY decoction, gene targets were obtained from TCMSP (https://tcmspw.com/index.php) and HERB (http://herb.ac.cn) databases. For compounds lacking target information, SMILES strings were obtained from PubChem (https://pubchem.ncbi.nlm.nih.gov/) and used in SwissTargetPrediction (http://www.swisstargetprediction.ch/), retaining the top five predicted targets for each compound. Official gene symbols were standardized using the UniProt (https://www.uniprot.org/) database.

Gene targets associated with human gastritis were identified based on data retrieved from the DisGeNet (http://www.disgenet.org/), GeneCards (https://www.genecards.org/), and MalaCards (www.malacards.org/) databases.

A Venn diagram was generated by importing the compounds and disease targets into the Venny 2.1.0 platform (https://bioinfogp.cnb.csic.es/tools/venny/). The PPI network was constructed using String 11.5 platform (https://www.string-db.org/) with the species set to *Homo sapiens* and confidence threshold set to >0.7. Subsequently, Cytoscape 3.9.1 with the CytoNCA plugin ((https://cytoscape.org/) was used to calculate the topological property parameters of the PPI network, including betweenness centrality, presence centrality, degree, local average connectivity, eigenvector, and network centrality.

The Metascape database (www.metascape.org/) was used to perform Gene Ontology (GO) and Kyoto Encyclopedia of Genes and Genomes (KEGG) pathway enrichment analyses. The p-value threshold of <0.01 was used for statistical significance. The top 10 GO terms and the top 20 KEGG pathways were selected based on ascending order of p-values.

3. Results and discussion

3.1. Optimization of HS-GC-MS analysis conditions

The effects of headspace sampling conditions, including split ratio, equilibrium temperature, and equilibrium time, on the HS–GC–MS analysis of DSY decoction were systematically investigated. Evaluation criteria included the peak areas of the five representative compounds with the highest response values (furfural, bornyl acetate, 2-methoxy-4-vinylphenol, α-santalol, and cis-nuciferol) and the total number of peaks detected under each condition. The examination results are shown in Figure 1 and Figure S1. Based on an overall evaluation of peak shape, peak area, and the number of peaks, the optimal analytical conditions were determined to be a split ratio of 1:20, an equilibrium temperature of 120°C, and an equilibrium time of 15 min.

3.2. Identification of volatile compounds in DSY decoction

A total of 15 volatile compounds were identified in the DSY decoction (Table 2). These compounds included five terpenoids, three furans, three aromatic hydrocarbons, two alcohols, and two ketones. The relative contents of each compound were calculated using peak area normalization. The results indicated that the contents of 1-oxo-di-epicatechuene, 2,4-di-tert-butylphenol, and camphor were present in relatively high concentrations. Comparison with the volatile profiles of individual herbs (Figure 2) revealed that most volatile compounds in DSY originated from DS, with 12 compounds found in both DS and DSY. However, in terms of their relative content, certain volatile compounds–such as diepicedrene-1-oxide and camphor–originating from TX accounted for 47.677% of the total volatile content in DSY. A detailed identification information of the volatile compounds for each individual herb is provided in Table S3 (DS), Table S4 (TX), and Table S5 (SR). I addition, the Soxhlet extraction method was employed to extract volatile oil from the aqueous extracts. However, the extraction yields of DSY, DS, SR, and TX were <0.1%.

These findings suggest that while the majority of identified volatile species are contributed by DS, the dominant contributors by concentration are compounds derived from TX. Liu *et al.*[23] demonstrated that TX facilitates small intestinal transit and accelerates gastric emptying in a murine model. Studies have indicated that prolonged exposure of the gastric mucosa to gastric acid and reduced gastric mucosal resistance may be the primary causes of gastric mucosal lesions.[24] Therefore, the volatile compounds in DSY decoction, particularly those derived from TX, may exert protective effects on the gastric mucosa by enhancing gastric motility and reducing acid retention.

3.3. Optimization of UHPLC-Orbitrap Exploris MS analysis conditions

To improve the accuracy of the systematic characterization of the nonvolatile compounds of DSY decoction, the chromatographic separation conditions and stationary phases were systematically optimized. Each experimental condition was replicated three times. In the mobile phase evaluation (Figure 3), it was observed that the peaks exhibited improved response and separation when 0.1%

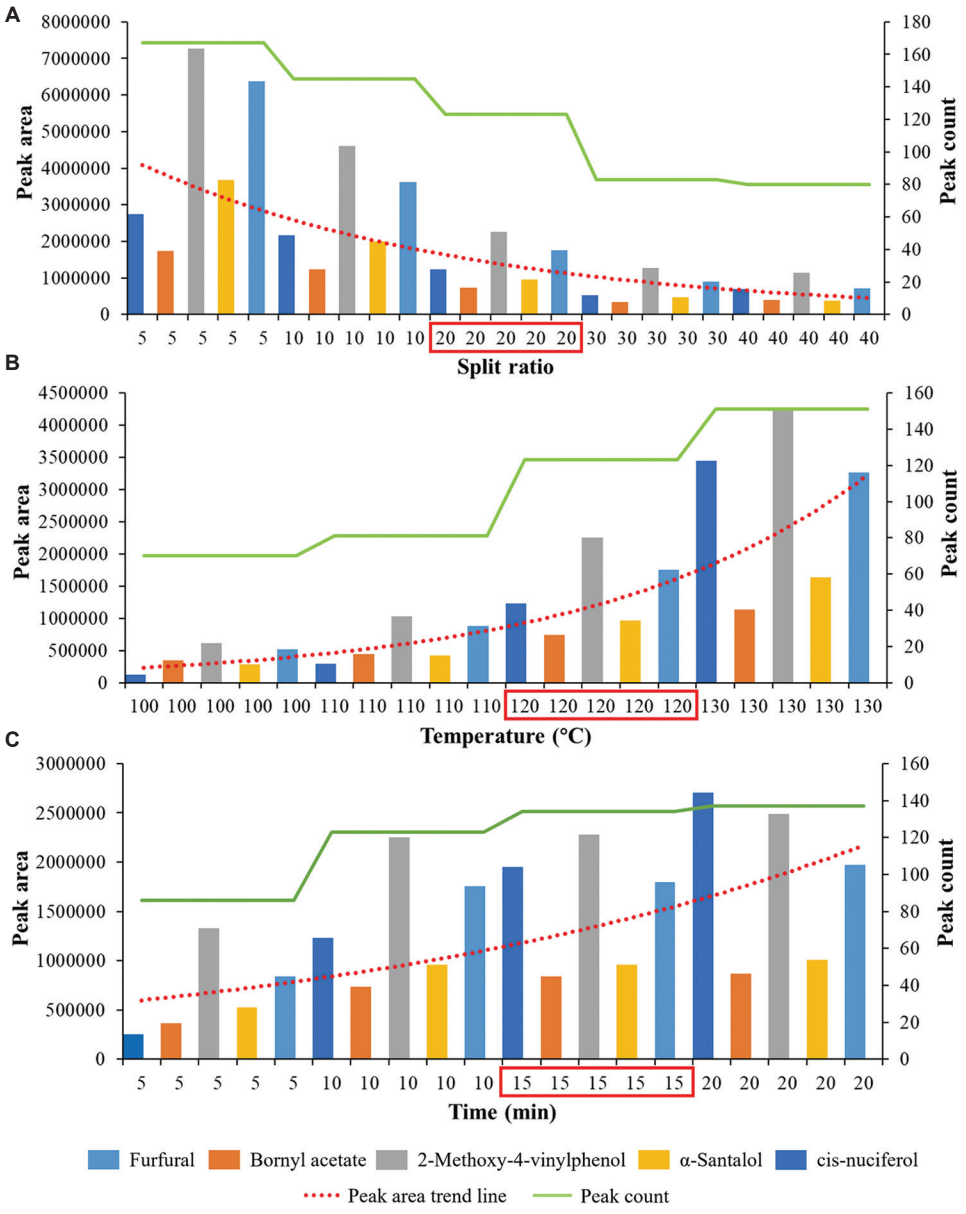


Figure 1. Optimization of GC-MS parameters for DSY decoction analysis. (A) Effect of the split ratio on peak profiles. (B) Effect of the equilibrium temperature on peak profiles. (C) Effect of the equilibrium time on peak profiles.
Abbreviations: GC-MS: Gas chromatography-mass spectrometry; DSY: Dan-Shen-Yin.

formic acid in a water-acetonitrile system was used. In addition, six kinds of chromatographic columns were examined, as shown in Figure 4. The results showed that Hypersil GOLD (Thermo) achieved the best peak separation and yielded the highest number of compounds–totaling 1,436–as determined by SIEVE software extraction in both positive and negative ion modes. Spray voltage, capillary temperature, and auxiliary gas temperature significantly affect the sensitivity and accuracy of mass spectrometry. Therefore, these parameters were optimized in this study, with results as shown in Figure 5. Salvinorin A, salvinorin B, epicatechin, and orientin were used to screen for the optimal spray voltage in the negative ion mode, while dihydrotanshinone I, cryptotanshinone (Cry), and tanshinone IIA were used for the positive ion mode. Based on the peak areas of these compounds, the optimal mass spectrometry parameters were determined as follows: spray voltages of 1.5 kV (positive mode) and 3 kV (negative mode), capillary temperature of 350°C, and auxiliary gas temperature of 400°C.

Table 2. Identification of volatile compounds in DSY decoction based on HS-GC-MS

No.	t_R (min)	Molecular formula	CAS number	Compound name	Match degree		Relative content (%)	Sources
					P. Match	R. Match		
1	4.240	$C_5H_6O_2$	98-00-0	2-Furanmethanol	803	830	1.065	DSY, SR, DS
2	5.444	$C_4H_6O_2$	96-48-0	Butyrolactone	860	966	0.947	DSY, SR, DS
3	8.787	C_8H_8O	122-78-1	Benzeneacetaldehyde	929	959	1.294	DSY, SR, DS
4	9.144	$C_6H_8O_3$	3658-77-3	Furaneol	810	836	0.410	DSY, DS
5	11.568	$C_6H_8O_4$	28564-83-2	4H-pyran-4-one, 2,3-dihydro-3,5-dihydroxy-6-methyl-	921	926	5.750	DSY, SR, DS
6	11.659	$C_{10}H_{16}O$	76-22-2	Camphor	811	906	2.138	DSY, TX
7	15.635	$C_{12}H_{20}O_2$	76-49-3	Bornyl acetate	834	834	0.666	DSY, SR, TX
8	18.588	$C_8H_8O_3$	621-59-0	Isovanillin	817	860	1.166	DSY, DS
9	19.016	$C_{14}H_{26}O_2$	126-86-3	2,4,7,9-Tetramethyl-5-decyn-4,7-diol	822	825	0.818	DSY, DS
10	21.126	$C_{14}H_{22}O$	96-76-4	2,4-Di-tert-butylphenol	938	941	4.684	DSY, DS
11	23.664	$C_{15}H_{26}O$	23811-08-7	Hinesol	854	889	0.565	DSY, DS
12	23.893	$C_{15}H_{26}O$	473-15-4	Beta-eudesmol	885	887	1.467	DSY, DS
13	27.793	$C_{15}H_{28}O_2$	4666-84-6	Cryptomeridiol	844	844	1.472	DSY, DS
14	30.888	$C_{17}H_{24}O_3$	82304-66-3	7,9-Di-tert-butyl-1- oxaspiro (4,5) deca-6,9-diene-2,8-dione	887	891	2.734	DSY, SR, DS
15	31.164	$C_{15}H_{24}O$	/	Diepicedrene-1-oxide	801	810	45.539	DSY, TX

Abbreviations: DS: *Salvia miltiorrhiza Bge.*; DSY: Dan-Shen-Yin; HS-GC-MS: Headspace gas chromatography–mass spectrometry; P.Match: Positive match score; R.Match: Reverse match score; SR: *Amomum villosum Lour.*; TX: *Santalum album L.*; t_R: Retention time.

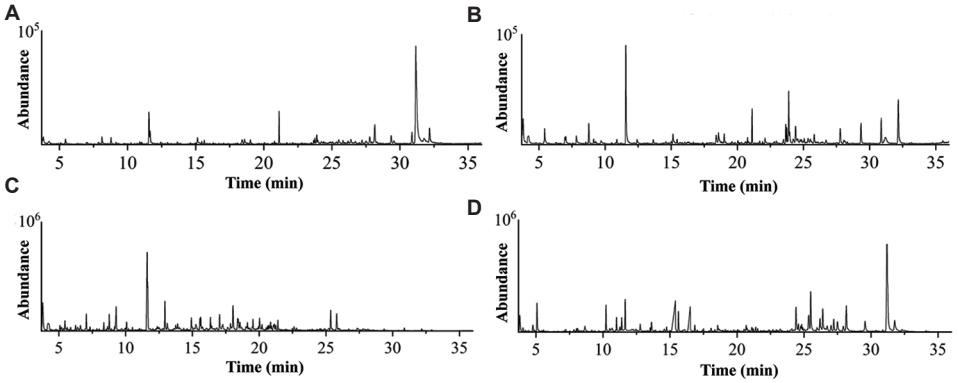


Figure 2. HS-GC-MS TIC diagram for DSY and its individual herbs. (A) DSY. (B) DS. (C) SR. (D) TX
Abbreviations: DS: *Salvia miltiorrhiza Bge.*; DSY: Dan-Shen-Yin; HS-GC-MS: Headspace gas chromatography–mass spectrometry; SR: *Amomum villosum Lour.*; TIC: Total ion chromatogram; TX: *Santalum album L.*

3.4. Identification of nonvolatile compounds in DSY decoction

A precursor ion list consisting of 304 ions (Figure 5D), including 163 $[M+H]^+$ and 141 $[M-H]^-$, was constructed to increase detection sensitivity for trace compounds. Based on reference compounds and an in-house database, 52 nonvolatile compounds in DSY were identified or confirmed through deduction (Figure 6A), including 22 phenylpropanoids, 10 phenols, eight flavonoids, eight diterpenes, two oligosaccharides, a carboxylic acid, and a benzoic acid (Table 3).

In addition, as shown in Figure 6B–D, the nonvolatile compounds in the individual herbs (DS, TX, and SR) were also identified, with details provided in Tables S6–S8. Among the 52 compounds, 42 were derived from DS, mainly phenolic acids such as salvianolic acid A, salvianolic acid B, rosmarinic acid, and lithospermic acid. Eight nonvolatile compounds were derived from SR (three of which were also found in DS), mainly proanthocyanidins. Five nonvolatile compounds were derived from TX, mainly flavonoids. Quantitative analysis of the original aqueous extract indicated that the proportions of nonvolatile components were 70%, 73%, 66.3%, and 55.8% for DSY, DS, TX, and SR, respectively.

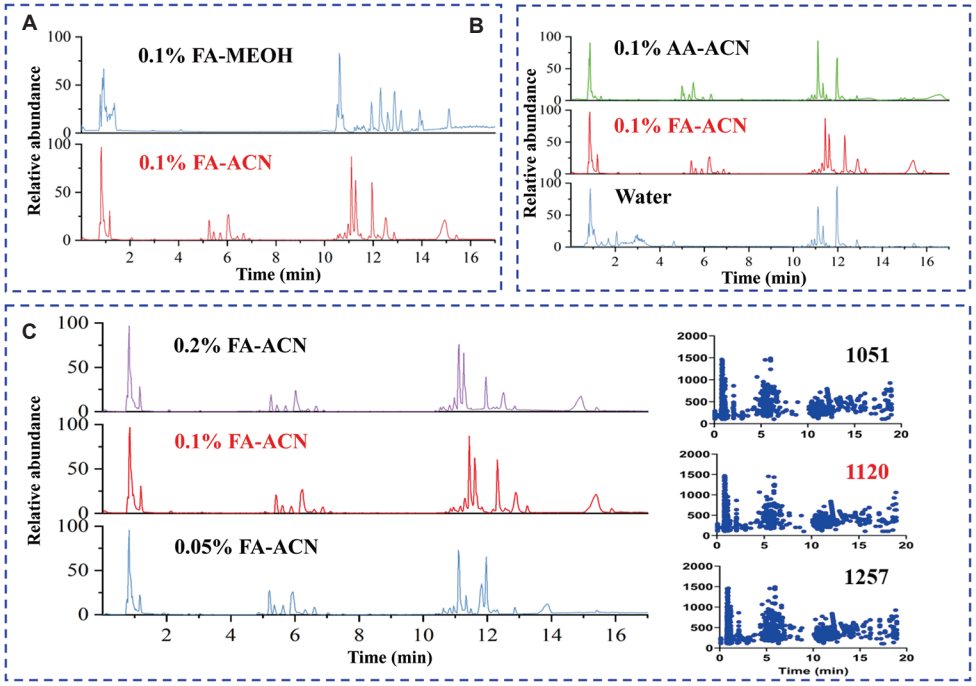


Figure 3. Optimization of mobile phase conditions of UHPLC-Orbitrap Exploris MS analysis. (A) Organic phases. (B) Aqueous phase. (C) Aqueous phase additives.
Abbreviations: AA: Acetic acid; CN: Acetonitrile; FA: Formic acid; MEOH: Methanol; MS: Mass spectrometry; UHPLC: Ultra-high performance liquid chromatography.

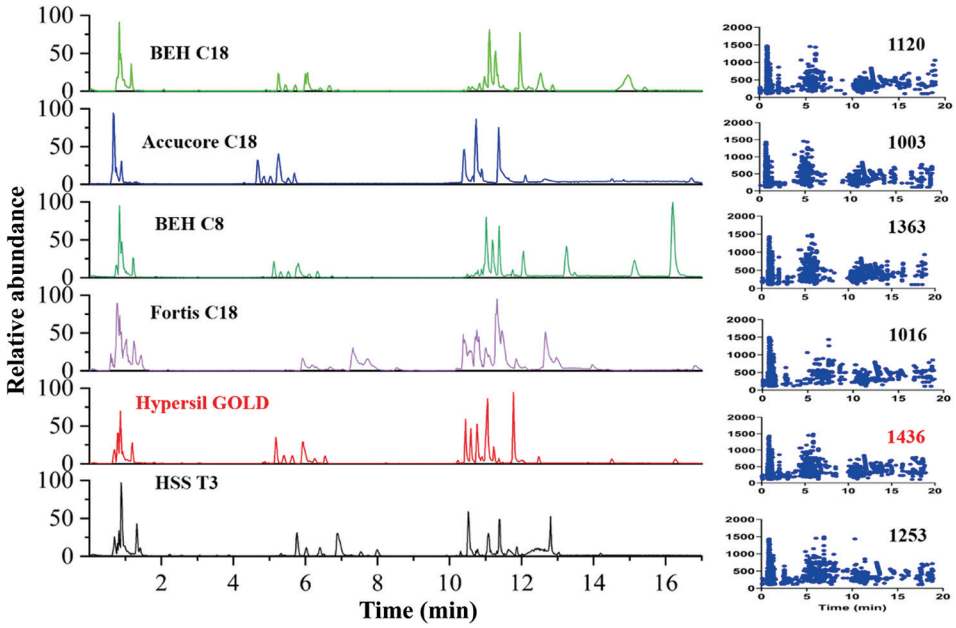


Figure 4. Detection results of UHPLC-Orbitrap Exploris MS analysis using different chromatographic columns
Abbreviations: MS: Mass spectrometry; UHPLC: Ultra-high performance liquid chromatography.

Therefore, the material basis of DSY decoction primarily consists of nonvolatile compounds, the majority of which originate from DS. Modern analytical chemistry and pharmacological studies have demonstrated that DS contains biologically active compounds such as salvianolic acids and tanshinones, which exhibit anti-

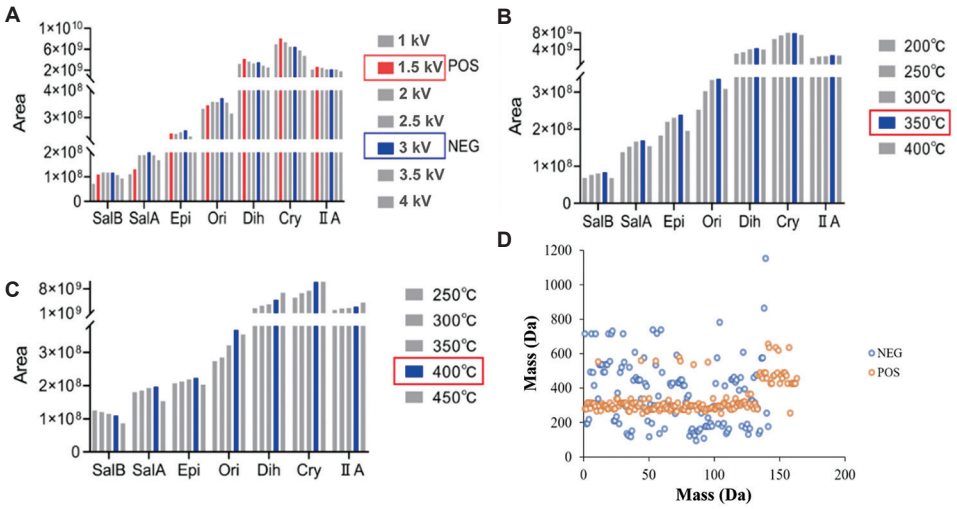


Figure 5. Optimization of key MS parameters for DSY decoction analysis. (A) Effect of spray voltage on peak area. (B) Effect of capillary temperature on peak area. (C) Effect of auxiliary gas temperature on peak area. (D) Distribution map of detected precursor ions in positive and negative ion modes.
Abbreviations: Cry: Cryptotanshinone; Dih: Dihydrotanshinone I; DSY: Dan-Shen-Yin; Epi: Epicatechin; II A: Tanshinone IIA; MS: Mass spectrometry; NEG: Negative ion mode; Ori: Orientin; POS: Positive ion mode; SalA: Salvianolic acid A; SalB: Salvianolic acid B.

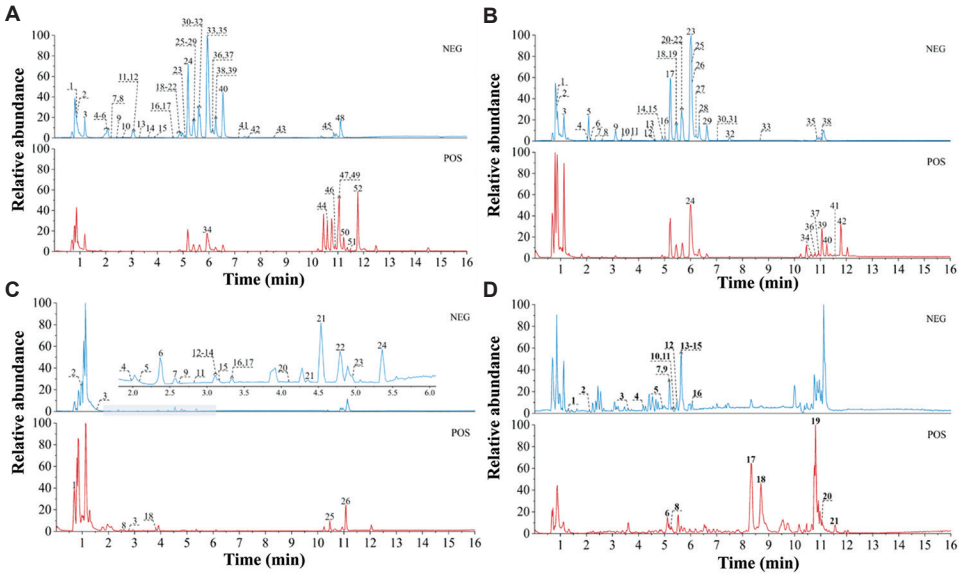


Figure 6. LC-MS TIC diagram positive and negative ion modes for DSY and its individual herbs. (A) DSY. (B) DS. (C) SR. (D) TX.
Abbreviations: DS: *Salvia miltiorrhiza Bge.*; DSY: Dan-Shen-Yin; LC-MS: Liquid chromatography–mass spectrometry; NEG: Negative ion mode; POS: Positive ion mode; SR: *Amomum villosum Lour.*; TIC: Total ion chromatogram; TX: *Santalum album L.*

inflammatory, antioxidant, antitumor, and antimetastatic properties.[25] Moreover, DS extract may serve as a potential chemopreventive agent against bile reflux-associated gastric cancer.[26] Danshensu, a major compound of DS extract, has been shown to prevent bile reflux-induced gastritis and gastric cancer by modulating multiple signaling pathways involved in inflammation, oxidative stress, DNA damage, and apoptosis.[25] Collectively, these findings underscore the significant role of DS-derived nonvolatile compounds in the treatment of gastritis and the prevention of gastric cancer.

3.5. Measurement and analysis of polysaccharides in DSY decoction

The contents of total sugar, uronic acid, and protein in DSY decoction and its individual herbs (DS, TX, and SR) are summarized in Figure 7. The sugar content in DSY was 45.70%, as determined using the phenol-sulfuric acid

Table 3. Identification of nonvolatile compounds in DSY decoction based on UHPLC-Orbitrap Exploris MS

No.	t_R (min)	Mass (ppm)	Molecular formula	Selected ion	ESI-MS^2 fragments	Compound name	Mass error (ppm)	Sources
1	0.83	665.2148	$C_{24}H_{42}O_{21}$	$[M-H]^-$	485.1528, 383.1202, 341.1098	Tetrose	1.948	DSY, DS
2	0.85	341.1090	$C_{12}H_{22}O_{11}$	$[M-H]^-$	179.0565	Disaccharide	3.436	DSY, DS
3	1.12	191.0197	$C_6H_8O_7$	$[M-H]^-$	173.0093, 111.0088	Citric acid	5.607	DSY, DS
4	1.92	329.0879	$C_{14}H_{18}O_9$	$[M-H]^-$	269.0666, 209.0457, 167.0351	Vanillin hexoside	0.166	DSY, SR
5	2.06	151.0402	$C_8H_8O_3$	$[M-H]^-$	123.0453	2-Anisic acid	8.272	DSY, DS
6	2.07	197.0455	$C_9H_{10}O_5$	$[M-H]^-$	179.0352, 135.0453, 123.0453, 72.9932	Danshensu*	−0.135	DSY, DS
7	2.16	151.0402	C8H8O3	$[M-H]^-$	136.0166	Vanillin	0.944	DSY, TX
8	2.18	167.0350	$C_8H_8O_4$	$[M-H]^-$	152.0114, 123.0452, 108.0217, 91.0191	Vanillic acid	0.287	DSY, SR
9	2.35	153.0193	$C_7H_6O_4$	$[M-H]^-$	109.0295, 91.0191	Protocatechuic acid	−0.274	DSY, DS, SR
10	2.63	181.0506	$C_9H_{10}O_4$	$[M-H]^-$	163.0402, 135.0453	3,4-Dihydroxyhydrocinnamic acid	7.538	DSY, DS
11	3.04	289.0710	$C_{15}H_{14}O_6$	$[M-H]^-$	245.0811, 205.0498, 151.0394, 123.0448, 109.0292	Epicatechin*	−2.807	DSY, SR
12	3.06	137.0245	$C_7H_6O_3$	$[M-H]^-$	119.0139, 108.0218, 91.0190	Protocatechualdehyde	0.273	DSY, DS, SR
13	3.27	193.0506	$C_{10}H_{10}O_4$	$[M-H]^-$	149.0608	Ferulic acid*	0.425	DSY, DS
14	3.63	179.0349	$C_9H_8O_4$	$[M-H]^-$	135.0436, 107.0487	Caffeic acid	−0.123	DSY, DS
15	3.81	289.0718	$C_{15}H_{14}O_6$	$[M-H]^-$	245.0811, 205.0494, 123.0447, 109.0291	Catechin*	0.064	DSY, SR
16	4.54	537.1043	$C_{27}H_{22}O_{12}$	$[M-H]^-$	493.1135, 295.0611, 185.0244, 109.0295	Salvianolic acid H	2.788	DSY, DS
17	4.58	313.0718	$C_{17}H_{14}O_6$	$[M-H]^-$	313.0717, 269.0821, 203.0352, 159.0453, 109.0296	Salvianolic acid F	0.059	DSY, DS
18	4.71	537.1043	$C_{27}H_{22}O_{12}$	$[M-H]^-$	493.1135, 295.0611, 185.0244, 109.0295	Salvianolic acid I	0.057	DSY, DS
19	4.86	431.0999	$C_{21}H_{20}O_{10}$	$[M-H]^-$	341.0645, 311.0563, 228.1595, 203.0871	Vitexin*	3.572	DSY, TX
20	4.90	493.1143	$C_{26}H_{22}O_{10}$	$[M-H]^-$	295.0612, 185.0244, 109.0295	Salvianolic acid A*	0.547	DSY, DS
21	4.91	537.1042	$C_{27}H_{22}O_{12}$	$[M-H]^-$	493.1135, 295.0611, 109.0295	Salvianolic acid U	0.634	DSY, DS
22	4.94	463.0884	$C_{21}H_{20}O_{12}$	$[M-H]^-$	300.0276, 271.0249, 243.0295, 151.0039	Quercitrin*	0.326	DSY, SR
23	5.00	537.1041	$C_{27}H_{22}O_{12}$	$[M-H]^-$	493.1135, 295.0611, 109.0295	Salvianolic acid T	0.392	DSY, DS
24	5.21	417.0829	$C_{20}H_{18}O_{10}$	$[M-H]^-$	197.0444, 175.0388	Salvianolic acid D*	0.408	DSY, DS
25	5.34	447.0944	$C_{21}H_{20}O_{11}$	$[M-H]^-$	332.0856, 228.1654, 203.0869	Orientin*	2.472	DSY, TX
26	5.37	447.0939	$C_{21}H_{20}O_{11}$	$[M-H]^-$	300.0278, 271.0252, 255.0303, 243.0298, 151.0039	Isoquercitrin	0.281	DSY, SR
27	5.38	447.0944	$C_{21}H_{20}O_{11}$	$[M-H]^-$	332.0856, 228.1654, 203.0869	Isoorientin*	0.773	DSY, TX
28	5.39	551.1198	$C_{28}H_{24}O_{12}$	$[M-H]^-$	353.0668, 321.0405	Monomethyl lithospermate	0.564	DSY, DS
29	5.44	717.1459	$C_{36}H_{30}O_{16}$	$[M-H]^-$	519.0937, 339.0511, 321.0405	Salvianolic acid B or its isomer	−0.234	DSY, DS
30	5.56	537.1041	$C_{27}H_{22}O_{12}$	$[M-H]^-$	493.1135, 295.0611, 185.0244, 109.0295	Salvianolic acid J	2.565	DSY, DS
31	5.66	359.0772	$C_{18}H_{16}O_8$	$[M-H]^-$	197.0444, 197.0444, 161.0230	Rosmarinic acid*	−0.002	DSY, DS
32	5.79	493.1142	$C_{26}H_{22}O_{10}$	$[M-H]^-$	295.0611, 185.0243, 109.0295	Salvianolic acid A or its isomer	0.365	DSY, DS
33	5.98	717.1460	$C_{36}H_{30}O_{16}$	$[M-H]^-$	295.0606, 519.0930, 339.0503, 321.0399	Salvianolic acid B or its isomer	−0.150	DSY, DS
34	5.99	339.0511	$C_{18}H_{12}O_7$	$[M+H]^-$	295.0615, 185.0244, 109.0295	Salvianolic acid G	0.262	DSY, DS
35	6.01	537.1041	$C_{27}H_{22}O_{12}$	$[M-H]^-$	493.1135, 295.0611, 185.0244, 109.0295	Lithospermic*	2.434	DSY, DS

(Cont'd...)

Table 3. *(Continued)*

No.	t_R (min)	Mass (ppm)	Molecular formula	Selected ion	ESI-MS² fragments	Compound name	Mass error (ppm)	Sources
36	6.06	431.0999	$C_{21}H_{20}O_{10}$	$[M-H]^-$	341.0645, 311.0563, 228.1595, 203.0871	Isovitexin*	3.572	DSY, TX
37	6.07	493.1142	$C_{26}H_{22}O_{10}$	$[M-H]^-$	295.0612, 185.0244, 109.0295	Salvianolic acid A or its isomer	0.304	DSY, DS
38	6.21	717.1459	$C_{36}H_{30}O_{16}$	$[M-H]^-$	519.0937, 339.0511, 321.0405	Salvianolic acid E	1.295	DSY, DS
39	6.33	717.1462	$C_{36}H_{30}O_{16}$	$[M-H]^-$	519.0937, 339.0511, 321.0405	Salvianolic acid B*	0.184	DSY, DS
40	6.64	493.1141	$C_{26}H_{22}O_{10}$	$[M-H]^-$	295.0612, 185.0244, 109.0295	Salvianolic acid A or its isomer	0.243	DSY, DS
41	7.16	493.1142	$C_{26}H_{22}O_{10}$	$[M-H]^-$	295.0611, 185.0243, 109.0295	Salvianolic acid A or its isomer	0.487	DSY, DS
42	7.50	491.0986	$C_{26}H_{20}O_{10}$	$[M-H]^-$	293.0455, 265.0506, 197.0455	Isosalvianolic acid C*	0.468	DSY, DS
43	8.65	491.0986	$C_{26}H_{20}O_{10}$	$[M-H]^-$	293.0455, 249.0555, 135.0451	Salvianolic acid C	0.529	DSY, DS
44	10.57	311.1277	$C_{19}H_{18}O_4$	$[M+H]^-$	267.1377, 203.0853	Tanshinaldehyde	-3.929	DSY, DS
45	10.80	327.1238	$C_{19}H_{20}O_5$	$[M-H]^-$	283.1340, 239.1441	1S-hydroxy-anhydride of 16Rcryptotanshinone	0.040	DSY, DS
46	10.83	311.1277	$C_{19}H_{18}O_4$	$[M+H]^-$	293.1191, 275.1058, 203.0852	Tanshinone IIB	−0.307	DSY, DS
47	10.94	309.1119	$C_{19}H_{16}O_4$	$[M+H]^-$	265.1223, 223.0755, 203.0854	Salvianolic aldehyde	−0.438	DSY, DS
48	11.03	313.1445	$C_{19}H_{22}O_4$	$[M-H]^-$	269.1543, 213.0914	Neocryptotanshinone*	−0.008	DSY, DS
49	11.04	297.1484	$C_{19}H_{20}O_3$	$[M+H]^-$	253.1586, 203.0853	Isocryptotanshinone	−0.674	DSY, DS
50	11.23	279.1014	$C_{18}H_{14}O_3$	$[M+H]^-$	261.0907, 203.0852	Dihydrotanshinone I*	−0.469	DSY, DS
51	11.51	295.1327	$C_{19}H_{18}O_3$	$[M+H]^-$	267.1379, 249.1266, 203.0853	Tanshinone IIA*	−4.431	DSY, DS
52	11.79	297.1482	$C_{19}H_{20}O_3$	$[M+H]^-$	279.1378, 203.0852	Cryptotanshinone*	−4.704	DSY, DS

Note: *Compared with reference compounds.

Abbreviations: DS: *Salvia miltiorrhiza Bge.*; DSY: Dan-Shen-Yin; ESI-MS2: Electrospray ionization tandem mass spectrometry; MS: Mass spectrometry; SR: *Amomum villosum Lour.*; TX: *Santalum album L.*; t_R: Retention time; UHPLC: Ultra-high performance liquid chromatography.

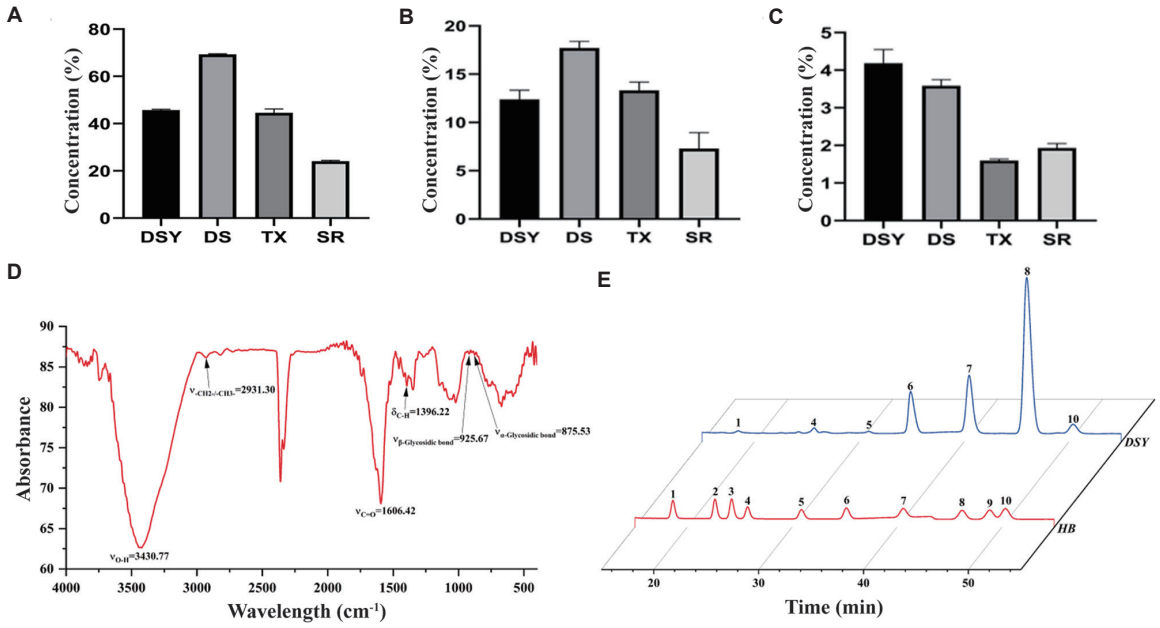


Figure 7. HPLC analysis of monosaccharide compositions of DSY decoction. (A) Total sugar content (mg/g). (B) The total uronic acid content (mg/g). (C) Total protein content (mg/g). (D) Infrared spectrum of the DSY polysaccharide. (E) HPLC chromatogram of the monosaccharide composition of DSY (1: Man 2: Lyx 3: Rib 4: Rha 5: GlcA 6: GalA 7: Glc 8: Gal 9: Xyl 10: Ara HB: Mixed standard).

Abbreviations: Ara: Arabinose; DS: *Salvia miltiorrhiza Bge.*; DSY: Dan-Shen-Yin; Gal: Galactose; GalA: Galacturonic acid; Glc: Glucose; GlcA: Glucuronic acid; HPLC: High performance liquid chromatography; Man: Mannose; Rha: Rhamnose; SR: *Amomum villosum Lour.*; TX: *Santalum album L.*

method. The contents of total uronic acid and proteins in DSY samples were 12.39% and 4.18%, respectively.

The monosaccharide composition of DSY polysaccharide was analyzed using complete acid hydrolysis followed by PMP derivatization and HPLC analysis. As shown in Figure 7D, seven kinds of monosaccharides were identified, including mannose, rhamnose, glucuronic acid, galacturonic acid, glucose, galactose, and arabinose. In addition, the molar percentages of monosaccharide composition were calculated based on their respective peak areas (Table 4). The results revealed that DSY polysaccharide is primarily composed of galactose, glucose, and galacturonic acid.

FTIR spectroscopy (Figure 7E) confirmed the presence of characteristic polysaccharide functional groups. The O–H stretching vibration at 3431 cm^{-1} indicates intermolecular hydrogen bonding. The peak at 2931 cm^{-1} corresponds to $–CH_2–$ or $–CH_3$ stretching vibrations, while the strong absorption at 1606 cm^{-1} indicates the C=O stretch of free carboxyl groups. The peaks at 1396 cm^{-1}, 926 cm^{-1}, and 871 cm^{-1} are assigned to C–H bending, β-glycosidic, and α-glycosidic bonds, respectively. These results are consistent with typical features of plant-derived polysaccharides.

The relative contents of crude polysaccharides in their respective aqueous extracts were 9.8% (DSY), 12.4% (DS), 16% (SR), and 6.4% (TX), indicating that polysaccharides are important components of DSY, primarily derived from SR and DS.

Although polysaccharide macromolecules have complex structures and poor oral absorbability, studies have found that plant polysaccharides can exhibit biological effects in the gastrointestinal tract.[27] DS polysaccharides have been shown to regulate the gut microbiota homeostasis.[28] Moreover, the findings of Gao *et al.*[29] suggest that disruption of the gut microbiota may be a key factor contributing to the worsening of gastric mucosal inflammation, and that restoring gut microbiota balance could be a significant approach to curing or preventing the progression from chronic atrophic gastritis to gastric cancer. In addition, Liu *et al.*[30] found that purified SR polysaccharide (AVLP-2) improved the oxidative stress status of the gastric mucosa by increasing superoxide dismutase activity and glutathione levels and inhibiting malondialdehyde accumulation. Therefore, in the treatment of gastritis, the polysaccharide of DSY may play a significant role. Despite this, polysaccharides have garnered limited attention in previous gastritis studies investigating DSY's mechanisms of action.

3.6. Network pharmacology analysis

A total of 1138 targets related to 67 compounds (15 volatile and 52 nonvolatile) were obtained through the TCMSP, HERB, and SwissTargetPrediction databases. Concurrently, 1719 targets related to gastritis were obtained through the DisGeNet, GeneCards, and MalaCards databases. Venn diagram analysis (Figure 8A) revealed 195 overlapping targets, representing potential therapeutic targets of DSY for treating gastritis. Subsequently, the compounds identified in DSY decoction and these overlapping targets were imported into Cytoscape 3.9.1 to construct a compound–target–disease interaction network (Figure 8B). Network topology parameters–degree, betweenness centrality, and closeness centrality value–were used to evaluate node importance in the network. As shown in Table 5, 22 compounds (5 volatile and 17 nonvolatile) exhibited values greater than the corresponding median values, suggesting their potential as key bioactive components of DSY in treating gastritis.

The shared targets DSY compounds and gastritis were imported to the STRING database, resulting in a PPI network containing 194 nodes and 1142 edges (Figure 8C). The CytoNCA plugin in Cytoscape was then used to assess the importance of each node. Filtering conditions were set as follows: betweenness centrality ≥median, closeness centrality ≥median, degree ≥median, local average connectivity ≥median, eigenvector ≥median, and network ≥median. Ultimately, 55 core targets, including TNF, IL2, IL6, AKT1, STAT3, and TP53, were screened from the 195 intersecting targets (Figure 8C).

The GO enrichment analysis of these 55 core targets returned 1373 terms, including 1234 biological processes, 52 cellular components, and 87 molecular functions. The top 10 terms in each category are shown in Figure 8D. In the biological process category, the therapeutic effects of DSY appear to involve a response to reactive oxygen species. Membrane raft, transcription regulator complex, side of membrane, and endoplasmic reticulum lumen were enriched in the cellular component category. In the molecular function category, protein kinase binding, DNA-

Table 4. Molar percentages of monosaccharide composition in DSY polysaccharide.

Monosaccharide	Mannose	Rhamnose	Glucuronic acid	Galacturonic acid	Glucose	Galactose	Arabinose
Molar %	0.21	0.53	0.15	4.12	6.24	18.07	0.84

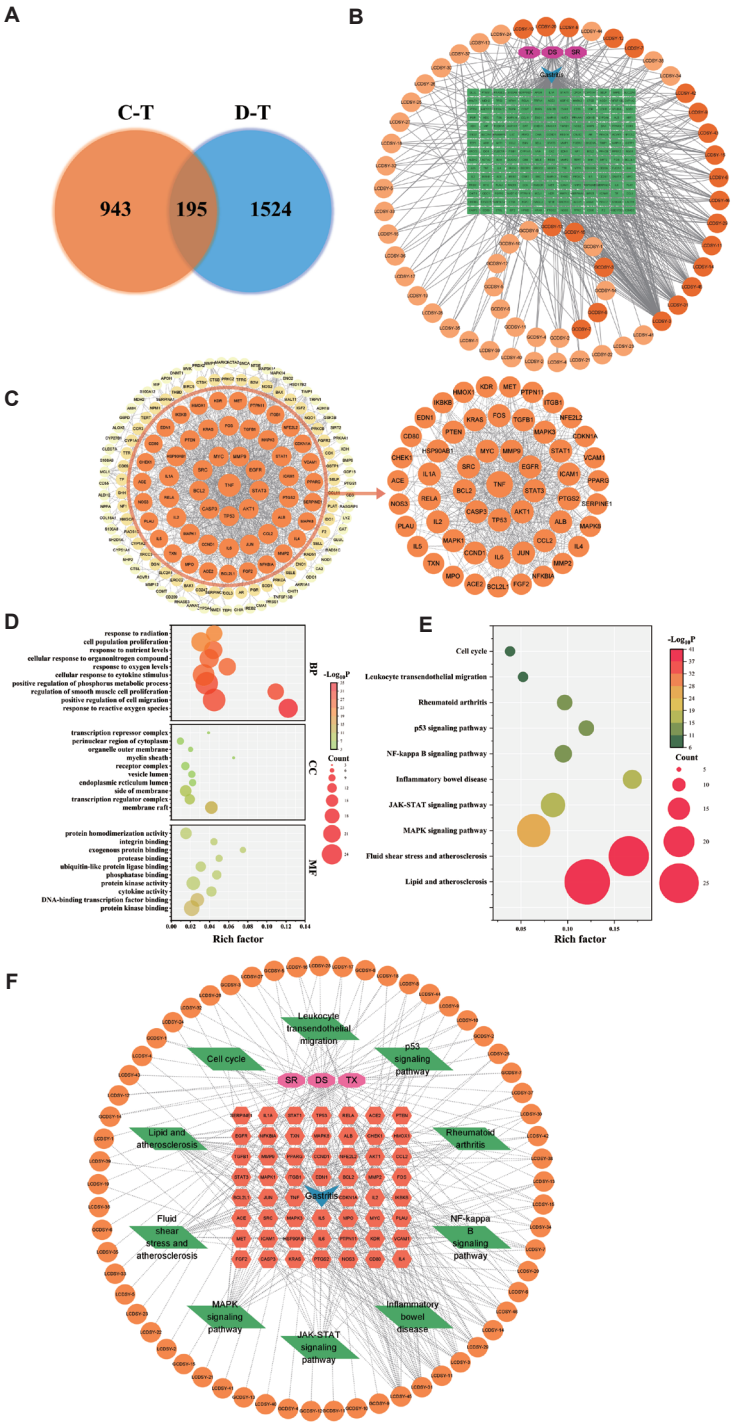


Figure 8. Network pharmacology-based prediction of the mechanisms of DSY in treating gastritis. (A) Venn diagram showing overlapping targets between DSY-related compounds and gastritis-related genes. (B) PPI network and core targets. (C) Compounds-potential targets-disease network. (D) Disease-core targets-compounds-pathways interaction network. (E) GO enrichment analysis of biological processes, molecular functions, and cellular components of core targets. (F) KEGG enrichment analysis of effect targets of pathways modulated by DSY compounds.
Abbreviations: CC: Cellular component; DS: *Salvia miltiorrhiza Bge.*; DSY: Dan-Shen-Yin; GO: Gene Ontology; IL2: Interleukin 2; IL6: Interleukin 6; JAK: Janus kinase; KEGG: Kyoto Encyclopedia of Genes and Genomes; MAPK: Mitogen-activated protein kinase; MF: Molecular function; NF-κB: Nuclear factor kappa B; PPI: Protein–protein interaction; STAT3: Signal transducer and activator of transcription 3; SR: *Amomum villosum Lour.*; TNF: Tumor necrosis factor; TP53: Tumor protein p53; TX: *Santalum album L.*

Table 5. Degree, betweenness, and closeness values of potential bioactive compounds in DSY targeting gastritis

Serial number	Compound name	Degree	Betweenness	Closeness	Sources
LCDSY-3	Citric acid	92	33661.1680	0.1223	DSY, DS
LCDSY-31	Rosmarinic acid	28	7463.3510	0.1155	DSY, DS
LCDSY-45	Tanshinone IIA	25	6402.2240	0.1144	DSY, DS
LCDSY-14	Caffeic acid	24	6760.6210	0.1158	DSY, DS
LCDSY-11	Epicatechin	24	5167.0913	0.1149	DSY, SR
LCDSY-46	Cryptotanshinone	16	2765.5713	0.1143	DSY, DS
LCDSY-29	Salvianolic acid B	16	5837.8240	0.1124	DSY, DS
LCDSY-6	Danshensu	13	2847.7444	0.1134	DSY, DS
LCDSY-15	Catechin	12	1437.6676	0.1137	DSY, SR
LCDSY-43	Isocryptotanshinone	11	1593.7957	0.1137	DSY, DS
LCDSY-42	Neocryptotanshinone	10	803.9311	0.1137	DSY, DS
LCDSY-9	Protocatechuic acid	9	1740.7864	0.1136	DSY, DS, SR
LCDSY-7	Vanillin	8	1034.0078	0.1136	DSY, TX
LCDSY-20	Salvianolic acid A	7	509.3273	0.1121	DSY, DS
LCDSY-10	3,4-Dihydroxyhydrocinnamic acid	7	717.6403	0.1128	DSY, DS
LCDSY-8	Vanillic acid	7	737.9602	0.1135	DSY, SR
LCDSY-12	Protocatechualdehyde	6	1142.4958	0.1123	DSY, DS, SR
GCDSY-8	Isovanillin	5	471.3908	0.1132	DSY, DS
GCDSY-7	Bornyl acetate	4	600.2523	0.1105	DSY, SR, TX
GCDSY-15	Diepicedrene-1-oxide	3	515.2957	0.1034	DSY, TX
GCDSY-3	Benzeneacetaldehyde	3	461.9877	0.1066	DSY, SR, DS
GCDSY-13	Cryptomeridiol	2	15.5880	0.1101	DSY, DS

Notes: Degree refers to the number of connections to other nodes in the network. Betweenness refers to the frequency of a node appearing on shortest paths between nodes. Closeness refers to the average shortest path from the node to all other nodes.
Abbreviations: DS: *Salvia miltiorrhiza Bge.*; DSY: Dan-Shen-Yin; SR: *Amomum villosum Lour.*; TX: *Santalum album L.*

binding transcription factor binding, cytokine activity, and protein kinase activity were enriched.

As shown in Figure 8F, the KEGG enrichment analysis indicated that 10 out of the top 20 pathways (total = 170 pathways) were associated with inflammation. These include lipid and atherosclerosis, fluid shear stress and atherosclerosis, MAPK signaling pathway, JAK-STAT signaling pathway, inflammatory bowel disease, nuclear factor-kappa B (NF-κB) signaling pathway, p53 signaling pathway, rheumatoid arthritis, leukocyte transendothelial migration, and cell cycle. A disease-core target-compound-pathway network constructed using Cytoscape 3.9.1 exhibited 134 nodes and 346 edges (Figure 8F). This network illustrates that one compound can act on multiple targets while multiple compounds act on a common target, and the targets are involved in different signaling pathways.

In summary, this study employed network pharmacology analysis based on the comprehensive characterization of DSY decoction, thereby elucidating its active compounds, core targets, and associated pathways involved in the treatment of gastritis. The analysis identified 22 bioactive compounds, potentially representing the key material basis by which DSY exerts its therapeutic effects. At present, most of these compounds have been previously reported in pharmacological studies to exhibit a range of activities relevant to the treatment of gastritis. For instance, rosmarinic acid has a significant gastric protective effect as it increases antioxidant defense and PGE_2 secretion.[31] Hiruma Lima *et al.*[32] found that Epi present in *Virola surinamensis* resin exhibits anti-ulcer activity. Catechin and isocryptotanshinone have the potential preventive effects against gastric carcinogenesis.[33,34] Cheng *et al.*[35] proposed that protocatechuic acid can treat oxidative stress-associated gastrointestinal ulcer diseases by inducing Parkinson disease protein 7 (DJ-1) expression. The results of Murakami *et al.*[36] indicated that salvianolic acid A shows antisecretory and anti-ulcer activity by inhibiting the gastric H^+, K^+-ATPase. Ren *et al.*,[37] using a rat model of chronic atrophic gastritis (CAG), demonstrated that tanshinone IIA may alleviate inflammation and cellular apoptosis by inhibiting the activation of the JAK2/

STAT3 signaling pathway and the nuclear translocation of NF-κB, thereby mitigating structural and functional damage to the gastric mucosa. Yang *et al.*[38] demonstrated that caffeic acid attenuates hydrochloric acid/ethanol-induced gastric inflammatory responses by inhibiting the JNK, IRAK1, and IRAK4 signaling pathways in a murine model. In addition, numerous studies have shown that Cry, salvianolic acid B, danshensu, neocryptotanshinone, vanillin, vanillic acid, and bornyl acetate have significant anti-inflammatory activities.[39-46] These findings suggest that DSY has a substantial material basis for the prevention and treatment of gastritis and its progression to gastric cancer. Moreover, the constructed disease-core target-compound-pathway interaction network suggests that DSY exerts its therapeutic effects through multiple targets and signaling pathways, which may underlie its notable clinical efficacy. Half of the top 20 pathways analyzed by KEGG enrichment were associated with inflammation. Among them, MAPK signaling pathway, NF-κB signaling pathway, p53 signaling pathway, and JAK-STAT signaling pathway are common signaling pathways targeted in CAG treatment.[47,48] In addition, previous studies have shown that pathways associated with inflammatory bowel disease, rheumatoid arthritis, leukocyte transendothelial migration, and cell cycle are strongly associated with gastritis caused by *H. pylori*.[49-52] These findings further demonstrate that DSY can effectively alleviate and protect against inflammatory injury of the gastric mucosa, thereby preventing or treating gastritis.

4. Conclusion

Clinical studies have shown that DSY demonstrates notable efficacy in the treatment of gastritis. As a multi-component compound preparation, DSY contains diverse chemical constituents, and reliance on a single detection method is insufficient to comprehensively elucidate its material basis. Therefore, this study characterized the nonvolatile compounds, volatile compounds, and polysaccharides in DSY decoction using UHPLC-Orbitrap Exploris MS, HS-GC-MS, and HPLC. Fifteen volatile and fifty-two nonvolatile compounds were identified in the DSY decoction, primarily originating from TX and DS. In addition, polysaccharides in the DSY decoction, primarily derived from SR and DS, consisted mainly of galactose, glucose, and galacturonic acid. Finally, based on a comprehensive characterization of DSY decoction, network pharmacology analysis identified 22 active compounds interacting with 55 core targets and modulating 10 inflammation-related signaling pathways, thereby elucidating the potential mechanisms underlying the therapeutic effects of DSY in treating gastritis. However, this study lacks a systematic quality assessment of DSY and does not include an analysis of its blood-absorbed (bioavailable) compounds. Quantifying the therapeutic efficacy by using selected active compounds as quality control markers can substantially improve the accuracy and reliability of DSY's quality evaluation. This study provides references and a basis for the development of such evaluation methods for DSY in the future. In addition, as a multi-component compound preparation, the mechanisms through which DSY treats gastritis and prevents its progression to gastric cancer warrant further investigation.

Acknowledgments

None.

Funding

This study was supported by the Science and Technology Program of Tianjin, China (Grant numbers: 24ZYJDSS00310 and 24ZYJDSS00300).

Conflict of interest

Miaomiao Jiang is an Editorial Board Member of this journal, but was not in any way involved in the editorial and peer-review process conducted for this paper, directly or indirectly. Separately, other authors declared that they have no known competing financial interests or personal relationships that could have influenced the work reported in this paper.

Author contributions

Conceptualization: Miaomiao Jiang
Formal analysis: Miaomiao Jiang, Jianbing Dong, Zhirong Zhou
Investigation: Jianbing Dong, Zhirong Zhou
Methodology: Jianbing Dong, Zhirong Zhou, Peng Lei
Writing–original draft: Jianbing Dong, Zhirong Zhou, Yi Chen
Writing–review & editing: Jianbing Dong, Zhirong Zhou, Yi Chen, Qingrui Zhang

Ethics approval and consent to participate

Not applicable.

Consent for publication

Not applicable.

Availability of data

Data is available from the corresponding author upon reasonable request.

References

1. Wafaey AA, El-Hawary SS, Abdelhameed MF, *et al.* Green synthesis of zinc oxide nanoparticles using ethanolic extract of *Gliricidia sepium* (Jacq.) kunth. Ex. Walp.,

stem: Characterizations and their gastroprotective effect on ethanol-induced gastritis in rats. *Bioorg Chem*. 2024;145:107225.

doi: 10.1016/j.bioorg.2024.107225

2. Gao X, Yin P, Ren Y, *et al*. Predicting personalized diets based on microbial characteristics between patients with superficial gastritis and atrophic gastritis. *Nutrients*. 2023;15(22):4738.

doi: 10.3390/nu15224738

3. López MJ, Carbajal J, Alfaro AL, *et al*. Characteristics of gastric cancer around the world. *Crit Rev Oncol Hematol*. 2023;181:103841.

doi: 10.1016/j.critrevonc.2022.103841

4. Li JX, Chen J, Lu B, Wang YG. Consensus on diagnosis and treatment of chronic atrophic gastritis with integrated traditional Chinese and western medicine (2017). *Chin J Integr Tradit West Med Dig*. 2018;26(2):121-131.

doi: 10.3969/j.issn.1671-038X.2018.02.03

5. Du LJ, Chen BR, Kim JJ, Kim S, Shen JH, Dai N. Helicobacter pylori eradication therapy for functional dyspepsia: Systematic review and meta-analysis. *World J Gastroenterol*. 2016;22(12):3486-3495.

doi: 10.3748/wjg.v22.i12.3486

6. Li Z, Wu C, Li L, *et al*. Effect of long-term proton pump inhibitor administration on gastric mucosal atrophy: A meta-analysis. *Saudi J Gastroenterol*. 2017;23(4):222-228.

doi: 10.4103/sjg.SJG-573-16

7. Liu M, Li Z, Yue O, *et al*. Material basis and integrative pharmacology of danshen decoction in the treatment of cardiovascular diseases. *Phytomedicine*. 2023;108:154503.

doi: 10.1016/j.phymed.2022.154503

8. Yu ZH. Observation on the therapeutic effect of modified danshen yin on chronic gastritis. *Chin J Clin Ration Drug Use*. 2012;5(4):86-87.

doi: 10.15887/j.cnki.13-1389/r.2012.04.017

9. Sun XN, Su YQ, Xu XQ, Zhao CP, Ji JL, Sun B. Treating gastric collaterals obstructed type of chronic gastritis with the danshen decoction by professor sun bin. *Clin J Chin Med*. 2021;13(14):69-72.

doi: 10.3969/j.issn.1674-7860.2021.14.020

10. Wang Df, Zhao M, Dong XY, Li XY. Clinical effect and mechanism of modified danshenyin against chronic atrophic gastritis with syndrome of stasis in stomach collateral: Based on theory of collateral diseases. *Chin J Exp Tradit Med Form*. 2022;28(23):122-127.

doi: 10.13422/j.cnki.syfjx.20221623

11. Li J, Chai JB. Experimental study on the mechanism of danshen yin in preventing pyloric ligation induced gastric ulcer in rats. *Chin Arch Tradit Chin Med*. 2006;(4):588-589.

doi: 10.3969/j.issn.1673-7717.2006.04.003

12. Zhang HQ, Liu L. Effects and mechanisms of danshenyin on accelerate gastric ulcer healing. *Chin J Clin Pharmacol Ther*. 2005;(7):812-818.

doi: 10.3969/j.issn.1009-2501.2005.07.022

13. Liu MN, Yuan G, Luo G, *et al*. Network pharmacology analysis and experimental verification strategies reveal the action mechanism of danshen decoction in treating ischemic cardiomyopathy. *Evid Based Complement Alternat Med*. 2022;2022:7578055.

doi: 10.1155/2022/7578055

14. Jing YS, Ma YF, Wang FF, Zhang YW, Wu LF, Zhang DS. Research progress on content determination, structural characterization and pharmacological activity of *Salvia miltiorrhiza* polysaccharides. *China Pharm*. 2020;31(16):2037-2042.

doi: 10.6039/j.issn.1001-0408.2020.16.22

15. Shan XX, Hong BZ, Liu J, *et al*. Review of chemical composition, pharmacological effects, and clinical review of chemical composition, pharmacological effects, and clinical. *China J Chin Mater Med*. 2021;46(21):5496-5511.

doi: 10.19540/j.cnki.cjcmm.20210630.203

16. Yang DS, Zhang Y, Shu Y, Cao H. Research progress on chemical constituents and pharmacological effects of *Amomum villosum*. *Guangdong Chem Ind*. 2022;49(8):111-114.

doi: 10.3969/j.issn.1007-1865.2022.08.035

17. Zhang W, Liu YY, Zou YC, Yu M, Zhan ZL, Xin GS. Advances on the investigation of phytochemistry and pharmacological activities of heartwood of *Santalum album* L. *World Sci Technol Modernization Tradit Chin Med*. 2020;22(12):4300-4307.

doi: 10.11842/wst.20200407016

18. Navarini L, Gilli R, Gombac V, Abatangelo A, Bosco M, Toffanin R. Polysaccharides from hot water extracts of roasted *Coffea arabica* beans: Isolation and characterization. *Carbohydr Polym*. 1999;40(1):71-81.

doi: 10.1016/S0144-8617(99)00032-6

19. Dubois M, Gilles KA, Hamilton JK, Rebers PA, Smith F. Colorimetric method for determination of sugars and related substances. *Anal Chem*. 1956;28(3):350-356.

doi: 10.1021/ac60111a017

20. Blumenkrantz N, Asboe-Hansen G. New method for quantitative determination of uronic acids. *Anal Biochem*. 1973;54(2):484-489.

doi: 10.1016/0003-2697(73)90377-1

21. Lowry OH, Rosebrough NJ, Farr AL, Randall RJ. Protein

measurement with the folin phenol reagent. *J Biol Chem*. 1951;193(1):265-275.

doi: 10.1016/S0021-9258(19)52451-6

22. Sun X, Wang H, Han X, Chen S, Zhu S, Dai J. Fingerprint analysis of polysaccharides from different *Ganoderma* by HPLC combined with chemometrics methods. *Carbohydr Polym*. 2014;114:432-439.

doi: 10.1016/j.carbpol.2014.08.048

23. Guo JS, Liu HY, Huang XJ, Zhang M, Chen J, Nie ZW. Effect of the different extracts of santali albi lignum on isolated the small intestine movement function and gastric emptying of mice. *Chin J Exp Tradit Med Form*. 2012;18(2):139-143.

doi: 10.3495/R.2011116.1422.001

24. Zhang HF, Xue YW. Empirical study in the relation of gastric mucosal lesion with gastric emptying and gastric acid secretion. *Zhonghua Wei Chang Wai Ke Za Zhi*. 2008;11(5):472-476.

25. Li J, Ren XJ, Lou Y. Research progress on the pathogenesis of gastric cancer induced by bile acids and the potential effects of *Salvia miltiorrhiza* extract. *J Chin Foreign Med Pharm Res*. 2024;3(8):156-158.

doi: 10.3969/j.issn.2096-6229.2024.08.052

26. Miao HX, Zhang HW, Wang J. Research progress on pharmacological mechanism of *Salvia miltiorrhiza* and its extracts in the treatment of oral malignant tumors. *Glob Tradit Chin Med*. 2023;16(3):565-570.

doi: 10.3969/j.issn.1674-1749.2023.03.038

27. Yu YY, Zhu YY, Zhang SC, *et al*. Research progress of plant polysaccharides in treatment of gastrointestinal diseases. *Chin Arch Tradit Chin Med*. 2024;42(4):194-199.

doi: 10.13193/j.issn.1673-7717.2024.04.038

28. Li L, Lan X, Peng X, *et al*. Polysaccharide from *Salviae miltiorrhizae* radix et rhizoma attenuates the progress of obesity-induced non-alcoholic fatty liver disease through modulating intestinal microbiota-related gut-liver axis. *Int J Mol Sci*. 2022;23(18):10620.

doi: 10.3390/ijms231810620

29. Gao BQ, Liu Y, Chen YH, Yang DC, Liu GP. Characteristics of gut microbiota in patients with chronic atrophic gastritis. *Chin J Microecol*. 2024;36(3):282-291.

doi: 10.3389/fcimb.2019.00369

30. Liu H, Zhuang S, Liang C, *et al*. Effects of a polysaccharide extract from *Amomum villosum* lour. on gastric mucosal injury and its potential underlying mechanism. *Carbohydr Polym*. 2022;294:119822.

doi: 10.1016/j.carbpol.2022.119822

31. Heidari F, Komeili-Movahhed T, Hamidizad Z, Moslehi A. The protective effects of rosmarinic acid on ethanol-induced gastritis in male rats: Antioxidant defense enhancement. *Res Pharm Sci*. 2021;16(3):305-314.

doi: 10.4103/1735-5362.314829

32. Hiruma-Lima CA, Batista LM, Almeida AB, *et al*. Antiulcerogenic action of ethanolic extract of the resin from *Virola surinamensis* warb. (*Myristicaceae*). *J Ethnopharmacol*. 2009;122(2):406-409.

doi: 10.1016/j.jep.2008.12.023

33. Chen ZM, Huang L, Li MM, Meng L, Ying SC, Xu AM. Inhibitory effects of isocryptotanshinone on gastric cancer. *Sci Rep*. 2018;8(1):9307.

doi: 10.1038/s41598-018-27638-0

34. Ohno T, Ohtani M, Suto H, *et al*. Effect of green tea catechins on gastric mucosal dysplasia in insulin-gastrin mice. *Oncol Rep*. 2016;35(6):3241-3247.

doi: 10.3892/or.2016.4717

35. Cheng YT, Lin JA, Jhang JJ, Yen GC. Protocatechuic acid-mediated DJ-1/PARK7 activation followed by PI3K/mTOR signaling pathway activation as a novel mechanism for protection against ketoprofen-induced oxidative damage in the gastrointestinal mucosa. *Free Radic Biol Med*. 2019;130:35-47.

doi: 10.1016/j.freeradbiomed.2018.10.415

36. Murakami S, Kijima H, Isobe Y, *et al*. Effect of salvianolic acid a, a depside from roots of *Salvia miltiorrhiza*, on gastric H+,K(+)-ATPase. *Planta Med*. 1990;56(4):360-363.

doi: 10.1055/s-2006-960982

37. Ren L, Wang LM, Zhang M. Study on the mechanism of tanshinone IIA alleviates gastric mucosal injury in rats with chronic atrophic gastritis by inhibiting JAK2/STAT3 pathway. *Tianjin J Tradit Chin Med*. 2024;41(7):914-921.

doi: 10.11656/j.issn.1672-1519.2024.07.19

38. Yang WS, Jeong S, Yi YS, *et al*. IRAK1/4-targeted anti-inflammatory action of caffeic acid. *Mediators Inflamm*. 2013;2013:518183.

doi: 10.1155/2013/518183

39. Ciciliato MP, Souza MCD, Tarran CM, Castilho ALTD, Vieira AJ, Rozza AL. Anti-inflammatory effect of vanillin protects the stomach against ulcer formation. *Pharmaceutics*. 2022;14(4):755.

doi: 10.3390/pharmaceutics14040755

40. Guo R, Li L, Su J, *et al*. Pharmacological activity and mechanism of tanshinone IIA in related diseases. *Drug Des Devel Ther*. 2020;14:4735-4748.

doi: 10.2147/dddt.s266911

41. Li J, Chen YH, Li LZ, *et al*. Omics and transgenic analyses reveal that salvianolic acid b exhibits its anti-inflammatory effects through inhibiting the mincle-syk-related pathway in

macrophages. *J Proteome Res*. 2021;20(7):3734-3748.

doi: 10.1021/acs.jproteome.1c00325

42. Wu C, Zhao W, Zhang X, Chen X. Neocryptotanshinone inhibits lipopolysaccharide-induced inflammation in RAW264.7 macrophages by suppression of NF-κB and iNOS signaling pathways. *Acta Pharm Sin B*. 2015;5(4):323-329.

doi: 10.1016/j.apsb.2015.01.010

43. Wu YH, Wu YR, Li B, Yan ZY. Cryptotanshinone: A review of its pharmacology activities and molecular mechanisms. *Fitoterapia*. 2020;145:104633.

doi: 10.1016/j.fitote.2020.104633

44. Yoo SR, Jeong SJ, Lee NR, Shin HK, Seo CS. Simultaneous determination and anti-inflammatory effects of four phenolic compounds in dendrobii herba. *Nat Prod Res*. 2017;31(24):2923-2926.

doi: 10.1080/14786419.2017.1300798

45. Zhang J, Zhang Q, Liu G, Zhang N. Therapeutic potentials and mechanisms of the Chinese traditional medicine danshensu. *Eur J Pharmacol*. 2019;864:172710.

doi: 10.1016/j.ejphar.2019.172710

46. Zhang T, Lu SH, Bi Q, *et al*. Volatile oil from amomi fructus attenuates 5-fluorouracil-induced intestinal mucositis. *Front Pharmacol*. 2017;8:786.

doi: 10.3389/fphar.2017.00786

47. Jia JH, Zhao H, Li F, *et al*. Research on drug treatment and the novel signaling pathway of chronic atrophic gastritis. *Biomed Pharmacother*. 2024;176:116912.

doi: 10.1016/j.biopha.2024.116912

48. Liu X, Wang S, Li J, Zhang J, Liu D. Regulatory effect of traditional Chinese medicines on signaling pathways of process from chronic atrophic gastritis to gastric cancer. *Chin Herb Med*. 2022;14(1):5-19.

doi: 10.1016/j.chmed.2021.10.008

49. Nagura H, Ohtani H, Sasano H, Matsumoto T. The immuno-inflammatory mechanism for tissue injury in inflammatory bowel disease and helicobacter pylori-infected chronic active gastritis. Roles of the mucosal immune system. *Digestion*. 2001;63 Suppl 1:12-21.

doi: 10.1159/000051905

50. Nakamura H, Mukai E, Hirano D, Matsuhisa T, Yamada N, Yoshino S. Gastrointestinal disorder and helicobacter pylori infection in patients with rheumatoid arthritis. *Mod Rheumatol*. 2001;11(1):23-27.

doi: 10.3109/s101650170039

51. Polat A, Cinel L, Dusmez D, Aydin O, Egilmez R. Expression of cell-cycle related proteins in helicobacter pylori gastritis and association with gastric carcinoma. *Neoplasma*. 2002;49(2):95-100.

doi: 10.1038/sj.neo.7900211

52. Suzuki T, Ina K, Nishiwaki T, *et al*. Differential roles of interleukin-1beta and interleukin-8 in neutrophil transendothelial migration in patients with helicobacter pylori infection. *Scand J Gastroenterol*. 2004;39(4):313-321.

doi: 10.1080/00365520310008610

ACCSCIENCE PUBLISHING

Eurasian Journal of Medicine and Oncology

ORIGINAL RESEARCH ARTICLE

Basic medication therapy based on target glycated hemoglobin levels in patients with ischemic heart disease and diabetes

Raisa Trigulova[1†], Alisher Ikramov[2,3†*], Dilnoza Alimova[1], Shukhrat Doniyorov[1], Dilafruz Akhmedova[1], and Shakhnoza Mukhtarova[4]

[1]Scientific Laboratory of Preventive Cardiology, The Republican Specialized Scientific-Practical Medical Center of Cardiology, Tashkent, Uzbekistan

[2]Department of Mathematics, School of Humanities, Natural, and Social Sciences, New Uzbekistan University, Tashkent, Uzbekistan

[3]Laboratory of Biomedical Informatics, V.I. Romanovskiy Institute of Mathematics, Uzbekistan Academy of Sciences, Tashkent, Uzbekistan

[4]Department of Pediatric Endocrinology, Medical-Pedagogical and Medical Faculty, Tashkent Pediatric Medical Institute, Tashkent, Uzbekistan

Abstract

Introduction: Type 2 diabetes mellitus (T2DM) and ischemic heart disease (IHD) are significant medical conditions. Research indicates that patients with T2DM have a substantially increased risk of developing cardiovascular diseases, necessitating meticulous monitoring and management of both diabetes and associated cardiovascular conditions. Achieving target glycated hemoglobin (HbA1c) levels is crucial for effective T2DM treatment.

Objective: This study investigates the prescribed basic medication therapy in patients with T2DM and IHD based on target HbA1c levels.

Methods: A prospective observational study was conducted at the Republican Specialized Scientific-Practical Medical Center of Cardiology in Uzbekistan from 2022 to 2024, involving 130 patients with T2DM and IHD. Clinical, functional, and instrumental parameters, including left ventricular ejection fraction and other metabolic indicators, were assessed. Data were collected using standardized questionnaires and analyzed using the Statistical Package for Social Sciences. Logistic and linear regression models were used to analyze the efficiency of medication treatment.

Results: Among the cohort, 56.9% achieved an HbA1c level ≤8%, while 43.1% had an HbA1c level ≥8%. Significant differences were observed in age, gender distribution, duration of diabetes, and IHD between the two groups. Medication therapy varied significantly, with higher usage of metformin and insulin in patients with an HbA1c level ≥8%. The linear regression model predicts HbA1c levels based on clinical data and dosages of prescribed medications with a root mean square error of 1.172 and a Spearman correlation coefficient of 0.826. The logistic regression model predicts achievement of target HbA1c levels with a receiver operating characteristic area under the curve value of 0.92.

Conclusion: The study highlights the importance of individualized medication therapy tailored to HbA1c levels to improve clinical outcomes in patients with T2DM and IHD. It also highlights differences in medication effects based on the target HbA1c levels in patients.

Keywords: Diabetes mellitus; Ischemic heart disease; Glycated hemoglobin; Medication therapy

†*These authors contributed equally to this work.*

***Corresponding author:**
Alisher Ikramov
(a.ikramov@newuu.uz)

Citation: Trigulova R, Ikramov A, Alimova D, Doniyorov S, Akhmedova D, Mukhtarova S. Basic medication therapy based on target glycated hemoglobin levels in patients with ischemic heart disease and diabetes. *Eurasian J Med Oncol.* 2025;9(3):185-196. doi: 10.36922/EJMO025160133

Received: April 18, 2025

Revised: May 8, 2025

Accepted: June 4, 2025

Published online: July 28, 2025

Copyright: © 2025 Author(s). This is an Open-Access article distributed under the terms of the Creative Commons Attribution License, permitting distribution, and reproduction in any medium, provided the original work is properly cited.

Publisher's Note: AccScience Publishing remains neutral with regard to jurisdictional claims in published maps and institutional affiliations.

1. Introduction

Type 2 diabetes mellitus (T2DM) and ischemic heart disease (IHD) are among the most prevalent chronic conditions worldwide, posing significant challenges to healthcare systems due to their high morbidity and mortality rates. The International Diabetes Federation estimates that the global prevalence of diabetes will continue to rise, reaching alarming levels by 2030.[1] Whiting *et al.*[1] provided global estimates of diabetes prevalence, highlighting the significant burden of DM and its complications. This increase underscores the urgent need for effective management strategies to mitigate the associated health risks.

Patients with T2DM are particularly vulnerable to cardiovascular diseases, including IHD, due to the complex interplay between hyperglycemia, insulin resistance, and cardiovascular risk factors. The United Kingdom Prospective Diabetes Study (UKPDS)[2] highlighted the critical role of blood-glucose control in reducing cardiovascular complications among patients with T2DM. Achieving target glycated hemoglobin (HbA1c) levels is a cornerstone of diabetes management, as it significantly lowers the risk of cardiovascular events.

HbA1c level serves as a reliable marker for long-term glycemic control, reflecting average blood glucose levels over the past 2 – 3 months. The American Diabetes Association recommends maintaining HbA1c levels below 7% to minimize the risk of diabetes-related complications. However, individual targets may vary based on patient characteristics, comorbidities, age, and treatment goals. Older adults with complex health conditions or intermediate health are advised to reach target levels of HbA1c below 8%.[3] Similarly, the Action to Control Cardiovascular Risk in Diabetes study analyzed the trajectory of HbA1c and its impact on cardiovascular outcomes, emphasizing the importance of maintaining optimal glycemic control.[4]

Medications used for glycemic control include sodium-glucose co-transporter 2 (SGLT2) inhibitors and glucagon-like peptide-1 (GLP-1) receptor agonists,[5-8] and metformin. The results of previous studies demonstrated that SGLT2 inhibitors significantly reduced the risk of major adverse cardiovascular events, heart failure hospitalization, and all-cause mortality; their combined use with GLP-1 receptor agonists is more effective than monotherapy. Metformin remains a cornerstone in T2DM management due to its proven efficacy in lowering HbA1c and reducing cardiovascular risk, as first demonstrated by the UKPDS. Insulin therapy is reserved for patients with suboptimal control despite oral medication, a pattern reflected in both the literature and the current study's findings.

In addition to antihyperglycemic medications, the use of cardiovascular drugs in managing IHD in diabetic patients is important. Previous studies emphasize the necessity of integrating antihypertensive therapy, particularly angiotensin-converting enzyme (ACE) inhibitors, angiotensin receptor blockers, and beta-blockers, into diabetes care.[9,10] Intensive glycemic control is linked to reduced cardiovascular and renal complications.[11-13] Most of these studies used structured clinical data, such as HbA1c levels, blood pressure, lipids, creatinine, and demographic variables, to construct predictive models of treatment efficacy or complication risk.[14-16] The data are usually used to train linear and logistic regression models, but recent works incorporate machine learning and metabolomic data to refine risk stratification.[17-21]

In addition, economic and systemic factors were also considered in diabetic management. Beran *et al.*[22] conducted a cost-effectiveness analysis of expanding access to newer antidiabetic medications in low- and middle-income countries, revealing that these therapies can be viable if priced appropriately. Nelson *et al.*[23] focused on the gaps in therapy adherence among insured United States patients with T2DM and cardiovascular disease, highlighting the discrepancy between guideline recommendations and real-world practice. These findings underscore the broader systemic and socioeconomic challenges that influence therapeutic outcomes.

2. Methodology

2.1. Patient selection and data collection

This study was performed at the Republican Specialized Scientific-Practical Medical Center of Cardiology in Uzbekistan from 2022 to 2024. A total of 130 patients previously diagnosed with T2DM and IHD were included in this study. The inclusion criteria for patients with T2DM were established according to the World Health Organization classification: (i) Patients with a left ventricular ejection fraction (LVEF) ≥50%, and (ii) patients with T2DM and heart failure with LVEF between 41% and 49%.

Patients were excluded if they had any of the following conditions: (i) A recent myocardial infarction (<3 months ago), (ii) chronic heart failure of New York Heart Association class III – IV, (iii) severe liver and kidney dysfunction, (iv) respiratory failure, (v) significant arrhythmias, and (vi) heart failure with LVEF ≤40%. Patients with lower levels of LVEF were excluded because they received a different treatment regimen in accordance with national standards of care in Uzbekistan, which could affect clinical outcomes and the extent of change in measured indicators.

Data were collected using standardized questionnaires administered to the patients during their hospital visits. The questionnaires included sections on demographic information, medical history, clinical parameters, and medication usage. It also included prescriptions issued within the hospital setting. Clinical, functional, and instrumental parameters, including LVEF and other metabolic indicators, were assessed.

2.2. Outcome measurement

We employed descriptive data analysis to examine changes in clinical characteristics over time. Changes were calculated by subtracting baseline (first observation) values from follow-up (second observation) values.

The primary outcome measure was the achievement of target HbA1c levels (≤8%) in patients with T2DM and IHD. This target level was selected according to the severity of IHD in patients and in compliance with Uzbekistan's and global treatment standards. Given that the patient population consisted primarily of older adults with complex/intermediate health, many of whom have pacemakers or are at risk of hypoglycemia, a target HbA1c below 8% was considered clinically appropriate. Moreover, as the study was conducted in a cardiological hospital, all admitted patients had IHD as their primary diagnosis, with T2DM as a comorbidity. Therefore, the target HbA1c levels used were not the same as those of a healthy population.

Secondary outcome measures included comparisons of demographic characteristics, clinical parameters, and medication usage between patients who achieved target HbA1c levels and those who did not. We also compared different medication types and outcomes using statistical analysis. We randomly permuted and split our dataset into training (70%) and test (30%) sets to construct linear regression and logistic regression models.

2.3. Statistical analysis

Data were analyzed using the Statistical Package for the Social Sciences version 23.0. Continuous variables were presented as mean ± standard deviation (SD). We applied *t*-tests and the Kruskal–Wallis test to compare variables. Categorical variables were presented as percentages and compared using Chi-squared tests. For non-parametric analysis of variance, we used Python 3.7 SciPy library (v1.15). Statistical significance was accepted at $p<0.05$. In addition, the multinomial logistic regression model from the Statsmodels library (v.0.15) was used.

2.4. Ethical considerations

The study was approved by the ethics committee of the Republican Specialized Scientific-Practical Medical Center of Cardiology (decision no. П3-202007041). All patients provided informed consent to participate in the study and received a full explanation of the study's objectives and methods. Confidentiality of data and the right to withdraw from the study were guaranteed to all participants. The study was conducted in accordance with the principles of the Declaration of Helsinki (as revised in 2013) and ethical guidelines for clinical research.

3. Results

The study included 130 patients diagnosed with T2DM and IHD. Table 1 presents the demographic and clinical characteristics of the cohort. A total of 75 patients achieved HbA1c levels ≤8% while 55 patients did not (≥8%).

3.1. Glycemic control and medication therapy

The study found significant differences in glycemic control and medication therapy between patients who achieved target HbA1c levels (≤8%) and those who did not (≥8%). The average age of participants with HbA1c levels ≤8% was significantly higher than those with HbA1c levels ≥8% (67.19 ± 9.73 years versus 63.48 ± 9.23 years, $t = 4.879$, $p=0.027$). In addition, a higher frequency of women was present in the HbA1c level ≥8% group compared to the HbA1c level ≤8% group during the second observation (62.5% vs. 48.6%, $t = 8.186$, $p=0.004$).

The duration of T2DM was higher among patients in the HbA1c level ≥8% group (11.12 ± 4.55 years) compared to the patients in the HbA1c level ≤8% group (7.04 ± 4.93 years, $t = 26.010$, $p=0.000$). Similarly, the duration of IHD was longer in the HbA1c level ≥8% group (8.38 ± 3.70 years) compared to the HbA1c level ≤8% group (6.93 ± 3.43 years, $t = 5.007$, $p=0.025$).

Table 2 shows the dosages of medications prescribed to patients. The duration of treatment before the second observation was 9.94±5.71 months (interquartile range = 6.00 – 12.00; minimum = 2.0, maximum = 31.0).

Medication therapy varied significantly between the two groups. Metformin was prescribed to 69.6% of patients with an HbA1c level ≥8%, compared to 35.1% of patients with an HbA1c level ≤8% ($t = 56.324$, $p=0.000$). Insulin therapy was also more common in the HbA1c level ≥8% group (41.1% vs. 9.5%, $t = 41.289$, $p=0.000$). Table 3 presents the distribution of antidiabetic medication prescriptions across patient groups, expressed as percentages.

Empagliflozin, a medication known for its cardiovascular benefits, was prescribed for all 130 patients in the study. Dipeptidyl peptidase-4 (DPP-4) inhibitors were more frequently prescribed to patients with an HbA1c

Table 1. Demographic and clinical characteristics of patients

Characteristic	HbA1c level ≤8% (*n*=75)	HbA1c level ≥8% (*n*=55)	*T*	*p*
Age, years (mean±standard deviation)	67.19±9.73	63.48±9.23	4.879	0.027
Female	48.6 (36)	62.5 (35)	8.186	0.004
Weight, kg (mean±standard deviation)	85.20±16.76	85.43±15.32	0.031	0.860
Height, cm (mean±standard deviation)	165.15±8.67	163.77±8.02	0.680	0.410
Body mass index, kg/m² (mean±standard deviation)	31.45±6.15	31.93±4.58	1.154	0.283
COVID-19 in anamnesis	48.6 (36)	58.9 (33)	4.366	0.037
Duration of diabetes, years (mean±standard deviation)	7.04±4.93	11.12±4.55	26.010	0.000
Duration of IHD, years (mean±standard deviation)	6.93±3.43	8.38±3.70	5.007	0.025
Atrial fibrillation	16.2 (12)	3.6 (2)	46.428	0.000
Mortality	0.0 (0)	1.8 (1)	1.818	0.178
History of myocardial infarction	35.1 (26)	35.7 (20)	0.015	0.904
History of PCI	29.7 (22)	28.6 (16)	0.066	0.798
History of CABG	10.8 (8)	7.1 (4)	2.028	0.154
History of Stroke	6.8 (5)	3.6 (2)	2.946	0.086
Proximal LAD Stenosis>50%	12.2 (9)	7.1 (4)	3.798	0.051
Complex 3-vessel disease	2.7 (2)	1.8 (1)	0.479	0.489

Note: Data are presented as *n* (%), unless stated otherwise.
Abbreviations: CABG: Coronary artery bypass grafting; HbA1c: Glycated hemoglobin; IHD: Ischemic heart disease; LAD: Left anterior descending; PCI: Percutaneous coronary intervention.

Table 2. Dosages of medications prescribed to patients during their first observation

Medication	HbA1c level ≤8% *n*=75				HbA1c level ≥8% *n*=55				*p*	Statistic
	Mean±SD	Q1 – Q3	Min; max	*n*	Mean±SD	Q1 – Q3	Min; max	*n*		
Valsartan	45.89±26.41	26.00 – 51.00	12.8; 103.0	21	34.33±11.79	26.00 – 44.75	26.0; 51.0	6	0.407	0.687
Fibrate	96.67±34.18	72.50 – 108.75	72.5; 145.0	3	96.67±34.18	72.50 – 126.88	72.5; 145.0	6	1.000	0.000
Rosuvastatin	15.54±4.85	10.00 – 20.00	5.0; 20.0	30	13.10±4.81	10.00 – 20.00	5.0; 20.0	29	0.052	3.769
Atorvastatin	15.00±5.00	10.00 – 20.00	10.0; 20.0	26	19.75±7.15	18.75 – 20.00	10.0; 40.0	20	0.023*	5.152
Beta-blockers	3.78±5.61	2.50 – 5.00	1.2; 47.5	68	3.76±2.42	2.50 – 5.00	1.2; 12.5	51	0.261	1.263
Other sartans	53.03±30.55	32.50 – 80.00	12.5; 160.0	30	48.42±37.34	21.25 – 50.00	7.5; 160.0	30	0.280	1.169
ACE inhibitors	4.07±2.15	2.50 – 5.00	1.2; 10.0	14	4.88±3.17	2.38 – 6.25	2.0; 10.0	4	0.912	0.012
GLP-1 agonists	0.60±0.00	0.60 – 0.60	0.6; 0.6	1	1.20±0.00	1.20 – 1.20	1.2; 1.2	1	0.317	1.000
Calcium channel blockers	23.50±23.97	2.00 – 37.50	2.0; 60.0	4	11.00±13.45	2.00 – 23.00	0.0; 30.0	6	0.356	0.851
Insulin	35.43±18.54	20.00 – 47.00	12.0; 64.0	7	26.87±15.78	15.00 – 37.00	8.0; 70.0	23	0.302	1.065
DPP-4 inhibitors	54.17±22.44	50.00 – 50.00	25.0; 100.0	6	72.50±26.10	50.00 – 100.00	25.0; 100.0	20	0.139	2.189
Metformin	775.00±420.81	500.00 – 850.00	250.0; 2000.0	27	1090.13±584.24	500.00 – 1,700.00	425.0; 2,000.0	38	0.012*	6.355
Empagliflozin	7.87±2.62	5.00 – 10.00	2.5; 12.5	75	8.61±4.88	5.00 – 10.00	2.5; 25.0	55	0.784	0.075

Notes: Patients are distributed in two groups based on their HbA1c levels during their second observation. The dosages are compared using the Kruskal–Wallis test. *Indicates statistical significance at $p<0.05$.
Abbreviations: ACE: Angiotensin-converting enzyme; DPP-4: Dipeptidyl peptidase-4; GLP-1: Glucagon-like peptide-1; HbA1c: Glycated hemoglobin; SD: Standard deviation.

level ≥8% (35.7%) compared to those with an HbA1c level ≤8% (8.1%). Figure 1 shows box plots for changes in fasting glucose and HbA1c levels in patients with regard to the prescribed antidiabetic medications.

3.2. Cardiovascular medications

We also analyzed the use of cardiovascular medications among the patients. ACE inhibitors were prescribed to 18.9% of patients with an HbA1c level ≤8%, compared to 7.1% in the HbA1c level ≥8% group (t = 20.908, p=0.000). Beta-blockers and loop diuretics were commonly used in both groups, with significant differences in their usage. Table 4 presents the distribution of cardiovascular medication prescriptions across patient groups, expressed as percentages.

Figure 2 shows the box plots illustrating the changes in urea, uric acid, and creatinine levels between the two observations, depending on the type of diuretics prescribed. We also calculated mean values and SDs for changes in critical clinical parameters according to the prescribed medications. Results are presented in Table 5.

The use of statins was significantly higher in the HbA1c level ≥8% group (87.5%) compared to the HbA1c level ≤8% group (75.7%, t = 12.783, p=0.000). Table 6 shows the results of this treatment on triglyceride levels, analyzed by gender across the two groups.

Table 3. Antihyperglycemic medications used in the study groups

Medication	HbA1c level ≤8% (%)	HbA1c level ≥8% (%)
Metformin	35.1	69.6
DPP-4 inhibitors	8.1	35.7
Sulfonylureas	5.4	8.9
GLP-1 agonists	1.4	1.8
Insulin	9.5	41.1

Abbreviations: DPP-4: Dipeptidyl peptidase-4; GLP-1: Glucagon-like peptide-1; HbA1c: Glycated hemoglobin.

3.3. Multinomial logistic regression and correlation of variables

Figure 3 demonstrates the cross-correlation between the study variables. The correlation between the durations of T2DM and IHD may be attributed to the simultaneous diagnosis of both conditions upon symptom presentation, resulting in the uncertainty of the actual duration of each disease. Understanding these durations is crucial for evaluating the course of treatment. Apart from the clear correlations between systolic and diastolic blood pressure, fasting glucose and HbA1c levels, and creatinine, uric acid, and urea levels, other variables exhibited sufficient independence.

We used the Statsmodels library (v.0.15) to train a multinomial logistic regression model. To enable interpretation of model coefficients as predictors of variable importance, we normalized all values before training and testing. The results are shown in Table 7. As anticipated, HbA1c levels during the first observation emerged as the most significant predictor. Although N-terminal pro-B-type natriuretic peptide (NT-proBNP) had a relatively small coefficient, its values varied significantly in the sample, even after normalization. Specifically, the maximum value of NT-proBNP reached 6.2, approximately 1.3 times higher than the maximum value of all other markers, explaining the disproportionately small coefficient. Other key predictors included urea levels, diastolic blood pressure, and duration of diabetes.

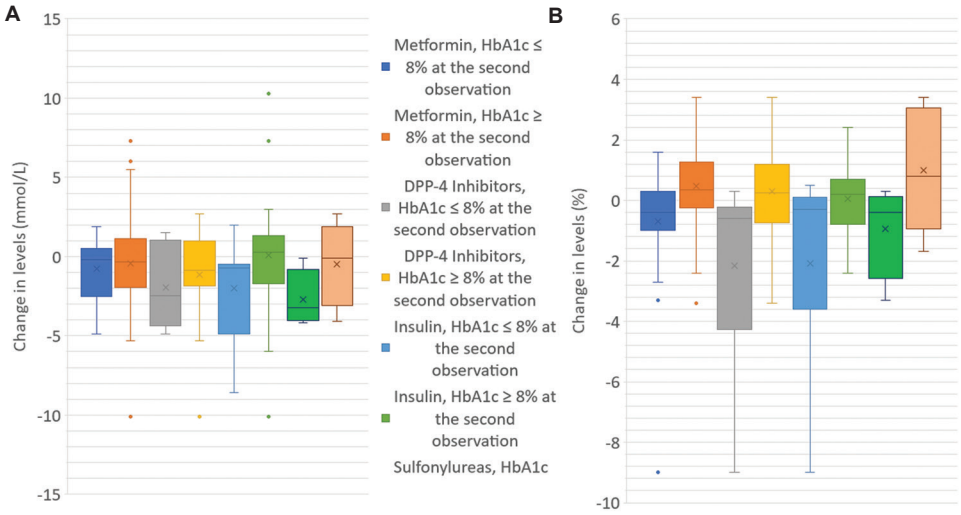


Figure 1. Box plots illustrating changes in (A) fasting glucose and (B) HbA1c levels in patients between two observations depending on the type of prescribed antidiabetic drugs. Group 1 is a group with HbA1c ≤8% during the second observation, and Group 2 consists of all remaining patients. The colors are consistent.
Abbreviations: DPP-4: Dipeptidyl peptidase-4; HbA1c: Glycated hemoglobin.

Table 4. Cardiovascular medications used in the study groups

Medication	HbA1c level ≤8% (%)	HbA1c level ≥8% (%)
ACE inhibitors	18.9	7.1
Angiotensin II receptor blockers	37.8	58.9
Beta-blockers	90.5	92.9
Mineralocorticoid receptor antagonists	68.9	51.8
Calcium channel blockers	44.6	48.2
Thiazide diuretics	9.5	16.1
Loop diuretics	71.6	46.4
Antiplatelet agents	100	100
Statins	75.7	87.5
Sacubitril/valsartan	28.4	10.7
Ivabradine	2.7	8.9

Abbreviations: ACE: Angiotensin-converting enzyme; HbA1c: Glycated hemoglobin.

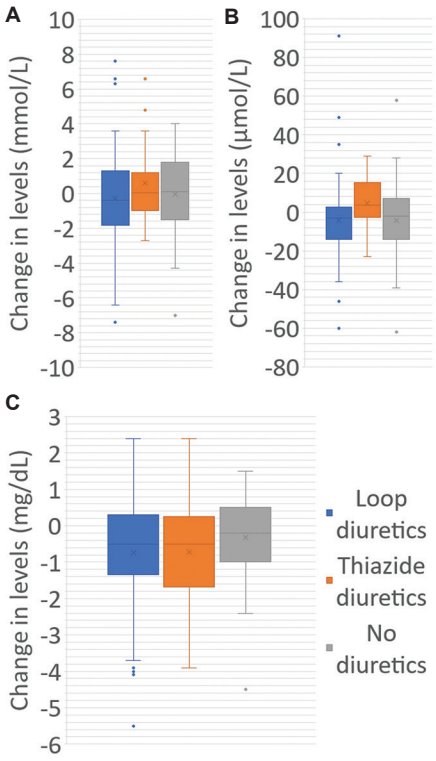


Figure 2. Box plots illustrating changes in (A) urea, (B) creatinine, and (C) uric acid levels in patients between two observations, depending on the type of prescribed diuretics. The colors are consistent.

We also constructed a linear regression model to predict HbA1c levels in patients based on their clinical data and dosages of prescribed medications. This model was trained on the training set and was tested using Spearman's correlation coefficient between predicted and actual levels of HbA1c during the second observation. This non-parametric measure was selected due to the non-linear relationship between medication dosage and glycemic response. The model achieved strong performance, with a correlation coefficient of 0.826 (p=2.3 × 10^{-22}). To understand the importance of each feature used in the model, all features were normalized before training. The description of the model is presented in Table 8. The root mean square error of the model on the test set was 1.172.

In addition, we found that patients with higher HbA1c levels (≥8%) were generally younger and had a longer duration of diabetes and IHD. These patients also required more aggressive antihyperglycemic therapy, including higher usage of metformin and insulin. The use of cardiovascular medications varied significantly between the groups, with higher usage of ACE inhibitors and statins in patients with higher HbA1c levels.

4. Discussion

The study revealed that patients with higher HbA1c levels (≥8%) were generally younger and were more likely to be female. This observation is consistent with related research indicating that younger patients with T2DM often struggle with glycemic control due to various factors, including lifestyle, adherence to treatment, and metabolic differences. Gale and Gillespie[12] discussed the impact of gender on diabetes management, noting that women may have a higher risk of poor glycemic control due to hormonal fluctuations and other physiological factors. However, we hypothesized that the primary contributing factor is the difference in life expectancy between men (72.1 years) and women (76.6 years) in Uzbekistan. The average age of women reaching the target levels was 69.2 years, whereas it was 65 years for men. The average age of women with an HbA1c level ≥8% was 66.7 years, and 58.4 years for men. Thus, the younger age in the second group is largely attributed to men with lower life expectancy. Failure to reach target levels poses a greater risk, with impaired survival being a key contributing factor to this outcome.

The longer duration of diabetes and IHD in patients with higher HbA1c levels suggests that disease duration significantly impacts glycemic control. The Diabetes Control and Complications Trial demonstrated that prolonged diabetes duration is associated with an increased risk of complications and poorer glycemic control. This study's findings underscore the importance of early and aggressive intervention to achieve and maintain target HbA1c levels. The multinomial logistic regression model revealed that the duration of T2DM has a negative impact, while the duration of IHD has a positive impact. Patients with a longer history of IHD were more likely to adhere to

Table 5. Changes in clinical characteristics by medication and HbA1c target achievement

Medication	Clinical characteristics	HbA1c level ≤8%	HbA1c level ≥8%	*H*	*p*-value
Metformin	NT-proBNP	−38.59±395.50	−121.79±207.95	0.021	0.884
	LVEF	1.62±4.23	2.11±4.37	1.192	0.275
	Systolic blood pressure	1.81±15.02	−5.39±14.16	3.880	0.049*
	Diastolic blood pressure	−2.04±9.26	−2.37±7.05	0.030	0.863
	Heart rate	−1.04±10.21	−3.79±10.96	0.010	0.920
DPP-4 inhibitors	NT-proBNP	−68.17±321.28	−98.30±226.65	0.370	0.543
	LVEF	0.93±3.48	1.75±4.38	0.675	0.411
	Systolic blood pressure	9.00±14.55	−3.50±15.58	2.700	0.100
	Diastolic blood pressure	−8.33±10.67	−3.00±7.14	1.499	0.221
	Heart rate	−1.83±5.37	−1.75±9.11	0.034	0.855
Insulin	NT-proBNP	−259.14±397.90	−86.14±780.08	0.376	0.540
	LVEF	−2.13±8.40	2.01±4.95	2.312	0.128
	Systolic blood pressure	5.57±21.92	−4.35±15.34	1.207	0.272
	Diastolic blood pressure	−7.14±17.50	−3.04±7.48	0.436	0.509
	Heart rate	1.86±6.64	−1.96±7.93	1.171	0.279
Sulfonylureas	NT-proBNP	−113.50±89.06	−44.20±82.43	1.830	0.176
	LVEF	1.94±3.42	2.12±5.19	0.000	1.000
	Systolic blood pressure	5.00±8.66	−6.00±10.20	2.055	0.152
	Diastolic blood pressure	−5.00±5.00	2.00±4.00	3.086	0.079
	Heart rate	−1.00±6.40	−8.20±11.57	0.549	0.459
ACE inhibitors	NT-proBNP	−170.64±235.10	−69.00±209.59	0.102	0.750
	LVEF	0.96±3.17	1.22±1.50	0.003	0.958
	Systolic blood pressure	6.07±17.34	5.00±20.62	0.003	0.957
	Diastolic blood pressure	3.21±10.96	0.00±7.07	0.200	0.654
	Heart rate	1.86±6.98	2.75±11.78	0.003	0.957
Angiotensin II receptor blockers	NT-proBNP	497.09±2136.96	−154.03±451.81	0.227	0.634
	LVEF	2.27±4.88	1.55±4.44	0.188	0.665
	Systolic blood pressure	−6.21±20.24	−8.75±11.25	0.498	0.480
	Diastolic blood pressure	−4.14±11.60	−2.81±6.72	0.474	0.491
	Heart rate	−2.52±10.84	−2.03±8.87	0.302	0.583
Beta-blockers	NT-proBNP	6.49±1204.74	−121.20±554.91	0.037	0.847
	LVEF	1.52±5.20	1.65±4.57	0.017	0.897
	Systolic blood pressure	−1.78±18.05	−5.29±14.93	1.498	0.221
	Diastolic blood pressure	−3.01±11.18	−2.75±7.69	0.108	0.743
	Heart rate	−1.49±9.85	−2.69±10.68	0.004	0.949
Mineralocorticoid receptor antagonists	NT-proBNP	28.02±1382.94	−233.66±470.53	0.343	0.558
	LVEF	1.72±5.92	1.57±3.83	0.261	0.610
	Systolic blood pressure	−2.08±19.42	−6.90±13.73	1.124	0.289
	Diastolic blood pressure	−3.73±11.54	−2.41±7.27	0.376	0.540
	Heart rate	−1.41±11.00	−2.86±9.05	0.003	0.960

Notes: Changes in clinical parameter levels are presented as mean±standard deviation. Kruskal–Wallis test's (non-parametric analysis of variance) results are statistics *H* and *P* value. *Indicates statistical significance at $p<0.05$.

Abbreviations: ACE: Angiotensin-converting enzyme; DPP-4: Dipeptidyl peptidase-4; HbA1c: Glycated hemoglobin; LVEF: Left ventricular ejection fraction; NT-proBNP: N-terminal pro-B-type natriuretic peptide.

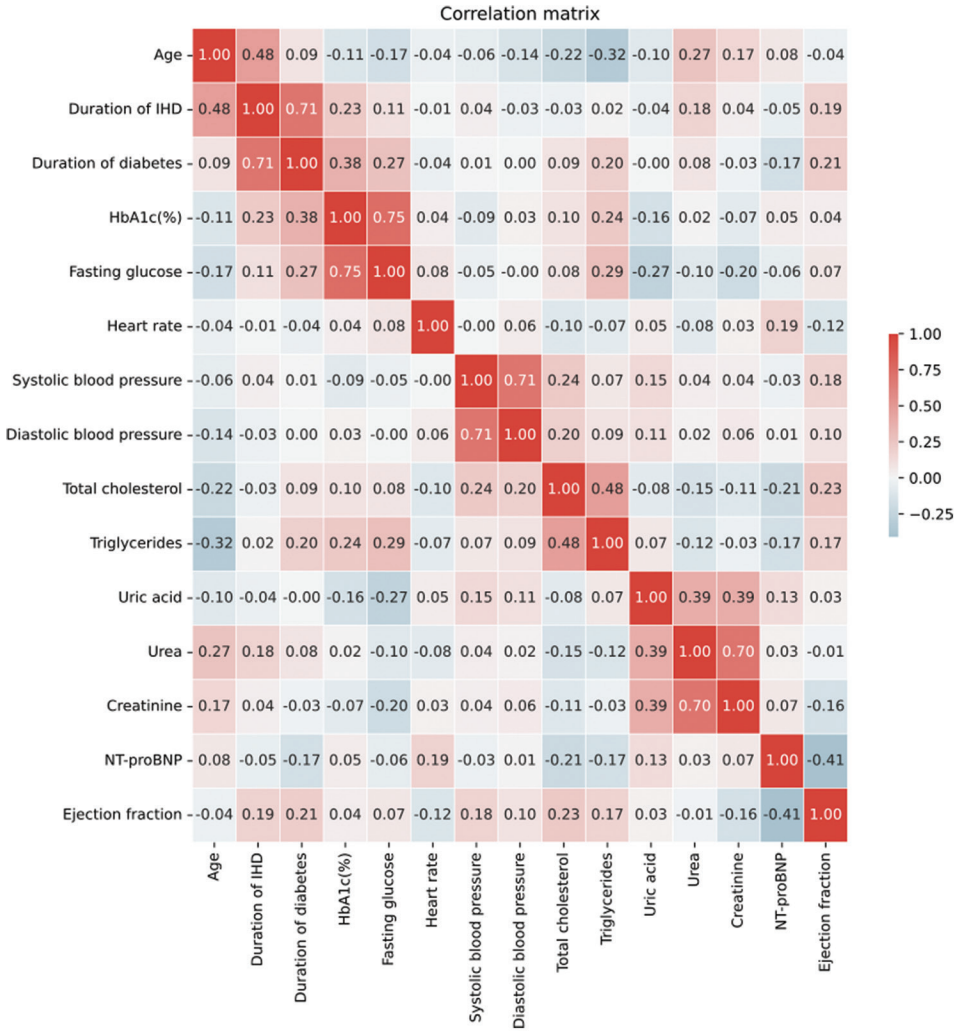


Figure 3. Correlation heatmap between primary variables in the study. Data from all patients on their first observation was used
Abbreviations: HbA1c: Glycated hemoglobin; IHD: Ischemic heart disease; NT-proBNP: N-terminal pro-B-type natriuretic peptide.

Table 6. Patients with triglyceride levels below the upper boundary based on gender

Gender	Reference value (mg/dL)	HbA1c level ≤8%		HbA1c level ≥8%		Chi-squared test	
		TG below limits (%)	TG above limits (%)	TG below limits (%)	TG above limits (%)	Statistics	*p*-value
Women	247	80.6	19.4	68.6	31.4	6.664	0.009
Men	288	74.4	25.6	55	45	29.009	0.000

Note: Pearson's Chi-squared test was used to verify the statistical significance of HbA1c control on levels of triglycerides.
Abbreviations: HbA1c: Glycated hemoglobin; TG: Triglyceride.

their prescribed medications due to their experience with the positive outcome of adherence.

4.1. Medication therapy

The significant differences in medication therapy between the two groups highlight the need for tailored treatment strategies based on individual patient characteristics and glycemic control. Patients with higher HbA1c levels required more aggressive antihyperglycemic therapy, including higher dosages of metformin and DPP-4 inhibitors (Table 2). This finding aligns with the results of Wilson et al.,[24] reporting that patients with poor glycemic control often require more complex treatment regimens.[24] We observed a statistically significant difference in the

Table 7. Multinomial logistic regression using primary variables

Variables	Coefficient	Standard error	z	$p>\|z\|$	Lower bound CI (0.025)	Upper bound CI (0.975)
Intercept	−0.4608	0.280	−1.644	0.100	−1.010	0.088
Age	−0.6777	0.393	−1.726	0.084	−1.447	0.092
Duration of IHD	−0.1246	0.506	−0.246	0.805	−1.116	0.866
Duration of diabetes	0.5746	0.445	1.292	0.196	−0.297	1.446
Heart rate	0.2971	0.302	0.983	0.326	−0.295	0.890
Systolic blood pressure	0.7056	0.417	1.693	0.091	−0.111	1.523
Diastolic blood pressure	−0.9186	0.436	−2.105	0.035	−1.774	−0.063
Fasting glucose	0.3378	0.453	0.747	0.455	−0.549	1.225
HbA1c level	1.5568	0.506	3.077	0.002	0.565	2.548
Total cholesterol	−0.3175	0.325	−0.978	0.328	−0.954	0.319
Triglycerides	0.4376	0.352	1.242	0.214	−0.253	1.128
Creatinine	−0.3337	0.418	−0.798	0.425	−1.153	0.485
Uric acid	−0.5615	0.340	−1.650	0.099	−1.229	0.106
Urea	0.9779	0.473	2.069	0.039	0.052	1.904
NT-proBNP	0.1777	0.423	0.420	0.675	−0.652	1.007
Ejection fraction	0.6635	0.338	1.963	0.050	0.001	1.326

Notes: The target was binary, indicating whether the patient failed to achieve an HbA1c level ≤8%. The receiver operating characteristic area under the curve value of the model was 0.92. The pseudo-R^2 was 0.4748.
Abbreviations: CI: Confidence interval; HbA1c: Glycated hemoglobin; IHD: Ischemic heart disease; NT-proBNP: N-terminal pro-B-type natriuretic peptide.

Table 8. Coefficients of the linear regression model

Parameters	Coefficient	Standard deviation
HbA1c level	0.81346	2.003743
Creatinine	−0.23825	36.639461
Triglycerides	0.10554	221.15185
Fasting blood glucose	0.16253	3.02244
Uric acid	0.01018	1.71296
Intercept	6.265236	-
Medication dosages		
Empagliflozin	−0.14453	3.76635
Metformin	0.19195	615.33906
DPP-4 inhibitors	−0.01531	29.76051
Insulin	0.10263	14.61167
Sulfonylureas	−0.02430	6.86299
GLP-1 agonists	0.00747	0.11685

Notes: Coefficients of linear regression model to predict levels of HbA1c in patients during their second observation based on their clinical data and dosages of hypoglycemic medications at their first observation.
Abbreviations: DPP-4: Dipeptidyl peptidase-4; GLP-1: Glucagon-like peptide-1; HbA1c: Glycated hemoglobin.

triglyceride levels between the two groups (Table 6). These results are consistent with other studies and could be attributed to dietary problems and differences in food preferences between women and men.

The use of empagliflozin, a medication known for its cardiovascular benefits, was higher in patients with better glycemic control (HbA1c levels ≤8%). This suggests that achieving target HbA1c levels may allow the use of medications with additional cardiovascular benefits, potentially improving overall patient outcomes. Our linear regression model attributed the decrease in HbA1c levels to higher dosages of empagliflozin. Sulfonylureas and DPP-4 inhibitors were also associated with decreases in HbA1c levels, albeit with smaller effect sizes. Interestingly, creatinine exhibited a negative coefficient, which may be explained by the prescription of more aggressive treatment for renal insufficiency in patients with low glomerular filtration rates, consequently leading to an improvement in their renal function by the time of the second observation.

We also found significant differences in the use of cardiovascular medications between the two groups. Patients with higher HbA1c levels were more likely to be prescribed ACE inhibitors and statins, reflecting the need for comprehensive management of cardiovascular risk factors in this patient population. Alpert *et al.*[10] emphasized the importance of controlled hypertension and lipid management in patients with diabetes to reduce cardiovascular risk.

Prescription of loop diuretics led to a decrease in creatinine levels in most patients. Ikramov *et al.*[25]

established it to be an important predictor of diastolic dysfunction in patients with T2DM.

4.2. Implications for clinical practice

The results of this study have significant implications for clinical practice. Lowering HbA1c levels below the threshold is substantial for mitigating the risk of cardiovascular complications in patients with T2DM and IHD. Healthcare providers should consider individualized treatment approaches based on patient characteristics, disease duration, and glycemic control. The use of medications with cardiovascular benefits, such as empagliflozin, should be prioritized in patients who achieve target levels of HbA1c.

The UKPDS demonstrated that intensive blood-glucose control significantly reduces the risk of cardiovascular events in patients with T2DM. The Action to Control Cardiovascular Risk in Diabetes study further emphasized the importance of maintaining optimal glycemic control to improve cardiovascular outcomes.

Recent advancements in diabetes treatment have introduced new classes of antihyperglycemic agents, such as GLP-1 receptor agonists and SGLT2 inhibitors, which have demonstrated better results in improving both glycemic control and cardiovascular outcomes. Joseph *et al.*[6] discussed management strategies for cardiovascular risk factors in adults with T2DM, underscoring the need for individualized treatment approaches. Johnson and Wang[7] and Smith and Patel[26] concluded that the combined use of these medications provides better cardiometabolic and renal outcomes than monotherapy.

4.3. Limitations

This study has several limitations that should be considered when interpreting its findings. The sample size was relatively small, and the study was conducted at a single center. Moreover, the patients in this study originate from various regions across the country, as the center serves as the primary cardiologic hospital in Uzbekistan. In addition, the observational nature of the study does not allow causal inferences to be made. The high costs of repeated laboratory tests constrained the frequency and scope of data collection.

Further limitations include potential confounding factors, such as patients' adherence, socioeconomic factors, dietary adherence, and stress. A more comprehensive analysis is required to account for these factors. However, the use of empagliflozin was well-monitored, as this medication was provided to patients by the center.

Empagliflozin was relatively recently approved by the Food and Drug Administration for the treatment of T2DM in patients with IHD. It was incorporated into the treatment standards in Uzbekistan in 2018. Consequently, the duration of observation for patients using empagliflozin was significantly limited.

5. Conclusion

This study investigated the prescribed basic medication therapy in relation to achieving target HbA1c levels in patients with T2DM and IHD. The findings revealed significant differences in demographic characteristics, duration of diabetes and IHD, and medication usage between patients who achieved target HbA1c levels (≤8%) and those who did not (≥8%). Reaching target levels of HbA1c is important for mitigating the risk of cardiovascular complications.

Patients with higher HbA1c levels had a longer duration of diabetes and IHD. Female patients with higher levels of HbA1c were older than male patients who did not reach target levels. These patients required more aggressive antihyperglycemic therapy, including higher usage of metformin and insulin. The use of cardiovascular medications varied significantly between the groups, with higher usage of ACE inhibitors and statins in patients with higher HbA1c levels.

Our logistic regression model demonstrated a very high receiver operating characteristic area under the curve value of 0.92 on the test set, effectively predicting whether the patient would achieve target HbA1c levels after treatment. In addition, the linear regression model was used to analyze the efficiency of hypoglycemic medications and their combination based on patients' data, yielding a Spearman's correlation coefficient of 0.82 on the test set.

Acknowledgments

None.

Funding

None.

Conflict of interest

The authors declare they have no competing interests

Author contributions

Conceptualization: Raisa Trigulova, Alisher Ikramov
Formal analysis: Shukhrat Doniyorov
Investigation: Dilnoza Alimova, Shakhnoza Mukhtarova
Methodology: Dilafruz Akhmedova
Writing – original draft: Raisa Trigulova
Writing – review & editing: Raisa Trigulova, Alisher Ikramov

Ethics approval and consent to participate

The study was approved by the Ethics Board of the Republican Specialized Scientific-Practical Medical Center of Cardiology in Uzbekistan (Approval ID: П3-202007041). Participants provided written consent to participate in the study.

Consent for publication

The participants provided written consent to use and publish the data and results.

Availability of data

Data can be obtained by request from the corresponding author.

References

1. Whiting DR, Guariguata L, Weil C, Shaw J. IDF diabetes atlas: Global estimates of the prevalence of diabetes for 2011 and 2030. *Diabetes Res Clin Pract*. 2011;94(3):311-321.

   doi: 10.1016/j.diabres.2011.10.029

2. Effect of intensive blood-glucose control with metformin on complications in overweight patients with type 2 diabetes (UKPDS 34). UK prospective diabetes study (UKPDS) Group. *Lancet*. 1998;352(9131):854-865.

3. American Diabetes Association. Glycemic goals and hypoglycemia: Standards of care in diabetes - 2025. *Diabetes Care*. 2025;48(Suppl 1):S128-S145.

   doi: 10.2337/dc25-S006

4. Wang JS, Liu WJ, Lee CL. HbA1c trajectory and cardiovascular outcomes: An analysis of data from the action to control cardiovascular risk in diabetes (ACCORD) study. *Ther Adv Chronic Dis*. 2021;12:20406223211026391.

   doi: 10.1177/20406223211026391

5. Nauck MA, Meier JJ. The incretin effect in healthy individuals and those with type 2 diabetes: Physiology, pathophysiology, and response to therapeutic interventions. *Lancet Diabetes Endocrinol*. 2016;4(6):525-536.

   doi: 10.1016/S2213-8587(15)00482-9

6. Joseph JJ, Deedwania P, Acharya T, *et al*. Comprehensive management of cardiovascular risk factors for adults with type 2 diabetes: A scientific statement from the American heart association. *Circulation*. 2022;145(9):e722-e759.

   doi: 10.1161/CIR.0000000000001040

7. Johnson L, Wang H. Cardioprotective effects of GLP-1 receptor agonists and SGLT2 inhibitors in T2DM patients. *J Diabetes Complications*. 2024;38(3):145-158.

   doi: 10.1016/j.jdiacomp.2024.01.005

8. Hou J, Ren L, Hou Q, *et al*. Efficacy and safety of sodium-glucose cotransporter 2 (SGLT2) inhibitors in patients with acute heart failure: A systematic review and meta-analysis. *Front Cardiovasc Med*. 2024;11:1388337.

   doi: 10.3389/fcvm.2024.1388337

9. Naha S, Gardner MJ, Khangura D, Kurukulasuriya LR, Sowers JR. Hypertension in Diabetes. In: Feingold KR, Ahmed SF, Anawalt B, *et al.*, editors. *Endotext*. MDText.com Inc.; 2000. Available from: https://www.ncbi.nlm.nih.gov/books/nbk279027 [Last accessed on 2024 Aug 07].

10. Alpert CM, Smith MA, Hummel SL, Hummel EK. Symptom burden in heart failure: Assessment, impact on outcomes, and management. *Heart Fail Rev*. 2017;22(1):25-39.

    doi: 10.1007/s10741-016-9581-4

11. Diabetes control and complications trial (DCCT): Results of feasibility study. The DCCT research group. *Diabetes Care*. 1987;10(1):1-19.

    doi: 10.2337/diacare.10.1.1

12. Gale EA, Gillespie KM. Diabetes and gender. *Diabetologia*. 2001;44(1):3-15.

    doi: 10.1007/s001250051573

13. Chou CL, Zheng CM, Chiu HW, *et al*. Impact of acute kidney injury, co-existing with and without chronic kidney disease on the short-term adverse outcomes following atherosclerotic cardiovascular disease events in patients with diabetes. *J Multidiscip Healthc*. 2025;18:2019-2037.

    doi: 10.2147/JMDH.S123456

14. Vloemans AF, Eilander MM, Rotteveel J, *et al*. Youth with type 1 diabetes taking responsibility for self-management: The importance of executive functioning in achieving glycemic control: Results from the longitudinal DINO study. *Diabetes Care*. 2019;42(2):225-231.

    doi: 10.2337/dc18-1143

15. Tucker B, Ong KL, Robledo K, Keech A, Patel S. Association of inflammation, triglycerides and lipoprotein(a) with cardiovascular events in the UK Biobank. *Eur Heart J*. 2024;45(Suppl 1):ehae666.2751.

    doi: 10.1093/eurheartj/ehae666.2751

16. Quispe R, Sweeney T, Varma B, Agarwala A, Michos ED. Recent updates in hypertriglyceridemia management for cardiovascular risk reduction. *Curr Atheroscler Rep*. 2022;24:52-64.

    doi: 10.1007/s11883-022-01052-4

17. Wu K, Chen J, Lin Y, Wang J. A cohort study on the correlation between serum Klotho levels and all-cause mortality in American diabetic populations. *Diabetol Metab Syndr*. 2025;17:124.

    doi: 10.1186/s13098-025-01686-9

18. Xie R, Seum T, Sha S, *et al*. Improving 10-year cardiovascular

risk prediction in patients with type 2 diabetes with metabolomics. *Cardiovasc Diabetol*. 2025;24:581.

doi: 10.1186/s12933-025-02581-3

19. Miller V, Micha R, Choi E, Karageorgou D, Webb P, Mozaffarian D. Evaluation of the quality of evidence of the association of foods and nutrients with cardiovascular disease and diabetes: A systematic review. *JAMA Network Open*. 2025;8(3):e2788634.

    doi: 10.1001/jamanetworkopen.2025.2788634.

20. Zhao C, Lin M, Yang Y, Yang H, Gao Z, Yan Z, *et al*. Association between dietary inflammatory index and cardiovascular-kidney-metabolic syndrome risk: A cross-sectional study. *Nutr J*. 2025;24:1127.

    doi: 10.1186/s12937-025-01127-3

21. Gupta A, Shah K, Gupta V. Interconnected epidemics: Obesity, metabolic syndrome, diabetes and cardiovascular diseases - insights from research and prevention strategies. *Discover Public Health*. 2025;22:106.

    doi: 10.1186/s12982-025-00496-8

22. Global Health and Population Project on Access to Care for Cardiometabolic Diseases (HPACC). Expanding access to newer medicines for people with type 2 diabetes in low-income and middle-income countries: A cost-effectiveness and price target analysis. Lancet Diabetes Endocrinol. 2021;9(12):825-836.

    doi: 10.1016/S2213-8587(21)00240-0

23. Nelson AJ, Ardissino M, Haynes K, *et al*. Gaps in evidence-based therapy use in insured patients in the United States with type 2 diabetes mellitus and atherosclerotic cardiovascular disease. *J Am Heart Assoc*. 2021;10(2):e016835.

    doi: 10.1161/jaha.120.016835

24. Wilson LM, Herzig SJ, Marcantonio ER, *et al*. Management of diabetes and hyperglycemia in the hospital: A systematic review of clinical practice guidelines. *Diabetes Care*. 2025;48(4):655-664.

    doi: 10.2337/dc24-2510

25. Ikramov A, Mukhtarova S, Trigulova R, Alimova D, Abdullaeva S. Prediction of glycosylated hemoglobin level in patients with cardiovascular diseases and type 2 diabetes mellitus with respect to anti-diabetic medication. *Front Endocrinol*. 2024;15:1305640.

    doi: 10.3389/fendo.2024.1305640

26. Smith J, Patel R. Real-world effectiveness of adding newer generation GLP-1RA to SGLT2i in T2DM patients with CHD. *Cardiovasc Diabetol*. 2024;23(4):237-250.

    doi: 10.1186/s12933-025-02737-1

ACCSCIENCE PUBLISHING

Eurasian Journal of Medicine and Oncology

ORIGINAL RESEARCH ARTICLE

Targeting the FN3K–Nrf2 axis: Discovery and pre-clinical evaluation of novel inhibitors for breast cancer therapy

Erica Alves, Gurupadayya Bannimath*, and Prabitha Prabhakaran

Department of Pharmaceutical Chemistry, JSS College of Pharmacy, JSS Academy of Higher Education & Research, Mysore, Karnataka, India

Abstract

Introduction: Fructosamine-3-kinase (FN3K), a deglycation enzyme implicated in redox regulation through the nuclear factor erythroid 2-related factor 2 (Nrf2) pathway, has emerged as a novel therapeutic target in breast cancer. Elevated FN3K activity enhances antioxidant defenses, promoting cancer cell survival and resistance to therapies. Pharmacological inhibition of FN3K may sensitize tumors to oxidative stress.
Objective: This study aimed to identify and validate potent FN3K inhibitors through structure-based virtual screening (SBVS) and *in vitro* evaluation in breast cancer models.
Methods: A homology-modeled FN3K structure was generated and validated using SWISS-MODEL, PROCHECK, and QMEAN. Compound libraries, including the Food and Drug Administration (FDA)-approved kinase inhibitors, World Health Organization (WHO) essential medicines, and anti-breast cancer agents, were screened using Schrödinger's Glide module. Top-ranked compounds were prioritized based on binding affinity, molecular interactions, absorption, distribution, metabolism, excretion, and toxicity (ADMET) profiling. *In vitro* validation in MCF-7, BT-474, T-47D, and Vero cell lines included MTT cytotoxicity assay and evaluation of FN3K and Nrf2 expression through quantitative PCR (qPCR) and Western blotting. Statistical analyses were performed to assess the significance of observed effects.
Results: Oxaliplatin, lansoprazole, and capivasertib exhibited strong binding affinities (Glide scores: –9.2 to –8.1 kcal/mol) and selective cytotoxicity in breast cancer cell lines ($IC_{50:}$ 90 – 110 µg/mL). qPCR analysis revealed >99% downregulation of FN3K, accompanied by significant suppression of Nrf2 in cancer cells. Minimal modulation was observed in Vero cells, indicating tumor selectivity. Western blotting further corroborated the downregulation of FN3K and Nrf2 at the protein level. Molecular dynamics (MD) simulations validated the binding stability of the lead small molecules, reinforcing their potential as effective inhibitors.
Conclusion: The integrated *in silico* and *in vitro* analysis supports FN3K as a viable therapeutic target in breast cancer. Oxaliplatin, lansoprazole, and capivasertib demonstrated strong FN3K inhibition and modulation of tumor redox homeostasis, suggesting their potential for further pre-clinical development as novel anti-cancer agents targeting metabolic adaptability.

Keywords: Breast neoplasms; Fructosamine-3-kinase; Nuclear factor erythroid 2-related factor 2 protein; Oxidative stress; Antineoplastic agents

***Corresponding author:**
Gurupadayya Bannimath
(bmgurupadayya@jssuni.edu.in)

Citation: Alves E, Bannimath G, Prabhakaran P. Targeting the FN3K–Nrf2 axis: Discovery and pre-clinical evaluation of novel inhibitors for breast cancer therapy. *Eurasian J Med Oncol*. 2025;9(3):197-225.
doi: 10.36922/EJMO025150114

Received: April 13, 2025

Revised: May 17, 2025

Accepted: June 4, 2025

Published online: July 28, 2025

Copyright: © 2025 Author(s). This is an Open-Access article distributed under the terms of the Creative Commons Attribution License, permitting distribution, and reproduction in any medium, provided the original work is properly cited.

Publisher's Note: AccScience Publishing remains neutral with regard to jurisdictional claims in published maps and institutional affiliations.

1. Introduction

Breast cancer persists as a predominant contributor to global cancer-related mortality, with the efficacy of present therapeutic modalities often constrained by systemic toxicities and the progressive development of multidrug resistance.[1] Recent global statistics indicate that, in 2022, breast cancer was diagnosed in approximately 2.3 million women worldwide, leading to more than 670,000 reported deaths.[1] Although incidence rates are higher in high-income countries, mortality remains disproportionately elevated in low-resource settings due to delayed diagnosis and limited access to effective treatment options. The complexity of breast cancer, encompassing diverse molecular subtypes, presents significant therapeutic challenges.[1]

Resistance to chemotherapeutic agents and targeted therapies continues to undermine treatment efficacy, underscoring the urgent need for novel therapeutic strategies. Emerging evidence underscores metabolic reprogramming as a critical driver of cancer progression and therapeutic resistance.[2] To sustain uncontrolled growth and adapt to the tumor microenvironment, cancer cells exhibit marked metabolic adaptability driven by alterations in glycolysis, glutamine utilization, lipid processing, and mitochondrial respiration.[2] Targeting key metabolic enzymes within these reprogrammed pathways – such as hexokinase II, glutaminase, and fatty acid synthase – has emerged as a promising therapeutic strategy, offering selectivity by exploiting cancer-specific metabolic dependencies.[2] However, the dynamic nature of metabolic adaptation highlights the need for combinatorial approaches and robust biomarkers to improve therapeutic efficacy.[2]

Fructosamine-3-kinase (FN3K) is a deglycating enzyme that catalyzes the phosphorylation of fructosamine adducts on glycated proteins, thereby promoting their elimination and aiding in protein quality control and repair. This enzymatic activity plays a crucial role in mitigating cellular damage associated with non-enzymatic glycation, oxidative stress, and metabolic dysregulation. A marked reduction in FN3K activity has been observed in breast cancer tissues compared to adjacent normal tissues, indicating its potential involvement in tumor progression and diminished defense against advanced glycation end products (AGEs).[3] Beyond its role in protein repair through deglycation, FN3K has been implicated in cancer progression by contributing to the stabilization of nuclear factor erythroid 2-related factor 2 (Nrf2), a key transcription factor governing antioxidant defense mechanisms. This stabilization enhances Nrf2-mediated transcription of cytoprotective genes, thereby promoting cancer cell proliferation, survival, and resistance to therapy. FN3K facilitates metabolic adaptability in cancer cells by alleviating oxidative stress and maintaining redox homeostasis, thereby underscoring its potential as an emerging therapeutic target in breast cancer.[4] FN3K modulates the activity of redox-sensitive transcription factors, such as Nrf2 by catalyzing the deglycation of essential lysine and arginine residues critical for transcriptional activation. Glycation of Nrf2 impairs its stability, nuclear translocation, and interaction with small musculoaponeurotic fibrosarcoma (sMAF) proteins, thereby attenuating its antioxidant transcriptional program. Conversely, FN3K overexpression maintains Nrf2 in a functional state, promoting redox homeostasis and facilitating tumor cell survival under oxidative stress. Elevated FN3K activity has been associated with enhanced Nrf2 signaling and poor prognosis in multiple cancer types, including breast cancer, underscoring its role in disease progression and therapy resistance.[5]

Using structure-based virtual screening (SBVS) combined with molecular docking, Beeraka *et al.*[5] reported that multiple anti-cancer compounds – including tyrosine kinase inhibitors, hormonal modulators, and immunosuppressants – exhibited strong modulatory effects on FN3K activity.[6] Beeraka *et al.*[5] also identified several anti-cancer agents – including gefitinib, sorafenib, neratinib, tamoxifen citrate, and cyclosporine A – as potent modulators of FN3K through SBVS and molecular docking approaches.[6] A separate study demonstrated a strong positive correlation between FN3K levels and Nrf2-target antioxidant gene expression signatures, implicating FN3K in sustaining redox homeostasis through Nrf2 pathway protection. Notably, elevated FN3K expression has been correlated with decreased disease-specific survival, indicating its potential relevance as a prognostic biomarker in breast cancer.[7] Yousefi *et al.*[2] conducted a comparative enzymatic analysis of FN3K activity in paired breast tumor and adjacent normal tissues, revealing a significant reduction in FN3K activity within tumor samples. This reduction may compromise cellular deglycation efficiency, leading to the accumulation of AGEs, which can disrupt protein function, elevate oxidative stress, and facilitate malignant transformation by driving metabolic reprogramming. These observations highlight FN3K as a potential regulator of metabolic pathways involved in the pathogenesis of breast cancer.[3] FN3K mediates a distinctive intracellular deglycation process by phosphorylating fructosamine adducts at the third carbon of the deoxyfructose ring, thereby promoting their spontaneous breakdown and restoring free amino groups. This enzymatic correction limits the formation of stable AGEs, which are associated with persistent oxidative stress and inflammation – key pathophysiological factors in cancer initiation and progression.[8]

Pharmacological inhibition of FN3K represents a novel therapeutic strategy to disrupt Nrf2-mediated antioxidant defense mechanisms that enable cancer cell survival, proliferation, and resistance to therapy. Inhibiting FN3K may preserve Nrf2 in its glycated and transcriptionally inactive form, thereby increasing cancer cell susceptibility to oxidative stress and potentially augmenting the therapeutic effectiveness of standard interventions, such as chemotherapy and radiotherapy. However, despite its therapeutic promise, FN3K remains an underexplored target in oncology, with limited progress in the identification and development of potent, selective small molecule inhibitors.[4] The pursuit of novel anti-cancer agents has been significantly accelerated by the emergence of SBVS, a pivotal component of computer-aided drug discovery. SBVS enables the high-throughput computational screening of large chemical libraries against well-defined biological targets, leveraging structural insights to identify potential lead compounds with enhanced specificity and binding affinity. Compared to traditional high-throughput screening methods, virtual screening (VS) offers substantial reductions in time, cost, and resource expenditure, while improving hit rates through rational design strategies. Moreover, recent advancements in docking algorithms, scoring functions, and ensemble-based receptor modeling have further enhanced the accuracy and success rate of SBVS in anti-cancer drug discovery.[9] In addition to its role in Nrf2 regulation, recent advances have clarified that FN3K plays a multifaceted role in cancer progression. FN3K deglycates key lysine and arginine residues on Nrf2, enhancing its nuclear stability and enabling antioxidant response element (ARE)-driven transcription of antioxidant and cytoprotective genes, such as heme oxygenase-1 (HO-1), NAD(P)H quinone dehydrogenase 1 (NQO1), and thioredoxin reductase 1 (TXNRD1), which collectively contribute to redox homeostasis, chemoresistance, and tumor survival.[3,4,10] Conversely, inhibiting FN3K impairs Nrf2's interaction with sMAF proteins, reduces nuclear translocation, and suppresses downstream antioxidant responses, thereby sensitizing cancer cells to oxidative stress.[4,5] Moreover, FN3K modulates broader signaling networks through glycation stress; the AGE and the receptor for AGE (AGE-RAGE) systems stimulate oncogenic cascades, including phosphoinositide 3-kinase/protein kinase B (PI3K/Akt), mitogen-activated protein kinase (MAPK), and Janus kinase/signal transducer and activator of transcription 3 (JAK/STAT3), promoting epithelial–mesenchymal transition, angiogenesis, and immune evasion.[3,10] Dual inhibition strategies (e.g., oxaliplatin + brusatol) have demonstrated enhanced reactive oxygen species (ROS)-mediated apoptosis, reduced migration and clonogenicity, and dose-sparing cytotoxic effects.[11] FN3K is also implicated in mitochondrial regulation, glutathione metabolism, and extracellular matrix (ECM) remodeling – hallmarks of tumor metabolic adaptation.[3] These findings position FN3K as a central modulator of cancer redox biology and metabolism, offering therapeutic leverage beyond Nrf2 regulation.

The present study investigates the therapeutic relevance of FN3K inhibition in breast cancer, aiming to evaluate its potential to overcome drug resistance and enhance treatment outcomes through an integrated *in silico*, *in vitro*, and *in vivo* approach. This study utilizes three curated and pharmacologically validated compound databases as the primary source for VS. The first database comprises the Food and Drug Administration (FDA)-approved kinase inhibitors, which are designed to modulate aberrant kinase signaling – a hallmark of various malignancies. Given the central role of protein kinases in regulating key cellular processes and their frequent dysregulation in cancer, this class of therapeutics represents one of the most extensively targeted mechanisms in oncology. As of 2024, 80 small molecule kinase inhibitors have received FDA approval, of which 69 are indicated for cancer treatment, underscoring their clinical relevance in oncology.[12] The second compound library was sourced from the World Health Organization (WHO) Model List of Essential Medicines, a globally endorsed collection of drugs selected based on their proven efficacy, safety, affordability, and significance to public health. These compounds are clinically relevant, possess well-documented safety profiles, and are widely applicable across diverse therapeutic settings.[13] The third dataset comprises FDA-approved therapeutics used in breast cancer management, including agents that act on various molecular targets, such as estrogen and progesterone receptors, human epidermal growth factor receptor 2 (HER2), and key regulators of the cell cycle. These drugs constitute the cornerstone of present treatment protocols and may present repurposing opportunities if found to inhibit FN3K. Such dual-function compounds hold promise in attenuating both breast cancer progression and FN3K-driven metabolic adaptability.[14]

This study employed SBVS to identify potential small molecule binders with strong affinity toward the FN3K enzyme. SBVS involves molecular docking techniques that simulate the interaction of candidate compounds within the enzyme's active site, assessing their steric and electrostatic compatibility. To predict binding affinities and rank potential candidates, a combination of scoring functions – spanning empirical methods, force field-based approaches, and knowledge-driven models – was utilized to evaluate the stability of ligand-enzyme

interactions. This approach facilitates rational drug design by streamlining lead identification from extensive chemical libraries, minimizing experimental workload, and improving hit enrichment.[15] Lead molecule selection for therapeutic development represents a critical phase in the drug discovery pipeline, necessitating the validation of computational predictions through robust experimental assays. Lead candidates were strategically selected from the initial SBVS hits by evaluating their predicted binding strength and structural compatibility with the FN3K enzyme. These candidates were then subjected to biological evaluation to confirm their ability to inhibit FN3K enzymatic activity.[16] The overarching aim was to identify potent inhibitors capable of suppressing FN3K function, thereby offering potential therapeutic benefit in the context of breast cancer management.

To confirm computational findings and evaluate the biological significance of the selected FN3K inhibitors, *in vitro* assays were performed using quantitative PCR (qPCR) and Western blotting. These assays were utilized to investigate the expression patterns of FN3K and the redox-responsive transcription factor Nrf2, a key regulator of cellular antioxidant defenses and chemoresistance. Earlier research has shown that abnormal elevation of Nrf2 expression promotes tumor cell survival in oxidative environments, while its suppression increases cancer cell vulnerability to chemotherapeutic agents. This study also investigated the relationship between FN3K and Nrf2 expression across various breast cancer subtypes, underscoring their potential co-regulatory involvement in redox homeostasis and tumor progression.[7,17] By identifying compounds that selectively inhibit FN3K activity, we aimed to uncover novel therapeutic agents with potential applications in breast cancer management. FN3K plays a pivotal role in cancer progression by stabilizing and enhancing the oncogenic potential of Nrf2 through deglycation, thereby enabling sustained activation of antioxidant and survival pathways in tumor cells. Therefore, targeting FN3K offers a promising therapeutic strategy to attenuate aberrant Nrf2 signaling, overcome drug resistance, and sensitize cancer cells to oxidative stress. The identification of promising lead compounds exhibiting strong FN3K-inhibitory activity lays the groundwork for the rational design of novel anti-cancer strategies, particularly in breast cancer, where FN3K overexpression has been linked to unfavorable clinical outcomes. Taken together, this work illustrates the effectiveness of combining computational approaches, such as VS, with *in vitro* validation to accelerate the identification of targeted therapeutic candidates. The FN3K–Nrf2 signaling axis emerges as a novel and relatively unexplored target in cancer research, with FN3K inhibition offering promising prospects for advancing personalized treatment modalities.[4]

2. Materials and methods

2.1. SBVS

2.1.1. Materials

2.1.1.1. Software

Schrödinger Maestro (Schrödinger, LLC, USA) was used as a comprehensive molecular modeling environment for preparing, visualizing, and analyzing molecular structures.[18] For molecular docking, the Schrödinger Glide module within Maestro, was employed, as it is widely used for VS and drug discovery.[19]

2.1.1.2. Datasets

Kinase inhibitors approved by the FDA are integral components of cancer treatment due to their targeted mechanisms of action.[12] The WHO Model Essential Medicines list comprises pharmacological agents recognized for their clinical efficacy, safety profile, and widespread use in medical practice, as endorsed by the WHO.[13] In addition, FDA-approved anti-breast cancer agents represent a curated list of approved drugs specifically targeting breast cancer, offering potential repositioning opportunities.[14]

2.1.1.3. Computational resources

A high-performance computing cluster or a powerful workstation with sufficient memory and processing power was used to handle molecular simulations and docking calculations.[20]

2.1.1.4. Protein and ligand data

The three-dimensional (3D) structure of the target protein was generated through comparative or homology modeling to enable precise molecular docking and reliable assessment of ligand–protein interactions.[21] Ligand datasets were obtained from reputable sources, such as DrugBank, PubChem, and the FDA, providing well-characterized small molecules for VS.[12-14]

2.1.2. Methods

2.1.2.1. Construction of the 3D structure of the protein

The 3D structure of human FN3K was constructed through a systematic multistep process. First, the amino acid sequence of human FN3K, consisting of 309 residues and indexed under UniProt ID Q9H479, was retrieved from the UniProt database.[22] Phylogenetic similarities among FN3K sequences were then assessed using Clustal Omega, a robust tool for multiple sequence alignment.[23] For homology

modeling, a suitable structural template for FN3K was generated using SWISS-MODEL, an automated web-based tool for protein structure prediction based on sequence homology.[24] The preliminary FN3K model was further refined using the GalaxyWEB server, a platform providing specialized tools for protein structure optimization.[25] To ensure reliability and precision, the refined FN3K model underwent rigorous validation through various analytical techniques. Ramachandran plot analysis was performed to evaluate the ϕ (phi) and ψ (psi) dihedral angles of amino acid residues, confirming their placement within sterically favorable regions of the protein structure.[26] PROCHECK, accessed through the SAVES server at UCLA (https://saves.mbi.ucla.edu/), was used to assess the stereochemical quality and geometric parameters of the model.[27] In addition, the Global Model Quality Estimation (GMQE) score provided by SWISS-MODEL was considered to gauge the predicted reliability of the generated model.[28] Finally, Qualitative Model Energy Analysis (QMEAN) values were examined to estimate overall model quality based on multiple scoring functions.[29,30]

2.1.2.2. Protein preparation

To prepare the protein structure constructed through homology modeling, the generated model was imported into Maestro. Using the Protein Preparation Wizard within Maestro, several essential steps were undertaken to refine the homology-modeled protein structures.[31]

2.1.2.3. Preparation of ligand libraries

In preparing the ligand libraries, ligand datasets were curated from databases, such as DrugBank, PubChem, and the FDA.[12,32,33] The selected ligand structures were then imported into Maestro, where the LigPrep tool was used to generate 3D conformations from the 2D structures.[34]

2.1.2.4. Identification of potential binding sites

Potential ligand-binding regions on the modeled FN3K structure were predicted using the SiteMap module integrated within the Maestro software suite. SiteMap is an advanced computational tool designed to detect and characterize binding pockets and cavities within a protein structure.[35]

2.1.2.5. Preparation of the receptor grid

Following the identification of potential binding sites using SiteMap, the next step involved the preparation of the receptor grid. The receptor grid generation tool in Maestro was used for this purpose.[34]

2.1.2.6. Docking

The molecular docking setup was initiated by selecting the standard-precision (SP) mode within Glide. Glide is a molecular docking tool that predicts the binding affinity and orientation of ligands within a receptor binding site.[36]

2.1.2.7. Post-docking analysis

The docking results generated by Glide were analyzed to identify hit molecules based on binding affinity (Glide score) and key interactions with the FN3K active site. Binding conformations were evaluated for key molecular interactions, including hydrogen bonding, hydrophobic contacts, and π-π stacking.[37]

2.1.2.8. Absorption, distribution, metabolism, excretion, and toxicity (ADMET) screening

The shortlisted hit molecules from the post-docking analysis underwent the ADMET screening to assess their drug-like properties and safety profiles. This filtering step ensured the identification of compounds with both high binding affinity and desirable pharmacokinetic properties for further consideration.[38]

2.2. In vitro screening studies

2.2.1. In vitro cytotoxicity evaluation

2.2.1.1. Cell lines and culture conditions

The cytotoxicity of the selected compounds was assessed using human breast cancer cell lines – MCF-7, T47D, and BT-474 – as well as non-malignant Vero cells. All cell lines were cultured in Dulbecco's Modified Eagle's Medium (DMEM) supplemented with 10% fetal calf serum (FCS), 100 U/mL penicillin, 100 µg/mL streptomycin, and 50 µg/mL kanamycin. Cells were maintained at 37°C in a humidified incubator containing 5% CO_2 until approximately 70% confluency was achieved.[39]

2.2.1.2. 3-[4,5-dimethylthiazol-2-yl]-2,5-diphenyl tetrazolium bromide (MTT) assay

The cytotoxic effects of 1-deoxy-morpholino-D-fructose (1-DMF), ritonavir, amiloride, lansoprazole, capivasertib, and oxaliplatin were investigated using the MTT assay, following the ISO 10993-5:2009 guidelines for *in vitro* cytotoxicity assessment.[40] Cells were dispensed into 96-well plates at a density of 1×10^4 cells per well and incubated for 24 h to allow adherence under standard conditions. Thereafter, cells were treated in triplicates with a range of compound concentrations (12.5 – 200 µg/mL), tailored to individual solubility and bioactivity profiles, and incubated for an additional 24-h period.[41]

Post-treatment, 20 µL of MTT solution at 5 mg/mL, prepared in phosphate-buffered saline (PBS), was added to each well, followed by a 4-h incubation at 37°C to allow for formazan crystal formation.[40] The resulting crystals were solubilized using 100 µL of isopropanol containing 0.04N

hydrochloric acid (HCl). Absorbance was then recorded at 570 nm using a microplate spectrophotometer. Untreated cells served as the negative control for determining relative cell viability.[41]

2.2.2. qPCR evaluation

2.2.2.1. Cell culture and treatment

MCF-7, BT-474, and T-47D human breast cancer cell lines, along with non-malignant Vero cells, were cultured as adherent monolayers in 25 cm^2 tissue culture flasks. The cells were maintained in DMEM supplemented with 10% FCS and antibiotics, including penicillin and streptomycin, under standard incubation conditions at 37°C with 5% CO_2 and high humidity. Cultures were allowed to grow until approximately 70% confluency was achieved.[42] Cells were gently rinsed with 1× PBS and subsequently detached using 0.2% trypsin-EDTA at a volume of 200 µL per flask for 5 min at room temperature. The dissociated cells were then seeded into 6-well plates at a volume of 1.0 mL per well. The cells were allowed to adhere and stabilize for 48 h before treatment.

2.2.2.2. Total RNA isolation

Cell pellets were resuspended in TRIzol reagent and mixed thoroughly, followed by the addition of 300 µL chloroform to each sample.[43] After brief vortexing, the samples were incubated at room temperature for 15 min. Phase separation was carried out by centrifugation at 14,000 rpm for 10 min at 4°C, and the resulting aqueous phase was carefully transferred to a new microcentrifuge tube. An equal volume of isopropanol was then added, mixed gently, and incubated at room temperature for 5 min to precipitate RNA, followed by centrifugation under the same conditions. The RNA pellet was washed with 70% ethanol, air-dried, and reconstituted in 100 µL of diethyl pyrocarbonate (DEPC)-treated water. RNA purity and concentration were then determined spectrophotometrically by measuring absorbance at 260 nm.[44]

2.2.2.3. Complementary DNA (cDNA) synthesis

First-strand cDNA synthesis was performed using 5 µg of total RNA according to standardized reverse transcription protocols. The reaction mixture was prepared by combining 2 µL of total RNA (~5 µg), 2 µL of random hexamer or oligo(dT) primers, 2 µL of 10 mM dNTP mix, and 4 µL of DEPC-treated water. This mixture was heated at 65°C for 2 min to denature secondary structures and then allowed to equilibrate to room temperature. Next, 2 µL of 10× reverse transcription buffer, 4 µL of 25 mM $MgCl_2$, 2 µL of 0.1 M DTT, and 1 µL of RNase inhibitor were added. The mixture was pre-incubated at 25°C for 2 min, after which 1 µL of SuperScript II Reverse Transcriptase (Invitrogen, USA) was added. The enzymatic reaction was carried out through a thermal program consisting of 10 min at 25°C, 90 min at 42°C, and 15 min at 70°C to inactivate the enzyme. After a brief centrifugation step, 1 µL of RNase H was added to degrade the RNA template, followed by incubation at 37°C for 30 min. The synthesized cDNA was stored at −20°C until further use.

2.2.2.4. qPCR Analysis

The cDNA was diluted 1:1 with DEPC-treated water before amplification.[45] Each 10 µL qPCR reaction consisted of 1 µL of diluted cDNA, 1 µL of gene-specific primer mix (forward and reverse), 5 µL of SYBR® Green Supermix (Bio-Rad; Cat. No. 172-5270, USA), and nuclease-free Milli-Q water to reach the final volume.

qPCR was conducted using the QuantStudio 5 Real-Time PCR System (Applied Biosystems, USA) under a thermal protocol comprising 40 amplification cycles. Cycle threshold (Ct) values were recorded for each target gene, and relative gene expression levels were quantified using the ΔΔCt method. This approach ensures precise normalization and reliable detection of low-abundance transcripts, minimizing technical variability.[46,47]

2.2.2.5. Primer sequences

The specific primer sequences used for the amplification of FN3K, Nrf2, and ACTB (Beta actin) genes were summarized in Table 1.

2.2.3. Western blot analysis

2.2.3.1. Cell culture and treatment

MCF-7, BT-474, and T-47D human breast cancer cell lines, along with non-malignant Vero cells, were cultured as adherent monolayers in 25 cm^2 tissue culture flasks. The cells were maintained in DMEM supplemented with 10% FCS, penicillin, and streptomycin under standard incubation conditions at 37°C with 5% CO_2 in a humidified atmosphere, until approximately 70% confluency was reached.[7]

Cells were then rinsed with 1× PBS and detached by treating with 0.2% trypsin-EDTA at a volume of 200 µL per flask for 5 min at room temperature. The detached cells were resuspended in complete DMEM containing 10% FCS and antibiotics, and subsequently seeded into 6-well plates at a volume of 1.0 mL per well. After a 48-h adherence period, the cells were treated for 24 h with selected compounds – amiloride, capivasertib, ritonavir, oxaliplatin, lansoprazole, and 1-DMF.

Following treatment, cells were harvested, washed once with 1× PBS, and resuspended in 500 µL of 1× PBS. To each

Table 1. Primer sequences used for amplification of *FN3K, Nrf2*, and *ACTB* genes

Gene	Forward primer (5' → 3')	Reverse primer (5' → 3')	Reference
FN3K	GGGTGCTGAGCCTCAGTATGTGG	CCTTCTCAATGAGGTCCAGCTGC	Designed using Primer-BLAST
Nrf2	CATCGAGAGCCCAGTCTTCATTTGC	GCTTGTCATTTTCAATATTAAGAC	Designed using Primer-BLAST
ACTB	CATGCCATCCTGCGTCTGGACCTG	GTCCAGGGCGACGTAGCACAGC	Housekeeping gene

sample, 500 µL of 3× Laemmli sample buffer (50 mM Tris-HCl, pH 6.8; 100 mM DTT; 7% SDS; 0.1% bromophenol blue; and 10% glycerol) was added. The mixture was then heat-denatured at 95°C for 5 min in preparation for sodium dodecyl-sulfate polyacrylamide gel electrophoresis (SDS-PAGE).

2.2.3.2. SDS-PAGE

SDS-PAGE was carried out following the Laemmli protocol using a vertical gel electrophoresis system with a discontinuous buffer setup. The resolving gel was prepared with 8% acrylamide in 0.375 M Tris-HCl buffer (pH 8.8) containing 0.1% SDS, while the stacking gel comprised 5% acrylamide in 0.125 M Tris-HCl buffer (pH 6.8) with 0.1% SDS. Polymerization was initiated by the addition of tetramethylethylenediamine (TEMED) and ammonium persulfate (APS).

Protein samples were loaded into the wells, and electrophoretic separation was conducted in a running buffer consisting of 0.025 M Tris-HCl, 0.192 M glycine, and 0.1% SDS (pH 8.3). A constant current of 20 mA was applied during the stacking phase, followed by 30 mA during the resolving phase. Following electrophoresis, proteins were transferred onto polyvinylidene difluoride (PVDF) membranes through electrophoretic transfer for subsequent Western blot analysis.[48]

2.2.3.3. Protein transfer to PVDF membrane]

Following electrophoresis, the gel was incubated in transfer buffer composed of 39 mM glycine, 48 mM Tris base, 0.0375% SDS, and 20% methanol for 10 min to facilitate equilibration. Proteins were then transferred onto a PVDF membrane, pre-activated with methanol, and equilibrated in the same buffer. The transfer was performed using a semi-dry electroblotting system operated at a constant current of 0.8 mA/cm^2 for 1.5 h.

Transfer efficiency was verified by staining the membrane with Ponceau S solution containing 0.2% in 3% trichloroacetic acid and 3% sulfosalicylic acid. The positions of the molecular weight markers were marked on the blot before immunodetection.[48]

2.2.3.4. Western blot analysis and chemiluminescence detection

The membrane was extensively rinsed with 1× PBS to eliminate residual Ponceau S stain, followed by a blocking step in 5% Blotto solution – comprising 5% non-fat dry milk dissolved in Tris-buffered saline containing 0.1% Tween-20 (TBST) – for 1 h at room temperature to minimize non-specific antibody binding. Following blocking, the membrane was washed with TBST and incubated overnight at 4°C with the appropriate primary antibodies, including anti-Nrf2 antibody (1:1000 dilution), anti-FN3K antibody (1:1000 dilution), and anti-beta actin antibody (1:5000 dilution) as a loading control. After overnight incubation, the membranes were washed three times with TBST for 5 – 10 min each wash to remove unbound antibodies. Subsequently, the blots were incubated for 1 h at room temperature with horseradish peroxidase-conjugated goat anti-rabbit IgG secondary antibody, diluted 1:5000 in TBST. Following thorough washes with TBST to eliminate excess secondary antibody, protein bands were detected using a chemiluminescent substrate according to the manufacturer's protocol. Chemiluminescence signals were captured using a digital imaging system, and band intensities were analyzed for quantification. Beta actin served as a loading control for normalization of protein expression levels.[49]

2.3. Statistical analysis

All statistical evaluations were performed using Python libraries, including SciPy and statsmodels,[50] to assess the differential expression of FN3K and Nrf2 across various treatment groups in MCF-7, T-47D, BT-474, and Vero cell lines.

2.3.1. Data processing and normalization

In qPCR analysis, relative gene expression levels were calculated using the $2^{-}\Delta\Delta Ct$ method, with ACTB served as the internal control for normalization.[47] Meanwhile, for Western blot analysis, densitometric quantification of FN3K and Nrf2 protein bands was carried out using ImageJ (National Institutes of Health, Bethesda, USA). The values were normalized to beta actin to account for loading variability, and the resulting relative expression levels were subjected to statistical analysis.[50]

2.3.2. Statistical tests applied

Welch's t-test was employed to evaluate treatment effects by independently comparing each experimental group with the untreated control group. This statistical test

accommodates unequal variances and is appropriate for datasets with small sample sizes.[51] To mitigate the risk of false positives due to multiple comparisons, the Benjamini-Hochberg procedure was applied to control the False Discovery Rate (FDR).[52]

2.3.3. Significance thresholds used

The following significance thresholds were applied in the analysis: $p<0.05$ (*; marginally significant), $p<0.01$ (**; significant), $p<0.001$ (***; highly significant), $p\geq0.05$ → (not significant). All statistical analyses were conducted in Python utilizing the SciPy and statsmodels libraries, with statsmodels. stats. multitest applied for FDR correction.

3. Results and discussion

3.1. SBVS

3.1.1. Template selection and model validation

Template selection for homology modeling of the human FN3K enzyme was carried out by aligning the target protein sequence with evolutionarily related structures available in the SWISS-MODEL template library. To identify suitable homologous templates, the FN3K amino acid sequence was queried against the PDB-BLAST database. This search initially yielded 5,643 potential templates that matched the target sequence. To refine this extensive list, a heuristic approach was employed, narrowing it down to 50 templates. Figure 1 illustrates the alignment of the human FN3K target sequence with one of the selected homologous templates, highlighting the conserved regions and secondary structural elements.

Quality assessment of these 50 templates was performed using QMEAN and GMQE scores. QMEAN evaluates the overall geometric and energetic quality of the model, while GMQE estimates the expected accuracy of the homology model. Templates were ranked based on these criteria, with the top three templates demonstrating the highest scores and best alignment with the target sequence. In the subsequent protein modeling, three homology models (Figure 2) were developed, and the first model, based on the template from *Arabidopsis thaliana* FN3K, exhibited a sequence similarity of 90.61% with human FN3K and was selected for the study. This model was evaluated using GMQE and QMEAN scoring functions, where values approaching 1.0 on a scale from 0 to 1 indicate high model quality. The modeled protein structure (Model-1) achieved satisfactory scores, meeting the quality attributes necessary for a reliable model.

Further validation was carried out using the PROCHECK tool to assess the stereochemical quality of the model. PROCHECK provided a Ramachandran plot (Figure 3), which is instrumental in evaluating the overall geometry of the protein model based on residue-by-residue analysis of backbone dihedral angles (ϕ and ψ). The Ramachandran plot analysis revealed that most of the residues were located in the favored regions, indicating energetically favorable conformations. None of the residues were found in the disallowed or forbidden regions,



Figure 1. Target-template sequence alignment of human FN3K with a selected homologous structure (PDB ID: A0A2Y9PDG6.1.A). The figure displays the sequence alignment between the target human FN3K protein and its template, color-coded by region. Secondary structural elements (β-sheets) are shown as arrows. Conserved residues and aligned motifs critical for structural and functional integrity are evident across the alignment. This visualization supports the selection of a high-quality template for building the 3D model during the homology modeling process
Abbreviations: FN3K: Fructosamine-3-kinase

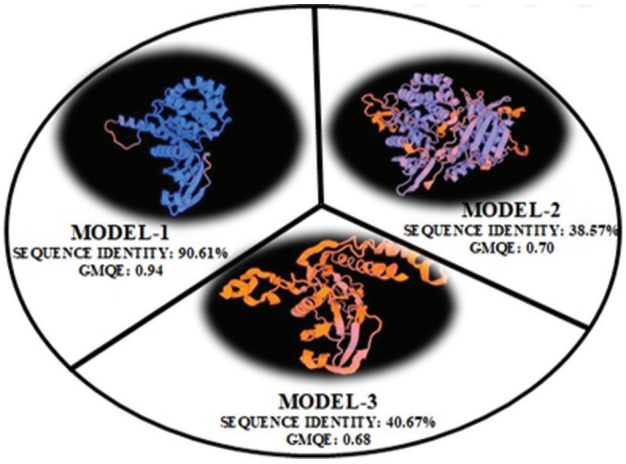


Figure 2. Comparative structural models of human FN3K derived from top-ranked homology templates. The figure illustrates three homology models generated during the structure prediction of human FN3K. Model-1 (top left): Based on a template from *Arabidopsis thaliana*, showing the highest sequence identity (90.61%) and a GMQE score of 0.94, indicating high structural reliability. Model-2 (top right): Built from a template with 38.57% sequence identity and a GMQE of 0.70. Model-3 (bottom): Constructed using a template with 40.67% identity and GMQE of 0.68
Abbreviations: FN3K: Fructosamine-3-kinase; GMQE: Global model quality estimation

confirming that the model meets the validation criteria for acceptable stereochemistry. Overall, the combination of high sequence similarity, favorable GMQE and QMEAN scores, and validation through PROCHECK suggests that Model-1 is a robust and accurate representation of the human FN3K enzyme structure. This structural model (Figure 4) provides a solid foundation for further computational and experimental studies aimed at understanding the functional implications and potential applications of human FN3K.

3.1.2. VS and docking results

SBVS yielded multiple candidate compounds with strong predicted binding affinities toward FN3K, as indicated by favorable docking scores. The selection criteria for potential hits included both numerical docking scores and qualitative assessments of key ligand–protein interactions, such as hydrogen bonding, hydrophobic contacts, and π–π stacking. Among the docked molecules, a subset exhibited significantly higher binding affinities and more favorable interaction profiles compared to others. To ensure the selection of the most potent inhibitors, a rank-based selection approach was applied, wherein the top 10% of ligands or the top 10 ranked compounds with the most negative Glide docking scores were shortlisted. This approach ensured that only the best-performing molecules – those predicted to have the highest binding affinity – were prioritized for

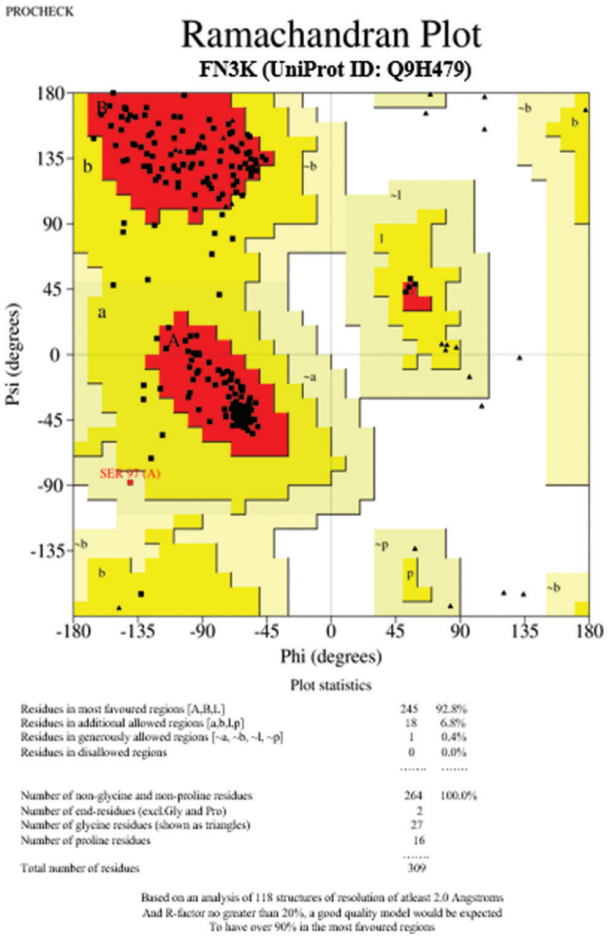


Figure 3. Ramachandran plot of the modeled human FN3K structure generated by PROCHECK. The plot depicts the distribution of backbone dihedral angles (ϕ and ψ) for amino acid residues in the modeled FN3K protein. Among 309 residues, 92.8% are located within the most favored regions, 6.8% within additionally allowed regions, and 0.4% within generously allowed regions. No residues were observed in disallowed regions, indicating the stereochemical validity of the predicted protein structure
Abbreviations: FN3K: Fructosamine-3-kinase

further evaluation. Table 2 summarizes the top six docked molecules, highlighting their docking scores, molecular weights, and specific amino acid interactions within the FN3K binding pocket. Notably, oxaliplatin, ritonavir, lansoprazole, and capivasertib demonstrated strong interactions with key residues, such as CYS A:24, LYS A:41, and ASP A:217 – suggesting a conserved binding motif critical for effective FN3K inhibition.

3.1.3. ADMET analysis of hit compounds

To further validate the potential hits, the top-ranked candidates were subjected to additional rounds of analysis. This included a review of their physicochemical properties

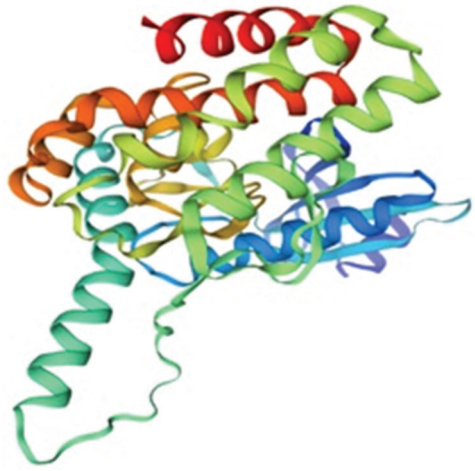


Figure 4. Three-dimensional structure of the final modeled human FN3K protein. The 3D structure is depicted using a rainbow color gradient, ranging from the N-terminus (blue) to the C-terminus (red), to illustrate the overall fold. The model features a compact globular conformation with prominent α-helices and β-sheets. Following validation by stereochemical and sequence-based assessments, this structure was chosen for subsequent molecular docking and functional analysis
Abbreviations: FN3K: Fructosamine-3-kinase

to ensure drug-likeness and a preliminary ADMET assessment to evaluate their pharmacokinetic profiles and safety considerations. The detailed results of the ADMET screening, including physicochemical properties, drug-likeness, solubility, gastrointestinal absorption, and cytochrome P450 (CYP) interactions, are provided in Supplementary Tables S1-S5 and Figure S1. These combined analyses enabled the exclusion of compounds with suboptimal properties or toxicity risks. Ultimately, the final selection of hit molecules was based on a holistic assessment encompassing VS performance, rank-based scoring, favorable physicochemical characteristics, and acceptable ADMET profiles. These molecules serve as promising leads for subsequent validation through *in vitro* enzyme inhibition assays and advanced computational analyses, aimed at substantiating their potential as therapeutic inhibitors of FN3K. Docking scores, expressed in kcal/mol, reflect the predicted binding affinity between ligand and target, with more negative values corresponding to stronger interactions.

3.1.4. Key findings from VS

Oxaliplatin (−9.2 kcal/mol) exhibited the highest binding affinity, forming stable interactions with residues CYS A:24, ILE A:25, LYS A:41, MET A:51, ASP A:217, and TRP A:219. These residues are likely critical for FN3K activity, suggesting a strong inhibitory potential. Lansoprazole (−8.6 kcal/mol) and capivasertib (−8.1 kcal/mol) also showed strong binding, interacting with CYS A:24, LYS A:41, and ASP A:217, which are key active site residues. This supports their potential as FN3K inhibitors. Ritonavir (−8.7 kcal/mol) demonstrated a strong binding score but interacted with fewer critical residues, indicating potential, but possibly with reduced specificity for FN3K inhibition. In contrast, amiloride (−6.9 kcal/mol) and 1-DMF (−6.1 kcal/mol) displayed weaker binding and fewer significant interactions, suggesting they may not be ideal candidates as FN3K inhibitor. The 3D and 2D protein–ligand interaction profiles of all six hit molecules, including their binding residues and docking scores, are presented in Figure S2.

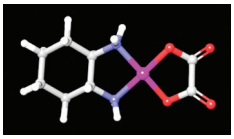
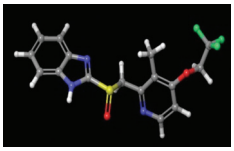
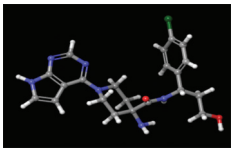
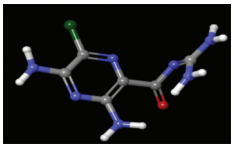
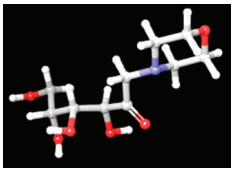
This study was intentionally structured as a focused drug repurposing investigation aimed at identifying clinically relevant FN3K inhibitors with high translational potential. The screening FDA-approved kinase inhibitors, WHO-listed essential medicines, and anti-breast cancer agents offers multiple advantages in oncology drug discovery, including established safety profiles, known pharmacokinetic properties, and regulatory familiarity – factors that collectively expedite the clinical translation process. This strategic approach allowed us to rapidly transition from *in silico* screening to *in vitro* validation across diverse breast cancer subtypes.

Our findings with oxaliplatin, lansoprazole, and capivasertib underscore the feasibility and effectiveness of this repurposing-centric approach. These compounds demonstrated strong FN3K inhibition, selective cytotoxicity toward malignant cells, and downregulation of redox-associated transcriptional programs, thereby validating their mechanistic relevance.

Nonetheless, we acknowledge that restricting the chemical library to approved drugs inherently limits the structural diversity and novelty of potential hits. Exploring broader chemical space, including natural product scaffolds, macrocyclic inhibitors, and *de novo* designed chemical entities, may uncover novel binding chemotypes and allosteric inhibitors with improved specificity and potency. Accordingly, future studies will integrate VS of natural compound libraries (e.g., NPASS, ZINC Natural Products), fragment-based approaches, and machine learning-assisted scaffold hopping to identify next-generation FN3K inhibitors.

Thus, while our repurposing approach lays a pragmatic foundation for translational success, it also opens avenues for expanded pharmacophore discovery and rational design of structurally novel inhibitors tailored to FN3K's catalytic and regulatory domains.

Table 2. Docking scores and key interactions of selected hits with FN3K

S. No.	Drug name	Chemical structure	Docking score (kcal/mol)	Interacting amino acids
1	Oxaliplatin Mol wt: 397.2		−9.2	CYS A: 24, ILE A: 25, LYS A: 41, MET A: 51, ASP A: 217, TRP A: 219
2	Ritonavir Mol wt: 720.31		−8.7	PHE A: 39, GLY A: 221
3	Lansoprazole Mol wt: 369.08		−8.6	CYS A: 24, LYS A: 41, ASP A: 217, TRP A: 219, HIS A: 288
4	Capivasertib Mol wt: 428.17		−8.1	CYS A: 24, LYS A: 41, ASP A: 217, GLY A: 221, ASN A: 222, ASP A: 234
5	Amiloride Mol wt: 229.05		−6.9	CYS A: 24, ILE A: 25, SER A: 26, LYS A: 41, GLU A: 55, GLY A: 152, ASN A: 222
6	1-DMF Mol wt: 249.12		−6.1	GLY A: 221, ASP A: 234

Abbreviations: 1-DMF: 1-deoxy-morpholino-D-fructose; Mol wt: Molecular weight.

3.2. *In vitro* screening studies

3.2.1. Half-maximal inhibitory concentration (IC50) determination and cytotoxicity analysis

The cytotoxic effects of six selected compounds – 1-DMF, ritonavir, amiloride, lansoprazole, capivasertib, and oxaliplatin – were assessed across three breast cancer cell lines (MCF-7, T47D, and BT-474) and one non-malignant Vero cells using the MTT assay. IC_{50} values were calculated based on the percentage of viable cells relative to untreated controls. The IC_{50} values for each compound across the individual cell lines are summarized in Table 3.

All tested compounds exhibited concentration-dependent cytotoxicity across the evaluated breast cancer cell lines. Among them, oxaliplatin and lansoprazole demonstrated the lowest IC_{50} values (90 – 110 µg/mL), indicating a higher potency against MCF-7, T47D, and BT-474 cells. These results suggest that both compounds

Table 3. IC_{50} values (µg/mL) of selected compounds across different cell lines

Compounds	MCF-7	T47D	BT-474	Vero
1-DMF	125	125	125	>150
Ritonavir	125 – 150	125 – 150	125 – 150	>150
Amiloride	125 – 150	125 – 150	125 – 150	>150
Lansoprazole	90 – 110	90 – 110	90 – 110	150
Capivasertib	100 – 125	100 – 125	100 – 125	>150
Oxaliplatin	90 – 110	90 – 110	90 – 110	140

Abbreviations: 1-DMF: 1-deoxy-1-morpholino-D-fructose; IC_{50}: Half-maximal inhibitory concentration.

may be effective at lower concentrations in reducing cell viability and warrant further investigation as potential anti-cancer agents targeting FN3K pathways.

Capivasertib showed moderate cytotoxicity, with IC_{50} values ranging from 100 – 125 μg/mL across the tested breast cancer cell lines. On the other hand, ritonavir, amiloride, and 1-DMF exhibited higher IC_{50} values (125 – 150 μg/mL), suggesting relatively lower cytotoxic potential. Interestingly, the non-malignant Vero cells showed markedly higher IC_{50} values (>150 μg/mL for most compounds), indicating selective cytotoxicity toward cancer cells. This selective response enhances the potential therapeutic index of the effective compounds. Although the IC_{50} values observed for oxaliplatin and lansoprazole (~90 – 110 μg/mL) and for capivasertib (100 – 125 μg/mL), indicate promising *in vitro* potency, their pharmacological relevance must be interpreted with caution. Drug concentrations required to achieve cytotoxic effects in monolayer culture systems are often higher than those effective *in vivo*, due to differences in drug metabolism, microenvironmental factors, and tumor tissue architecture. Moreover, *in vitro* IC_{50} values do not account for sustained exposure, tissue retention, or intracellular accumulation – all of which significantly influence therapeutic outcomes in clinical settings.

For instance, oxaliplatin forms DNA adducts that persist long after plasma clearance, contributing to prolonged anti-tumor activity.[53] Capivasertib has demonstrated efficacy in breast cancer clinical trials with intermittent oral dosing (400 – 480 mg BID), showing favorable toxicity profiles.[54] Lansoprazole, although not classified as an anti-cancer drug, has exhibited synergistic effects with chemotherapeutics in pre-clinical models due to its modulation of lysosomal pH and autophagy.[55]

Therefore, while the IC_{50} values provide a useful benchmark for early-stage screening, *in vivo* pharmacokinetic and tumor accumulation studies are essential for confirming therapeutic relevance. Our future animal studies will evaluate FN3K–Nrf2 axis modulation, assess systemic toxicity, and establish optimal dosing strategies to bridge the current gap between *in vitro* and *in vivo* findings.

To further assess treatment-induced effects, microscopic images of both treated and untreated cells were captured. These images, provided in Supplementary Figures S3 and S4, depict the cellular morphological changes observed post-treatment. However, as this study primarily focuses on the molecular downregulation of FN3K expression, further analyses were conducted using qPCR and Western blot techniques.

3.2.2. qPCR analysis

3.2.2.1. FN3K and Nrf2 expression in MCF-7 Cells

qPCR was conducted to assess the modulatory effects of six tested compounds on the gene expression levels of FN3K and Nrf2 in MCF-7 breast cancer cells. The integrity of the isolated RNA was validated through agarose gel electrophoresis (Supplementary Figure S5).

The expression patterns of FN3K and Nrf2 were evaluated across different treatment conditions, revealing distinct regulatory effects. In the untreated control, FN3K and Nrf2 exhibited baseline expression levels of 1.000 and 1.020, respectively. Among the tested compounds, oxaliplatin, lansoprazole, and capivasertib emerged as potent FN3K inhibitors. Oxaliplatin exhibited the most significant suppression, reducing FN3K expression by nearly 99.99% (2.0×10^{-5}), along with a moderate Nrf2 suppression (0.032). Similarly, lansoprazole showed strong FN3K inhibition, with a 99.90% reduction (0.001), accompanied by a mild decrease in Nrf2 expression (0.015). Capivasertib also demonstrated substantial FN3K suppression (0.000), along with moderate Nrf2 inhibition (0.063), making its efficacy comparable to that of the other top inhibitors. These findings confirm that oxaliplatin, lansoprazole, and capivasertib act as effective FN3K inhibitors, capable of significantly reducing FN3K expression with varying degrees of Nrf2 suppression. This is illustrated in Supplementary Figure S6, which presents qPCR gel images of FN3K and Nrf2 expression.

Conversely, amiloride, ritonavir, and 1-DMF did not exhibit strong FN3K inhibition, with some compounds showing unexpected regulatory effects. Amiloride led to a 157.0% increase in FN3K expression (2.570), while simultaneously inducing marked suppression of Nrf2 (7.4×10^{-5}), suggesting a potential inverse regulatory mechanism. Similarly, ritonavir induced a slight upregulation of FN3K (1.220), along mild Nrf2 suppression (0.001), indicating no inhibitory effect on FN3K. Meanwhile, 1-DMF displayed moderate FN3K suppression (0.176), but only weak inhibition of Nrf2 (0.022), making it less potent compared to oxaliplatin, lansoprazole, and capivasertib.

Since FN3K inhibition was the primary objective of this study, only compounds demonstrating significant FN3K downregulation in MCF-7 cells were selected for further qPCR analysis. Among the six tested compounds, oxaliplatin, lansoprazole, and capivasertib exhibited potent FN3K suppression (≥99.6%), whereas amiloride and ritonavir failed to inhibit FN3K, and 1-DMF showed only moderate inhibition.

To substantiate these observations and examine the consistency of FN3K inhibition across distinct breast

cancer subtypes, qPCR analysis was further performed on T-47D and BT-474 cell lines. Vero cells were incorporated as a non-malignant control model to evaluate the selectivity of the tested compounds toward malignant cells.

3.2.2.2. FN3K and Nrf2 expression in T-47D Cells

The impact of oxaliplatin, lansoprazole, and capivasertib on the expression of FN3K and Nrf2 was assessed in T-47D cells, demonstrating a consistent downregulation of FN3K, comparable to the pattern observed in MCF-7 cells. In the untreated control group, baseline expression levels were recorded as 1.010 for FN3K and 1.060 for Nrf2. Among the tested compounds, lansoprazole displayed the highest degree of FN3K inhibition, reducing expression by 99.99% (1.00×10^{-4}), along with significant suppression of Nrf2 (0.029, ↓97.2%). Oxaliplatin also exhibited potent FN3K downregulation (↓99.6%), reducing FN3K expression to 0.004, with corresponding Nrf2 suppression of 0.028 (↓97.3%). Similarly, capivasertib strongly inhibited FN3K expression (↓99.97%), reducing it to 2.60×10^{-4}, with a moderate suppression of Nrf2 (0.056, ↓94.7%).

These results indicate that FN3K suppression by lansoprazole, oxaliplatin, and capivasertib in T-47D cells is consistent with trends observed in MCF-7 cells. Notably, lansoprazole demonstrated the highest FN3K inhibition in T-47D (↓99.99%), exceeding its effect in MCF-7 cells, further reinforcing its potential as a potent FN3K inhibitor. Similarly, oxaliplatin and capivasertib maintained strong FN3K suppression across both cell lines (↓99.6 – 99.99%), confirming their effectiveness in targeting FN3K-dependent pathways. These findings suggest that FN3K inhibition by these compounds is not restricted to a specific cell line but represents a consistent biological response, further validating their therapeutic relevance.

3.2.2.3. FN3K and Nrf2 expression in BT-474 Cells

The expression patterns of FN3K and Nrf2 were analyzed in BT-474 cells following treatment with oxaliplatin, lansoprazole, and capivasertib, revealing strong and consistent downregulation of FN3K across all tested conditions. In the untreated control group, baseline expression levels of FN3K and Nrf2 were 1.020 and 1.050, respectively. Lansoprazole demonstrated the most potent FN3K inhibition, reducing its expression by 99.98% to 0.000, while also significantly suppressing Nrf2 to 0.060, representing a 94.3% reduction. Oxaliplatin also showed strong FN3K suppression, reducing expression by 99.7% to 0.003, with Nrf2 downregulated to 0.104, corresponding to a 90.1% decrease. Similarly, capivasertib exhibited substantial FN3K inhibition of 99.88%, lowering expression to 0.001, and moderately suppressing Nrf2 to 0.067, representing a 93.5% reduction.

These findings further reinforce the consistency of FN3K inhibition across multiple breast cancer cell lines. Lansoprazole consistently exhibited the highest FN3K suppression across MCF-7, T-47D, and BT-474 models, with inhibition levels ranging from 99.98% to 99.99%. Similarly, oxaliplatin and capivasertib maintained robust and reproducible FN3K inhibition across all cell lines, with suppression levels ranging from 99.6% to 99.99%. The consistency of these results across various breast cancer subtypes – including ER-positive, HER2-positive, and triple-negative models – indicates the broad-spectrum potential of these compounds as FN3K inhibitors, thereby reinforcing their prospective therapeutic value in various breast cancer settings.

3.2.2.4. FN3K and Nrf2 expression in Vero cells

The expression patterns of FN3K and Nrf2 in Vero cells were assessed following treatment with oxaliplatin, lansoprazole, and capivasertib. In contrast to the strong inhibitory effects observed in breast cancer cell lines, these compounds exhibited minimal to no suppression of FN3K in Vero cells. In the untreated control group, baseline expression levels of FN3K and Nrf2 were 1.040 and 1.000, respectively. Oxaliplatin resulted in a modest 12% reduction in FN3K expression, lowering it to 0.880, while Nrf2 remained unchanged at 1.010, indicating no significant impact on this pathway. Lansoprazole caused a slight FN3K suppression of 9%, reducing expression to 0.910, and also mildly inhibited Nrf2 to 0.890, representing an 11% decrease. Capivasertib did not alter FN3K expression, which remained at 1.010, and induced only a minor suppression in Nrf2 to 0.950, representing a 5% decrease.

These results suggest that FN3K inhibition by oxaliplatin, lansoprazole, and capivasertib is not prominent in non-malignant Vero cells, in stark contrast to their effects in breast cancer models. The lack of substantial FN3K suppression in Vero cells indicates a degree of specificity toward malignant cells, as observed in MCF-7, T-47D, and BT-474. Furthermore, the minimal changes in Nrf2 expression across treatments further support the idea that these compounds may exert selective effects depending on the cellular context. These observations underscore the differential regulatory effects of the tested compounds on FN3K and Nrf2 expression in cancerous versus non-cancerous cell lines, supporting their therapeutic potential in cancer management while indicating a comparatively minimal impact on normal cells.

3.2.3. Comparative analysis of FN3K and Nrf2 downregulation: Cancer vs. normal cells

qPCR was employed to investigate the expression patterns of FN3K and Nrf2 in three human breast cancer cell lines

– MCF-7, T-47D, and BT-474 – as well as in the non-malignant Vero cell line. This analysis aimed to explore the differential modulation of FN3K and Nrf2 following treatment with oxaliplatin, lansoprazole, and capivasertib, thereby evaluating both the selectivity and efficacy of these agents in targeting cancerous versus non-cancerous cells.

As shown in Table 4, all three compounds significantly suppressed FN3K and Nrf2 expression in the breast cancer cell lines, with lansoprazole and oxaliplatin showing the most potent effects. Notably, the FN3K fold changes in cancer cells decreased by more than 99% across all three treatments, while expression in Vero cells remained largely unaffected, highlighting their selective activity toward malignant cells. Similar trends were observed for Nrf2, with up to 98.5% downregulation in cancer lines and only minimal suppression observed in the Vero cell line.

This comparative analysis provides critical insights into the therapeutic potential of FN3K-targeted inhibition and its downstream impact on Nrf2-regulated oxidative stress pathways, which are often upregulated in cancer cells to promote survival and resistance to therapy.

3.2.3.1. FN3K inhibition exhibits high selectivity for cancer cells with minimal effects in normal cells

As shown in Table 4, oxaliplatin, lansoprazole, and capivasertib all demonstrated strong FN3K downregulation (↓99.6 – 99.99%) in breast cancer cell lines. In contrast, FN3K expression in non-malignant Vero cells remained largely unaffected, with only a modest reduction of 9 – 12%. These findings indicate that FN3K inhibition by these compounds exhibits tumor-selective activity, potentially minimizing the risk of off-target effects in non-cancerous cells.

3.2.3.2. Nrf2 inhibition follows FN3K suppression selectively in cancer cells

In cancer cells, Nrf2 expression was significantly downregulated (↓90.1 – 98.5%) following treatment with the tested compounds. In Vero cells, however, Nrf2 expression level remained unchanged or was only mildly suppressed (↓5 – 11%). This pattern further supports the selectivity of FN3K-targeting compounds for tumor suppression.

3.2.3.3. Capivasertib demonstrates the highest FN3K selectivity among the tested compounds

Among the three compounds, capivasertib exhibited the greatest selectivity. In breast cancer cells (MCF-7, T-47D, BT-474), capivasertib strongly inhibited FN3K expression (↓99.88 – 99.98%). In contrast, FN3K expression in Vero cells remained unchanged, indicating no significant impact on non-malignant cells. This suggests that capivasertib may serve as the most specific FN3K inhibitor among the three.

3.3. Statistical analysis

3.3.1. Differential expression of FN3K and Nrf2 in MCF-7 Cells

qPCR analysis of FN3K and Nrf2 gene expression in MCF-7 breast cancer cells treated with oxaliplatin, lansoprazole, capivasertib, amiloride, ritonavir, and 1-DMF demonstrated notable alterations in transcript levels. Statistical evaluation was performed using either Welch's

Table 4. Comparative qPCR analysis of FN3K and Nrf2 downregulation in cancer (MCF-7, T-47D, BT-474) versus normal (Vero) cells

Treatment	FN3K fold change (MCF-7)	FN3K fold change (T-47D)	FN3K fold change (BT-474)	FN3K fold change (Vero)	Interpretation
Untreated (control)	1.00	1.01	1.02	1.04	Baseline expression in all cell lines.
Oxaliplatin	0.00002 (↓99.99%)	0.0039 (↓99.6%)	0.0029 (↓99.7%)	0.88 (↓12%)	Selective FN3K inhibition in cancer cells, minimal effect in Vero cells.
Lansoprazole	0.00097 (↓99.90%)	0.0001 (↓99.99%)	0.0002 (↓99.98%)	0.91 (↓9%)	Highly selective FN3K inhibition in cancer cells, minimal suppression in Vero cells.
Capivasertib	0.00017 (↓99.98%)	0.00026 (↓99.97%)	0.0012 (↓99.88%)	1.01 (No change)	Strong FN3K suppression in cancer cells, no effect in Vero cells.
Treatment	Nrf2 fold change (MCF-7)	Nrf2 fold change (T-47D)	Nrf2 fold change (BT-474)	Nrf2 fold change (Vero)	Interpretation
Untreated (Control)	1.02	1.06	1.05	1.00	Baseline expression in all cell lines.
Oxaliplatin	0.0318 (↓96.8%)	0.0283 (↓97.3%)	0.1041 (↓90.1%)	1.01 (No change)	Selective Nrf2 inhibition in cancer cells, no effect in Vero cells.
Lansoprazole	0.0152 (↓98.5%)	0.0289 (↓97.2%)	0.0595 (↓94.3%)	0.89 (↓11%)	Strong Nrf2 inhibition in cancer cells, mild effect in Vero cells.
Capivasertib	0.0629 (↓93.8%)	0.0563 (↓94.7%)	0.0673 (↓93.5%)	0.95 (↓5%)	Significant Nrf2 suppression in cancer cells, minimal effect in Vero cells.

Note: ↓indicates percent downregulation in gene expression relative to control (untreated) levels.
Abbreviation: FN3K: Fructosamine-3-kinase.

t-test or the Mann-Whitney U test, with adjustments for multiple comparisons made through FDR correction.

3.3.1.1. FN3K expression analysis

The expression of FN3K was significantly downregulated upon treatment with oxaliplatin, lansoprazole, and capivasertib, with all three compounds showing highly significant reductions (p<0.001; Figure 5). In contrast, 1-DMF exhibited a marginally significant reduction in FN3K expression (p<0.05). Neither amiloride (p=0.092) nor ritonavir (p=0.199) significantly altered FN3K expression following FDR correction. These findings suggest that oxaliplatin, lansoprazole, and capivasertib act as effective FN3K inhibitors, whereas amiloride and ritonavir do not substantially influence FN3K levels in MCF-7 cells.

3.3.1.2. Nrf2 expression analysis

The expression of Nrf2 was significantly downregulated by lansoprazole, amiloride, and ritonavir, with all three compounds demonstrating highly significant reductions (p<0.001; Figure 5). Oxaliplatin also suppressed Nrf2 expression but to a lesser extent, with statistical significance at p<0.01. Meanwhile, 1-DMF exhibited a marginally significant reduction (p<0.05). Capivasertib, however, did not significantly alter Nrf2 expression (p=0.171). Interestingly, although amiloride and ritonavir did not significantly impact FN3K expression, both compounds caused a pronounced suppression of Nrf2, suggesting a potential alternative regulatory mechanism.

These results highlight that oxaliplatin, lansoprazole, and capivasertib effectively inhibit FN3K, while lansoprazole, amiloride, and ritonavir strongly suppress Nrf2. The differential effects observed indicate that while some compounds act directly on FN3K, others may influence Nrf2 independently, warranting further mechanistic exploration.

3.3.2. Differential expression of FN3K and Nrf2 in T-47D Cells

3.3.2.1. FN3K expression analysis

The expression of FN3K was significantly downregulated by oxaliplatin, lansoprazole, and capivasertib, with all three treatments displaying highly significant reductions (p<0.001; Figure 6). This strong statistical significance indicates that these compounds may act as potent FN3K inhibitors in T-47D cells, reinforcing their inhibitory effects observed in other breast cancer cell models.

3.3.2.2. Nrf2 expression analysis

Oxaliplatin, lansoprazole, and capivasertib all significantly downregulated Nrf2 expression, with p-values falling below the 0.01 threshold after FDR correction (Figure 6).

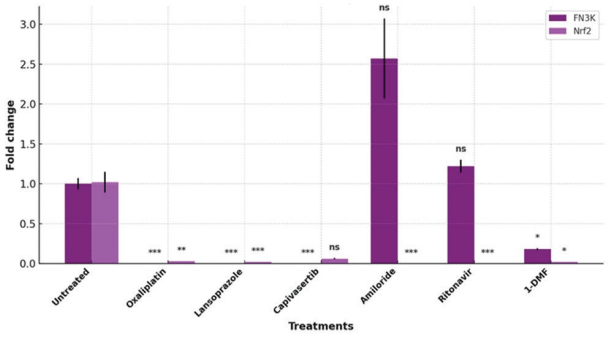


Figure 5. Treatment-specific expression of *FN3K* and *Nrf2* genes in MCF-7 cells. The bar graph illustrates the fold change in FN3K and Nrf2 expression following treatment with oxaliplatin, lansoprazole, capivasertib, amiloride, ritonavir, and 1-DMF. Significant downregulation of FN3K was observed with oxaliplatin, lansoprazole, and capivasertib (p<0.001), while Nrf2 expression was significantly reduced by lansoprazole, amiloride, and ritonavir (p<0.001)
Abbreviations: 1-DMF: 1-deoxy-1-morpholino-D-fructose; FN3K: Fructosamine-3-kinase; Nrf2: Nuclear factor erythroid 2-related factor 2; ns: Not significant

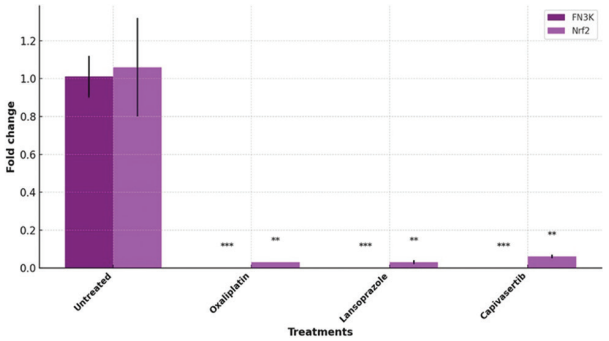


Figure 6. Treatment-specific expression of *FN3K* and *Nrf2* genes in T-47D cells. FN3K and Nrf2 expression were significantly reduced in response to oxaliplatin, lansoprazole, and capivasertib (p<0.001 for FN3K; p<0.01 for Nrf2), suggesting a strong inhibitory effect
Abbreviations: FN3K: Fructosamine-3-kinase; Nrf2: Nuclear factor erythroid 2-related factor 2

This consistent suppression of Nrf2 suggests that these compounds may exert a dual effect by not only inhibiting FN3K but also reducing Nrf2 levels in T-47D cells. The concurrent inhibition of both FN3K and Nrf2 may enhance the therapeutic relevance of these compounds by targeting key regulatory pathways involved in cancer progression.

3.3.3. Differential expression of FN3K and Nrf2 in BT-474 Cells

3.3.3.1. FN3K expression analysis

The expression of FN3K was significantly downregulated by oxaliplatin, lansoprazole, and capivasertib, with all three treatments displaying highly significant reductions

(p<0.001; Figure 7). The strong statistical significance across these treatments suggests that these compounds act as potent FN3K inhibitors in BT-474 cells, consistent with findings in other breast cancer models. This reinforces their potential as effective FN3K-targeting agents.

3.3.3.2. Nrf2 expression analysis

Oxaliplatin, lansoprazole, and capivasertib all significantly downregulated Nrf2 expression, with p-values falling below 0.01 after FDR correction (Figure 7). This suggests that these compounds not only inhibit FN3K but also reduce Nrf2 levels in BT-474 cells. The simultaneous suppression of FN3K and Nrf2 may enhance their therapeutic potential by targeting key pathways involved in tumor progression, further supporting their role as promising candidates for cancer therapy.

3.3.4. Differential expression of FN3K and Nrf2 in Vero Cells

3.3.4.1. FN3K expression analysis

FN3K expression did not show significant downregulation in response to oxaliplatin, lansoprazole, or capivasertib, as all treatments resulted in p-values greater than 0.05, indicating no statistical significance (Figure 8). This suggests that these compounds do not significantly affect FN3K expression in Vero cells, a non-malignant model. The absence of FN3K suppression in normal cells further supports the hypothesis that the inhibitory effects observed in breast cancer models may be tumor-specific.

3.3.4.2. Nrf2 expression analysis

Similarly, no significant downregulation of Nrf2 expression was observed in response to oxaliplatin, lansoprazole, or capivasertib, with all p-values exceeding 0.05 (Figure 8). This indicates that these compounds do not exhibit inhibitory effects on Nrf2 expression in Vero cells. Given that Vero cells are non-malignant, these findings reinforce the idea that FN3K and Nrf2 inhibition observed in breast cancer models may be selective for cancerous cells, further strengthening their potential relevance in oncological applications.

3.4. Western blot

Western blot analysis was conducted to quantify FN3K and Nrf2 protein expression levels in MCF-7, BT-474, and T-47D breast cancer cell lines, as well as in Vero cells to assess specificity. The initial analysis was performed in MCF-7 cells to evaluate the expression levels of FN3K and Nrf2 following treatment with six hit molecules identified from the *in silico* VS. Based on the expression patterns observed, a subset of these compounds was chosen for

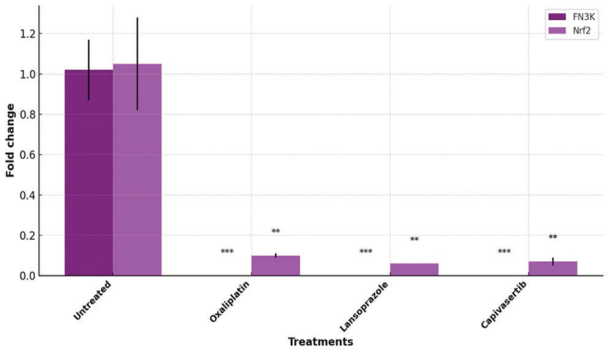


Figure 7. Treatment-specific expression of *FN3K* and *Nrf2* genes in BT-474 cells. The expression levels of FN3K and Nrf2 were significantly downregulated following treatment with oxaliplatin, lansoprazole, and capivasertib (p<0.001 for FN3K; p<0.01 for Nrf2)
Abbreviations: FN3K: Fructosamine-3-kinase; Nrf2: Nuclear factor erythroid 2-related factor 2

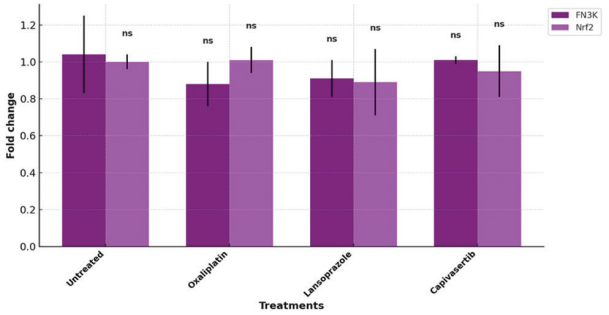


Figure 8. Treatment-specific expression of FN3K and Nrf2 in Vero cells. The bar graph represents the fold change in expression levels upon treatment with oxaliplatin, lansoprazole, and capivasertib. No statistically significant changes were observed across treatments
Abbreviations: FN3K: Fructosamine-3-kinase; Nrf2: Nuclear factor erythroid 2-related factor 2; ns: Not significant

further validation in BT-474 and T-47D breast cancer cell lines to assess the consistency of their effects across different breast cancer models. In addition, the selected compounds were tested in Vero cells to evaluate their specificity and ensure that the observed effects were cancer cell-specific rather than a generalized cellular effect.

3.4.1. Western blot analysis of FN3K and Nrf2 expression in MCF-7 Cells

Western blot analysis revealed distinct expression patterns of FN3K and Nrf2 across different treatment groups, highlighting potential mechanisms of action for the tested compounds. The primary FN3K inhibitors demonstrated substantial downregulation of FN3K (Figure 9), whereas the impact on Nrf2 varied among treatments (Figure 10), indicating distinct regulatory influences on metabolic and oxidative stress pathways.

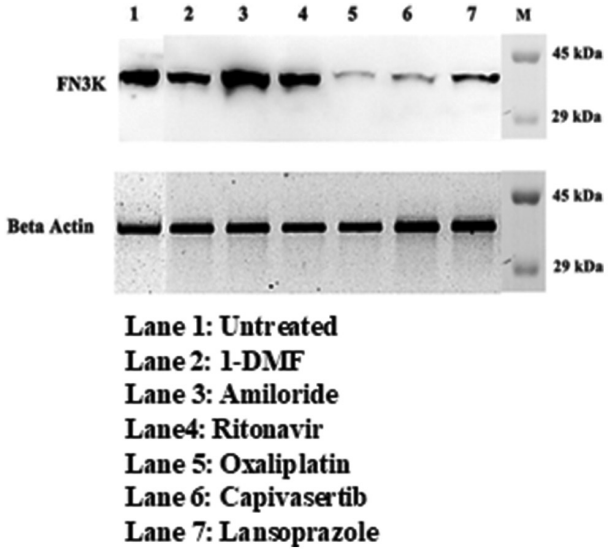


Figure 9. Representative Western blot showing FN3K protein expression following treatment with various compounds. Cell lysates were subjected to SDS-PAGE and probed with anti-FN3K antibody. Beta actin was used as a loading control. A molecular weight marker (lane M) is included for size reference (29 kDa and 45 kDa)
Abbreviations: 1-DMF: 1-deoxy-1-morpholino-D-fructose; FN3K: Fructosamine-3-kinase

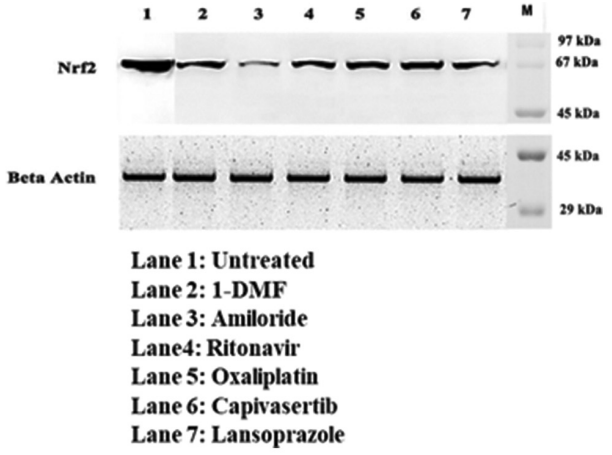


Figure 10. Representative Western blot showing Nrf2 protein expression under different treatment conditions. Cell lysates were analyzed by SDS-PAGE and immunoblotted with an anti-Nrf2 antibody. Beta actin was used as a loading control. A molecular weight marker (lane M) was included for reference, indicating band positions at 29, 45, 67, and 97 kDa
Abbreviations: 1-DMF: 1-deoxy-1-morpholino-D-fructose; Nrf2: Nuclear factor erythroid 2-related factor 2

3.4.1.1. FN3K expression analysis

FN3K expression was markedly reduced by oxaliplatin (0.322), capivasertib (0.317), and lansoprazole (0.457), indicating a strong inhibitory effect (Figure 9). Among these, oxaliplatin exhibited the most potent suppression, reducing FN3K levels by approximately 66% relative to the untreated control, closely followed by capivasertib. These findings suggest that FN3K inhibition may be a key mechanism underlying the anti-cancer activity of oxaliplatin and capivasertib. Moderate suppression of FN3K expression was observed with 1-DMF (0.636) and ritonavir (0.834), indicating a less pronounced but still notable inhibitory effect. This suggests that while these compounds interfere with FN3K function, their effects are weaker compared to oxaliplatin and capivasertib. In contrast, amiloride (0.976) had minimal impact on FN3K expression, implying that its mechanism of action does not involve FN3K inhibition and may instead act through alternative metabolic or signaling pathways.

3.4.1.2. Nrf2 expression analysis

Nrf2 expression exhibited the most significant reduction following treatment with amiloride (0.393), representing nearly a 60% decrease relative to the untreated control (Figure 10). This drastic downregulation suggests that amiloride may interfere with oxidative stress-related pathways, potentially sensitizing MCF-7 cells to oxidative stress and impairing adaptive responses that promote chemoresistance.

Moderate reductions in Nrf2 expression were observed with 1-DMF (0.639), ritonavir (0.584), and lansoprazole (0.683). The suppression induced by lansoprazole (~30% reduction) aligns with previous studies suggesting that proton pump inhibitors can modulate oxidative stress and apoptosis-related mechanisms. In contrast, oxaliplatin (0.818) and capivasertib (0.812) did not significantly suppress Nrf2 expression, with levels remaining close to those of the untreated control. This suggests that while these compounds effectively inhibit FN3K, they do not substantially impair oxidative stress defenses, indicating a more selective mechanism of action. The observed variations in FN3K and Nrf2 expression across different treatment conditions provide valuable insights into the mechanistic pathways influenced by these compounds. The differential effects on FN3K and Nrf2 suggest potential therapeutic implications, with some compounds acting primarily as FN3K inhibitors, while others modulating oxidative stress responses, both of which may contribute to their overall anti-cancer potential.

3.4.2. Western blot analysis of FN3K and Nrf2 expression in T-47D Cells

Western blot analysis was carried out to quantify FN3K and Nrf2 protein expression in T-47D cells following treatment with the selected compounds. The result revealed distinct expression patterns of FN3K and Nrf2 across the different

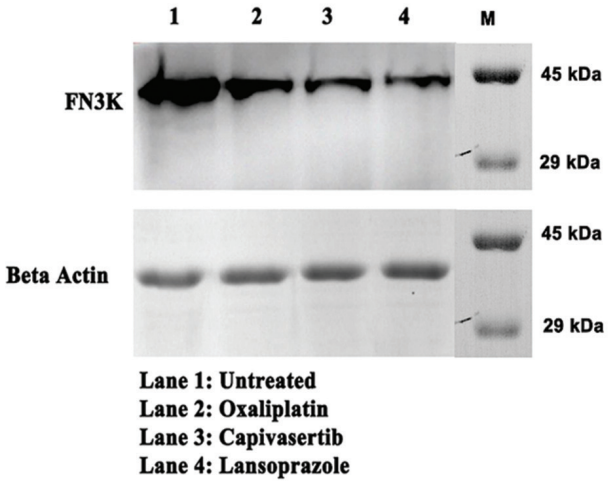


Figure 11. Representative Western blot showing FN3K protein levels in T47D cells treated with different compounds. T47D cell lysates were subjected to SDS-PAGE and immunoblotted using an anti-FN3K antibody. Beta actin was used as a loading control. A molecular weight marker (lane M) is included for size reference (29 kDa and 45 kDa)
Abbreviations: FN3K: Fructosamine-3-kinase

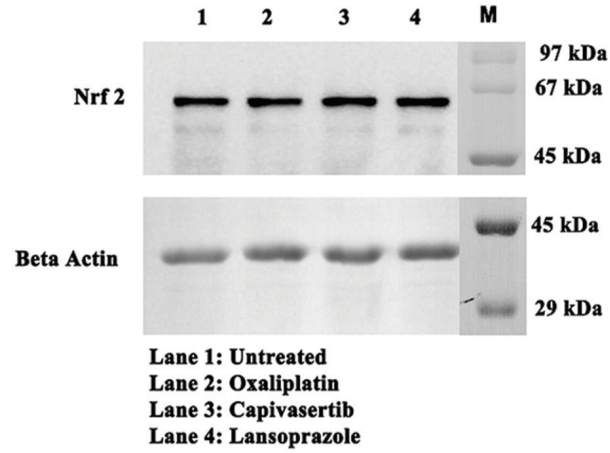


Figure 12. Representative Western blot showing Nrf2 protein expression in T47D cells treated with selected compounds. Western blot analysis was performed using T47D cell lysates probed with an anti-Nrf2 antibody. Beta actin was used as the internal loading control. A molecular weight marker (M) indicates bands at 29, 45, 67, and 97 kDa
Abbreviations: Nrf2: Nuclear factor erythroid 2-related factor 2

treatment groups, highlighting potential mechanisms of action for the tested compounds, as depicted in Figures 11 and 12.

3.4.2.1. FN3K expression analysis

Oxaliplatin exhibited the most substantial reduction in FN3K expression, decreasing its levels to 0.677, which representing approximately a 30% suppression compared to the untreated control (Figure 11). This suggests that oxaliplatin may act as a strong FN3K inhibitor in T-47D cells, potentially influencing metabolic regulation. In contrast, capivasertib (0.979) and lansoprazole (0.876) induced only minimal reductions in FN3K expression, with lansoprazole showing a modest ~10% decrease, while capivasertib had a negligible effect. These findings indicate that while these compounds may modulate FN3K expression, their impact is less pronounced than that observed with oxaliplatin. The untreated control (0.967) served as a baseline reference for comparison.

3.4.2.2. Nrf2 expression analysis

Nrf2 expression remained largely unaffected across all treatment groups, with oxaliplatin (0.909), capivasertib (0.979), and lansoprazole (0.886) showing values close to or slightly below control levels (1.049; Figure 12). This suggests that, in T-47D cells, these compounds do not significantly influence Nrf2 expression, contrasting with their observed effects in other cell models.

A notable difference was observed when comparing these findings to MCF-7 cells, where amiloride significantly suppressed Nrf2 expression (~60% reduction), and both oxaliplatin and capivasertib induced moderate reductions (~20%). In T-47D cells, however, none of the tested compounds produced significant Nrf2 downregulation, indicating potential cell-line-specific resistance mechanisms or a lack of regulatory dependency between FN3K suppression and Nrf2 modulation in this model. These findings highlight differences in FN3K and Nrf2 regulatory pathways between MCF-7 and T-47D cells, suggesting that cell-line-specific responses should be considered when evaluating FN3K inhibitors for therapeutic applications.

3.4.3. Western blot analysis of FN3K and Nrf2 expression in BT-474 Cells

Western blot analysis was conducted to evaluate FN3K and Nrf2 expression levels in BT-474 cells under different treatment conditions. The results (Figures 13 and 14) illustrate distinct regulatory effects, with FN3K expression exhibiting variable suppression across treatments, while Nrf2 levels remained largely stable.

3.4.3.1. FN3K expression analysis

Oxaliplatin exhibited the most pronounced suppression of FN3K expression, reducing its levels to 0.681, corresponding to an approximately 30% reduction compared to the untreated control (Figure 13). This suggests that oxaliplatin effectively inhibits FN3K,

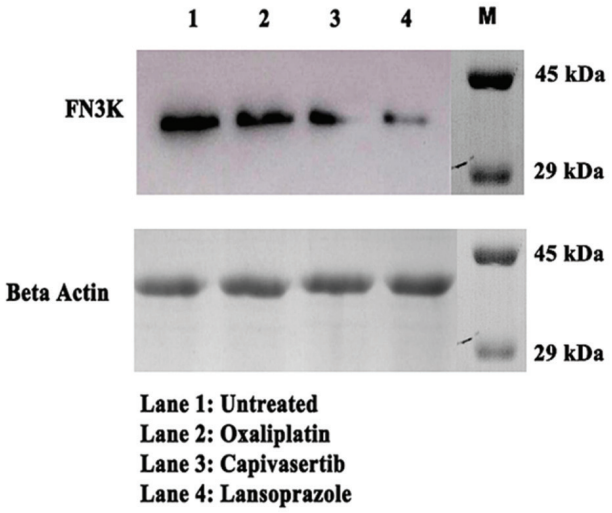


Figure 13. Representative Western blot showing FN3K expression in BT474 cells treated with different compounds. Protein lysates from BT474 cells were separated by SDS-PAGE and immunoblotted with an anti-FN3K antibody. Beta actin served as the internal loading control. A molecular weight marker (lane M) is included for size reference (29 kDa and 45 kDa)
Abbreviations: FN3K: Fructosamine-3-kinase

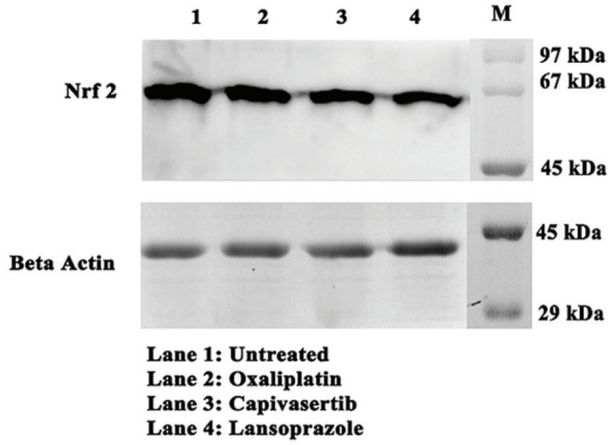


Figure 14. Representative Western blot showing Nrf2 protein expression in BT474 cells after compound treatment. BT474 cell lysates were analyzed by SDS-PAGE and probed with an anti-Nrf2 antibody. Beta actin was used as a loading control. A molecular weight marker (M) indicates bands at 29, 45, 67, and 97 kDa
Abbreviations: Nrf2: Nuclear factor erythroid 2-related factor 2

potentially disrupting metabolic adaptation mechanisms in BT-474 cells. Lansoprazole (0.802) induced a moderate reduction (~17% decrease), indicating some level of inhibition, though less pronounced than oxaliplatin. In contrast, capivasertib (0.991) resulted in a negligible reduction (~2% decrease), suggesting that it does not significantly affect FN3K levels in BT-474 cells.

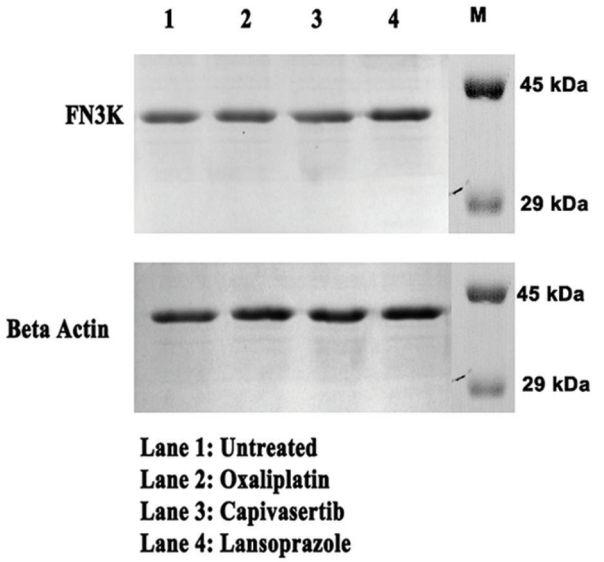


Figure 15. Representative Western blot showing FN3K expression in Vero cells after treatment with selected compounds. Vero cell lysates were subjected to SDS-PAGE and immunoblotting using an anti-FN3K antibody. Beta actin served as a loading control. A molecular weight marker (lane M) is included for size reference (29 kDa and 45 kDa)
Abbreviations: FN3K: Fructosamine-3-kinase

3.4.3.2. Nrf2 expression analysis

Nrf2 expression remained largely unchanged across all treatment groups, with oxaliplatin (0.917), capivasertib (1.008), and lansoprazole (0.964) displaying values close to those of the untreated control (1.049; Figure 14). This indicates that these compounds do not significantly downregulate Nrf2 in BT-474 cells. The stability of Nrf2 levels suggests the presence of a resistance mechanism in this cell line that prevents oxidative stress suppression, distinguishing BT-474 from other models.

These findings underscore the distinct regulatory responses in BT-474 cells compared to MCF-7 and T-47D, emphasizing the importance of considering cell-line-specific variations in FN3K and Nrf2 modulation when evaluating therapeutic strategies.

3.4.4. Western blot analysis in Vero cells: Assessing specificity and off-target effects

Vero cells, derived from the kidney epithelium of the African green monkey, serve as a non-malignant control model in comparative studies. Unlike cancer cells, Vero cells exhibit distinct metabolic and oxidative stress response mechanisms, allowing them suitable for assessing potential off-target effects and the cancer selectivity of tested compounds. Evaluating FN3K and Nrf2 modulation in Vero cells following treatment with oxaliplatin, capivasertib, and lansoprazole provides valuable insights

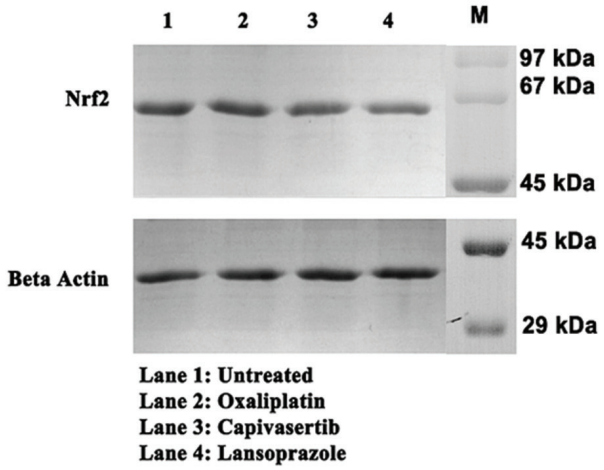


Figure 16. Representative Western blot showing Nrf2 expression in Vero cells treated with selected compounds. Vero cell lysates were analyzed by SDS-PAGE followed by immunoblotting with an anti-Nrf2 antibody. Beta actin was used as the internal loading control. A molecular weight marker (M) indicates bands at 29, 45, 67, and 97 kDa
Abbreviations: Nrf2: Nuclear factor erythroid 2-related factor 2

into the tumor-specific targeting of these compounds, as depicted in Figures 15 and 16.

3.4.4.1. FN3K expression analysis

FN3K expression remained largely unchanged across all treatment groups (Figure 15), with oxaliplatin (1.024) and capivasertib (0.980) showing minimal deviation from the untreated control (0.967). Lansoprazole induced a slight increase in FN3K expression (1.036), representing an approximate 7% upregulation, which is unlikely to have a biologically significant impact. These findings suggest that FN3K-dependent metabolic pathways in normal Vero cells are not strongly affected by these compounds, reinforcing the notion that FN3K inhibition is more relevant in cancer-specific metabolic adaptations.

Comparison with FN3K expression patterns in MCF-7, T-47D, and BT-474 cells reveals that baseline FN3K expression in Vero cells is inherently lower than in cancerous models. This observation supports the hypothesis that FN3K is upregulated in cancer cells as part of metabolic reprogramming, making it a viable tumor-specific target.

3.4.4.2. Nrf2 expression analysis

Nrf2 expression remained relatively stable across all conditions (Figure 16), with only minor variations observed. Oxaliplatin (0.929) led to a slight reduction (~11%), while capivasertib (1.008) and lansoprazole (0.946) showed no significant alterations in expression levels compared to the untreated control (1.049). These findings suggest that the

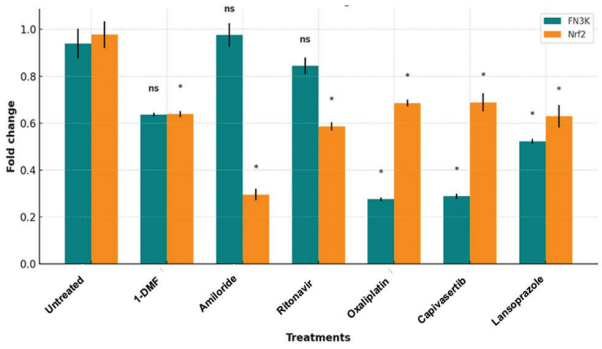


Figure 17. Western blot densitometric analysis of FN3K and Nrf2 expression in MCF-7 cells. Protein expression levels were normalized to beta actin. Welch's t-test with Benjamini-Hochberg correction was applied for statistical analysis. Significant changes ($p<0.05$) are marked with an asterisk (*), while non-significant changes are labeled as ns
Abbreviations: 1-DMF: 1-deoxy-1-morpholino-D-fructose; FN3K: Fructosamine-3-kinase; Nrf2: Nuclear factor erythroid 2-related factor 2

tested compounds do not strongly modulate Nrf2-driven oxidative stress responses in non-cancerous cells.

Notably, Nrf2 expression in untreated Vero cells was already high, indicating strong intrinsic antioxidant defenses typical of normal kidney-derived cells. This aligns with previous findings that non-cancerous epithelial cells rely on robust basal Nrf2 activity to counter oxidative stress, further distinguishing their regulatory mechanisms from those of cancer cells.

3.5. Overall implications

Across all tested breast cancer cell lines, oxaliplatin consistently demonstrated the strongest FN3K inhibition, followed by lansoprazole and capivasertib, with varying degrees of suppression depending on the cell type. The absence of FN3K inhibition in Vero cells confirms that the inhibitory effects observed in MCF-7, T-47D, and BT-474 are cancer-specific rather than the result of generalized cytotoxicity. These findings suggest that FN3K inhibitors preferentially target metabolic pathways in breast cancer cells while sparing normal tissues, highlighting their potential therapeutic relevance.

As this study primarily focused on FN3K inhibition, changes in Nrf2 expression were not a direct objective. According to the proposed mechanism, FN3K inhibition is expected to reduce Nrf2 deglycation, thereby preventing its activation and nuclear translocation. Consequently, Nrf2 expression itself should remain unchanged or show slight upregulation, which is consistent with the observed results. The absence of significant Nrf2 downregulation across all tested cell lines further supports the hypothesis that FN3K inhibition selectively disrupts Nrf2 activation without directly altering its expression levels. These findings

reinforce FN3K as a promising therapeutic target, with minimal impact on oxidative stress regulatory pathways.

3.6. Statistical analysis of FN3K and Nrf2 expression in MCF-7 Cells

Statistical evaluation of FN3K and Nrf2 protein expression across various treatment groups was performed using Welch's t-test, with multiple testing corrections applied through the Benjamini-Hochberg method to control the FDR. Protein levels were normalized against beta actin, and all statistical analyses were carried out using the SciPy and statsmodels libraries in Python. The resulting statistical metrics and significance thresholds are illustrated in Figure 17.

3.6.1. FN3K expression analysis

Oxaliplatin, capivasertib, and lansoprazole significantly downregulated FN3K expression ($p<0.05$), indicating a strong inhibitory effect on this metabolic enzyme (Figure 17). In contrast, 1-DMF ($p=0.060$), amiloride ($p=0.678$), and ritonavir ($p=0.341$) did not significantly alter FN3K expression, suggesting minimal or no impact on this pathway in MCF-7 cells.

3.6.2. Nrf2 expression analysis

All tested compounds, including 1-DMF, amiloride, ritonavir, oxaliplatin, capivasertib, and lansoprazole, significantly suppressed Nrf2 expression ($p<0.05$; Figure 17). This suggests a potential mechanistic link between FN3K inhibition and oxidative stress modulation, reinforcing the idea that these compounds may influence tumor progression through metabolic and redox regulatory pathways.

These findings highlight that oxaliplatin, capivasertib, and lansoprazole effectively target FN3K while also reducing Nrf2 expression. Meanwhile, although 1-DMF, amiloride, and ritonavir did not significantly impact FN3K levels, their ability to suppress Nrf2 suggests possible alternative mechanisms of action related to oxidative stress and redox balance in MCF-7 cells.

3.7. Statistical analysis of FN3K and Nrf2 expression in T-47D Cells

In T-47D cells, statistical analysis of FN3K and Nrf2 protein expression was conducted using Welch's t-test, with FDR correction applied for multiple comparisons. Protein levels were normalized to beta actin, and a p-value below 0.05 was considered statistically significant, as presented in Figure 18.

3.7.1. FN3K expression analysis

Oxaliplatin significantly downregulated FN3K expression ($p=0.048$), suggesting an inhibitory effect on this metabolic enzyme in T-47D cells (Figure 18). In contrast, capivasertib ($p=0.864$) and lansoprazole ($p=0.072$) did not induce statistically significant FN3K suppression, indicating minimal or inconsistent effects on FN3K expression in this cell line.

3.7.2. Nrf2 expression analysis

Nrf2 expression remained largely unaffected across all treatment groups (Figure 18), with oxaliplatin ($p=0.300$), capivasertib ($p=0.657$), and lansoprazole ($p=0.552$) showing no statistically significant changes compared to the untreated control. This suggests that, in T-47D cells, these compounds do not strongly influence oxidative stress regulatory pathways.

These findings highlight a differential regulatory response in T-47D cells compared to MCF-7, where FN3K inhibition was more pronounced and Nrf2 suppression was significant across multiple treatments. The lack of

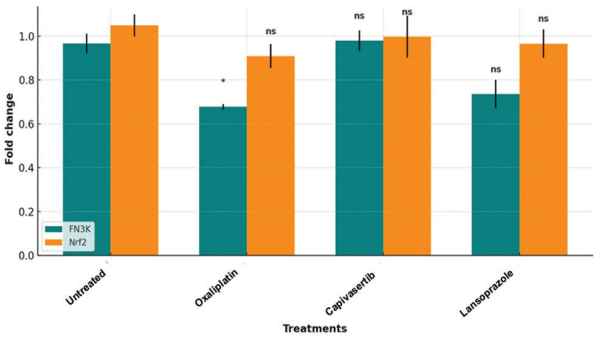


Figure 18. Western blot densitometric analysis of FN3K and Nrf2 expression in T-47D cells. Protein expression levels were normalized to beta actin. Welch's t-test with Benjamini-Hochberg correction was applied. Significant changes ($p<0.05$) are marked with an asterisk (*), while non-significant changes are labeled as ns
Abbreviations: FN3K: Fructosamine-3-kinase; Nrf2: Nuclear factor erythroid 2-related factor 2

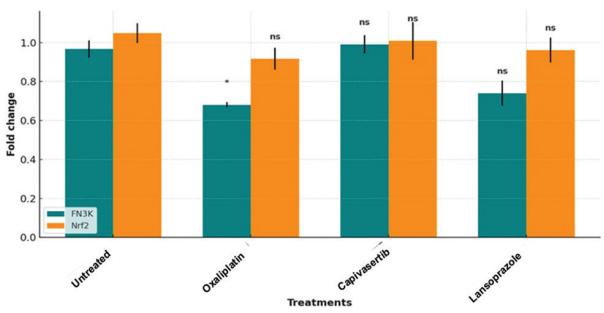


Figure 19. Western blot densitometric analysis of FN3K and Nrf2 expression in BT-474 cells. Protein expression levels were normalized to beta actin. Welch's t-test with Benjamini-Hochberg correction was applied. Significant changes ($p<0.05$) are marked with an asterisk (*), while non-significant changes are labeled as ns
Abbreviations: FN3K: Fructosamine-3-kinase; Nrf2: Nuclear factor erythroid 2-related factor 2

significant Nrf2 modulation in T-47D cells suggests that FN3K suppression in this model may not directly impact oxidative stress signaling, reinforcing the importance of cell-line-specific responses in evaluating potential therapeutic targets.

3.8. Statistical analysis of FN3K and Nrf2 expression in BT-474 Cells

Protein expression changes of FN3K and Nrf2 in BT-474 cells were statistically analyzed using Welch's t-test, with FDR correction applied for multiple testing. Beta actin was used for normalization, and statistical significance was defined as $p<0.05$, as depicted in Figure 19.

3.8.1. FN3K expression analysis

Oxaliplatin induced a marginally significant reduction in FN3K expression ($p=0.049$), suggesting a moderate inhibitory effect on FN3K expression in BT-474 cells (Figure 19). However, capivasertib ($p=0.725$) and lansoprazole ($p=0.077$) did not significantly alter FN3K expression, indicating statistically no significance impact on this pathway in this cell line.

3.8.2. Nrf2 expression analysis

Nrf2 expression remained unchanged across all treatment groups (Figure 19), with oxaliplatin ($p=0.300$), capivasertib ($p=0.739$), and lansoprazole ($p=0.521$) showing no significant differences compared to the untreated control. These results align with trends observed in T-47D cells, where FN3K suppression did not correlate with notable Nrf2 modulation.

These findings suggest that while oxaliplatin exerts a measurable inhibitory effect on FN3K expression in BT-474 cells, capivasertib and lansoprazole do not significantly impact this metabolic enzyme in this context.

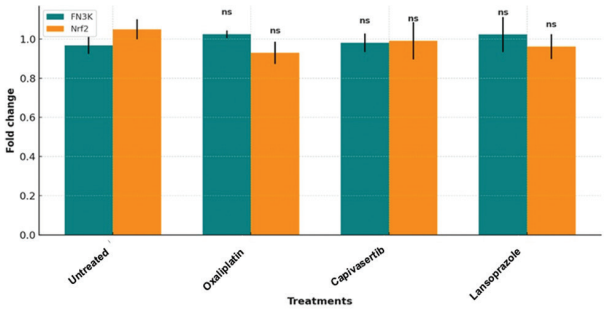


Figure 20: Western blot densitometric analysis of FN3K and Nrf2 expression in Vero cells. Protein expression levels were normalized to beta actin. Welch's t-test with Benjamini-Hochberg correction was applied. No significant changes were observed across treatments, as indicated by the non-significant (ns) labels
Abbreviations: FN3K: Fructosamine-3-kinase; Nrf2: Nuclear factor erythroid 2-related factor 2

In addition, the lack of significant Nrf2 suppression across treatments implies that oxidative stress regulatory pathways in BT-474 cells may be less responsive to these compounds, further reinforcing the importance of considering cell-line-specific variations in therapeutic response.

3.9. Selective FN3K inhibition in cancer: Lack of significant modulation in non-malignant Vero cells

Statistical analysis of Western blot data was performed using Python-based tools, with appropriate tests applied for normality assessment and pairwise comparisons. Multiple comparison correction was implemented to ensure statistical robustness (Figure 20).

3.9.1. FN3K expression analysis

Treatment with oxaliplatin ($p=0.846$), capivasertib ($p=0.846$), and lansoprazole ($p=0.846$) did not result in statistically significant alterations in FN3K expression levels in Vero cells (Figure 20). These results indicate that none of the tested compounds exert an inhibitory effect on FN3K in this non-malignant cell line, further reinforcing the selective suppression of FN3K in cancerous models.

3.9.2. Nrf2 expression analysis

Similarly, Nrf2 expression remained unaffected across all treatment conditions (Figure 20), with oxaliplatin ($p=0.600$), capivasertib ($p=0.624$), and lansoprazole ($p=0.600$) showing no statistically significant changes compared to the untreated control. The absence of Nrf2 modulation suggests that oxidative stress pathways in Vero cells are not significantly influenced by these compounds.

These findings confirm that FN3K inhibition is primarily a cancer-specific event, with minimal impact on non-malignant cell lines, such as Vero cells. The lack of significant FN3K and Nrf2 modulation in these normal cells supports the hypothesis that FN3K suppression occurs preferentially in tumor-specific contexts, reinforcing its potential as a selective therapeutic target in oncology.

3.10. Crosstalk between FN3K and redox-sensitive pathways

While Nrf2 suppression emerged as a consistent downstream effect of FN3K inhibition in our study, we recognize that Nrf2 is a master regulator of cellular redox balance, and its modulation may impact multiple overlapping pathways. FN3K has been shown to deglycate lysine and arginine residues on Nrf2, enhancing its nuclear translocation, sMAF binding, and transcriptional activation of ARE-driven genes, such as *NQO1*, *HO-1*, and *TXNRD1*.[3,10] Our *in vitro* results confirmed FN3K and Nrf2 co-downregulation in breast cancer cells, supporting this mechanistic link. However, Nrf2 activity intersects with a wide array of signaling

cascades – including PI3K/Akt, nuclear factor kappa B (NF-κB), glucose-6-phosphate dehydrogenase (G6PD), hypoxia-inducible factor 1-alpha (HIF1α), and Notch – which govern tumor proliferation, inflammation, and immune evasion.[56,57]

Inhibition of FN3K may thus have pleiotropic effects, not only attenuating Nrf2's antioxidant defense but also disrupting cellular metabolism, mitochondrial function, and DNA repair responses through its deglycation activity on other substrates. FN3K-sensitive proteins include ribosomal subunits, translation factors, histones, and glycolytic enzymes, implying that FN3K may act as a redox-modifying hub beyond Nrf2 stabilization. Moreover, accumulation of AGEs due to reduced FN3K activity can activate RAGE-mediated pathways (PI3K, MAPK, NF-κB), promoting angiogenesis, drug resistance, and cancer progression.[3,10]

While our findings emphasize Nrf2 suppression as a prominent outcome of FN3K inhibition, we acknowledge the possibility of off-target redox modulation. Further pathway-mapping studies are warranted to profile global transcriptional changes, ROS accumulation, and metabolic shifts induced by FN3K inhibition in tumor and normal tissues. These insights will be crucial for identifying synergistic targets and ensuring safety in future pre-clinical development.

3.11. Translational relevance and clinical integration

The repositioning of oxaliplatin, lansoprazole, and capivasertib as FN3K-targeted inhibitors necessitates careful evaluation of their clinical applicability, particularly in breast cancer settings. Oxaliplatin, a third-generation platinum-based chemotherapeutic, has shown efficacy beyond colorectal cancer, including promising results in platinum-pretreated breast and ovarian cancers. Despite dose-limiting peripheral neuropathy, novel strategies, such as chronomodulated delivery and calcium–magnesium infusions have been explored to mitigate toxicity.[53,58,59] Its potential in redox-sensitive tumors supports dose-sparing strategies when used in combination with targeted agents, such as FN3K inhibitors.

Capivasertib, a selective pan-AKT inhibitor, has been validated in hormone receptor-positive and triple-negative breast cancer (TNBC) through trials, such as CAPItello-291, which demonstrated a significant progression-free survival advantage when combined with fulvestrant in patients harboring PI3K/AKT/PTEN alterations. The intermittent 4-days-on/3-days-off (400–480 mg BID) dosing regimen was optimized based on exposure–response modeling to balance efficacy and tolerability, minimizing adverse events like hyperglycemia, rash, and diarrhea.[60] These pharmacological characteristics support its rational inclusion in redox-modulatory and kinase-targeted regimens, including FN3K-focused strategies.

Lansoprazole, traditionally used as a proton pump inhibitor (PPI), has demonstrated potent anti-tumor effects, including HDAC2 inhibition, autophagy modulation, and reversal of drug sequestration in acidic endosomal compartments. Its synergy with chemotherapeutic agents, such as doxorubicin and metronomic cyclophosphamide underscores its capacity to enhance intratumoral drug distribution and overcome microenvironment-induced resistance.[61-64] Importantly, lansoprazole has a wide therapeutic window, favorable oral bioavailability, and a well-established safety profile, making it a viable candidate for combination therapies targeting the FN3K–Nrf2 axis.

Collectively, the clinical readiness of these agents, coupled with their distinct mechanisms of action, offers a pragmatic advantage for rapid translation. Future trials should focus on dose-optimization, toxicity reduction through combination strategies, and patient stratification based on FN3K and Nrf2 expression to ensure precision-guided therapy in breast cancer.

3.12. Statistical limitations and power considerations

Although the experimental results – particularly qPCR and Western blot analyses – revealed statistically significant downregulation of FN3K and Nrf2 across multiple breast cancer cell lines, it is important to acknowledge that this study did not include a formal a priori power analysis. Given the exploratory nature of the study, a fixed number of biological replicates (n = 3 per group) was used, which is consistent with standard practice for preliminary *in vitro* screening studies. Welch's t-test was employed to accommodate unequal variance assumptions, and FDR correction was applied to manage Type I errors in multiple comparisons. However, the small sample size may reduce the power to detect subtle biological effects and increase the risk of false negatives (Type II errors).

Power analysis, which estimates the minimum required sample size to achieve a desired statistical power (commonly 80%) at a defined effect size and significance level (typically $\alpha = 0.05$), is a critical component of confirmatory pre-clinical studies. In this preliminary work, our objective was to identify FN3K-inhibitory candidates and assess differential expression patterns across redox-responsive signaling pathways. The findings from this phase now provide the effect size estimates that will inform formal sample size calculations in subsequent confirmatory studies.

Future validation studies – including *in vivo* tumor xenograft models and expanded *in vitro* assays with dose–response replicates – will incorporate a priori power analyses to optimize statistical robustness, minimize sampling bias, and ensure reproducibility. This stepwise

integration of statistical planning from exploratory to confirmatory phases aligns with best practices in translational cancer research and ensures rigorous evidence generation in subsequent stages of drug development.

3.13. Scope and generalizability of findings

The present study employed three molecularly distinct breast cancer cell lines – MCF-7 (luminal A, ER^+/PR^+), T-47D (luminal B, $ER^+/PR^+/HER2^-$), and BT-474 ($HER2^+$ subtype) – to explore the role of FN3K inhibition across hormone-driven and HER2-amplified breast cancer models. This experimental design was intended to capture a broad segment of the clinical breast cancer spectrum, particularly those subtypes where redox adaptation contributes to treatment resistance.

However, we acknowledge that these models do not encompass the full heterogeneity of breast cancer, especially TNBC, which exhibits distinct redox vulnerabilities and metabolic plasticity. In addition, cancer types outside the breast tissue may exhibit different dependencies on FN3K or Nrf2 signaling, potentially limiting the generalizability of our present findings.

This study was conceptualized as a focused proof-of-concept investigation into the feasibility of repurposing FN3K-targeted agents in selected breast cancer subtypes. Moving forward, we aim to expand our experimental scope by incorporating TNBC cell lines and non-breast cancer models with known oxidative stress signatures, such as lung, liver, and pancreatic cancers. These comparative studies will enable systematic mapping of FN3K expression, redox pathway activation, and drug responsiveness across cancer types.

4. Molecular dynamics (MD) simulations of lead molecules

Following *in vitro* confirmation of FN3K inhibition by lansoprazole, capivasertib, and oxaliplatin, MD simulations were employed to gain deeper insight into their binding stability, conformational behavior, and key molecular interactions within the FN3K active site. Simulations were conducted using Desmond version 13.7 (Schrödinger, LLC, USA) with the OPLS5 force field, placing the complexes in an orthorhombic simulation box solvated with TIP3P water molecules. The system was initially energy-minimized and subsequently equilibrated under NPT ensemble conditions at 300 K and 1 atm pressure. A production simulation was carried out for 200 ns with a 2-femtosecond timestep, applying the Particle Mesh Ewald (PME) method for long-range electrostatics and a 9 Å cutoff for van der Waals interactions. Post-simulation trajectory analyses – including root mean square deviation (RMSD), root mean square fluctuation (RMSF), radius of gyration (rGyr), and hydrogen bond occupancy – were performed to evaluate complex stability and dynamic binding features, offering comprehensive insights into the affinity and interaction profiles of the selected lead compounds.[65]

4.1. Selection of lead molecules for MD simulations

The selection of lansoprazole, capivasertib, and oxaliplatin for MD simulations was based on three primary criteria. First, all three compounds demonstrated strong FN3K inhibition, with reductions ranging from 99.6% to 99.99% across multiple breast cancer cell lines (MCF-7, T-47D, BT-474). Second, these compounds exhibited minimal off-target effects in non-malignant Vero cells, reinforcing their tumor-selective properties. Finally, their favorable ADMET profiles further supported their candidacy: Capivasertib and lansoprazole showed high gastrointestinal absorption, while oxaliplatin demonstrated high solubility, making all three suitable for further evaluation through MD simulations.

4.2. Objective of MD simulations

To investigate the molecular interactions and dynamic stability of the lead candidates – lansoprazole, capivasertib, and oxaliplatin – in complex with FN3K, MD simulations were conducted for 200 ns using Desmond. Several key parameters were evaluated to characterize the behavior and binding profiles of the complexes. RMSD was employed to monitor the overall structural stability of the protein-ligand complex throughout the simulation, while RMSF assessed the flexibility and mobility of amino acid residues, particularly within the active site, in response to ligand binding. Hydrogen bond analysis was performed to examine the consistency and strength of hydrogen bonding interactions between the ligand and FN3K over the simulation trajectory. In addition, binding free energy was calculated using MM-GBSA or MM-PBSA methods to estimate the thermodynamic favorability and strength of binding for each compound. Finally, total energy calculations were conducted within Desmond to analyze the system's potential and interaction energies, offering insights into conformational stability and favorable binding orientations.

Findings from the MD simulations offer valuable mechanistic insights into FN3K inhibition, supporting the therapeutic relevance of the identified lead compounds. The full simulation trajectories and detailed parameter-specific results – such as RMSD, RMSF, rGyr, hydrogen bonding, and MM-GBSA binding energy analyses – are presented in Supplementary Figures S7-S40.

5. Future perspectives

The findings of this study provide a strong foundation for exploring FN3K inhibition as a novel therapeutic strategy

for breast cancer. However, several critical avenues remain to be explored to fully establish its clinical relevance. First, while the study establishes the inhibitory effects of selected FN3K inhibitors on breast cancer cell lines, further in-depth mechanistic investigations are required to elucidate the precise molecular role of FN3K in cancer progression. These should include studies on FN3K-mediated metabolic adaptations and its impact on oxidative stress pathways beyond Nrf2 signaling; as such investigations would provide deeper insights into its therapeutic potential. Secondly, *in vivo* studies and pharmacokinetics are critical; although initial *in vivo* validation demonstrated significant tumor growth suppression, comprehensive pharmacokinetic and toxicological evaluations in animal models are essential. Determining the bioavailability, metabolic stability, and potential off-target effects of FN3K inhibitors will be crucial before progressing to clinical trials. In addition, the development of selective FN3K inhibitors from existing FDA-approved drugs, future efforts should focus on rational drug design to develop more selective inhibitors with minimal off-target effects. Computational approaches, such as MD simulations and free energy perturbation studies can aid in optimizing lead compounds for enhanced specificity and efficacy. Furthermore, exploration of combination therapies is warranted. Given the role of FN3K in modulating oxidative stress responses, investigating its inhibition in combination with chemotherapeutic agents or targeted therapies could provide synergistic effects. Evaluating the impact of FN3K inhibitors on drug resistance mechanisms may reveal novel combination strategies to enhance treatment efficacy. For clinical translation and biomarker development, studies should assess FN3K expression patterns in patient-derived tumor samples and correlate them with disease progression and treatment response. Identifying reliable biomarkers associated with FN3K inhibition will be instrumental in patient stratification and personalized therapy approaches. Finally, CRISPR/Cas9-based gene editing approaches, including knockout or knockdown studies in breast cancer models, can help validate the direct contribution of FN3K to tumorigenesis. Functional studies in FN3K-deficient models will clarify its essentiality in breast cancer survival and progression.

By addressing these critical aspects, FN3K-targeted therapy can move closer to clinical application, offering a promising avenue for breast cancer treatment.

6. Conclusion

The present study underscores the therapeutic potential of targeting FN3K in breast cancer management. By integrating *in silico* virtual screening with *in vitro* validation, we identified lead compounds – oxaliplatin, lansoprazole, and capivasertib – that significantly inhibited FN3K expression and function. This inhibition was corresponded with suppression of Nrf2-mediated antioxidant signaling and reduced cancer cell viability, supporting the role of FN3K in tumor progression and redox adaptation.

Importantly, all three compounds demonstrated strong selectivity toward breast cancer cells with minimal cytotoxicity in normal cells, indicating a favorable therapeutic index. These findings collectively support the FN3K–Nrf2 axis as a promising molecular target in redox-driven breast cancer subtypes.

While the present findings are encouraging, we acknowledge the limitation that *in vivo* validation was not included in this phase of the study. To address this, future experiments are already planned to assess the efficacy and safety of FN3K inhibition in xenograft tumor models. These will include evaluation of tumor growth suppression, pharmacokinetic profiles, and modulation of the FN3K–Nrf2 axis in excised tumor tissues. In addition, downstream molecular pathway mapping, ADME optimization, and combinatorial strategies with standard therapeutics will be explored to facilitate translational relevance.

Overall, this work establishes FN3K inhibition as a viable therapeutic strategy for breast cancer and provides a strong foundation for future *in vivo* and clinical investigations. Based on the present stage of validation, oxaliplatin, lansoprazole, and capivasertib should be regarded as promising pre-clinical candidates for FN3K-targeted intervention, rather than as definitive therapeutic options. Further *in vivo* and combination therapy studies are required to fully determine their clinical applicability.

Acknowledgments

The authors acknowledge the JSS Academy of Higher Education and Research and the JSS College of Pharmacy for providing institutional support. The Department of Computer Aided Drug Design is gratefully acknowledged for providing the computational resources essential for the *in silico* studies. The authors also express their sincere thanks to Dr. Subramanyam P, Muppandal Genomics and Immunologicals Pvt. Ltd., Hyderabad, for his technical assistance in conducting the *in vitro* biological experiments and supporting data validation.

Funding

The work was supported by the Council of Scientific and Industrial Research, Human Resource Development Group (CSIR-HRDG), New Delhi, India (Grant No.111-5634- 11759/2023/1 dated February 19th, 2024).

Conflict of interest

The authors have no relevant financial or non-financial interests to disclose.

Author contributions

Conceptualization: Gurupadayya Bannimath, Prabitha Prabhakaran
Data curation: Erica Alves
Formal analysis: Erica Alves, Prabitha Prabhakaran
Investigation: Erica Alves
Methodology: Erica Alves
Software: Erica Alves
Validation: Erica Alves, Prabitha Prabhakaran
Writing – original draft: Erica Alves
Writing – review & editing: Erica Alves

Ethics approval and consent to participate

Not applicable.

Consent for publication

Not applicable.

Availability of data

All data generated or analyzed during this study are included in this published article and its supplementary files, which can be accessed in https://docs.google.com/document/d/1KTlZzQXsTetJk5wVh7Hyw6cdw6UK0HRl/edit?usp=sharing&ouid=103717361144569370602&rtpof=true&sd=true Additional datasets supporting the findings of this study are available from the corresponding author upon reasonable request.

References

1. Tufail M, Jiang CH, Li N. Altered metabolism in cancer: Insights into energy pathways and therapeutic targets. *Mol Cancer.* 2024;23(1):203.

   doi: 10.1186/s12943-024-02119-3

2. Yousefi T, Pasha ARG, Kamrani G, *et al.* Evaluation of fructosamine 3-kinase and glyoxalase 1 activity in normal and breast cancer tissues. *Biomedicine (Taipei).* 2021;11(3):15-22.

   doi: 10.37796/2211-8039.1130

3. Alves E, Bannimath G, Prabhakaran P, Beeraka NM. The FN3K-Nrf2 axis: A novel therapeutic target in cancer metabolism. *Eurasian J Med Oncol.* 2024;8(4):338-339.

   doi: 10.14744/ejmo.2024.20665

4. Sanghvi VR, Leibold J, Mina M, *et al.* The oncogenic action of NRF2 depends on de-glycation by fructosamine-3-kinase. *Cell.* 2019;178(4):807-819.e21.

   doi: 10.1016/j.cell.2019.07.031

5. Beeraka NM, Zhang J, Mandal S, *et al.* Screening fructosamine-3-kinase (FN3K) inhibitors, a deglycating enzyme of oncogenic Nrf2: Human FN3K homology modelling, docking and molecular dynamics simulations. *PLoS One.* 2023;18(11):e0283705.

   doi: 10.1371/journal.pone.0283705

6. Beeraka NM, Zhang J, Uthaiah CA, *et al.* Expression patterns and relevance of FN3K, Nrf2, and NQO1 in breast cancers. *Eurasian J Med Oncol.* 2024;8(1):88-105.

   doi: 10.14744/ejmo.2024.61033

7. Delpierre G, Collard F, Fortpied J, Van Schaftingen E. Fructosamine 3-kinase, an enzyme involved in protein deglycation. *Biochem Soc Trans.* 2004;32(6):813-816.

   doi: 10.1042/bst0320813

8. Lionta E, Spyrou G, Vassilatis DK, Cournia Z. Structure-based virtual screening for drug discovery: Principles, applications and recent advances. *Curr Top Med Chem.* 2014;14(16):1923-1938.

   doi: 10.2174/1568026614666140929124445

9. Roskoski R Jr. Properties of FDA-approved small molecule protein kinase inhibitors: A 2023 update. *Pharmacol Res.* 2023;187:106552.

   doi: 10.1016/j.phrs.2023.106552

10. Beeraka NM, Bovilla VR, Doreswamy SH, Puttalingaiah S, Srinivasan A, Madhunapantula SV. The taming of nuclear factor erythroid-2-related factor-2 (Nrf2) deglycation by fructosamine-3-kinase (FN3K)-inhibitors-a novel strategy to combat cancers. *Cancers (Basel).* 2021;13(2):281.

    doi: 10.3390/cancers13020281

11. Beeraka NM, Zhang J, Zhao D, *et al.* Combinatorial implications of Nrf2 inhibitors with FN3K inhibitor: *In vitro* breast cancer study. *Curr Pharm Des.* 2023;29(30):2408-2425.

    doi: 10.2174/0113816128261466231011114600

12. Carles F, Bourg S, Meyer C, Bonnet P. PKIDB: A curated, annotated and updated database of protein kinase inhibitors in clinical trials. *Molecules.* 2018;23(4):908.

    doi: 10.3390/molecules23040908

13. World Health Organization. *WHO Model Lists of Essential Medicines. 23rd List*; 2023. Available from: https://www.who.int/publications/i/item/WHO-MHP-HPS-EML-2023.01 [Last accessed on 2025 Mar 14].

14. National Cancer Institute. *Breast Cancer Treatment Drugs*. Bethesda, MD: National Cancer Institute. Available from: https://www.cancer.gov/about-cancer/treatment/drugs/breast [Last accessed on 2025 Mar 14].

15. Cheng T, Li Q, Zhou Z, Wang Y, Bryant SH. Structure-based virtual screening for drug discovery: A problem-centric review. *AAPS J.* 2012;14(1):133-141.

doi: 10.1208/s12248-012-9322-0

16. Hevener KE, Pesavento R, Ren J, Lee H, Ratia K, Johnson ME. Hit-to-lead: Hit validation and assessment. *Methods Enzymol.* 2018;610:265-309.

doi: 10.1016/bs.mie.2018.09.022

17. Wang XJ, Sun Z, Villeneuve NF, *et al.* Nrf2 enhances resistance of cancer cells to chemotherapeutic drugs, the dark side of Nrf2. *Carcinogenesis.* 2008;29(6):1235-1243.

doi: 10.1093/carcin/bgn095

18. Schrödinger LLC. *Maestro: Schrödinger Release 2024-1*. New York, NY: Schrödinger, LLC; 2024. Available from: https://www.schrodinger.com/maestro [Last accessed on 2025 Feb 21].

19. Friesner RA, Murphy RB, Repasky MP, *et al.* Extra precision glide: Docking and scoring incorporating a model of hydrophobic enclosure for protein-ligand complexes. *J Med Chem.* 2006;49(21):6177-6196.

doi: 10.1021/jm051256o

20. Liu T, Lu D, Zhang H, *et al.* Applying high-performance computing in drug discovery and molecular simulation. *Natl Sci Rev.* 2016;3(1):49-63.

doi: 10.1093/nsr/nww003

21. UniProt Consortium. UniProt: A worldwide hub of protein knowledge. *Nucleic Acids Res.* 2019;47(D1):D506-D515.

doi: 10.1093/nar/gky1049

22. UniProt. *FN3K Fructosamine-3-Kinase Homo Sapiens (Human)*. UniProtKB; 2025. Available from: https://www.uniprot.org/uniprotkb/q9H479/entry [Last accessed on 2025 Mar 15].

23. Sievers F, Higgins DG. Clustal Omega for making accurate alignments of many protein sequences. *Protein Sci.* 2018;27(1):135-145.

doi: 10.1002/pro.3290

24. Schwede T, Kopp J, Guex N, Peitsch MC. SWISS-MODEL: An automated protein homology-modeling server. *Nucleic Acids Res.* 2003;31(13):3381-3385.

doi: 10.1093/nar/gkg520

25. Ko J, Park H, Heo L, Seok C. GalaxyWEB server for protein structure prediction and refinement. *Nucleic Acids Res.* 2012;40(Web Server issue):W294-W297.

doi: 10.1093/nar/gks493

26. Kleywegt GJ, Jones TA. Phi/Psi-chology: Ramachandran revisited. *Structure.* 1996;4(12):1395-1400.

doi: 10.1016/S0969-2126(96)00147-5

27. University of California, Los Angeles (UCLA). *SAVES - Structure Analysis and Verification Server*. Available from: https://saves.mbi.ucla.edu [Last accessed on 2025 Mar 15].

28. Biasini M, Bienert S, Waterhouse A, *et al.* SWISS-MODEL: Modelling protein tertiary and quaternary structure using evolutionary information. *Nucleic Acids Res.* 2014;42(Web Server issue):W252-W258.

doi: 10.1093/nar/gku340

29. Benkert P, Tosatto SC, Schomburg D. QMEAN: A comprehensive scoring function for model quality assessment. *Proteins.* 2008;71(1):261-277.

doi: 10.1002/prot.21715

30. Benkert P, Biasini M, Schwede T. Toward the estimation of the absolute quality of individual protein structure models. *Bioinformatics.* 2011;27(3):343-350.

doi: 10.1093/bioinformatics/btq662

31. Schrödinger LLC. *Protein Preparation Workflow*. Schrödinger. Available from: https://www.schrodinger.com/life-science/learn/white-papers/protein-preparation-workflow [Last accessed on 2025 Mar 15].

32. National Center for Biotechnology Information (NCBI). PubChem. Available from: https://pubchem.ncbi.nlm.nih.gov [Last accessed on 2025 Mar 15].

33. Knox C, Wilson M, Klinger CM, *et al.* DrugBank 6.0: The drugbank knowledgebase for 2024. *Nucleic Acids Res.* 2024;52(D1):D1265-D1275.

doi: 10.1093/nar/gkad976

34. Sahayarayan JJ, Rajan KS, Vidhyavathi R, *et al. In-silico* protein-ligand docking studies against the estrogen protein of breast cancer using pharmacophore based virtual screening approaches. *Saudi J Biol Sci.* 2021;28(1):400-407.

doi: 10.1016/j.sjbs.2020.10.023

35. Ge Y, Pande V, Seierstad MJ, Damm-Ganamet KL. Exploring the application of sitemap and site finder for focused cryptic pocket identification. *J Phys Chem B.* 2024;128(26):6233-6245.

doi: 10.1021/acs.jpcb.4c00664

36. Elekofehinti OO, Iwaloye O, Josiah SS, Lawal AO, Akinjiyan MO, Ariyo EO. Molecular docking studies, molecular dynamics and ADME/tox reveal therapeutic potentials of STOCK1N-69160 against papain-like protease of SARS-CoV-2. *Mol Divers.* 2021;25:1761-1773.

doi: 10.1007/s11030-020-10151-w

37. Park MS, Dessal AL, Smrcka AV, Stern HA. Evaluating docking methods for prediction of binding affinities of small molecules to the G protein betagamma subunits. *J Chem Inf Model.* 2010;49(2):437-443.

doi: 10.1021/ci800412z

38. Daina A, Michielin O, Zoete V. SwissADME: A free web tool to evaluate pharmacokinetics, drug-likeness and medicinal chemistry friendliness of small molecules. *Sci Rep.* 2017;7:42717.

doi: 10.1038/srep42717

39. Li W, Zhou J, Xu Y. Study of the *in vitro* cytotoxicity testing of medical devices. *Biomed Rep.* 2015;3(5):617-620.

doi: 10.3892/br.2015.481

40. International Organization for Standardization. *ISO 10993-5:2009. Biological Evaluation of Medical Devices-Part 5: Tests for In Vitro Cytotoxicity.* 3rd ed. Geneva: ISO; 2009.

41. Senthilraja P, Kathiresan K. *In vitro* cytotoxicity MTT assay in vero, HepG2 and MCF-7 cell lines study of marine yeast. *J Appl Pharm Sci.* 2015;5(3):80-84.

doi: 10.7324/JAPS.2015.50313

42. Freshney RI. *Culture of Animal Cells: A Manual of Basic Technique and Specialized Applications.* 6th ed. Hoboken, NJ: Wiley-Blackwell; 2010.

43. Chomczynski P, Sacchi N. Single-step method of RNA isolation by acid guanidinium thiocyanate-phenol-chloroform extraction. *Anal Biochem.* 1987;162(1):156-159.

doi: 10.1016/0003-2697(87)90021-2

44. Rio DC, Ares M Jr., Hannon GJ, Nilsen TW. Determining the yield and quality of purified RNA. *Cold Spring Harb Protoc.* 2010;2010(6).

doi: 10.1101/pdb.top82

45. Taylor SC, Laperriere G, Germain H. Droplet digital PCR versus qPCR for gene expression analysis with low abundant targets: From variable nonsense to publication quality data. *Sci Rep.* 2017;7(1):2409.

doi: 10.1038/s41598-017-02217-x

46. Livak KJ, Schmittgen TD. Analysis of relative gene expression data using real-time quantitative PCR and the 2−ΔΔCt method. *Methods.* 2001;25(4):402-408.

doi: 10.1006/meth.2001.1262

47. Pfaffl MW. A new mathematical model for relative quantification in real-time RT-PCR. *Nucleic Acids Res.* 2001;29(9):e45.

doi: 10.1093/nar/29.9.e45

48. Mahmood T, Yang PC. Western blot: Technique, theory, and trouble shooting. *N Am J Med Sci.* 2012;4(9):429-434.

doi: 10.4103/1947-2714.100998

49. Taylor SC, Posch A. The design of a quantitative western blot experiment. *Biomed Res Int.* 2014;2014:361590.

doi: 10.1155/2014/361590

50. Virtanen P, Gommers R, Oliphant TE, *et al.* SciPy 1.0: Fundamental algorithms for scientific computing in python. *Nat Methods.* 2020;17(3):261-272.

doi: 10.1038/s41592-019-0686-2

51. Ahad NA, Syed Yahaya SS. Sensitivity analysis of Welch's t-test. *AIP Conf Proc.* 2014;1605:888-893.

doi: 10.1063/1.4887707

52. Lee S, Lee DK. What is the proper way to apply the multiple comparison test. *Korean J Anesthesiol.* 2018;71(5):353-360.

doi: 10.4097/kja.d.18.00242

53. Kasi A. Oxaliplatin. In: *StatPearls*. Treasure Island, FL: StatPearls Publishing; 2025. Available from: https://www.ncbi.nlm.nih.gov/books/nbk557690 [Last accessed on 2023 May 16].

54. Fernandez-Teruel C, Cullberg M, González-García I, Schiavon G, Zhou D. An exposure-safety analysis to support the dosage of the novel AKT inhibitor capivasertib. *Cancer Chemother Pharmacol.* 2025;95:48.

doi: 10.1007/s00280-025-04775-8

55. Ahmed A, Clarke JO. Proton Pump Inhibitors (PPI). In: *StatPearls*. Treasure Island, FL: StatPearls Publishing; 2025. Available from: https://www.ncbi.nlm.nih.gov/books/nbk557385 [Last accessed on 2023 May 01].

56. Lau A, Villeneuve NF, Sun Z, Wong PK, Zhang DD. Dual roles of Nrf2 in cancer. *Pharmacol Res.* 2008;58(5-6):262-270.

doi: 10.1016/j.phrs.2008.09.003

57. Kumar H, Kumar RM, Bhattacharjee D, Somanna P, Jain V. Role of Nrf2 signaling cascade in breast cancer: Strategies and treatment. *Front Pharmacol.* 2022;13:720076.

doi: 10.3389/fphar.2022.720076

58. Bogliolo S, Cassani C, Gardella B, *et al.* Oxaliplatin for the treatment of ovarian cancer. *Expert Opin Investig Drugs.* 2015;24(9):1275-1286.

doi: 10.1517/13543784.2015.1062874

59. Innominato PF, Karaboué A, Focan C, *et al.* Efficacy and safety of chronomodulated irinotecan, oxaliplatin, 5-fluorouracil and leucovorin combination as first- or second-line treatment against metastatic colorectal cancer: Results from the international EORTC 05011 trial. *Int J Cancer.* 2021;148(10):2512-2521.

doi: 10.1002/ijc.33422

60. Rugo HS, Oliveira M, Howell SJ, *et al.* Capivasertib and fulvestrant for patients with hormone receptor-positive advanced breast cancer: Characterization, time course, and management of frequent adverse events from the phase III CAPItello-291 study. *ESMO Open.* 2024;9(9):103697.

doi: 10.1016/j.esmoop.2024.103697

61. Khadempar S, Lotfi M, Haghiralsadat F, Saidijam M, Ghasemi N, Afshar S. Lansoprazole as a potent HDAC2 inhibitor for treatment of colorectal cancer: An *in-silico* analysis and experimental validation. *Comput Biol Med.* 2023;166:107518.

doi: 10.1016/j.compbiomed.2023.107518

62. Spugnini EP, Buglioni S, Carocci F, *et al.* High dose lansoprazole combined with metronomic chemotherapy: A phase I/II study in companion animals with spontaneously occurring tumors. *J Transl Med.* 2014;12:225.

doi: 10.1186/s12967-014-0225-y

63. Fais S, De Milito A, You H, Qin W. Targeting vacuolar H^+-ATPases as a new strategy against cancer. *Cancer Res.* 2007;67(22):10627-10630.

doi: 10.1158/0008-5472.CAN-07-1805

64. Kao HW, Tsai KW, Lin WC. Synergistic effect of metformin and lansoprazole against gastric cancer through growth inhibition. *Int J Med Sci.* 2023;20(6):717-724.

doi: 10.7150/ijms.82407

65. Salo-Ahen OMH, Alanko I, Bhadane R, *et al.* Molecular dynamics simulations in drug discovery and pharmaceutical development. *Processes.* 2021;9(1):71.

doi: 10.3390/pr9010071

ACCSCIENCE PUBLISHING

Eurasian Journal of Medicine and Oncology

ORIGINAL RESEARCH ARTICLE

Critical care pharmacists in intensive care units: A meta-analysis of their impact on mortality and adverse drug events

Mohamed S. Imam[1]*, Khalid Nassir Almurayeh[2], Abdulrahman Saeed M. Okshah[2], Fawaz Saad Yahya Thabit[2], Amal Ali Al Thabet[2], Abdullah Abduh Ali Hijazy[2], Shahad Abdullah Ali Alahmari[2], Faisal Saeed Mohammed Hatab[2], Sadeem Nawaf A. Alotaibi[3], Ruba Hamoud Mohammed Alshahrani[3], and Ranaa Abdullah Saleh Alamri[4]

[1]Department of Clinical Pharmacy, National Cancer Institute, Cairo University, Cairo, Egypt

[2]College of Pharmacy, King Khalid University, Abha, Asir, Saudi Arabia

[3]College of Pharmacy, Taif University, Taif, Mecca, Saudi Arabia

[4]College of Pharmacy, King Saud University, Riyadh, Saudi Arabia

Abstract

Introduction: Critical care pharmacists (CCPs) are increasingly integrated into intensive care unit (ICU) teams to enhance medication safety and improve outcomes. However, their effect on mortality and adverse drug events (ADEs) remains inadequately studied.

Objective: This study aimed to evaluate the impact of CCP involvement in ICU care on patient mortality and ADEs.

Methods: A comprehensive systematic review and meta-analysis were performed, encompassing studies published through January 2025. The literature search was conducted in multiple databases, such as PubMed, Embase, and the Cochrane Library.

Results: A total of 16 eligible studies were identified, collectively involving 37,925 ICU patients. To evaluate outcomes, odds ratios (ORs) and corresponding 95% confidence intervals (CIs) were calculated utilizing either fixed-effects or random-effects models, depending on heterogeneity levels. Patients in ICUs with CCPs experienced significantly reduced mortality (OR: 0.72; 95% CI: 0.56 – 0.92; p=0.01) and fewer ADEs (OR: 0.39; 95% CI: 0.21 – 0.70; p=0.002) compared to controls. Despite notable heterogeneity, findings were consistent in sensitivity analyses. No significant publication bias was detected.

Conclusion: The inclusion of CCPs in ICU teams is associated with lower mortality and fewer ADEs. These findings support expanding the role of pharmacists in critical care settings.

Keywords: Critical care pharmacists; Pharmacotherapy; Intensive care unit; Adverse drug events; Mortality; Interdisciplinary care

***Corresponding author:**
Mohamed S. Imam
(imammohamed311@gmail.com)

Citation: Imam MS, Almurayeh KN, Okshah ASM, *et al*. Critical care pharmacists in intensive care units: A meta-analysis of their impact on mortality and adverse drug events. *Eurasian J Med Oncol*. 2025;9(3):226-238.
doi: 10.36922/EJMO025150116

Received: April 13, 2025

1st revised: June 24, 2025

2nd revised: June 26, 2025

Accepted: July 3, 2025

Published online: August 4, 2025

Copyright: © 2025 Author(s). This is an Open-Access article distributed under the terms of the Creative Commons Attribution License, permitting distribution, and reproduction in any medium, provided the original work is properly cited.

Publisher's Note: AccScience Publishing remains neutral with regard to jurisdictional claims in published maps and institutional affiliations.

1. Introduction

In the evolving landscape of critical care, intensivist-led multidisciplinary teams have become a cornerstone of best practices in the intensive care unit (ICU).[1] These teams are designed to deliver timely, accurate, and collaborative care to critically ill patients, thereby

improving patient recovery and minimizing excessive consumption of healthcare resources. Among the essential, yet sometimes underappreciated, members of these teams are critical care pharmacists (CCPs).[2] Their integration into ICU care has increasingly been recognized as an indispensable strategy to enhance therapeutic outcomes and reduce medication-related risks.[3-5] Moreover, the evolving landscape of intensive care presents increasingly complex pharmacotherapeutic challenges, driven by the rapid development of new drugs, emerging antimicrobial resistance patterns, and high rates of comorbidities among ICU patients.[6-8] CCPs are uniquely positioned to address these dynamics by ensuring the implementation of up-to-date medication practices, assessing evolving pharmacokinetics in critically ill patients, and managing drug-related toxicities.[9,10] Their expertise in emergency drug resuscitation protocols and knowledge of high-alert medications further reinforces their critical contribution to ICU safety.[11]

CCPs possess specialized training and clinical expertise in pharmacotherapy, particularly in high-acuity settings. Their roles transcend traditional pharmacy duties, encompassing real-time decision-making, participation in multidisciplinary rounds, individualization of medication regimens, dose adjustments based on organ function, management of drug interactions, and oversight of medication safety protocols.[12,13] This allows for a more proactive approach to patient care in the ICU, where complex drug regimens and rapid physiological changes demand constant monitoring and adjustment.[2]

Evidence suggests that the involvement of CCPs leads to a higher implementation rate of pharmacotherapeutic recommendations.[14] These interventions include dosage adjustments, therapeutic drug monitoring, and the prevention or resolution of adverse drug events (ADEs). In addition, CCPs serve as valuable resources in formulating and adhering to institutional guidelines, conducting staff education, and contributing to antimicrobial stewardship initiatives, all of which are vital in managing critically ill patients, particularly those with sepsis, multi-organ failure, or polypharmacy.[15,16]

A growing body of literature supports the contribution of CCPs to improved patient outcomes in the ICU. Previous studies have shown that their participation reduces preventable ADEs, medication errors, and overall hospital costs. For example, a frequently referenced meta-analysis conducted by Wang *et al.*[14] reported a significant decrease in ADEs following pharmacist-led interventions. However, the study did not find a definitive impact on the incidence of medication errors. It is worth noting that the patient populations analyzed were not limited to the ICU; instead, they largely encompassed individuals from general medical and surgical wards. This broader scope limits the direct relevance of the findings to critically ill populations, where clinical dynamics and pharmacotherapeutic challenges differ substantially.

Furthermore, the aforementioned meta-analysis[14] faced limitations related to small sample sizes, study heterogeneity, and a high risk of bias, which called into question the strength and generalizability of its conclusions. In addition, these earlier evaluations lacked a focus on mortality outcomes and did not disaggregate results by clinical setting. As a result, the true impact of CCPs in the ICU remains inadequately quantified, particularly with regard to patient survival and the incidence of medication-related problems (MRPs).

Beyond reducing ADEs, CCPs are also believed to contribute indirectly to lowering ICU mortality rates.[3,17,18] Their recommendations often lead to more appropriate and timely initiation of therapies such as antibiotics, vasopressors, or anticoagulants, which are critical in managing life-threatening conditions. For example, inappropriate antimicrobial therapy has been linked to increased mortality in sepsis patients; thus, pharmacist-led antimicrobial stewardship can be life-saving.[15] Moreover, by assuming responsibilities related to medication safety and efficacy, CCPs allow intensivists and nurses to focus more on other aspects of patient care, potentially reducing the risk of oversight and burnout among ICU staff.[2,19]

Despite these potential benefits, the extent of CCPs' influence on clinical outcomes such as ADEs and mortality has not been thoroughly evaluated in a comprehensive, ICU-specific meta-analysis. Previous studies have either lacked adequate statistical power, failed to isolate the ICU as a unique clinical environment, or focused only on surrogate outcomes like cost savings or error rates rather than clinically significant endpoints.

This knowledge gap underscores the need for more rigorous evaluation. To date, no meta-analysis has been exclusively dedicated to assessing the influence of CCPs on both mortality and ADEs in ICU populations. Therefore, the current study aims to address this gap by conducting a comprehensive meta-analysis focused specifically on the inclusion of CCPs in ICU teams and their impact on these two critical outcomes.

The objective of this meta-analysis is to systematically assess and quantify the impact of CCPs on clinical outcomes among ICU patients, with a primary focus on mortality and ADEs. In addition to these primary endpoints, the study also explores secondary outcomes where data are available, including ICU length of stay,

ventilator days, cost-related implications, and the broader clinical roles of CCPs such as antimicrobial stewardship, pharmacotherapy optimization, and interdisciplinary care contributions. This comprehensive approach aims to inform evidence-based policy and practice regarding the integration of pharmacists into critical care teams.

2. Methods

2.1. Study design

This investigation was designed as a systematic review and meta-analysis, adhering to both the Meta-analysis of Observational Studies in Epidemiology framework and the Preferred Reporting Items for Systematic Reviews and Meta-Analyses guidelines.[20] Its primary aim was to consolidate and evaluate existing evidence on the clinical impact of integrating CCPs within ICU teams, specifically focusing on two key outcomes: patient mortality and the incidence of ADEs. The study is registered in the International Prospective Register of Systematic Reviews under the number CRD420251080799.

2.2. Eligibility criteria

Study selection was guided by clearly defined inclusion and exclusion criteria established in advance to maintain methodological integrity and ensure the relevance of the included research.

Inclusion criteria were as follows:

(i) The analysis encompassed a range of study designs, including randomized controlled trials, prospective cohort studies, and retrospective observational investigations.
(ii) The patient population consisted exclusively of individuals admitted to ICUs.
(iii) The intervention involved the integration or presence of CCPs as active members of the ICU care team.
(iv) The study reported clinical outcomes, specifically mortality and/or ADEs, comparing an intervention group (with CCPs) against a control group (without CCP involvement).

Exclusion criteria were as follows:

(i) Studies that did not explicitly evaluate the impact of CCPs on either mortality or ADEs.
(ii) Studies where the intervention involved pharmacy services not specific to critical care or not clearly involving pharmacists embedded in ICU teams.
(iii) Publications lacking a comparison group, such as single-arm studies, editorials, review articles, conference abstracts, commentaries, or letters to the editor.

2.3. Literature search strategy

The search strategy was based on the PICOS framework: P (Population): ICU patients; I (Intervention): involvement of CCPs; C (Comparison): care without CCPs; O (Outcomes): mortality and ADEs; S (Study Design): randomized controlled trials, prospective cohort studies, and retrospective observational studies.[21] A comprehensive and systematic literature search was performed across three major electronic databases: PubMed, Embase, and the Cochrane Library. The search spanned from database inception through January 2025. Keywords and Medical Subject Headings included "intensive care unit," "critical care pharmacists," "adverse drug events," "death," and "multidisciplinary." The specific search strategies for each database are detailed in Table 1. Boolean operators (AND and OR) were employed to ensure a sensitive and inclusive search.

Duplicate entries were removed using EndNote software, after which two reviewers independently screened the remaining titles and abstracts. Full-text versions of studies deemed potentially eligible were retrieved and evaluated for inclusion according to the predefined criteria.

2.4. Data collection and quality evaluation

Data were systematically collected using a standardized and pre-tested data extraction form. From each eligible study, the following key information was obtained:

(i) First author and publication year
(ii) Country and healthcare setting
(iii) Study design and duration
(iv) Number of participants in the intervention and control groups
(v) Patient characteristics
(vi) Nature of the pharmacist intervention
(vii) Clinical outcomes (mortality and ADEs)
(viii) Reported effect sizes and confidence intervals (CIs).

Table 1. Structured search strategies used across selected databases

Database	Search strategy
PubMed	#1 "critical care pharmacists" (MeSH Terms) OR "intensive care unit" (MeSH Terms) OR "adverse drug events" (All Fields) #2 "multi-disciplinary" (MeSH Terms) OR "death" (All Fields) #3 #1 AND #2
Embase	"critical care pharmacists"/exp OR "intensive care unit"/exp OR "adverse drug events"/exp #2 "multidisciplinary"/exp OR "death"/exp #3 #1 AND #2
Cochrane Library	#1 (critical care pharmacists): ti, ab, kw OR (intensive care unit): ti, ab, kw OR (adverse drug events): ti, ab, kw (Word variations have been searched) #2 (multidisciplinary): ti, ab, kw OR (death): ti, ab, kw (Word variations have been searched) #3 #1 AND #2

Abbreviation: MeSH: Medical Subject Headings.

Methodological quality was evaluated using the Cochrane Risk of Bias Tool for randomized controlled trials, and an adapted version of the Newcastle-Ottawa Scale was employed for observational studies. Risk of bias assessments were independently performed by two reviewers to ensure objectivity and consistency.[22] Any disagreements were resolved through consensus between the reviewers, and, when necessary, a third reviewer was consulted to reach a final decision.

Bias levels were rated as low, moderate, or high, based on how adequately studies addressed core methodological elements, including participant selection, intervention implementation, outcome measurement, attrition handling, and reporting transparency.

2.5. Statistical analysis

The meta-analysis was performed using Review Manager version 5.3, provided by the Nordic Cochrane Centre. For binary outcomes such as mortality and ADEs, odds ratios (ORs) with corresponding 95% CIs were calculated using either fixed-effects or random-effects models, depending on the degree of heterogeneity among the included studies.

Heterogeneity was quantified using the I^2 statistic, interpreted as follows:[23]

- I^2 value of 0% indicates no observed heterogeneity
- I^2 value of 25% reflects low heterogeneity
- I^2 value of 50% suggests a moderate level of heterogeneity
- I^2 value of 75% or higher represents substantial or high heterogeneity.

When the I^2 statistic exceeded 50%, indicating moderate to high heterogeneity, a random-effects model was employed to account for inter-study variability. For lower levels of heterogeneity, a fixed-effects model was applied. Where data permitted, subgroup analyses were planned to investigate potential sources of variability across studies.

To evaluate the robustness of the results, sensitivity analyses were performed by excluding studies deemed to have a high risk of bias or those with small sample sizes ($n \leq 100$). Potential publication bias was assessed visually through funnel plot inspection and statistically using Egger's regression test.[24] A p=0.05 or higher was interpreted as no significant publication bias.

2.6. Outcome measures

The primary outcomes assessed were:

(i) Mortality: Defined as all-cause in-hospital or ICU death, as reported in each study.

(ii) ADEs: Defined as any harm associated with medication use, including medication errors, adverse drug reactions, or other preventable injuries, according to the criteria specified in each individual study.

All outcomes were reported as aggregate effect sizes, and subgroup comparisons were performed where data were available.

3. Results

3.1. Study selection and characteristics

Out of a total of 3,301 unique records identified through the comprehensive database search, 16 studies met the predefined eligibility criteria and were included in the final meta-analysis (Figure 1).[25-40] These studies were published between 1999 and 2022 and collectively enrolled 37,925 patients admitted to ICUs. Of these, 23,060 patients received care involving CCPs, while 14,865 patients served as controls (i.e., managed without the involvement of CCPs).

The included studies varied in design, comprising both prospective and retrospective observational cohorts, as well as interventional trials, and were conducted across multiple countries, including the United States, China, Belgium, Thailand, Egypt, and India. Sample sizes of individual studies ranged widely, from as few as 70 patients to as many as 30,032 (Table 2). The interventions performed by CCPs included direct participation in ICU rounds, antimicrobial stewardship, pain and sedation management, prevention of drug interactions, and optimization of pharmacotherapy in critical illness.

3.2. Impact on mortality

A pooled analysis of all 16 studies demonstrated a significant reduction in mortality associated with the inclusion of CCPs in ICU teams. The overall OR for mortality was 0.72, with a 95% CI of 0.56 – 0.92 (p=0.01), favoring the intervention group (Figure 2). Patients receiving care with CCP involvement had a 28% lower likelihood of mortality compared to those managed without pharmacist involvement.

Nonetheless, the analysis demonstrated substantial heterogeneity across the included studies, as reflected by an I^2 statistic of 78% (Figure 2). This considerable variation in effect sizes is likely attributable to differences in study methodologies, patient populations, and the nature of pharmacist-led interventions. As a result, the use of a random-effects model was deemed appropriate to account for this variability.

3.3. Impact on ADEs

The meta-analysis also revealed a substantial reduction in the incidence of ADEs among patients managed with CCP

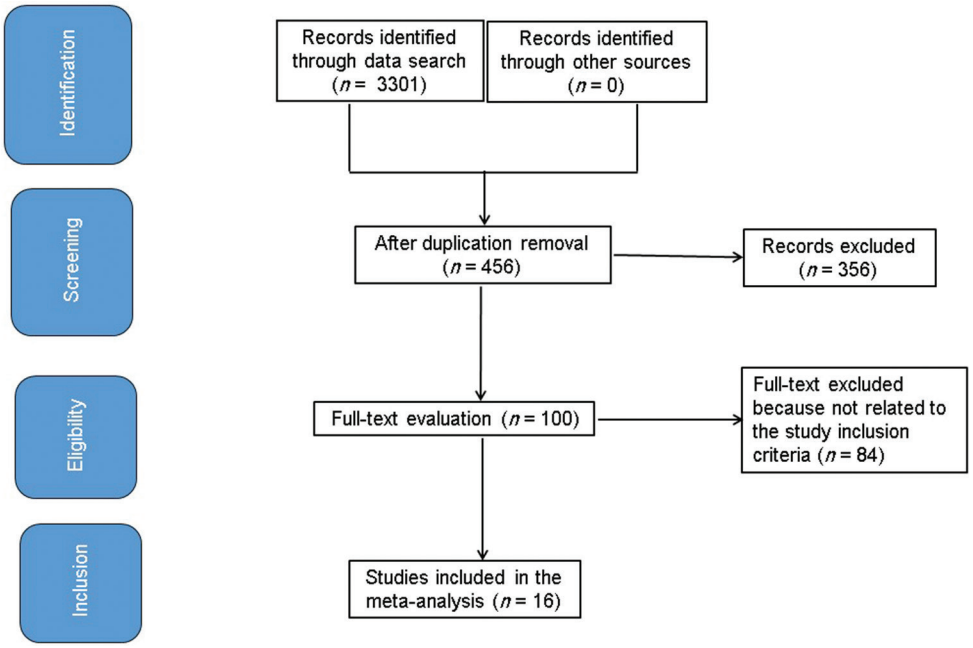


Figure 1. Preferred reporting items for systematic reviews and meta-analyses flow diagram illustrating the study selection process for the meta-analysis

Table 2. Summary of key characteristics of studies included in the meta-analysis

Study	Country	Total	Critical care pharmacist	Control
Leape *et al.*[25]	USA	150	75	75
MacLaren *et al.*[37]	USA	30,023	18,804	11,219
Rivkin and Yin[26]	USA	266	137	129
Jiang *et al.*[27]	China	144	73	71
Jiang, *et al.*[38]	China	180	93	87
Jiang, *et al.*[28]	China	209	106	103
Claus *et al.*[29]	Belgium	155	80	75
Oxman *et al.*[30]	USA	92	42	50
Hammond *et al.*[31]	USA	219	118	101
Li *et al.*[32]	China	577	353	224
Dilokpattanamongkol *et al.*[39]	Thailand	156	66	90
Louzon *et al.*[33]	USA	70	35	35
Gu *et al.*[34]	China	2,872	1,436	1,436
Aghili and Kasturirangan[35]	India	228	211	17
Toukhy *et al.*[36]	Egypt	2,480	1,379	1,101
Mohammad *et al.* [40]	USA	104	52	52
Total		37,925	23,060	14,865

Abbreviation: USA: United States of America.

involvement. The pooled OR for ADEs was 0.39 (95% CI: 0.21 – 0.70, p=0.002), indicating a 61% reduction in the odds of experiencing an ADE when CCPs were integrated into the ICU care team (Figure 3).

As with mortality, the analysis of ADE outcomes showed significant heterogeneity (I^2 = 83%), prompting the use of a random-effects model to account for inter-study differences. Despite this heterogeneity, the association remained statistically robust, supporting the positive role of CCPs in minimizing MRPs in critical care settings.

3.4. Publication bias and funnel plot analysis

To assess the risk of publication bias, funnel plots were constructed for both mortality and ADE outcomes (Figures 4 and 5). The plots appeared symmetric, and Egger's regression test yielded a p=0.87, suggesting no significant publication bias for either outcome.

3.5. Sensitivity analysis

Sensitivity analyses were conducted to evaluate the stability of the results. Excluding studies with small sample sizes ($n \leq 100$) and those with a high risk of bias did not materially alter the overall findings, thereby reinforcing the reliability of the conclusions.

3.6. Subgroup observations

Although data limitations prevented formal subgroup analyses by age, gender, or ethnicity, a narrative synthesis of selected studies highlighted consistent benefits of CCP inclusion across different regions and ICU types (e.g., medical, surgical, and trauma). Furthermore, studies incorporating CCPs with well-defined clinical roles, such as daily patient rounds and antimicrobial stewardship,

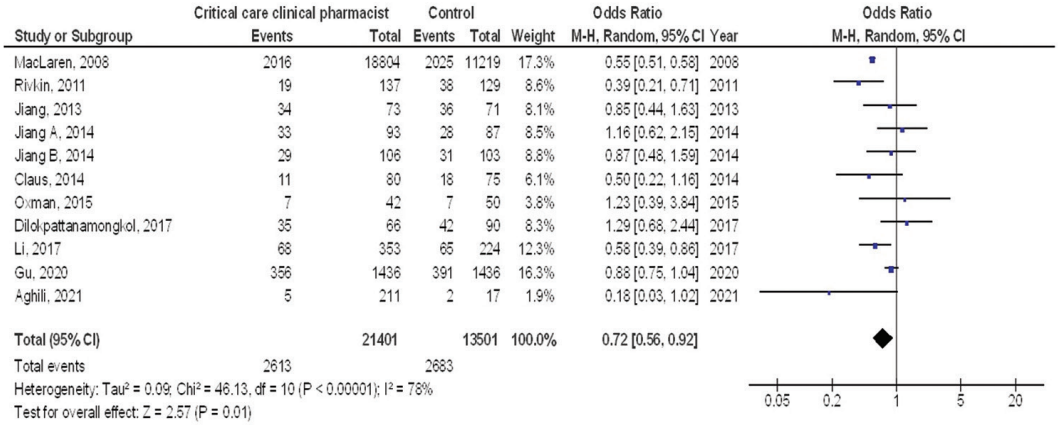


Figure 2. Forest plot comparing intensive care unit mortality rates between patients managed with and without critical care pharmacist involvement

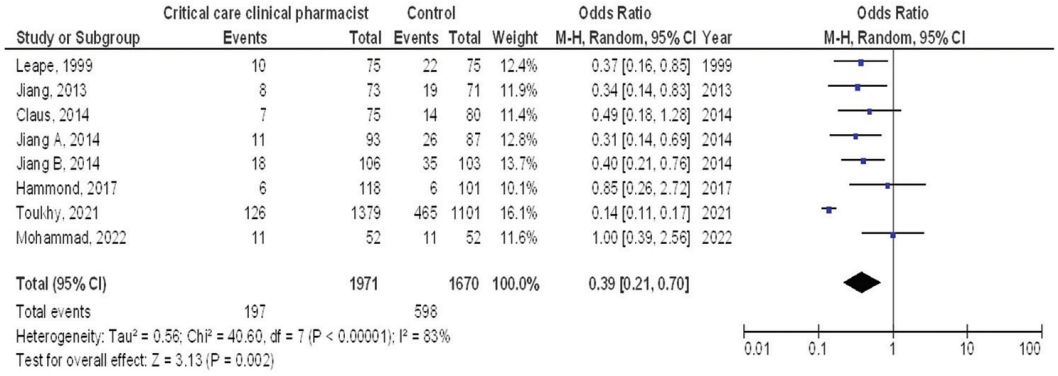


Figure 3. Forest plot illustrating the effect of critical care pharmacist involvement on the rate of adverse drug events among intensive care unit patients, compared to standard care without pharmacist participation

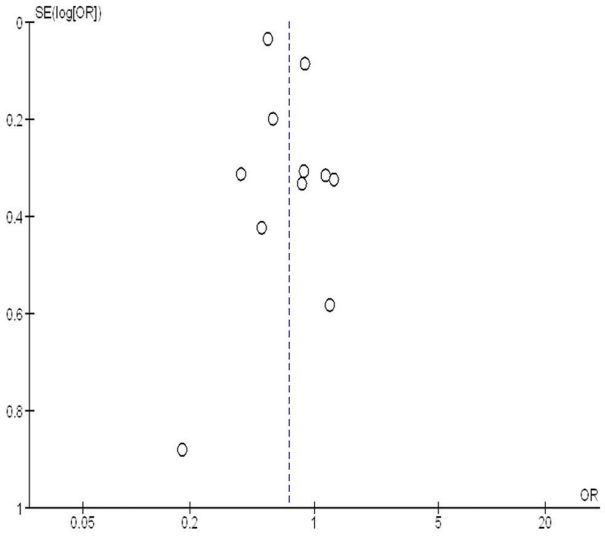


Figure 4. Funnel plot evaluating potential publication bias in mortality outcomes
Abbreviations: OR: Odds ratio; SE: Standard error

reported more pronounced improvements in mortality and ADEs.

3.7. Summary of study characteristics

Detailed characteristics of the included studies are presented in Table 2. Most studies were conducted in tertiary academic centers, and the interventions typically involved CCPs making direct pharmacotherapeutic recommendations during interdisciplinary rounds. Several studies also documented CCP contributions to institutional policy development, formulary management, and healthcare staff education, all of which may have contributed to improved outcomes.

4. Discussion

This meta-analysis, involving 16 studies and 37,925 ICU patients, presents strong evidence that integrating CCPs into ICUs is significantly associated with reduced mortality and a lower incidence of ADEs. The findings

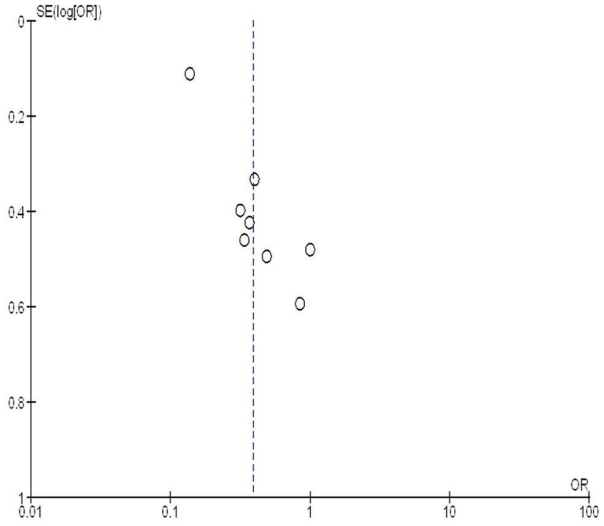


Figure 5. Funnel plot examining potential publication bias associated with adverse drug event outcomes
Abbreviations: Or: Odds ratio; SE: Standard error

support previous literature and underscore the clinical and operational value of pharmacist-led interventions in high-acuity environments. Clinicians in the ICU face difficult-to-manage situations and complex patients daily, and without appropriate pharmacological oversight, these challenges can lead to fatal complications.[41] CCPs with particular experiences can help decrease complex MRPs when integrated into ICU teams.[42]

The inclusion of CCPs may also decrease the workload of other ICU staff by redistributing responsibilities.[41] Reduced workloads have been associated with lower ICU mortality by minimizing medical errors and improving access to critical equipment.[43] By contributing to an interdisciplinary team, CCPs can play a vital role in reducing mortality, which is a key indicator of ICU care quality.[44] Moreover, ADEs are often fatal in critically ill patients,[45] reinforcing the importance of medication safety interventions.

The 28% reduction in mortality observed in ICUs with CCP involvement is particularly noteworthy. Mortality in critical care is influenced by multiple intersecting variables, including disease severity, timeliness and appropriateness of treatment, comorbidities, and care coordination. Pharmacists help optimize several of these factors, especially through the identification and prevention of drug-related problems, timely therapeutic adjustments, and reduction of iatrogenesis harm. The mortality benefit observed in this analysis likely reflects CCPs' proactive role in early pharmacotherapy optimization in the clinical trajectory, which is essential in conditions such as sepsis, acute respiratory distress syndrome, or multi-organ failure.

This study revealed that ICU team care involving CCPs decreased the occurrence of ADEs. The incidence of ADEs is influenced by the clinical setting and the nature of interventions. ADEs contribute significantly to healthcare costs, particularly through insurance claims; therefore, reducing their occurrence represents a major advantage for ICU patients.[46] The observed 61% reduction in ADEs supports the role of CCPs in improving medication safety. In the ICU, ADEs are frequently linked to polypharmacy, organ dysfunction, drug–drug interactions (DDIs), and medications with narrow therapeutic indices. CCPs bring specialized expertise to address these challenges, ensuring appropriate dosing and monitoring of medications. Their interventions range from preventing nephrotoxic drug combinations to adjusting antibiotic regimens based on pharmacokinetic parameters, actions that directly mitigate the risk of ADEs.

These findings align with earlier meta-analyses. For example, Wang *et al.*[14] demonstrated that CCP interventions were effective in reducing ADEs in general hospital settings. However, their analysis did not show a significant effect on mortality and did not focus specifically on ICU populations. Our results not only reaffirm the benefit of CCPs in reducing ADEs but also extend prior research by demonstrating a clear mortality advantage specific to ICU settings, which represent the most complex and high-risk environment for medication management.

In a more recent systematic review, Lee *et al.*[3] highlighted improvements in ICU outcomes when pharmacists participated in multidisciplinary care. However, their analysis did not quantify ADEs, and the mortality data were more limited. Our work thus provides a more comprehensive synthesis of both safety and survival endpoints and fills an important evidence gap in the literature on ICU pharmacotherapy.

The study by Rivkin and Yin[26] demonstrated that CCPs significantly reduce clinically important DDIs in medical ICU patients. Prospective pharmacist review during rounds led to a 65% reduction in severe DDIs requiring therapy modification or avoidance (classified as categories D and X; $p<0.01$), with an 82% acceptance rate of pharmacist recommendations. Notably, fewer DDIs were associated with shorter ICU length of stay ($p<0.01$), though the direct impact on mortality was not statistically significant ($p=0.09$). The intervention group had a lower mortality rate (13.9% vs. 29.5%, $p=0.01$), suggesting broader benefits of pharmacist involvement beyond DDI management. This highlights the pharmacist's role in mitigating MRPs and optimizing ICU outcomes through proactive, team-based interventions.

Aghili and Kasturirangan[35] investigated the role of clinical pharmacists in managing DDIs among

critically ill patients with chronic kidney disease (CKD), demonstrating their significant impact on medication safety. The study identified 273 DDIs in 76 patients (83.5% of participants), with 63.7% requiring close monitoring and 30% necessitating therapy modification or drug discontinuation. Pharmacist interventions, including dosage adjustments (19.4%), drug discontinuation (17.2%), and enhanced monitoring (41%), were highly accepted by prescribers (92%). Notably, 22% of DDIs caused temporary harm or prolonged hospitalization, but pharmacist involvement mitigated severe outcomes, such as life-threatening hypotension from contraindicated combinations (e.g., nitroglycerine-sildenafil). The study also highlighted that advanced CKD stages (e.g., stage 5) and polypharmacy significantly increased DDI risk ($p<0.05$). These findings underscore the critical role of pharmacists in preventing ADEs through proactive DDI management, particularly in high-risk CKD populations, though their impact on mortality remains unexplored.

Dilokpattanamongkol *et al.*[39] evaluated the impact of pharmacist-led pharmaceutical care on pain and agitation management in a Thai medical ICU, demonstrating significant improvements in clinical outcomes. The study found that pharmacist involvement in analgesic/sedative selection reduced median ICU length of stay (from 10.00 to 6.50 days, $p=0.002$), hospital stay (from 30.50 to 17.50 days, $p<0.001$), and ventilator days (from 14.00 to 8.50 days, $p=0.008$). Pharmacists optimized therapy by promoting opioid-based regimens over benzodiazepines, which decreased adverse events like prolonged sedation (from 24.44% to 4.55%, $p=0.001$) and hemodynamic instability (from 18.89% to 3.03%, $p=0.003$). However, mortality rates remained unchanged (53.03% vs. 46.67%, $p=0.432$), likely due to the multifactorial nature of ICU mortality. The study highlights the role of CCPs in protocol-driven sedation management to enhance recovery and resource utilization, though their impact on survival may require broader multidisciplinary interventions.

The study by Louzon *et al.*[33] demonstrated the significant impact of CCPs in managing pain, agitation, and delirium through multidisciplinary ABCDE bundle rounds. Their two-phase initiative showed that pharmacist-directed sedation management reduced continuous sedation exposure by 46%, decreased ICU length of stay by 5 days, and lowered hospital costs by $1.2 million. In addition, the expanded ABCDE bundle program further improved outcomes, including a reduction in mean ventilator days from 5.6 to 4.0 days and a significant decline in mortality Acute Physiology and Chronic Health Evaluation ratios from 1.26 to 0.75. These findings underscore the role of pharmacists in optimizing clinical outcomes and reducing resource utilization in ICUs, aligning with broader evidence supporting their integration into critical care teams.

Mohammad *et al.*[40] evaluated the role of clinical pharmacists in an interprofessional ICU recovery clinic, demonstrating their effectiveness in addressing MRPs among ICU survivors. The study found that pharmacist interventions led to a significant reduction in MRPs between initial and six-month follow-up visits (from 3.5 ± 1.7 to 2.4 ± 1.3 per patient, $p=0.025$), with common interventions including patient education (91.3%), medication changes (73.9%), and care coordination (73.9%). Although no significant difference in MRPs was observed between the intervention and control groups, the high acceptance of pharmacist recommendations (e.g., addressing safety-related issues, drug interactions, and adherence) underscores their value in post-ICU care. The authors emphasized the pharmacist's role in comprehensive medication management, particularly for complex sepsis or respiratory failure survivors, highlighting potential long-term benefits in reducing preventable readmissions and optimizing recovery. These findings align with broader evidence supporting pharmacist integration in critical care transitions to mitigate ADEs and improve patient outcomes.

The study by Oxman *et al.*[30] evaluated the impact of pharmacist-driven interventions on antibiotic de-escalation in suspected ventilator-associated pneumonia cases. Pharmacist involvement significantly improved the rate of appropriate antibiotic targeting based on culture results (59% pre-intervention vs. 91% post-intervention, $p=0.003$), demonstrating their role in optimizing antimicrobial stewardship. However, the intervention did not significantly increase early antibiotic discontinuation in low-risk patients (19% vs. 23%, $p=0.767$), suggesting physician reluctance to stop empiric therapy despite clinical indicators. While mortality rates remained unchanged (14% vs. 16.7%, $p=0.72$), the study highlights the pharmacist's ability to enhance evidence-based antibiotic use in critical care, particularly in tailoring therapy to microbiological data.

The study by Jiang *et al.*[28] highlights the role of CCPs in optimizing antimicrobial dosing for patients undergoing continuous venovenous hemofiltration (CVVH), demonstrating significant reductions in ADEs and cost savings. Pharmacist interventions, including daily dosing adjustments based on dynamic CVVH parameters, led to a 2.36-fold decrease in antimicrobial-related ADEs (11 vs. 26 events, $p=0.002$) and cost savings of £1637.7 per patient. Notably, β-lactams accounted for 51.2% of dosing errors, underscoring the complexity of antimicrobial management in renal replacement therapy. While mortality and ICU length of stay remained unchanged, the study emphasizes

the pharmacist's impact on preventing preventable ADEs (4 vs. 14 events, p=0.006) and reducing drug costs, reinforcing their value in multidisciplinary ICU teams.

The study by Hammond *et al.*[31] evaluated the impact of pharmacist-led educational interventions on the appropriateness of stress ulcer prophylaxis (SUP) in critically ill patients. The intervention, which included guideline-based education and pocket cards for physicians, significantly reduced inappropriate initiation of acid suppression therapy (AST) from 23% to 11% (p=0.012). While no differences were observed in mortality or adverse events (e.g., pneumonia, *Clostridium difficile* infection), the study demonstrated that pharmacist involvement in education improved adherence to evidence-based SUP practices. This highlights the role of CCPs in optimizing medication safety and reducing unnecessary therapy, though broader interventions may be needed to address inappropriate continuation of AST beyond the ICU.

In a study performed by Pronovost *et al.*,[1] apposite pharmacist recommendations for antibiotic treatment in critically ill patients were associated with a decline in ventilator-related pneumonia, which is often linked to higher mortality. Furthermore, a study by Kim *et al.*[47] showed that, compared to patients who did not receive team-based care with CCP, mortality was lower among those managed by an ICU team that incorporated CCPs.

An earlier meta-analysis focusing on the influence of ICU CCPs' interventions on medication errors and ADEs showed a decrease in ADEs when a CCP was added to the team.[14] However, the data were derived from subjects admitted to general medical or surgical units rather than ICU settings, and the definition of medication errors was unclear.

A previous study by Leape *et al.*[25] demonstrated the significant impact of integrating pharmacists into ICU rounds, showing a 66% reduction in preventable ADEs, from 10.4 to 3.5/1,000 patient-days, after implementing pharmacist participation. The study, conducted in a medical ICU, highlighted that nearly all (99%) of the pharmacists' recommendations were accepted by physicians, with interventions ranging from dose corrections to identifying drug interactions and allergies. The authors estimated annual cost savings of approximately $270,000 due to prevented ADEs, underscoring the pharmacist's role in error prevention, interception, and systems improvement. These findings support the value of pharmacists as active members of the ICU team in enhancing medication safety and reducing harm.

Several mechanisms likely explain the observed outcomes:

(i) Medication error prevention: CCPs review and reconcile medications daily, preventing errors in dosing, duplications, and omissions, especially during care transitions.
(ii) Therapeutic optimization: Pharmacists tailor treatments based on patient-specific variables, including renal/hepatic function, weight, drug levels, and drug interactions.
(iii) Antimicrobial stewardship: Several studies (e.g., Jiang *et al.*[27,28,38] and Li *et al.*[32]) in this meta-analysis demonstrated that CCP-led antimicrobial programs reduced inappropriate antibiotic use and potentially minimized resistance patterns, leading to improved infection-related outcomes.
(iv) Education and protocol development: CCPs contribute to policy and protocol development and offer bedside education, increasing adherence to evidence-based guidelines.
(v) Interdisciplinary synergy: Pharmacists free up physician time by managing medication-related tasks, contributing to more efficient workflows and reducing clinician burnout, a factor indirectly tied to fewer clinical errors.

A notable strength of this meta-analysis is its inclusion of studies from diverse regions, such as North America, Asia, Europe, and Africa. This diversity supports the global applicability of the findings. Even in middle-income countries, such as Egypt and India, where resource constraints may be more prominent, CCPs demonstrated measurable improvements in patient safety and outcomes. This suggests that pharmacist integration is not only a high-income health system luxury but also a universally impactful intervention when appropriately implemented.

In resource-limited settings, CCPs may have even greater importance, given the scarcity of intensivists, suboptimal nurse-to-patient ratios, and high patient turnover. The pharmacist's vigilance and expertise can serve as a vital safety net in such environments.

This study demonstrated a significant association between the inclusion of CCPs in ICU teams and reductions in both mortality and ADEs. However, further high-quality trials are needed to clarify the specific clinical contexts and mechanisms through which these benefits occur. In addition, our meta-analysis did not identify any significant associations between outcomes and patient characteristics such as age, ethnicity, or gender. This finding is consistent with previous meta-analyses, which also reported no clear influence of these demographic factors on the observed outcomes.[3,48]

Incorporating CCPs should be considered a standard component of ICU staffing models, especially given

the magnitude of benefit demonstrated. Policymakers and healthcare leaders should advocate for expanding pharmacist roles in the ICU beyond the traditional scope. Furthermore, educational and professional development programs must be tailored to produce pharmacists with the advanced competencies required for critical care practice. This integration may also be cost-effective. Although our analysis did not focus on economic outcomes, prior studies have shown that pharmacist interventions lead to reduced length of stay, MRPs, and lower hospital readmissions, all contributing to healthcare cost savings.[48,49]

5. Limitations

Despite the compelling results, several limitations should be acknowledged:

(i) Heterogeneity: There was significant heterogeneity among the included studies in terms of design, sample size, CCP roles, and outcome definitions. While random-effects modeling mitigates this statistically, clinical heterogeneity remains a consideration.

(ii) Study design: Only a few of the included studies were randomized trials; most were observational, potentially introducing bias.

(iii) Inadequate subgroup data: The inability to perform subgroup analyses based on variables such as age, gender, severity scores, ICU type (e.g., medical vs. surgical), and comorbidities limits the granularity of the findings.

(iv) Lack of long-term outcomes: Most studies reported only in-hospital outcomes. The long-term impact of CCPs on quality of life, post-ICU syndrome, or 90-day mortality remains to be clarified.

(v) Economic evaluation: While improved clinical outcomes often translate to cost savings, this analysis did not explore cost-effectiveness, which is an essential consideration for implementation.

6. Conclusion

This systematic review and meta-analysis provide compelling evidence that the incorporation of CCPs into ICU teams is associated with significantly lower mortality and fewer ADEs among critically ill patients. The findings reinforce the importance of pharmacist-led pharmacotherapy optimization, antimicrobial stewardship, and interdisciplinary collaboration in intensive care settings. Given the clinical relevance of these outcomes and the increasing complexity of ICU pharmacotherapy, healthcare institutions and policymakers should consider the routine deployment of CCPs as a strategic priority. Future studies should aim to address remaining gaps, including the cost-effectiveness of CCP services, long-term patient outcomes, and their impact across various ICU subtypes and demographic groups. Ultimately, integrating CCPs represents not only a pharmacological intervention but also a structural advancement in ICU team-based care, contributing to safer, more efficient, and outcome-driven patient management.

Acknowledgments

None.

Funding

None.

Conflict of interest

The authors declare no conflicts of interest.

Author contributions

Conceptualization: Mohamed S. Imam, Fawaz Saad Yahya Thabit
Data curation: All authors
Writing – original draft: All authors
Writing – review & editing: All authors

Ethics approval and consent to participate

Not applicable.

Consent for publication

Not applicable.

Availability of data

The data analyzed in this meta-analysis were extracted from publicly available publications, with full citations and article links provided in the references section.

References

1. Pronovost PJ, Angus DC, Dorman T, Robinson KA, Dremsizov TT, Young TL. Physician staffing patterns and clinical outcomes in critically ill patients: A systematic review. *JAMA*. 2002;288(17):2151-2162.

   doi: 10.1001/jama.288.17.2151

2. Arredondo E, Udeani G, Horseman M, Hintze TD, Surani S. Role of clinical pharmacists in intensive care units. *Cureus*. 2021;13(9):e17929.

   doi: 10.7759/cureus.17929

3. Lee H, Ryu K, Sohn Y, Kim J, Suh GY, Kim E. Impact on patient outcomes of pharmacist participation in multidisciplinary critical care teams: A systematic review and meta-analysis. *Crit Care Med*. 2019;47(9):1243-1250.

   doi: 10.1097/CCM.0000000000003830

4. Jacobi J, Kane-Gill S, Boucher B. Critical care pharmacists have a rich history and evolving roles. *J Am Coll Clin Pharm*.

2023;6(8):934-941.

doi: 10.1002/jac5.1840

5. Aljuhani O. The role of critical care pharmacists beyond intensive care units: A narrative review on medication management for ICU survivors. *Braz J Pharm Sci*. 2022;58:e21012.

doi: 10.1590/s2175-97902022e21012

6. Park TY, Lee SM, Kim SE, *et al*. Pharmacotherapeutic problems and pharmacist interventions in a medical intensive care unit. *Korean J Crit Care Med*. 2015;30(2):82-88.

doi: 10.4266/kjccm.2015.30.2.82

7. Agarwal J, Singh V, Das A, Nath SS, Kumar R, Sen M. Reversing the trend of antimicrobial resistance in ICU: Role of antimicrobial and diagnostic stewardship. *Indian J Crit Care Med*. 2021;25(6):635.

doi: 10.5005/jp-journals-10071-23861

8. Esper AM, Martin GS. The impact of comorbid [corrected] conditions on critical illness. *Crit Care Med*. 2011;39(12):2728-2735.

doi: 10.1097/CCM.0b013e318236f27e

9. Chiang LH, Huang YL, Tsai TC. Clinical pharmacy interventions in intensive care unit patients. *J Clin Pharm Ther*. 2021;46(1):128-133.

doi: 10.1111/jcpt.13265

10. Ayhan YE. Role of clinical pharmacists in intensive care unit. In: *The Roles and Responsibilities of Clinical Pharmacists in Hospital Settings*. Sharjah: Bentham Science Publishers; 2024. p. 83-108.

11. Aradhya PJ, Ravi R, Chandra BJ, Ramesh M, Chalasani SH. Assessment of medication safety incidents associated with high-alert medication use in intensive care setting: A clinical pharmacist approach. *Indian J Crit Care Med*. 2023;27(12):917-922.

doi: 10.5005/jp-journals-10071-24588

12. Xu P, Yi Q, Wang C, *et al*. Pharmacist-led intervention on the inappropriate use of stress ulcer prophylaxis pharmacotherapy in intensive care units: A systematic review. *Front Pharmacol*. 2021;12:741724.

doi: 10.3389/fphar.2021.741724

13. Buckley MS, Roberts RJ, Yerondopoulos MJ, Bushway AK, Korkames GC, Kane-Gill SL. Impact of critical care pharmacist-led interventions on pain, agitation, and delirium in mechanically ventilated adults: A systematic review. *J Am Coll Clin Pharm*. 2023;6(9):1041-1052.

doi: 10.1002/jac5.1778

14. Wang T, Benedict N, Olsen KM, *et al*. Effect of critical care pharmacist's intervention on medication errors: A systematic review and meta-analysis of observational studies. *J Crit Care*. 2015;30(5):1101-1106.

doi: 10.1016/j.jcrc.2015.06.018

15. Hashimoto M, Asai S, Umezawa K, *et al*. Impact of ward pharmacist-led antimicrobial stewardship in intensive care units. *J Chemother*. 2023;35(3):188-197.

doi: 10.1080/1120009X.2022.2087652

16. Van Den Bergh D, Messina AP, Goff DA, *et al*. A pharmacist-led prospective antibiotic stewardship intervention improves compliance to community-acquired pneumonia guidelines in 39 public and private hospitals across South Africa. *Int J Antimicrob Agents*. 2020;56(6):106189.

doi: 10.1016/j.ijantimicag.2020.106189

17. Nili-Ahmadabadi B, Luisetto M, Nili-Ahmadabadi H, Nasser H, Mashori GR, Nili-Ahmadabadi M. Clinical impact of pharmacist presence in ICU medical team on mortality rate. *Clin Teamwork*. 2016;1:15-33.

18. Alsayed HAH, Sharif-Askari FS, Sharif-Askari NS, Halwani R. Clinical pharmacist interventions in an intensive care unit reduces ICU mortality at a tertiary hospital in Dubai, United Arab Emirates. *Explor Res Clin Soc Pharm*. 2024;14:100431.

doi: 10.1016/j.rcsop.2024.100431

19. Albayrak A, Başgut B, Bıkmaz GA, Karahalil B. Clinical pharmacist assessment of drug-related problems among intensive care unit patients in a Turkish university hospital. *BMC Health Serv Res*. 2022;22(1):79.

doi: 10.1186/s12913-022-07494-5

20. Page MJ, McKenzie JE, Bossuyt PM, *et al*. The PRISMA 2020 statement: An updated guideline for reporting systematic reviews. *BMJ*. 2021;372:n71.

doi: 10.1136/bmj.n71

21. Saaiq M, Ashraf B. Modifying "Pico" question into "Picos" model for more robust and reproducible presentation of the methodology employed in a scientific study. *World J Plast Surg*. 2017;6(3):390-392.

22. Collaboration C. *RoB 2: A revised Cochrane Risk-of-Bias Tool for Randomized Trials*; 2020. Available from: https://www.com/bias/resources/rob-2-revised-cochrane-risk-bias-tool-randomized-trials [Last accessed on 2019 Dec 06].

23. Higgins JP, Thompson SG, Deeks JJ, Altman DG. Measuring inconsistency in meta-analyses. *BMJ*. 2003;327(7414):557-560.

doi: 10.1136/bmj.327.7414.557

24. Gupta A, Das A, Majumder K, *et al*. Obesity is independently associated with increased risk of hepatocellular cancer-related mortality: A systematic review and meta-analysis. *Am J Clin Oncol*. 2018;41(9):874-881.

doi: 10.1097/COC.0000000000000388

25. Leape LL, Cullen DJ, Clapp MD, *et al*. Pharmacist participation on physician rounds and adverse drug events

in the intensive care unit. *JAMA*. 1999;282(3):267-270.

doi: 10.1001/jama.282.3.267

26. Rivkin A, Yin H. Evaluation of the role of the critical care pharmacist in identifying and avoiding or minimizing significant drug-drug interactions in medical intensive care patients. *J Crit Care*. 2011;26(1):104.e1-e6.

doi: 10.1016/j.jcrc.2010.04.014

27. Jiang SP, Zhu ZY, Ma KF, Zheng X, Lu XY. Impact of pharmacist antimicrobial dosing adjustments in septic patients on continuous renal replacement therapy in an intensive care unit. *Scand J Infect Dis*. 2013;45(12):891-899.

doi: 10.3109/00365548.2013.827338

28. Jiang SP, Xu YY, Wu WF, *et al*. Improving antimicrobial dosing in critically ill patients receiving continuous venovenous hemofiltration and the effect of pharmacist dosing adjustment. *Eur J Intern Med*. 2014;25(10):930-935.

doi: 10.1016/j.ejim.2014.08.001

29. Claus BO, Robays H, Decruyenaere J, Annemans L. Expected net benefit of clinical pharmacy in intensive care medicine: A randomized interventional comparative trial with matched before-and-after groups. *J Eval Clin Pract*. 2014;20(6):1172-1179.

doi: 10.1111/jep.12289

30. Oxman DA, Adams CD, Deluke G, *et al*. Improving antibiotic de-escalation in suspected ventilator-associated pneumonia: An observational study with a pharmacist-driven intervention. *J Pharm Pract*. 2015;28(5):457-461.

doi: 10.1177/0897190014527316

31. Hammond DA, Killingsworth CA, Painter JT, *et al*. Impact of targeted educational interventions on appropriateness of stress ulcer prophylaxis in critically ill adults. *Pharm Pract (Granada)*. 2017;15(3):948.

doi: 10.18549/pharmpract.2017.03.948

32. Li Z, Cheng B, Zhang K, *et al*. Pharmacist-driven antimicrobial stewardship in intensive care units in East China: A multicenter prospective cohort study. *Am J Infect Control*. 2017;45(9):983-989.

doi: 10.1016/j.ajic.2017.02.021

33. Louzon P, Jennings H, Ali M, Kraisinger M. Impact of pharmacist management of pain, agitation, and delirium in the intensive care unit through participation in multidisciplinary bundle rounds. *Am J Health Syst Pharm*. 2017;74(4):253-262.

doi: 10.2146/ajhp150942

34. Gu H, Sun L, Sheng B, Gu X, Wang S, Chen W. *Effect of Critical Care Pharmacist on Antibiotic Medication Optimizations, Reduce Drug Costs But not Increase Mortality: A Retrospective Cohort Study in the Real World Research*. United States: Research Square; 2020.

35. Aghili M, Kasturirangan MN. Management of drug-drug interactions among critically ill patients with chronic kidney disease: Impact of clinical pharmacist's interventions. *Indian J Crit Care Med*. 2021;25(11):1226-1231.

doi: 10.5005/jp-journals-10071-23919

36. Toukhy A, Fayed S, Sabry N, Shawki M. The impact of an established pharmaceutical care pathway on drug related problems in an intensive care unit. *Am J Med Sci*. 2021;362(2):143-153.

doi: 10.1016/j.amjms.2021.03.007

37. MacLaren R, Bond CA, Martin SJ, Fike D. Clinical and economic outcomes of involving pharmacists in the direct care of critically ill patients with infections. *Crit Care Med*. 2008;36(12):3184-3189.

doi: 10.1097/CCM.0b013e31818f2269

38. Jiang SP, Zhu ZY, Wu XL, Lu XY, Zhang XG, Wu BH. Effectiveness of pharmacist dosing adjustment for critically ill patients receiving continuous renal replacement therapy: A comparative study. *Ther Clin Risk Manag*. 2014;10:405-412.

doi: 10.2147/TCRM.S59187

39. Dilokpattanamongkol P, Tangsujaritvijit V, Suansanae T, Suthisisang C. Impact of pharmaceutical care on pain and agitation in a medical intensive care unit in Thailand. *Int J Clin Pharm*. 2017;39:573-581.

doi: 10.1007/s11096-017-0456-0

40. Mohammad RA, Eze C, Marshall VD, *et al*. The impact of a clinical pharmacist in an interprofessional intensive care unit recovery clinic providing care to intensive care unit survivors. *J Am Coll Clin Pharm*. 2022;5(10):1027-1038.

doi: 10.1002/jac5.1671

41. Donovan AL, Aldrich JM, Gross AK, *et al*. Interprofessional care and teamwork in the ICU. *Crit Care Med*. 2018; 46(6):980-990.

doi: 10.1097/CCM.0000000000003067

42. Devlin JW, McKenzie C. Expanding the reach of critical care pharmacists globally. *Crit Care Med*. 2018;46(2):328-330.

doi: 10.1097/CCM.0000000000002879

43. Donchin Y, Gopher D, Olin M, *et al*. A look into the nature and causes of human errors in the intensive care unit. 1995. *Qual Saf Health Care*. 2003;12(2):143-147; discussion 147-8.

doi: 10.1136/qhc.12.2.143

44. Brinkman S, Abu-Hanna A, De Jonge E, De Keizer NF. Prediction of long-term mortality in ICU patients: Model validation and assessing the effect of using in-hospital versus long-term mortality on benchmarking. *Intensive Care Med*. 2013;39(11):1925-1931.

doi: 10.1007/s00134-013-3042-5

45. Michalets E, Creger J, Shillinglaw WR. Outcomes of

expanded use of clinical pharmacist practitioners in addition to team-based care in a community health system intensive care unit. *Am J Health Syst Pharm*. 2015;72(1):47-53.

doi: 10.2146/ajhp140105

46. Kopp BJ, Erstad BL, Allen ME, Theodorou AA, Priestley G. Medication errors and adverse drug events in an intensive care unit: Direct observation approach for detection. *Crit Care Med*. 2006;34(2):415-425.

doi: 10.1097/01.CCM.0000198106.54306.D7

47. Kim MM, Barnato AE, Angus DC, Fleisher LA, Kahn JM. The effect of multidisciplinary care teams on intensive care unit mortality. *Arch Intern Med*. 2010;170(4):369-376.

doi: 10.1001/archinternmed.2009.521

48. Baudouin A, Herledan C, Poletto N, *et al*. Economic impact of clinical pharmaceutical activities in hospital wards: A systematic review. *Res Social Adm Pharm*. 2021;17(3):497-505.

doi: 10.1016/j.sapharm.2020.07.016

49. Dawoud DM, Smyth M, Ashe J, *et al*. Effectiveness and cost effectiveness of pharmacist input at the ward level: A systematic review and meta-analysis. *Res Soc Adm Pharm*. 2019;15(10):1212-1222.

doi: 10.1016/j.sapharm.2018.10.006

ACCSCIENCE PUBLISHING

Eurasian Journal of Medicine and Oncology

ORIGINAL RESEARCH ARTICLE

Perception of advance health-care directives among nursing students in oncology and palliative care settings: An Italian pre–post study

Diego Lopane[1,2†], Sara Morales Palomares[3†], Alessandra Dacomi[1], Daniela Cattani[1], Simone Cosmai[2], Chiara Provasoli[1], Sarah Scollo[2], Mauro Parozzi[4], Giovanni Cangelosi[5*], Stefano Mancin[1], Emanuela Morenghi[1,2‡], and Beatrice Mazzoleni[2‡]

[1]Scientific Institute for Research, Hospitalization and Healthcare, Humanitas Research Hospital, Milan, Milano, Italy

[2]Department of Biomedical Sciences, Faculty of Nursing, Humanitas University, Milan, Milano, Italy

[3]Department of Pharmacy, Health and Nutritional Sciences, Faculty of Health Sciences, University of Calabria, Rende, Cosenza, Italy

[4]Department of Medicine and Surgery, Faculty of Medicine and Surgery, University of Parma, Parma, Parma, Italy

[5]Department of Experimental Medicine and Public Health, School of Pharmacy, University of Camerino, Macerata, Macerata, Italy

(This article belongs to the *Special Issue: Nursing Care in Cancer*)

Abstract

Introduction: Advance health-care directives (AHDs) empower individuals to express treatment preferences in anticipation of future incapacity and play a crucial role in ensuring patient-centered end-of-life care. However, nursing students often report limited training and discomfort when addressing these issues.

Objective: This study aims to assess the impact of an oncology palliative care module on nursing students' knowledge and perceptions of AHDs.

Methods*:* In a pre–post observational design, 39 3rd-year nursing students completed questionnaires immediately before (pre-test) and after (post-test) a 75-h oncology palliative care module that included lectures, case discussions, and active learning methods. Sociodemographic and attitudinal data were analyzed using descriptive statistics.

Results: After the module, students showed an increased preference for refusing non-beneficial treatments (from 63.6% to 71.4%) and reported heightened awareness of the need for proactive communication regarding therapies and pain management. While willingness to donate organs remained high (94.9% vs. 92.3%), students exhibited increased caution regarding the involvement of minors in end-of-life discussions. Openness to spiritual support also rose, alongside slight increases in preferences for cremation and body donation. Although these changes did not reach statistical significance, the consistency index indicated generally stable ethical orientations, with emerging trends toward deeper reflection and heightened awareness.

Conclusion: Although no statistically significant differences were observed, the educational intervention on AHDs appeared to influence certain perceptions and attitudes among nursing students toward end-of-life decisions. Integrating structured AHD training into nursing curricula may enhance students' awareness and ability to support patient self-determination in clinical practice.

Keywords: Advance health-care directives; Nursing education; Patient self-determination; Clinical ethics; End-of-life care

†*These authors contributed equally to this work.*

‡*These authors contributed equally as senior authors.*

***Corresponding author:**
Giovanni Cangelosi
(giovanni01.cangelosi@unicam.it)

Citation: Lopane D, Palomares SM, Dacomi A, *et al.* Perception of advance health-care directives among nursing students in oncology and palliative care settings: An Italian pre–post study. *Eurasian J Med Oncol.* 2025;9(3):239-249. doi: 10.36922/EJMO025250263

Received: June 18, 2025

1st revised: July 15, 2025

2nd revised: July 21, 2025

Accepted: July 23, 2025

Published online: August 14, 2025

Copyright: © 2025 Author(s). This is an Open-Access article distributed under the terms of the Creative Commons Attribution License, permitting distribution, and reproduction in any medium, provided the original work is properly cited.

Publisher's Note: AccScience Publishing remains neutral with regard to jurisdictional claims in published maps and institutional affiliations.

1. Introduction

The progressive aging of the population and the increasing incidence of chronic and degenerative diseases are reshaping global health-care priorities. In 2021, the World Health Organization estimated that by 2050, the proportion of individuals over the age of 60 will double, reaching 22% of the total population.[1] In Europe, more than 70% of deaths are attributable to non-communicable chronic diseases, such as cancer, cardiovascular, and respiratory conditions, many of which require advance care planning.[2] Studies conducted in Europe highlight that a substantial number of patients die without receiving adequate palliative care despite having complex needs.[3] In Italy, the Higher Institute of Health reports that approximately 30% of dying patients require palliative care, but only a minority receives it.[4] According to data from the 2022 Italian National Institute of Statistics, fewer than 10% of citizens have signed an Advance Treatment Directive (*Disposizioni Anticipate di Trattamento* [DAT]), indicating limited cultural familiarity and dissemination of this tool, even among health-care professionals.[5]

The promotion of patient autonomy in clinical settings has been legally recognized in many countries. In the United States, the Patient Self-Determination Act of 1990 introduced the requirement for health-care institutions to inform patients about their right to express advance health-care directives (AHDs).[6] In Europe, regulation is not uniform—some countries, such as Germany and Spain, legally recognize advance directives, whereas others, such as the Netherlands and Belgium, also allow euthanasia or medically assisted suicide.[7-9]

In Italy, Law No. 219/2017 introduced the DAT, officially recognizing citizens' rights to express their wishes concerning medical treatment in the event of future incapacity, including the option to designate a health-care proxy.[10] In addition to codifying the principle of informed consent, the law aims to enhance the therapeutic relationship and communication among patients, families, and healthcare professionals. However, the implementation of DAT in clinical practice remains limited, hindered by cultural resistance, lack of information, and operational uncertainty among health-care providers.[11,12]

Nurses play a crucial role in supporting patients at the end of life, assisting them in articulating their individual values and preferences.[13,14] Nevertheless, several studies report a lack of preparation among nursing students regarding the ethical-legal aspects of end-of-life decision-making.[15,16] Barriers such as insecurity, fear of addressing sensitive topics, and limited knowledge of the legislation restrict their ability to support patients in advance care planning.[17-19] Therefore, several studies advocate for the inclusion of specific modules within university curricula that incorporate active learning methodologies, simulation, and ethical reflection.[20,21]

Building on these premises, it is worth exploring how targeted educational interventions can bridge existing gaps in nursing students' knowledge and attitudes concerning end-of-life care. Accordingly, the present study seeks to address the following research question: "To what extent can a structured educational module on AHDs influence nursing students' attitudes, knowledge, and ethical orientation toward end-of-life decision-making?"

The primary objective is to evaluate the impact of a targeted educational intervention on students' knowledge regarding therapeutic self-determination by examining changes in awareness, preferences, and ethical sensitivity before and after the training. Ultimately, this study aims to contribute to the development of more effective educational strategies that promote ethical competence, relational awareness, and empathy in supporting patients during the final stage of life.

2. Materials and methods

2.1. Study design

A pre–post observational study design was employed to evaluate the impact of an educational intervention on nursing students' understanding and attitudes toward AHDs. This exploratory study involved a single cohort of nursing students recruited through convenience sampling. The sample size was determined by the number of eligible participants who enrolled in the module. This study adhered to the Strengthening the Reporting of Observational Studies in Epidemiology guidelines[22] for reporting observational research.

2.2. Setting and participants

The study was conducted during the second semester of the 2024/2025 academic year at Humanitas University, Italy, within the Bachelor's Degree in Nursing program. The target population consisted of 3rd-year students enrolled in the palliative care module. Inclusion criteria required attendance at a minimum of 75% of the total module hours and mandatory participation in the final two lessons. Exclusion criteria included failure to meet attendance requirements or being absent during the final sessions. A total of 39 students met the inclusion criteria and completed all study phases.

2.3. Educational intervention

The educational module comprised 75 h of instruction on palliative care and integrated lectures, case discussions, and active learning methodologies. A dedicated session

on AHDs was incorporated, emphasizing the legal, ethical, and practical aspects related to AHDs. The curriculum was designed to enhance students' knowledge, foster positive attitudes, and develop communication skills relevant to end-of-life care.

2.4. Data collection

Data were collected using structured, anonymous questionnaires administered immediately before (pre-test) and after (post-test) the educational intervention. The survey instrument included sections on sociodemographic characteristics (e.g., age, gender, and previous exposure to end-of-life care discussions) as well as knowledge of AHDs and relevant legal frameworks. Data collection was conducted using the VIDAS AHD Module, ensuring alignment with standardized national guidelines on end-of-life care documentation.

2.5. Ethical statement

The study received ethical approval from the Humanitas University Ethics Committee in Milan (Protocol CLI_RIC_14). All participants provided informed consent, and confidentiality was maintained in accordance with the Declaration of Helsinki.[23] Data privacy and participant anonymity were strictly ensured throughout the research process.

2.6. Study procedures

Before the intervention, an introductory session was held to explain the study objectives, ethical considerations, and methodological procedures to all potential participants. Clear instructions were provided regarding voluntary participation, data protection, and the right to withdraw at any time without academic penalty. This initial briefing ensured informed and voluntary participation while helping establish a climate of academic integrity and trust. Participants then completed the pre-intervention questionnaire, attended the educational sessions, and subsequently completed the post-intervention assessment.

2.7. Evaluation instruments

For the evaluation of students' knowledge, attitudes, and perceptions regarding AHDs, the study employed the official Italian AHD Module, made available through the Ministry of Health and municipal services, in accordance with national guidelines for end-of-life care documentation.[24] This structured and standardized questionnaire was specifically designed to explore individual preferences concerning end-of-life care, therapeutic choices, and personal attitudes toward critical issues such as organ donation, the refusal of therapeutic obstinacy, and funeral practices, in line with the provisions of Italian Law No. 219/2017.

The instrument collected sociodemographic information, including age, gender, and previous exposure to end-of-life care discussions. It also assessed students' knowledge regarding the legal and ethical aspects of AHDs, as well as their attitudes toward advance directives and communication with healthcare professionals. In addition, it explored personal preferences related to end-of-life decisions, such as willingness to donate organs and the choice between cremation and traditional burial.

The adoption of the VIDAS AHD module enabled a culturally sensitive, legally coherent, and methodologically standardized evaluation, ensuring the reliability of both pre- and post-intervention measurements. This approach provided a comprehensive understanding of the educational intervention's impact on students' awareness and attitudes toward end-of-life care planning. While the questionnaire was based on the VIDAS module and the official AHD template, no formal psychometric validation (e.g., reliability testing or factor analysis) was performed.

2.8. Statistical analysis

Descriptive statistics (e.g., mean, standard deviation, median, and interquartile range) were used to characterize the sample and summarize pre- and post-intervention responses. McNemar's test was applied to paired binary variables (e.g., willingness to donate organs and preference for life-sustaining treatments), and odds ratios were calculated to explore directional tendencies. Only participants who provided complete and valid responses for both the pre- and post-intervention phases were included in each pairwise comparison. Consequently, the number of observations analyzed with McNemar's test varied by item and was sometimes lower than the total sample size (n = 39), which ensured methodological rigor while preserving internal validity.

A consistency index (range: 0–7) was computed by summing the number of identical responses across seven dichotomous items administered pre- and post-intervention. Although not derived from a validated scale, the index was constructed based on item-level concordance, a method commonly employed in preference-sensitive research to describe decision stability. The index should be interpreted as an exploratory tool intended to describe trends in response stability rather than as a validated outcome measure.

Pearson's correlation coefficient was used to explore the association between consistency (index score) and age, as both were continuous variables. Gender was dummy-coded (0 = female, 1 = male) and included in the correlation

and regression models as an independent variable. However, it was excluded from the correlation analysis due to insufficient variability. To identify predictors of post-intervention willingness to donate organs, a binary logistic regression model was conducted, including age, gender, and consistency as independent variables.

Finally, thematic analysis of open-ended responses was performed, followed by frequency analysis and graphical visualization of thematic shifts. All analyses were conducted using R version 4.3.2 (R Core Team, Vienna, Austria). A two-tailed $p<0.05$ was considered statistically significant.

3. Results

3.1. Sample characteristics

A total of 39 3rd-year nursing students participated in this study, with a mean age of 22.4 ± 1.8 years, and 74.6% were female. All participants completed both the pre- and post-module questionnaires, yielding a fully paired dataset. The homogeneity of the academic level and the narrow age range helped control for extraneous variability, although the predominance of female respondents reflects the broader gender distribution typical within nursing cohorts. All data are presented in Tables S1-S6.

3.2. Advance disclosure of health status

Before the educational intervention, nearly all students (n = 36, 92.3%) reported feeling comfortable authorizing disclosure of their health status and life expectancy to their parents. This proportion decreased slightly to 34 (87.2%) after the module. In contrast, the willingness to share such information with siblings increased slightly from 31 (79.5%) to 32 (82.1%) students, while authorization for friends rose from 19 (48.7%) to 20 (51.3%) students. The most pronounced change occurred regarding participants' own children: initial willingness was 16 (41.0%) but decreased significantly to 8 (20.5%) post-intervention, suggesting that students reconsidered the ethical and emotional appropriateness of involving minors in end-of-life discussions. Authorization to inform partners remained largely unchanged, shifting from 27 (69.2%) to 26 (66.7%) participants.

3.3. Preferences for life-sustaining treatments in irreversible conditions

When asked about specific life-sustaining interventions in the context of an irreversible illness, students' responses remained remarkably consistent. Cardiopulmonary resuscitation was accepted by 14 students (35.9%) out of 39, both before and after the module. Mechanical ventilation showed a slight reduction in approval, from 12 (30.8%) student's pre-module to 11 (28.2%) post-module. Approval of artificial nutrition increased slightly from 14 (35.9%) students to 15 (38.5%), whereas acceptance of deep sedation increased from 29 (74.4%) students to 30 (76.9%). Preferences for dialysis remained unchanged (n = 11, 28.2%) at both time points, mirroring approval for emergency surgery (n = 13, 33.3%). Finally, support for blood transfusions increased from 12 (30.8%) students to 14 (35.9%), and antibiotic therapy rose from 16 (41.0%) students to 17 (43.6%). These marginal shifts underscore that, even after targeted palliative care education, core attitudes toward these critical treatments were largely stable. Preferences for cardiopulmonary resuscitation and dialysis demonstrated a non-significant increase after the intervention (odds ratio [OR] = 2.50 and 2.00, respectively), whereas palliative sedation remained unchanged (OR = 1.00). These findings may indicate a trend toward greater therapeutic openness, although this change was not statistically significant (Table 1).

3.4. Religious support and funeral arrangements

The module appeared to affect students' views on spiritual care and post-mortem planning. Before instruction, 5 (12.8%) participants opted against any religious assistance at the end of life. However, after completing the module, none (n = 0, 0%) chose "no religious assistance," indicating a unanimous openness to spiritual support. In parallel, the proportion selecting a religious funeral increased from 28 (71.8%) participants to 32 (82.1%), suggesting that the educational content may have highlighted the role of faith and tradition in holistic palliative care. In addition, the proportion choosing "other" types of assistance decreased slightly from 3 (7.7%) to 2 (5.1%), whereas non-response rates increased from 4 (10.3%) to 5 (12.8%). These shifts suggest not only a growing preference for formal religious rites but also a modest consolidation of opinions, with fewer participants opting for unspecified options.

3.5. Post-mortem dispositions

Students' post-mortem preferences also shifted to a limited extent. Support for organ donation for transplant remained nearly universal, declining only slightly from 37 participants (94.9%) before the module to 36 (92.3%) afterward (χ^2 [1 =1.778, p=0.182), indicating stable attitudes toward this option. Willingness to donate one's body for scientific purposes increased from 14 (35.9%) pre-module to 16 (41.0%) post-module, and preference for cremation increased from 18 (46.2%) to 21 (53.8%) (χ^2 [1 = 0.205, p=0.651). In contrast, the choice of inhumation remained unchanged, shifting from 10 (25.6%) before to 9 (23.1%).

These patterns suggest that the educational content may have influenced less familiar dispositions—particularly

Table 1. Preferences for life-sustaining treatments

Treatment	Odds ratio	*p*-value	Interpretation
Resuscitation	2.50	0.450	Slight post-intervention increase[a]
Dialysis	2.00	0.683	Non-significant variation[a]
Sedation	1.00	1.000	No change observed[a]

Notes: Odds ratio values indicate the likelihood of post-intervention endorsement relative to pre-intervention responses. [a]No statistically significant difference. Life-sustaining treatments were evaluated in the context of irreversible clinical conditions. Only items with a sufficient number of paired binary responses (pre/post) are included. Data are based on 3rd-year nursing students (n=39) who completed both assessments.

body donation and cremation—while attitudes toward organ donation and traditional burial remained largely unchanged. McNemar's test revealed no statistically significant changes in students' post-mortem decisions following the educational module: preferences for organ donation (p=0.248), body donation (p=1.000), cremation (p=1.000), and traditional burial (p=0.480) did not reach significance. Although some response trends shifted, no variable met the threshold for statistical significance (Table 2).

3.6. Consistency and predictive modeling

The consistency index ranged from 3 to 7, with most students showing a high level of decision stability. Pearson's correlation revealed a weak positive association between consistency and age (r = 0.23), suggesting that older participants may demonstrate more stable preferences. Gender was excluded from the analysis due to insufficient variability.

A binary logistic regression (Table 3) was conducted to predict willingness to donate organs post-intervention. Although no predictor reached statistical significance, higher consistency was associated with an increased likelihood of organ donation (β = 1.98, p=0.105), whereas age showed a mild negative trend (β = –0.0028, p=0.102), and gender did not contribute significantly (β = –0.134, p=0.811).

Thematic analysis of open-ended responses revealed recurring themes, including requests for "no resuscitation," preferences for "organ donation," and references to "spiritual needs." These responses reflect students' evolving ethical reflections and are illustrated through frequency graphs.

4. Discussion

The present study suggests that a targeted oncology palliative care module may meaningfully influence nursing students' knowledge and attitudes toward AHDs.

Table 2. Pre/post changes in post-mortem dispositions

Variable	Pre→post (b)	Post→pre (c)	*p*-value	Odds ratio
Organ donation	0	3	0.248	0.00
Body donation	3	3	1.000	1.00
Cremation	3	4	1.000	0.75
Burial	0	2	0.480	0.00

Notes: The number of observations included in each comparison is based only on participants with paired valid responses. This explains the variability in the total n across items. "b" indicates the number of participants who changed their response from "Yes" (pre) to "No" (post), whereas "c" denotes number of participants who changed their response from "No" (pre) to "Yes" (post).

Table 3. Logistic regression predicting organ donation post-intervention

Variable	Estimate (β)	Standard error	*z*-value	*p*-value
Intercept	–5.734	4.793	–1.196	0.232
Age	–0.0028	0.00174	–1.634	0.102
Consistency	+1.984	1.225	+1.620	0.105

Note: No statistically significant predictors at P=0.05. However, consistency showed a near-significant trend.

The observed increase in the preference to refuse non-beneficial treatments aligns with previous findings that activate learning strategies in enhancing self-efficacy.[18,25] By engaging students in case discussions and role-plays, the intervention appears to have strengthened their ability to support patient autonomy, a crucial mediator of clinical behavior.

Systematic evaluations further demonstrate that palliative care education not only improves immediate learning outcomes but also fosters long-term retention of competencies. For example, Gupta *et al.*[26] reported that Indian nurses who completed the End-of-Life Care Nursing Education Consortium program maintained significant gains in knowledge, attitudes, and practices up to 18 months post-training. Similarly, Hökkä *et al.*[27] found that pedagogical strategies—particularly interactive methods such as simulations and small-group discussions—were associated with sustained improvements among nursing and medical students. These findings suggest that integrating AHD content longitudinally throughout the nursing curriculum, rather than concentrating it in a single standalone module, could promote more enduring competence.

The slight decline in willingness to donate organs observed in this study (from 94.9% to 92.3%) diverges from previous research that reported stable or increased intent after organ-donation education.[28,29] One possible interpretation is that exposure to values-clarification

exercises, which emphasize both procedural knowledge and moral reasoning,[30] may have fostered deeper ethical reflection. Embedding structured discussions on the ethical complexities of organ donation could therefore be essential to balance factual instruction with personal and cultural exploration.

The module's emphasis on simulation and role-play likely contributed to students' increased awareness of communication needs regarding therapies and pain management. Previous research confirms that experiential learning promotes both practical skill acquisition and empathic engagement.[20] Future curricular initiatives could further enhance these outcomes by integrating high-fidelity simulations and standardized patient encounters to strengthen skills in navigating difficult conversations.

Interprofessional learning is increasingly recognized as a best practice in palliative care education, promoting collaboration and role clarity among future health-care teams.[31] Expanding educational modules to include joint sessions with medical, social work, and allied health students may foster more holistic, patient-centered approaches to end-of-life care.

The module's impact on students' spiritual perspectives also deserves attention. The unanimous shift away from "no religious assistance" reflects the importance of addressing cultural and spiritual diversity in palliative training. Studies have shown that spiritual beliefs and family dynamics strongly influence end-of-life decisions.[13,16] Incorporating multicultural case vignettes and discussions could better prepare students to honor each patient's unique worldview.

The thematic content of the free-text responses provided valuable insight into students' evolving views, particularly regarding dignity, autonomy, and spirituality. Even without statistical significance, these narratives enhance our understanding of how students internalize end-of-life concepts.

To move beyond attitudinal change, it is crucial to assess whether these educational interventions translate into measurable effects on clinical practice. Audit-and-feedback interventions have been shown to improve nursing compliance with documentation practices, with post-intervention rates exceeding 70% in several educational settings.[32-35] Embedding structured audits of AHD-related conversations during clinical placements, coupled with individualized feedback, could provide objective evidence linking student participation in such training to improvements in both the quality and frequency of end-of-life discussions.

Moreover, blended learning approaches—which combine asynchronous e-learning with face-to-face experiential activities—have demonstrated preliminary trends of superior effectiveness compared to traditional methods, with a standardized mean difference of 0.73 in knowledge outcomes.[36] Applying this model to AHD education could increase accessibility, reinforce key concepts through spaced learning, and optimize long-term retention as well as real-world application.

Integrating behavioral audit strategies alongside innovative blended delivery models could therefore enable nursing programs not only to foster attitudinal change but also to achieve measurable improvements in the quality of advance-care conversations, ultimately enhancing patient-centered care at the end of life.

An additional priority is fostering emotional resilience. Palliative care environments expose nurses to profound ethical and emotional challenges, and resilience skills are crucial for sustaining professional well-being. Rushton *et al.*[37] proposed a collaborative model for building moral resilience through structured debriefings and peer support. Embedding such reflective practices into palliative care education, especially after high-intensity simulations, may help students process difficult emotions, mitigate moral distress, and promote long-term professional sustainability.

Taken together, the findings support the strategic incorporation of AHD education within broader palliative care training, emphasizing active, reflective, and interprofessional methodologies to prepare nursing students for the complex realities of end-of-life care.

Although the open-ended responses yielded valuable insights into students' evolving perspectives, the qualitative analysis was intentionally kept descriptive rather than interpretive. Rather than applying a formal coding framework, the analysis focused on identifying the most frequent semantic patterns to capture emerging sentiments across the cohort. This approach allowed for an overview of key conceptual areas such as dignity, autonomy, and spirituality; however, it limited the interpretive depth typically afforded by more structured qualitative methodologies such as reflexive thematic analysis[38,39] or framework analysis.[40,41] In addition, the absence of triangulation and peer debriefing may have constrained the trustworthiness of the findings.[42-44] Future studies should therefore consider incorporating rigorous qualitative designs—including iterative coding, inter-rater reliability checks, and deeper contextual interpretation—to more fully explore the moral reasoning and emotional responses elicited by end-of-life training.

4.1. Limitations and future directions

This study presents several limitations that should be acknowledged. First, no data were collected on the disease

status or medical background of the participants' family members, which could have influenced students' emotional responses and preferences regarding end-of-life decisions. This represents a potential unmeasured confounding factor. While the homogeneity of the cohort (3rd-year nursing students from the same institution) ensured internal consistency, it also limited external validity, particularly in relation to diverse cultural or institutional contexts.

Second, the short-term nature of the assessment—conducted immediately before and after the educational intervention—precludes drawing conclusions regarding the long-term retention of knowledge or sustained changes in attitudes and behavior. Third, although the study included a thematic analysis of open-ended responses, it lacked in-depth qualitative data (e.g., interviews or focus groups) that could have provided richer insights into the students' emotional and ethical reasoning processes.

Furthermore, the study did not collect data on participants' ethnicity or geographic origin. While this reflects the relatively homogeneous composition of the nursing student cohort, it limits the analysis of cultural differences in perceptions of AHDs. The relatively small sample size also limited the statistical power of the study, and the absence of statistically significant findings may be attributable to this limitation. It is also important to note that no a priori power analysis was conducted to determine the minimum required sample size. Another limitation concerns the use of a non-validated instrument. Although grounded in national guidelines, the lack of psychometric evaluation could reduce the interpretability and generalizability of the findings.

Future research should address these limitations by employing multicenter randomized controlled trials with larger sample sizes and more diverse educational settings. Longitudinal follow-up studies are also warranted to assess the durability of attitudinal and behavioral changes over time, particularly during clinical placements or post-graduation. Moreover, incorporating qualitative methodologies, such as narrative interviews or focus groups, could provide deeper insights into the nuanced ways in which educational interventions shape students' moral development and communication strategies in end-of-life care.

4.2. Clinical and educational implications

The findings of this study have significant implications for both nursing education and clinical practice. Integrating AHD content longitudinally into nursing curricula, rather than confining it to isolated modules, is a key educational strategy. This approach supports the reinforcement of ethical principles, communication skills, and reflective competencies throughout the course of study, as supported by Dimoula *et al.*[18] and Muliira *et al.*[25]

The results also highlight the value of active learning strategies, such as case discussions, simulation, and role-play. These pedagogical methods have been shown to deepen understanding and foster empathy, particularly in emotionally complex contexts of end-of-life care.[20,27] By confronting students with complex scenarios, they help them develop confidence and relational competence when addressing sensitive issues such as therapeutic limitation and patient autonomy.

Shifts in students' views on spiritual and post-mortem preferences suggest the importance of providing culturally sensitive education that incorporates spiritual beliefs, personal values, and family dynamics as integral aspects of holistic palliative care. The literature confirms that cultural and spiritual factors profoundly influence end-of-life decisions.[13,16] Educational interventions that use intercultural case vignettes and facilitate structured ethical reflection may better prepare students to support patients from diverse backgrounds with cultural humility.

Another important implication is the need to integrate interprofessional education into palliative care training. Learning environments that bring together students of nursing, medicine, social work, and other allied health professions can enhance communication skills, clarify professional roles, and foster collaboration—key elements for delivering integrated and patient-centered care in multiple clinical settings.[31,45-49]

Finally, the emotional demands of palliative care call for strategies that promote emotional resilience and moral integrity among nursing students. Incorporating structured debriefings, peer support mechanisms, and guided ethical discussion, particularly after emotionally intense learning experiences, can help mitigate moral distress and prepare students for the psychological challenges of end-of-life care. As emphasized by Rushton *et al.*,[37] cultivating moral resilience is essential for sustaining compassionate and ethically grounded nursing practice over time.

5. Conclusion

This study suggests that a targeted oncology palliative care module may enhance nursing students' understanding and attitudes toward AHDs, although the observed changes were not statistically significant. Key outcomes included an increased preference for refusing non-beneficial treatments and heightened awareness of the need for improved communication regarding therapies and pain management. Although a slight decline in willingness to donate organs was observed—potentially reflecting

deeper ethical engagement—overall, the results indicate that structured, active-learning strategies may strengthen students' ability to support patient self-determination.

These results carry meaningful implications for the broader academic and professional nursing community. Educators and curriculum developers should consider integrating AHD content longitudinally within palliative care pathways, using interactive strategies such as simulation, case-based learning, and interprofessional collaboration. Institutions should also invest in training frameworks that address cultural and spiritual diversity, promote ethical reflection, and build emotional resilience among students facing the challenges of end-of-life care.

This study highlights the urgent need for further multicenter, longitudinal research to evaluate the long-term impact of AHD education on clinical practice and to explore how these educational interventions translate into real-world behaviors, such as documentation of patient preferences and the quality of end-of-life communication. By aligning educational innovation with empirical validation, the nursing profession can strengthen its role in safeguarding patient autonomy and dignity across care settings.

Acknowledgments

The authors thank the 3rd-year nursing students of Humanitas University for their participation and thoughtful contributions to the study. The authors also acknowledge the faculty and administrative staff for their logistical support during data collection.

Funding

None.

Conflict of interest

Giovanni Cangelosi and Stefano Mancin are Guest Editors of this special issue. The authors declared that they have no known competing financial interests or personal relationships that could have influenced the work reported in this paper.

Author contributions

Conceptualization: Simone Cosmai, Sarah Scollo, Stefano Mancin, Giovanni Cangelosi, Emanuela Morenghi, Beatrice Mazzoleni,

Formal analysis: Sarah Scollo, Mauro Parozzi, Emanuela Morenghi

Investigation: Sarah Scollo, Giovanni Cangelosi, Emanuela Morenghi, Beatrice Mazzoleni

Methodology: Simone Cosmai, Stefano Mancin, Emanuela Morenghi, Beatrice Mazzoleni

Project administration: Emanuela Morenghi, Beatrice Mazzoleni

Supervision: Sarah Scollo, Giovanni Cangelosi

Writing–original draft: Diego Lopane, Sara Morales Palomares

Writing–review & editing: Alessandra Dacomi, Daniela Cattani, Chiara Provasoli, Sarah Scollo, Mauro Parozzi, Emanuela Morenghi, Beatrice Mazzoleni,

Ethics approval and consent to participate

The study received ethical approval from the Humanitas University Ethics Committee in Milan (Protocol CLI_RIC_14). All participants provided informed consent, and confidentiality was maintained in accordance with the Declaration of Helsinki. Data privacy and participant anonymity were strictly ensured throughout the research process.

Consent for publication

All participants provided written informed consent before enrollment in the study. No identifiable personal data or images were collected or published.

Availability of data

The datasets generated and analyzed during the current study are available from the corresponding author upon reasonable request.

References

1. World Health Organization. *World Report on Ageing and Health*. World Health Organization; 2021. Available from: https://www.who.int/publications/i/item/9789241565042 [Last accessed on 2025 May 01].

2. European Union. *Health at a Glance: Europe 2022*. State of Health in the EU Cycle, OECD. Available from: https://www.oecd.org/en/publications/health-at-a-glance-europe-2022_507433b0-en.html [Last accessed on 2025 May 01].

3. Abarshi E, Echteld M, Van den Block L, *et al.* Use of palliative care services and general practitioner visits at the end of life in The Netherlands and Belgium. *J Pain Symptom Manage*. 2011;41(2):436-448.

   doi: 10.1016/j.jpainsymman.2010.04.016

4. Governo Italiano. *Ministero della Salute. Disposizioni Anticipate di Trattamento - DAT*. Available from: https://www.salute.gov.it/new/it/faq/faq-disposizioni-anticipate-di-trattamento [Last accessed on 2025 May 01].

5. Governo Italiano. *Ministero Della Salute. Banche Dati Delle DAT*. Available from: https://www.salute.gov.it/new/it/tema/disposizioni-anticipate-di-trattamento-dat/banca-dati-delle-dat/?paragraph=4 [Last accessed on 2025 May 01].

6. Teno JM, Sabatino C, Parisier L, Rouse F, Lynn J. The impact

of the patient self-determination act's requirement that states describe law concerning patients' rights. *J Law Med Ethics*. 1993;21(1):102-108.

doi: 10.1111/j.1748-720x.1993.tb01235.x

7. Zweifel P, Felder S, Meiers M. Ageing of population and health care expenditure: A red herring? *Health Econ*. 1999;8(6):485-496.

doi: 10.1002/(sici)1099-1050(199909)8:6<485:aid-hec461>3.0.co;2-4

8. Mercadante S, Lo Cascio A, Casuccio A. Mortality rate and palliative sedation in an acute palliative care unit. *BMJ Support Palliat Care*. 2025;15(4):526-529.

doi: 10.1136/spcare-2023-004669

9. Anquinet L, Rietjens JA, Seale C, Papavasiliou E, Sterckx S, Deliens L. The practice of continuous deep sedation until death in Flanders (Belgium), the Netherlands, and the U.K.: A comparative study. *J Pain Symptom Manage*. 2012;44(1):33-43.

doi: 10.1016/j.jpainsymman. 2011.07.007

10. Presidenza del Consiglio dei Ministri. *Legge 22 dicembre 2017, n. 219, "Norme in Materia di Consenso Informato e di Disposizioni Anticipate di Trattamento"*. Available from: https://www. normattiva.it/uri-res/N2Ls?urn: nir:stato: legge:2017;219 [Last accessed on 2025 May 10].

11. Mignani V, Ingravallo F, Mariani E, Chattat R. Perspectives of older people living in long-term care facilities and of their family members toward advance care planning discussions: A systematic review and thematic synthesis. *Clin Interv Aging*. 2017;12:475-484.

doi: 10.2147/cia.s128937

12. Montanari Vergallo G, Spagnolo AG. Informed consent and advance care directives: Cornerstones and outstanding issues in the newly enacted Italian legislation. *Linacre Q*. 2019;86(2-3):188-197.

doi: 10.1177/0024363919837863

13. Periyakoil VS, Stevens M, Kraemer H. Multicultural long-term care nurses' perceptions of factors influencing patient dignity at the end of life. *J Am Geriatr Soc*. 2013;61(3):440-446.

doi: 10.1111/jgs.12145

14. Brännström M, Boman K. Effects of person-centred and integrated chronic heart failure and palliative home care. PREFER: A randomized controlled study. *Eur J Heart Fail*. 2014;16(10):1142-1151.

doi: 10.1002/ejhf.151

15. Cogo SB, Lunardi VL, Quintana AM, Girardon-Perlini NM, Silveira RS. Challenges to implementation of advance directives of will in hospital practice. *Rev Bras Enferm*. 2016;69(6):1031-1038.

doi: 10.1590/0034-7167-2016-0085

16. Poveda-Moral S, De la Casa PJM, Sánchez-Valero P, Roldán-Valero A. Association between knowledge and attitudes towards advance directives in emergency services. *BMC Med Ethics*. 2021;22(1):75.

doi: 10.1186/s12910-021-00646-y

17. Cantrell ML, Meyer SL, Mosack V. Effects of simulation on nursing student stress: An integrative review. *J Nurs Educ*. 2017;56(3):139-144.

doi: 10.3928/01484834-20170222-04

18. Dimoula M, Kotronoulas G, Katsaragakis S, Christou M, Siskou O. Undergraduate nursing students' knowledge about palliative care and attitudes towards end-of-life care: A three-cohort, cross-sectional survey. *Nurse Educ Today*. 2019;74:7-14.

doi: 10.1016/j.nedt.2018.11.025

19. Korfage IJ, Rietjens JA, Overbeek A, Jabbarian LJ, Billekens P, Van der Heide A. Preferences of the dutch general public for a good death and associations with attitudes towards end-of-life decision-making. *Palliat Med*. 2010;24(3):242-250.

doi: 10.1177/0269216306070241

20. Novaes LMS, Paiva EMC, O'Mahony A, Garcia ACM. Roleplay as an educational strategy in palliative care: A systematic integrative review. *Am J Hosp Palliat Care*. 2022;39(5):570-580.

doi: 10.1177/10499091211036703

21. Rosa WE, Ferrell BR, Mazanec P. Global integration of palliative nursing education to improve health crisis preparedness. *J Contin Educ Nurs*. 2021;52(3):130-135.

doi: 10.3928/00220124-20210216-07

22. Vandenbroucke JP, Von Elm E, Altman DG, *et al*. Strengthening the reporting of observational studies in epidemiology (STROBE): Explanation and elaboration. *PLoS Med*. 2007;4(10):e297.

doi: 10.1371/journal.pmed.0040297

23. World Medical Association. World medical association declaration of helsinki. Ethical principles for medical research involving human subjects. *Nurs Ethics*. 2002;9(1):105-109.

doi: 10.1191/0969733002ne486xx

24. Ministero Della Salute. *Disposizioni Anticipate di Trattamento - DAT*. Available from: https://dat.salute.gov.it/portale-dat [Last accessed on 2025 May 25].

25. Muliira JK, Lazarus ER, Mirafuentes EC. A countrywide assessment of Omani undergraduate nursing students' palliative care knowledge and attitudes towards end-of-life care. *J Cancer Educ*. 2023;38(3):781-788.

doi: 10.1007/s13187-022-02184-6

26. Gupta M, Pruthi G, Singh K. Long-term impact of the end-

of-life care nursing education consortium on knowledge, attitudes, and practice (KAP) of Indian nurses working in non-palliative care settings: A KAP-GAP analysis. *Am J Hosp Palliat Care*. 2024;41(12):1380-1390.

doi: 10.1177/10499091231225739

27. Hökkä M, Rajala M, Kaakinen P, Rissanen C, Holopainen A. The effect of teaching methods in palliative care education for undergraduate nursing and medical students: A systematic review. *Int J Palliat Nurs*. 2022;28(6):245-253.

doi: 10.12968/ijpn.2022.28.6.245

28. Fontana F, Massari M, Giovannini L, Alfano G, Cappelli G. Knowledge and attitudes toward organ donation in health care undergraduate students in Italy. *Transplant Proc*. 2017;49(9):1982-1987.

doi: 10.1016/j.transproceed.2017.09.029

29. Kurz JM. Impact of organ donation education on US undergraduate nursing students. *Prog Transplant*. 2014;24(2):211-217.

doi: 10.7182/pit2014624

30. Mercadante S, Bellaviam G, Cascio AL, *et al.* The use of complementary alternative medicines in advanced cancer patients followed at home. *Support Care Cancer*. 2022;30(3):2003-2008.

doi: 10.1007/s00520-021-06580-4

31. Kirkpatrick AJ, Donesky D, Kitko LA. A systematic review of interprofessional palliative care education programs. *J Pain Symptom Manage*. 2023;65(5):e439-e466.

doi: 10.1016/jjpainsymman.2023.01.022

32. Mancin S, Cangelosi G, Sguanci M, *et al.* Integrating active learning methodologies into clinical nutrition education for nursing students: A quasi-experimental study. *Nurs Rep*. 2025;15(3):77.

doi: 10.3390/nursrep15030077

33. Lomuscio S, Capogna E, Sironi S, *et al.* Debriefing methodologies in nursing simulation: An exploratory study of the Italian settings. *Nurs Rep*. 2024;15(1):7.

doi: 10.3390/nursrep15010007

34. Bunting J, De Klerk M. Strategies to improve compliance with clinical nursing documentation guidelines in the acute hospital setting: A systematic review and analysis. *SAGE Open Nurs*. 2022;8:23779608221075165.

doi: 10.1177/23779608221075165

35. Assolari F, Mancin S, Lopane D, *et al.* Advanced practice nursing in surgery: A scoping review of roles, responsibilities, and educational programs. *Int Nurs Rev*. 2025;72(3):e13045.

doi: 10.1111/inr.13045

36. Cook DA, Levinson AJ, Garside S, Dupras DM, Erwin PJ, Montori VM. Internet-based learning in the health professions: A meta-analysis. *JAMA*. 2008;300(10):1181-1196.

doi: 10.1001/jama.300.10.1181

37. Rushton CH, Schoonover-Shoffner K, Kennedy MS. A collaborative state of the science initiative: Transforming moral distress into moral resilience in nursing. *Am J Nurs*. 2017;117(2 Suppl 1):S2-S6.

doi: 10.1097/01.naj.0000512203.08844.1d

38. Mercadante S, Grassi Y, Cascio A, Restivo V, Casuccio A. Characteristics of untreated cancer patients admitted to an acute supportive/palliative care unit. *J Pain Symptom Manage*. 2023;65(6):e677-e682.

doi: 10.1016/j.jpainsymman.2023.01.010

39. Connelly DM, Guitar NA, Atkinson AN, Janssen SM. Learnings from nursing bridging education programs: A scoping review. *Nurse Educ Pract*. 2023;73:103833.

doi: 10.1016/j.nepr.2023.103833

40. Gale NK, Heath G, Cameron E, Rashid S, Redwood S. Using the framework method for the analysis of qualitative data in multi-disciplinary health research. *BMC Med Res Methodol*. 2013;13:117.

doi: 10.1186/1471-2288-13-117

41. Yoong SQ, Wang W, Seah ACW, *et al.* Nursing students' experiences with patient death and palliative and end-of-life care: A systematic review and meta-synthesis. *Nurse Educ Pract*. 2023;69:103625.

doi: 10.1016/j.nepr.2023.103625

42. Lorelli SN, Jill MN, White DE, Moules NJ. Thematic analysis: Striving to meet the trustworthiness criteria. *Int J Qual Methods*. 2017;16:1-13.

doi: 10.1177/1609406917733847

43. Yang A, Fernando S, Tighe J, O'Halloran M, Morphet J, Kumar A. Impact of an interprofessional surgical skills workshop on undergraduate medical and nursing student interest in a career in surgery: A thematic analysis. *J Surg Educ*. 2021;78(3):905-913.

doi: 10.1016/j.jsurg.2020.09.014

44. Lavery J, Henshall C. First year pre-registration nursing student perceptions of community nursing roles: A thematic analysis. *Br J Community Nurs*. 2022;27(4):172-179.

doi: 10.12968/bjcn.2022.27.4.172

45. Eddy K, Jordan Z, Stephenson M. Health professionals' experience of teamwork education in acute hospital settings: A systematic review of qualitative literature. *JBI Database Syst Rev Implement Rep*. 2016;14(4):96-137.

doi: 10.11124/jbisrir-2016-1843

46. Tarot A, Pithon M, Ridley A, *et al.* Experiencing and enduring patient distress: The distress of palliative care patients and its emotional impact on physicians in training.

BMC Med Educ. 2024;24(1):696.

doi: 10.1186/s12909-024-05668-9

47. Andreoli D, Morales Palomares S, Mancin S, *et al.* Exploring the competencies of nephrology nurses: A comprehensive scoping review. *Int Nurs Rev*. 2025;72(1):e13085.

doi: 10.1111/inr.13085

48. Mancin S, Bragaglia F, Andreoli D, *et al.* Nursing care and postgraduate education of nephrology and dialysis nurses in Italy. *G Ital Nefrol*. 2024;41(5):2024-vol5.

doi: 10.69097/41-05-2024-12

49. Usman FM, Jalal A, Bansal M, *et al.* The role of simulation in oncology nursing: A systematic review. *Nurse Educ Pract*. 2025;87:104466.

doi: 10.1016/j.nepr.2025.104466

ACCSCIENCE PUBLISHING

Eurasian Journal of Medicine and Oncology

ORIGINAL RESEARCH ARTICLE

Enhanced expression of metastasis-associated genes in colorectal cancer

Adeodatus Yuda Handaya[1,2]*, Hendra Susanto[3], and Moch Sholeh[4]

[1]Department of Surgery, Faculty of Medicine, Universitas Gadjah Mada, Yogyakarta, Indonesia

[2]Digestive Surgery Division, Sardjito Hospital, Yogyakarta, Indonesia

[3]Department of Biology, Faculty of Mathematics and Natural Sciences, Universitas Negeri Malang, Malang, East Java, Indonesia

[4]Department of Biomedical Sciences, Faculty of Medicine, Universitas Brawijaya, Malang, Indonesia

Abstract

Introduction: Globally, colorectal cancer (CRC) continues to be a major cause of cancer-related morbidity and death, with metastasis—particularly to the liver—significantly worsening patient outcomes.

Objective: The aim of this study was to investigate the expression of key epithelial-mesenchymal transition (EMT) transcription factors (Snail family transcriptional repressor 1 [SNAI1], zinc finger e-box binding homeobox 1 [ZEB1], Slug, Twist, and metastasis-associated protein 3 [MTA3]) and the pro-inflammatory cytokine tumor necrosis factor-alpha (TNF-α) in CRC cases with and without metastasis to the liver.

Methods: A total of 41 CRC patients (20 non-metastatic, 21 with liver metastasis) from Dr. Sardjito General Hospital, Yogyakarta, were examined utilizing reverse transcription quantitative polymerase chain reaction of the adjacent normal tissues and the tumors.

Results: SNAI1, ZEB1, Slug, Twist, and TNF-α were significantly upregulated in metastatic CRC, while MTA3 was downregulated. Expression of these markers correlated with body mass index, liver enzymes (aspartate aminotransferase), and cancer stage.

Conclusion: These findings highlight the central role of EMT-related transcription factors and inflammatory signaling in CRC metastasis and suggest that targeting these pathways could offer novel therapeutic strategies for metastatic CRC.

Keywords: Colorectal cancer; Liver metastasis; Body weight loss; Metastasis marker

***Corresponding author:**
Adeodatus Yuda Handaya
(yudahandaya@ugm.ac.id)

Citation: Handaya AY, Susanto H, Sholeh M. Enhanced expression of metastasis-associated genes in colorectal cancer. *Eurasian J Med Oncol*. 2025;9(3):250-260. doi: 10.36922/EJMO025210202

Received: May 19, 2025

Revised: June 23, 2025

Accepted: July 23, 2025

Published online: August 18, 2025

Copyright: © 2025 Author(s). This is an Open-Access article distributed under the terms of the Creative Commons Attribution License, permitting distribution, and reproduction in any medium, provided the original work is properly cited.

Publisher's Note: AccScience Publishing remains neutral with regard to jurisdictional claims in published maps and institutional affiliations.

1. Introduction

Colorectal cancer (CRC), the third most common malignancy and the second leading cause of cancer-related deaths worldwide, is one of the most common cancers.[1] Incidence rates vary widely across different regions, with a higher prevalence observed in developed countries compared to developing countries. The etiology of CRC is multifactorial, involving a combination of genetic predispositions, lifestyle factors such as diet and physical inactivity, and environmental influences. Notably, polymorphisms in several genes have been studied for their potential association with CRC risk, although findings regarding their significance have been mixed.[2-5] Pathologically, CRC typically

arises from adenomatous polyps through the adenoma-carcinoma sequence (ACS), characterized by genetic mutations that lead to uncontrolled cell growth.[6,7] This development shows the importance of early detection and screening strategies in reducing CRC-related mortality.[7-9]

In addition to genetic and epigenetic alterations, metabolic reprogramming has emerged as a hallmark of CRC progression. Cancer cells frequently undergo metabolic shifts to meet the increased energy demands and biosynthetic needs associated with rapid proliferation and metastasis.[10] For instance, enhanced glycolysis, known as the Warburg effect, supports tumor growth even in the presence of oxygen.[10] Moreover, alterations in lipid metabolism and amino acid utilization have been implicated in CRC aggressiveness. These metabolic adaptations not only sustain tumor cell survival but also modulate the immune microenvironment, influencing the recruitment and function of immune cells such as tumor-associated macrophages and myeloid-derived suppressor cells.[11] Therapeutic strategies targeting metabolic vulnerabilities of CRC cells hold promise for disrupting tumor progression and overcoming resistance to existing treatments.

Chronic conditions and external stressors can significantly influence the metastasis of CRC, often leading to considerable morbidity and mortality. The metastatic process is influenced by various factors, including chronic inflammation, which can be exacerbated by conditions such as chronic hepatitis B (CHB) and psychological stress.[12,13] Paradoxically, CHB may also protect against colorectal liver metastasis due to its sclerosing effect on the liver and certain immune-mediated mechanisms.[14] Psychological stress and a perturbed gut microbiome can promote CRC growth and metastasis.[15] Single-cell RNA sequencing has revealed that chronic stress can induce an immunosuppressive environment that encourages CRC metastasis.[16] Studies have shown that chronic inflammation can activate oncogenic pathways, promoting tumor growth and metastasis.[17] Furthermore, the tumor microenvironment plays an important role in the progression of CRC, with immune cells like tumor-associated macrophages recruited to support metastatic spread.[18] Research indicates that chronic stress can alter the gut microbiome, further enhancing the metastatic potential of CRC.[19] Understanding these mechanisms is vital for developing targeted therapies, such as inhibition of related genes in CRC, aimed at preventing or reducing metastasis in patients with chronic CRC.

CRC progression and metastasis are governed by a complex interplay of genetic, epigenetic, and microenvironmental factors, each contributing to the disease's heterogeneity and clinical outcomes.[7] Beyond the classical ACS and the role of epithelial-mesenchymal transition (EMT) regulators, recent research has illuminated several additional mechanisms that underpin CRC advancement and metastatic spread.[7] One critical aspect is the dysregulation of multiple cellular signaling pathways, which orchestrate the malignant transformation and dissemination of CRC cells. Notably, the Wnt/β-catenin pathway is frequently activated in CRC, driving uncontrolled proliferation and survival of tumor cells.[20] Mutations in key genes can disrupt cellular homeostasis, thereby facilitating the accumulation of genetic changes that drive tumorigenesis. Snail family transcriptional repressor 1 (SNAI1), zinc finger e-box binding homeobox 1 (ZEB1), Slug, Twist, metastasis-associated protein 3 (MTA3), as transcription factors, and tumor necrosis factor-alpha (TNF-α), a pro-inflammatory cytokine signaling are also shown to be involved in CRC progression and metastasis.[21-23] In particular, SNAI1, Slug, and MTA3 are pivotal regulators of EMT, a process that enables cancer cells to acquire migratory properties. They are also members of the metastasis-associated protein family.[24,25] TNF-α has been shown to induce EMT in CRC cells by stabilizing SNAI1 through the AKT/GSK-3β signaling pathway.[26] This pathway enhances SNAI1's nuclear localization and promotes the switch from E-cadherin to N-cadherin expression, a hallmark of EMT.[21] Meanwhile, ZEB1 and Twist also contribute to this process by responding to various microenvironmental signals and facilitating the transition of epithelial cells into mesenchymal-like cells.[27] The interplay between these factors not only drives tumor invasion but also correlates with unfavorable clinical outcomes in CRC patients, underscoring their potential as targets for therapy in managing cancer metastasis.

Clinically, advancements in molecular profiling have enabled the stratification of CRC patients based on genetic and epigenetic signatures, allowing for more personalized therapeutic approaches. Biomarkers such as SNAI1, ZEB1, Slug, Twist, MTA3, and TNF-α are increasingly used to guide treatment decisions, particularly regarding the selection of targeted agents and immunotherapies. Immune checkpoint inhibitors have shown remarkable efficacy in a subset of CRC patients with high expression, highlighting the potential of immunotherapeutic approaches in against this disease.[28,29] However, resistance mechanisms and the limited response in tumor microenvironment remain challenges that necessitate further investigation. The interplay of these pathways not only promotes tumor growth but also provides potential therapeutic targets for intervention.

In summary, the progression and metastasis of CRC are driven by a complex interplay of genetic mutations,

epigenetic alterations, and dynamic interactions within the tumor microenvironment. Understanding these mechanisms is essential for developing effective diagnostic, prognostic, and therapeutic strategies. Ongoing research into the molecular and cellular mechanisms underlying CRC will continue to inform the development of targeted interventions, aiming to improve both survival and quality of life for those affected by this formidable disease.

2. Materials and methods

2.1. Respondents

This descriptive clinical study used 41 patients as respondents during the period 2021–2022 at Dr. Sardjito General Hospital, Yogyakarta. This study obtained ethical approval through the Institutional Review Board (IRB), Faculty of Medicine, Universitas Gadjah Mada, Indonesia (ethics number: KE/FK/0938/EC/2021). The respondents consisted of 20 CRC patients without metastasis and 21 CRC patients with liver metastasis. Then, each group was also compared with adjacent normal tissue. The study's inclusion criteria encompassed patients diagnosed with cancer, whether metastatic or non-metastatic, who had completed the diagnostic phase, had been declared as surgery candidates, and possessed comprehensive medical records. Patients with incomplete data, lung metastasis, or refused to participate in the study were excluded from the study. Confirmation and classification of samples were based on histopathology data and computed tomography scans assessed by medical personnel at the hospital. Basic patient information was extracted from the patient's medical records. Primary tumor samples were stored in the Biobank of the Faculty of Medicine, Public Health and Nursing, Universitas Gadjah Mada, and sent to the Molecular Biology Laboratory, Universitas Negeri Malang, for further analysis.

2.2. Marker expression analysis

The mRNA expression levels of SNAI1, ZEB1, Slug, Twist, MTA3, and TNF-α were measured by reverse transcription quantitative polymerase chain reaction (RT-qPCR). Total RNA was extracted from fresh frozen tissue samples (100 mg) using the TRISURE™/Qiazol Total RNA Isolation Kit (Bio line, UK) and stored at −80°C for subsequent analysis. RNA purity was evaluated by determining the A260/280 ratio (acceptable range: 1.8–2.0) using a Nanodrop spectrophotometer, and residual genomic DNA (gDNA) was removed by treatment with RNAse-free DNase enzyme (Invitrogen, US).

Complementary DNA (cDNA) synthesis was performed using the High-Capacity ReverTra Ace® qPCR RT Master Mix with gDNA Remover (Toyobo, Japan) following the manufacturer's protocol, using 2 μg of total RNA. The reaction mixture was processed in a PCR thermocycler (Applied Biosystems, US) with the following steps: denaturation at 65°C for 5 min, gDNA elimination at 37°C for 5 min, followed by cDNA synthesis at 37°C for 15 min, 50°C for 5 min, and 98°C for 5 min, then held at 4°C. The resulting cDNA was diluted to 0.5 μg/μL to be used as a template for subsequent RT-qPCR analysis.

PCR samples were prepared using the SensiFAST SYBR Green No-ROX kit (Bioline, UK) and analyszed on an Analytic Jena qTower instrument. Relative quantification of PCR products was performed using the $2^{-\Delta\Delta CT}$ method. Primers from Integrated DNA Technologies through Genetika Science Indonesia, Singapore, were used as follows: TNF-α, forward 5'- CCTGCCCCAATCCCTTTATT -3' and reverse 5'- CCCTAAGCCCCCAATTCTCT -3'; SNAI1, forward 5'- ACTGCAACAAGGAATACCTCAG -3' and reverse 5'- GCACTGGTACTTCTTGACATCTG -3'; ZEB1, forward 5'- AGCAGTGAAAGAGAAGGGAATGC -3' and reverse 5'- GGTCCTCTTCAGGTGCCTCAG -3'; Slug, forward 5'- ATCTGCGGCAAGGCGTTTTCCA -3' and reverse 5'- GAGCCCTCAGATTTGACCTGTC -3'; Twist, forward 5'- GCAGGACGTGTCCAGCTC -3' and reverse 5'- CTGGCTCTTCCTCGCTGTT -3'; MTA3, forward 5'- TATCAGGGGAAAGTGCAGTGTTG -3' and reverse 5'- AACAGCATTTCTGGAATGTCTGC -3'; and GAPDH, forward 5'- TGCACCACCAACTGCTTAGC -3' and reverse 5'- GGCATGGACTGTGGTCATGA -3'. The mRNA expression levels of target genes were normalized to GAPDH expression.

2.3. Statistical analysis

Data distribution was evaluated using the Kolmogorov-Smirnov normality test. Demographic features were analyzed using ANOVA test. Comparisons between groups were conducted using the independent samples t-test. Associations among variables such as body mass index (BMI), carcinoembryonic antigen (CEA), alanine aminotransferase (ALT), and aspartate aminotransferase (AST) were assessed using Pearson correlation and univariate linear regression analysis, while the staging parameters (T, N, and M) were analyzed using ordinal regression. A significance level of 5% was applied, and data are presented as mean ± standard error of the mean.

3. Results

The interplay among SNAI1, ZEB1, Slug, Twist, MTA3, and TNF-α in colon cancer involves a complex regulatory network driving EMT, metastasis, and therapeutic resistance. The results of this study provide compelling evidence for the intricate molecular interplay underlying EMT and metastatic progression in colon cancer. The

significant upregulation of SNAI1, Slug, ZEB1, Twist, and TNF-α in the liver metastasis group, as compared to both non-liver metastasis patients and adjacent normal tissue, underscores the central roles of these transcription factors and inflammatory mediators in facilitating metastatic dissemination. This pattern of expression aligns with the well-established understanding that EMT is a pivotal driver in cancer metastasis, endowing tumor cells with enhanced migratory and invasive properties. The concurrent downregulation of MTA3 in the liver metastasis group is particularly noteworthy, as it suggests a loss of EMT suppression, further promoting a pro-metastatic phenotype. The following presents a structured framework based on mechanistic insights supported by research evidence:

This framework (Table 1) highlights the central roles of SNAI1, Slug, ZEB1, and Twist in EMT, supported by stromal interactions and pro-inflammatory mediators such as TNF-α, whereas MTA3 acts as a suppressive regulator. Targeting these molecular nodes may disrupt metastatic progression in colon cancer.

Three patients in the non-liver metastasis group had a history of diabetes mellitus (DM), four had hypertension, 19 followed a high-protein diet, and two had cardiovascular disease (CVD), according to the patients' medical records. In the liver metastasis group, two individuals had a history of DM, one had hyperlipidemia, two had hypertension, six had a history of smoking, fifteen followed a high-protein diet, and two had CVD. None of the participants had a history of hepatitis or alcohol consumption. There were no significant differences ($p \geq 0.05$) between the two groups in terms of hemoglobin, hematocrit, white blood cells, red blood cells, platelets, fasting blood glucose, albumin, blood urea nitrogen, creatinine, systolic blood pressure, diastolic blood pressure, and age. However, individuals with liver metastases from CRC exhibited higher levels of circulating fasting blood glucose, albumin, platelets, and blood urea nitrogen. Notably, CEA, ALT, AST, and BMI showed significant differences between the groups ($p<0.05$) as detailed in Table 2.

It was observed that SNAI1, Slug, ZEB1, Twist, and TNF-α were most highly expressed in the liver metastasis group, whereas MTA3 was markedly decreased in this group (Figure 1). The expression levels were significantly different when compared to both the non-liver metastasis group and adjacent normal tissue. Further analysis using univariate linear regression revealed that SNAI1, ZEB1, Slug, Twist, and TNF-α markers were significantly correlated with BMI ($p \leq 0.05$), while AST was correlated with SNAI1, Slug, Twist, and TNF-α only. Notably, MTA3 showed no correlation with any of the four basic clinical characteristics (Table 3). Furthermore, each marker's association with cancer staging (T, N, and M) was specifically assessed. As presented in Table 4, all markers were found to significantly affect cancer stage. It is worth noting that MTA3 exhibited a negative Wald value, which indicates an inverse relationship with cancer staging.

The correlation between the expression of EMT markers (SNAI1, Slug, ZEB1, Twist, and TNF-α) and BMI highlights a potential link between metabolic status and the molecular mechanisms underlying metastasis (Table 3). Obesity and metabolic dysregulation have been increasingly recognized as risk factors for cancer progression, and our findings provide molecular evidence supporting this association. Elevated BMI may create a microenvironment conducive to EMT and metastasis, possibly through mechanisms such

Table 1. Framework summary of marker correlations

Marker	Role in colon cancer	Interaction partners	Clinical relevance
SNAI1	Drives EMT, stemness, and stromal remodeling; upregulated by tumor ECM	TWIST1, PDGF-BB, and TGF-β1[30,31]	Poor prognosis, metastasis[31,32]
Twist	Enhances EMT and lymph node metastasis; synergizes with SNAI1	SNAI1, ALDH1[33]	Reduced survival[33]
Slug	Supports EMT and stemness; context-dependent expression	SNAI1[34]	Clinical aggressiveness of tumors and poor patient survival[34,35]
ZEB1	Sustains mesenchymal state; potential downstream effector of SNAI1/TWIST1	SNAI1, TWIST1[36]	Promotes the proliferation and invasion of cancer[37]
MTA3	Represses SNAI1; loss of MTA3 promotes	SNAI1[31]	Metastasis suppression[31]
TNF-α	Pro-inflammatory cytokine inducing EMT via NF-κB; modulates stromal-tumor crosstalk	SNAI1, TWIST1[38,39]	Linked to advanced disease[40]

Abbreviations: ALDH1: Aldehyde Dehydrogenase 1, ECM: Extracellular matrix; EMT: Epithelial-mesenchymal transition; MTA3: Metastasis-associated protein 3; NF- κB: Nuclear factor kappa B; PDGF-BB; Platelet-derived growth factor subunit B; SNAI1: Snail family transcriptional repressor 1; TGF-β1: Transforming growth factor-beta 1; TNF-α: Tumor necrosis factor-alpha; ZEB1: Zinc finger e-box binding homeobox 1.

Table 2. Basic demographic and clinical features of the study groups

Parameters	Groups	
	Non-metastasis (*n*=20)	Metastasis (*n*=21)
Age (years)	54.50±3.12	57.08±2.99
BMI (kg/m^2)	23.41±1.19	18.92±0.49*
ALT (U/L)	11.65±1.74	28.25±5.12*
AST (U/L)	21.35±4.51	47.92±10.71*
CEA (µg/L)	14.36±5.51	307.53±1.27*
Stage (average from T, N, and M)	4	2
Tumor	3	5
Node	1	2
Metastasis	0	2
DM		
Yes	3	2
No	17	19
Hyperlipidemia		
Yes	0	1
No	20	20
Hypertension		
Yes	4	2
No	16	19
Smoking		
Yes	0	6
No	20	15
Alcoholism		
Yes	0	0
No	20	21
High protein diet		
Yes	19	15
No	1	6
Hepatitis		
Yes	0	0
No	20	21
CVD		
Yes	2	2
No	18	19

Notes: Independent sample t-test was used to compare differences among groups. Data are presented as mean ± standard error of the mean. *Significant value of each parameter compared to the non-metastasis group by ANOVA Test ($p \leq 0.05$). The value or grading of the TNM stage is divided into three components of colon cancer, namely, T (Tumor), N (Node), and M (Metastasis). T consists of levels 0–5, N: levels 0–6, and M: levels 0–4. This grading is then used to determine the stages of cancer, including low, well, moderate, and poor differentiation.[41]
Abbreviations: ALT: Alanine aminotransferase; AST: Aspartate aminotransferase; BMI: Body mass index; CEA: Carcinoembryonic antigen; CVD: Cardiovascular disease; DM: Diabetes mellitus.

Table 3. Univariate linear regression analysis

Response	Predictor	Estimate (B)	*p*-value
BMI	SNAI1	−3.156	0.012*
CEA	SNAI1	81.303	0.501
ALT	SNAI1	10.025	0.065
AST	SNAI1	11.982	0.046*
BMI	ZEB1	−5.501	0.029*
CEA	ZEB1	70.112	0.524
ALT	ZEB1	11.383	0.070
AST	ZEB1	9.117	0.055
BMI	Slug	−6.813	0.042*
CEA	Slug	56.118	0.174
ALT	Slug	5.293	0.091
AST	Slug	7.231	0.042*
BMI	Twist	−4.532	0.021*
CEA	Twist	61.002	0.407
ALT	Twist	11.015	0.060
AST	Twist	12.740	0.048*
BMI	MTA3	1.241	0.104
CEA	MTA3	10.203	0.075
ALT	MTA3	5.746	0.081
AST	MTA3	15.801	0.159
BMI	TNF-α	−9.725	0.033*
CEA	TNF-α	51.118	0.235
ALT	TNF-α	18.964	0.136
AST	TNF-α	11.507	0.046*

Note: *Significant with $p \leq 0.05$.
Abbreviations: ALT: Alanine aminotransferase; AST: Aspartate aminotransferase; BMI: Body mass index; CEA: Carcinoembryonic antigen; MTA3: Metastasis-associated protein 3; SNAI1: Snail family transcriptional repressor 1; TNF-α: Tumor necrosis factor-alpha; ZEB1: Zinc finger e-box binding homeobox 1.

as chronic low-grade inflammation or altered adipokine signaling, which could upregulate the expression of EMT-promoting genes. The specific association of AST with SNAI1, Slug, Twist, and TNF-α further suggest the role of liver function and systemic metabolic changes are intertwined with the molecular events that drive metastatic colonization of the liver.

In addition, the observed differences in clinical and biochemical parameters between the non-liver metastasis and liver metastasis groups further contextualize the molecular findings. The significant elevations in CEA, ALT, AST, and BMI among patients with liver metastasis reflect both increased tumor burden and the systemic impact of metastatic disease. Taken together with the gene

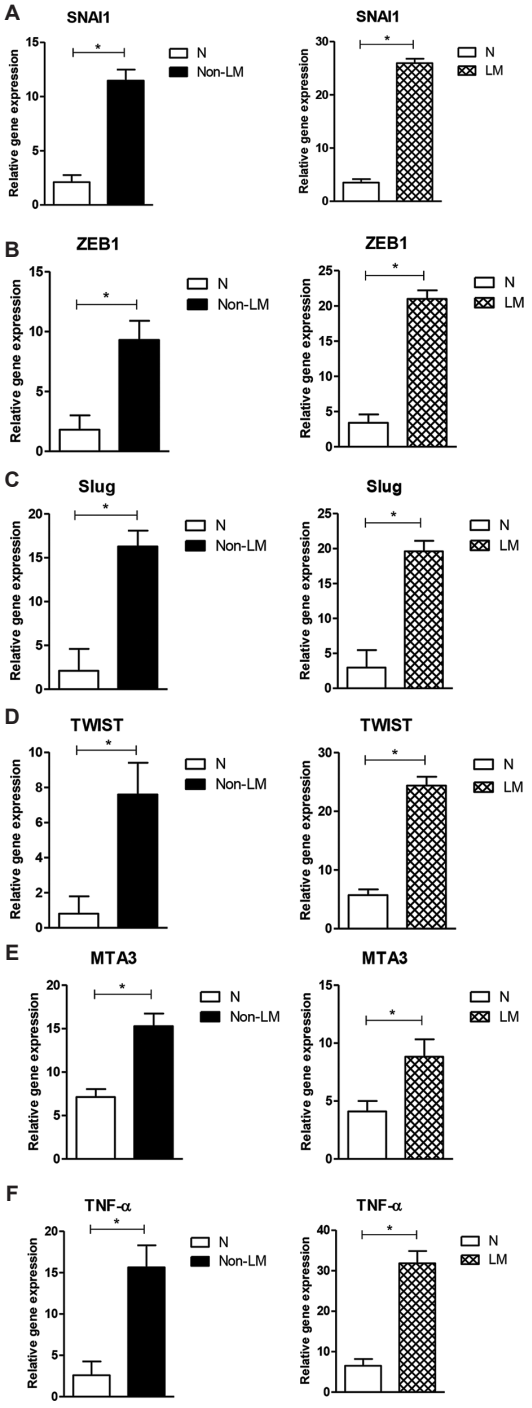


Figure 1. (A-F) Relative gene expression of markers in CRC patients with non-liver and liver metastasis, measured by RT-qPCR and compared with adjacent normal tissue

Note: *Significant difference between groups by independent sample t-test ($p \leq 0.05$).

Abbreviations: CRC: Colorectal cancer; LM: Liver metastasis; MTA3: Metastasis-associated protein 3; N: Adjacent normal tissue; Non-LM:Non-livermetastasis;SNAI1:Snailfamilytranscriptionalrepressor1; TNF-α: Tumor necrosis factor-alpha; ZEB1: Zinc finger e-box binding homeobox 1.

Table 4. Ordinal regression analysis

Response	Predictor	Wald value	*p*-value
Stage (TNM)	SNAI1	3.006	0.022*
Stage (TNM)	ZEB1	1.725	0.031*
Stage (TNM)	Slug	2.018	0.016*
Stage (TNM)	Twist	1.922	0.028*
Stage (TNM)	MTA3	−3.443	0.035*
Stage (TNM)	TNF-α	5.813	0.006*

Note: * Significant with $p \leq 0.05$.

Abbreviations: M: Metastasis; MTA3: Metastasis-associated protein 3; N: Node; SNAI1: Snail family transcriptional repressor 1; T: Tumor; TNF-α: Tumor necrosis factor-alpha; ZEB1: Zinc finger e-box binding homeobox 1.

expression profiles, these clinical markers may serve as a potential composite biomarker panel for risk stratification and early detection of metastatic spread.

The clinical significance of these molecular findings is reinforced by the ordinal regression analysis, which demonstrated that all examined markers significantly influence cancer stage (T, N, M). The negative Wald value for MTA3 is particularly intriguing, indicating that higher MTA3 expression is associated with a lower cancer stage and, conversely, that its downregulation is linked to more advanced disease. This inverse relationship supports the hypothesis that MTA3 acts as a tumor suppressor by antagonizing EMT and maintaining epithelial integrity. Therapeutically, restoring MTA3 function or mimicking its activity could represent a novel strategy to impede metastatic progression in colon cancer.

4. Discussion

Beyond the molecular insights, the clinical translation of these findings holds significant promise for improving patient outcomes in CRC. The identification of SNAI1 as a central regulator of EMT and chemoresistance suggests that SNAI1-targeted therapies could be developed to overcome treatment resistance, a major challenge in advanced CRC. Small molecule inhibitors or RNA interference strategies aimed at reducing SNAI1 expression, or disrupting its stabilization pathways such as the AKT/GSK-3β axis, may sensitize tumors to conventional chemotherapeutics.[7] Furthermore, the interplay between SNAI1 and inflammatory cytokines such as TNF-α highlights the potential for combinatorial therapies that simultaneously target both EMT and inflammation. For instance, anti-TNF-α agents, already in clinical use for inflammatory bowel disease, could be repurposed or combined with EMT inhibitors to suppress tumor progression and metastasis in CRC patients with elevated TNF-α signaling.

The roles of SNAI1, ZEB1, Slug, Twist, and TNF-α in colon cancer progression reveal complex interactions between EMT-related transcription factors and inflammatory signaling, as shown in recent studies. Overexpression of SNAI1 induces partial or complete EMT in colon cancer cells, correlating with chemoresistance, reduced apoptosis, and increased tumor growth.[42,43] Mechanistically, TNF-α stabilizes SNAI1 protein through the AKT/GSK-3β signaling, bypassing transcriptional upregulation.[44] In addition, phosphorylation of sirtuin 1 at Ser27 further stabilizes SNAI1, enhancing its deacetylase activity and promoting interleukin-6 and interleukin-8-mediated tumor progression.[45] These findings position SNAI1 as a critical node in EMT regulation, with its expression levels dictating phenotypic outcomes.[46] As shown in Figure 1, SNAI1 expression is highest in the liver metastasis group. This indicates the role of SNAI1 as a central driver of EMT and chemoresistance.

The context-dependent roles of ZEB1 and Slug in colon cancer, as revealed in this study, also underscore the necessity for patient stratification in future therapeutic interventions. Since ZEB1 and Slug expression is elevated in liver metastatic lesions, their detection could serve as biomarkers of aggressive disease and guide the application of more intensive or targeted therapeutic regimens.[47] Liquid biopsy approaches, such as the measurement of circulating tumor cells or cell-free nucleic acids expressing these EMT-transcription factors (EMT-TFs), may provide non-invasive means for real-time disease monitoring and early detection of metastasis. Although ZEB1 and Slug contribute to EMT in other cancers, their involvements in colon cancer appear context-dependent.[48,49] For instance, TNF-α induces Slug in papillary thyroid cancer, while in colon cancer, SNAI1 predominates in regulating EMT. Some herbal or natural bioactive compounds have been shown to suppress SNAI1 through NF-κB inhibition, highlighting SNAI1's primacy over other EMT-TFs in therapeutic targeting.[50,51] As in Figure 1, it is clear that ZEB1 and Slug expression increase in the liver metastasis group.

Although less studied in colon cancer, Twist has also been implicated in contributing to metastasis by promoting cancer stem cell-like traits. Another study found that Manuka honey downregulates Twist, Slug, and SNAI1 in colonospheres, thereby reducing migration and angiogenesis.[52] This suggests that combinatorial targeting of EMT-TFs could enhance therapeutic efficacy. TNF-α also orchestrates a pro-metastatic niche by stabilizing SNAI1 and activating stromal fibroblasts expressing SNAI1, which, in turn, enhances cancer cell proliferation and invasion.[21,53] This stromal-epithelial crosstalk underscores the importance of microenvironmental inflammation in colon cancer progression. Therefore, TNF-α has a dual role in both inflammation and EMT, with both showing a similar expression pattern in the liver metastasis group.

In addition, the observed downregulation of MTA3 in metastatic cases suggests a tumor-suppressive function. Restoring MTA3 activity could thus represent another avenue for therapeutic intervention. Epigenetic drugs that modulate MTA3 expression or activity warrant further investigation in preclinical CRC models. While MTA3 has not been directly addressed in the recent studies, its known role in repressing SNAI1 in breast cancer suggests a potential cross-talk in colon cancer.[54] Future studies should explore whether MTA3 loss contributes to SNAI1 activation in colorectal tumors. In this study, MTA3 expression was found to be decreased in the liver metastasis group and elevated in the non-metastasis group (Table 1), supporting its proposed role as a metastasis suppressor.

The correlation of SNAI1, ZEB1, Slug, Twist, and TNF-α with BMI and AST in cancer involves their roles in EMT, cancer progression, and inflammation, though direct correlations with BMI and AST specifically are not extensively detailed in the provided sources. However, based on the results of this study, these markers were found to correlate with BMI and AST (Table 3). The decrease in BMI, as shown in Table 2, indicates the occurrence of cachexia in the subjects studied. Cachexia in colon cancer involves complex interactions between transcription factors and inflammatory mediators, with SNAI1, ZEB1, Twist1, and TNF-α playing significant roles.[55-57] Cachexia progression in colon cancer involves energy metabolism disruption (e.g., impaired amino acid metabolism) and elevated serum lysine/acetate, which may serve as diagnostic biomarkers.[58] EMT-related transcription factors (ZEB1, Twist1, and SNAI1) contribute to tumor resilience and metastasis, indirectly perpetuating cachexia by sustaining tumor-derived catabolic signals (e.g., activin A).[55-57] ZEB1, Twist1, and SNAI1 drive tumor progression and cachexia in colon cancer through EMT, anti-apoptotic signaling, and muscle degradation pathways, while TNF-α and systemic inflammation amplify these effects.

According to another study, TNF-α also showed a direct, concentration-dependent correlation with AST.[59] The relationship of AST was not directly correlated with SNAI1, ZEB1, Slug, and Twist, but these markers contribute to the development of cancer and liver-related pathologies, potentially increasing AST through metastasis, immune infiltration, or hepatocyte damage. The prognostic value of an increased AST ratio independently predicted the risk and mortality of cancer, which underlines the need to monitor liver function in cancer patients.[60] This is in line

with the results obtained in this study, where AST levels were higher in the metastasis group than in the non-metastasis group (Table 2).

Therapeutic implications for targeting SNAI1, ZEB1, Slug, Twist, MTA3, and TNF-α or their regulators show promise. Natural compounds sensitize cells to chemotherapy by disrupting EMT and inhibiting cancer development, while stromal inhibition of SNAI1, ZEB1, Slug, Twist, MTA3, and TNF-α could mitigate pro-tumorigenic signaling. However, partial EMT states may persist as reservoirs for recurrence, necessitating combination therapies. As shown in Table 4, the markers used in this study affect cancer development, as expressed in the T, N, and M (stage) grading scores.

In conclusion, SNAI1 emerges as the dominant EMT-TF in colon cancer, modulated by TNF-α and stromal interactions. ZEB1, Slug, and Twist play ancillary roles, while MTA3's involvement remains speculative. Therapeutic strategies must account for SNAI1's multifaceted regulation and the complexity of the tumor microenvironment. However, we recognize several limitations in this study, including: (a) the lack of a comprehensive database for patient baseline data, and (b) the focus on profiling the expression of several markers in CRC patient tumors without supporting or validating data from additional tests, such as somatic mutation analysis. Future studies should involve larger sample sizes, comparisons across racial groups of clinical patients, and further laboratory analysis. A comprehensive correlational approach that includes microscopic, serological, and bioinformatics analysis will be essential to support these initial findings.

5. Conclusion

Through this study, it was found that SNAI1, ZEB1, Slug, Twist, and TNF-α were associated with cancer progression toward metastasis, as their expression levels increased accordingly. In contrast, MTA3, a known metastasis suppressor, showed relatively lower expressing during metastasis progression. In addition, SNAI1, ZEB1, Slug, Twist, and TNF-α were also correlated with BMI and AST levels

Acknowledgments

The authors would like to express our deepest gratitude to the PhD Biotechnology team at Malang State University for conducting this research, as well as to our partners from the Division of Digestive Surgery, Department of Surgery, Faculty of Medicine, Public Health and Nursing, Gadjah Mada University, and Dr. Sardjito General Hospital, Yogyakarta, Indonesia, for their assistance with clinical support and respondent preparation.

Funding

None.

Conflict of interest

The authors declared that there were no conflict of interest in this work.

Author contributions

Conceptualization: Adeodatus Yuda Handaya, Hendra Susanto
Formal analysis: All authors
Investigation: All authors
Methodology: Hendra Susanto, Adeodatus Yuda Handaya
Writing–original draft: Adeodatus Yuda Handaya, Moch Sholeh
Writing–review & editing: Adeodatus Yuda Handaya, Moch Sholeh

Ethics approval and consent to participate

The participants consented to complete the informed consent form for the clinical observational study. With the certificate of ethics number: KE/FK/0938/EC/2021, this clinical study was authorized by the IRB, Faculty of Medicine, Universitas Gadjah Mada, Indonesia, in accordance with the Declaration of Helsinki.

Consent for publication

Not applicable, because the respondents' identities have been completely masked, and they have also agreed in the "written consent to participate" section that the samples will be used for further research purposes.

Availability of data

All the datasets generated in the current study are available from the corresponding author based on reasonable request.

References

1. Klimeck L, Heisser T, Hoffmeister M, Brenner H. Colorectal cancer: A health and economic problem. *Best Pract Res Clin Gastroenterol.* 2023;66:101839.

   doi: 10.1016/j.bpg.2023.101839

2. Sharzehan MAK, Sito H, Abdullah N, *et al.* Association between CYP2E1 polymorphisms and colorectal cancer risk: A systematic review and meta-analysis. *Sci Rep.* 2022;12(1):20149.

   doi: 10.1038/s41598-022-24398-w

3. Islam MR, Aziz MA, Shahriar M, Islam MS. Polymorphisms in IL-17A gene and susceptibility of colorectal cancer in bangladeshi population: A case-control analysis. *Cancer*

Control. 2022;29:1-11.

doi: 10.1177/10732748221143879

4. Diao YE, Xu Q. CASR rs1801725 polymorphism is associated with the risk and prognosis of colorectal cancer: A case-control study. *J Clin Lab Anal*. 2020;34(11):e23463.

doi: 10.1002/jcla.23463

5. Yi C, Li T, Shen Y, *et al*. Polymorphisms of nucleotide excision repair genes associated with colorectal cancer risk: Meta-analysis and trial sequential analysis. *Front Genet*. 2022;13:1009938.

doi: 10.3389/fgene.2022.1009938

6. Nguyen LH, Goel A, Chung DC. Pathways of colorectal carcinogenesis. *Gastroenterology*. 2020;158(2):291-302.

doi: 10.1053/j.gastro.2019.08.059

7. Li Q, Geng S, Luo H, *et al*. Signaling pathways involved in colorectal cancer: Pathogenesis and targeted therapy. *Sig Transduct Target Ther*. 2024;9(1):266.

doi: 10.1038/s41392-024-01953-7

8. Li J, Ma X, Chakravarti D, Shalapour S, DePinho RA. Genetic and biological hallmarks of colorectal cancer. *Genes Dev*. 2021;35(11-12):787-820.

doi: 10.1101/gad.348226.120

9. Shweikeh F, Zeng Y, Jabir AR, *et al*. The emerging role of blood-based biomarkers in early detection of colorectal cancer: A systematic review. *Cancer Treat Res Commun*. 2024;42:100872.

doi: 10.1016/j.ctarc.2025.100872

10. Schiliro C, Firestein BL. Mechanisms of metabolic reprogramming in cancer cells supporting enhanced growth and proliferation. *Cells*. 2021;10(5):1056.

doi: 10.3390/cells10051056

11. Pascual G, Benitah SA. Lipids in the tumor microenvironment: Immune modulation and metastasis. *Front Oncol*. 2024;14:1435480.

doi: 10.3389/fonc.2024.1435480

12. Zhang YH, Chen XL, Wang YR, Hou YW, Zhang YD, Wang KJ. Prevention of malignant digestive system tumors should focus on the control of chronic inflammation. *World J Gastrointest Oncol*. 2023;15(3):389-404.

doi: 10.4251/wjgo.v15.i3.389

13. Varghese N, Majeed A, Nyalakonda S, Boortalary T, Halegoua-DeMarzio D, Hann HW. Review of related factors for persistent risk of hepatitis b virus-associated hepatocellular carcinoma. *Cancers (Basel)*. 2024;16(4):777.

doi: 10.3390/cancers16040777

14. Kaur A, Azeez GA, Thirunagari M, *et al*. Association of chronic hepatitis B with colorectal cancer and its dual impact on colorectal liver metastasis: A narrative review. *Cureus*. 2024;16(12):e76079.

doi: 10.7759/cureus.76079

15. Zhao L, Hou X, Feng Y, *et al*. A chronic stress-induced microbiome perturbation, highly enriched in Ruminococcaceae_UCG-014, promotes colorectal cancer growth and metastasis. *Int J Med Sci*. 2024;21(5):882-895.

doi: 10.7150/ijms.90612

16. Shi X, Wang X, Yao W, *et al*. Mechanism insights and therapeutic intervention of tumor metastasis: Latest developments and perspectives. *Signal Transduct Target Ther*. 2024;9(1):1-46.

doi: 10.1038/s41392-024-01885-2

17. Zhao H, Wu L, Yan G, *et al*. Inflammation and tumor progression: Signaling pathways and targeted intervention. *Signal Transduct Target Ther*. 2021;6(1):1-46.

doi: 10.1038/s41392-021-00658-5

18. Hou S, Zhao Y, Chen J, Lin Y, Qi X. Tumor-associated macrophages in colorectal cancer metastasis: Molecular insights and translational perspectives. *J Transl Med*. 2024;22(1):62.

doi: 10.1186/s12967-024-04856-x

19. Yang S, Li Y, Zhang Y, Wang Y. Impact of chronic stress on intestinal mucosal immunity in colorectal cancer progression. *Cytokine Growth Factor Rev*. 2024;80:24-36.

doi: 10.1016/j.cytogfr.2024.10.007

20. Xue C, Chu Q, Shi Q, Zeng Y, Lu J, Li L. Wnt signaling pathways in biology and disease: Mechanisms and therapeutic advances. *Signal Transduct Target Ther*. 2025;10:106.

doi: 10.1038/s41392-025-02142-w

21. Wang H, Wang HS, Zhou BH, *et al*. Epithelial-mesenchymal transition (EMT) induced by TNF-α requires AKT/GSK-3β-mediated stabilization of snail in colorectal cancer. *PLoS One*. 2013;8(2):e56664.

doi: 10.1371/journal.pone.0056664

22. Buyuk B, Jin S, Ye K. Epithelial-to-mesenchymal transition signaling pathways responsible for breast cancer metastasis. *Cel Mol Bioeng*. 2022;15(1):1-13.

doi: 10.1007/s12195-021-00694-9

23. Lu J, Kornmann M, Traub B. Role of epithelial to mesenchymal transition in colorectal cancer. *Int J Mol Sci*. 2023;24(19):14815.

doi: 10.3390/ijms241914815

24. Ribatti D, Tamma R, Annese T. Epithelial-mesenchymal transition in cancer: A historical overview. *Transl Oncol*. 2020;13(6):100773.

doi: 10.1016/j.tranon.2020.100773

25. Georgakopoulos-Soares I, Chartoumpekis DV, Kyriazopoulou V, Zaravinos A. EMT factors and metabolic pathways in cancer. *Front Oncol*. 2020;10:499.

doi: 10.3389/fonc.2020.00499

26. Bhat AA, Nisar S, Singh M, *et al*. Cytokine- and chemokine-induced inflammatory colorectal tumor microenvironment: Emerging avenue for targeted therapy. *Cancer Commun (Lond)*. 2022;42(8):689-715.

doi: 10.1002/cac2.12295

27. Lu J, Fei F, Wu C, Mei J, Xu J, Lu P. ZEB1: Catalyst of immune escape during tumor metastasis. *Biomed Pharmacother*. 2022;153:113490.

doi: 10.1016/j.biopha.2022.113490

28. Shiravand Y, Khodadadi F, Kashani SMA, *et al*. Immune checkpoint inhibitors in cancer therapy. *Curr Oncol*. 2022;29(5):3044-3060.

doi: 10.3390/curroncol29050247

29. Rahimi A, Baghernejadan Z, Hazrati A, *et al*. Combination therapy with immune checkpoint inhibitors in colorectal cancer: Challenges, resistance mechanisms, and the role of microbiota. *Biomed Pharmacother*. 2025;186:118014.

doi: 10.1016/j.biopha.2025.118014

30. Herrera A, Herrera M, Guerra-Perez N, *et al*. Endothelial cell activation on 3D-matrices derived from PDGF-BB-stimulated fibroblasts is mediated by snail1. *Oncogenesis*. 2018;7(9):76.

doi: 10.1038/s41389-018-0085-z

31. Zhang X, Luo Y, Cen Y, *et al*. MACC1 promotes pancreatic cancer metastasis by interacting with the EMT regulator SNAI1. *Cell Death Dis*. 2022;13(11):923.

doi: 10.1038/s41419-022-05285-8

32. Hu X, Zhu X, Chen Y, *et al*. Senescence-related signatures predict prognosis and response to immunotherapy in colon cancer. *J Gastrointest Oncol*. 2024;15(3):1020-1034.

doi: 10.21037/jgo-24-339

33. Kim YH, Kim G, Kwon CI, Kim JW, Park PW, Hahm KB. TWIST1 and SNAI1 as markers of poor prognosis in human colorectal cancer are associated with the expression of ALDH1 and TGF-β1. *Oncol Rep*. 2014;31(3):1380-1388.

doi: 10.3892/or.2014.2970

34. Marques-Magalhães Â, Monteiro-Ferreira S, Canão PA, *et al*. Patient-derived colorectal cancer extracellular matrices modulate cancer cell stemness markers. *Int J Mol Sci*. 2025;26(7):2890.

doi: 10.3390/ijms26072890

35. Qian J, Liu H, Chen W, *et al*. Knockdown of Slug by RNAi inhibits the proliferation and invasion of HCT116 colorectal cancer cells. *Mol Med Rep*. 2013;8(4):1055-1059.

doi: 10.3892/mmr.2013.1604

36. Brzozowa M, Michalski M, Wyrobiec G, *et al*. The role of Snail1 transcription factor in colorectal cancer progression and metastasis. *Contemp Oncol (Pozn)*. 2015;19(4):265-270.

doi: 10.5114/wo.2014.42173

37. Lindner P, Paul S, Eckstein M, *et al*. EMT transcription factor ZEB1 alters the epigenetic landscape of colorectal cancer cells. *Cell Death Dis*. 2020;11(2):1-13.

doi: 10.1038/s41419-020-2340-4

38. Li CW, Xia W, Huo L, *et al*. Epithelial-mesenchyme transition induced by TNF-α requires NF-κB-mediated transcriptional upregulation of Twist1. *Cancer Res*. 2012;72(5):1290-1300.

doi: 10.1158/0008-5472.can-11-3123

39. Wu Y, Zhou BP. TNF-α/NF-κB/Snail pathway in cancer cell migration and invasion. *Br J Cancer*. 2010;102(4):639-644.

doi: 10.1038/sj.bjc.6605530

40. Al Obeed OA, Alkhayal KA, Al Sheikh A, *et al*. Increased expression of tumor necrosis factor-α is associated with advanced colorectal cancer stages. *World J Gastroenterol*. 2014;20(48):18390-18396.

doi: 10.3748/wjg.v20.i48.18390

41. Derwinger K, Kodeda K, Bexe-Lindskog E, Taflin H. Tumour differentiation grade is associated with TNM staging and the risk of node metastasis in colorectal cancer. *Acta Oncologica*. 2010;49(1):57-62.

doi: 10.3109/02841860903334411

42. Liaghat M, Ferdousmakan S, Mortazavi SH, *et al*. The impact of epithelial-mesenchymal transition (EMT) induced by metabolic processes and intracellular signaling pathways on chemo-resistance, metastasis, and recurrence in solid tumors. *Cell Commun Signal*. 2024;22(1):575.

doi: 10.1186/s12964-024-01957-4

43. Hoffmann H, Wartenberg M, Vorlova S, *et al*. Normalization of Snai1-mediated vessel dysfunction increases drug response in cancer. *Oncogene*. 2024;43(35):2661-2676.

doi: 10.1038/s41388-024-03113-1

44. Dong B, Wu Y. Epigenetic regulation and post-translational modifications of SNAI1 in cancer metastasis. *Int J Mol Sci*. 2021;22(20):11062.

doi: 10.3390/ijms222011062

45. Liao Z, Cai X, Zheng Y, *et al*. Sirtuin 1 in osteoarthritis: Perspectives on regulating glucose metabolism. *Pharmacol Res*. 2024;202:107141.

doi: 10.1016/j.phrs.2024.107141

46. Tsirigoti C, Ali MM, Maturi V, Heldin CH, Moustakas A. Loss of SNAI1 induces cellular plasticity in invasive triple-negative breast cancer cells. *Cell Death Dis*. 2022;13(9):832.

doi: 10.1038/s41419-022-05280-z

47. Zhang GJ, Zhou T, Tian HP, Liu ZL, Xia SS. High expression of ZEB1 correlates with liver metastasis and poor prognosis in colorectal cancer. *Oncol Lett*. 2013;5(2):564-568.

doi: 10.3892/ol.2012.1026

48. Parfenyev SE, Daks AA, Shuvalov OY, *et al*. Dualistic role of ZEB1 and ZEB2 in tumor progression. *Biol Direct*. 2025;20(1):32.

doi: 10.1186/s13062-025-00604-3

49. El-Deek HEDM, El-Naggar MS, Morsy AMM, Sedik MF, Osman HA, Ahmed AM. P4HA2 involved in SLUG-associated EMT predicts poor prognosis of patients with KRAS-positive colorectal cancer. *Med Mol Morphol*. 2024;57(3):167-176.

doi: 10.1007/s00795-024-00385-0

50. Lautert-Dutra W, Melo CM, Chaves LP, *et al*. Investigating the role of SNAI1 and ZEB1 expression in prostate cancer progression and immune modulation of the tumor microenvironment. *Cancers (Basel)*. 2024;16(8):1480.

doi: 10.3390/cancers16081480

51. Tong J, Shen Y, Zhang Z, Hu Y, Zhang X, Han L. Apigenin inhibits epithelial-mesenchymal transition of human colon cancer cells through NF-κB/Snail signaling pathway. *Biosci Rep*. 2019;39(5):BSR20190452.

doi: 10.1042/bsr20190452

52. Cianciosi D, Forbes-Hernandez T, Armas Diaz Y, *et al*. Manuka honey's anti-metastatic impact on colon cancer stem-like cells: Unveiling its effects on epithelial-mesenchymal transition, angiogenesis and telomere length. *Food Funct*. 2024;15(13):7200-7213.

doi: 10.1039/d4fo00943f

53. Herrera A, Herrera M, Alba-Castellón L, *et al*. Protumorigenic effects of Snail-expression fibroblasts on colon cancer cells. *Int J Cancer*. 2014;134(12):2984-2990.

doi: 10.1002/ijc.28613

54. Liu Y, Lu T, Li R, *et al*. Discovery of Jaspamycin from marine-derived natural product based on MTA3 to inhibit hepatocellular carcinoma progression. *Sci Rep*. 2024;14(1):25294.

doi: 10.1038/s41598-024-75205-7

55. Guo C, Ma J, Deng G, *et al*. ZEB1 promotes oxaliplatin resistance through the induction of epithelial - mesenchymal transition in colon cancer cells. *J Cancer*. 2017;8(17):3555-3566.

doi: 10.7150/jca.20952

56. Qing F, Xue J, Sui L, *et al*. Intestinal epithelial SNAI1 promotes the occurrence of colorectal cancer by enhancing EMT and Wnt/β-catenin signaling. *Med Oncol*. 2023;41(1):34.

doi: 10.1007/s12032-023-02253-w

57. Razzaque MS, Atfi A. Regulatory role of the transcription factor Twist1 in cancer-associated muscle cachexia. *Front Physiol*. 2020;11:662.

doi: 10.3389/fphys.2020.00662

58. Qiu X, Lu R, He Q, Chen S, Huang C, Lin D. Metabolic signatures and potential biomarkers for the diagnosis and treatment of colon cancer cachexia. *Acta Biochim Biophys Sin (Shanghai)*. 2023;55(12):1913-1924.

doi: 10.3724/abbs.2023151

59. Zhao S, Jiang J, Jing Y, *et al*. The concentration of tumor necrosis factor-α determines its protective or damaging effect on liver injury by regulating Yap activity. *Cell Death Dis*. 2020;11(1):70.

doi: 10.1038/s41419-020-2264-z

60. Chen W, Wang W, Zhou L, *et al*. Elevated AST/ALT ratio is associated with all-cause mortality and cancer incident. *J Clin Lab Anal*. 2022;36(5):e24356.

doi: 10.1002/jcla.24356

ACCSCIENCE PUBLISHING

Eurasian Journal of Medicine and Oncology

ORIGINAL RESEARCH ARTICLE

Identification and validation of relevant diagnostic biomarkers for osteoporosis by Weighted Gene Co-expression Network Analysis and machine learning

Cuicui Zhou[1,2], Zarina Awang[1], and Farra Aidah Jumuddin[1]*

[1]Department of Clinical Medicine, Faculty of Medicine, Lincoln University College, Petaling Jaya, Selangor, Malaysia

[2]Department of Orthopaedic Surgery, The Second Affiliated Hospital of Nanyang Medical College, Nanyang, Henan, China

Abstract

Introduction: Osteoporosis (OP) is a systemic metabolic bone disease characterized by complex pathogenesis and high prevalence. Current diagnostic and therapeutic approaches have limited effectiveness, and new biomarkers are needed to improve the treatment and diagnosis of OP.

Objective: The present study aimed to identify novel diagnostic biomarkers for OP through integrated bioinformatics analysis.

Methods: We performed an integrative bioinformatics analysis combining Weighted Gene Co-expression Network Analysis and machine learning on two Gene Expression Omnibus datasets (GSE35958, GSE35956). Differentially expressed genes (DEGs) were identified using "limma" package of R software, followed by module construction and key gene screening via Least Absolute Shrinkage and Selection Operator (LASSO) regression. Functional enrichment, immune infiltration, and drug prediction analyses were conducted to explore biological mechanisms and therapeutic potential.

Results: Differential expression analysis identified 1,020 DEGs, from which 10 co-expression modules were constructed. The blue module demonstrated the strongest correlation with OP ($r = 0.99$, $p<0.0001$). LASSO regression analysis prioritized seven candidate genes (LOC286177, nucleobindin 1 [NUCB1], peroxisomal biogenesis factor 19 [PEX19], metastasis associated 1 [MTA1], DRA aassociated protein 1 [DRAP1], protocadherin gamma A1 [PCDHGA1], and pre-mRNA processing factor 39 [PRPF39]), with subsequent validation confirming NUCB1, PEX19, MTA1, DRAP1, and PCDHGA1 as robust diagnostic biomarkers (Area under the curve > 0.85). Functional enrichment implicated these genes in endoplasmic reticulum stress, Wnt/β-catenin signaling, and immune regulatory pathways. Immune profiling further revealed significant perturbations in T-cell and macrophage populations in OP. The Coremine Medical database was leveraged to predict potential therapeutic agents, including both small-molecule and phytochemical candidates.

Conclusion: The present study identified NUCB1, PEX19, MTA1, DRAP1, and PCDHGA1 as promising OP diagnostic markers and explored their roles in bone metabolism. The findings offer insights for early diagnosis and targeted therapy but require further clinical validation.

Keywords: Osteoporosis; Gene Expression Omnibus; Weighted Gene Co-expression Network Analysis; Least Absolute Shrinkage and Selection Operator; Biomarker

***Corresponding author:**
Farra Aidah Jumuddin
(farraaiadah@lincoln.edu.my)

Citation: Zhou C, Awang Z, Jumuddin FA. Identification and validation of relevant diagnostic biomarkers for osteoporosis by Weighted Gene Co-expression Network Analysis and machine learning. *Eurasian J Med Oncol.* 2025;9(3):261-276.
doi: 10.36922/EJMO025240252

Received: June 09, 2025

Revised: July 25, 2025

Accepted: July 29, 2025

Published online: September 9, 2025

Copyright: © 2025 Author(s). This is an Open-Access article distributed under the terms of the Creative Commons Attribution License, permitting distribution, and reproduction in any medium, provided the original work is properly cited.

Publisher's Note: AccScience Publishing remains neutral with regard to jurisdictional claims in published maps and institutional affiliations.

1. Introduction

Osteoporosis (OP) is a systemic metabolic bone disorder characterized by decreased bone mineral density (BMD) and microarchitectural deterioration, predisposing patients to fragility fractures at high-risk sites including the hip, spine, and wrist.[1] These fractures frequently lead to chronic pain, functional impairment, and irreversible skeletal damage, collectively contributing to reduced quality of life.[2-4] OP currently affects approximately 200 million individuals globally, with a prevalence of 30% in women and 20% in men aged over 50 years.[5] Furthermore, demographic aging is projected to escalate the annual healthcare costs of osteoporotic fractures to hundreds of billions of USD by 2050.[6] Together, these pathophysiological and epidemiological features establish OP as a major global public health challenge requiring urgent intervention.

The pathogenesis of OP is multifactorial, with immune and inflammatory responses playing pivotal roles in disrupting bone homeostasis.[5] Chronic inflammatory states activate the nuclear factor kappa B (NF-κB) signaling pathway and promote the release of pro-inflammatory cytokines such as interleukin-6 (IL-6) and tumor necrosis factor-alpha (TNF-α), which enhance osteoclast activity and suppress osteoblast function, thereby accelerating bone loss.[6,7] In addition, genetic predisposition, hormonal changes, nutritional status, and lifestyle factors contribute significantly to the development of OP. [8-10] In recent years, therapeutic strategies for OP have primarily included bisphosphonates, selective estrogen receptor modulators (SERMs), and monoclonal antibodies. While these agents effectively inhibit bone resorption, their long-term use may be associated with adverse effects and fails to fully restore bone microstructure and function.[11,12] Moreover, the absence of definitive diagnostic criteria and targeted therapies complicates early intervention and personalized treatment.[13] Therefore, identifying diagnostic biomarkers holds substantial clinical significance for early screening, risk prediction, and the discovery of therapeutic targets in OP.[14]

Bioinformatics approaches have become instrumental in elucidating core disease mechanisms. Weighted Gene Co-expression Network Analysis (WGCNA) enables the systematic identification of disease-associated modules and hub genes from high-throughput data, with demonstrated applications in OP and other metabolic disorders.[15,16] As a classical machine learning method, Least Absolute Shrinkage and Selection Operator (LASSO) regression employs L1 regularization to enhance model interpretability by selecting the most predictive features while reducing overfitting.[17] This approach has been widely adopted in biomarker discovery due to its ability to handle high-dimensional omics data and identify robust disease-associated signatures.[17] In particular, LASSO regression has demonstrated scientific reliability in screening biomarkers for complex diseases, including oncology, cardiovascular disorders, and, more recently, bone metabolic diseases.[18,19] In the present study, we aim to combine WGCNA and LASSO regression to systematically analyze gene expression data related to OP, identifying and validating diagnostic biomarkers and potential drug targets. Through this research, we seek to provide novel scientific insights and references for the clinical diagnosis and treatment of OP. The analysis flowchart is shown in Figure 1.

2. Materials and methods

2.1. Sample sources

Transcriptome profiles were retrieved from the NCBI Gene Expression Omnibus (GEO) repository via the GEOquery R package (v2.66.0). Two datasets generated on the Affymetrix Human Genome U133 Plus 2.0 Array (GPL570) were selected to serve as discovery and validation cohorts, respectively: GSE35958, which included four healthy controls and five OP cases, and GSE35956, used as the validation set with five controls and five cases.

Raw CEL files were downloaded and subjected to stringent quality control using the affyQC-Report R package (v1.72.0), with no samples excluded on the basis of normalized unscaled standard errors (>1.05) or relative log expression dispersion criteria. Probe-level data were background-corrected, quantile-normalized, and log2-transformed using the affy and "limma" packages. Non-specific filtering was applied to retain only probes with an average intensity ≥4 in at least 20% of arrays. Probe sets were collapsed to unique Entrez gene symbols using the annotate package (max mean probe per gene). The two datasets were processed independently to preserve their mutual independence for downstream machine learning modeling and subsequent enrichment analyses.

2.2. Differential analysis

To identify differentially expressed genes (DEGs) associated with OP, we conducted a comprehensive analysis of the GSE35958 and GSE35956 datasets utilizing the "limma" package in R. The criteria for selecting DEGs were established based on a stringent threshold of |log fold change (FC)| > 0.5 and a significance level of $p<0.05$. Specifically, genes with log FC > 0.5 and $p<0.05$ were classified as upregulated, whereas those with log FC < −0.5 and $p<0.05$ were categorized as downregulated. For visualization, we generated heatmaps using the "pheatmap" package, and volcano plots were constructed using "ggplot2" to illustrate the distribution of DEGs.

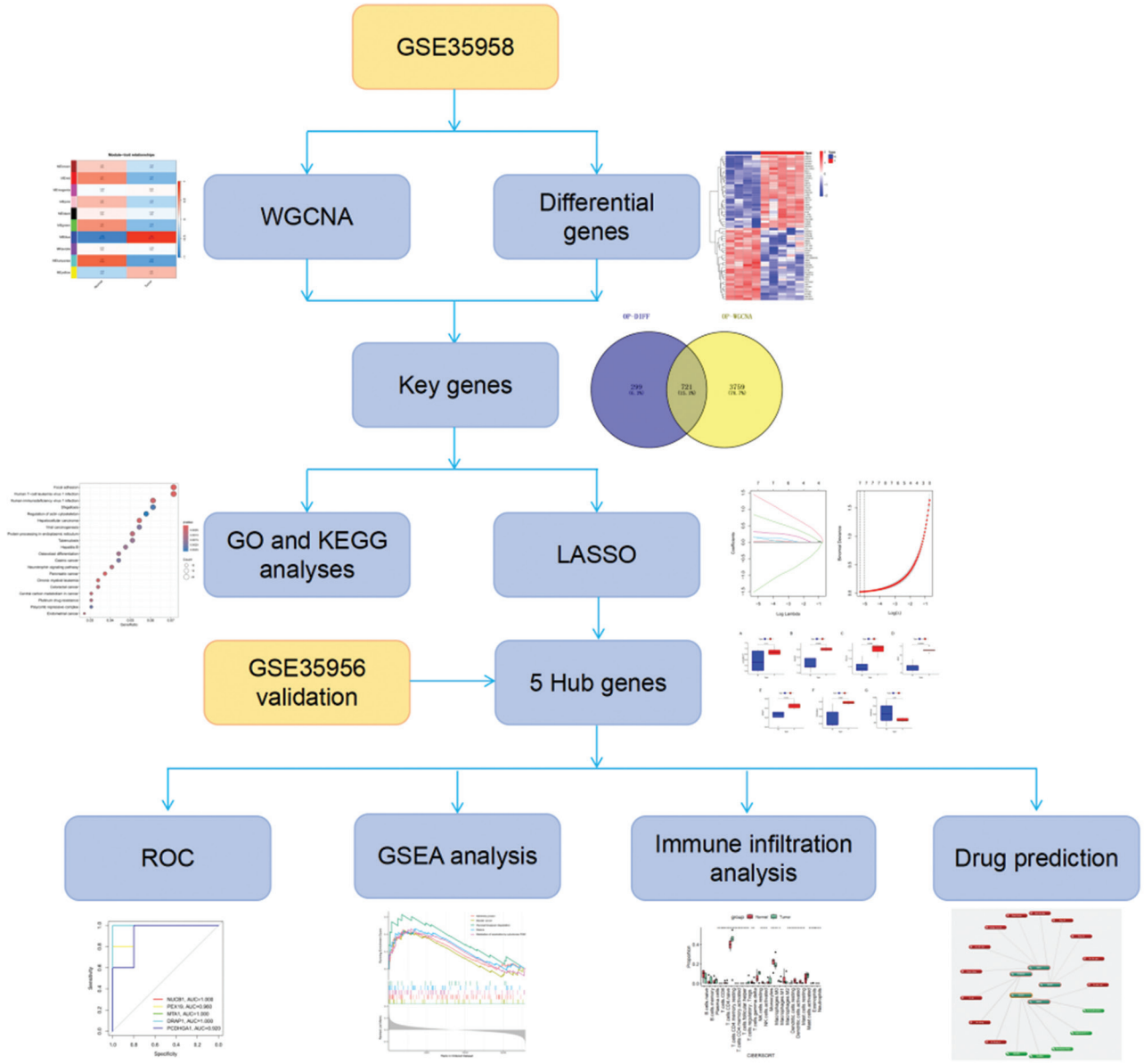


Figure 1. The flowchart of the integrative bioinformatics analysis
Abbreviations: GO: Gene ontology; GSEA: Gene Set Enrichment Analysis; KEGG: Kyoto encyclopedia of genes and genomes; LASSO: Least Absolute Shrinkage and Selection Operator; ROC: Receiver operating characteristic; WGCNA: Weighted Gene Co-expression Network Analysis.

2.3. WGCNA

Co-expression network analysis was conducted using the WGCNA package (v1.72) in R on the GSE35958 expression dataset. The adjacency matrix was constructed with a soft-threshold power (β) of 7, determined by scale-free topology fitting index ($R^2 > 0.85$). Network topology was calculated using unsigned topological overlap matrices (TOMType = "unsigned") with the following parameters: minModuleSize = 50 to ensure biological relevance, mergeCutHeight = 0.6 for module consolidation, and recreateThreshold = 0 to maintain original clustering. Non-expressed genes (standard deviation = 0) were excluded from the analysis. Module-trait relationships were assessed through Pearson's correlation, and modules with significant associations ($|r| > 0.5$, false discovery rate [FDR]-adjusted $p<0.01$) were selected for downstream biomarker analysis.[15] Finally, DEGs were intersected with genes contained within the key WGCNA modules using the "Venn" package in R. The intersected genes were analyzed in the next step of the study.

2.4. Enrichment analysis

To systematically dissect the biological relevance of the identified gene lists, we conducted gene ontology (GO) and Kyoto Encyclopedia of Genes and Genomes (KEGG) pathway enrichment analyses. Gene symbols were first converted to Entrez IDs using the org.Hs.eg.db annotation package (v3.17.0). The clusterProfiler package (v4.8.1) was then used to query three GO domains—biological process (BP), molecular function, and cellular component (CC)—as well as the KEGG PATHWAY database (release 104.0). Enrichment analysis was performed using the enrichGO and enrichKEGG functions, with a p-value cutoff of 0.05 after Benjamini–Hochberg FDR correction, and gene sets restricted to sizes between 10 and 500 genes. Redundant GO terms were collapsed with the simplify function (q-value cutoff = 0.05). To quantify the enrichment strength, normalized enrichment scores (NES) and gene ratios were extracted for each term.

The resulting GO and KEGG terms were visualized using the "ggplot2" (v3.4.2) and "enrichplot" (v1.18.3) packages. Bubble plots and cnet plots were generated to depict the top 20 most significantly enriched terms, ranked by adjusted p-value.

2.5. Screening and validation of key genes through machine learning

To identify the minimal set of genes that robustly discriminates OP from healthy bone, we applied LASSO penalized logistic regression to the GSE35958 discovery cohort (n = 9). Prior to modeling, the expression matrix was variance-stabilized using the voom transformation and z-score normalized across samples. The optimal λ value was determined by 10-fold cross-validation (CV) with 1,000 repetitions, selecting the λ within one standard error of the minimum mean cross-validated deviance. Genes retaining non-zero regression coefficients at the optimal λ were designated as core genes. All LASSO analyses were implemented using the glmnet package (v4.1-8) in R (v4.3.0).

For internal validation, expression levels of the core genes in GSE35958 dataset were visualized using box plots and dot plots generated with the "ggpubr" package (v0.6.0). For external validation, the same core gene set was projected onto the independent GSE35956 dataset (n = 10). Differential expression between OP and control groups was quantified by the two-sided Wilcoxon rank-sum test and corrected for multiple comparisons using the Benjamini–Hochberg (FDR < 0.05).

To assess the discriminatory capacity of the core gene signatures, receiver operating characteristic (ROC) curves were constructed for both datasets using the "pROC" package (v1.18.4). The area under the ROC curve (area under the curve [AUC]) and the corresponding 95 % confidence intervals were computed by DeLong's method. An AUC >0.85 was considered indicative of excellent predictive accuracy.

2.6. Gene Set Enrichment Analysis (GSEA)

GSEA was performed to systematically explore the potential BPs and signaling pathways associated with the hub gene of interest. The entire transcriptome was first ranked according to the Pearson's correlation coefficient between the hub gene and all other expressed genes. Next, singlegene GSEA was conducted with the "GSEA" function implemented in the clusterProfiler R package against the Molecular Signatures Database (MSigDB, v7.x) "c2.cp.kegg" and "c5.go" collections. To ensure statistical robustness, 10,000 phenotype-based permutations were executed, and gene set sizes were restricted to between 10 and 200 genes. Pathways with a ($|NES|$) ≥ 1 and an adjusted p-value (FDR) <0.05 were considered significantly enriched. The leading-edge genes driving each enriched gene set were extracted, and the results were visualized using the "gseaplot2" function from the "enrichplot" R package.

2.7. Immune infiltration analysis

To quantify the landscape of tumor-infiltrating immune cells, we applied "CIBERSORT" R package calculation to perform *de novo* enumeration of 22 human immune cell subsets through a ν-support vector regression algorithm trained on the LM22 signature matrix, which consisted of 547 genes. The analysis was carried out using default parameters: 1,000 permutations, quantile normalization disabled, and batch correction activated. Samples with a deconvolution p<0.05 were retained for downstream analysis to ensure high fidelity of the inferred fractions.

Subsequently, the relative proportions of immune cell subsets, such as $CD8^+$ T cells, M2 macrophages, and regulatory T cells, were compared between normal and OP samples using a two-sided Wilcoxon rank-sum test with Benjamini–Hochberg correction (FDR < 0.05). Compositional shifts were visualized using the "ggplot2" and "pheatmap" R packages, whereas intercellular correlation networks ($|r|$ > 0.4 and p<0.05) were constructed using the "igraph" package to explore potential immune cell crosstalk.

2.8. Potential drug prediction

The OP core genes (Entrez IDs) were imported into Coremine Medical (http://www.coremine.com/medical), where the platform's text-mining engine was queried under the "herb–gene–disease" relationship layer to retrieve botanical entities statistically linked to both the gene set

and the MeSH term "osteoporosis." Statistical significance was assessed by a one-tailed Fisher's exact test and corrected for multiple comparisons using the Benjamini–Hochberg method; an adjusted $p<0.05$ was required for retention. For CV, the Latin binomials of the prioritized herbs were subsequently queried in the HERB database (http://herb.ac.cn) to confirm their documented therapeutic relevance to OP. Only records that were manually curated from peer-reviewed publications within the last decade were retained, ensuring the highest level of evidence.

3. Results

3.1. Identification of DEGs

In the study, we first performed batch effect correction and normalization on the raw data extracted from the GEO dataset GSE35958. The results showed that the distribution of expression profiles of all the samples generally converged after batch correction and log-normalization (Figure 2A). Subsequently, differential expression analysis was conducted between the control and OP groups, resulting

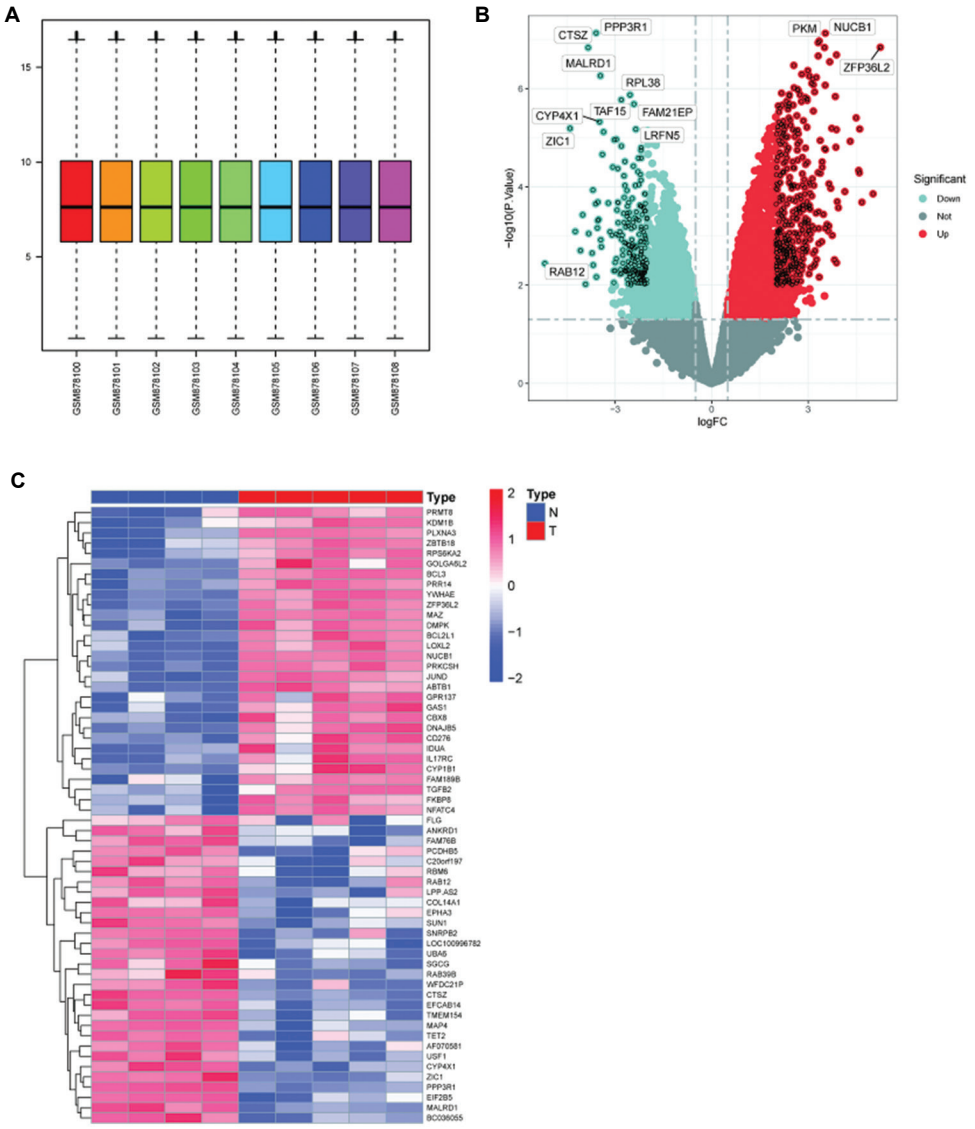


Figure 2. Identification of DEGs. (A) Normalized gene expression data from the GSE35958 dataset. (B) Volcano plot of DEGs in GSE35958. Red dots indicate upregulated genes, blue dots indicate downregulated genes, and gray dots indicate genes without significant differential expression. (C) Heatmap of DEGs in the GSE30528 dataset.
Abbreviations: DEGs: Differentially expressed genes. Group description: N, normal group; T, test group comprising osteoporosis (OP) patients.

in the identification of a total of 1,020 DEGs. In addition, a volcano plot (Figure 2B) and a heatmap (Figure 2C) were then generated to visualize the distribution of DEGs.

3.2. Construction of weighted gene co-expression networks

To investigate the association among OP-associated DEGs, we constructed a weighted gene co-expression network using the WGCNA package. The optimal soft-threshold power was determined to be 7 (Figure 3A), and a total of 10 distinct co-expression modules were identified (Figure 3B-D). Among these, the black module exhibited the strongest correlation with OP (correlation coefficient = 0.99, $p<0.0001$), establishing it as the key module. Subsequent intersection analysis between the OP-associated DEGs and the genes within the WGCNA module revealed 721 core candidate genes (Figure 3E).

3.3. Functional enrichment analysis

Subsequently, we performed GO and KEGG enrichment analysed on the 721 key genes. In the BP assessment, they were mainly associated with functions such as regulation of response to endoplasmic reticulum (ER) stress and small GTPase-mediated signal transduction. In the CC assessment, they were mainly enriched in the ER-Golgi intermediate compartment and the RNA polymerase II transcription regulator complex. In the MM assessment, they were mainly associated with DNA-binding transcription factor binding and chromatin DNA binding (Figure 4A). KEGG pathway analysis revealed significant enrichment in pathways including human T-cell leukemia virus 1 infection, human immunodeficiency virus 1 infection, and focal adhesion (Figure 4B-D).

3.4. Machine learning screening and expression validation of pivotal genes

To further screen the pivotal genes, we analyzed 721 key genes using the LASSO regression algorithm, identifying seven pivotal genes, namely LOC286177, nucleobindin 1 (NUCB1), peroxisomal biogenesis factor 19 (PEX19), metastasis associated 1 (MTA1), DRA aassociated protein 1 (DRAP1), protocadherin gamma A1 (PCDHGA1), and pre-mRNA processing factor 39 (PRPF39) (Figure 5A and B).

Next, we validated these seven hub genes in both the GSE35958 dataset and an independent OP dataset, GSE35956. In the GSE35958 dataset, the expression levels of LOC286177, NUCB1, PEX19, MTA1, DRAP1, and PCDHGA1 were significantly elevated in the OP group compared with normal controls, while PRPF39 expression was significantly decreased (Figure 6A-G). In the GSE35956 dataset, consistent elevation of NUCB1, PEX19, MTA1, DRAP1, and PCDHGA1 was also observed in the OP group, whereas LOC286177 and PRPF39 shosed no significant differential expression (Figure 7A-G). Therefore, subsequent analyses focused on the five validated genes, including NUCB1, PEX19, MTA1, DRAP1, and PCDHGA1.

3.5. ROC curve analysis

Next, we performed ROC curve analysis to evaluate the diagnostic performance of the five hub genes. In the GSE35958 dataset, all five genes such as NUCB1, PEX19, MTA1, DRAP1, and PCDHGA1 demonstrated excellent diagnostic accuracy, each achieving an AUC of 1.000 (Figure 8A). In the GSE35956 dataset, NUCB1, MTA1, and DRAP1 also achieved AUCs of 1.000, while PEX19 and PCDHGA1 showed AUCs of 0.960 and 0.920, respectively (Figure 8B). In both datasets, the AUC values of all five genes were >0.7, suggesting strong diagnostic potential.

3.6. GSEA

To explore the potential pathways of these five hub genes, we performed single-gene GSEA. The results showed that the high-expression group of NUCB1 was highly enriched in the galactose metabolism, starch and sucrose metabolism pathways (Figure 9A). The high-expression group of PEX19 was highly enriched in the adherens junction and metabolism of xenobiotics by cytochrome P450 pathways (Figure 9B). Both MTA1 and DRAP1 high expression groups were highly enriched in phenylalanine metabolism and SNARE interactions in vesicular transport pathways (Figure 9C and D). The high-expression group of PCDHGA1 was highly enriched in glycosaminoglycan degradation and vasopressin-regulated water reabsorption pathways (Figure 9E).

3.7. Immune infiltration analysis

To analyze the differences in immune levels between osteoporotic and normal conditions, we analyzed immune cell infiltration in the control and OP groups using the GSE35958 dataset. The results showed that T cell subsets and macrophage subsets were the major subpopulations of immune cells in both groups (Figure 10A). Notably, the expression levels of $CD4^+$ T cells, regulatory T cells, M0, M1, and M2 macrophages, and several other immune cell types were significantly altered in OP samples compared to normal samples (Figure 10B).

3.8. Potential targeted drug prediction and identification of core components

To explore potential therapeutic drugs for OP, we predicted potential Chinese or Western therapeutic drugs for these five genes by screening them with $p<0.05$ as a criterion through Coremine Medical database. The results showed

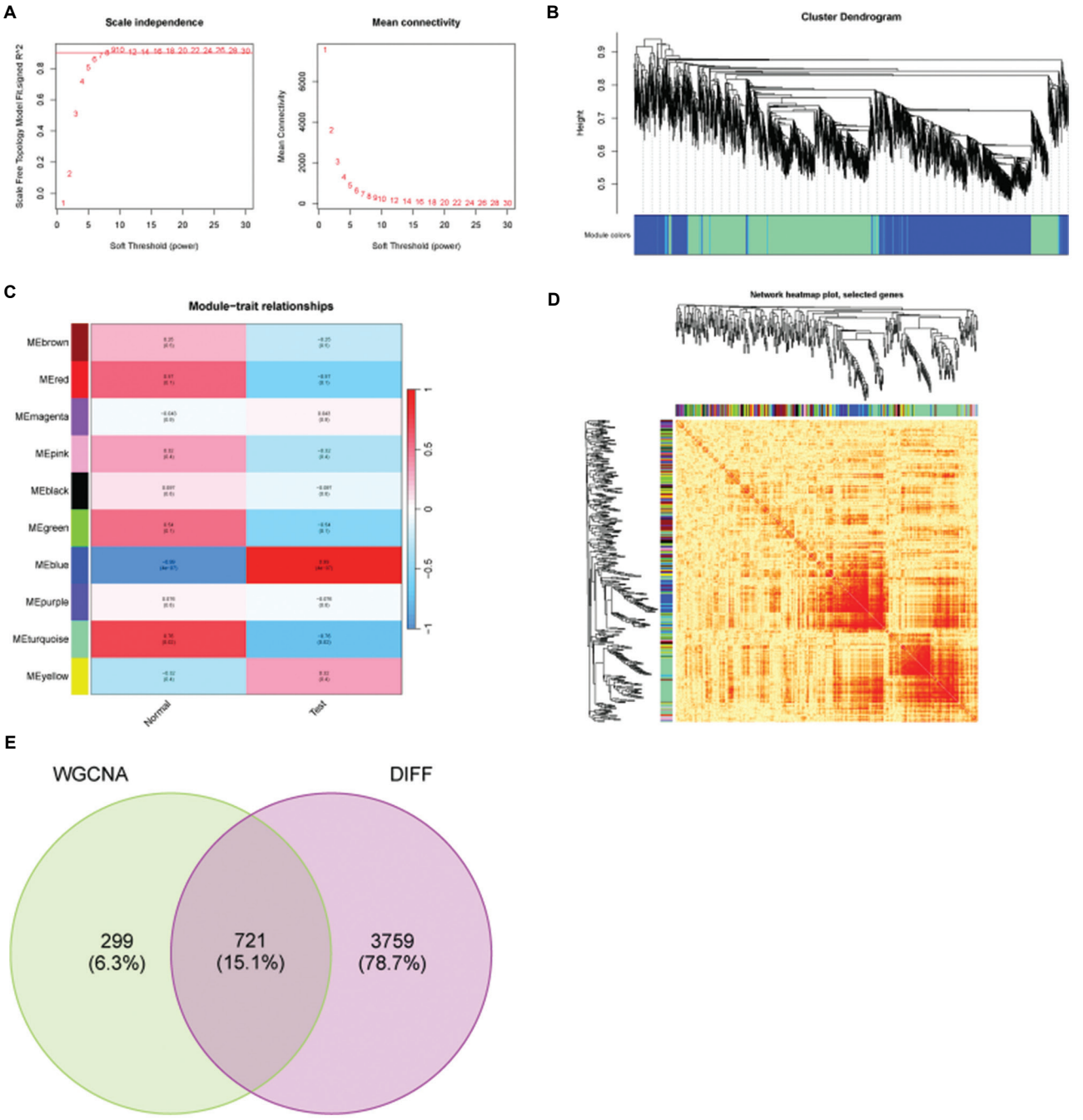


Figure 3. Construction of weighted gene co-expression networks. (A) Scale independence and mean connectivity were used to determine the optimal soft-threshold power. (B) Hierarchical clustering tree dendrogram showing co-expression modules identified by WGCNA. (C) Module-trait relationship heatmap displaying 10 gene modules (y-axis) and clinical modules (x-axis). The numbers in each cell indicate the Pearson's correlation coefficient (r) and the corresponding *p*-value. (D) Heatmap displaying the TOM among all genes. (E) Venn diagrams of 721 DEGs.
Abbreviations: DEGs: Differentially expressed genes; OP: Osteoporosis; TOM: Topological overlap matrices; WGCNA: Weighted Gene Co-expression Network Analysis.

that NUCB1, MTA1, DRAP1, and PCDHGA1 were associated with four, five, one, and two potential therapeutic Chinese medicines, respectively, while PEX19 was not associated with any. Notably, PEX19 was associated with five potential therapeutic Western medicines, as identified through Western medicine screening (Figure 11).

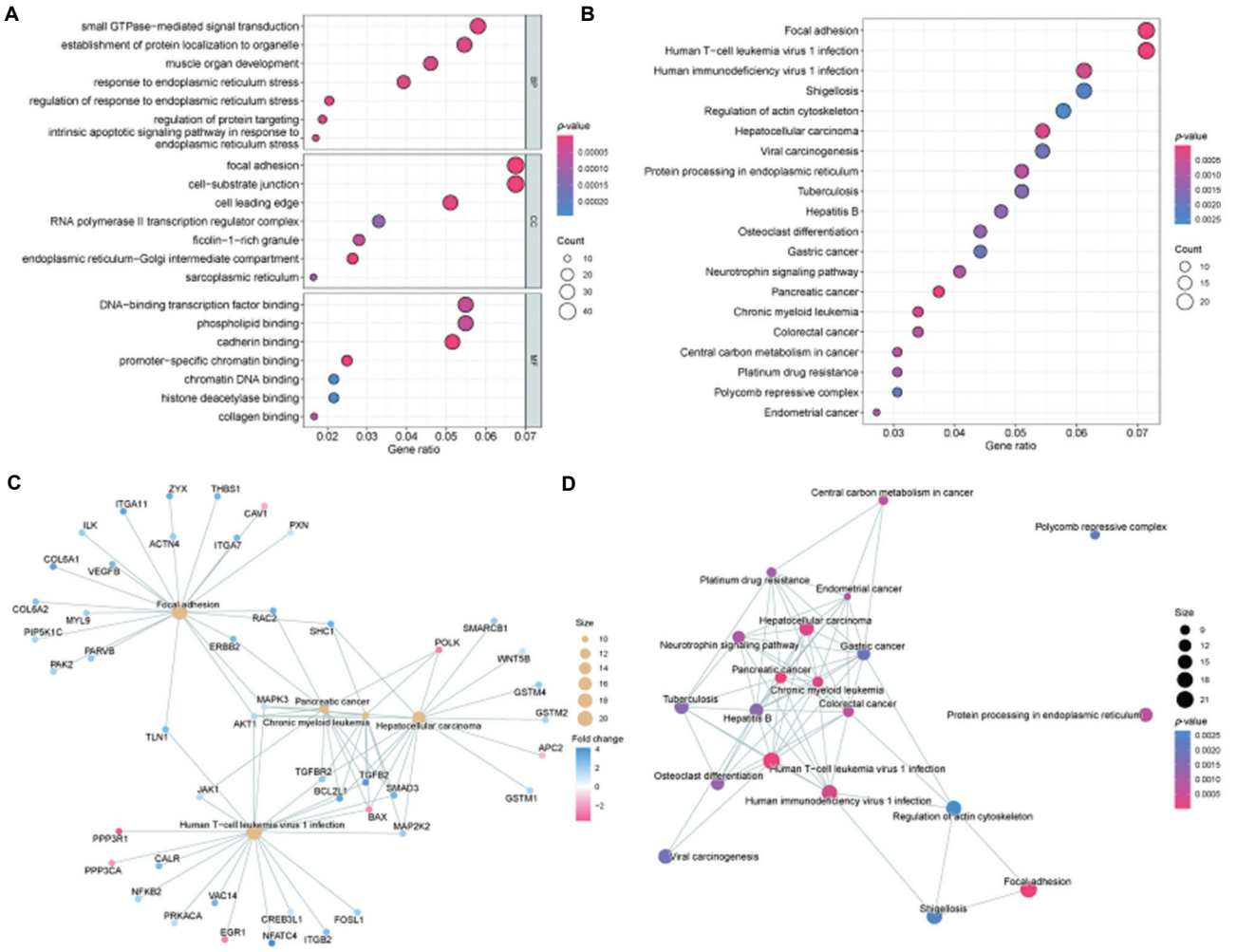


Figure 4. Functional enrichment analysis. (A) GO enrichment analysis of key genes. (B) KEGG pathway enrichment analysis. (C and D) Visualization of KEGG-enriched pathways and the related genes.
Abbreviations: GO: Gene ontology; KEGG: Kyoto encyclopedia of genes and genomes.

4. Discussion

Current diagnostic methods for OP primarily rely on dual-energy X-ray absorptiometry for BMD measurement and clinical fracture risk assessment tools such as FRAX. However, these approaches exhibit limitations, including insufficient sensitivity, high cost, and an inability to detect early-stage bone metabolism imbalances.[20] Moreover, due to the insidious nature of early OP symptoms, delayed intervention can lead to irreversible bone loss and fragility fractures, increasing disability, mortality, and socioeconomic burdens.[11] Consequently, identifying sensitive and specific molecular diagnostic markers is critical for early screening and targeted intervention. In the present study, we integrated WGCNA and LASSO regression to screen transcriptomic data from OP patients, identifying five key genes (*NUCB1*, *PEX19*, *MTA1*, *DRAP1*, and *PCDHGA1*). These genes were significantly upregulated in OP datasets ($p<0.01$) and demonstrated high diagnostic efficacy in ROC curve analysis (AUC > 0.85). While these findings suggest their potential as novel diagnostic biomarkers, the limited sample size (training: $n = 9$; validation: $n = 10$) necessitates further large-scale validation to evaluate possible overfitting.

NUCB1 is a calcium-binding protein predominantly localized in the Golgi apparatus of neurons.[21] It functions as a calcium-dependent guanine nucleotide dissociation inhibitor (GDI) for Gαi1, regulating G-protein-mediated signaling pathways.[22] In addition, NUCB1 modulates the unfolded protein response by inhibiting ATF6 activation, thereby influencing ER stress adaptation.[23] Emerging evidence suggests that dysregulated calcium signaling and ER stress contribute to bone metabolism disorders,

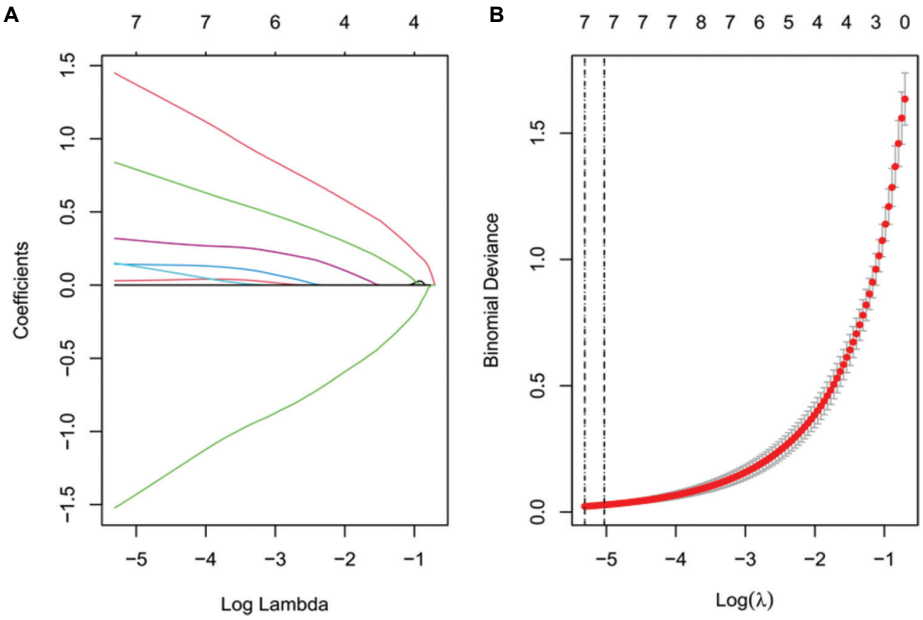


Figure 5. Machine learning screening using LASSO regression model. (A) The coefficient profiles were plotted based on the log (lambda) sequence. (B) A 10-fold CV plot for optimal λ selection.
Abbreviations: CV: Cross-validation; LASSO: Least Absolute Shrinkage and Selection Operator.

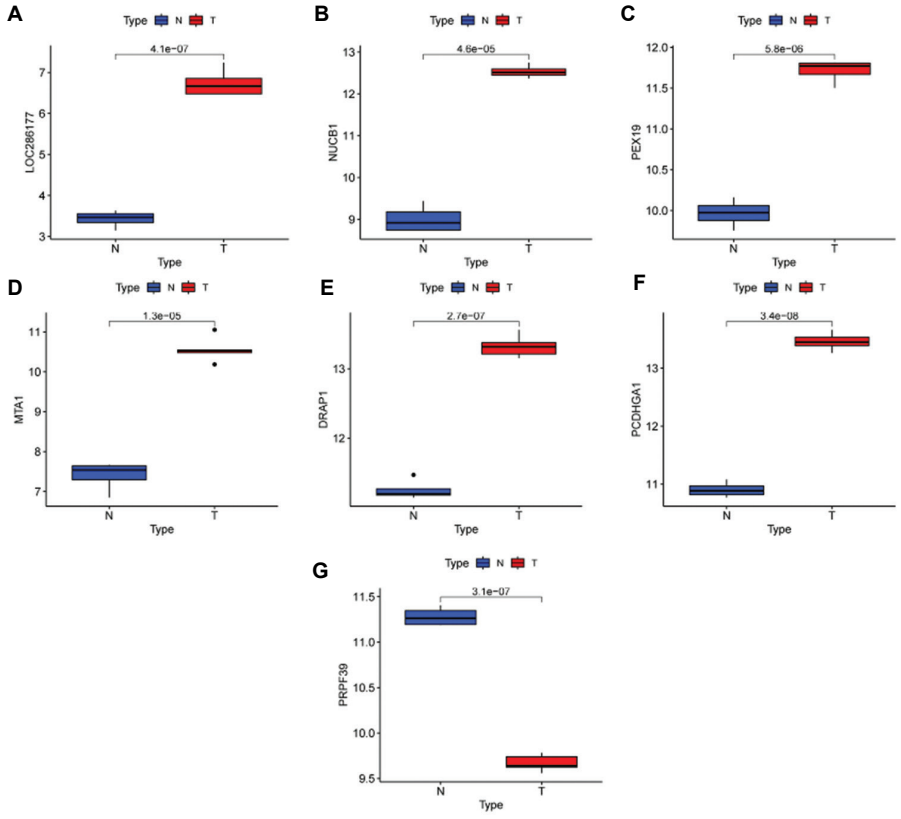


Figure 6. Validation of hub gene expression in the GSE35958 dataset. Differential analysis of (A) LOC286177, (B) NUCB1, (C) PEX19, (D) MTA1, (E) DRAP1, (F) PCDHGA1, and (G) PRPF39 expresison between healthy and OP groups. Group description: N, normal group; T, test group comprising osteoporosis (OP) patients.
Abbreviations: NUCB1: Nucleobindin 1; PEX19: Peroxisomal biogenesis factor 19; MTA1: Metastasis associated 1; DRAP1: DRA aassociated protein 1; PCDHGA1: Protocadherin gamma A1; PRPF39: Pre-mRNA processing factor 39.

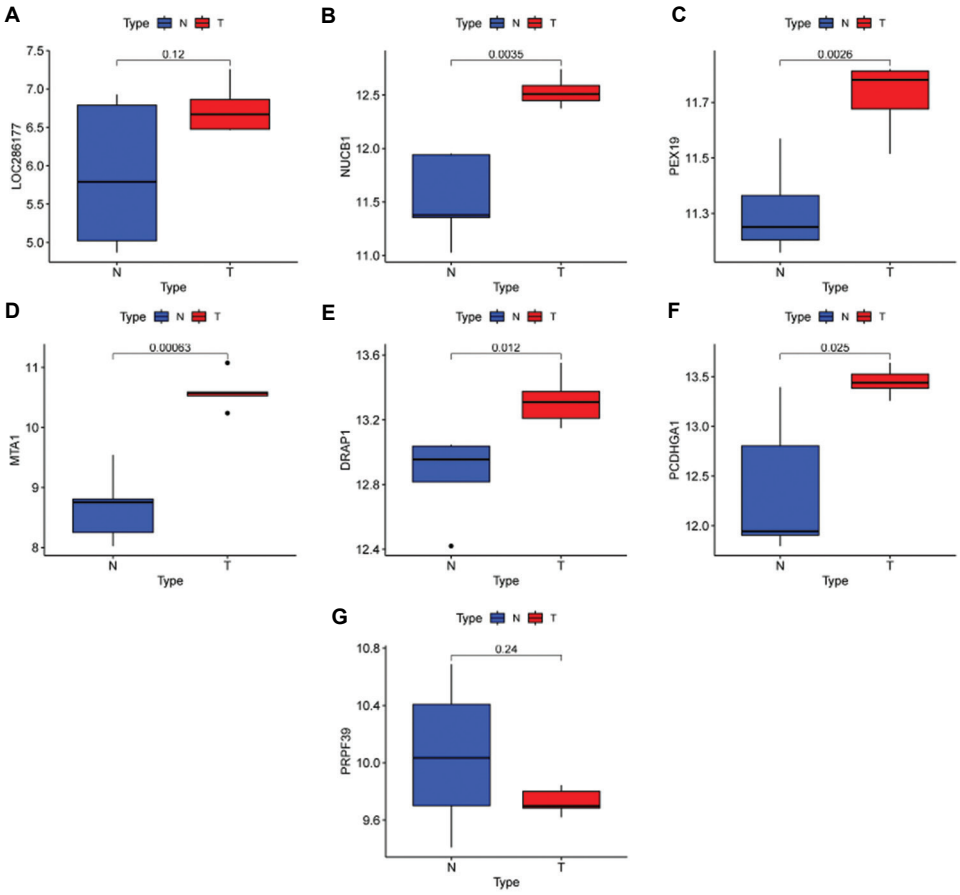


Figure 7. Validation of hub gene expression in an external GSE35956 dataset. Differential analysis of (A) LOC286177, (B) NUCB1, (C) PEX19, (D) MTA1, (E) DRAP1, (F) PCDHGA1, and (G) PRPF39 expresison between healthy and OP groups. Group description: N, normal group; T, test group comprising osteoporosis (OP) patients.
Abbreviations: NUCB1: Nucleobindin 1; PEX19: Peroxisomal biogenesis factor 19; MTA1: Metastasis associated 1; DRAP1: DRA aassociated protein 1; PCDHGA1: Protocadherin gamma A1; PRPF39: Pre-mRNA processing factor 39.

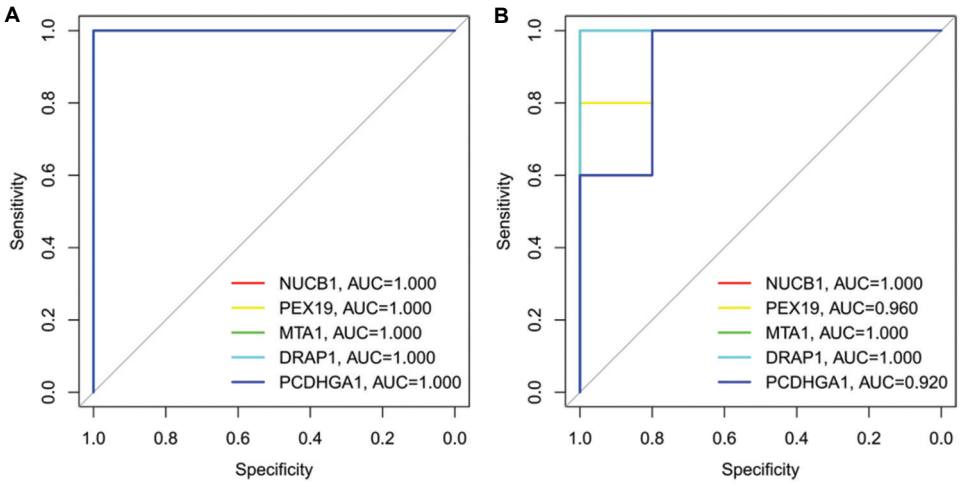


Figure 8. ROC curve analysis. ROC curve evaluating the diagnostic performance of hub genes in the (A) GSE35958 and (B) GSE35956 datasets.
Abbreviations: AUC: Area under the curve; ROC: Receiver operating characteristic.

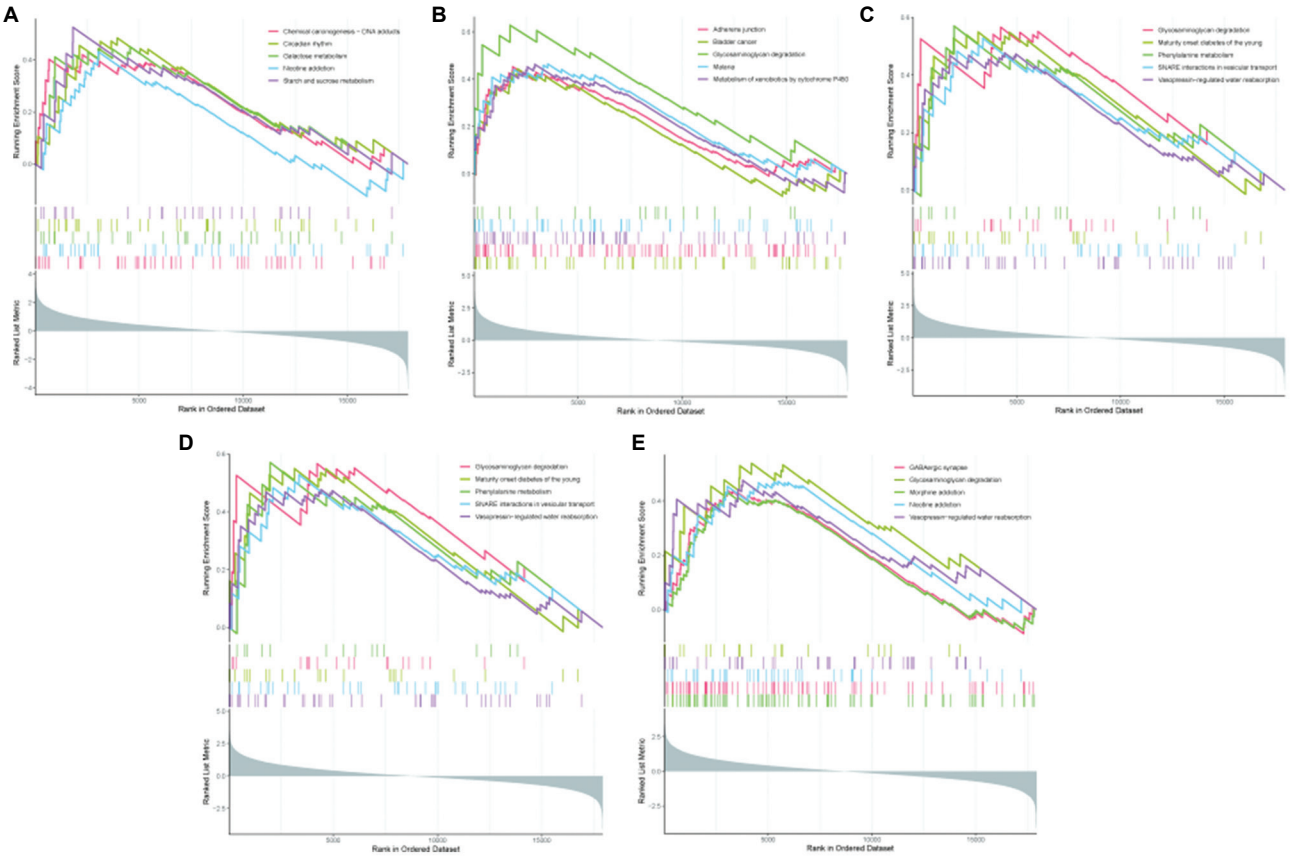


Figure 9. Enrichment results of GSEA to identify the potential pathways that differentiate the healthy and OP groups. Overview of the upper five pathways obtained from GSEA of (A) NUCB1, (B) PEX19, (C) MTA1, (D) DRAP1, and (E) PCDHGA1.
Abbreviations: GSEA: Gene Set Enrichment Analysis; OP: Osteoporosis; NUCB1: Nucleobindin 1; PEX19: Peroxisomal biogenesis factor 19; MTA1: Metastasis associated 1; DRAP1: DRA aassociated protein 1; PCDHGA1: Protocadherin gamma A1; PRPF39: Pre-mRNA processing factor 39.

including OP.[24,25] Although NUCB1 has not been directly linked to bone remodeling, its role in calcium homeostasis and stress response pathways raises the possibility of its involvement in osteoclast/osteoblast regulation. Further studies are required to determine whether NUCB1-mediated calcium signaling or ER stress modulation affects bone mineralization processes.

PEX19 is an essential chaperone for peroxisome membrane assembly and protein import, critical for peroxisome biogenesis.[26] Recent studies have demonstrated that PEX19 deficiency impairs peroxisomal β-oxidation of very-long-chain fatty acids, resulting in intracellular lipid accumulation and excessive reactive oxygen species (ROS) generation.[27] Emerging evidence indicates that ROS promote osteoclast differentiation and enhance bone resorption activity,[28] suggesting that PEX19 dysfunction may contribute to OP through ROS-mediated osteoclast activation. Furthermore, impaired peroxisomal metabolism may reduce endogenous fatty acid availability, potentially compromising osteoblast bioenergetics and bone formation.[29]

MTA1 is a core component of the nucleosome remodeling and histone deacetylation complex, which regulates gene expression through histone deacetylation (HDAC) modification.[30] HDAC plays an important role in regulating osteogenic differentiation and bone formation in bone marrow stromal cells,[31] which may provide research clues for MTA1 to activate osteoclastogenesis through epigenetic inhibition of osteogenic differentiation. In addition, modern studies have found that MTA1 can be involved in mediating the inactivation of the Wnt/β-catenin pathway,[32] and the imbalance of the Wnt/β-catenin pathway is closely related to the occurrence and development of OP,[33] which may also be a potential mechanism of MTA1-mediated OP.

DRAP1 is a transcriptional coregulator that forms a functional complex with DR1 to modulate gene expression programs.[34] Recent mechanistic studies revealed that the DRAP1/DR1 complex potentiates mTOR signaling activity, thereby promoting tumor progression and influencing therapeutic responses in triple-negative

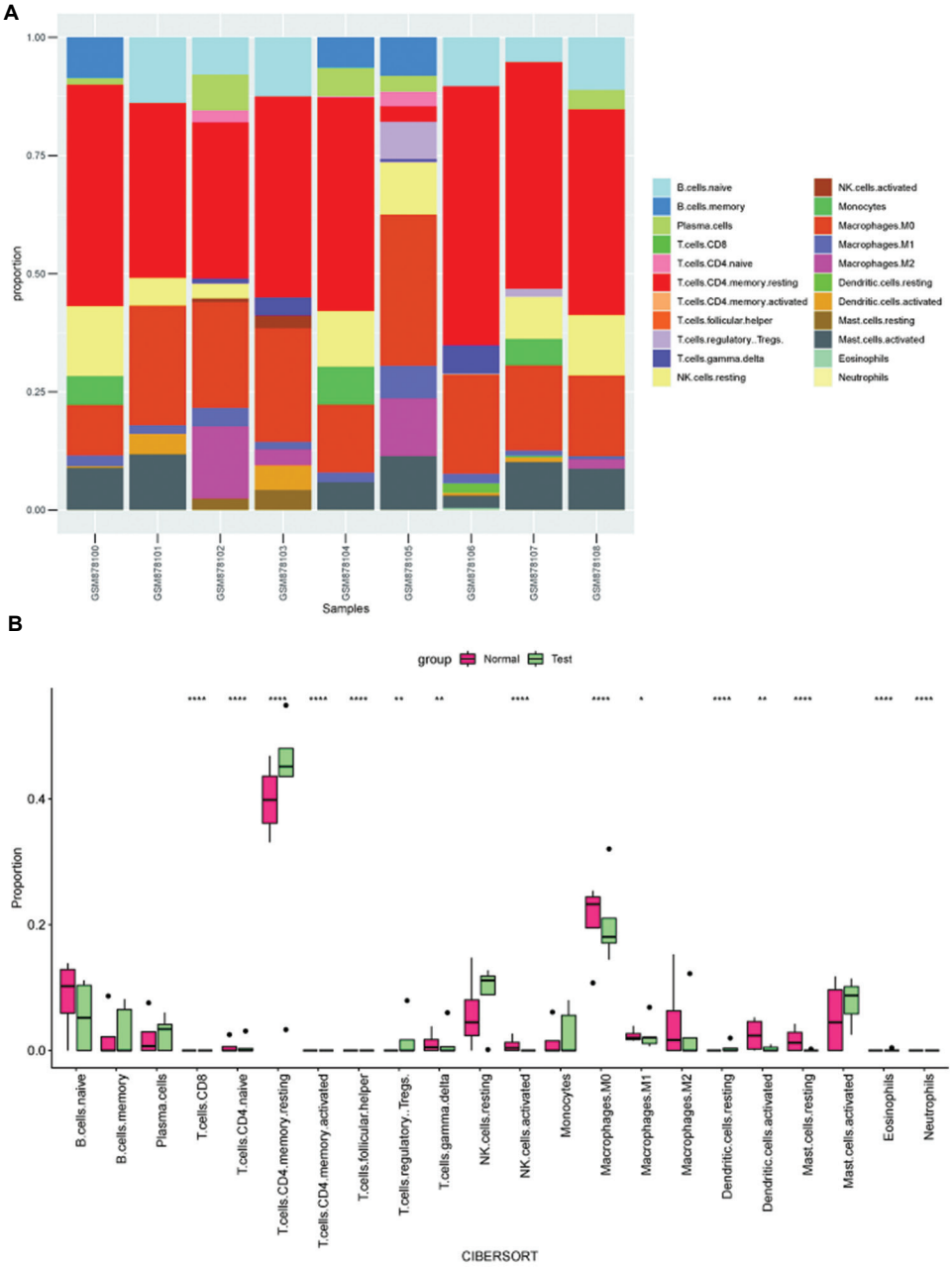


Figure 10. Immune infiltration analysis. (A) The bar plot showing the content of immune cell subsets in the OP and the control groups. Different colors represent different immune cell types. (B) Box plot showing the different distribution of immune cells between the OP and control groups.
Abbreviation: OP: Osteoporosis.

breast cancer.[34] The mTOR pathway is known to regulate fundamental cellular processes, including autophagy and mitophagy,[35] which are critically involved in maintaining bone homeostasis. Evidence from bone biology research demonstrates that mTOR signaling coordinates osteoblast-mediated bone formation and osteoclast-mediated bone resorption.[35] While these findings suggest a potential regulatory role for DRAP1 in bone metabolism through mTOR pathway modulation, direct experimental evidence establishing this connection remains to be documented.

PCDHGA1, a neural cadherin family member, mediates calcium-dependent cell adhesion.[36] Recent studies identified its expression in osteoblasts and its association with mineralization capacity.[37] Genetic analyses have linked protocadherin loci to BMD variations.[38]

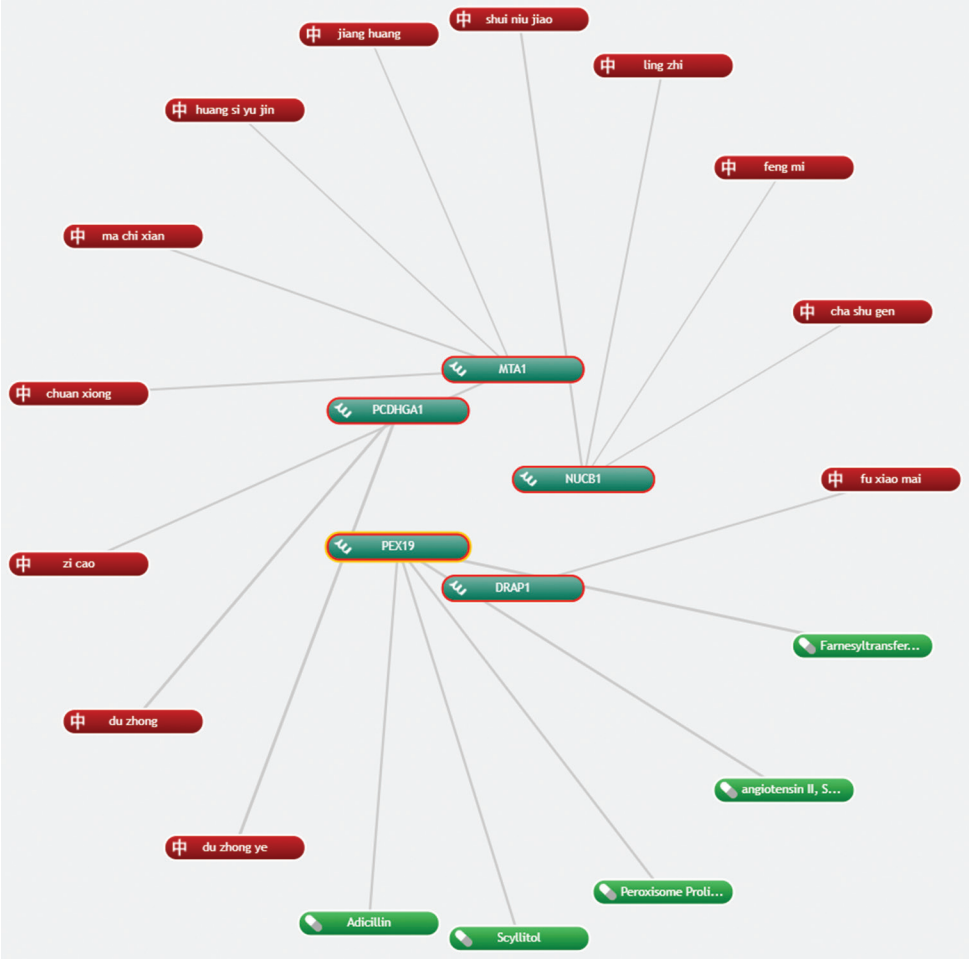


Figure 11. Potential targeted drug prediction and core components identification. Dark green boxes represent biomarkers; red boxes represent potentially therapeutic herbal medicines; green boxes represent potentially therapeutic Western medicines.

While these findings suggest PCDHGA1 involvement in bone metabolism, direct evidence for its role in OP pathogenesis remains unavailable. Future studies should characterize its function in bone remodeling and examine potential interactions with osteogenic pathways.

The present study has several limitations that should be considered. First, the exclusive reliance on computational analyses of public datasets (GSE35958: n = 9; GSE35956: n = 10) without wet laboratory or clinical validation represents a significant constraint. Second, the small sample sizes may compromise the statistical power and generalizability of the identified biomarkers (NUCB1, PEX19, MTA1, DRAP1, PCDHGA1). Third, the transcriptomic focus precluded integration with proteomic or metabolomic data, limiting systems-level understanding. Despite these limitations, this work provides the first computational evidence for these five biomarkers in OP diagnosis. To address these gaps, we propose a three-phase validation roadmap: (1) *in vitro* functional validation using osteoblast/osteoclast cultures to assess biomarker roles in bone remodeling; (2) preclinical validation in OP animal models with longitudinal biomarker monitoring; and (3) clinical validation through prospective cohort studies measuring biomarker performance against gold-standard diagnostics. These studies should be complemented by multiomics integration to elucidate the biomarkers' mechanistic pathways and regulatory networks.

5. Conclusion

This study identifies NUCB1, PEX19, MTA1, DRAP1, and PCDHGA1 as potential diagnostic biomarkers for OP through integrative bioinformatics and machine learning. These genes, found to be upregulated in OP and linked to ER stress, Wnt/β-catenin signaling, and immune dysregulation, and they demonstrate strong diagnostic accuracy (AUC > 0.85). Immune infiltration analysis further supports their role in OP-associated microenvironmental changes. While computational predictions suggest therapeutic

candidates, further experimental and clinical validation is essential to confirm their mechanistic roles and translational value. These findings provide potential directions for developing diagnostic and therapeutic strategies for OP.

Acknowledgments

None.

Funding

None.

Conflict of interest

The authors declare they have no competing interests.

Author contributions

Conceptualization: Farra Aidah Jumuddin
Formal analysis: Zarina Awang
Investigation: Cuicui Zhou
Methodology: Cuicui Zhou, Farra Aidah Jumuddin
Writing–original draft: Cuicui Zhou
Writing–review & editing: Cuicui Zhou, Zarina Awang

Ethics approval and consent to participate

Not applicable.

Consent for publication

Not applicable.

Availability of data

Data is available from the corresponding author upon reasonable request.

References

1. Gómez O, Talero AP, Zanchetta MB, *et al*. Diagnostic, treatment, and follow-up of osteoporosis-position statement of the Latin American federation of endocrinology. *Arch Osteoporos.* 2021;16(1):114.

   doi: 10.1007/s11657-021-00974-x

2. Gao S, Zhao Y. Quality of life in postmenopausal women with osteoporosis: A systematic review and meta-analysis. *Qual Life Res.* 2023;32(6):1551-1565.

   doi: 10.1007/s11136-022-03281-1

3. Compston JE, McClung MR, Leslie WD. Osteoporosis. *Lancet.* 2019;393(10169):364-376.

   doi: 10.1016/s0140-6736(18)32112-3

4. Clynes MA, Harvey NC, Curtis EM, Fuggle NR, Dennison EM, Cooper C. The epidemiology of osteoporosis. *Br Med Bull.* 2020;133(1):105-117.

   doi: 10.1093/bmb/ldaa005

5. Wu D, Cline-Smith A, Shashkova E, Perla A, Katyal A, Aurora R. T-cell mediated inflammation in postmenopausal osteoporosis. *Front Immunol.* 2021;12:687551.

   doi: 10.3389/fimmu.2021.687551

6. Fischer V, Haffner-Luntzer M. Interaction between bone and immune cells: Implications for postmenopausal osteoporosis. *Semin Cell Dev Biol.* 2022;123:14-21.

   doi: 10.1016/j.semcdb.2021.05.014

7. Tyagi AM, Srivastava K, Mansoori MN, Trivedi R, Chattopadhyay N, Singh D. Estrogen deficiency induces the differentiation of IL-17 secreting Th17 cells: A new candidate in the pathogenesis of osteoporosis. *PLoS One.* 2012;7(9):e44552.

   doi: 10.1371/journal.pone.0044552

8. Management of osteoporosis in postmenopausal women: The 2021 position statement of The North American menopause society. *Menopause.* 2021;28(9):973-997.

   doi: 10.1097/gme.0000000000001831

9. Reid IR. Vitamin D effect on bone mineral density and fractures. *Endocrinol Metab Clin North Am.* 2017;46(4):935-945.

   doi: 10.1016/j.ecl.2017.07.005

10. Weaver CM, Gordon CM, Janz KF, *et al*. The national osteoporosis foundation's position statement on peak bone mass development and lifestyle factors: A systematic review and implementation recommendations. *Osteoporos Int.* 2016;27(4):1281-1386.

    doi: 10.1007/s00198-015-3440-3

11. LeBoff MS, Greenspan SL, Insogna KL, *et al*. The clinician's guide to prevention and treatment of osteoporosis. *Osteoporos Int.* 2022;33(10):2049-2102.

    doi: 10.1007/s00198-021-05900-y

12. Johnston CB, Dagar M. Osteoporosis in older adults. *Med Clin North Am.* 2020;104(5):873-884.

    doi: 10.1016/j.mcna.2020.06.004

13. Eastell R, Szulc P. Use of bone turnover markers in postmenopausal osteoporosis. *Lancet Diabetes Endocrinol.* 2017;5(11):908-923.

    doi: 10.1016/s2213-8587(17)30184-5

14. Li H, Xiao Z, Quarles LD, Li W. Osteoporosis: Mechanism, molecular target and current status on drug development. *Curr Med Chem.* 2021;28(8):1489-1507.

    doi: 10.2174/0929867327666200330142432

15. Lo HJ, Tsai CH, Huang TW. Apoptosis-associated genetic mechanisms in the transition from rheumatoid arthritis to osteoporosis: A bioinformatics and functional analysis approach. *APL Bioeng.* 2024;8(4):046107.

    doi: 10.1063/5.0233961

16. Xu M, Zhou H, Hu P, *et al*. Identification and validation of immune and oxidative stress-related diagnostic markers for diabetic nephropathy by WGCNA and machine learning. *Front Immunol.* 2023;14:1084531.

doi: 10.3389/fimmu.2023.1084531

17. Jiang F, Zhou H, Shen H. Identification of critical biomarkers and immune infiltration in rheumatoid arthritis based on WGCNA and LASSO algorithm. *Front Immunol.* 2022;13:925695.

doi: 10.3389/fimmu.2022.925695

18. Wang T, Dai L, Shen S, *et al*. Comprehensive molecular analyses of a macrophage-related gene signature with regard to prognosis, immune features, and biomarkers for immunotherapy in hepatocellular carcinoma based on WGCNA and the LASSO algorithm. *Front Immunol.* 2022;13:843408.

doi: 10.3389/fimmu.2022.843408

19. Liu F, Huang Y, Liu F, Wang H. Identification of immune-related genes in diagnosing atherosclerosis with rheumatoid arthritis through bioinformatics analysis and machine learning. *Front Immunol.* 2023;14:1126647.

doi: 10.3389/fimmu.2023.1126647

20. Carey JJ, Chih-Hsing Wu P, Bergin D. Risk assessment tools for osteoporosis and fractures in 2022. *Best Pract Res Clin Rheumatol.* 2022;36(3):101775.

doi: 10.1016/j.berh.2022.101775

21. Tulke S, Williams P, Hellysaz A, Ilegems E, Wendel M, Broberger C. Nucleobindin 1 (NUCB1) is a golgi-resident marker of neurons. *Neuroscience.* 2016;314:179-188.

doi: 10.1016/j.neuroscience.2015.11.062

22. Kapoor N, Gupta R, Menon ST, Folta-Stogniew E, Raleigh DP, Sakmar TP. Nucleobindin 1 is a calcium-regulated guanine nucleotide dissociation inhibitor of G{alpha}i1. *J Biol Chem.* 2010;285(41):31647-31660.

doi: 10.1074/jbc.M110.148429

23. Tsukumo Y, Tomida A, Kitahara O, *et al*. Nucleobindin 1 controls the unfolded protein response by inhibiting ATF6 activation. *J Biol Chem.* 2007;282(40):29264-29272.

doi: 10.1074/jbc.M705038200

24. Proudfoot D. Calcium signaling and tissue calcification. *Cold Spring Harb Perspect Biol.* 2019;11(10):a035303.

doi: 10.1101/cshperspect.a035303

25. Li HJ, Goff A, Rudzinskas SA, *et al*. Altered estradiol-dependent cellular Ca^{2+} homeostasis and endoplasmic reticulum stress response in premenstrual dysphoric disorder. *Mol Psychiatry.* 2021;26(11):6963-6974.

doi: 10.1038/s41380-021-01144-8

26. Agrawal G, Shang HH, Xia ZJ, Subramani S. Functional regions of the peroxin Pex19 necessary for peroxisome biogenesis. *J Biol Chem.* 2017;292(27):11547-11560.

doi: 10.1074/jbc.M116.774067

27. Sarkar C, Lipinski MM. Role and function of peroxisomes in neuroinflammation. *Cells.* 2024;13(19):1655.

doi: 10.3390/cells13191655

28. Agidigbi TS, Kim C. Reactive oxygen species in osteoclast differentiation and possible pharmaceutical targets of ROS-mediated osteoclast diseases. *Int J Mol Sci.* 2019;20(14):3576.

doi: 10.3390/ijms20143576

29. Nandy A, Helderman RCM, Thapa S, *et al*. Lipolysis supports bone formation by providing osteoblasts with endogenous fatty acid substrates to maintain bioenergetic status. *Bone Res.* 2023;11(1):62.

doi: 10.1038/s41413-023-00297-2

30. Li DQ, Pakala SB, Nair SS, Eswaran J, Kumar R. Metastasis-associated protein 1/nucleosome remodeling and histone deacetylase complex in cancer. *Cancer Res.* 2012;72(2):387-394.

doi: 10.1158/0008-5472.Can-11-2345

31. Wang J, Wang CD, Zhang N, *et al*. Mechanical stimulation orchestrates the osteogenic differentiation of human bone marrow stromal cells by regulating HDAC1. *Cell Death Dis.* 2016;7(5):e2221.

doi: 10.1038/cddis.2016.112

32. Lu Y, Wei C, Xi Z. Curcumin suppresses proliferation and invasion in non-small cell lung cancer by modulation of MTA1-mediated Wnt/β-catenin pathway. *In Vitro Cell Dev Biol Anim.* 2014;50(9):840-850.

doi: 10.1007/s11626-014-9779-5

33. Gao Y, Chen N, Fu Z, Zhang Q. Progress of wnt signaling pathway in osteoporosis. *Biomolecules.* 2023;13(3):483.

doi: 10.3390/biom13030483

34. Huang MY, Hu SY, Dong J, *et al*. The DRAP1/DR1 repressor complex increases mTOR activity to promote progression and confer everolimus sensitivity in triple-negative breast cancer. *Cancer Res.* 2024;84(16):2660-2673.

doi: 10.1158/0008-5472.Can-23-2781

35. Wang S, Deng Z, Ma Y, *et al*. The role of autophagy and mitophagy in bone metabolic disorders. *Int J Biol Sci.* 2020;16(14):2675-2691.

doi: 10.7150/ijbs.46627

36. Wu Q, Maniatis T. A striking organization of a large family of human neural cadherin-like cell adhesion genes. *Cell.* 1999;97(6):779-790.

doi: 10.1016/s0092-8674(00)80789-8

37. Guan M, Pan D, Zhang M, Leng X, Yao B. The aqueous extract of eucommia leaves promotes proliferation, differentiation,

and mineralization of osteoblast-like MC3T3-E1 cells. *Evid Based Complement Alternat Med*. 2021;2021:3641317.

doi: 10.1155/2021/3641317

38. Estrada K, Styrkarsdottir U, Evangelou E, *et al*. Genome-wide meta-analysis identifies 56 bone mineral density loci and reveals 14 loci associated with risk of fracture. *Nat Genet*. 2012;44(5):491-501.

doi: 10.1038/ng.2249

ACCSCIENCE PUBLISHING

Eurasian Journal of Medicine and Oncology

ORIGINAL RESEARCH ARTICLE

Efficacy of preperitoneal local anesthetic infiltration on post-operative analgesia following laparoscopic cholecystectomy

Noha Mohamed Abdelwahab Elsaid[1]*, Ain El-Marwa Abdelmonem Abdallah Hassan[1], Ahmed Mohamed Said[2], Mostafa R. Bakry[3], Doaa Mohamed Almonayery Ibrahim[1], Marwa Ibrahim Eid[1], Hayam Shaaban Soliman Morsy[4], Mostafa Mohamed Elsayed[1], Nashwa Mohammed Ibrahiem[1], Gihan Eissa Zahran[1], Nahla Mohammed Eldeeb[1], Mayada Yahia Elbohouty[1], Heba Atwa Ahmed Atwa[2], Gehan Abd Elrhman Eldesoky[1], Eman A. Salem[1], Samia Sayed Ahmed[1], Warda Demerdash Khalifa Ali[4], and Tarek Abdelmonem Abdelzaher[5]

[1]Department of Anesthesia, ICU and Pain Management, Faculty of Medicine, Al-Azhar University, Cairo, Egypt

[2]Department of General Surgery, Faculty of Medicine, Al-Azhar University, Cairo, Egypt

[3]Department of Reproductive Medicine and IVF, Dar-Al Nokhba Infertility and IVF Center, Cairo, Egypt

[4]Department of Anesthesia, ICU and Pain Management, Faculty of Medicine, Al-Azhar University, Assiut, Egypt

[5]Department of Anesthesia, ICU and Pain Management, Faculty of Medicine, Minia University, Minia, Egypt

***Corresponding author:**
Noha Mohamed Abdelwahab Elsaid (nohamohamed.medg@azhar.edu.eg)

Citation: Elsaid NMA, Hassan AAA, Said AM, *et al*. Efficacy of preperitoneal local anesthetic infiltration on post-operative analgesia following laparoscopic cholecystectomy. *Eurasian J Med Oncol*. 2025;9(3):277-286. doi: 10.36922/EJMO025180164

Received: May 2, 2025

Revised: June 7, 2025

Accepted: August 1, 2025

Published online: September 23, 2025

Copyright: © 2025 Author(s). This is an Open-Access article distributed under the terms of the Creative Commons Attribution License, permitting distribution, and reproduction in any medium, provided the original work is properly cited.

Publisher's Note: AccScience Publishing remains neutral with regard to jurisdictional claims in published maps and institutional affiliations.

Abstract

Introduction: Post-operative pain significantly impairs recovery, delaying hospital discharge after laparoscopic cholecystectomy. Effective pain management facilitates early ambulation, which diminishes the probability of post-operative complications.
Objective: This study compares the analgesic efficacy of preperitoneal bupivacaine infiltration with dexamethasone and the transversus abdominis plane (TAP) block.
Methods: This prospective, randomized, double-blinded study included 40 patients undergoing laparoscopic cholecystectomy. Group 1 (n = 20) received a TAP block, while Group 2 (n = 20) received preperitoneal bupivacaine for analgesia. The primary outcomes were (i) the level of post-operative pain, assessed using the Visual Analog Scale every 15 min in the 1st post-operative hour, at 2-h intervals up to 12 h, and at 6-h intervals up to 24 h; (ii) time to first request for rescue analgesia; and (iii) the total dose of analgesia. Secondary outcomes included patient-reported sleep quality and the incidence of post-operative nausea and vomiting.
Results: The study found that the TAP block provided superior post-operative pain relief compared to preperitoneal infiltration with bupivacaine in patients who underwent laparoscopic cholecystectomy. The TAP block group exhibited significantly lower pain scores at 8 and 12 h postoperatively and experienced a delayed first request for rescue analgesia at 14.6 ± 2.52 h on average, compared with 7.1 ± 1.02 h in the preperitoneal group.
Conclusion: The findings establish that TAP block is a more effective analgesic technique than preperitoneal infiltration with bupivacaine for managing post-operative pain in laparoscopic cholecystectomy. Patients receiving TAP block

required fewer opioids, had delayed onset of rescue analgesia, and reported lower pain scores at critical post-operative intervals.

Keywords: Transversus abdominis plane block; Preperitoneal space; Cholecystectomy; Analgesia

1. Introduction

Laparoscopic cholecystectomy is a commonly performed procedure, typically associated with a short post-operative hospital stay.[1] Although laparoscopic cholecystectomy operations result in less post-operative pain than open cholecystectomy operations, severe and moderate pain are the most common concerns, particularly during the first 24 h. A critical objective for early hospital discharge is implementing appropriate pain management.[2] In general, multimodal analgesic techniques, such as intravenous patient-controlled analgesia and thoracic epidural analgesia, are implemented to mitigate pain.[3] A regional nerve blockade method known as the transversus abdominis plane (TAP) block, which has recently acquired popularity, is now a frequently used multimodal approach element in post-operative pain management.[4]

The TAP block is a regional anesthesia technique that involves injecting local anesthetics into the TAP, located between the transversus abdominis and internal oblique muscles. This technique has gained popularity due to its effectiveness in reducing post-operative pain and opioid consumption, particularly when ultrasound guidance is used to enhance precision. Studies have demonstrated that TAP block significantly prolongs the duration of analgesia, delaying the first request for rescue analgesia and improving overall patient comfort. However, its primary limitation is its inability to provide visceral pain relief, as it primarily targets somatic pain from the abdominal wall. In addition, its efficacy is highly operator-dependent, requiring technical expertise and ultrasound guidance for optimal results.[5]

Preperitoneal infiltration involves the administration of local anesthetics into the preperitoneal space, effectively targeting nociceptive pathways to reduce post-operative pain. This technique offers several advantages, including ease of administration under direct laparoscopic visualization and reduced dependence on specialized equipment like ultrasound. Furthermore, preperitoneal infiltration can minimize opioid requirements, thereby reducing the incidence of opioid-related side effects such as post-operative nausea and vomiting (PONV) and sedation. However, its analgesic duration is shorter than the TAP block, often necessitating earlier rescue analgesia. In addition, the potential risk of inadvertent intraperitoneal injection or inconsistent drug spread may limit its effectiveness.[6,7]

Both TAP block and preperitoneal infiltration are associated with minimal complications. TAP block has been reported to have a favorable safety profile, with rare but potential risks including inadvertent needle injury to adjacent structures such as the liver or bowel. In addition, improper administration may result in incomplete analgesia or block failure. Preperitoneal infiltration, a simpler technique, carries a lower risk of technical complications but may be less effective in managing pain at later post-operative stages.[8]

This study compares the analgesic efficacy of preperitoneal infiltration with bupivacaine and dexamethasone and the TAP block in patients undergoing laparoscopic cholecystectomy. This comparison is based primarily on post-operative pain scores (Visual Analog Scale [VAS]) and the time for first request for rescue analgesia, which are critical metrics for evaluating pain management strategies.

2. Methodology

This randomized, prospective, double-blinded study was performed at the Department of Anesthesia and General Surgery of Al-Zahraa University Hospital and Minia University Hospital, Egypt. This study was approved by the Institutional Review Board and the Ethical Committee of the Faculty of Medicine for Girls, Al-Azhar University (Approval Number 1784/2023), and additionally by the Institutional Review Board of Minia University Hospital, according to the WMA Declaration of Helsinki. It was approved by the Ethical Committee of Al-Azhar Faculty of Medicine. The study was conducted for 6 months from February 2023 to August 2023. The trial was filed at the Pan African Clinical Trial Registry (pactr.samrc.ac.za) database (PACTR202504865598437).

The participants were informed of the study's objectives and instruments. This investigation was conducted with the approval of the institutional review board of the Faculty of Medicine for Girls Al-Azhar University (1784/2023).

The study was voluntary, and each participant had to provide informed written consent before enrollment. Each

participant was entitled to decline participation or resign from the study at any time without providing a rationale or affecting their right to medical care. In addition, participants' confidentiality was guaranteed through anonymous and coded data.

2.1. Inclusion criteria

The study included adult patients undergoing elective laparoscopic cholecystectomy. Participants were required to have normal laboratory parameters, including a complete blood count, coagulation profile, and normal liver and kidney function. They had to meet the American Society of Anesthesiologists' physical status classification of I or II and be willing to provide informed consent.

2.2. Exclusion criteria

Patients who refused and those with a history of allergic reactions to local anesthetic drugs, a history of chronic pain, a history of drug addiction, and those who had undergone complicated surgery were excluded from the study.

Complicated surgery refers to laparoscopic cholecystectomy procedures involving additional challenges beyond standard conditions, such as severe intra-abdominal adhesions, conversion to open surgery, significant bleeding requiring transfusion, and difficult anatomical variations that prolong operative time.[9] These cases were excluded to ensure homogeneity and minimize variables that could affect post-operative outcomes.

2.3. Randomization and blinding

The study employed a prospective, randomized, double-blind design. Using a computer-generated randomization sequence, participants were randomly allocated into two equal groups (TAP block or preperitoneal infiltration). Allocation concealment was maintained using sealed, opaque envelopes opened only by a designated team member uninvolved in patient care. Both patients and outcome assessors were blinded to group allocation. The anesthesiologist administering the block and the surgeon performing the infiltration were aware of the allocation but did not participate in outcome assessment, ensuring unbiased data collection.

Although the study is described as "double-blind," it is important to clarify that the blinding was maintained between the patients and the outcome assessors, not the surgical or anesthesia team. The surgeon and anesthesiologist were necessarily unblinded due to the nature of the interventions—TAP block and preperitoneal infiltration—which require direct procedural knowledge and expertise.

However, to minimize bias, outcome assessors (those collecting VAS scores, analgesic use, and post-operative metrics) were blinded to group assignment, and patients were unaware of their group allocation.

2.4. Allocation concealment

Allocation concealment was ensured via sealed opaque envelopes, and the treatment was administered by personnel not involved in outcome measurement. Forty adult cases had a laparoscopic cholecystectomy. The patients were randomly allocated into two equal groups.

2.4.1. TAP block group

The group was given a bilateral ultrasound-guided TAP block with 18 mL of the local anesthetic 0.25% bupivacaine and 8 mg of dexamethasone (total volume 20 mL).

2.4.2. Preperitoneal group

The group was preoperatively injected with local anesthetic through a preperitoneal local instillation of 18 mL of the local anesthetic 0.25% bupivacaine and 8 mg of dexamethasone (total volume 20 mL).

Preoperatively, laboratory investigations, such as a complete blood profile, coagulation profile, liver and kidney function, and age and weight, were conducted for all patients as part of their routine preoperative investigations. The patient had been fasting for 8 h before the procedure.

Patients enrolled were advised to have a fasting period of at least 8 h before surgery. All patients were given 8 mg of intravenous ondansetron 15 min before surgery, before the induction of anesthesia. Standard monitoring included pulse oximetry (Drager Fabius plus monitor, Drager Medical System, Inc., United States), electrocardiography, and non-invasive blood pressure measurement. General anesthesia was induced after 3 min of preoxygenation by intravenous injection of 1–2 μg/kg fentanyl (Sunny Pharmaceutical, Egypt), 2–3 mg/kg of propofol (B. Braun, Germany), and an induction dose of 0.5 mg/kg of atracurium (Sunny Pharmaceutical, Egypt). An endotracheal tube was inserted, and volume-controlled mechanical ventilation was initiated.

Anesthesia was maintained with sevoflurane 2% with controlled mechanical ventilation with 3L of oxygen and a maintenance dose of 0.1 mg/kg of atracurium. Positive pressure ventilation was initiated with an 8 mL/kg tidal volume and an altered respiratory rate to preserve end-tidal carbon dioxide between 45 and 35 mmHg. Baseline heart rate and mean arterial pressure measurements were documented and recorded every 10 min.

The surgery was conducted under general anesthesia by a single general surgeon, who adhered to a standardized

surgical approach. The intra-abdominal pressure was kept at 12 mm Hg for all cases. Before skin incision, the procedure was performed in the operating room using a fully aseptic technique.

For the TAP block group, a unilateral TAP block was performed on the surgery site utilizing 18 mL of 0.25% bupivacaine and 8 mg of dexamethasone (total volume of 20 mL) through a midaxillary approach under ultrasound guidance. The probe was positioned transversely between the costal margin and the iliac crest. The 22-G echogenic spinal needle, which was 8 cm long, was advanced in-plane. After the needle point reached the plane, the correct placement was confirmed by instilling 2 mL of anesthetic solution to view the hydrodissection. Subsequently, the entire drug volume was administered, resulting in the formation of a meniscus between the planes. To minimize operator variability, all TAP blocks were performed by the same consultant anesthesiologist with over 5 years of experience in ultrasound-guided regional anesthesia.

Preperitoneal infiltration was performed immediately after induction of general anesthesia. The procedure was performed under laparoscopic visualization after insertion of trocars and carbon dioxide gas insufflation. Digital pressure was applied to identify the injection site, and a blind injection was then performed, advancing the needle inserted until its tip was visible at the peritoneum. The needle was then withdrawn gently for about 0.5 cm, and the local anesthetic was injected. The surgeon administered 18 mL of 8 mg dexamethasone and 0.25% bupivacaine (total volume 20 mL) under laparoscopic vision.

To ensure that no intraperitoneal injections were administered, the injection site within the peritoneal cavity was examined, with an internal protrusion, also known as Doyle's bulge, serving as the definitive procedural landmark. To minimize operator variability, all preperitoneal infiltrations were conducted by the same senior laparoscopic surgeon under direct laparoscopic visualization. The injection site was identified after trocar insertion and insufflation.

Sevoflurane administration was discontinued at the conclusion of surgery, and spontaneous breathing resumed. The gas flow rate was increased to 7 L/min of oxygen, and the neuromuscular blockade was reversed with a standard dose of atropine (0.01 mg/kg) and neostigmine (0.05 mg/kg). The patient was extubated when they were able to respond to a verbal request and were able to breathe spontaneously with a tidal volume of 5–8 mL/kg. Subsequently, they were transferred to the recovery room.

While the TAP block used real-time imaging and the preperitoneal technique relied on visual laparoscopic guidance, the involvement of experienced specialists and standardized procedural steps helped ensure consistency. We acknowledge that differing guidance methods (ultrasound vs. laparoscopic) may affect the reproducibility and accuracy of anesthetic spread, and we have added this as a potential limitation in the discussion section.

2.5. Protocol for post-operative analgesia

Additional analgesia was administered when patients reported a VAS score of ≥4, indicating moderate to severe pain. The first-line rescue analgesic used was intravenous paracetamol (1 g) administered every 6 h, as needed. If pain persisted despite paracetamol, intravenous pethidine (50 mg) was given as a second-line agent. For each patient, the total dosage and frequency of administration were recorded to evaluate cumulative analgesic use.

2.6. Outcomes

2.6.1. Primary outcomes

2.6.1.1. Visual Analog Scale scores

Pain intensity was measured using the VAS at six post-operative time points: 0, 2, 4, 8, 12, and 24 h. Patients rated their pain on a scale from 0 (no pain) to 10 (worst pain imaginable). This provided an objective assessment of pain severity over time for comparison between the two groups.

2.6.1.2. Time to first rescue analgesia

The duration from the end of surgery until the patient's first request for additional analgesia was recorded. This measure reflects the analgesic efficacy and duration of pain relief provided by the intervention.

2.6.1.3. Total analgesic dose

The cumulative dose of opioids required within the first 24 h postoperatively was documented. Lower opioid consumption indicated better pain control and effectiveness of the analgesic technique.

2.6.2. Secondary outcomes

2.6.2.1. PONV

The occurrence of nausea and vomiting was monitored in both groups, as these are common side effects of anesthesia and opioid use. PONV incidences were compared to evaluate the influence of the analgesic technique on this outcome.

2.6.2.2. Sleep quality

Post-operative sleep quality was assessed using a subjective scoring system, where patients rated their sleep on a scale from 0 (poor sleep) to 10 (excellent sleep). This score was

collected during the structured interview on the first post-operative morning. Patients were asked to consider factors such as ease of falling asleep, frequency of waking, and overall restfulness during the night.[4]

2.7. Sample size

Sample size calculation was based on the difference in post-operative pain incidence between the group with preperitoneal bupivacaine infiltration and the placebo group, retrieved from previous research.[10] The G*Power program version 3.1.9.4 was used to calculate the sample size based on an expected 27% difference and a large effect size (f = 1.061195). Using a two-tailed test, α error = 0.05, and power = 90.0%, the total calculated sample size was 40 patients, divided into two equal groups (Figure 1).

2.8. Statistical analysis

The Statistical Package for the Social Sciences, version 23.0 (SPSS Inc., United States), was employed to analyze the recorded data. Parametric quantitative data distribution was represented as mean ± standard deviation and ranges. Conversely, non-parametric variables were represented as median with inter-quartile range (IQR). In addition, qualitative variables were presented as percentages and numbers. The Shapiro–Wilk test and Kolmogorov–Smirnov test were employed to investigate the normality of the data.

The Mann–Whitney U test was performed for two-group comparisons in non-parametric data, while the independent-sample t-test of significance was employed when comparing two means. The Chi-square and Fisher's exact tests were performed to compare groups with qualitative data, except when the expected count in any cell was <5. The margin of error accepted was 5%, and the confidence interval was 95%. Therefore, a p<0.05 was deemed significant.

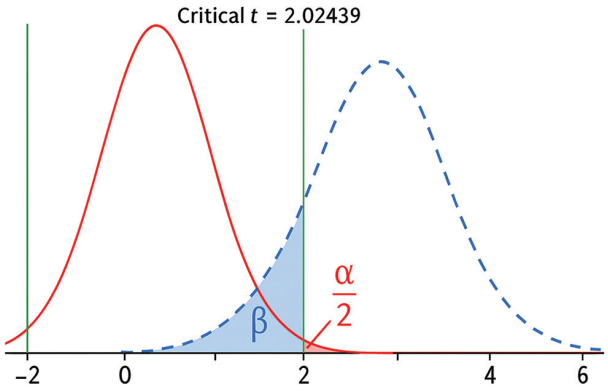


Figure 1. Distributions in a two-tailed t-test

3. Results

The subsequent tables and figures illustrate the findings of the current investigation. Table 1 reveals no significant differences in demographic characteristics between the TAP block and preperitoneal groups. Both groups were comparable in age, sex distribution, body mass index, American Society of Anesthesiologists physical status classification, and sleep quality. For instance, the average age in the TAP block group was 42.45 ± 12.37 years; in the preperitoneal group, it was 41.80 ± 10.86 years (p=0.861). Similarly, the body mass index was 23.60 ± 2.04 kg/m^2 in the TAP block group and 24.20 ± 2.98 kg/m^2 in the preperitoneal group (p=0.462).

Table 2 reveals no statistically significant difference in sleep quality between groups (p>0.05).

Table 3 and Figure 2 indicate that the VAS scores for post-operative pain were assessed at various intervals (0, 2, 4, 8, 12, and 24 h). Significant differences were observed at the 8- and 12-h marks, with the preperitoneal group reporting higher median pain scores than the TAP block group. At 8 h, the median VAS score was 3 (IQR 3–3) for the TAP block group and 4 (IQR 4–5) for the preperitoneal group (p=0.027). At 12 h, the median VAS score was 3 (IQR 3–4) in the TAP block group and 5 (IQR 4–6) in the preperitoneal group (p=0.019). The differences were not statistically significant at other time intervals (0, 2, 4, and 24 h).

Table 4 reveals no significant difference between the two groups regarding the occurrence of PONV. In the TAP block group, 60% of patients experienced PONV, compared to 50% in the preperitoneal group (p=0.525). This suggests that both analgesic techniques have a similar impact on PONV, highlighting that the advantage of TAP block lies primarily in its pain-relieving efficacy rather than in mitigating nausea or vomiting.

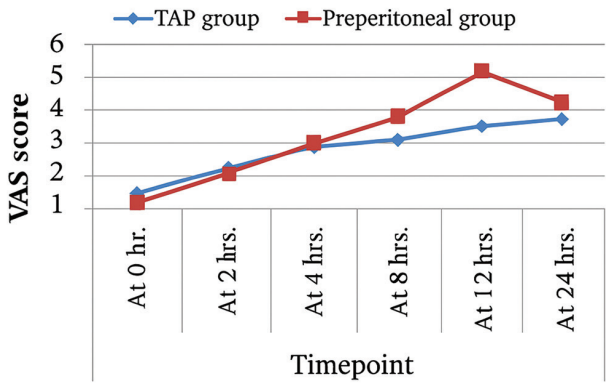


Figure 2. Comparison of the Visual Analog Scale between the transversus abdominis plane block and preperitoneal groups
Abbreviation: hrs.: Hours

Table 1. Demographic characteristics of the patient groups

Demographic data	TAP block group (*n*=20)	Preperitoneal group (*n*=20)	Test value	*p*-value
Age (years)	20–60 (42.45±12.37)	20–60 (41.80±10.86)	0.031	0.861
Sex (%)				
Female	3 (15.0)	5 (25.0)	0.625	0.429
Male	17 (85.0)	15 (75.0)		
Body mass index (kg/m^2)	20–26 (23.60±2.04)	20–29 (24.20±2.98)	0.552	0.462
ASA classification				
ASA1, *n* (%)	11 (55.0)	13 (65.0)	0.417	0.519
ASA2, *n* (%)	9 (45.0)	7 (35.0)		
Operative time (minutes)	33–51 (42.27±6.43)	34–54 (44.34±7.26)	0.955	0.346
Block duration (minutes)	4–7 (5.90±1.03)	5–8 (6.32±1.14)	1.223	0.229

Note: Data presented as range (mean±standard deviation), unless stated otherwise. Independent sample *t*-test for mean±standard deviation; Chi-square test for number (%) or Fisher's exact test, when appropriate.
Abbreviations: ASA: American Society of Anesthesiologists; TAP: Transversus abdominis plane.

Table 2. Comparison of sleep quality between groups

Group	Sleep quality score	Test value	*p*-value
TAP block group	5–9 (7.05±1.23)	0.129	0.721
Preperitoneal group	5–10 (7.20±1.40)		

Note: Data presented as range (mean±standard deviation), unless stated otherwise.
Abbreviation: TAP: Transversus abdominis plane.

Table 3. Comparison of the Visual Analog Scale between groups

Visual Analog Scale measurement timepoints	TAP block group (*n*=20)	Preperitoneal group (*n*=20)	Test value	*p*-value
0-h			1.862	0.572
Mean±SD	1.45±1.00	1.25±0.79		
Median (IQR)	2 (0–2)	2 (1–2)		
Range	0–3	0–3		
2-h			0.958	0.762
Mean±SD	2.04±0.82	1.95±0.69		
Median (IQR)	3 (2–3)	3 (1–3)		
Range	1–3	1–3		
4-h			1.175	0.386
Mean±SD	2.85±0.59	3.02±0.44		
Median (IQR)	3 (2–3)	3 (3–4)		
Range	1–4	3–4		
8-h			2.793	0.027*
Mean±SD	2.90±0.31	3.80±0.41		
Median (IQR)	3 (3–3)	4 (4–5)		
Range	2–3	3–4		
12-h			2.975	0.019*
Mean±SD	3.30±0.57	5.10±0.85		
Median (IQR)	3 (3–4)	5 (4–6)		
Range	2–4	3–7		
24-h			1.376	0.291
Mean±SD	3.50±1.00	4.05±0.89		
Median (IQR)	4 (3–4)	5 (3–5)		
Range	1–5	2–6		

Note: Statistical analysis conducted using the Mann–Whitney test for non-parametric data. *indicates statistical significance at $p<0.05$.
Abbreviations: IQR: Interquartile; SD: Standard deviation; TAP: Transversus abdominis plane.

Table 5 shows that the time to the first request for analgesia was significantly longer in the TAP block group compared to the preperitoneal group. Patients in the TAP block group required rescue analgesia after an average of 14.6 ± 2.52 h, whereas those in the preperitoneal group requested it after 7.1 ± 1.02 h ($p<0.001$). This highly significant result underscores the prolonged analgesic effect of the TAP block, providing extended pain relief and delaying the need for additional pain management interventions. In addition, there was a statistically significantly higher total dose of analgesia in the pre-peritoneal group compared to the TAP block group, with a $p<0.05$. Narcotics requirement was significantly less frequent among the TAP block group (Table 6). In addition, the total dose of opioids was significantly lower in the TAP block group (Table 7).

4. Discussion

Cholecystectomy is one of the most commonly performed surgical procedures. The laparoscopic approach is becoming progressively popular due to its earlier recovery and shorter hospital stay, as well as its reduced post-operative pain and morbidity compared to open cholecystectomy surgery.[2]

During laparoscopic cholecystectomy, various perioperative causes, including pneumo-peritoneum,

intra-abdominal cavity elongation, amount of blood left in the abdomen, and pelvic region dissection, may induce distinct types of pain.[2] Furthermore, patients who underwent laparoscopic procedures, which are renowned for their reduced pain, were found to experience excessive post-operative pain and receive inadequate pain alleviation in comparison to aggressive major operations.[9,11] Despite the procedure's minimal invasive nature, the post-operative pain that follows laparoscopic cholecystectomy is frequently difficult to manage, leading to delayed hospital discharge and increased opioid use.[12] In addition, patients who undergo abdominal interventions experience significant distress that is linked to somatic pain signals that originate from the abdominal wall.[13] A prolonged hospital stay, myocardial ischemia, delirium, respiratory complications, and an elevated probability of chronic pain are among the numerous undesirable post-operative consequences that may result from poorly controlled pain following abdominal surgery, in addition to patient suffering and distress.[14]

Advantages of effective post-operative analgesia include reduced post-operative morbidity and stress response, increased patient satisfaction, and enhanced patient outcome.[14]

In this investigation, 40 patients were scheduled for laparoscopic cholecystectomy surgery and were categorized into two groups. The preperitoneal group (n = 20) underwent trocar infiltration of local anesthetic, while the TAP block group (n = 20) was given a TAP block under ultrasound guidance.

Our findings show no significant difference in sleep quality between the TAP block and preperitoneal groups. Moreover, regarding VAS and the first request of analgesia, the results showed that the 8- and 12-h VAS scores had a higher median value in the preperitoneal group than the TAP block group, with a statistically significant difference. The parameters were insignificant at 0-, 2-, and 4-h.

This study compared the analgesic efficacy of the TAP block and preperitoneal infiltration with bupivacaine in patients undergoing laparoscopic cholecystectomy. The findings demonstrated that the TAP block provided superior pain relief, as evidenced by significantly lower VAS scores at 8- and 12-h post-operation and a longer time to first rescue analgesia (14.6±2.52 h in the TAP block group vs. 7.1 ± 1.02 h in the preperitoneal group, p<0.001). In addition, patients in the TAP block group required

Table 4. Comparison of post-operative nausea and vomiting between groups

Presence of post-operative nausea and vomiting	TAP block group (n=20) (%)	Preperitoneal group (n=20) (%)	Test value	p-value
No	8 (40.0)	10 (50.0)	0.404	0.525
Yes	12 (60.0)	10 (50.0)		

Note: Chi-square test for number (%) or Fisher's exact test, when appropriate.
Abbreviation: TAP: Transversus abdominis plane.

Table 5. Comparison of time to first request for rescue analgesia between groups

Group	Time to first request for rescue analgesia (hours)	Test value	p-value
TAP block group	12–18 (14.60±2.52)	5.027	0.001*
Preperitoneal group	6–8 (7.10±1.02)		

Note: Data presented as range (mean±standard deviation), unless stated otherwise. Independent sample t-test for mean±standard deviation.* indicates statistical significance.
Abbreviation: TAP: Transversus abdominis plane.

Table 6. Opioid requirements and dosage among the studied groups

Opioid requirement	TAP block group (n=20) (%)	Preperitoneal group (n=20) (%)	p-value	Effect size, relative risk (95% confidence interval)
Required	2 (10.0)	5 (25.0)	0.037*	0.51 (0.23–1.09)
Not required	18 (90.0)	15 (75.0)		

Note: Effect size refers to the effect of the TAP block group relative to the preperitoneal group. *indicates statistical significance.
Abbreviation: TAP: Transversus abdominis plane.

Table 7. Opioid total dose in cases that required analgesia among the studied groups

Group	Opioid total dose (mg)	p-value	Effect size, mean±standard error (95% confidence interval)
TAP block group (n=2)	50.0–75.0 (55.0±11.2)	0.007*	−27.7±9.0 (−46.9–−8.5)
Preperitoneal group (n=5)	50.0–100.0 (82.7±18.8)		

Note: Statistical analysis using an independent t-test. Effect size refers to the effect of the TAP block group relative to the control. *indicates statistical significance.
Abbreviation: TAP: Transversus abdominis plane.

significantly less total opioid consumption within the first 24 h postoperatively.

The results of our study agree with the findings of El sharkwy *et al*.[15] They determined that the TAP block is more efficacious in the early post-operative period in terms of pain scores and analgesia consumption than preperitoneal infiltration in surgical laparoscopy. Ghisi *et al*.,[16] discovered that the pain scores at rest and through movement were not lowered by ultrasound-guided TAP block through the first 24 h following laparoscopic hysterectomy, in contrast to the control group that received morphine patient-controlled analgesia as a treatment. This is in stark contrast to the findings of El sharkwy *et al*.[15], who demonstrated the superiority of the TAP block over preperitoneal infiltration during the early post-operative period.

In a retrospective cohort study by Rivard *et al*.,[17] the intraperitoneal bupivacaine administration was associated with reduced post-operative narcotic use and lower patient-reported pain scores in minimally invasive surgery, such as cancer staging and hysterectomy. With respect to post-operative complications, no significant difference in PONV was indicated between the preperitoneal group and the TAP block group.

Badawy[18] compared the intraperitoneal local analgesia instillation before the trocars' removal in laparoscopic hysterectomy cases to the control group. Pain scores were significantly decreased within the first 24 h after surgery when an intraperitoneal local anesthetic was administered. This was demonstrated by the reduction in opioid consumption and post-operative analgesia. In addition, there was a reduction in the incidence of PONV.

None of the complications associated with the TAP block was encountered during our investigation. Furthermore, the TAP block has not been associated with any complications in the preponderance of all other studies. The primary benefit of the TAP block is its safety profile, although researchers have documented the incidence of liver and colon injury.[19]

In contrast, wound infiltration utilization by local anesthetics through laparoscopic surgery to mitigate post-operative pain has been documented since the early 1990s. Dec and Andruszkiewicz[20] were the first to disclose the use of wound infiltration by local anesthetics for minimally invasive cholecystectomies in the general surgery literature in 2016. A meta-analysis of 30 studies featuring laparoscopic cholecystectomies revealed a reduction in the quantity of analgesics administered postoperatively and a decrease in post-operative pain scores. Yoshiyama *et al*.,[21] found that the posterior TAP block was more efficient than the lateral TAP block in providing pain relief to patients who underwent laparoscopic gynecologic surgery.

While our findings indicate that the TAP block provided longer-lasting analgesia and reduced opioid consumption compared to preperitoneal infiltration, it is important to emphasize that both techniques were clinically effective in managing post-operative pain following laparoscopic cholecystectomy.

Although the differences in VAS scores at 8 and 12 h were statistically significant, the absolute differences were modest. This suggests that while the TAP block may offer an advantage in the duration of pain relief, preperitoneal infiltration remains a viable and practical alternative, particularly when ultrasound resources or expertise are limited. These findings support the inclusion of either technique within a multimodal analgesia strategy, tailored to the clinical setting, provider experience, and patient-specific factors.

4.1. Strengths

The study's randomized, double-blinded design enhances the reliability and validity of the findings by reducing selection and observer biases. Using objective measures, such as the VAS for pain assessment and quantification of opioid consumption, adds rigor to the evaluation of the analgesic techniques. Furthermore, the direct comparison between the TAP block and preperitoneal infiltration offers a practical perspective on optimizing pain management strategies. The study also controlled key procedural variables, such as surgical and anesthetic protocols, ensuring that observed differences were attributable to the analgesic methods rather than external factors. These methodological strengths provide a robust foundation for the study's conclusions.

4.2. Limitations

Despite its strengths, the study has notable limitations. A notable limitation of this study is its relatively small sample size, which may reduce the generalizability of the findings and the statistical power to detect smaller but clinically meaningful differences. Although the observed trends favor the TAP block in terms of analgesic duration and opioid-sparing effect, these results should be interpreted with caution. The study focuses exclusively on laparoscopic cholecystectomy, and its applicability to other surgical procedures remains uncertain. The study examined only short-term outcomes within the first 24 h, omitting the potential for long-term complications, chronic pain, or extended recovery metrics. The homogeneity of the study population, with limited diversity in demographics or comorbidities, further narrows the scope of the conclusions.

Finally, while complications associated with TAP block were minimal in this study, it does not extensively address rare but potentially severe risks, such as inadvertent organ injury.

To validate these preliminary findings and better understand the comparative efficacy of these techniques, we recommend conducting larger, multicenter randomized controlled trials. Future studies should also explore long-term outcomes, cost-effectiveness, and patient satisfaction to provide more comprehensive clinical guidance.

5. Conclusion

The findings establish that the TAP block is a more effective analgesic technique compared to preperitoneal infiltration with bupivacaine for managing post-operative pain in laparoscopic cholecystectomy. Patients receiving TAP block required fewer opioids, had delayed onset of rescue analgesia, and reported lower pain scores at critical post-operative intervals. These results underline the TAP block's potential to enhance patient recovery by minimizing opioid-related side effects and expediting discharge. The study highlights the need to integrate the TAP block into routine perioperative care for laparoscopic procedures to improve pain control and patient outcomes.

Future research should focus on expanding the study to include larger and more diverse populations to validate these findings and assess their applicability to other surgical contexts. Long-term studies are necessary to explore the impact of these analgesic techniques on chronic pain, quality of life, and recovery trajectories. Moreover, conducting a cost-effectiveness analysis of TAP block versus other analgesic methods would provide a comprehensive understanding of its economic and clinical benefits.

Acknowledgments

None.

Funding

None.

Conflict of interest

The authors have no conflicts of interest to declare.

Author contributions

Conceptualization: Noha Mohamed Abdelwahab Elsaid, Ain EL-Marwa Abdelmonem Abdallah, Ahmed Mohamed Said, Mostafa Mohamed Elsayed, Nashwa Mohammed Ibrahiem, Gihan Eissa Zahran

Formal analysis: Noha Mohamed Abdelwahab Elsaid, Ain El-Marwa Abdelmonem Abdallah Hassan, Ahmed Mohamed Said, Eman A. Salem, Tarek Abdelmonem Abdelzaher, Warda Demerdash Khalifa Ali

Investigation: Noha Mohamed Abdelwahab Elsaid, Ain El-Marwa Abdelmonem Abdallah Hassan, Ahmed Mohamed Said, Doaa Mohamed Almonayery Ibrahim, Marwa Ibrahim Eid, Hayam Shaaban Soliman Morsy

Methodology: Mostafa R. Bakry, Noha Mohamed Abdelwahab Elsaid, Ain EL-Marwa Abdelmonem Abdallah, Ahmed Mohamed Said, Mayada Yahia Elbohouty, Heba Atwa Ahmed Atwa, Gehan Abd Elrhman Eldesoky, Nahla Mohammed Eldeeb

Writing–original draft: Mostafa R. Bakry, Noha Mohamed Abdelwahab Elsaid, Ain El-Marwa Abdelmonem Abdallah Hassan, Ahmed Mohamed Said

Writing–review & editing: Mostafa R. Bakry, Noha Mohamed Abdelwahab Elsaid, Ain El-Marwa Abdelmonem Abdallah Hassan

Ethics approval and consent to participate

This study was approved by the Institutional Review Board and the Ethical Committee of the Faculty of Medicine for Girls, Al-Azhar University (Approval Number 1784/2023), and additionally by the Institutional Review Board of Minia University Hospital, according to the WMA Declaration of Helsinki. Each participant was required to provide an informed written consent before enrollment.

Consent for publication

Each participant was required to provide verbal consent before publication.

Availability of data

The data used in the study are available from the corresponding author upon reasonable request.

References

1. Molfino S, Botteri E, Baggi P, *et al*. Pain control in laparoscopic surgery: A case-control study between transversus abdominis plane-block and trocar-site anesthesia. *Updates Surgery*. 2019;71:717-722.

   doi: 10.1007/s13304-018-00615-y

2. Suragul W, Tantawanit A, Rungsakulkij N, *et al*. Effect of local anaesthetic infiltration on postoperative pain after laparoscopic cholecystectomy: Randomized clinical trial. *BJS Open*. 2022;6(3):zrac066.

   doi: 10.1093/bjsopen/zrac066

3. Ali Esmail AM, Seleem TAE, Mohammad ES, El-Sayed MMM. Comparative Study between ultrasound guided quadratus lumborum block versus ultrasound guided transversus abdominis plane block for postoperative pain relief in patients undergoing unilateral inguinal surgeries.

Al-Azhar Med J. 2020;49(3):1231-1244.

doi: 10.21608/amj.2020.91642

4. Ram D, Sistla SC, Karthikeyan VS, Ali SM, Badhe AS, Mahalakshmy T. Comparison of intravenous and intraperitoneal lignocaine for pain relief following laparoscopic cholecystectomy: A double-blind, randomized, clinical trial. *Surg Endosc*. 2014;28:1291-1297.

doi: 10.1007/s00464-013-3325-5

5. Peng K, Ji FH, Liu HY, Wu SR. Ultrasound-guided transversus abdominis plane block for analgesia in laparoscopic cholecystectomy: A systematic review and meta-analysis. *Med Princ Pract*. 2016;25(3):237-246.

doi: 10.1159/000444688

6. El-Misady MM, Abd El-Rahman AS, Abd El-Latif Shabayek I. Comparison between ultrasound guided transversus abdominis plane (Tap) block and local anesthetic infiltration in patients undergoing laparoscopic cholecystectomy. *Al-Azhar Med J*. 2023;52:1107-1118.

doi: 10.21608/amj.2023.326881

7. Herrador-Benito J, Páramo-Zunzunegui J, Rodríguez-Caravaca G, Durán-Poveda M. Pre-incisional local infiltration with levobupivacaine in laparoscopic cholecystectomy: A randomized and clinical trial. *Cir Cir*. 2024;92(1):69-76.

doi: 10.24875/ciru.230000221

8. Malallah ZZ, Al-Mafrachi KKR. The use of local anesthesia for relief of postoperative pain after laparoscopic cholecystectomy. *Iraqi J Med Sci*. 2022;20(1):98-105.

doi: 10.22578/IJMS.20.1.13

9. Warren JA, Carbonell AM, Jones LK, *et al*. Length of stay and opioid dose requirement with transversus abdominis plane block vs epidural analgesia for ventral hernia repair. *J Am Coll Surg*. 2019;228(4):680-686.

doi: 10.1016/j.jamcollsurg.2018.12.017

10. Boerboom SL, de Haes A, Vd Wetering L, *et al*. Preperitoneal bupivacaine infiltration reduces postoperative opioid consumption, acute pain, and chronic postsurgical pain after bariatric surgery: A randomized controlled trial. *Obes Surg*. 2018;28(10):3102-3110.

doi: 10.1007/s11695-018-3341-6

11. D'Cunha D, Somayaji AS. Intraperitoneal instillation versus port-site infiltration or subcostal transversus abdominis plane block for post-operative analgesia following laparoscopic cholecystectomy. *Res Opin Anesth Intensive Care*. 2024;11(2):116-124.

doi: 10.4103/roaic.roaic_45_23

12. Leitao MM Jr., Malhotra V, Briscoe G, *et al*. Postoperative pain medication requirements in patients undergoing computer-assisted ("Robotic") and standard laparoscopic procedures for newly diagnosed endometrial cancer. *Ann Surg Oncol*. 2013;20:3561-3567.

doi: 10.1245/s10434-013-3064-9

13. Shian B, Larson ST. Abdominal wall pain: Clinical evaluation, differential diagnosis, and treatment. *Am Fam Physician*. 2018;98(7):429-436.

14. Mishra M, Mishra SP. Transversus abdominis plane block: The new horizon for postoperative analgesia following abdominal surgery. *Egypt J Anaesth*. 2016;32(2):243-247.

doi: 10.1016/j.egja.2015.12.003

15. El sharkwy IA, Noureldin EH, Mohamed EA, Mohamed AA. Laparoscopic-guided transversus abdominis plane block versus trocar site local anesthetic infiltration in gynecologic laparoscopy. *Gynecol Surg*. 2018;15:1-6.

doi: 10.1186/s10397-018-1047-3

16. Ghisi D, Fanelli A, Vianello F, *et al*. Transversus abdominis plane block for postoperative analgesia in patients undergoing total laparoscopic hysterectomy: A randomized, controlled, observer-blinded trial. *Anesth Analg*. 2016;123(2):488-492.

doi: 10.1213/ANE.0000000000001267

17. Rivard C, Vogel RI, Teoh D. Effect of intraperitoneal bupivacaine on postoperative pain in the gynecologic oncology patient. *J Minim Invasive Gynecol*. 2015;22(7):1260-1265.

doi: 10.1016/j.jmig.2015.07.013

18. Badawy AM. Intraperitoneal analgesia to reduce pain after laparoscopic hysterectomy. *Int J Reprod Contracept Obstet Gynecol*. 2017;6(8):3235-3241.

doi: 10.18203/2320-1770.ijrcog20173444

19. Young MJ, Gorlin AW, Modest VE, Quraishi SA. Clinical implications of the transversus abdominis plane block in adults. *Anesthesiol Res Pract*. 2012;2012(1):731645.

doi: 10.1155/2012/731645

20. Dec M, Andruszkiewicz P. Anaesthesia for minimally invasive surgery. *Wideochir Inne Tech Maloinwazyjne*. 2015;10(4):509-514.

doi: 10.5114/wiitm.2015.56411

21. Yoshiyama S, Ueshima H, Sakai R, Otake H. A posterior TAP block provides more effective analgesia than a lateral TAP block in patients undergoing laparoscopic gynecologic surgery: A retrospective study. *Anesthesiol Res Pract*. 2016;2016(1):4598583.

doi: 10.1155/2016/4598583

ACCSCIENCE PUBLISHING

Eurasian Journal of Medicine and Oncology

SHORT COMMUNICATION

Causal links between *Helicobacter pylori* infection and Alzheimer's disease: Insights from genome-wide summary data-based Mendelian randomization

Yuan Xin Hou[1,2], Ao Wang[1], and Ke Yi[1,2]*

[1]Key Laboratory of Obstetrics and Gynecologic and Pediatric Diseases and Birth Defects of Ministry of Education, West China Second University Hospital, Sichuan University, Chengdu, Sichuan, China

[2]Department of Operation Management, Hubei Provincial Key Laboratory of Occurrence and Intervention of Rheumatic Diseases/Hubei Provincial Clinical Research Center for Nephrology, Minda Hospital of Hubei Minzu University, Hubei Minzu University, Enshi, Hubei, China

Abstract

Introduction: *Helicobacter pylori* infection is associated with various illnesses like Alzheimer's disease (AD).

Objective: The purpose of this work is to utilize Mendelian randomization (MR) methods to examine the possible link between AD and *H. pylori* infection.

Methods: We utilized information from the Finngen database and the UK Biobank for MR analysis. Six antibodies related to *H. pylori* were assessed for their association with AD. The MR analysis involved two-sample methods, while generalized summary data-based MR (GSMR) was employed to analyze genetic data for a robust causal inference.

Results: The two-sample MR investigation exhibited a strong link among AD and anti-*H. pylori* UREA antibodies, with an odds ratio (OR) of 1.076 (95% confidence interval [CI] = 1.010 – 1.147; p=0.024). Similarly, GSMR confirmed this relationship, showing an OR of 1.071 (95% CI = 1.004 – 1.143; p=0.038). No notable correlations were seen with other antibodies.

Conclusion: Our findings suggest that *H. pylori* infection may be related to a higher likelihood of AD development, particularly through anti-*H. pylori* UREA antibodies.

Keywords: *Helicobacter pylori*; Infection; Alzheimer's disease; Mendelian randomization; Genome-wide summary data-based Mendelian randomization

***Corresponding author:**
Ke Yi
(yike@scu.edu.cn)

Citation: Hou YX, Wang A, Yi K. Causal links between *Helicobacter pylori* infection and Alzheimer's disease: Insights from genome-wide summary data-based Mendelian randomization. *Eurasian J Med Oncol*. 2025;9(3):287-293. doi: 10.36922/EJMO025140087

Received: April 4, 2025

Revised: April 27, 2025

Accepted: May 6, 2025

Published online: May 22, 2025

Copyright: © 2025 Author(s). This is an Open-Access article distributed under the terms of the Creative Commons Attribution License, permitting distribution, and reproduction in any medium, provided the original work is properly cited.

Publisher's Note: AccScience Publishing remains neutral with regard to jurisdictional claims in published maps and institutional affiliations.

1. Introduction

The Gram-negative, spiral-shaped bacterium *Helicobacter pylori* is commonly found in the human stomach and is widely recognized as a primary pathogen responsible for chronic gastritis and peptic ulcers.[1,2] In addition, a substantial correlation exists between *H. pylori* infection and the development of stomach cancer.[3] While the bacterium's effects have traditionally been associated with the gastrointestinal system, recent studies have begun to explore its potential links to neurological disorders.[4,5]

Alzheimer's disease (AD) is a neurodegenerative illness that causes memory loss and gradual decline in cognitive abilities, severely compromising patients' day-to-day

activities and overall life quality.[6] AD's clinical importance is highlighted by its high prevalence and the substantial burden it places on affected individuals and their families.[7,8] Understanding the potential risk factors for AD becomes increasingly imperative for guiding early intervention and therapeutic strategies as the world's population ages.[9,10]

Current investigation on the correlation between AD and infection is increasingly highlighting *H. pylori*'s potential role in AD's development.[11,12] Meta-analysis findings reveal that *H. pylori* infection raises AD risk, with an OR of 1.40 in these patients, indicating a correlation between the two.[13] In addition, co-infection with periodontal pathogens further exacerbates this risk, as seen in studies where specific pathogens interact synergistically with *H. pylori* to influence AD incidence.[14] Mechanistically, *H. pylori* can cause increased β-amyloid deposition in the brain by altering the gut flora and causing chronic low-grade inflammation.[15] Through the oropharyngeal olfactory route, the bacteria's metabolites can reach the central nervous system, promoting neurodegenerative processes.[16] Moreover, the buildup of β-amyloid plaques, which are closely linked to the pathological features of AD, may be facilitated by the chronic inflammatory state linked to *H. pylori* infection.[17] However, numerous studies have predominantly employed observational designs, which are inherently constrained by potential biases and confounding variables. In addition, variations in sample selection may limit the result's generalizability, as certain populations could not fully reflect the larger population. Furthermore, reliance on specific instrumental variables (IVs) in prior analyses may undermine the validity of causal inferences. It is imperative that these methodological constraints are addressed to improve our comprehension of the intricate relationship between infection and AD.

To elucidate the correlation between them, our study employed Mendelian randomization (MR) analysis, which employs genetic variations as key variables to deduce causal relationships. A significant advantage of MR is its capacity to simulate the conditions of a randomized controlled trial, thereby addressing the constraints of observational studies.[18] Weighted median estimation, inverse variance weighting (IVW), weighted mode, and MR-Egger regression are examples of common two-sample MR techniques. These approaches are used to improve the findings' reliability as well as robustness. Generalized summary data-based MR (GSMR) presents distinct advantages over traditional MR. By taking into account linkage disequilibrium (LD) among genetic variants, GSMR improves analytical efficiency.[19] Furthermore, it employs or heterogeneity in dependent instruments (HEIDI) test to identify instrumental outliers and exclude pleiotropic single-nucleotide polymorphisms (SNPs).[20] Utilizing genetic data, MR analysis provides compelling evidence that the pathogenesis of AD may be directly influenced by *H. pylori* infection. This methodology not only enriches our comprehension of the etiological role of the infection in AD but also holds substantial promise for informing future therapeutic interventions.

2. Materials and methods

2.1. Data source

The data on *H. pylori* infection in this study is sourced from the literature by Butler-Laporte *et al.*[21] We examined six antibodies related to *H. pylori* infection: Anti-*H. pylori* CagA, Catalase, GroEL, OMP, UREA, and VacA, which correspond to genome-wide association studies (GWAS) database IDs GCST90006911 through GCST90006916. The study sample is composed of European ancestry people, with sample size details presented in Table 1. IVs for AD were extracted from the Finngen database, comprising 11,755 AD cases and 441,978 European ancestry controls. All AD cases adhered to the criteria set by the International Classification of Diseases (ICD-10).

2.2. MR analysis

To determine the correlation among *H. pylori* infection and AD, we conducted GSMR and a two-sample MR investigation. SNPs were analyzed as IVs.[22] During the whole procedure, it is crucial to validate three important hypotheses to ensure optimal outcome accuracy.[23] The first step involves confirming that the chosen IVs exhibit a direct association with the *H. pylori* infection. Second, it is essential to establish the IVs' independence from potential confounders impacting both exposure and outcome. Finally, ensuring that the IVs affect AD solely through their influence on the risk factor.

We primarily employed the IVW approach as our MR analysis strategy. To fully evaluate the possible association,

Table 1. Baseline characteristics for participants

Exposure/ Outcome	Data source	Phenotype	Sample size*
Alzheimer's disease	The FinnGen consortium	Alzheimer's disease	11,755/441,978
Antibodies against *H. pylori*	Butler-Laporte *et al.*[21]	CagA	985
		Catalase	1558
		GroEL	2716
		OMP	2640
		UREA	2251
		VacA	1571

Note: *Sample size shown as a total number for quantitative traits and cases/controls for binary traits.

we also used four more useful techniques: MR-Egger, weighted median, weighted mode, and simple mode. SNPs with genome-wide significance ($p<5 \times 10^{-6}$) were selected as IVs for both anti *H. pylori* antibodies and AD. The F-statistic for each SNP was calculated to assess the strength of the selected instruments. SNPs with an F-statistic <10 were excluded to avoid bias from weak instruments. The LD threshold was established at $r^2 < 0.001$, with a genetic distance of 10,000 kb, to guarantee SNP independence. We computed the F-statistic for the selected SNPs, applying a threshold of >10 to evaluate the strength of the IVs. To evaluate pleiotropy and heterogeneity, we used Cochran's Q statistic as well as the MR-Egger test, respectively.

2.3. GSMR analysis

GSMR is an advanced analytical method that integrates genome-wide summary data from multiple independent studies, flexibly utilizing several relatively independent IVs for MR analysis. This approach aims to analyze the causal links among various illnesses and exposure determinants, providing more reliable inference results.[19] For the genetic instruments associated with anti-*H. pylori* antibodies, we employed a clumping algorithm to identify SNPs that are genome-wide significant for each trait, applying an LD threshold of $r^2 = 0.001$ and a significance threshold of $p<5 \times 10^{-6}$. The reference for LD estimation was derived from the 1000 Genomes Project (1000G) phase 3 European samples. In the reverse analysis, we selected independent SNPs from the GWAS summary statistics for AD by establishing a LD threshold of $r^2 < 0.001$ and a significance threshold of $p<5 \times 10^{-6}$. We established a HEIDI outlier threshold of 0.01 to exclude instruments with significant putative pleiotropic effects.

2.4. Sensitivity analyses

We carried out a comprehensive set of sensitivity tests to confirm the causal impact of *H. pylori* infection on AD. Cochran's Q statistic was applied to analyze any possible heterogeneity in the data.[24] Horizontal pleiotropy was analyzed by employing the MR-Egger intercept analysis. Furthermore, by systematically excluding each SNP, a leave-one-out investigation was carried out to see whether any single SNP had a considerable influence on the results. RStudio and R (version 4.2.0) were used for all analyses, including the R packages gsmr, TwoSampleMR, and MR-PRESSO.

3. Results

3.1. Causal effect of *H. pylori* infection on AD

In our initial investigation, we utilized GSMR to examine the correlation among AD and six anti-*H. pylori* antibodies. Anti-*H. pylori* UREA was found to raise AD risk (odds ratio [OR] = 1.071; 95% confidence interval (CI) = 1.004 – 1.143; p=0.038) (Figure 1).

Anti-*H. pylori* UREA and AD were found to be similarly associated in the two-sample MR analysis, with an OR of 1.076 (95% CI = 1.010 – 1.147; p=0.024) (Figure 2). Detailed information on F-values as well as LD independent SNPs related to exposure (*H. pylori* antibodies) can be found in Tables S1-S6 (available in Supplementary File).

3.2. Reverse MR analysis

In the reverse MR study exploring the correlation among *H. pylori* and AD, both the two-sample MR and GSMR analyses failed to identify a meaningful correlation among the two. These results indicate that AD does not appear to influence *H. pylori* infection risk. Further details are presented in Tables S7 and S8 (Supplementary File).

3.3. Sensitivity analysis

The assessment of *H. pylori* infection's effect on AD revealed no substantial heterogeneity, as per the Cochran's Q test. The MR-Egger intercept test also found no proof of horizontal pleiotropy. Scatter plots demonstrated the impact of the infection on AD across five MR approaches, with a positive slope indicating a direct correlation (Figure S1 in Supplementary File). Furthermore, as indicated by leave-one-out analysis, specific SNPs are unlikely to significantly influence the causal estimates (Figure S2 in Supplementary File). Together, these findings strengthen the robustness of the observed associations.

4. Discussion

This study explored the causal link of *H. pylori* infection with AD. Employing MR techniques, a substantial positive association was found between AD and anti-*H. pylori* UREA antibodies, with an OR of 1.071 (95% CI = 1.004 – 1.143, p=0.038). This result highlights that higher levels of these antibodies may correlate with a higher chance of AD development, thereby offering new insights for clinical and public health interventions. Importantly, the notable association with anti-*H. pylori* UREA underscores its distinct function in AD pathogenesis, which may inform future therapeutic and preventive approaches to mitigate the impact of this neurodegenerative disorder.

The strong correlation between the two suggests that *H. pylori* infection is critical in the etiology of AD. Investigations indicated that *H. pylori* can induce chronic inflammation and immune responses, potentially resulting in neural damage.[25] Moreover, the infection may release neurotoxic substances that impair neuronal function and survival, thereby accelerating cognitive decline.[26] Although

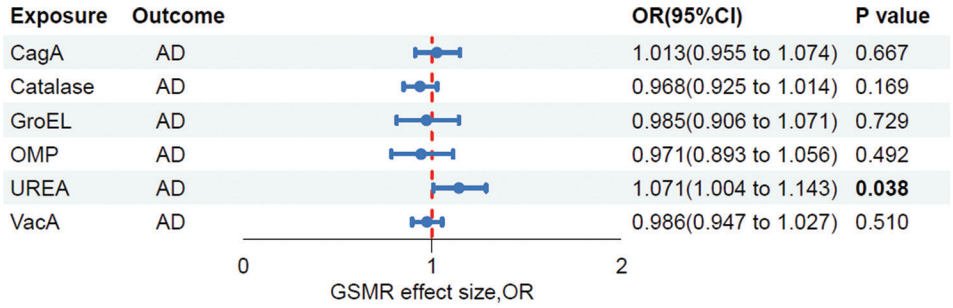


Figure 1. Forest plot for the GSMR effect of antibodies against *Helicobacter pylori* on Alzheimer's disease
Note: *p*-value in boldface indicates anti-*H. pylori* UREA was found to be significantly associated with an increased risk of AD in GSMR.
Abbreviations: AD: Alzheimer's disease; CI: Confidence interval; GSMR: Generalized summary data–based Mendelian randomization; OR: Odds ratio.

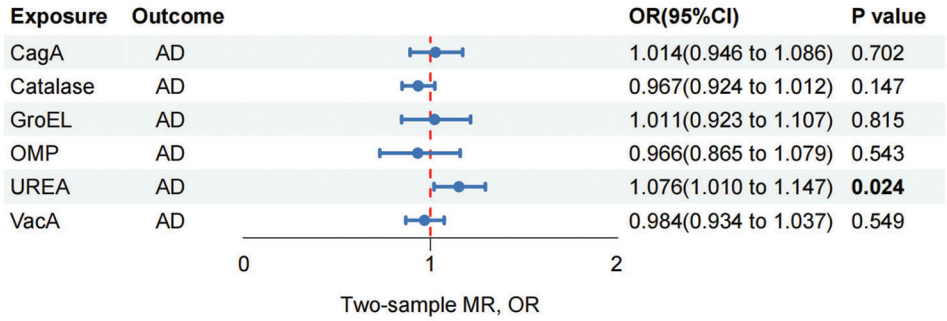


Figure 2. Forest plot for two-sample Mendelian randomization effect of antibodies against *Helicobacter pylori* on Alzheimer's disease
Note: *p*-value in boldface indicates anti-*H. pylori* UREA was found to be significantly associated with an increased risk of AD in Two-sample MR.
Abbreviations: AD: Alzheimer's disease; CI: Confidence interval; OR: Odds ratio.

our reverse MR analysis found no significant impact of AD on *H. pylori* infection, this does not diminish the potential of *H. pylori* as an intervenable risk factor for AD. Therefore, further investigation into the causal link and underlying mechanisms between AD and *H. pylori* is essential to enhance prevention and treatment strategies for AD.

In this study, we identified a strong correlation among AD and anti-*H. pylori* UREA antibodies, which aligns with prior research examining the correlation between neurodegenerative disorders and *H. pylori* infection.[27-29] Numerous studies indicate that this infection may raise AD risk by inducing chronic inflammation and immune responses that adversely affect neuronal function and viability.[30,31] However, the discrepancies in findings across various studies necessitate further examination. For example, some investigations have not demonstrated a direct correlation among AD and *H. pylori* infection,[32] potentially attributable to variations in sample selection, study design, and methodologies. In addition, differences in *H. pylori* strains may result in distinct pathogenic mechanisms, thereby influencing the strength of the association with neurodegenerative diseases. Factors such as individual genetic predispositions, environmental influences, and lifestyle choices may also contribute to these inconsistent results. Consequently, future research should account for these variables to further elucidate the precise role played by *H. pylori* infection in the etiology of neurodegenerative disorders and the inherent complexities involved.

A significant advantage of this work is the use of advanced MR techniques, specifically GSMR and two-sample MR. These methodologies utilize information from large-scale genome-wide association investigations, thereby enhancing both the statistical power and reliability of the findings. In addition, GSMR facilitates the flexible use of multiple independent IVs, resulting in more robust causal inferences. The implementation of these techniques establishes a solid theoretical foundation and analytical framework for investigating the correlation among AD and *H. pylori* infection.

Despite the strengths of this study, several limitations must be acknowledged. First, reliance on specific SNPs as IVs may restrict the generalizability of the findings.

If these SNPs do not adequately represent the genetic architecture of *H. pylori* infection, the validity of the causal inferences could be compromised. Second, the potential for residual confounding remains a significant concern, as unmeasured factors may simultaneously influence both AD and *H. pylori* infection, complicating result interpretation. In addition, despite the strengths of MR in reducing confounding, it is important to note that potential confounders, such as microbial communities and lifestyle factors, may still affect both AD and *H. pylori* infection. These factors were not included in our analysis, which could influence the explanatory power. Moreover, the fact that the population in this study is exclusively European limits the generalizability of the findings to other racial and ethnic groups. It remains unclear whether the results would hold true for populations with different genetic backgrounds or environmental exposures. To shed light on the interactions between *H. pylori* and neurodegenerative illnesses, future studies should employ bigger, more varied cohorts and longitudinal data.

5. Conclusion

This investigation indicates a strong correlation among AD and anti-*H. pylori* UREA antibodies, suggesting a potential role of *H. pylori* infection in the etiology of AD. These findings suggest *H. pylori* as a modifiable risk factor, emphasizing the necessity for additional investigations to clarify causal mechanisms and address existing limitations.

Acknowledgments

None.

Funding

None.

Conflict of interest

The authors declare that they have no conflict of interest.

Author contributions

Conceptualization: Ke Yi
Formal analysis: Yuan Xin Hou, Ke Yi
Methodology: Yuan Xin Hou, Ke Yi
Writing – original draft: Yuan Xin Hou, Ao Wang
Writing – review & editing: Yuan Xin Hou, Ao Wang

Ethics approval and consent to participate

Not applicable.

Consent for publication

Not applicable.

Availability of data

Original data generated and analyzed during this study are included in this published article or supplementary material. Further inquiries can be directed to the corresponding author.

References

1. Malfertheiner P, Camargo MC, El-Omar E, *et al*. *Helicobacter pylori* infection. *Nat Rev Dis Primers*. 2023;9(1):19.

   doi: 10.1038/s41572-023-00431-8

2. Usui Y, Taniyama Y, Endo M, *et al*. *Helicobacter pylori*, homologous-recombination genes, and gastric cancer. *N Engl J Med*. 2023;388(13):1181-1190.

   doi: 10.1056/NEJMoa2211807

3. Salvatori S, Marafini I, Laudisi F, Monteleone G, Stolfi C. *Helicobacter pylori* and gastric cancer: Pathogenetic mechanisms. *Int J Mol Sci*. 2023;24(3):2895.

   doi: 10.3390/ijms24032895

4. Gorlé N, Bauwens E, Haesebrouck F, Smet A, Vandenbroucke RE. *Helicobacter* and the potential role in neurological disorders: There is more than *Helicobacter pylori*. *Front Immunol*. 2020;11:584165.

   doi: 10.3389/fimmu.2020.584165

5. Ju Z, Shen L, Zhou M, *et al*. *Helicobacter pylori* and Alzheimer's disease-related metabolic dysfunction: Activation of TLR4/Myd88 inflammation pathway from p53 perspective and a case study of low-dose radiation intervention. *ACS Chem Neurosci*. 2022;13(7):1065-1081.

   doi: 10.1021/acschemneuro.2c00082

6. Scheltens P, De Strooper B, Kivipelto M, *et al*. Alzheimer's disease. *Lancet*. 2021;397(10284):1577-1590.

   doi: 10.1016/s0140-6736(20)32205-4

7. Tatulian SA. Challenges and hopes for Alzheimer's disease. *Drug Discov Today*. 2022;27(4):1027-1043.

   doi: 10.1016/j.drudis.2022.01.016

8. Trejo-Lopez JA, Yachnis AT, Prokop S. Neuropathology of Alzheimer's disease. *Neurotherapeutics*. 2022;19(1):173-185.

   doi: 10.1007/s13311-021-01146-y

9. Rostagno AA. Pathogenesis of Alzheimer's disease. *Int J Mol Sci*. 2022;24(1):107.

   doi: 10.3390/ijms24010107

10. Vaz M, Silvestre S. Alzheimer's disease: Recent treatment strategies. *Eur J Pharmacol*. 2020;887:173554.

    doi: 10.1016/j.ejphar.2020.173554

11. Cuomo P, Papaianni M, Sansone C, *et al*. An *in vitro* model to

investigate the role of *Helicobacter pylori* in type 2 diabetes, obesity, Alzheimer's disease and cardiometabolic disease. *Int J Mol Sci*. 2020;21(21):8369.

doi: 10.3390/ijms21218369

12. Kandpal M, Baral B, Varshney N, *et al*. Gut-brain axis interplay via STAT3 pathway: Implications of *Helicobacter pylori* derived secretome on inflammation and Alzheimer's disease. *Virulence*. 2024;15(1):2303853.

doi: 10.1080/21505594.2024.2303853

13. Fu P, Gao M, Yung KKL. Association of intestinal disorders with Parkinson's disease and Alzheimer's disease: A systematic review and meta-analysis. *ACS Chem Neurosci*. 2020;11(3):395-405.

doi: 10.1021/acschemneuro.9b00607

14. Beydoun MA, Beydoun HA, Weiss J, Hossain S, El-Hajj ZW, Zonderman AB. *Helicobacter pylori*, periodontal pathogens, and their interactive association with incident all-cause and Alzheimer's disease dementia in a large national survey. *Mol Psychiatry*. 2021;26(10):6038-6053.

doi: 10.1038/s41380-020-0736-2

15. Wang XL, Zeng J, Feng J, *et al*. *Helicobacter pylori* filtrate impairs spatial learning and memory in rats and increases β-amyloid by enhancing expression of presenilin-2. *Front Aging Neurosci*. 2014;6:66.

doi: 10.3389/fnagi.2014.00066

16. Pauwels EKJ, Boer GJ. Friends and foes in Alzheimer's disease. *Med Princ Pract*. 2023;32(6):313-322.

doi: 10.1159/000534400

17. Kuźniar J, Kozubek P, Czaja M, Leszek J. Correlation between Alzheimer's disease and gastrointestinal tract disorders. *Nutrients*. 2024;16(14):2366.

doi: 10.3390/nu16142366

18. Walker VM, Zheng J, Gaunt TR, Smith GD. Phenotypic causal inference using genome-wide association study data: Mendelian randomization and beyond. *Annu Rev Biomed Data Sci*. 2022;5:1-17.

doi: 10.1146/annurev-biodatasci-122120-024910

19. Zhu Z, Zheng Z, Zhang F, *et al*. Causal associations between risk factors and common diseases inferred from GWAS summary data. *Nat Commun*. 2018;9(1):224.

doi: 10.1038/s41467-017-02317-2

20. Liu Y, Li B, Ma Y, Huang Y, Ouyang F, Liu Q. Mendelian randomization integrating GWAS, eQTL, and mQTL data identified genes pleiotropically associated with atrial fibrillation. *Front Cardiovasc Med*. 2021;8:745757.

doi: 10.3389/fcvm.2021.745757

21. Butler-Laporte G, Kreuzer D, Nakanishi T, Harroud A, Forgetta V, Richards JB. Genetic determinants of antibody-mediated immune responses to infectious diseases agents: A genome-wide and HLA association study. *Open Forum Infect Dis*. 2020;7(11):ofaa450.

doi: 10.1093/ofid/ofaa450

22. Lawlor DA, Harbord RM, Sterne JA, Timpson N, Davey Smith G. Mendelian randomization: Using genes as instruments for making causal inferences in epidemiology. *Stat Med*. 2008;27(8):1133-1163.

doi: 10.1002/sim.3034

23. Davies NM, Holmes MV, Davey Smith G. Reading Mendelian randomisation studies: A guide, glossary, and checklist for clinicians. *BMJ*. 2018;362:k601.

doi: 10.1136/bmj.k601

24. Bowden J, Del Greco MF, Minelli C, *et al*. Improving the accuracy of two-sample summary-data Mendelian randomization: Moving beyond the NOME assumption. *Int J Epidemiol*. 2019;48(3):728-742.

doi: 10.1093/ije/dyy258

25. Kountouras J, Gavalas E, Zavos C, *et al*. Alzheimer's disease and *Helicobacter pylori* infection: Defective immune regulation and apoptosis as proposed common links. *Med Hypotheses*. 2007;68(2):378-388.

doi: 10.1016/j.mehy.2006.06.052

26. Park AM, Tsunoda I. *Helicobacter pylori* infection in the stomach induces neuroinflammation: The potential roles of bacterial outer membrane vesicles in an animal model of Alzheimer's disease. *Inflamm Regen*. 2022;42(1):39.

doi: 10.1186/s41232-022-00224-8

27. Kountouras J, Deretzi G, Gavalas E, *et al*. A proposed role of human defensins in *Helicobacter pylori*-related neurodegenerative disorders. *Med Hypotheses*. 2014;82(3):368-373.

doi: 10.1016/j.mehy.2013.12.025

28. Kountouras J, Doulberis M, Papaefthymiou A, *et al*. Controlling the impact of *Helicobacter pylori*-related hyperhomocysteinemia on neurodegeneration. *Medicina (Kaunas)*. 2023;59(3):504.

doi: 10.3390/medicina59030504

29. Wang XL, Zeng J, Yang Y, *et al*. *Helicobacter pylori* filtrate induces Alzheimer-like tau hyperphosphorylation by activating glycogen synthase kinase-3β. *J Alzheimers Dis*. 2015;43(1):153-165.

doi: 10.3233/jad-140198

30. Noori M, Mahboobi R, Nabavi-Rad A, *et al*. *Helicobacter pylori* infection contributes to the expression of Alzheimer's disease-associated risk factors and neuroinflammation. *Heliyon*. 2023;9(9):e19607.

doi: 10.1016/j.heliyon.2023.e19607

31. Douros A, Ante Z, Fallone CA, *et al*. Clinically apparent *Helicobacter pylori* infection and the risk of incident Alzheimer's disease: A population-based nested case-control study. *Alzheimers Dement*. 2024;20(3):1716-1724.

doi: 10.1002/alz.13561

32. Shiota S, Murakami K, Yoshiiwa A, *et al*. The relationship between *Helicobacter pylori* infection and Alzheimer's disease in Japan. *J Neurol*. 2011;258(8):1460-1463.

doi: 10.1007/s00415-011-5957-5

ACCSCIENCE PUBLISHING

Eurasian Journal of Medicine and Oncology

SHORT COMMUNICATION

Fertility outcomes of macroscopic tubal reanastomosis through mini-laparotomy: A retrospective case series study

Dilay Gök Korucu[1]*, Esra Koşucu[1], Şükran Doğru[2], and Oğuzhan Günenç[1]

[1]Department of Obstetrics and Gynecology, Konya City Hospital, University of Health Sciences, Konya, Türkiye

[2]Department of Perinatology, Konya City Hospital, University of Health Sciences, Konya, Türkiye

Abstract

Introduction: Tubal ligation reversal is a surgical option for restoring fertility, with outcomes influenced by technique, surgeon expertise, and patient factors.

Objective: This study evaluates the fertility outcomes of macroscopic tubal reanastomosis through mini-laparotomy.

Methods: This retrospective study analyzed medical records of women who had previously undergone tubal ligation either during cesarean sections or through laparoscopic electrocoagulation at a tertiary hospital in Türkiye between 2019 and 2022. The primary surgical approach involved a mini-laparotomy, and the anastomosis was performed macroscopically—without the use of an operating microscope—relying instead on direct visual inspection to access and reconnect the fallopian tubes. The suitability of the tubes for reanastomosis was assessed based on the length of the tubes, the presence of adhesion, and the condition of the fimbriae. Fertility outcomes, including live birth rates and time to conception, and surgical success rates, were measured.

Results: The data of 23 patients were retrospectively reviewed. The surgical success rate was 78.2% (unilateral or bilateral reanastomosis of the tubas), with a pregnancy rate of 43.5% and a live birth rate of 34.8%. The mean time to conception was 3.73 months.

Conclusion: Despite lower pregnancy rates compared with the broader literature, these outcomes are deemed acceptable, particularly for centers lacking facilities for more advanced surgical options. Therefore, macroscopic tubal reanastomosis through mini-laparotomy emerges as a feasible alternative for surgeons with limited experience in more intricate microsurgical techniques, providing a viable pathway to restoring fertility with reasonable success.

Keywords: Sterilization reversal; Laparotomy; Fallopian tube reanastomoses; Pregnancy rate

***Corresponding author:**
Dilay Gök Korucu
(dilaygok@yahoo.com)

Citation: Korucu DG, Koşucu E, Doğru S, Günenç O. Fertility outcomes of macroscopic tubal reanastomosis through mini-laparotomy: A retrospective case series study. *Eurasian J Med Oncol*. 2025;9(3):294-299.
doi: 10.36922/EJMO025150111

Received: April 12, 2025

1st revised: May 13, 2025

2nd revised: July 3, 2025

Accepted: August 1, 2025

Published online: September 3, 2025

Copyright: © 2025 Author(s). This is an Open-Access article distributed under the terms of the Creative Commons Attribution License, permitting distribution, and reproduction in any medium, provided the original work is properly cited.

Publisher's Note: AccScience Publishing remains neutral with regard to jurisdictional claims in published maps and institutional affiliations.

1. Introduction

Female sterilization through bilateral tubal ligation (BTL) is a leading method of contraception worldwide, used by nearly 25% of women aged 15–44 years (approximately 200 million globally), with the prevalence in the United States for the same age group at

22%.[1,2] Despite its widespread use, BTL must be presented to patients as a permanent method during counseling. The potential for reversal is limited, as success is not guaranteed and depends on factors such as the original surgical technique and the patient's fertility status. Moreover, reversal procedures represent a significant financial barrier, as they are rarely covered by health insurance. Emphasizing these points before agreeing to this procedure is essential to ensure informed consent and minimize future regret.

Interestingly, 5–20% of women who underwent sterilization later regret their choice, and only 1–2% seek to have the procedure reversed.[3] Regret over sterilization often stems from changes in marital status, the death of a child, or shifts in personal perspectives. Key predictors of dissatisfaction with the decision to undergo sterilization include being young, having a new partner, experiencing the loss of a child, or the desire to have more children, with some individuals hoping to become pregnant again.[4] For women who have undergone tubal sterilization, there are two main options for achieving pregnancy: laparoscopic microsurgical reversal and *in vitro* fertilization (IVF) therapy. An American Society for Reproductive Medicine (ASRM) report emphasizes the importance of considering factors such as a woman's age, sperm quality, desire for children, the extent of tubal disease, and the surgeon's experience when treating tubal infertility. While there are not enough studies comparing pregnancy rates between laparoscopic microsurgical reversal and IVF therapy, IVF offers higher per-cycle pregnancy rates. On the other hand, tubal anastomosis for reversing tubal sterilization provides higher cumulative pregnancy rates compared to IVF, with microsurgical anastomosis being the recommended technique. Hence, both treatment options should be evaluated based on patient preferences and clinical factors.[5] Moon *et al.*[6] discussed the comparison of microsurgical tubal reanastomosis and IVF for fertility restoration after BTL. They highlighted that while IVF is commonly preferred for its higher per-cycle pregnancy rates, tubal reanastomosis could provide better cumulative outcomes in specific cases, such as younger women or those wanting multiple children. Despite the dominance of IVF, they suggested that tubal reanastomosis remains a cost-effective and viable option, especially if training for microsurgical techniques is enhanced. Their study advocated for recognizing tubal reanastomosis as a feasible alternative to IVF in modern fertility treatments.

Tubal reanastomosis surgery has seen various technological advances over the years. Initially performed through laparotomy by Garcia[7] in 1972, the procedure was later adapted to laparoscopic methods by Sedbon *et al.*[8] in 1989, and subsequently, robotic techniques were introduced by Falcone *et al.*[9] in 1998. The success rates of these surgeries, varying by the specific surgical method employed, have been reported to range between 57% and 84%.[10] This article aims to share our experiences and present the pregnancy rates of our patients who underwent macroscopic tubal reanastomosis with mini-laparotomy.

2. Materials and methods

This retrospective study reviewed 23 patients admitted to Konya City Hospital, University of Health Sciences between 2019 and 2022 who requested tubal reanastomosis, which was performed macroscopically through mini-laparotomy. This study was conducted in compliance with the Declaration of Helsinki. The data of the patients were obtained from patient files and computer records. Written and verbal consents are routinely obtained from all patients admitted to our hospital for use in scientific publications.

The inclusion criteria were women with prior tubal ligation, either through the Pomeroy technique during cesarean section or through laparoscopic electrocoagulation, who subsequently desired fertility restoration. All participants underwent comprehensive fertility assessments, including day-3 hormone analysis, baseline ultrasonography, and pelvic examination, to exclude other infertility factors. Normal semen analysis of male partners was mandatory to rule out male factor infertility. Surgical candidates were required to have macroscopically suitable fallopian tubes with adequate length (>4 cm), minimal adhesions, and healthy fimbriae, with no contraindications for mini-laparotomy, such as severe pelvic adhesions and significant comorbidities. Patients were excluded from the study for several reasons: male factor infertility (abnormal semen parameters); other infertility causes, including ovarian dysfunction (e.g., diminished reserve or polycystic ovary syndrome); uterine abnormalities (e.g., fibroids or adhesions); endometriosis; or pelvic inflammatory disease affecting tubal function. In addition, women with unfavorable tubal conditions, including hydrosalpinx and extensive adhesions preventing safe anastomosis, as well as those with medical contraindications to surgery (e.g., uncontrolled diabetes and cardiovascular disease), were not considered candidates. This study specifically focused on Pomeroy and laparoscopic electrocoagulation sterilization methods, excluding other techniques such as clips and rings. Live birth outcomes were the primary outcome, while the mean age of the patients, success rates of tubal reversal (patients with at least one open tube on hysterosalpingography [HSG]), and time to pregnancy were secondary outcomes.

In the Pomeroy technique, a segment of the fallopian tube is isolated and looped. A suture is then placed around

the base of the looped segment, and the encircled portion of the tube is excised. The ends of the tube are then left to heal separately, effectively preventing the passage of an oocyte from the ovaries to the uterus, thus inhibiting fertilization and pregnancy. On the other hand, laparoscopic tubal ligation is a minimally invasive procedure that involves accessing the fallopian tubes through small incisions in the abdomen. During the procedure, the fallopian tubes are cauterized to prevent oocytes released from the ovaries from reaching the uterus. This blockage effectively stops sperm from meeting oocytes, thereby preventing fertilization and subsequent pregnancy.

2.1. Surgical method

All patients were positioned in lithotomy, and the bladders were emptied using a urinary catheter. After administering either general or spinal anesthesia, the abdomens were accessed through a mini-laparotomy in accordance with surgical protocol. A surgical exploration of the abdomen was performed. Suitability of the tubes for reanastomosis, the length of the tubes, adhesions with surrounding tissues, the condition of the fimbriae, and the relationship between the tubes and ovaries were assessed.

Initially, the opposing ends of the ligated tubes were identified, and the fibrotic tissues were excised from both ends using scissors. An 18-gauge epidural catheter was advanced from the fimbrial end and inserted into the lumen of the opposite tube, which had been opened with scissors, and then pushed toward the uterus. The tubes were sutured using the single-layer, four-suture technique described by Berge *et al.*,[11] with 5-0 Prolene sutures aligning the serosal and muscular layers in a single layer. Subsequently, methylene blue dye was administered through a vaginal Rubin cannula to check for patency from the tubes into the abdominal cavity, while keeping the epidural catheter stationary. Following hemostasis, the abdomen was gently closed, and the ends of the epidural catheter were secured to the skin surface. The epidural catheter was completely removed after 48 h, and the patients were discharged 48 h later. They were recalled for an HSG test after 2 months. Patients whose at least one tube was found to be patent were considered part of the successful surgical group and were allowed to pursue spontaneous pregnancy processes.

2.2. Statistical analysis

All data analyses in this study were performed using SPSS version 26 (IBM Corp., US). The data were assessed for normal distribution using histograms, Kolmogorov–Smirnov, and Shapiro–Wilk tests. Normally distributed data were presented as mean ± standard deviation. Categorical data were analyzed using the Chi-squared or Fisher's exact test, and results were expressed as *n* (%). $p<0.05$ was considered statistically significant.

3. Results

The analysis of data from 23 patients revealed that the mean age was 33.8 ± 6.3 years. Of these patients, 18 patients (78.3%) underwent tubal ligation through the Pomeroy technique during cesarean section, while 5 patients (21.7%) had laparoscopic tubal ligation with electrocoagulation. The mean duration between sterilization and tubal reanastomosis was 70.43 ± 40.01 months. These patient characteristics are summarized in Table 1. Regarding surgical outcomes, tubal reversal was successful in 18 patients (78.3%), with 11 (47.8%) achieving bilateral reversal and 7 (30.4%) unilateral reversal. The overall pregnancy rate post-reversal was 43.5% (10 patients), with a live birth rate of 34.8% (8 patients). The average time to conception after the reversal procedure was 3.73 ± 5.29 months.

4. Discussion

In this study, where reanastomosis of the fallopian tubes was performed macroscopically through mini-laparotomy, 78.3% of patients had their bilateral or unilateral tubal patency, which were detectable on HSG, successfully opened (47.8% bilateral, 30.4% unilateral). Of the 23 patients, 10 (43.5%) achieved pregnancy, and 8 (34.8%) had live births.

Tubal reanastomosis can be performed using three different techniques: (i) microsurgical method, (ii) laparoscopic method, or (iii) robotic method. The laparoscopic method offers several benefits, including reduced post-operative pain and the need for pain relief, decreased hospitalization duration, faster recovery, and improved cosmetic outcomes.[6] Nevertheless, laparoscopic microsurgery requires a significant amount of time and faces certain technical challenges.[12] Similarly, robotic surgery, while highly costly, also extends the duration of the operation and elevates the risk of complications during the procedure.[13]

The 2021 ASRM Committee Opinion recommended microsurgical anastomosis as the preferred method for reversing tubal ligation.[5] Mini-laparotomy appears to have similar pregnancy rates to laparoscopy, ranging from 54% to 88% versus 31% to 85%, respectively.[4] A previous study compared pregnancy outcomes after tubal reanastomosis using laparotomic, laparoscopic, or robotic methods among women desiring pregnancy after tubal sterilization.[10] Although the percentage of pregnancy was lowest in the laparotomy group with 52.6%, there were no significant differences in pregnancy rates among the three surgical

Table 1. Patient characteristics

Parameters	Number (n=23)	
Age (years)	33.8±6.3	
Tubal ligation method (%)		
C/S (Pomeroy)	18 (78.3)	
L/S BTL	5 (21.7)	
Interval between sterilization and reversal (months)	70.43±40.01	
Successful reversal of tubes by HSG (%)		
Bilateral	11 (47.8)	
Unilateral	7 (30.4)	
No passing	5 (21.7)	
Overall pregnancy	10 (43.5)	
Tubal ligation method (%)		
C/S (Pomeroy)	7 (70)	p=0.401
L/S BTL	3 (30)	
Abortion (%)	2 (8.7)	
Live birth (%)	8 (34.8)	

Notes: Data of age and interval between sterilization and reversal are represented as mean±standard deviation; data of other parameters are expressed as *n* (%).
Abbreviations: C/S: Cesarean section; HSG: Hysterosalpingography; L/S BTL: Laparoscopic bilateral tubal ligation.

methods. The overall pregnancy rate in the current study was 43.5%, which was lower than the pregnancy rate in the laparotomy tubal reanastomosis group in the previous study. In addition, laparoscopic surgery may be preferred due to a shorter hospitalization duration. Nonetheless, a surgeon's preference and experience, as well as hospital conditions, are the prominent factors in choosing tubal reanastomosis methods.

Every surgical method for tubal reanastomosis has a generally acceptable success rate range. A 2017 systematic review of pooled data reported consistent pregnancy rates ranging from 42%, 68% to 65% for laparotomic macrosurgical, laparotomic microsurgical, laparoscopic microsurgical, and robotic technique, respectively.[14] Pregnancy outcomes after tubal reanastomosis, however, are influenced by more than just surgical technique. The mother's age is the primary determinant.[15] Data from over 14,000 individuals suggest that pregnancy rates are higher among younger women.[16] Specifically, the pregnancy rate for women under 30 was 76.3% (confidence interval: 53.0–99.5%), and it declined with age: 60.6% for women aged 30–35, 59.4% for women aged 36–39, and 52.4% for women aged 40 years and older. In the present study, the mean patient age was 33.8 ± 6.3 years, and the pregnancy rate was 43.5%, slightly lower than previously reported.

Previous studies have shown that tubal reanastomosis outcomes largely depend on several key factors. For example, younger women tend to have higher pregnancy rates.[17] Other favorable factors include shorter intervals since sterilization, longer post-operative oviduct lengths (>7 cm), and the site of anastomosis, with isthmus–isthmus connections proving most effective. In addition, another study suggests that the type of original sterilization method also plays a critical role—less invasive methods, such as clips or rings, are associated with higher reversal success rates than electrocautery.[13] A remaining tubal length of at least 4 cm after reversal is also associated with better pregnancy outcomes. Collectively, these factors are key determinants of fertility restoration success after tubal reversal.

At present, IVF is frequently selected as the initial treatment after tubal ligation. The primary factor in deciding between tubal reanastomosis and IVF is the likelihood of achieving pregnancy, as the ultimate aim is to conceive. Direct comparison of pregnancy outcomes is challenging because IVF pregnancy reports are either mandatory or standardized, unlike those for tubal reanastomosis. Thus, outcomes should be evaluated on an individual basis, considering additional factors, such as cost-effectiveness, ease of the procedure, potential complications, side effects, personal preference, coexisting infertility factors, and the availability of skilled surgeons. Only two studies have compared the pregnancy outcomes of tubal reanastomosis and IVF for women seeking conception after tubal ligation. Boeckxstaens *et al.*[18] reported live birth rates per patient of 59.5% for tubal reanastomosis and 52.0% for IVF, with no significant difference. A meta-analysis by van Seeters *et al.*[14] found that both pregnancy and live birth rates were generally higher in the tubal reanastomosis group than in the IVF group. In women over 40, one study found that although tubal reanastomosis historically showed higher pregnancy rates, IVF now achieves competitive success rates, is often more cost-effective, and carries lower procedural risks.[19] IVF also offers the advantage of embryo cryopreservation for future use, despite potential increases in obstetric complications and the risks associated with multiple pregnancies. The choice between IVF and tubal reanastomosis should consider the individual's fertility circumstances and preferences, with IVF generally recommended for its efficiency and safety in older women. On the other hand, the benefits of tubal reanastomosis include being a one-time, typically minimally invasive outpatient procedure, where patients can try to conceive monthly without additional interventions and potentially achieve multiple pregnancies.

While tubal reanastomosis offers a viable path to restoring natural fertility, the inherent risk of ectopic

pregnancy is a significant consideration that must not be overlooked during counseling. The literature reported varying rates for this complication, ranging from 2% to 7%. For example, Karayalcin *et al.*[20] observed an ectopic pregnancy rate of 3.7%, whereas Barac *et al.*[21] reported a higher incidence of 8.53%. This risk may also be influenced by surgical factors, with Barac *et al.*[21] noting a significantly higher incidence when anastomosis was performed closer to the fimbrial end of the tube. A notable limitation of the present study is the inability to track ectopic pregnancy rates. Due to the retrospective design, comprehensive follow-up on pregnancies that did not result in live births at our institution, including potential ectopic pregnancies, was unavailable. Therefore, although acknowledging this well-documented risk from the literature, the present study cannot contribute data on this complication, which should be considered a limitation.

This study has other limitations. First, the conclusion is based on a relatively small sample size of 23 patients, limiting the generalizability of the findings to a broader population. Second, being a retrospective study, the findings are subject to potential biases related to data collection and selection. Prospective studies are needed to confirm these results and allow for more controlled assessments of outcome variables. Third, without a comparison group, such as patients undergoing alternative surgical techniques or IVF, it is challenging to directly attribute observed outcomes solely to macroscopic tubal reanastomosis through mini-laparotomy. Finally, although the study focuses on mini-laparotomy, variations in surgical technique and surgeon experience were not controlled, which may have influenced the results.

5. Conclusion

Macroscopic tubal reanastomosis through mini-laparotomy was successful in 78.2% patients, with an overall post-reversal pregnancy rate of 43.5% and a mean time to achieve pregnancy of 3.73 ± 5.29 months. Although the pregnancy rate achieved in this study is lower than that reported in the literature, it is still considered acceptable. Therefore, this approach can be recommended as an alternative method for surgeons lacking extensive experience in laparoscopic microsurgery for tubal reanastomosis.

Acknowledgments

None.

Funding

None.

Conflict of interest

The authors declare that there are no conflicts of interest.

Author contributions

Conceptualization: Dilay Gök Korucu, Şükran Doğru
Data curation: Dilay Gök Korucu
Methodology: Dilay Gök Korucu, Şükran Doğru
Writing–original draft: Dilay Gök Korucu
Writing–review & editing: Esra Koşucu, Şükran Doğru, Oğuzhan Günenç

Ethics approval and consent to participate

This study was conducted with the approval of the Konya City Hospital Local Committee (Date: 06.03.2025; number: 09-58). Patients provided verbal and written consent to participate in this study.

Consent for publication

Patients provided verbal and written consent for publication on registration into our hospital.

Availability of data

Data are available from the corresponding author on request.

References

1. Stuart GS, Ramesh SS. Interval female sterilization. *Obstet Gynecol*. 2018;131(1):117-124.

   doi: 10.1097/AOG.0000000000002376.

2. Centers for Disease Control and Prevention. *National Center for Health Statistics (NCHS). National Health and Nutrition Examination Survey Questionnaire (or Examination Protocol, or Laboratory Protocol*); 2006. Available from: https://www.cdc.gov [Last accessed on 2025 Jul 01].

3. Salehjawich A, Günther V, Ruchay Z, *et al*. Robot-assisted tubal reanastomosis after sterilization: A choice for family planning. *J Clin Med*. 2022;11(15):4385.

   doi: 10.3390/jcm11154385

4. Godin PA, Syrios K, Rege G, Demir S, Charitidou E, Wery O. Laparoscopic reversal of tubal sterilization; a retrospective study over 135 cases. *Front Surg*. 2018;5:79.

   doi: 10.3389/fsurg.2018.00079

5. Practice Committee of the American Society for Reproductive Medicine. Electronic address: ASRM@asrm.org 1. Role of tubal surgery in the era of assisted reproductive technology: A committee opinion. *Fertil Steril*. 2021;115(5):1143-1150.

   doi: 10.1016/j.fertnstert.2021.01.051

6. Moon HS, Joo BS, Kim SG, Nam KI, Koo JS. Where microsurgical tubal reanastomosis stands in the *in vitro* fertilization era. *Gynecol Minim Invasive Ther*. 2024;13(2):71-78.

   doi: 10.4103/gmit.gmit_43_23

7. Garcia CR. Oviductal anastomosis procedures. In: *Human Sterilization*. Springfiled: Thomas Charle; 1972. p. 116.

8. Sedbon E, Delajolinieres JB, Boudouris O, Madelenat P. Tubal desterilization through exclusive laparoscopy. *Hum Reprod*. 1989;4(2):158-159.

doi: 10.1093/oxfordjournals.humrep.a136862

9. Falcone T, Goldberg JM, Margossian H, Stevens L. Robotic-assisted laparoscopic microsurgical tubal anastomosis: A human pilot study. *Fertil Steril.* 2000;73(5):1040-1042.

doi: 10.1016/s0015-0282(00)00423-4

10. Elci G, Elci E, Sayan S, Hanligil E. Is there any difference between pregnancy results after tubal reanastamosis performed laparotomically, laparoscopically, and robotically? *Asian J Endosc Surg*. 2022;15(2):261-269.

doi: 10.1111/ases.12991

11. Berger GS, Thorp JM Jr., Weaver MA. Effectiveness of bilateral tubotubal anastomosis in a large outpatient population. *Hum Reprod*. 2016;31(5):1120-1125.

doi: 10.1093/humrep/dew038

12. Koh CH, Janik GM. Laparoscopic microsurgery: Current and future status. *Curr Opin Obstet Gynecol*. 1999;11(4):401-407.

doi: 10.1097/00001703-199908000-00007

13. Madison A, Alamri L, Schwartz A, Brolinson M, DeCherney A. Conventional laparoscopy is the better option for tubal sterilization reversal: A closer look at tubal reanastomosis. *Womens Health Rep* (*New Rochelle*). 2021;2(1):375-380.

doi: 10.1089/whr.2021.0039

14. van Seeters JAH, Chua SJ, Mol BWJ, Koks CAM. Tubal anastomosis after previous sterilization: A systematic review. *Hum Reprod Update*. 2017;23(3):358-370.

doi: 10.1093/humupd/dmx003

15. Kim SH, Shin CJ, Kim JG, Moon SY, Lee JY, Chang YS. Microsurgical reversal of tubal sterilization: A report on 1,118 cases. *Fertil Steril*. 1997;68(5):865-870.

doi: 10.1016/s0015-0282(97)00361-0

16. Sastre J, Mínguez JA, Alcázar JL, Chiva L. Microsurgical anastomosis of the fallopian tubes after tubal ligation: A systematic review and meta-analysis. *Eur J Obstet Gynecol Reprod Biol*. 2023;291:168-177.

doi: 10.1016/j.ejogrb.2023.10.017

17. Feng Y, Zhao H, Xu H, *et al*. Analysis of pregnancy outcome after anastomosis of oviduct and its influencing factors. *BMC Pregnancy Childbirth*. 2019;19(1):393.

doi: 10.1186/s12884-019-2469-2

18. Boeckxstaens A, Devroey P, Collins J, Tournaye H. Getting pregnant after tubal sterilization: Surgical reversal or IVF? *Hum Reprod*. 2007;22(10):2660-2664.

doi: 10.1093/humrep/dem248

19. Peregrine J, McGovern PG, Brady PC, Ginsburg ES, Schlaff W. Restoring fertility in women aged 40 years and older after tubal ligation: tubal anastomosis versus *in vitro* fertilization. *Fertil Steril*. 2020;113(4):735-742.

doi: 10.1016/j.fertnstert.2020.01.041

20. Karayalcin R, Ozcan S, Tokmak A, Gürlek B, Yenicesu O, Timur H. Pregnancy outcome of laparoscopic tubal reanastomosis: Retrospective results from a single clinical centre. *J Int Med Res*. 2017;45(3):1245-1252.

doi: 10.1177/0300060517709815

21. Barac S, Jiga LP, Rata A, Sas I, Onofrei RR, Ionac M. Role of reconstructive microsurgery in tubal infertility in young women. *J Clin Med*. 2020;9(5):1300.

doi: 10.3390/jcm9051300

ACCSCIENCE PUBLISHING

Eurasian Journal of Medicine and Oncology

LETTER TO EDITOR

Ferroptosis inhibition: New insights for the treatment of acute lung injury

Xuhan Chen and Jinhe Guo*

Department in Traditional Chinese Medicine, College of Traditional Chinese Medicine, Tianjin University of Traditional Chinese Medicine, Tianjin, China

Dear Editor,

In recent years, the incidence of acute lung injury (ALI) during clinical treatment has shown a notable upward trend. The aging of the global population, the widespread use of mechanical ventilation, and the emergence of novel pathogens have further exacerbated this situation, posing a severe threat to public health. Consequently, identifying new drug targets and treatment strategies for ALI has become an urgent challenge in the medical field.

Ferroptosis, a distinct form of programmed cell death characterized by iron dependence and lipid peroxidation, differs fundamentally from apoptosis, necrosis, and autophagy, representing a unique mechanism of cell demise.[1] Research indicates that ferroptosis is involved in the occurrence and progression of ALI induced by various factors, such as radiation-induced ALI, ischemia-reperfusion ALI, and lipopolysaccharide (LPS)-induced ALI.[2,3] In a sepsis-induced ALI rat model, abnormal expression of ferroptosis-associated proteins was detected in lung tissues. Notably, pharmacological or genetic inhibition of ferroptosis led to a marked alleviation of ALI symptoms, suggesting that targeted modulation of ferroptosis could be a promising therapeutic approach for ALI.[4,5]

Nuclear factor erythroid 2-related factor 2 (Nrf2) and heme oxygenase-1 (HO-1) play pivotal roles as antioxidant regulators, modulating intracellular iron concentration and metabolism, protecting cells from oxidative stress damage, and inhibiting ferroptosis.[4] The downstream factor solute carrier family 7 member 11 (SLC7A11), a downstream effector of this regulatory network, is recognized for its inhibitory function in ferroptosis. As a key subunit of the cystine/glutamate antiporter system (system xc^-), SLC7A11 facilitates the uptake of extracellular cystine into cells. In addition, glutathione peroxidase 4 (GPX4) is a key protein that inhibits ferroptosis. Regulating certain pathways or directly targeting the activation of Nrf2 can inhibit ferroptosis and reduce lung injury. For example, obacunone can target and activate Nrf2, inhibit the ubiquitination hydrolysis of Nrf2, and improve the antioxidant capacity of lung tissue. Similarly, pachymic acid, glycyrrhizic acid, curcumin, and marmesin regulate different signaling pathways to upregulate the expression of Nrf2, HO-1, GPX4, and SLC7A11 or downregulate the expression of kelch-like ECH-associated protein 1 to reduce ferroptosis levels.

While the concept of ferroptosis is not explicitly defined within the theoretical framework of traditional Chinese medicine (TCM), the application of TCM decoctions has demonstrated beneficial effects of inhibiting ferroptosis in the treatment of ALI. For instance, Huanglian-Jie-du Tang (HLJDD) has been utilized in the management of sepsis-induced ALI, Ganlu Qingwen Fang in LPS-induced ALI, and modified Taoren Chengqi in ventilator-induced lung injury (VILI). Modern pharmacological investigations have revealed that quercetin, a primary monomeric component of HLJDD, exhibits notable

***Corresponding author:**
Jinhe Guo
(guojinhe@tjutcm.edu.cn)

Citation: Chen X, Guo J. Ferroptosis inhibition: New insights for the treatment of acute lung injury. *Eurasian J Med Oncol*. 2025;9(3):300-301. doi: 10.36922/EJMO025090043

Received: February 28, 2025

Accepted: March 10, 2025

Published Online: April 4, 2025

Copyright: © 2025 Author(s). This is an Open-Access article distributed under the terms of the Creative Commons Attribution License, permitting distribution, and reproduction in any medium, provided the original work is properly cited.

Publisher's Note: AccScience Publishing remains neutral with regard to jurisdictional claims in published maps and institutional affiliations.

ferroptosis-inhibitory properties.[6] Ganlu Qingwen Fang has been shown to mitigate inflammatory responses and oxidative stress in rats, thereby conferring protection against ALI, potentially through the modulation of the Nrf2/GPX4 ferroptosis pathway.[7] Modified Taoren Chengqi may ameliorate VILI in rats by activating the Nrf2/GPX4 pathway, consequently inhibiting ferroptosis.[8]

Ferroptosis represents a promising therapeutic target for various pulmonary disorders, including ALI, chronic obstructive pulmonary disease, pulmonary fibrosis, lung infections, and asthma, all of which exhibit ferroptosis during their pathogenesis, thereby influencing the initiation and progression of the diseases.[9] Thus, future investigations should aim to elucidate the specific roles of ferroptosis or crosstalk between different cell death pathways in sepsis-induced ALI and to explore their comprehensive signaling pathways and correlation with disease prognosis. Such research endeavors hold the potential to unveil novel therapeutic targets and strategies for the management of ALI.

Funding

The Science & Technology Development Fund of Tianjin Education Commission for Higher Education (2023KJ131).

Conflict of interest

The authors declare no competing interests.

References

1. Zhao L, Ge G, Li J, Han X. The improvement effect of osthole on lung injury in rats with mycoplasma pneumoniae pneumonia through the Nrf2-Gpx4 ferroptosis pathway. *ZCY*. 2023;45(1):48-54.
2. Zhang H, Zhang Y, Fu J, *et al*. Research progress on the induction of ferroptosis in tumor cells by active ingredients of traditional Chinese medicine. *Chin J Exp Tradit Med Formul*. 2024;30(9):245-253.

   doi: 10.13422/j.cnki.syfjx.20232121
3. Chen Z, Tang H, Gan S, *et al*. Ferroptosis mediates airway epithelial E-cadherin dysfunction in LPS-induced acute lung injury. *Pulm Pharmacol Ther*. 2024;84:102284.

   doi: 10.1016/j.pupt.2023.102284
4. Zhang J, Zheng Y, Wang Y, *et al*. YAP1 alleviates sepsis-induced acute lung injury via inhibiting ferritinophagy-mediated ferroptosis. *Front Immunol*. 2022;13:884362.

   doi: 10.3389/fimmu.2022.884362
5. Wang Y, Chen D, Xie H, *et al*. AUF1 protects against ferroptosis to alleviate sepsis-induced acute lung injury by regulating NRF2 and ATF3. *Cell Mol Life Sci*. 2022;79(5):228.

   doi: 10.1007/s00018-022-04248-8
6. Li C, Wang H, He Q, Guo X, Jiang T, Guo Y. Study on the effect and mechanism of quercetin in inhibiting the proliferation of A549 cells by inducing ferroptosis. *Chin Herb Med*. 2022;53(22):7112-7120.
7. Li J, Li Z, Li X, Liang Q, Liao C, Li F. Exploration of the protective effect of Ganlu Qingwen formula on rats with acute lung injury based on the Nrf2/GPX4 ferroptosis pathway. *ZCY*. 2024;47(2):596-600.
8. Sun Z, Wang L, Suo H, Li H, Chen Q. Exploration of the protective effect of jiawei taoren chengqi decoction on rats with ventilator-associated lung injury based on the Nrf2/GPX4 ferroptosis pathway. *Tradit Chin Drug Res Clin Pharmacol*. 2024;35(9):1281-1288.

   doi: 10.19378/j.issn.1003-9783.2024.09.001
9. Zhao L, Ge G, Li J, Han X. The improvement effect of osthole on lung injury in rats with mycoplasma pneumoniae pneumonia through the Nrf2-Gpx4 ferroptosis pathway. *ZCY*. 2023;45(1):48-54.

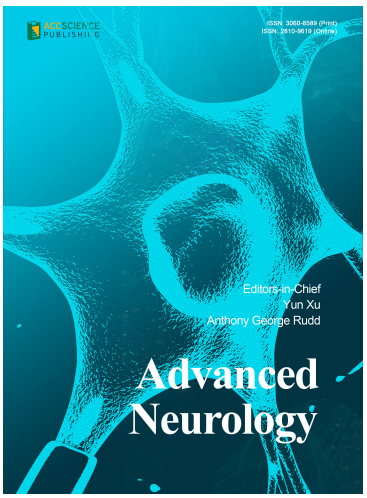
Our Journals



Organoid Research (OR) is an international, peer-reviewed journal dedicated to advancing the field of organoid science by publishing high-quality research articles, reviews, and perspectives. The journal focuses on studies that provide significant conceptual, experimental, and translational advances in the development and application of organoid technologies.

OR welcomes submissions spanning diverse areas of organoid science, including but not limited to stem cell biology, tissue engineering, regenerative medicine, disease modeling, and drug discovery. The journal encourages papers that explore bioengineered organoids, organoid-based systems biology, and the integration of organoids with clinical research. Special emphasis is placed on contributions that advance novel approaches to organoid development, including the use of cutting-edge bioengineering techniques, materiobiology, and integrative technologies such as artificial intelligence, high-throughput screening, and precision medicine. Additionally, the journal values research that delves into ethical considerations and challenges related to the clinical translation of organoid systems.

Advanced Neurology is a peer-reviewed and open-access journal that aims to publish and disseminate novel research in the breadth of neurology and neuroscience. The journal aims to advance our understanding in the nervous system and provide a platform to neuroscientists and physicians to showcase their findings in original fundamental and clinical research as well as to present new ideas that highlight the changes in the neurological clinical practice.



Advanced Neurology covers subject areas, including but not limited to the following:

- Neurological disorders
- Neurodegenerative disease
- Cerebrovascular disease
- Epilepsy and movement disorders
- Neuroimmune disease
- Neurological infections
- Muscle disease
- Molecular and cellular neuroscience
- Systems neuroscience
- Cognitive neuroscience
- Computational modeling of nervous system

Start a new journal

Write to us via email if you are interested to start a new journal with AccScience Publishing. Please attach your CV, professional profile page and a brief pitch proposal in your email. We shall inform you of our decision whether we are interested to collaborate in starting a new journal.

Contact: info@accscience.com

https://accscience.com/journal/EJMO



Contact

www.accscience.com

9 Raffles Place, Republic Plaza 1 #06-00 Singapore 048619

E-mail: editorial@accscience.com

Phone: +65 8182 1586